Multigene Metabolic Engineering for the Increase of Photosynthetic Efficiency

Beatriz Moreno García

University College

University of Oxford

A thesis submitted for the degree of

Doctor of Philosophy

Michaelmas 2020

Annihilating all that's made
To a green thought in a green shade.

— Andrew Marvell, *The Garden*

Acknowledgements

I am immensely grateful to Prof. Lee Sweetlove as my thesis supervisor. Thank you for your continuous guidance and advice, showing me how amazing photosynthesis and plant metabolism are, and believing in me to pursue such an awesome project. I have learnt a lot from you and I am particularly grateful for you teaching me the way towards becoming an independent researcher.

I would like to extend my thanks to Prof. Liam Dolan and Prof. Renier van der Hoorn from the Department of Plant Sciences at the University of Oxford for providing invaluable advice at key stages during my DPhil. I sincerely acknowledge Dr Nick Kruger and Dr Alistair McCormick for an intellectually stimulating DPhil viva and helpful comments and suggestions on this thesis.

I deeply acknowledge Prof. Ralph Bock and his team at the Max Planck Institute of Molecular Plant Physiology in Potsdam-Golm (Germany) for their contribution to this project and for hosting me at their Institute. Thank you to Margit Röβner, Claudia Hasse, and Dr Stephanie Ruf from the Transformation Team for performing the transformation and regeneration of the transgenic tobacco combinatorial library. I would like to thank Dr Szymon Kubiszewski-Jakubiak and Dr José Vallarino for assisting in the cloning and subsequent high light screen.

I am also grateful to Dr Patricia López Calcagno and Prof. Christine Raines from the School of Life Sciences at the University of Essex in Colchester (UK) for providing the synthetic Golden Gate modules and assisting in the generation of the multigene constructs used for tobacco transformation. I also wish to thank Dr Sanu Shameer for the modelling work on which this strategy was based, and for always being genuinely interested in my progress. I would like to acknowledge Dr Mark Fricker for his assistance in the confocal imaging of Arabidopsis. I appreciate the help of András Sándor and Alexander Bones with explant regeneration while I was in Germany. I am grateful to Dr John Walsby-Tickle and Prof. James McCullagh from the Chemistry Research Laboratory at the University of Oxford for providing training on the use of the Seahorse Extracellular Flux Analyser and helping me to adapt it to plant measurements. Thank you to Edward Smith for making it possible to run the last batch of plates when access to labs was restricted due to the COVID-19 pandemic.

I would like to thank the members of the Department of Plant Sciences at the University of Oxford for making it such a great place to work. Many thanks to Pedro Bota for providing technical support throughout my time at the Department. Thank you to everyone at the Biochemistry floor and the Sweetlove group for being a wonderful group of friends.

My gratitude extends to the Interdisciplinary Bioscience (BBSRC Doctoral Training Partnership) and the Doctoral Training Centre at the University of Oxford for funding, training, and support throughout my doctoral studies. Many thanks to Prof. Gail Preston for ongoing support and encouragement. I wish to acknowledge University College for financial support and providing an environment in which to thrive. Thank you, Univ, for being our home away from home.

I also wish to thank current and past mentors for encouraging my scientific curiosity and enthusiasm for Plant Biotechnology research and supporting me to get where I am today.

Thank you to my family and friends for making my time at Oxford so amazing. I will fondly remember chats over lunch, tea, and dinner, walks, formal halls, pub trips, concerts, visits to London, the 2018 trip to the Chalet des Anglais, runs in town and Port Meadow, kayaking on the Thames, our plot at Cripley Meadow, rowing with Univ, climbing, squash, punting...

I am deeply grateful to my family for their visits, trips with us, countless calls, postcards, and letters. Thank you to those who have left us and who would have been so proud. My heartfelt gratitude to my parents, Lola and Fernando, and siblings, Bárbara and Daniel, for their unconditional love and support and always being there for me. To Juan, thank you for your love, patience, and encouragement during the last four years (and always) and for being the best companion to this adventure (and everything).

Abstract

Improving photosynthesis is one of the most promising approaches to increase crop yield. To date, most efforts to enhance photosynthesis have focused on single-gene approaches. However, from a theoretical and experimental perspective, it is evident that multigene manipulations could lead to a greater impact. This DPhil project sets out to implement two innovative multigene metabolic engineering strategies for improved photosynthesis in *Nicotiana tabacum*. Firstly, combinatorial co-transformation was used with 12 transgenes, chosen to increase source leaf photosynthesis and downstream carbon metabolism. A library of metabolic phenotypes was recovered, from which five lines were selected for showing increased stem growth under high light conditions. This phenotype was not reproducible in subsequent experiments, but further characterisation of the selected lines suggested that their specific transgene combinations may not have been beneficial for growth due to transgene interference effects. Secondly, a diel flux balance analysis model of primary metabolism in Arabidopsis leaves was used to design a novel metabolic engineering strategy for improved leaf-energy efficiency and photosynthesis. A five-gene construct was generated that was predicted to result in increased mitochondrial ATP production, reduced chloroplast ATP export, and increased chloroplast NAD(P)H export. Contrary to the model predictions, transgene expression was found to correlate negatively with plant growth and photosynthesis. One possible explanation was a detrimental effect caused by the increased capacity of the chloroplast malate valve. This thesis constitutes one of the first investigations into the multigene engineering of photosynthesis and energy metabolism. Together, the results of this thesis highlight the complexity of manipulating plant central metabolism, particularly when targeting multiple transgenes, and suggests that further scrutiny of network behaviour and testing of transgene combinations will be needed to enhance photosynthesis and achieve the yield increases required to feed a growing population.

Contents

List of Figures

List of Tables

List of Abbreviations

ADP . . . . . Adenosine diphosphate

AGPase . . . . Adenosine diphosphate-glucose pyrophosphorylase

ANOVA . . . . Analysis of variance

ATP . . . . . Adenosine 5'-triphosphate

CaMV . . . . . Cauliflower mosaic virus

CBB . . . . . Calvin-Benson-Bassham

CO_2 . . . . . Carbon dioxide

cyFBPase . . . Cytosolic fructose 1,6-bisphosphatase

Cyt . . . . . Cytochrome

ddH_2O . . . . Double distilled water

EDTA . . . . . Ethylenediaminetetraacetic acid

EF-1α . . . . . Elongation factor-1α

F_0 . . . . . Minimum fluorescence intensity

FBA . . . . . Flux balance analysis

FBPA . . . . . Fructose 1,6-bisphosphate aldolase

FBPase . . . . Fructose 1,6-bisphosphatase

FCCP . . . . . Carbonyl cyanide 4-(trifluoromethoxy)phenylhydrazone

FIS1A . . . . . Fission 1A

F_m . . . . . Maximum fluorescence intensity

F_v . . . . . Maximum variable fluorescence intensity

F_v/F_m . . . . . Maximum quantum yield of primary photosystem II photochemistry

GAPC . . . . . Phosphorylating NAD-dependent glyceraldehyde 3-phosphate dehydrogenase

GC-MS . . . . Gas chromatography mass spectrometry

GDC-H . . . . Glycine decarboxylase H-protein

ICTB . . . . . Inorganic carbon transporter B

L25 . . . . . L25 ribosomal protein

LB . . . . . Luria-Bertani

mC . . . . . mCherry

MDH . . . . . Malate dehydrogenase

mMDH . . . . Mitochondrial malate dehydrogenase

MS . . . . . Murashige and Skoog

Mt . . . . . Million tonnes

NAD(H) . . . Nicotinamide adenine dinucleotide

NADP(H) . . Nicotinamide adenine dinucleotide phosphate

NPQ . . . . . Non-photochemical quenching

OCR . . . . . Oxygen consumption rate

PAR . . . . . Photosynthetically active radiation

PC . . . . . Principal component

PCA . . . . . Principal component analysis

PCR . . . . . Polymerase chain reaction

PetC . . . . . Rieske FeS protein

PFLP . . . . . Plant ferredoxin-like protein

3-PGA . . . . 3-Phosphoglyceric acid

P_i . . . . . Inorganic phosphate

pOMT . . . . . Plastidic 2-oxoglutarate/malate transporter

PPase . . . . . Pyrophosphatase

PP_i . . . . . Inorganic pyrophosphate

PS . . . . . Photosystem

ΦPSII . . . . . Efficiency of photosystem II photochemistry or quantum yield

qRT-PCR . . . Quantitative real-time polymerase chain reaction

RuBisCO . . . Ribulose 1,5 bisphosphate carboxylase-oxygenase

RuBP . . . . . Ribulose 1,5- bisphosphate

SBPase . . . . Sedoheptulose 1,7-bisphosphatase

SE . . . . . Standard error

SUT/SUC . . Sucrose transporter

SWEET . . . . Sugars Will Eventually be Exported Transporter

TAE . . . . . Tris-acetate-Ethylenediaminetetraacetic acid

TAIR . . . . . The Arabidopsis Information Resource

TCA . . . . . Tricarboxylic acid

TMRM . . . . Tetramethylrhodamine methyl ester

TPT . . . . . Triose phosphate/phosphate translocator

Ts . . . . . T-Sapphire

WT . . . . . Wild type

Chapter 1
General Introduction

Contents

1.1 Thesis scope and objectives

Global food production needs to increase by 25-70% to meet the projected demand in 2050 [1, 2]. Engineering photosynthesis is currently one of the most promising strategies for increasing crop productivity in a sustainable way, with potential yield gains associated with photosynthesis amounting from 12% [3] to 50% [4] in C_3 plants.

Comprehensive reviews have been published in the last decade that explore potential targets for improved yield [5–7] and photosynthetic capacity in C_3 species (see references [8–21] for selected reviews of particular relevance). A number of these targets have successfully been manipulated in plants, including an increased capacity of carbon fixation [19, 22, 23], or the use of alternative photorespiratory pathways, which have led to a remarkable increase in biomass of up to 37% in field trials in *Nicotiana tabacum* (tobacco hereafter) [24] and 14–35% in *Oryza sativa* (rice) [25]. Other more ambitious strategies are underway, such as the introduction of C_4 photosynthesis in C_3 plants, but are not expected to be readily available in the short-term [4].

The yield gains associated with these individual targets are appreciable but, to date, do not match the required increases to feed an ever-growing population. There remains scope for further increases in photosynthesis for the development of higher-yielding crops.

Given that (a) no single strategy for crop improvement will suffice to meet the demand on its own, and (b) novel targets could further increase photosynthetic capacity and yield, **the primary objective of the work presented in this thesis was to explore innovative strategies for improved photosynthesis**, with the following specific objectives:

1. **To simultaneously manipulate several metabolic pathways in source leaves by overexpressing transgenes that are established as effective individual targets for photosynthesis improvement**. This was achieved

by generating a library of transgenic plants using biolistic combinatorial co-transformation. Chapter 3 outlines the generation of the library of combinatorial transformants. The combinatorial plant lines overexpressed an array of transgene combinations that have previously been reported to improve photosynthetic capacity and/or plant growth. The target pathways comprise the photosynthetic electron transport chain, the Calvin-Benson-Bassham (CBB) cycle, photorespiration, leaf sucrose biosynthesis, and sucrose export into the phloem.

2. **To identify and characterise high performing lines in the library of combinatorial transformants.** A screen of the transgenic library of combinatorial plants for improved photosynthetic capacity and/or plant growth was performed in order to identify successful transgene combinations. Chapter 3 reports the results of the screen of the combinatorial library and Chapter 4 expands on the further characterisation of selected lines.

3. **To implement and test a novel, computationally-predicted strategy for photosynthetic improvement.** For this purpose, a computational model of leaf primary metabolism was used to conceive new targets for improved photosynthesis, entailing a subcellular rearrangement of energy and reductant fluxes in the mesophyll. Transgenes associated with the predicted target pathways were introduced in plants in combination in order to test the suitability of the predicted changes to increase photosynthetic capacity and plant growth. Chapter 5 describes the generation of transgenic plants carrying a multigene construct with the selected transgenes and an assessment of photosynthetic and respiratory capacity and plant growth of these transgenic plants.

1.2 Background

1.2.1 Food security in the context of overpopulation and climate change

Food security is defined by the Food and Agriculture Organization of the United Nations as '*a situation that exists when all people, at all times, have physical, social and economic access to sufficient, safe and nutritious food that meets their dietary needs and food preferences for an active and healthy life*' [26]. Based on this definition, four food security dimensions can be identified: food availability, economic and physical access to food, food utilisation, and stability over time [26]. Having been declared as the second Sustainable Development Goal for 2030 by the United Nations, preceded by ending poverty, food security is one of the most pressing challenges of the twenty-first century [27].

The global population is expected to grow by 26% in the next three decades, from the current 7.7 billion to 9.6 billion by 2050 [28]. The projected increases in global population are matched with an increase in global crop demand of up to 70% from current levels [1, 2, 29, 30].

Crop yield is defined as the harvested production per unit area of crop products [31]. Four crops contribute to two-thirds of the global calorie consumption [32], namely maize (*Zea mays*, with 1149 million tonnes (Mt) produced in 2019), wheat (*Triticum aestivum*, 766 Mt), paddy rice (756 Mt), and soybean (*Glycine max*, 334 Mt) [33]. However, the rate of year on year yield increases of these major crops is now stagnating [32].

Since crop yield is directly linked to food availability, there will be enormous pressure on agricultural food production in the coming decades. This pressure will be aggravated by climate change, leading to increased incidence of extreme weather events [32] that add large uncertainty over crop production. With additional pressure for sustainability in the food chain, there is a reluctance to clear further land for agricultural food production [34]. This means that there is a striking

need to increase crop yield towards achieving the sustainable intensification of agricultural production [35].

1.2.2 Improving photosynthesis for increased crop yield potential

Crop yield potential (Y_p) is '*the yield of a cultivar when grown in environments to which it is adapted, with nutrients and water non-limiting and with pests, diseases, weeds, lodging, and other stresses effectively controlled*' [36]. It can be calculated as harvest yield (MJm^{-2}) by adapting Monteith's equation [21, 37]:

$$Y_p = 0.487 \times S_t \times \epsilon_i \times \epsilon_c \times \epsilon_p$$

where S_t (GJm^{-2}) is the total incident solar radiation across the growing season, ϵ_i is light interception efficiency of photosynthetically active radiation (PAR, 400–700 nm), ϵ_c is conversion efficiency — also termed radiation use efficiency — or the ratio of biomass energy produced over a given period to the radiative energy intercepted by the canopy over the same period, and ϵ_p is partitioning efficiency — also termed harvest index — or the amount of the total biomass energy partitioned into the harvested portion of the crop [4, 5, 15, 21]. Approximately 10% of the PAR is transmitted by leaves ($>$ 700 nm). This represents about half the energy of sunlight, so S_t is halved to account for the fraction of transmitted light.

Crop yield saw an extraordinary increase during the Green Revolution. This sharp rise was possible thanks to improved agricultural practices (a more extended application of fertiliser and better protection against diseases) and an increase of genetic yield potential [38]. As illustrated by Zhu, Long, and Ort [21] the latter was mediated by an improvement of light interception efficiency (larger-leafed cultivars) and resource partitioning efficiency (dwarfing).

Light intercepted shows limited prospects for further improvement since modern cultivars of food crops already intercept most of the available radiation within their growing season and harvest index is considered to be at its maximum potential limit because some biomass must be allocated to non-harvestable plant tissues [4,

21]. With these parameters being now close to their biological limits, conversion efficiency is the only determinant of yield potential that could be enhanced for increased productivity [14, 39]. As a result, attention has been turned to improve photosynthesis in crops for increased biomass, which has been estimated at less than half the theoretical maximum [40]. In C_3 crops, it is estimated that conversion efficiency is about 0.5%, while the biological limit is 4.5% [41].

Attempts to improve conversion efficiency have largely been focused on increasing leaf photosynthesis since the conversion of intercepted radiation into biomass energy depends directly on photosynthetic efficiency. This strategy for increased productivity remains debated [4, 42–44] given previous observations showing that leaf photosynthetic rate did not correlate with crop yield. Nonetheless, several carbon dioxide (CO_2) enrichment experiments have proven otherwise. As an example, CO_2 enrichment experiments in field-grown soybean have demonstrated increases in leaf photosynthesis of 22.6% over the growing season, which correlates to an 18.8% increase in conversion efficiency and an 18.2% increase in total biomass [4].

An additional line of evidence for the importance of photosynthesis as a determinant of crop yield is C_4 photosynthesis. Plants performing C_4 photosynthesis, typically grown in environments of high light and temperature, such as tropical grasses, have higher photosynthetic efficiency under these conditions and this correlates to substantial increases in biomass content compared to their C_3 counterparts [8].

1.2.3 Determination of photosynthetic capacity in plants

The determination of photosynthetic rates in plants is usually done by measuring CO_2 exchange, oxygen (O_2) evolution, or chlorophyll fluorescence [45].

Infrared gas analysers measure CO_2 exchange (or gas exchange), the plant's uptake of CO_2, by determining CO_2 concentrations spectroscopically via the absorbance of infrared wavelengths within an enclosed chamber. This leads to an estimate of the rate of net CO_2 uptake or assimilation (A) and the CO_2 concentration in the substomatal cavity (Ci). The so-called A/C_i curves provide information about the biochemical and stomatal limitations on photosynthesis as per the model depicted by Farquhar *et al* [46]. Measurements of gas exchange can be done under varying conditions of CO_2 concentrations, light, or temperature [45].

The measurement of chlorophyll fluorescence is performed with light-based biophysical probes and allows the determination of the efficiency of the photosynthetic machinery, particularly the photochemistry of photosystem (PS) II. This is based on the three fates that light follows as it is absorbed by chlorophyll molecules: (i) the excitation energy passes to PS II and it is used to drive photosynthesis, where electrons are transferred from water through to plastoquinone (photochemistry). Excess energy (ii) is re-emitted or dissipated as heat (non-photochemical quenching, NPQ), or (iii) is re-emitted as light of a shifted wavelength (chlorophyll fluorescence) [47]. The three processes occur in competition, and so the deconvolution of the fluorescence signals allows to establish photochemistry and thus the efficiency of PS II. Figure 1.1 represents a stylised chlorophyll fluorescence trace of a typical experiment using dark-adapted leaf material to measure photochemical and non-photochemical parameters. During the measurement, light pulses of different intensities are applied to a leaf that has been adapted to darkness: by applying a beam of light, a measurement of the minimum level of fluorescence takes place (F_0). A pulse of saturating light is then applied, allowing the measurement of the maximum level of fluorescence (F_m), and the variable fluorescence (F_v) which represents the difference between F_0 and F_m [47]. This rise in fluorescence can be explained by the so-called Kautsky effect: as the leaf transitions from the dark

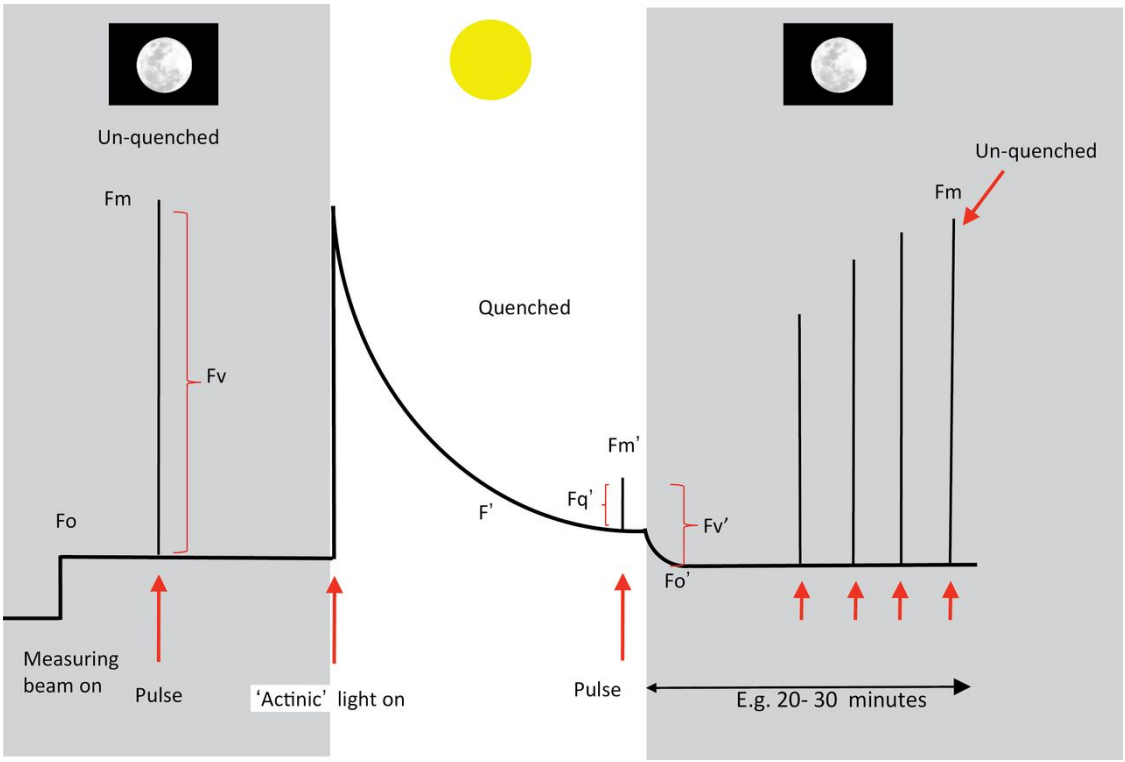

Figure 1.1: A stylized chlorophyll fluorescence trace of a typical experiment using dark-adapted leaf material to measure photochemical and non-photochemical parameters as per Murchie and Lawson [47]. Fluorescence levels are measured to obtain information about the performance of photosystem II whilst exposing the leaf to a combination of actinic lights, darkness, and saturating pulses. The minimum (F_0), maximum (F_m), and variable (F_v) levels of fluorescence are obtained by illuminating a dark-adapted leaf (un-quenched). A reduction in fluorescence due to photochemistry takes place after turning on the actinic light (quenched), and light-adapted values for maximum (F_m'), and variable fluorescence (F_v') are obtained, along with F_q', calculated as the difference between F' and F_m'. After switching off the actinic light, the decay in fluorescence provides a measurement of light-adapted minimum fluorescence (F_0'), and can be followed by dark adaptation. Reprinted by permission from Oxford University Press (`https://academic.oup.com/jxb`): Oxford University Press, Journal of Experimental Botany, (*Chlorophyll fluorescence analysis: a guide to good practice and understanding some new applications*, Erik H. Murchie, Tracy Lawson), Copyright © 2013 Oxford University Press.

to the light-adapted state, reaction centres close, which reduces the efficiency of photochemistry and increases chlorophyll fluorescence [48]. The measurement of F_m is followed by application of an actinic light (i.e. light that drives photochemistry) and a flash of saturating light, which lead to the value for maximum fluorescence in the light (F_m'). The removal of actinic light after the flash allows the determination of minimum fluorescence in the light (F_0') [47]. If the leaf has not been dark-

adapted for sufficient time, only measurements of F_m' and F_0' will be possible. A number of parameters can be derived from the measurements of minimum and maximum chlorophyll fluorescence, with the most useful being the efficiency of PS II photochemistry or quantum yield (ΦPSII, which corresponds to F_q'/F_m') and the maximum efficiency of PS II (F_v/F_m, where $F_v = F_m - F_0$).

In addition to the probing of PS II photochemistry, other spectral signatures can provide information about the photosynthetic electron transport chain, particularly with regard to cyclic electron flow and the activity of the chloroplast ATP synthase. The efficiency of PS I can be calculated from the redox status of its reaction centre, P700, by measuring shifts in absorbance at 800-850 nm after rapid light-saturating pulses. Besides, the electrochromic pigment absorbance shift of carotenoids (embedded in the thylakoid membranes) at an absorbance of 520 nm senses the electric field across the thylakoid membrane. In particular, the relaxation of the electrochromic shift in the dark is proportional to the proton motive force and its decay kinetics provide information on the conductivity of ATP synthase, as reviewed by Walker *et al.* [45].

Gas exchange is perhaps the most widely used technique (e.g. [22, 24, 49] to name a few) because it allows the determination of carbon fixation. On the other hand, the determination of chlorophyll fluorescence has gained popularity as a non-invasive tool, mainly because of its lower cost and speed of measurement compared to gas exchange. However, the combination of infrared gas exchange and chlorophyll fluorescence imaging techniques can also be applied as a powerful research tool since it allows the simultaneous determination of the photosynthetic electron transport chain, CBB cycle activity, and diffusion limitations on photosynthesis. For example, the reduction of the O_2 concentration in the infrared gas analyser chamber enables the direct correlation of PS II efficiency to CO_2 assimilation by eliminating photorespiration [47].

1.2.4 History of photosynthesis research

Photosynthesis is considered the most important process on the biogeosphere in terms of carbon flux and is currently known in more detail than any other plant process. It is the major plant metabolic pathway in leaves, converting inorganic CO_2 into organic compounds (triose phosphates), which are ultimately used as the building blocks of carbohydrates such as fructose, glucose, sucrose and starch.

The process of photosynthesis was unravelled by research done from the seventeenth to the early nineteenth centuries. Hill provided a historical perspective on that early research [50], highlighting the pivotal work done by Joseph Priestley (1776) on oxygen and the interdependence between plants and animals, Jean Senebier (1782) in establishing CO_2 as the source of carbon in plants, Jan Ingen-Housz (1773) on plant's need for light in order to release oxygen and the importance of the green colour, Nicholas de Saussure (1804) in assembling a more complete picture plant nutrition, and Robert Mayer (1845) in establishing that plants convert light energy into chemical energy.

Later in the nineteenth and twentieth century, the involvement of chlorophyll and chloroplasts was described. Of crucial importance was the work of Emerson and Arnold (1932) in describing that circa 2400 chlorophyll molecules are needed to evolve one molecule of O_2, which was the basis for the concept of reaction centres (described by Gaffron and Wohl (1936) as 'photosynthetic units') [51]. This was followed by advances in the physiology and biochemistry of photosynthesis which led to a relatively complete picture of the process by the 1960s, including the generation of nicotinamide adenine dinucleotide phosphate (NADP) in its reduced form (NADPH) and adenosine 5-triphosphate (ATP) in the light-dependent phase and their consumption in the CBB cycle [51]. The division of photosynthesis into 'light' and 'dark' (later corrected to 'carbon-reaction', since it is light-dependent too) phases was first described by Frederick Frost Blackman (1905). Robert Hill (1937) then found that the light and carbon-reaction phases can occur independently, using isolated chloroplasts which were able to evolve O_2 in the presence of artificial electron acceptors and despite a lack of CO_2 [51]. The use of ^{14}C was crucial in

deciphering the carbon-phase of CO_2 reduction in photosynthetic organisms, with work by Andrew Benson, Melvin Calvin, and James Bassham in the 1950s [51, 52].

1.2.5 Transgenic interventions in leaf photosynthesis and primary carbon metabolism

The potential for photosynthesis to improve yield was proposed in the 1990s, as the yield increases achieved during the Green Revolution began to stagnate [4]. With most genes, proteins, and metabolites involved in photosynthesis having been described and the availability of plant transformation techniques, various molecular targets in photosynthetic metabolism have been established as a means for improved photosynthetic efficiency: (i) the capacity of the chloroplast electron transport chain [22, 53]; (ii) the catalytic properties of ribulose 1,5-biphosphate (RuBP) carboxylase-oxygenase (RuBisCO) [54, 55] and RuBisCO activase [56]; (iii) the capacity of enzymes of the CBB cycle for an increased rate of RuBP regeneration [57–59]; (iv) the introduction of CO_2 concentrating mechanisms from cyanobacterial or algal systems [60–65]; (v) the speed of relaxation of the NPQ cycle at PS II [66]; (vi) the process of photorespiration via alternative photorespiratory pathways [24, 67–70] or accelerating flux through the native pathway [71]; and (vii) carbohydrate export from the leaves [72]. Additionally, ambitious research programmes are underway to avoid photorespiration altogether by introducing C_4 photosynthesis into C_3 crops [73, 74]. Experimentally, many studies, outlined in the following sections, have succeeded in manipulating these photosynthetic targets.

Photosynthetic electron transport

Photosynthesis starts with light absorption by the light-harvesting complexes, which leads to electron excitation and transfer through the photosynthetic electron transport chain in the thylakoid membranes of chloroplasts (Figure 1.2).

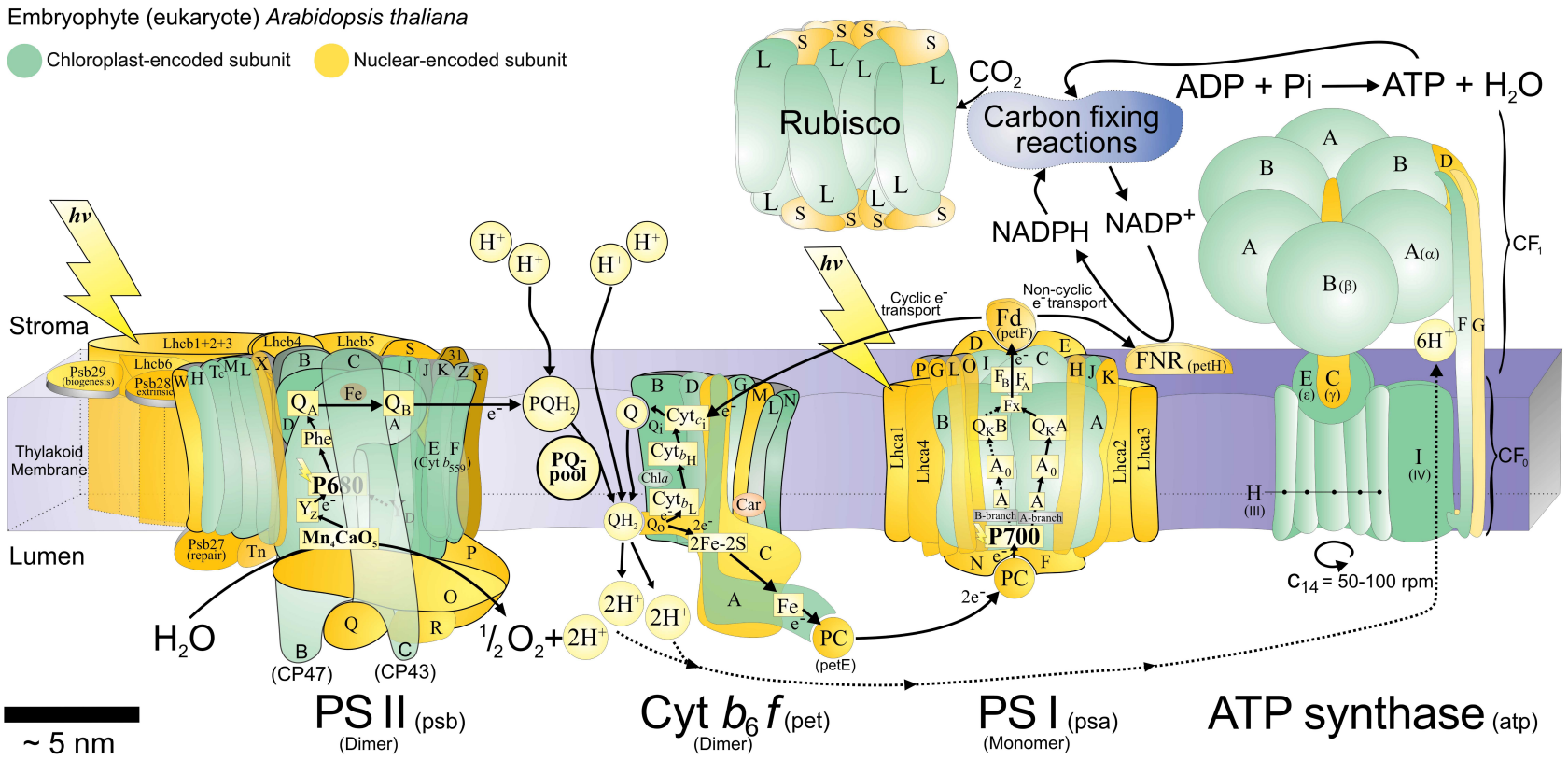

Figure 1.2: Schematic representation of the photosynthetic electron transport chain apparatus in the chloroplast of a higher plant exemplified by *Arabidopsis thaliana* as per [75]. Main proteins and complexes: Photosystem II (PS II); cytochrome b_6f (Cyt b_6f); photosystem I (PS I); adenosine 5-triphosphate (ATP) synthase; and RuBisCO. Subunit abbreviations: psa for photosystem I; psb for photosystem II; pet (photosynthetic electron transport) for the cytochrome b_6f complex and secondary electron carriers; atp for the ATP synthase; and rbc for RuBisCO. Reprinted by permission from Elsevier (`https://www.cell.com/trends/plant-science/home`): Elsevier, Trends in Plant Science, (*A structural phylogenetic map for chloroplast photosynthesis*, John F. Allen, Wilson B.M. de Paula, Sujith Puthiyaveetil, Jon Nield.), Copyright © 2011 Elsevier Ltd.

Soluble electron transport proteins were established as targets for manipulation when the hemeprotein cytochrome (Cyt) c_6 from the red alga *Porphyra yezoensis* was expressed ectopically in *Arabidopsis thaliana* (Arabidopsis hereafter) [76]. In cyanobacteria and some eukaryotic algae, both Cyt c_6 and/or plastocyanin can act as an electron carrier between the Cyt b_6f complex and the PS I reaction centre [77]. The Cyt c_6 has been lost in higher plants and only plastocyanin performs this step. With both proteins exhibiting a similar midpoint redox potential, Chida and coworkers examined the electron transfer capacity of the algal Cyt c_6 to the endogenous Arabidopsis PS I *in vitro* [76]. Not only was Cyt c_6 sufficient for electron transport but it also showed a faster electron transport rate than the Arabidopsis plastocyanin. Arabidopsis plants overexpressing this gene in the chloroplast showed accelerated electron transport, an increase in CO_2 assimilation capacity of 31%, and enhanced growth at early stages of development. Similarly, the overexpression of the gene coding for Cyt c_6 from the green alga *Ulva fasciata* in tobacco led to an increase in electron transport rate which was accompanied by an increase in chlorophyll content and biomass [78]. Importantly, the increased photosynthetic efficiency and biomass conferred by the overexpression of *Porphyra umbilicalis* Cyt c_6 in tobacco have been tested in the field [23].

The Cyt b_6f complex comprises four large subunits (Cyt f, Cyt b_6, Rieske FeS protein and subunit IV) and couples electron and proton transfer between PS I and II. This complex was identified as exerting substantial control over RuBP regeneration by targeted reductions of the protein complexes using inhibitors [79] and by antisense suppression of the Rieske FeS gene [53, 80, 81]. The resulting decrease in the accumulation of the Rieske FeS protein led to decreased electron transport capacity and growth [53, 80, 82]. Based on these studies, Simkin *et al.* reasoned that increased levels of the Cyt b_6f complex could potentially increase photosynthetic electron flow and flow. Overexpression of the nuclear gene *AtPetC*, which encodes the Rieske FeS protein in Arabidopsis, increased electron transport rate and CO_2 assimilation, along with biomass in tobacco [22].

Photosystem I donates electrons directly to ferredoxin. Reduced ferredoxin is a key component in photosynthesis, interacting with ferredoxin-dependent enzymes such as ferredoxin:$NADP^+$ reductase, responsible for the production of NADPH, or ferredoxin:thioredoxin reductase, responsible for the activation of four critical enzymes of the CBB cycle, including fructose 1,6-bisphosphatase (FBPase), sedoheptulose 1,7-bisphosphatase (SBPase), phosphoribulokinase, and glyceraldehyde 3-phosphate dehydrogenase [83]. The gene coding for the plant ferredoxin-like protein (PFLP), isolated from sweet pepper (*Capsicum annuum*), has been widely studied in the context of pathogen-resistance studies [84–86]. Additionally, its role in the alteration of photosynthetic capacity has been recently reported in rice [49]. The constitutive overexpression of PFLP from sweet pepper was shown to increase photosynthetic efficiency, sugar production and crop yield via an enhanced electron transport efficiency and gas exchange rate and higher transcription levels of carbohydrate metabolism-related genes [49].

Leaf carbon assimilation

The photosynthetic electron transport chain powers ATP production via the chloroplast ATP synthase complex and provides reducing power in the form of NADPH for the photosynthetic carbon reduction in the CBB cycle.

RuBisCO initiates the CBB cycle by catalysing the carboxylation of RuBP with CO_2 (Figure 1.3). The products of this reaction are two molecules of 3-phosphoglycerate, which are metabolised in the CBB cycle for the regeneration of RuBP (about five-sixths [87]) or exported as triose phosphates (one-sixth). This pathway was first described in 1950 through analyses of paper chromatography and autoradiography in algal suspensions fed with $^{14}CO_2$ [52]. RuBisCO can react with O_2 to produce one molecule of 3-phosphoglycerate (3-PGA) and one molecule of 2-phosphoglycerate. In the 1970s, gas exchange experiments showed that higher plants take up O_2 and release CO_2 at ambient CO_2 concentrations and that the rate of photosynthesis was inhibited by O_2, manifested by an increase in the CO_2 compensation point [88]. These experiments provided the link between

RuBisCO's carboxylation activity and photorespiration and led to the identification of RuBisCO's oxygenic activity [89] (see Section 1.2.5). Since then, RuBisCO has become one of the most extensively studied enzymes.

RuBisCO has a slow catalytic turnover number (K_{cat}), partly compensated for by a substantial nitrogen investment in RuBisCO protein [90, 91]. In addition, because it evolved in non-oxygenic prokaryotes 3.8-2.5 billions of years ago in a high CO_2 atmosphere, RuBisCO shows low substrate specificity for CO_2, which is exacerbated as temperature rises [92]. Modelling work suggests that introducing a RuBisCO enzyme with higher catalytic rates could boost conversion efficiency by 31% [4]. As a result, RuBisCO has been the focus of most efforts to improve photosynthesis [93].

Historically, RuBisCO was thought to be the major rate-limiting factor controlling CO_2 fixation [83, 94]. Subsequent studies using antisense technology proved otherwise, leading to the surprising finding that antisense plants with 40% less amount of RuBisCO protein than the control maintained similar rates of assimilation than non-transformed plants [94]. These studies showed that RuBisCO's control was variable depending on the growth and analysis conditions, with limitations of photosynthesis by a reduction in RuBisCO being more pronounced in conditions of high light and temperature, as reviewed in [83]. However, modelling work has suggested an increased protein investment in RuBisCO protein as a potential target for maximised photosynthetic rate [95]. The overexpression of RuBisCO with the assembly chaperone RAF1 led to increases in RuBisCO content and increased CO_2 assimilation rate [55]. A recent field study has shown how the overexpression of the small subunits of RuBisCO can increase yields in rice, when enough nitrogen fertilisation was applied [96].

The use of antisense transgenic plants targeting additional enzymes participating in the CBB cycle allowed an evaluation of their contribution to the CBB cycle and the rate of photosynthesis [87, 94]. Among the CBB cycle enzymes, fructose 1,6-bisphosphate aldolase (FBPA), SBPase, and transketolase were found to be of crucial importance. Small reductions in the levels and activities of these enzymes negatively affected growth and carbohydrate accumulation [83]. This came as

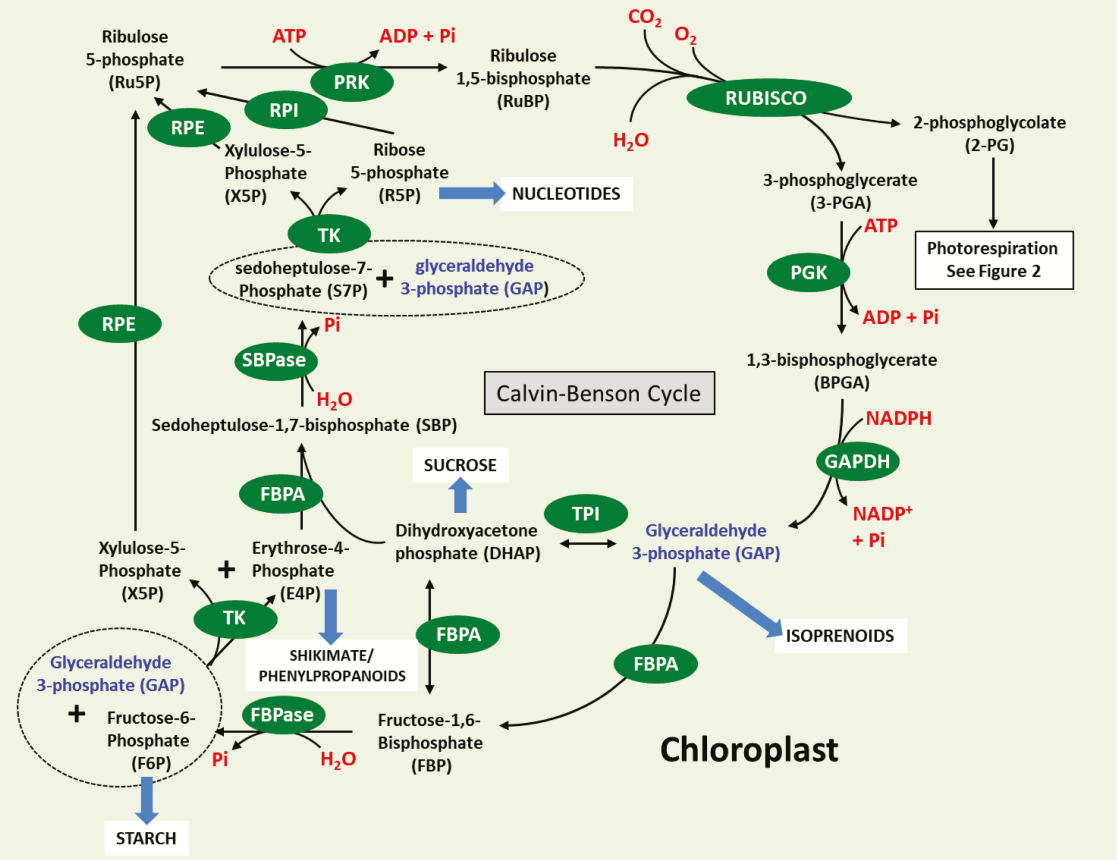

Figure 1.3: Schematic representation of the Calvin-Benson-Bassham cycle as per Simkin, Lopez-Calcagno, and Raines [19] Sedoheptulose-1,7-bisphosphatase (SBPase: EC 3.1.3.37), fructose-1,6-bisphosphate aldolase (FBPA: EC 4.1.2.13), fructose-1,6-bisphosphatase (FBPase; EC 3.1.3.11), transketolase (TK; EC 2.2.1.1), phosphoribulokinase (PRK; EC 2.7.1.19), ribulose-phosphate 3-epimerase (RPE; EC 5.1.3.1), triosephosphate isomerase (TPI; EC 5.3.1.1), glyceraldehyde 3-phosphate dehydrogenase (GAPDH; EC 1.2.1.12), phosphoglycerate kinase (PGK; EC 2.7.2.3), ribose 5-phosphate isomerase A (RPI; EC.5.3.1.6), RuBisCO (EC 4.1.1.39). Reprinted from Oxford University Press, Journal of Experimental Botany, (*Feeding the world: improving photosynthetic efficiency for sustainable crop production*, Andrew J. Simkin, Patricia E. López-Calcagno, Christine A. Raines), 2019. Open access article.

a surprise since it was assumed that highly regulated enzymes such as FBPase, glyceraldehyde 3-phosphate dehydrogenase or phosphoribulokinase would be the ones exerting the most control over the rate of the CBB cycle. On the contrary, reductions in the activities of these three enzymes resulted in little to no reductions on CO_2 assimilation.

The higher flux control values of SBPase (up to 0.75 [83]), along with non-regulated enzymes such as FBPA (up to 0.55 [83]) and transketolase (up to 1 [83]),

suggested that increasing the amount and activity of these enzymes could increase carbon fixation capacity. This was first proven in tobacco plants overexpressing a bifunctional FBPase/SBPase from *Synechococcus elongatus* PCC 7942 in chloroplasts, which displayed an increase in RuBisCO activity, carbon fixation, and dry matter [97]. Later studies showed how increased activity of SBPase [57, 58] and FBPA [98] resulted in enhanced growth and biomass yield in tobacco. Increased activity of SBPase was shown to lead to significant improvements in photosynthetic capacity and, importantly, to increases in grain yield of 30-40% in wheat [99]. Other studies have tested the effect of combining an increased activity of both enzymes simultaneously, demonstrating that multigene manipulations could lead to greater increases in photosynthetic capacity than single manipulations. The combination of increased activity of SBPase with FBPA and the expression of the H-protein of the photorespiratory enzyme glycine decarboxylase (GDC-H) [59] or the putative cyanobacterial inorganic carbon transporter B (ICTB) [100] significantly stimulated photosynthesis and growth in Arabidopsis and tobacco. As an example, the simultaneous overexpression of *SBPase*, *FBPA*, and *GDC-H* led to increases in biomass of 70% with respect to the control, while either of the three transgenes alone led to comparatively lower increases, which varied from 30 to 50%. Glycine decarboxylase is discussed in Section 1.2.5 below. The combined overexpression of the bifunctional FBPase/SBPase from *Synechocystis* and Cyt c_6 from *P. umbilicalis* was recently tested in tobacco [23], showing for the first time that the simultaneous stimulation of photosynthetic electron transport and RuBP regeneration can be more efficient for photosynthetic improvement than targeting each process alone.

Regarding ICTB, Arabidopsis and tobacco plants ectopically expressing the cyanobacterial protein ICTB were shown to have enhanced photosynthesis and increased biomass by 20% [101]. These effects were translated into rice [102], where biomass was increased by 20%, and soybean [63], where seed yield was increased by 30% at ambient temperature. ICTB was first described as an inorganic carbon transporter in a high-CO_2 requiring mutant of *Synechococcus* PCC 7942 impaired in bicarbonate uptake [103]. However, it was later shown that it does not

function as a bicarbonate transporter in a study where all known cyanobacterial inorganic carbon transporters were mutated, and CO_2 and bicarbonate uptake were fully impaired [104]. Therefore, the role of ICTB in cyanobacteria and the mechanism by which it improves photosynthesis is not clear. It has been suggested that it somehow concentrates internal CO_2 around RuBisCO, leading to an increased RuBisCO activation [101].

Unlike FBPA and SBPase, the overexpression of transketolase did not result in improved photosynthetic capacity. The activity of transketolase requires thiamine pyrophosphate as a co-factor. Increased availability and activity of transketolase in the plastid of tobacco involved an increased demand for thiamine, which ultimately led to thiamine deficiency in the seeds and reduced plant growth and chlorosis in later developmental stages in the transgenic tobacco plants [105].

Photorespiration

Photorespiration is the process which, following RuBisCO's oxygenation reaction, recycles 2-phosphoglycolate back to 3-PGA which can be used to regenerate RuBP. This pathway is biochemically complex, comprising eight enzymes in the core cycle and several auxiliary enzymes distributed among chloroplasts, peroxisomes, mitochondria, and the cytosol (Figure 1.4). Photorespiration recovers 75% of the carbon lost during the oxygenation reaction (one carbon atom is lost as CO_2) and 12.25 ATP molecules are required for the recycling of each 2-phosphoglycolate molecule [106]. Photorespiration interacts with various central metabolic pathways such as the CBB cycle, nitrogen assimilation, mitochondrial respiration and one-carbon (C_1) metabolism, and amino acid and phospholipid biosynthesis [107, 108]. Research on photorespiration has historically been based on the establishment of mutant plants defective in specific photorespiratory enzymes, leading to the discovery of the enzymatic steps in the pathway and providing evidence that an intact photorespiratory metabolism is essential. These mutants demonstrate a so-called photorespiratory phenotype, being unable to survive in normal air

(showing chlorosis and necrosis) but rescued in low O_2 or high CO_2 conditions where photorespiration is low [109].

Photorespiratory losses typically amount to 20% of net CO_2 assimilation although this is dependent on environmental conditions such as temperature and humidity, and can reach 50% [110]. As a result, photorespiration has been the target of several approaches with the aim of increasing plant yield. Among these strategies are photorespiratory bypasses, consisting of the introduction of alternative synthetic routes to decrease photorespiratory losses by genetic engineering [111]. A total of three bypasses were initially tested in the model systems Arabidopsis [67, 69], tobacco [68] and *Camelina sativa* [70]. A modified version of the Maier bypass [69] was successfully tested in the field in tobacco, leading to improvements in quantum yield of PS II by 20% and biomass productivity by 40% [24]. Importantly, a similar bypass was implemented in rice, showing that the benefits of circumventing photorespiration were translated into grain yield under specific environmental conditions [25], although the gains were not as high as in the tobacco field trials. In addition to the reported photorespiratory bypasses, another promising approach would be to design completely novel metabolic routes using the huge variety of enzyme activities found in bacteria, algae and Archaea [15].

An alternative strategy has been increasing the rate of photorespiratory enzymes, with the objective of increasing the rate of conversion of 2-phosphoglycolate to 3-PGA. The rationale behind this is that, since 2-phosphoglycolate is a potent enzyme inhibitor of triose phosphate isomerase, SBPase, and phosphofructokinase [108], a more rapid metabolisation can be beneficial to reduce its toxicity and increase the rate of return of 3-PGA to the CBB cycle [17]. These efforts have focused on glycine decarboxylase, with the accumulation of the L-protein and the H-proteins having shown to increase photosynthetic capacity and plant growth [59, 71, 112, 113].

Leaf sucrose and starch biosynthesis

The product of the CBB cycle, glyceraldehyde-3-phosphate, is subsequently exported from the chloroplast via triose phosphate/phosphate translocators (TPT), thus

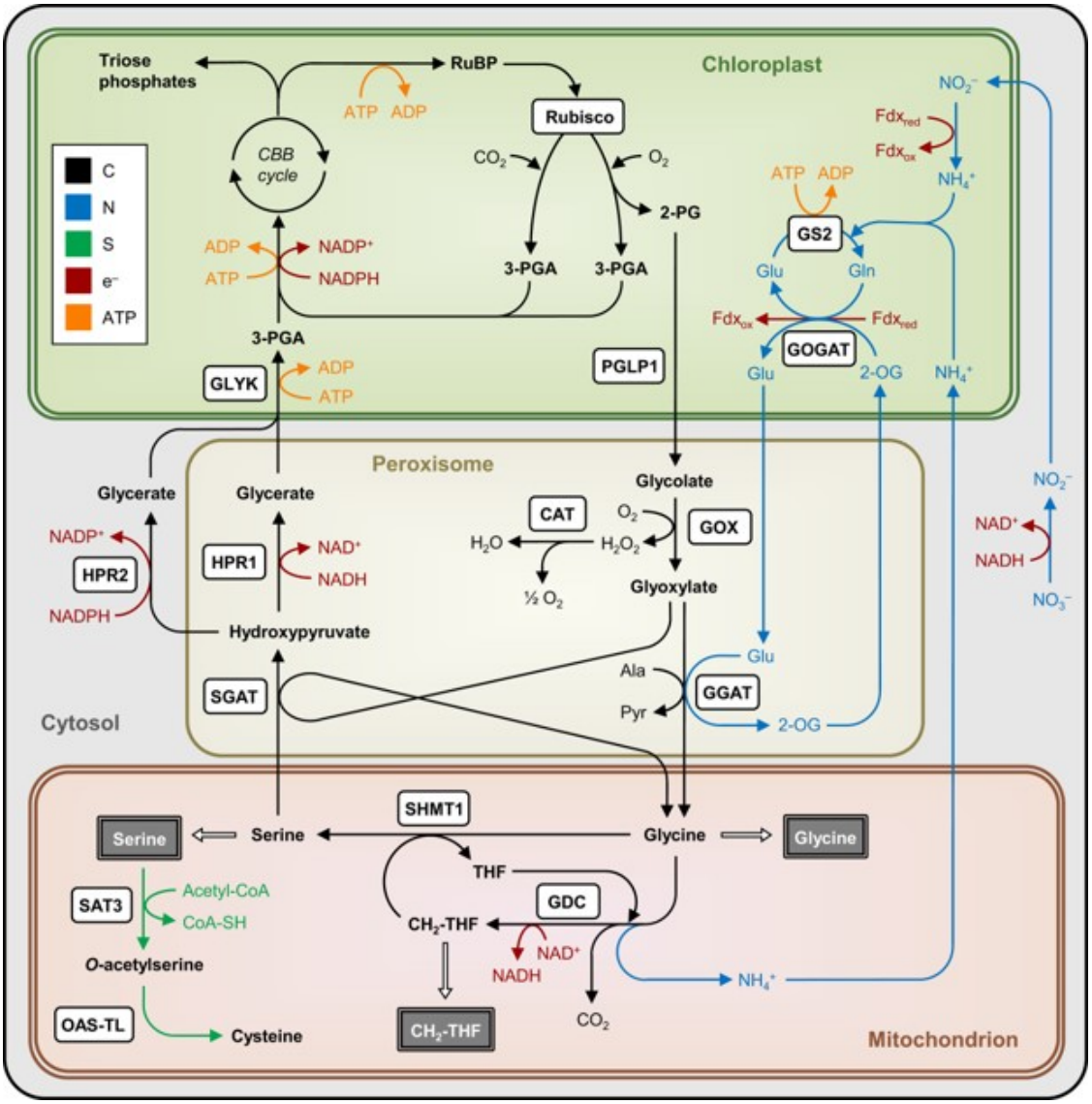

Figure 1.4: Schematic representation of the photorespiratory metabolism as depicted by Busch [108]. The movement of carbon along the photorespiratory pathway (black arrows) and the metabolites involved (bold font) are shown in the context of nitrogen (blue) and sulfur metabolism (green). Redox reactions involving NAD, NADP, or ferredoxin (Fdx) are shown in red and ATP-consuming processes in orange. Photorespiratory carbon leaves the pathway as CO_2 during the glycine decarboxylation step or is returned to the CBB cycle as 3-PGA. Carbon may also be exported from the photorespiratory pathway (white arrows) in the form of the amino acids glycine and serine, or as CH2-THF, which supplies one-carbon (C_1) units to the C_1 metabolism (grey boxes). 2-OG, 2-oxoglutarate; 2-PG, 2-phosphoglycolate; 3-PGA, 3-phosphoglycerate; CAT, catalase; GDC, glycine decarboxylase complex; GGAT, glutamate:glyoxylate aminotransferase; GLYK, glycerate kinase; GOGAT, glutamine:oxoglutarate aminotransferase; GOX, glycolate oxidase; GS2, glutamine synthetase; HPR1, hydroxypyruvate reductase 1; HPR2, hydroxypyruvate reductase 2; OAS-TL, O-acetylserine (thiol) lyase; PGLP1, phosphoglycolate phosphatase 1; SAT3, serine O-acetyltransferase; SGAT, serine:glyoxylate aminotransferase; SHMT1, serine hydroxymethyltransferase 1. Reprinted by permission from John Wiley & Sons Ltd (`https://onlinelibrary.wiley.com/journal/1365313x`): John Wiley & Sons Ltd, The Plant Journal, (*Photorespiration in the context of RuBisCO biochemistry, CO_2 diffusion and metabolism*, Florian A. Busch), © 2020 The Plant Journal, John Wiley & Sons Ltd.

providing the cytosol with precursors for sucrose biosynthesis (Figure 1.5). Located in the chloroplast inner membrane, TPTs mediate the passive exchange of stromal triose-phosphates and cytosolic phosphate ions (P_i) and have been found to exert significant control over sucrose synthesis [114]. Triose-phosphates are then converted into fructose 6-phosphate by the cytosolic FBPase (cyFBPase), which converts fructose 1,6-bisphosphate into fructose 6-phosphate, with the release of P_i. Fructose 6-phosphate is then used to generate sucrose via the sucrose phosphate synthase in the cytosol.

The simultaneous overexpression of Arabidopsis *cyFBPase* and *TPT* was shown to impact plant growth through an increase in source capacity, manifested by improved CO_2 assimilation capacity, increased accumulation of leaf soluble sugars, and increased shoot fresh weight [116]. The activity of cyFBPase is stimulated by the availability of glyceraldehyde-3-phosphate, which inhibits the synthesis and stimulates the degradation of cyFBPase's inhibitor fructose 2,6-bisphosphate [87]. In fact, the activity of cyFBPase strongly increases once a threshold concentration of triose phosphates is reached [87]. Therefore, increased availability of triose phosphates in the cytosol, mediated by TPT, resulted in a highly stimulated cyFBPase activity. Increased cyFBPase activity led to increased availability of P_i, which in turn stimulated TPT activity.

Soluble pyrophosphatases (PPases) catalyse the hydrolysis of inorganic pyrophosphate (PP_i), generating two P_i. In the process of sucrose synthesis, PP_i is produced by uridine diphosphate-glucose pyrophosphorylase, which catalyses the conversion of glucose-1-phosphate into UDP-glucose, which is then coupled with fructose 6-phosphate for the production of sucrose. In parallel, fructose 6-phosphate can be converted into glucose-1-phosphate, the precursor of adenosine diphosphate (ADP)-glucose, which generates starch via the ADP-glucose pyrophosphorylase (AGPase) for its transient storage in the chloroplast (Figure 1.5).

Both sucrose phosphate synthase and AGPase exert significant control over sucrose and starch biosynthesis, respectively [87]. The sucrose phosphate synthase from maize was overexpressed constitutively in tobacco, inducing acceleration in

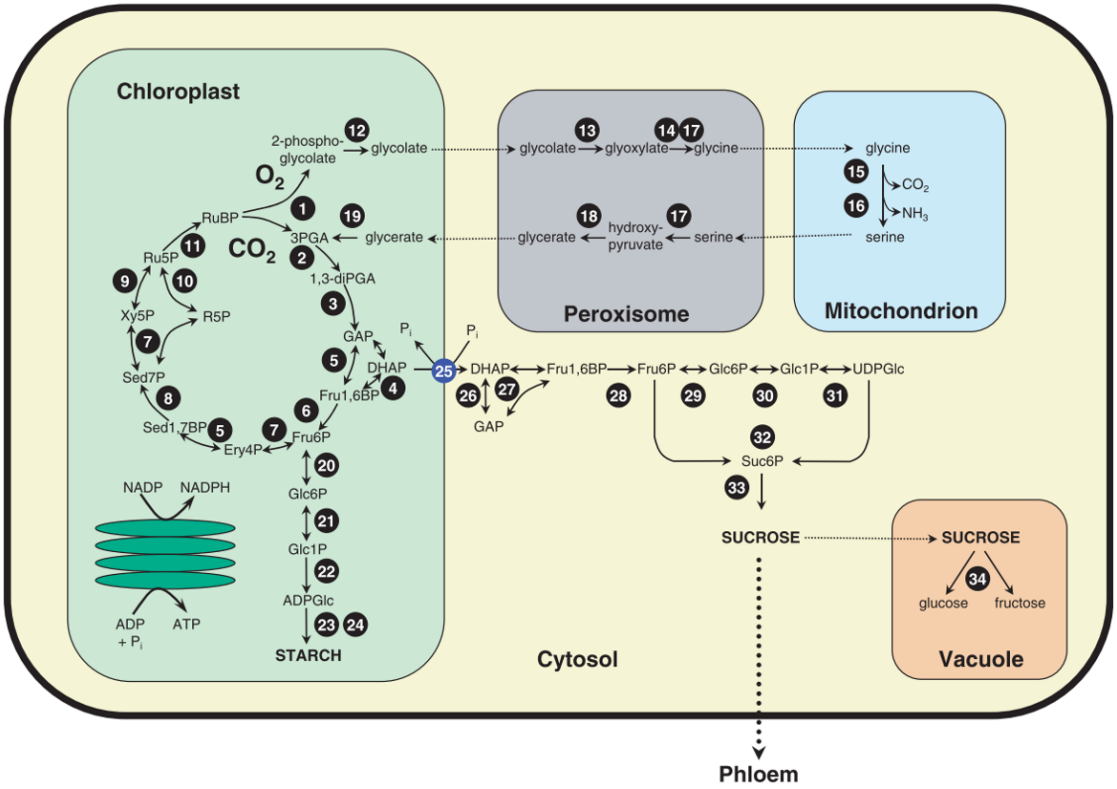

Figure 1.5: Schematic of photosynthetic carbon metabolism in Arabidopsis and other C_3 plants as depicted by Stitt *et al.* [115]. CO_2 fixation via the Calvin–Benson cycle in the chloroplasts is tightly integrated with the photorespiratory pathway, and with synthesis of the main end products of photosynthesis – starch and sucrose. The reactions are catalysed by the following enzymes: (1) RuBisCO; (2) phosphoglycerate kinase; (3) NADP-glyceraldehyde phosphate dehydrogenase; (4) plastidic triose phosphate isomerase; (5) plastidic aldolase; (6) plastidic fructose-1,6-bisphosphatase; (7) transketolase; (8) sedoheptulose-1,7-bisphosphatase; (9) ribulose phosphate epimerase; (10) phosphoriboisomerase; (11) phosphoribulokinase; (12) phosphoglycolate phosphatase; (13) glycolate oxidase; (14) glutamate:glyoxalate aminotransferase; (15) glycine decarboxylase; (16) serine hydroxymethyl transferase, (17) serine:glyoxylate aminotransferase; (18) hydroxypyruvate reductase; (19) glycerate kinase; (20) plastidic phosphoglucoisomerase; (21) plastidic phosphoglucomutase; (22) ADP-glucose pyrophosphorylase; (23) starch synthase; (24) starch branching enzyme; (25) triose phosphate translocator; (26) cytosolic triose phosphate isomerise; (27) cytosolic aldolase; (28) cytosolic fructose-1,6-bisphosphatase; (29) cytosolic phosphoglucoisomerase; (30) cytosolic phosphoglucomutase; (31) UDP-glucose pyrophosphorylase; (32) sucrose phosphate synthase; (33) sucrose-6-phosphate phosphatase; (34) vacuolar invertase. For simplicity, only the main pathway of carbon is shown, and the use of dihydroxyacetone (DHAP) as a substrate in the two transketolase reactions, and of glyceraldehyde-3-phosphate (GAP) as a substrate in the second aldolase reaction leading to the formation of sedoheptulose-1,7-bisphosphate (Sed1,7BP) has been omitted. Reprinted by permission from John Wiley & Sons Ltd (`https://onlinelibrary.wiley.com/journal/1365313x`): John Wiley & Sons Ltd, The Plant Journal, (*Arabidopsis and primary photosynthetic metabolism – more than the icing on the cake*, Mark Stitt, John Lunn, Björn Usadel), © 2010 The Plant Journal, John Wiley & Sons Ltd.

plant growth caused by earlier flowering, a higher number of flowers, overall higher sucrose-to-starch ratio, and increased photosynthesis in older leaves. Besides, the overexpression of maize AGPase small (Shrunken2, *Sh2*) and large (Brittle2, *Bt2*) subunits as a mechanism for increasing sink strength in rice leaves led to increased biomass [117]. Additionally, the overexpression of the *Escherichia coli* inorganic pyrophosphatase (*EcPPase*) gene in potato leaves (*Solanum tuberosum*) was shown to double tuber starch yield by re-routing photoassimilates to sink organs at the expense of starch accumulation in leaves [118].

Phloem sucrose loading

Sucrose is the major transport form of carbon between source and sink tissues and for short-distance travel within the plant. As a result, phloem sucrose loading is a key step for the transport of photoassimilates that support growth and maintenance of sink tissues. Sucrose travels from mesophyll cells to bundle sheath cells and the phloem parenchyma via plasmodesmata. In apoplastic loaders, such as Arabidopsis, tobacco, maize and most crops, efflux into the cell wall space is a prerequisite for phloem loading. From the phloem parenchyma, sucrose is exported to the phloem apoplast by the SUGARS WILL EVENTUALLY BE EXPORTED TRANSPORTERs (SWEETs) family of uniporters. Subsequent loading of sucrose into the sieve element/companion cell complex takes place by active, energy-dependent transport against the concentration gradient by the SUCROSE TRANSPORTERs (SUTs or SUCs).

Among the SWEET family of transporters, SWEET11 and SWEET12 are considered of particular importance to the first step of phloem loading. In Arabidopsis, *AtSWEET11* and *AtSWEET12* are highly expressed in leaves and co-express with other genes involved in sucrose biosynthesis (sucrose phosphate synthase) and phloem loading (SUT transporters) [119]. No detrimental effects in growth were observed in the Arabidopsis *Atsweet11* or *Atsweet12* mutants, but the double mutant *Atsweet11Atsweet12* was defective in phloem loading and showed stunted growth, mild chlorosis, and sucrose accumulation in the leaves [119], which reflects

the importance of both transporters in apoplastic phloem loading. SUT1 (known as SUC2 in Arabidopsis) encodes the predominant SUT [120], a sucrose-H^+ co-transporter which catalyses phloem loading. Mutants in *suc2* showed severely stunted growth, accumulated anthocyanin and starch in mature leaves, and were unable to export radiolabeled sucrose from source leaves [121–123].

1.2.6 The need for multigene engineering strategies

The previous section provided an account of the most relevant transgenic interventions of photosynthesis and related processes. While most of these studies focused on single transgene interventions, it transcends from several multigene studies, such as those by Cho *et al.* [116], Simkin *et al.*, [59, 100] and López-Calcagno *et al.* [23], that the stacking of successful transgenes can lead to better outcomes than those of individual transgenes. The following section expands on the theoretical background that provides the basis for multigene engineering strategies, drawing from the complexity of the plant metabolic network.

The plant metabolic network

Metabolism consists of an interconnected network of reactions that occurs within a cell. As sessile organisms, plants have developed the potential to produce several thousand metabolites depending on the species [124]. This entails a very complex metabolome, which is why, traditionally, reactions have been grouped into metabolic pathways, with the set of individual pathways forming the plant metabolic network.

Metabolic pathways are classified into central or primary metabolism and secondary metabolism. In plants, primary metabolites are directly involved in growth, development and defence, with photosynthesis being at the core of the primary metabolism, while secondary metabolites are non-essential for survival but can provide a competitive adaptation.

The complexity of the plant metabolic network makes plants able to survive in a wealth of environments and cope with biotic and abiotic stresses. Plants show a high degree of redundancy in pathway functions, with multiple enzyme

isoforms, which contributes to their metabolic plasticity. Despite the flexibility that this metabolic complexity brings to plants, it makes it difficult to design rational interventions of metabolism, particularly within central metabolism which is highly interconnected and is subject to multiple layers of regulation which function to control metabolic homeostasis [125]. There are the questions of predicting which targets to prioritise, how the corresponding genes would interact when combined, and how the system would be affected by these manipulations.

It was a long-held belief that a key, rate-limiting enzyme could be attributed all the control within a metabolic pathway and that manipulating that single enzyme could lead to significant changes in flux. However, in the 1970s, it was formalised that this was not the case for most metabolic pathways.

Metabolic control analysis

Metabolic control analysis theory provides an experimental-theoretical framework that describes how the control through a metabolic pathway is generally controlled by multiple enzymes, which will contribute to flux through the pathway in different degrees [126]. As such, there is not a single key enzyme or rate-limiting step that controls each metabolic pathway, but a network of enzymes sharing flux control among interconnected reactions. This implies that altering a particular enzyme or pathway in isolation is unlikely to have a strong effect as it tends to be compensated for unless that enzyme has a very high control, but the distribution of control depends on the conditions [94].

The degree of control that a given enzyme exerts on the flux (J) through a given metabolic pathway is calculated per flux control coefficients (C_E^J) as the ratio of the percentage change in flux ($\delta J/J$) that is obtained for a percentage change in enzyme activity ($\delta E/E$) [127]:

$$C_E^J = \frac{\delta J/J}{\delta E/E}$$

Flux control coefficients can vary from zero, where an enzyme exerts no control on the flux through the metabolic pathway, to one, where an enzyme exerts total control on the flux.

Flux control coefficients have been elucidated for certain enzymes. As an example, the flux control through the CBB cycle has been elucidated via the generation of antisense transgenic plants with reduced levels of individual enzymes [83], as described in Section 1.2.3. Namely, FBPA, SBPase, and transketolase exert the largest control among the pathway enzymes [83]. Notably, increases in the levels of FBPase and SBPase have led to appreciable improvements in photosynthetic capacity and biomass production in transgenic plants. However, increased flux manipulation could be achieved by intervening multiple pathways in the network. Metabolic control analysis theory proves that increasing the capacity of one enzyme in a network increases the flux control coefficient of others because control is shared [128]. In other words, relieving one enzyme-capacity bottleneck by overexpression will create bottlenecks elsewhere in the system [129, 130], with early studies having predicted that single enzyme manipulations are likely to give disappointing results [131, 132].

Therefore, substantial interventions in flux through the metabolic network would require a multisite manipulation of several target pathways simultaneously. A greater impact would be expected by combining several targets simultaneously [133]. Hence, effective engineering of photosynthetic efficiency and capacity calls for the introduction of multiple transgenes targeting several sites in the leaf metabolic network [87, 125]. This view is supported by experimental strategies involving the simultaneous manipulation of several transgenes. An example of this was provided by Fell and Thomas [128] with the tryptophan biosynthesis pathway, where the flux increase that resulted from changing all pathway enzymes together was much greater than manipulating single enzymes. More recent examples have shown how increasing the amount of SBPase, FBPA, and ICTB leads to further increases in biomass in contrast to manipulating each protein individually [100]. Similarly, the simultaneous overexpression of SBPase, FBPA, and GDC-H in Arabidopsis led to cumulative increases on leaf area and biomass [59]. Recently, the beneficial effects of simultaneously manipulating photosynthetic electron transport and the CBB cycle were tested in the field with tobacco plants overexpressing the algal Cyt c_6 and the cyanobacterial bifunctional FBPase/SBPase [23]. This proves that multisite

manipulation can be a more effective way of increasing photosynthetic capacity and crop yield than manipulating single targets.

1.2.7 Strategies for multigene engineering in plants

The introduction of multiple transgenes in plants takes place through transgene pyramiding, also known as transgene stacking, which allows the simultaneous or sequential integration of transgenes. Transgene pyramiding is widely used for conferring resistance against plant pathogens to overcome single-gene resistance [134], as well as for increased tolerance against abiotic stresses [135], or both [134]. Commercial transgenic crops with stacked traits (insect resistance and herbicide tolerance) were introduced in the market in 1996 and their global area has increased steadily ever since [136]. In 2018, 80.5 million hectares of biotech crops with stacked traits were grown worldwide, representing 42% of the global biotech crops area [136].

Transgene stacking can be performed by (i) simultaneous introduction of multiple transgenes in single or multiple separate plasmids, (ii) re-transforming a transgenic plant with additional targets of interest, or (iii) sexual crossing between transgenic plants carrying different transgenes of interest [137, 138]. The last two methods are significantly slower than the first and require different selection markers for each transformation event, as well as the availability of previous transformants with transgenes of interest.

Different methods are available for the simultaneous introduction of multiple transgenes [139, 140]. A Golden Gate assembly protocol arose as a tool for the rapid cloning of multiple transgenes in a single vector [141, 142]. Based on the use of type IIS restriction enzymes (which cleave outside of their recognition sequence), Golden Gate cloning allows rapid subcloning of multiple transgenes. Three sets of cloning vectors (level 0, 1 or 2) are used in two consecutive assembly steps. Level 0 constructs contain DNA fragments with basic cloning modules (such as promoters, untranslated regions, signal peptides, coding regions or terminators). These modules are used in a first assembly reaction, giving rise to level 1 constructs which accommodate expression cassettes consisting of single transcriptional units.

Hereafter, level 2 plasmids consisting of multigene constructs can be generated within a second assembly reaction [142]. More recently, a combinatorial DNA assembly protocol using Golden Gate emerged, allowing DNA shuffling [143]. A a set of cloning plasmids and standardised parts was also developed to enable Golden Gate construction of multigene constructs for plant transformation [144], that is used in this thesis.

Biolistic combinatorial co-transformation is a plant transformation technique that allows the introduction of a large number of transgenes in a single delivery process and generates transformants carrying different transgene combinations. This technique has been used to transform a wide range of plant species, such as soybean [145], rice [146], maize [147], tobacco [148], and others [138]. It emerged from initial efforts to develop standardised particle bombardment transformation protocols for commercially important crops, such as soybean [149, 150] and rice [151], not amenable to *Agrobacterium tumefaciens* (*Agrobacterium* hereafter) or protoplast-based transformation. These involved the co-transformation of different selection markers in separate plasmids, which were found to behave as a single dominant locus and followed Mendelian segregation patterns [150, 152]. They were gradually optimised [153, 154] and characterised with an increasing number of genes [145, 146].

In biolistic combinatorial co-transformation, gold or tungsten particles are coated with equimolar quantities of the plasmids to be delivered, each harbouring a single expression cassette which comprises the gene of interest flanked by a promoter and a terminator sequence [137]. Transgene integration follows a two-phase model: in the pre-integration phase, rearrangements between constructs lead to transgene concatenation via ligation. This is followed by the integration phase which consists of the second round of ligation in double-stranded breaks in the host genome, which act as hot spots favouring the integration of the concatenated constructs in a single transgenic locus [130, 155]. Because transgene integration occurs much more frequently during S-phase than at any other stage of the cell cycle, integration sites are often located in double-stranded breaks (such as DNA topoisomerase binding sites) and could be mediated by illegitimate recombination caused by microhomology

between the transgene cassettes and the host genome [130, 155]. Possible models for multigene integration at a single locus via biolistic combinatorial co-transformation were illustrated by Gelvin [156] (Figure 1.6).

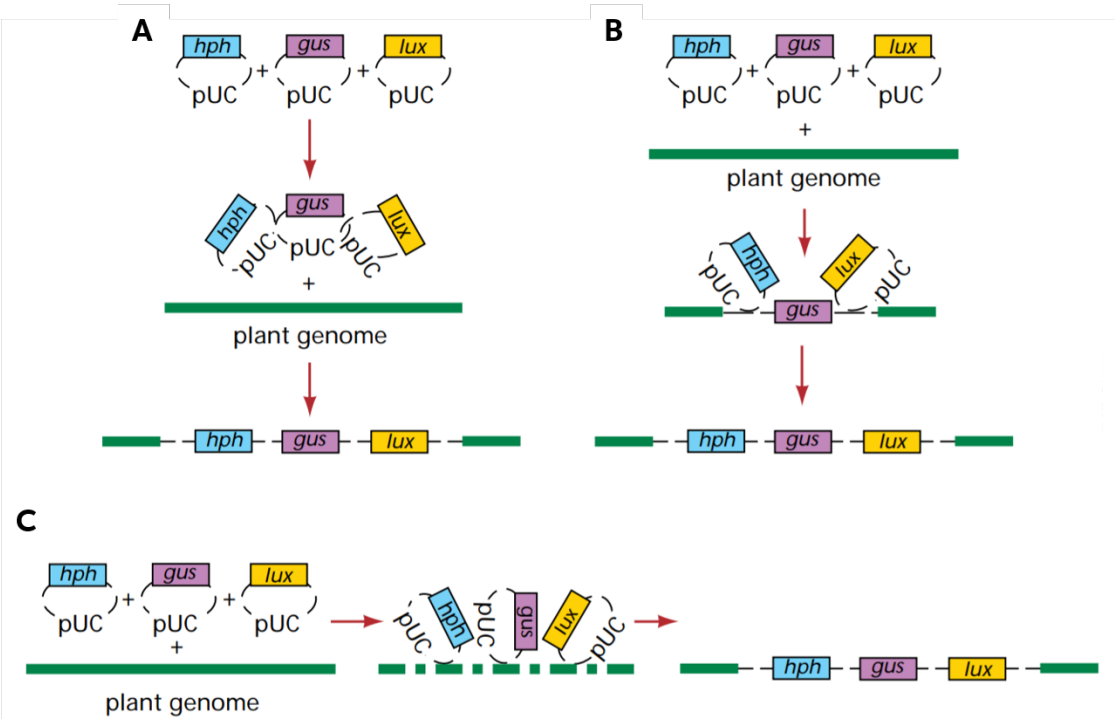

Figure 1.6: Models for multigene integration at a single genetic locus in combinatorial co-transformation as depicted by Gelvin [156]. For simplicity, only three genes (*hph*, hygromycin phosphotransferase; *gus*, b-glucuronidase; *lux*, firefly luciferase) are shown. The pUC vector sequences common to all plasmids are shown as a thin broken line. The plant genome is represented by a thick solid line. **A**. The three plasmids recombine, using homology within the pUC sequences, before integration of the unit into the plant genome. **B**. One plasmid (gus) first integrates into the plant genome, after which the other plasmids integrate using homology to the integrated pUC sequences. **C**. All three plasmids integrate directly into a region of the genome that may be damaged and attract DNA repair enzyme complexes. Reprinted by permission from Springer Nature (`https://www.nature.com/nbt/`): Springer Nature, Nature Biotechnology, (*Multigene plant transformation: More is better!*, Stanton B. Gelvin), Copyright © 1998, Springer Nature.

Golden Gate cloning requires that a decision be made on which transgene combinations are to be cloned. With individual transgene choice already carrying a bias [157], deciding which transgenes to combine on paper may be even riskier for the identification of successful transgene combinations. More importantly, this requires that each construct carrying combinations of n transgenes is used in

individual transformation events, which complicates the delivery and regeneration processes significantly. Besides, there is an intrinsic limitation in the number of transgenes that can be introduced in a single plasmid. In contrast, combinatorial co-transformation allows the introduction of a large number of transgenes with a single selection marker and transgenes are co-integrated, producing combinatorial variability [137, 139, 156]. Co-transformation has been adapted to different delivery methods, with reports of successful transformation using both *Agrobacterium* [158] and biolistics [145, 146]. The maximum number of co-integrated transgenes reported to date is 20 [159], with a previous study having reached 13 [146].

Applications of biolistic combinatorial co-transformation have focused on the accumulation of secondary metabolites of commercial interest such as carotenoids and vitamins [147, 160], and artemisin [148]. Other reports of combinatorial co-transformation using *Agrobacterium* involved the production of tobacco and aspen (*Populus tremuloides*) trees with reduced lignin content for improved efficiency in the wood production process [158]. Combinatorial co-transformation has also been suggested as an effective way of producing a functional carbon-concentrating mechanism in the chloroplast by expressing combinations of the different parts [64] and of finding targets for increased yield in the context of source-sink relationships [161]. Recently, combinatorial co-transformation was used for the simultaneous manipulation of carbon and nitrogen flow between source and sink tissues in *Solanum lycopersicum* (tomato) [159]. In their study, transgenes were targeted to tomato leaves, phloem transport, and fruits, and yield increases of up to 23% were observed as a result of a more efficient transfer of photoassimilate between leaves and fruit tissues [159].

1.2.8 Computational approaches for the identification of metabolic engineering targets

Rational engineering of plant metabolic pathways requires an understanding of the plant metabolic network. Models, defined as '*representations of a system or process by a mathematical formalism, programming language, or both*' [162], are a key tool to guide experimental designs in metabolic engineering. While the previous sections have mostly focused on metabolic engineering targets identified from empirical studies, computational approaches are increasingly becoming pivotal to the identification of novel targets.

Models of photosynthesis

Photosynthesis models have been historically invaluable for their association between the biochemistry of photosynthesis and plant photosynthetic rates [46, 163]. In particular, the Farquhar, von Caemmerer and Berry model [46], which consisted of a steady-state biochemical model of C_3 leaf photosynthesis, laid the foundation for many subsequent models of photosynthesis and has been widely used and validated. Several mathematical models that described the responses of photosynthetic carbon assimilation based on differential equations were then developed. These initially included the CBB cycle only [164, 165] but then increased their scope to include photosynthetic electron transport, sucrose biosynthesis, starch biosynthesis and degradation [166], and triose-phosphate export [167].

More recently, computational simulations of light-saturated photosynthetic rates have been key for the identification of engineering targets for the optimal allocation of resources [14, 95, 168]. Markedly, an advanced kinetic model of photosynthetic carbon metabolism was applied to optimise protein allocation between enzymes [95]. This dynamic model described all 38 enzymes participating from the CBB cycle, photorespiration, and sucrose and starch biosynthesis. The results of this study questioned current C_3 nitrogen partitioning, proposing that there is an over-investment of protein in photorespiratory enzymes and an under-investment in RuBisCO, SBPase, and FBPA [95]. Solving the differential equations towards

the objective function for a maximised photosynthetic rate under light-saturation was a considerable achievement which led to the authors identifying targets for improved photosynthetic capacity. This model is an example of the suitability of metabolic modelling for the identification of engineering targets, which were subsequently tested *in planta*. As predicted, increased amounts of the SBPase and FBPA in transgenic in combination with other photosynthesis-related proteins led to improved photosynthetic capacity and biomass yield in tobacco [59] and Arabidopsis [100], as examined in Section 1.2.3.

These models of photosynthesis have served as platforms to guide the manipulation of the core metabolic pathways in photosynthesis. Nevertheless, they do not account for the rest of leaf metabolism (e.g. nitrogen metabolism, respiration, etc). Increasingly, it has been stressed that metabolic engineering strategies should then be based on a systems-level perspective, particularly in the case of multisite manipulations and synthetic biology procedures.

Metabolic flux analysis and flux balance modelling

Traditionally, metabolic flux analysis has been extensively used to estimate the fluxes of reactions in the metabolic network *in vivo* and to construct flux maps [169]. In this approach, the system is fed with a substrate labelled with a stable isotope, often ^{13}C. As this precursor is processed through the metabolic network, the label becomes incorporated into other metabolites. The isotope redistribution is analysed using mass spectrometry and/or nuclear magnetic resonance. Flux maps can be inferred at a system-level based on fitting the labelling patterns of the metabolites to a model of the carbon transitions in the metabolic network [170, 171].

More recently, detailed computational models have emerged as an alternative tool for the prediction of metabolic fluxes. Computational metabolic models capture the complexity of the metabolic network, allowing accurate network-level predictions of alternative flux routes *in silico* that can direct and test wet lab metabolic engineering efforts [131].

Computational metabolic modelling can generally be divided into kinetic and stoichiometric models. Kinetic modelling contains details on metabolite concentrations and reaction fluxes as functions of time; stoichiometric modelling is defined at steady-state (metabolite concentrations not changing over time) in terms of the reactions' stoichiometry without any kinetic information [172]. Stoichiometric modelling lacks the time-dependent and metabolic control analysis capabilities of kinetic modelling but given that it does not require feeding with detailed kinetic parameters, it can capture a wider network [173]. This often entails around 1000 reactions (in contrast to 10-50 reactions in kinetic models) [131] which are organised in a stoichiometric matrix in which each metabolite is represented in a row and its stoichiometry in columns. As a result, stoichiometric modelling allows the inspection of the metabolic network at a wider level.

The construction of the model is followed by its analysis, for which flux balance analysis (FBA) is commonly applied in large-scale networks [162, 170, 171]. FBA finds a range of flux distributions that will satisfy a given objective function. The objective function may vary from maximising biomass output, to maximising growth rate, to maximal ATP yield [162, 171].

Flux-balance models have been constructed at different scales for Arabidopsis [174–176], maize [177], barley [178], and other plant species. The Sweetlove Research Group has generated and analysed computational stoichiometric models of leaf metabolism using FBA to capture day-night simulations of C_3 and crassulacean acid metabolism photosynthesis [179–181]. Recently, a stoichiometric model of primary metabolism in leaves was constructed that explores metabolic and energetic interactions between chloroplasts and mitochondria [182].

1.2.9 The link between chloroplast and mitochondrial metabolism

The previous sections have focused on direct manipulations of photosynthesis and downstream metabolic processes in the plant leaf. However, photosynthetic metabolism is highly intertwined with mitochondrial metabolism. While most of

the photosynthate produced in chloroplasts is used as a carbon backbone for plant growth, its re-oxidation to CO_2 during mitochondrial respiration is essential to provide the energy that powers metabolic pathways and transport processes in the form of ATP. Mitochondrial respiration comprises the tricarboxylic acid (TCA) cycle, which is coupled to oxidative phosphorylation through the mitochondrial electron transport chain. In addition to ATP production, mitochondria have important functions that contribute to the maintenance of photosynthetic rates, mainly the dissipation of excess reducing equivalents generated by the photochemical reactions, which are oxidised by the mitochondrial electron transport chain.

1.2.10 The role of mitochondria during the day

In photosynthetic cells, mitochondrial respiration is mainly active during the night, with respiratory CO_2 release in the light period being around 25% of that of the dark period [183]. Nevertheless, mitochondria play essential functions to support photosynthesis and other metabolic processes during the day. Some of the roles of mitochondria in the light involve: (i) glycine oxidation via GDC as part of the photorespiratory pathway, which is an important source of nicotinamide adenine dinucleotide (NAD) in its reduced form (NADH), (ii) the provision of ATP and NADH for biosynthesis reactions in the cytosol such as sucrose synthesis, (iii) the provision of carbon skeletons from the TCA cycle for ammonium assimilation and fatty acid elongation in the cytosol, and (iv) the dissipation of excess reducing equivalents from photosynthesis to prevent photoinhibition [184]. The extent to which mitochondrial respiration occurs in the light is thus likely to depend on the demand for reducing equivalents and carbon skeletons. It is estimated that 50-75% of the reducing equivalents produced in mitochondria remain in the mitochondrial matrix and are used for ATP synthesis, and 25-50% are exported to the cytosol via the malate/oxaloacetate shuttle [183]. With plant membranes being essentially impermeable to $NAD(P)^+$ and NAD(P)H, malate shuttles, which also occur in peroxisomes and chloroplasts, mediate the indirect exchange of reducing equivalents and are crucial to organelle communication [185]. The exported reducing equivalents

have been suggested to participate in nitrate reduction and in the peroxisomal hydroxypyruvate reduction. With the same amount of NADH being produced by GDC and consumed by hydroxypyruvate reductase in the peroxisome [186, 187], it has been suggested that photorespiration is the main pathway through which NADH is produced in mitochondria during the day [181].

Chloroplasts are able to contribute to the cytosolic demand for reducing equivalents via the dissipation of excess reductants. This helps to prevent photoinhibition, as electrons would otherwise accumulate in the chloroplast leading to the formation of reactive oxygen species, which inhibit the repair of PS II [188]. The dissipation of reducing equivalents is partly mediated by the chloroplast malate valve, a malate/oxaloacetate shuttle comprising a dual malate/oxaloacetate and 2-oxoglutarate/malate transporter located in the chloroplast inner envelope and malate dehydrogenase enzymes in the stroma and the cytosol [188, 189]. An additional mechanism for the export of excess reductants in chloroplasts is mediated by the TPT. Apart from its role in exchanging triose-phosphates and P_i for sucrose synthesis, it can exchange triose-phosphates with 3-PGA. The exported triose-phosphates can be oxidised by the non-phosphorylating NADP-dependent glyceraldehyde 3-phosphate dehydrogenase (NADP-G3PDH), producing 3-PGA and NADPH [189]. Triose-phosphates can also be used for the production of 3-PGA, ATP and NADH via the phosphorylating NAD-dependent glyceraldehyde 3-phosphate dehydrogenase (NAD-G3PDH, GAPC hereafter) and phosphoglycerate kinase [190].

1.2.11 A diel FBA model of primary metabolism of Arabidopsis leaves

Shameer *et al.* explored the contributions of chloroplasts and mitochondria to the energetic balance of leaves in a computational model of Arabidopsis metabolism [182]. The authors hypothesised that the extent to which mitochondria contribute to the export of reducing equivalents in photosynthesising leaves depends on the light conditions and the subsequent energetic balance of the cell. They developed a stoichiometric model of leaf primary metabolism in mature (source) and growing

(sink) leaves, comprising 647 reactions and including subcellular compartments and transport processes. The model was charge- and proton-balanced and the production of energy (in the form of ATP) and reducing power (in the form of NAD(P)H) was balanced by their consumption. The model included reactions for the biosynthesis of cell wall, lipids, proteins, and nucleotides, as well as the mitochondrial and chloroplast electron transport chains, including alternative electron transport modes such as cyclic electron flow around PS I and uncoupled mitochondrial respiration [182]. Diel FBA (accounting for light and dark conditions) was used to analyse the energetic balance of the system under different scenarios of light conditions and energy utilisation.

Firstly, it was observed that it was possible to achieve experimental rates of net CO_2 assimilation without any flux through the mitochondrial electron transport chain or ATP synthesis if enough light energy was available, in source leaves (supplied with at least 200 µmol (photons) m^{-2} s^{-1}) and sink leaves (with at least 400 µmol m^{-2} s^{-1}). This would mean that, if the minimum demand for light energy is met, the cytosolic demand for ATP is met by chloroplasts instead of mitochondria. In the model, this demand could be met via the chloroplast phosphoenolpyruvate-pyruvate shuttle, which couples phosphoenolpyruvate-pyruvate exchanges with the export of ATP from the chloroplast to the cytosol, and, to a much smaller extent, via the triose phosphate-3-PGA shuttle. In this scenario, in the sink leaf model, the chloroplast malate valve was also activated to meet the peroxisomal demand for NADH in the form of malate.

Next, the capacity of the chloroplast shuttles to export ATP to the cytosol was limited using experimental estimates, since the authors reasoned that it is likely that their actual catalytic rates restrict their capacity to support ATP export. These limitations switched the flux from the phosphoenolpyruvate-pyruvate to the triose phosphate-3-PGA shuttle, with barely any flux being detected in the phosphoenolpyruvate-pyruvate shuttle. Because the triose phosphate-3-PGA shuttle is a source of not only ATP but also NAD(P)H, this contributed to meeting the NADH demand in the peroxisome. The capacity limits in these shuttles meant

that mitochondrial ATP production was increased to meet the cytosolic demand for ATP [182]. This was more energy efficient since the mitochondrial ATP synthase has a superior H^+-ATP stoichiometry than the chloroplast one, with 10 and 14 protons required to make three ATP molecules, respectively [191]. As a result, the use of mitochondrial ATP production to satisfy cytosolic demand resulted in a more energy-use-efficient state of the leaf metabolic system in both source and sink leaves, with the light utilisation rate being lower when mitochondrial ATP synthesis is operative [182].

The implications of these analyses were (i) that the main role of mitochondria during the day is to use photorespiratory glycine to provide NADPH for ATP production, with only a minor role in supporting the peroxisomal demand for NADH and (ii) that the chloroplast malate valve and other shuttle systems that export reducing equivalents to the cytosol are key to achieve a balanced energy status [182].

The findings of the Shameer model implied a high degree of energetic coupling between organelles in leaves. This energetic coupling between chloroplasts and mitochondria was recently described in diatoms [192], where the exchange of ATP and reducing equivalents between chloroplasts and mitochondria were found to be crucial to ensure the fuelling of carbon assimilation. Taken together, these results suggest that an optimal leaf energy balance, mediated by an increased mitochondrial ATP production and increased activity in chloroplast shuttles, could be paramount to support photosynthetic processes and overall productivity. This would be particularly beneficial in conditions of low light, where the system would benefit from a more energetically-efficient use of light. Indeed, diatoms, in which the energetic coupling between organelles has been observed, live in marine, low-light environments.

In this thesis, a multigene metabolic engineering approach was designed based on the predictions of the Shameer model [182] to support a more energy-efficient leaf with the ultimate aim of improving photosynthetic capacity. An increased mitochondrial respiratory capacity would support cytosolic ATP demand through the use of photorespiratory glycine as a source of NADH, while chloroplasts would

be responsible for the transfer of reducing power to the peroxisomes, and plastidic ATP export would be suppressed.

1.3 Thesis layout

This thesis is structured in six chapters, including this General Introduction and the General Discussion. This first chapter aimed to provide a theoretical background to the experimental work done during my D.Phil research by including a review of the relevant literature and available methodologies and highlighting the gaps within them. The details of the methodology used to conduct this research are provided in the second chapter. The following three results chapters present an introduction to each of the topics covered, followed by a description of the results and a discussion.

Chapter 2
Materials and Methods

Contents

2.1 Microbiological methods

2.1.1 Bacterial strains and plasmids

The bacterial strains used in this study are described in Table 2.1. *E. coli* and *Agrobacterium* were grown in Luria-Bertani (LB) broth [193] at 37 °C and 28 °C, respectively. The plasmids used in this study are described in Tables A.1 to A.5. Antibiotics were used at the following final concentrations (mg L^{-1}): ampicillin, 50; cefotaxime, 400; kanamycin, 50; rifampicin, 60; spectinomycin, 50; streptomycin, 100.

Table 2.1: Bacterial strains used in this study. Strain, species, genotype, use, and source are indicated.

Strain	Species	Genotype	Use	Source
Alpha-select DH5-α	*Escherichia coli*	Chemically competent strain; F^- deoR endA1 recA1 relA1 gyrA96 hsdR17 (rk^-, mk^+) supE44 thi-1 phoA Δ(lacZYA argF)U169 Φ80lacZM15 λ^-	Plasmid amplification (cloning)	Bioline (London, UK)
One Shot TOP10		Chemically competent strain; F^- mcrA recA1 Δ(mrr-hsdRMS-mcrBC) Φ80lacZM15 ΔlacX74 araD139 Δ(araleu)7697 galU galK rpsL (StrepR) endA1 nupG	Plasmid amplification (cloning)	Thermo Fisher Scientific (MA, USA)
GV3101	*Agrobacterium tumefaciens*	C58 (RifR) Ti pMP90 (pTiC58DT-DNA) (GentR) Nopaline	Arabidopsis transformation	Provided by Paul Jarvis (Department of Plant Sciences, University of Oxford, Oxford, UK)
LBA4404		Ach5 (RifR) Ti pAL4404 (StrepR) Octopine	Tobacco transformation	Provided by Christine Raines (School of Life Sciences, University of Essex, Colchester, UK)

2.1.2 Bacterial transformation

The plasmids resulting from the cloning reactions were used to transform Alpha-Select DH5-α Chemically Competent Cells or One Shot TOP10 Chemically Competent *E. coli* (Table 2.1) by heat shock using the Hanahan method [194, 195]. Briefly, an aliquot of 50–100 µL of competent cells was thawed on ice. Plasmid DNA was added to the cells and the tube was mixed gently and incubated on ice for 30 min. The cells were transformed by applying a heat shock of 45 s at 37 °C, then placed back on ice before plating onto LB agar plates.

Transformation of *Agrobacterium* strains GV3101 and LBA4404 (Table 2.1) was performed using the freeze-thaw method [196]. Briefly, 250 µL of competent cells of the specified strains was thawed on ice and mixed with 1 µL of the plasmid of interest. The mixture was transferred to liquid nitrogen, then incubated for 5 min at 37 °C. Each tube was supplemented with 1 mL of LB medium and incubated at 28 °C for 3 h with gentle shaking. Cells were collected by spinning at 2,400 x *g* for 30 s and spread on LB agar plates with the appropriate antibiotics. Cells were grown for two days at 28 °C.

Transformants were selected for their ability to grow on the respective antibiotic(s), as specified in Tables A.1 to A.5.

2.1.3 Plasmid DNA extraction

Plasmid DNA from 2 mL LB broth overnight cultures of selected antibiotic-resistant clones was purified by alkaline lysis. Half the volume of the overnight broth was centrifuged for 1 min at 11,000 x *g*, and the supernatant was carefully removed. The remaining cell pellet was resuspended in 100 µL of 50 mM glucose, 10 mM ethylenediaminetetraacetic acid (EDTA), 25 mM Tris-HCl (pH 8.0) and 100 µg mL^{-1} of RNase-A. Cell lysis was performed by adding 200 µL of 0.2 M NaOH-1% sodium dodecyl sulfate (v/v) and incubating for 5 min at room temperature. Precipitation of cell lysate was obtained using 150 µL of 3 M potassium acetate (pH 4.8). This solution was incubated on ice for 10 min, and centrifuged for another 10 min at 11,000 x *g* and 4 °C. Plasmid DNA was recovered from the resulting supernatant

by ethanol precipitation and dissolved in 50 µL of sterile double distilled water (ddH_2O). The presence of the appropriate construct was confirmed in the selected colonies by restriction digest or polymerase chain reaction (PCR), and sequencing.

2.2 Bioinformatics analyses

2.2.1 DNA sequence retrieval of transgenes and transit peptides

Genes for combinatorial co-transformation

The sequences corresponding to each of the transgenes (Table 2.2) and chloroplast transit peptides (Table 2.3) were retrieved from the National Center for Biotechnology Information Genbank nucleotide database (`https://www.ncbi.nlm.nih.gov/genbank/`) [197] or The Arabidopsis Information Resource (TAIR, `https://www.arabidopsis.org/`). In the case of tobacco plastocyanin chloroplast transit peptide, the mRNA sequence was retrieved from the National Center for Biotechnology Information Genbank nucleotide database and the sequence for the signal peptide was predicted using the TargetP-2.0 server (`https://services.healthtech.dtu.dk/service.php?TargetP-2.0`).

Genes for *Agrobacterium*-mediated transformation

The sequences for the genes coding for the plastidic 2-oxoglutarate/malate transporter (*AtpOMT1*, AT5G12860) and the mitochondrial fission regulator FISSION1A (*AtFIS1A*, AT3G57090) were retrieved from TAIR. The sequence for the biosensor *c-Peredox-mCherry* was based on the plasmid GW1-Peredox-mCherry (Addgene plasmid #32380) as per [198]. The native DNA sequences for these three genes were found to contain restriction sites of type IIS restriction enzymes, either BsaI, BpiI, or EspI3, which are incompatible with Golden Gate modular cloning. Therefore, the DNA sequences corresponding to *AtpOMT1*, *AtFIS1A*, and *c-Peredox-mCherry* were modified to eliminate these restriction sites and codon-optimised for expression in tobacco. These gene sequences were artificially synthesised by

Bio Basic (Ontario, Canada) in the pUC57 plasmid for the generation of the corresponding transgene overexpression cassettes.

The sequences corresponding to the genes coding for the tobacco mitochondrial malate dehydrogenase (*mMDH*) and cytosolic glyceraldehyde 3-phosphate dehydrogenase (*GAPC*) to be silenced via antisense technology were identified as tobacco orthologues of their annotated versions in Arabidopsis. The full-length coding sequence and protein sequences for *AtmMDH1* (AT1G53240) and *AtGAPC* (AT1G13440 and AT3G04120, two annotated subunits) from Arabidopsis were retrieved from TAIR [199]. These were used to identify corresponding orthologues in tobacco using Basic Local Alignment Search Tool (BLAST) against the *N. tabacum* BX and TN90 Sierro 2014 versions of the tobacco genome [200] at the Sol Genomics Network database [201]. For each of the Arabidopsis genes, there were several mRNA matches of different sequence length in tobacco. In the case of *AtGAPC*, the matches were the same when using either of the Arabidopsis subunits (AT1G13440 or AT3G04120). Because of the high sequence similarity between mRNA sequences in tobacco, it was not possible to distinguish between orthologues of *AtmMDH1* and *AtmMDH2* or *AtGAPC1* and *AtGAPC2*. The top matches in the nucleotide and protein BLAST results were chosen for each gene. The selected tobacco sequences were *mRNA_92827_cds* for *mMDH* and *mRNA_81739_cds* for *GAPC*.

Table 2.2: Details of transgenes used for tobacco combinatorial co-transformation. Details of target transgenes, including source organism, abbreviation, molecular size (in base pairs, bp), choice of promoter, and sequence identifier (TAIR (`https://www.arabidopsis.org/`) for Arabidopsis genes and GenBank (`https://www.ncbi.nlm.nih.gov/genbank/`) for other species). Promoters are as follows: *pAtRbcS*, Arabidopsis RuBisCO small subunit (RbcS) promoter; *pCaMV35S*, CaMV 35S promoter; *pSlRbcS*, *S. lycopersicum* (tomato) RbcS promoter; *pStcyFBP*, *S. tuberosum* (potato) cytosolic fructose 1,6-bisphosphatase promoter; *pCoYMV*, commelina yellow mottle virus (*CoYMV*) promoter.

Transgene product	Source organism	Abbreviation	Molecular size (bp)	Promoter	Sequence identifier
Cytochrome b_6f Rieske FeS protein	*Arabidopsis thaliana*	*AtPetC*	756	*pAtRbcS*	AT4G03280.1
Cytochrome c_6	*Porphyra yezoensis*	*Pyc6*	546	*pAtRbcS*	AB040818.1
Ferredoxin-like protein	*Capsicum annuum*	*CaPFLP*	447	*pCaMV 35S*	AF039662.1
Putative bicarbonate transporter	*Synechococcus* PCC7942	*SeictB*	1584	*pCaMV 35S*	U62616.1
Fructose 1,6-bisphophate aldolase	*Arabidopsis thaliana*	*AtFBPA*	1197	*pSlRbcS*	AT4G38970
Sedoheptulose 1,7-bisphosphatase	*Arabidopsis thaliana*	*AtSBPase*	1182	*pCaMV 35S*	NM_115438.4
Glycine decarboxylase-H protein	*Flaveria pringlei*	*FpGLDH*	489	*pSlRbcS*	Z25856.1
Chloroplast triose-phosphate/ phosphate translocator	*Arabidopsis thaliana*	*AtTPT*	1248	*pStcyFBP*	AT5G46110
Cytosolic fructose 1,6-bisphosphatase	*Arabidopsis thaliana*	*AtcFBPase*	1026	*pStcyFBP*	AT1G43670
Cytosolic pyrophosphatase	*Escherichia coli*	*EcPP*	531	*pStcyFBP*	M23550.1
Passive sucrose transporter	*Arabidopsis thaliana*	*AtSWEET11*	1538	*pCoYMV*	NM_114733.4
Sucrose/H^+ importer	*Arabidopsis thaliana*	*AtSUC2*	870	*pSlRbcS*	NM_102118.4

Table 2.3: Details of transit peptides used for chloroplast targeting in the tobacco combinatorial co-transformation experiment. Details of chloroplast transit peptides, including source organism, molecular size (in bp), and identifier are included.

Source gene	Source organism	Molecular size (bp)	GenBank identifier
Plastocyanin	*Nicotiana tabacum*	204	XM_016614988.1
RuBisCO small subunit (RbcS)	*Pisum sativum*	249	GU269269.1

Table 2.4: Details of transgenes used for *Agrobacterium*-mediated transformation of tobacco. Details of target transgenes, including strategy (overexpression/knock-down antisense silencing), source organism, abbreviation, molecular size (in bp), choice of promoter, and sequence identifier (TAIR (`https://www.arabidopsis.org/`) or Addgene (`https://www.addgene.org/`). Promoters are as follows: *pCaMV2x35S*, double-enhancer *CaMV35S* promoter; *pAtLhb1B1*, Arabidopsis light-harvesting chlorophyll-protein complex II subunit B1 promoter; *pSlRbcS2*, *S. lycopersicum* (tomato) RbcS2 promoter; *pStLS1*, *S. tuberosum* (potato) leaf and stem-specific promoter; *pAtRbcS2*, Arabidopsis RuBisCO small subunit 2 (*RbcS*) promoter.

Transgene product	**Strategy**	**Source organism**	**Abbreviation**	**Molecular size (bp)**	**Promoter**	**Identifier**
Cytosolic NADH:NAD+ biosensor	Overexpression	Synthetic	*c-Peredox-mCherry*	2769	*CaMV2x35S*	Addgene #32380
Fission 1A/bigyin	Overexpression	*Arabidopsis thaliana*	*FIS1A*	513	*AtLhb1B1*	AT3G57090
Glyceraldehyde 3-phosphate dehydrogenase	Antisense silencing	*Nicotiana tabacum*	*GAPC*	437*	*SlRbcS2*	AT1G13440/ AT3G04120
Mitochondrial malate dehydrogenase	Antisense silencing	*Nicotiana tabacum*	*mMDH*	639*	*StLS1*	AT1G53240
Plastidic 2-oxoglutarate/ malate transporter	Overexpression	*Arabidopsis thaliana*	*pOMT*	1674	*AtRbcS2*	AT5G12860

2.3 Nucleic acid manipulations

2.3.1 Preparation of overexpression constructs for combinatorial co-transformation of tobacco

Individual plasmids carrying single transgene expression cassettes were generated to perform tobacco combinatorial co-transformation, as per [137]. The plasmids were generated using restriction-ligation DNA cloning, with the target transgenes either amplified via PCR or synthesised artificially. Some of the plasmids used for the combinatorial co-transformation experiment were provided by collaborators, as specified in Table A.2.

DNA amplification and purification

The regions corresponding to the genes *AtFBPA*, *AtTPT* and *AtcyFBPase* were amplified via PCR using 200 ng of cDNA from Arabidopsis leaves, corresponding primers (labelled as cloning primers in Table A.6) and the Phusion Hot Start II High-Fidelity DNA Polymerase (Thermo Fisher Scientific, MA, USA). PCR conditions consisted of initial denaturation at 98 °C for 30 s; 30–40 cycles of denaturation at 98 °C for 10 s, primer annealing at 55 °C for 30 s, extension at 72 °C for 1 min; and a final extension at 72 °C for 10 min. Each 20 µL reaction contained 1X Phusion Green High-Fidelity Buffer (Thermo Fisher Scientific, MA, USA), 2 mM dNTPs, 0.5 µM of each primer, 0.1-0.2 µL of genomic DNA, 0.5 µL Phusion Hot Start II High-Fidelity DNA Polymerase, and ddH_2O.

All amplifications were performed in a Mastercycler ep Gradient S (Eppendorf, Hamburg, Germany). Agarose gel electrophoresis was used to separate the PCR products: 1% (w/v) agarose gels were prepared by dissolving the agarose in 1X Tris-acetate-EDTA (TAE) buffer (40 mM Tris-base, 20 mM (glacial) acetic acid and 1 mM EDTA (pH 8.0)). Ethidium bromide was used to visualise the DNA. Electrophoresis was performed at 100 V. DNA was detected using UV light and the size of the DNA was determined using the GeneRuler 1 kb DNA Ladder (Thermo Fisher Scientific, MA, USA). DNA fragments corresponding to the genes of interest were purified from agarose gels prior to further use using the NucleoSpin

Gel and PCR Clean-up kit (Macherey-Nagel, Berlin, Germany), following the manufacturer's instructions and eluting in 16 µL of ddH_2O.

Custom DNA synthesis

DNA corresponding to the *AtPetC*, *Pyc6*, *CaPFLP* and *SeictB* genes was artificially synthesised by Biomatik Corporation (Ontario, Canada) in the pUC57 plasmid. Their gene sequences were codon optimized for tobacco using CodonworkBench 0.8.2 (`http://www.buba-basis.de/software/cwb/cwb.html`). Restriction sites were included in the flanking regions. In order to target the gene products to the chloroplast lumen, the tobacco chloroplast transit peptide from plastocyanin was introduced in the N-terminal region of the *Pyc6* gene sequence, and the native chloroplast transit peptide in *AtPetC* gene was exchanged with the tobacco chloroplast transit peptide from plastocyanin. The pea ribulose bisphosphate carboxylase small chain (*RbcS*) chloroplast transit peptide was included in the N-terminal region of the *SeictB* gene to target its product to the stroma.

DNA restriction digest

Restriction digests of the purified PCR products or synthesised genes (inserts), as well as their corresponding plasmid DNA vectors, were completed using 1 µg of DNA, 10X FastDigest Green Buffer (Thermo Fisher Scientific, MA, USA), and 1 µL of each enzyme (FastDigest, Thermo Fisher Scientific, MA, USA; Table A.1). Samples were incubated at 37 °C for 30–60 min and the resulting digestion product was confirmed by agarose electrophoresis. DNA fragments corresponding to each insert and vector were purified from agarose gels using the NucleoSpin Gel and PCR Clean-up kit (Macherey-Nagel, Berlin, Germany) and eluting in 10 µL of ddH_2O prior to further use. Once the ligation reaction was performed and antibiotic-resistant colonies were obtained, the extracted pDNA was digested with the same restriction enzymes to confirm the presence of the insert by agarose electrophoresis.

Ligation

The DNA corresponding to each insert was subcloned into its corresponding plasmid using the T4 DNA ligase (Invitrogen, CA, USA). The molar ratio of vector:insert DNA was calculcated based on the manufacturer's instructions. The ligation reaction was incubated for at least 30 min at room temperature and at least 30 min at 16 °C before transforming *E. coli* competent cells.

2.3.2 Preparation of *AtFIS1A* overexpression construct for *Agrobacterium*-mediated transformation of Arabidopsis

DNA amplification and purification

To amplify the region corresponding to the gene *AtFIS1A*, PCR amplification was performed using 10 ng of cDNA from Arabidopsis, *AtFIS1A*-specific primers (Table A.7), and the Phusion Hot Start II High-Fidelity DNA Polymerase (Thermo Fisher Scientific, MA, USA). PCR conditions consisted of initial denaturation at 98 °C for 30 s; 30 cycles of denaturation at 98 °C for 10 s, primer annealing at 55°C for 30 s, extension at 72 °C for 70 s; and a final extension at 72 °C for 5 min. Each 50 µL reaction contained 1X Phusion Green High-Fidelity Buffer (Thermo Fisher Scientific, MA, USA), 2 mM dNTPs, 0.5 µM of each primer, 1 µL of genomic DNA, 0.5 µL Phusion Hot Start II High-Fidelity DNA Polymerase, and ddH_2O.

Amplifications were performed in a Mastercycler ep Gradient S (Eppendorf, Hamburg, Germany). Agarose gel electrophoresis (1% (w/v) agarose, 100 V) was used to separate the PCR products. SYBR Safe DNA Gel Stain (Thermo Fisher Scientific, MA, USA) was used to visualise the DNA. DNA was detected using UV light and the size of the DNA was determined using the Hyperladder I (Bioline, London, UK). DNA fragments corresponding to the genes of interest were purified from agarose gels using the QIAquick Gel Extraction Kit (Qiagen, Hilden, Germany) and eluting in 30 µL of ddH_2O prior to further use.

DNA cloning — TOPO cloning

Adenosine overhangs were added in the 3' end of the purified DNA after amplification for its cloning into the Gateway entry vector pCR8/GW/TOPO (Invitrogen, CA, USA) following the user's guide. The gel-purified PCR product (29 µL) was mixed in a 50 µL reaction with the following: 5 µL of 10X NH_4 buffer (Bioline, London, UK), 10 µL of 1 mM dATP (New England Biolabs, MA, USA), 3 µL of 50 mM $MgCl_2$ (Bioline, London, UK), and 0.5 units of the non-proofreading Taq BIOTAQ (Bioline, London, UK). The reaction was incubated at 72 °C for 20 min and used in the topoisomerase-based TOPO cloning reaction. The TOPO cloning reaction consisted of 4 µL of the PCR product (including 3' adenosine overhangs), 1 µL of salt solution (1.2 M NaCl; 0.06 M $MgCl_2$), and 10 ng of the pCR8/GW/TOPO entry vector. These were mixed and incubated at room temperature for 5 min, before proceeding to transform *E. coli* competent cells with 2 µL of the TOPO cloning reaction.

Single, antibiotic-resistant colonies were picked and diluted in a PCR tube containing 40 µL of LB liquid medium with spectinomycin and analysed via colony PCR using the 2X PCRBIO Taq Mix Red (PCR Biosystems, London, UK) and *AtFIS1A* primers. PCR conditions consisted of initial denaturation at 95 °C for 1 min; 40 cycles of denaturation at 95 °C for 15 s, primer annealing at 55 °C for 15 s, extension at 72 °C for 8 s. The 50 µL reaction consisted of 1 µL of the bacterial solution, 0.4 µM of each primer, 25 µL of 2X PCRBIO Taq Mix Red, and 20 µL of ddH_2O. Two putative pCR8/GW/TOPO-AtFIS1A colonies, positive for the presence of the insert in the colony PCR, were subjected to plasmid DNA extraction and sequence analysis.

DNA cloning — Gateway LR recombination reaction

Both the entry vector pCR8/GW/TOPO and the destination vector pK7WG2 [202] conferred resistance to the same antibiotic, spectinomycin. Plasmid DNA for pCR8/GW/TOPO-AtFIS1A, extracted from colonies confirmed via PCR and sequence analysis, was linearised before proceeding to perform the LR reaction. Linearisation consisted of a restriction digest with PvuI (New England Biolabs,

MA, USA), a single cutter whose restriction site sits specifically in the sequence corresponding to the gene conferring antibiotic resistance. This ensured that any spectinomycin-resistant colonies resulting from the transformation of *E. coli* cells with the product of the LR reaction would only be carrying the destination vector. The 20 µL digest reaction consisted of 10 µL of pCR8/GW/TOPO-AtFIS1A pDNA, 2 µL of FastDigest Green Buffer (10X) (Thermo Fisher Scientific, MA, USA), 1 µL of FastDigest PvuI (Thermo Fisher Scientific, MA, USA), and 7 µL of ddH_2O. Samples were incubated at 37 °C for 3 h and the resulting digests were confirmed by agarose electrophoresis. DNA fragments corresponding to the linearised vector were purified from the agarose gel using the QIAquick Gel Extraction Kit (Qiagen, Hilden, Germany), following the manufacturer's instructions.

The Gateway LR reaction (Invitrogen, CA, USA) is catalysed by the LR clonase and consists of the recombination between the *attL* sites of the generated entry clone and the *attR* sites of the destination vector, which results in an expression clone with the DNA of interest flanked by *attB* sites. The LR reactions (20 µL) were performed as per the manufacturer's instructions (Invitrogen, CA, USA), using 200 ng of the entry clone pCR8/GW/TOPO-AtFIS1A, 300 ng of the destination vector pK7WG2, 4 µL of the LR enzyme mix, and Tris-EDTA buffer (10 mM Tris-HCl (pH 8.0), 1 mM EDTA). These were incubated at 25 °C for 1 h when 4 µg of proteinase K was added to stop the reactions. Finally, samples were incubated at 37 °C for 10 min and the LR reaction products were used to transform competent cells of *E. coli*.

Spectinomycin-resistant colonies were subjected to plasmid DNA extraction and sequence analysis before proceeding to transform *Agrobacterium* with the confirmed *pK7WG2::AtFIS1A* plasmid.

2.3.3 Preparation of multigene constructs for *Agrobacterium*-mediated transformation of tobacco

DNA amplification and purification

Specific primers were designed to amplify the tobacco genes *mMDH* and *GAPC* using the sequences *mRNA_92827_cds* (Solyc12g014180.1.1) and *mRNA_81739_cds* (Solyc05g014470.2.1), respectively, retrieved from the Sol Genomics Network database [201]. The reverse complement DNA sequence was used to generate antisense constructs. Similarly, the position of the Golden Gate adapter sites, which contain BsaI restriction sites and are used for their cloning into level 1 vectors, was inverted. Two pairs of primers were designed for each gene and combined to amplify four distinct fragments of different sizes (Table A.7).

Each PCR amplification reaction (50 µL) consisted of 1X Phusion High-Fidelity Buffer (Thermo Fisher Scientific, MA, USA), 2 mM dNTPs, 0.5 µM of each primer, 2.5 µL of tobacco cDNA (synthesized from 1 µg of total RNA), 1 µL Phusion Hot Start II High-Fidelity DNA Polymerase, and ddH_2O. PCR conditions consisted of initial denaturation at 98 °C for 30 s; 35 cycles of denaturation at 98 °C for 10 s, primer annealing at 62 °C for 30 s, extension at 72 °C for 20 s; and a final extension at 72 °C for 10 min.

The purified DNA amplicons were used to build the level 0 Golden Gate modules. The level 0 Golden Gate modules were the purified PCR products in the case of *NtGAPC* and a *pCR8/GW/TOPO-NtmMDH* construct in the case of *NtmMDH* because the level 0 assembly was not successful using the PCR product directly in the case of *NtmMDH*.

Custom DNA synthesis

DNA corresponding to the *AtpOMT1*, *AtFIS1A*, and *c-Peredox-mCherry* genes, flanked by Golden Gate adapter sites, was artificially synthesised by Bio Basic (Ontario, Canada) in the pUC57 plasmid.

Golden Gate cloning

The Golden Gate modular cloning toolbox for plants [144] was used to build multigene constructs for plant transformation. The Golden Gate level 1 assembly reaction (7.5 µL) contained 0.5 µL of the T4 DNA ligase, 0.75 µL of the 10X T4 DNA ligase reaction buffer containing ATP, 0.5 µL of 100X BSA, 0.5 µL of BsaI, ddH_2O, and 100 ng of pDNA of each module component (i.e. promoter, terminator, coding sequence (PCR amplified or artificially synthesised), and the level 1 destination plasmid backbone). Reagents were purchased from New England Biolabs (MA, USA). The reaction mix was incubated in a thermocycler, with the following program: 25 cycles of 3 min at 37 °C and 4 min at 16 °C (restriction-ligation), followed by 5 min at 50 °C and 5 min at 80 °C (inactivation). This was followed by transformation of *E. coli* with 1 µL of the assembly reaction product. The level 1 plasmid backbones contained a lactose (*lac*) operon, which enabled the identification of putative positive colonies through a blue-white screen. White colonies, potentially containing the transcriptional unit of interest, were analysed using colony PCR followed by plasmid preparation and sequencing. Level 1 plasmids are described in Table A.4.

Level 2 constructs, comprising of two to six transcriptional units, were assembled as above, using BpiI. Each level 2 assembly reaction (7.5 µL) contained 0.5 µL of the T4 DNA ligase, 0.75 µL of the 10X T4 DNA ligase reaction buffer containing ATP, 0.08 µL of 100X BSA, 0.5 µL of BpiI, ddH_2O, and 100 ng of pDNA of each level 1 plasmid. The level 1 transcriptional units assembled into each level 2 construct are specified in Table A.5. The incubation and bacterial transformation steps were as indicated for the level 1 assembly.

2.3.4 Plant genomic DNA extraction

Genomic DNA was isolated from young leaves of two-week-old Arabidopsis and six-week-old tobacco plants using the cetyltrimethylammonium bromide (CTAB) method [203].

2.3.5 RNA extraction and cDNA synthesis

For total RNA extraction, 300—400 mg samples of frozen powdered plant material were prepared with the peqGOLD Trifast reagent or the TRIzol reagent (Thermo Fisher Scientific, MA, USA), following the manufacturer's instructions. The RNA pellet was resuspended in 50 µL of autoclaved, DEPC-treated ddH_2O, and immediately treated with DNase I (TURBO DNA-Free Kit, Ambion, Thermo Fisher Scientific, MA, USA). RNA was stored at -80 °C until further use.

After spectrophotometric quantification, RNA was used for cDNA synthesis, as follows: 0.5 µg of RNA were incubated with 0.5 µL of oligo(dT)20 primer (50 µM) and 0.5 µL of dNTPs (10 mM) for 5 min at 65 °C. Then, 3.5 µL of a master mix was added to the annealed RNA (2 µL of 5X SSIV buffer, 0.5 µL of 0.1 M DTT, 20 U of RNaseOUT Recombinant Ribonuclease Inhibitor (Thermo Fisher Scientific, MA, USA) and 100 U SuperScript IV Reverse Transcriptase (Thermo Fisher Scientific, MA, USA) and incubated for 10 min at 55 °C, followed by an inactivation step of 10 min at 80 °C. The cDNA was diluted in 70 µL of ddH_2O and stored at -20 °C.

2.3.6 Quantitative real-time PCR analyses

Quantitative real-time PCR (qRT-PCR) was performed in a StepOnePlus system (Thermo Fisher Scientific, MA, USA) using 1 µL of cDNA as template in 20 µL reactions containing 10 µL of the 2X qPCRBIO SyGreen Mix HI-ROX (PCR Biosystems, London, UK), corresponding primers (Table A.8), and ddH_2O. Three biological (independent plants) and two or three technical replicates were analysed per line. Results were normalised to the average of the mRNA levels of the housekeeping genes *L25 ribosomal protein* (*L25*) and *Elongation Factor-1α* (*EF-1α*) [204]. The relative transcript levels were determined as fold-change ($2^{-\Delta\Delta Ct}$) as per

Pfaffl [205], where $2^{-\Delta\Delta Ct} = 2^{Ct_x - Ct_y}/2^{Ct_a - Ct_b}$, Ct_x is the cycle threshold (Ct) of the transgene in the wild type (WT), Ct_y is the Ct of the transgene in the corresponding transgenic line, Ct_a is the average Ct of the housekeeping genes in the WT, and Ct_b is the average Ct of the housekeeping genes in the corresponding transgenic line.

2.3.7 Nucleic acid determination and sequencing

Nucleic acid quantification was performed using a NanoPhotometer P300 (Implen, CA, USA). All cloning constructs were confirmed by Sanger sequencing using the services of Eurofins Genomics (Hamburg, Germany) and Source BioScience (Nottingham, UK). Subsequent bioinformatics analysis was carried out using Clustal Omega [206] and Benchling (`benchling.com`). The multiple sequence alignments shown in the appendices were generated in Benchling using the MAFFT algorithm (MAFFT version 7 [207]), and MView [208] was used to visualise and reformat the alignments as presented in this thesis.

2.4 Plant materials and methods

2.4.1 Plant growth conditions

Plants were grown under axenic conditions for both the preparation of explants for plant transformation and the germination of transgenic seed on selection media. Tobacco (*Nicotiana tabacum* cv. Petit Havana SR1) and Arabidopsis (*Arabidopsis thaliana)* ecotype Columbia-0 (Col-0) plants were grown on agar-solidified Murashige and Skoog (MS) medium (Duchefa Biochemie, Harleem, Netherlands) and the appropriate antibiotics. Six-week-old tobacco leaves were used for plant transformation, irrespective of the transformation method.

The T_1 seeds were surface sterilised with 70% (v/v) ethanol for 2 min and 6% (v/v) bleach for 3 min, followed by 6-8 washes with sterile ddH_2O and stratification at 4 °C for three days. Seeds were germinated on antibiotic-containing media for two weeks to select for transgenic plants (hetero- and homozygous) before transferring them to soil. Growth chamber conditions (Sanyo mlR-350H, Sanyo,

Osaka, Japan) consisted of a long day photoperiod of 16 h of light and 8 h of dark and a day/night temperature cycle of 22 °C/14 °C, with light conditions reaching <200 µmol (photons) m^{-2} s^{-1}.

Transgenic plants were grown in containment glasshouses at the Department of Plant Sciences, University of Oxford, Oxford (UK), with long-day photoperiod conditions and a day/night temperature cycle of 22 °C/18 °C. Soil composition consisted of a mixture of three parts by volume of Levington M2 compost (tobacco) or Levington F2 compost (Arabidopsis) and one part of vermiculite, along with 0.4 g L^{-1} of the insecticide Exemptor (ICL, Ipswich, UK). Square, 9 cm square, black, plastic pots were used. The soil was kept well moistened with regular watering. Water was supplemented weekly with a standard fertiliser, Miracle Gro (Scotts Miracle-Gro Company, OH, USA), for the development of the primary tobacco transformants (T_0). An additional glasshouse growth experiment was performed with selected tobacco combinatorial lines at the Max Planck Institute of Molecular Plant Physiology, Potsdam-Golm (Germany), with equivalent experimental conditions.

For the high light primary screen of the combinatorial tobacco transformants, plants were first transferred to round, 6 cm, plastic pots and grown under low light conditions ('nursery', <120 µmol (photons) m^{-2} s^{-1}), with a long day photoperiod, a day/night temperature cycle of 22 °C/14 °C, and 75% humidity. After two weeks, plants were transplanted to 13 cm-diameter round pots and grown in Conviron growth chambers (Conviron, Winnipeg, Canada) with a long day photoperiod and a day/night temperature cycle of 22 °C/14 °C a light intensity of 600 µmol (photons) m^{-2} s^{-1}. Relative humidity was set to 75% during the day and 70% at night. Hakaphos fertiliser (Compo Expert, Grupa Azoty, Tarnow, Poland) was applied with every watering to ensure an adequate supply of nutrients.

An additional experiment was performed with selected tobacco combinatorial lines in an outdoor polytunnel (non-controlled conditions), where temperature, light, humidity and photoperiod were weather-dependent but, contrary to a field experiment, plants were watered regularly and grown in pots of 18 cm diameter.

The plant age for each specific measurement is indicated in the corresponding results section.

2.4.2 Biolistic combinatorial co-transformation

This experiment was performed by Margit Roessner, Claudia Hasse, and Dr Stephanie Ruf from the Transformation Team at the Max Planck Institute of Molecular Plant Physiology, Potsdam-Golm (Germany), as previously described [209]. Tobacco leaves grown under axenic conditions were harvested and bombarded with plasmid DNA-coated 0.6 µm gold particles (Bio-Rad, CA, USA) using the DuPont PDS-1000/He biolistic gun with the Hepta Adaptor setup (Bio-Rad, CA, USA). The plasmids specified in Table A.2 were mixed in equimolar quantities at a concentration of 2 µg μL^{-1} and the mixture was used to coat the gold particles. An additional plasmid carrying the *nptII* gene, conferring kanamycin resistance, was included in the mixture. Two shots were performed.

Shoots were regenerated on agar-solidified regeneration medium, containing, per L, 4.4 g of MS elements including modified vitamins (Duchefa Biochemie, Harleem, Netherlands), 30% sucrose, 0.1 g L^{-1} of α-naphthaleneacetic acid, 1 mg L^{-1} of 6-benzylaminopurine, and 50 mg L^{-1} kanamycin. Samples from antibiotic-resistant calli or regenerating shoots were transferred onto fresh selection medium for the elimination of escapes and further propagation of nuclear transformants.

2.4.3 *Agrobacterium*-mediated transformation

Arabidopsis floral dip transformation

Four-week-old Arabidopsis plants grown under glasshouse conditions were transformed with *Agrobacterium* strain GV3101 harbouring the construct *pK7WG2-AtFIS1A* using the floral dip method [210]. Three days before the transformation, the main inflorescence shoots were trimmed off to encourage the development of secondary shoots. An *Agrobacterium* culture was prepared containing 250 mL of LB and antibiotics at an optical density of 0.8 absorbance units at a wavelength of 600 nm. Cells were collected at 2,400 x *g* for 8 min, and resuspended in 400 mL of

infiltrating solution containing 5% (w/v) sucrose with 300 µL L^{-1} of Silwet L-77. The aerial parts of the plants were dipped into the infiltration solution for 5 min, with gentle shaking. The transformed plants were covered in plastic wrap to ensure high humidity for a day and grown under plant growth chamber conditions (as specified in Section 2.4.1) until they set seeds.

Tobacco leaf disc transformation

Tobacco leaf discs were transformed using *Agrobacterium* strain LBA4404 harbouring the plasmids of interest, LS0201 and LS0207, following the Horsch method [211]. Briefly, an *Agrobacterium* culture was prepared in 150 mL of medium containing LB and antibiotics. Cells were collected by spinning at 3,000 x *g* for 20 min, and resuspended in MS medium mineral elements. Leaf explants were prepared and mixed with the *Agrobacterium* suspension culture for 30 min. Co-culture of the leaf pieces and *Agrobacterium* took place on medium containing 4.4 g L^{-1} of MS medium mineral elements including modified vitamins (Duchefa Biochemie, Harleem, Netherlands), 30% sucrose, 0.1 g L^{-1} of α-naphthaleneacetic acid, and 1 mg L^{-1} of 6-benzylaminopurine over two days in a plant growth chamber. Explants were then washed in liquid MS medium mineral elements to remove the excess of *Agrobacterium* and moved to fresh medium. Shoots were regenerated on agar-solidified regeneration medium containing 4.4 g of MS elements including modified vitamins (Duchefa Biochemie, Harleem, Netherlands), 30% sucrose, 0.1 g L^{-1} of α-naphthaleneacetic acid, 1 mg L^{-1} of 6-benzylaminopurine, hygromycin (20 mg L^{-1}), and cefotaxime (to kill the *Agrobacterium* cells, 400 mg L^{-1}) for two weeks. Thereafter, the leaf discs were transferred to medium containing increased concentration of 6-benzylaminopurine (2.5 mg L^{-1}) and 0.2 mg L^{-1} of indole-3-acetic acid. Juvenile shoots derived from somatic embryos were then isolated and cultivated on MS-based media with antibiotic selection until roots developed. Putative transformants were transferred to soil and used for molecular analysis.

2.5 Plant growth measurements

Plant growth was evaluated by measuring plant height, leaf number, and fresh biomass. Plant height was determined from the base to the top of the shoot. Leaf number count consisted of all leaves, excluding cotyledons.

Determination of fresh weight aboveground biomass involved all aerial tissues, including leaves, the main and lateral shoots, flowers, and flower buds. To distinguish between leaves and stem biomass, leaves were detached from the plant and weighed separately from the stem. Stem biomass included inflorescences, where present. Root biomass was not determined.

2.6 Analyses of photosynthetic capacity

Photosynthetic capacity was evaluated in transgenic tobacco plants using a range of chlorophyll fluorescence-based measurements and chlorophyll content determination. Chlorophyll *a* emission was measured from the upper surface of the leaf using different instruments and techniques, as follows.

2.6.1 Light response curve

During the high light primary screen of the tobacco combinatorial transgenic library, a light response curve was used to determine *in vivo* chlorophyll fluorescence. Chlorophyll *a* fluorescence emission was measured with a pulsed amplitude modulation fluorometer PAM-2500 (Walz, Effeltrich, Germany) from the youngest fully expanded leaf (leaf blade > 15 cm long), 2-8 h into the light period. Each data acquisition took approximately 15 min. To generate a light response curve, plants were first dark-adapted for 15 min. Afterwards, F_0, F_m, maximum quantum yield of PS II and relative electron transport rates were evaluated every 2 min at photosynthetic photon flux densities of 0, 7, 32, 65, 142, 272, 475, 786, 1161, 1664, and 2016 µmol photons m^{-2} s^{-1}. Maximum relative electron transport rate reached during the recording of the light curve was calculated using the light curve fit feature as part of the PamWin 3 software (Walz, Effeltrich, Germany).

2.6.2 Chlorophyll fluorescence-based measurements using the MultispeQ instrument

The transgenic tobacco combinatorial lines selected in the high light primary screen were analysed for increased photosynthetic capacity in a glasshouse experiment in Oxford. Chlorophyll *a* fluorescence-based measurements were carried out using a hand-held MultispeQ v1.0 device controlled by the PhotosynQ platform software [212]. The MultispeQ is a hand-held instrument that combines a pulse-amplitude-modulated fluorometer, a chlorophyll meter, and a spectrometer, allowing the rapid measurement of photosynthetic parameters based on chlorophyll fluorescence [212]. Three measurements were taken per plant, one per leaf in the three upper-most leaves, which were averaged in the analyses. Measurements were done 2–4 h into the light period, in light-adapted plants. Each measurement took approximately 15 s. The Leaf Photosynthesis MultispeQ protocol V1.0 was used to assess a wide range of plant photosynthetic parameters, which were automatically calculated as per [212]. Saturation pulse chlorophyll fluorescence yield parameters (F_s, F_m', F_0') were measured by pulsed amplitude modulation fluorometry. From these measurements, estimations of F_v' ($F_m' - F_0'$), F_v/F_m, and the quantum yield of PS II ($F_m' - F_s'/F_m'$) were estimated. The fraction of open PS II centres (qL) was calculated as $(F_m' - F_s')/(F_m' - F_0') \times (F_0'/F_s)$. Linear electron flux was estimated based on the incident PAR as $LEF = \Phi PSII \times PAR \times 0.45$, where 0.45 is a factor that accounts for the leaf absorptance of PAR and the fraction of light absorbed by PS II, and relative chlorophyll content was calculated based on transmittance at 940 and 650 nm.

2.6.3 OJIP fluorescence transient

The tobacco multigene transgenic lines were subjected to chlorophyll *a* fluorescence-based analysis using a PAR-FluorPen FP 110 (Photon Systems Instruments, Drasov, Czech Republic) pulsed amplitude modulation fluorometer. The youngest fully expanded leaf of each plant was dark-adapted for 15 min with a detachable leaf clip. A super pulse of 455 nm was applied to induce an OJIP transient fluorescence rise,

where fluorescence intensity rises from the first measured minimal level (equivalent to F_0, O stands for origin) to a maximum level (equivalent to F_m, P stands for peak) via two intermediate levels J and I [213]. The optimal intensity of the pulse, where the F_v/F_m value has highest, was determined as 30%. Each measurement took approximately 1 min. The OJIP protocol included the following measured parameters: F_0, fluorescence intensity at 50 µs; F_j, fluorescence intensity at J-step (2 ms); F_i, fluorescence intensity at I-step (30 ms); and F_m, maximum fluorescence intensity. From these, a number of estimated parameters were calculated as per Strasser *et al.* [214].

2.6.4 Determination of chlorophyll contents

Leaf material (*circa* 0.1 g) was sampled after the determination of chlorophyll *a* fluorescence in the high light primary screen of the tobacco combinatorial transgenic library, in the same region of the leaf blade, and immediately frozen in liquid nitrogen. Leaf samples were ground in a retch mill (TissueLyser, Qiagen, Hilden, Germany). To the finely ground tissue, 2 mL of acetone 80% (v/v) was added and the mixture was transferred to a 15 mL Falcon tube, to which an additional 8 mL of acetone 80% (v/v) was added. A 1.5 mL aliquot of this was centrifuged in a tabletop centrifuge for 90 s at 12,100 x *g* and 1 mL of the resulting supernatant was used to determine chlorophyll absorbance in a Jasco F-6500 fluorometer (Jasco Inc., MD, USA), following the equations described by Porra, Thomson and, Kriedemann [215].

2.7 Analyses of dark respiration

The respiratory capacity of transgenic plants carrying the construct *pK7WG2::AtFIS1A* and the multigene construct LS0201 was evaluated by measuring oxygen consumption in leaf discs.

2.7.1 Leaf respiration measurement using a Clark-type oxygen electrode

The oxygen consumption rate (OCR) of Arabidopsis leaf discs was measured using a liquid-phase DW1/AD Oxygraph Plus system (Hansatech Instruments, Norfolk, United Kingdom). The electrode disc was assembled using commercial cigarette paper and a piece of polytetrafluorethylene membrane, which was wet with saturated KCl based on the manufacturer's instructions (see [216] for video instructions). The prepared electrode disc was assembled into the electrode chamber. A water bath, set to 25 °C, was used to circulate water through the electrode chamber jacket to maintain a stable temperature. Before the measurement, the electrode was calibrated by the addition of sodium dithionite to 1 mL of aerated autoclaved water to completely deplete oxygen in the chamber's reaction vessel and establish zero oxygen conditions. The reaction vessel was then washed with distilled water three times, then filled with 2 mL leaf respiration buffer, consisting of 50 mM hydroxyethyl piperazineethanesulfonic acid, 10 mM 2-(N-morpholino)ethanesulfonic acid (pH 6.6, adjusted with NaOH) and 2 mM $CaCl_2$ [217]. Three 6.5-mm-diameter leaf discs totalling around 20 mg fresh weight were kept immersed in the respiration buffer with the help of a mesh. Continuous stirring was provided with a magnetic stirrer to avoid the formation of air bubbles. Foil was used to cover the chamber to ensure darkness in the reaction vessel. Measurements of uncoupled dark respiration were taken at 25 °C by measuring OCR for at least 10 min after the addition of the uncoupler carbonyl cyanide 4-(trifluoromethoxy)phenylhydrazone (FCCP, Sigma Aldrich, MI, USA) to a final concentration of 10 µM. The amount of oxygen being consumed by the leaf discs was recorded using the Oxygraph Plus v2.26 software (Hansatech Instruments), and the OCR (nmol O_2 m^2 s^{-1}) was calculated according to the area of the leaf discs. Each measurement consisted of three leaf discs from three different plants of the same line and was repeated three times. Plants were 4–6 h into the dark phase of the photoperiod when the measurements were taken.

2.7.2 Leaf respiration measurements using the Seahorse XFe24 Extracellular Flux Analyser

An oxygen consumption assay was developed for tobacco leaf discs following [218, 219], with modifications. The Seahorse Bioscience XFe24 Extracellular Flux Analyser (Seahorse Bioscience, MA, USA) was used to determine real-time fluorimetric detection of oxygen levels in a microtiter plate. As oxygen quenches the fluorescence of a fluorescein complex, fluorescence is detected by a fibre-optic wave guide and converted into OCR.

The sensor cartridge was hydrated the day before the measurements by applying 1 mL of XF Calibrant Solution (Seahorse Bioscience) to each well of the XFe24 utility plate (Seahorse Bioscience) and incubating at 25 °C overnight. On the day after, sample plates were prepared as follows: leaf discs were excised from the youngest fully expanded leaf with a 5 mm-diameter cork borer, and the fresh weight of each disc was determined for normalisation. Veins were avoided, as the respiration rate in that area of the leaf is higher than that of adjacent parts in the leaf blade [219]. Commercial glue (Gorilla Super Glue Gel, Gorilla Glue Company, OH, USA) was used to attach the leaf discs to the bottom of the wells, which is key to ensure correct OCR measurements as the run protocol involves mixing steps and the immersion of the sensors into the wells. A small amount of Gorilla Super Glue Gel (Gorilla Glue Company, OH, USA), a cyanoacrylate-based glue, was applied to the adaxial side of the leaf disc with a cotton bud, and the disc was positioned at the bottom of the well with forceps, pressing gently with a cotton bud. Immediately after, 1 mL of respiration buffer (50 mM hydroxyethyl piperazineethanesulfonic acid, 10 mM 2-(N-morpholino)ethanesulfonic acid, and 2 mM $CaCl_2$ (pH 6.6, adjusted with NaOH)) was added carefully to each well [217, 219]. The plates were then covered in aluminium foil for 1 h to ensure dark adaptation of the leaf discs before the OCR measurement.

The sensor cartridge was calibrated following the manufacturer's instructions. A 30 min wait step was included between the calibration and measurement steps to ensure stabilisation of OCR after calibration. The protocol for respiration

measurements consisted of the following steps: mix (3 min), wait (2 min), measure (3 min). The method allowed for 10 cycles of mixing, waiting, and measuring, reaching a duration of 48 min per plate.

The OCR of single leaf discs was recorded by the Wave software version 2.6.0.31 (Agilent Technologies, CA, USA) and the same software was used to calculate the normalised OCR values of each transgenic line.

Each 24-well plate contained four discs per line, each coming from the youngest fully expanded leaf of an independent plant. Four wells were used as blanks to determine the background levels of OCR, each containing a small amount of Gorilla Super Glue Gel and 1 mL of respiration buffer. Single-gene transgenic plants overexpressing the c-Peredox-mCherry biosensor were used as control lines.

2.8 Confocal laser scanning microscopy

Confocal imaging of four-week-old Arabidopsis plants was performed using a Zeiss Laser Scanning Microscope 880, Axio Imager 2 (Zeiss, Oberkochen, Germany). Leaves were vacuum infiltrated with 1 mL of a mitochondria labelling solution containing 10 µM MitoTracker Green (Thermo Fisher Scientific, MA, USA) and 100 nM tetramethylrhodamine methyl ester (TMRM, Sigma Aldrich). Labelling was allowed for 3 h before the leaves were mounted for imaging. One leaf was used per line, and three z-stacks were done per sample. Excitation/emission wavelengths were: 490 nm/516 nm for MitoTracker Green, 561 nm/566-631 nm for TMRM, and 650 nm for chlorophyll.

2.9 Plate reader fluorimetry assay

The fluorescence emission spectra of the ratiometric c-Peredox-mCherry sensor was used to determine the *in vivo* status of the redox couple NADH/NAD^+ using a plate reader fluorimetry assay, based on [220, 221].

Three-week-old transgenic plants carrying the c-Peredox-mCherry sensor and WT control plants were used. Leaf discs with a 6-mm diameter, each corresponding

to a different plant, were laid at the bottom of each well (abaxial face up) in Nunclon 96-well, flat-bottom, transparent microplates (Thermo Fisher Scientific, MA, USA). A total volume of 200 µL assay medium (10 mM 2-(N-morpholino)ethanesulfonic acid, 5 mM KCl, 10 mM $MgCl_2$, 10 mM $CaCl_2$, pH 5.8 adjusted with KOH) was added to each well. Plates were kept in the dark for at least 2 h before recording fluorescence to minimise potential effects of active photosynthesis. The fluorophores Ts and mC were excited at 400 ± 9 nm and 570 ± 9 nm, respectively, and emission collected at 520 ± 20 nm and 610 ± 20 nm in a Tecan Infinite 200 (Tecan, Zurich, Switzerland) using top optics, 30 °C incubation temperature, well-multichromatic monitoring, 25 flashes per well, and measuring cycle with orbital averaging. The gain was manually set as 162 for Ts and 188 for mC to allow data to be compared between different experiments and subsequent batches of plants. Each experiment was independently repeated twice to validate the results, and the results of both experiments were averaged in the analyses.

2.10 Metabolite profiling

This experiment was performed by Dr Jose Vallarino from the Max Planck Institute of Molecular Plant Physiology, Potsdam-Golm (Germany). Tobacco leaf samples were harvested and immediately frozen in liquid nitrogen during the high light primary screen of the transgenic combinatorial library. After sample grinding, metabolite extraction using methanol-chloroform and derivatisation, relative metabolite levels were obtained by gas chromatography time-of-flight mass spectrometry (GC-MS) [222]. Chromatograms and mass spectra were evaluated using ChromaTOF v.4.51.6 (LECO Corp., MI, USA) and TagFinder v.4.0. [223]. Each compound was annotated based on its unique mass spectrum [224].

2.11 Data analysis

Statistical analyses were performed using R [225] in RStudio version 1.2.5033 [226]. Statistical differences between groups were determined using two-tailed unpaired T-test (*t.test* function) or one-way analysis of variance (ANOVA; *res.aov* function) followed by post hoc Tukey test (*TukeyHSD* function) for normally distributed data. When ANOVA assumptions were not met, a non-parametric alternative, the Kruskal-Wallis rank sum test (*kruskal.test* from the *stats* package and *multcompBoxplot* function from the *multcompView* package) was used instead. The R packages *FactoMineR* (for data analysis) and *factoextra* (for data visualisation) were used to perform principal component analysis (PCA). Spearman correlation tests were done using the *ggscatter* function from the *ggpubr* package. Figure preparation was done using the R packages *ggplot2* and *ggpubr*. The specific statistical methods, exact n values, and P-values used in each figure are described in the figure legends. Error bars represent the standard error of the mean (SE). Significance was reported as "***" for P-value<0.001, "**" for P-value<0.01, or "*" for P-value<0.05.

Chapter 3

Generation and screen of a library of tobacco combinatorial transformants

Contents

3.1 Aims and objectives

This chapter outlines the generation and screen of a library of combinatorial tobacco plants overexpressing different combinations of a selection of transgenes. The objectives of the work described in this chapter were:

1. To generate a library of tobacco combinatorial transgenic lines overexpressing different combinations of transgenes. The target pathways comprised the photosynthetic electron transport chain, the CBB cycle, photorespiration, leaf sucrose biosynthesis, and sucrose export into the phloem.

2. To identify potential lines with successful transgene combinations through a primary screen of the transgenic combinatorial library for improved photosynthetic capacity and/or plant growth.

3.2 Introduction and rationale

Individual transgenic manipulations have led to appreciable improvements in photosynthetic capacity and plant growth. Yet, the introduction of multigene transgenes targeting several sites within the leaf metabolic network could allow a greater impact to be achieved, as argued in Section 1.2.6.

In an attempt to boost photosynthetic efficiency, transgene targets for increased photosynthetic capacity and plant growth were identified through a systematic literature review. Twelve transgenes were chosen, involved in different metabolic pathways within the mesophyll and phloem companion cells (Figure 3.1). Tables 3.1, 3.2, and 3.3 outline the effects achieved by individual targets in photosynthetic capacity and yield, which justifies the choice of targets.

However, more than a billion transgene combinations are theoretically possible when manipulating 12 transgenes simultaneously. In addition, despite the selected transgenes having been reported to improve photosynthetic efficiency when manipulated individually, it is uncertain how they would behave when combined due to the complexity of the central metabolic network [125].

To overcome the issues associated with producing each possible combination and choosing the ones to be delivered into the plant, a combinatorial co-transformation approach was implemented. This transformation technique allowed the generation of a plant library, with each transgenic line carrying a different transgene combination. Individual constructs containing one transgene each were generated. These, along with an additional plasmid harbouring a gene conferring kanamycin resistance, were introduced in the nuclear genome of tobacco plants using biolistic combinatorial co-transformation. The combinatorial library was then screened to identify the best-performing lines and the underpinning transgene combination.

Tobacco is considered a model species in photosynthesis research. It is one of the most widely cultivated industrial crops worldwide (7 Mt in 2019 [33]), with a relatively short life cycle and transformation protocols readily available [209, 227].

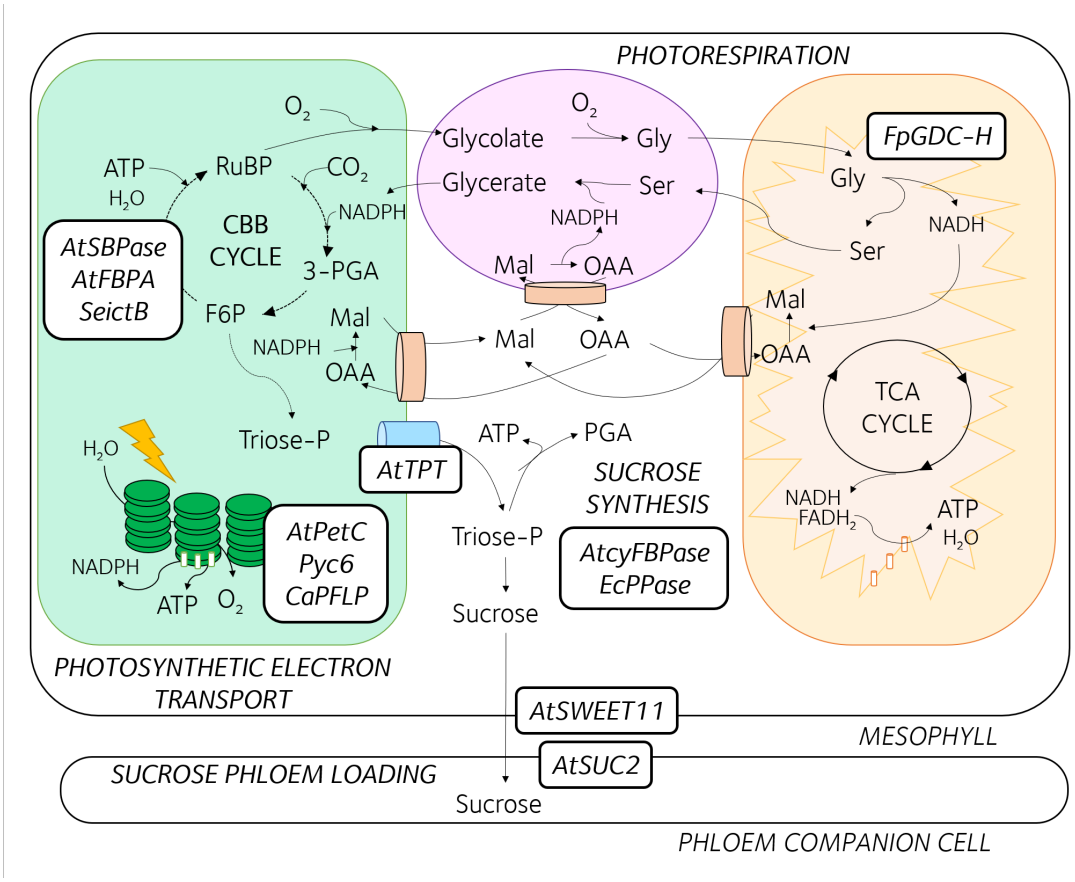

Figure 3.1: Selected transgene targets and metabolic pathways for the combinatorial co-transformation of tobacco. Schematic representation of a mesophyll cell and a phloem companion cell, depicting selected transgene targets and their corresponding metabolic pathways, namely the photosynthetic electron transport chain, the Calvin-Benson-Bassham (CBB) cycle, photorespiration, sucrose synthesis, and sucrose phloem loading. Abbreviations: *AtcyFBPase*, cytosolic fructose 1,6-bisphosphatase; *AtFBPA*, fructose 1,6-bisphosphate aldolase; *AtPetC*, cytochrome b_6f Rieske FeS protein; *AtSBPase*, sedoheptulose 1,7-bisphosphatase; *AtSUC2*, sucrose/H^+ importer; *AtSWEET11*, passive sucrose transporter; *AtTPT*, triose-phosphate/phosphate translocator; *CaPFLP*, ferredoxin-like protein; *EcPPase*, cytosolic pyrophosphatase; *FpGDC-H*, glycine decarboxylase-H protein; *Pyc6*, cytochrome c_6; *SeictB*, putative bicarbonate transporter.

The next section elaborates on the generation of the synthetic overexpression constructs for the 12 selected transgenes and their delivery into tobacco. The phenotype of the primary transformants (T_0 generation) and the results of the primary screen of the combinatorial library (T_1 generation) are then illustrated and assessed.

Table 3.1: Rationale for transgenes, selected from single targeted manipulations of photosynthetic electron transport. Details of manipulations are provided, including targeted metabolic pathways, transgene names and products, plant species tested, and their biological outcomes. Experiments described consist of overexpression unless otherwise stated.

Manipulation	Transgene	Transgene product	Species	Functional description	References
Photosynthetic electron transport	*PetC*	Rieske FeS protein	Arabidopsis	Increased electron transport rate and CO_2 fixation rate, increased chlorophyll content. Increases in biomass of 30-70% and seed yield up to 50%.	[22]
	Cyt c_6	Cytochrome c_6	Arabidopsis	Increased CO_2 fixation by 31%, accompanied by increases in chlorophyll and starch content. Increases in height of 30%.	[76]
			Tobacco	Increases in CO_2 assimilation rate and chlorophyll content. Increased height by up to 50%.	[23, 78]
	PFLP	Ferredoxin-like protein	Rice	Electron transport rate and CO_2 assimilation increase by 30%. Increased seed yield and panicle weight by 50 and 30%.	[49]

Table 3.2: Rationale for transgenes, selected from single targeted manipulations of putative carbon transport and Calvin-Benson-Bassham cycle. Details of manipulations are provided, including targeted metabolic pathways, transgene names and products, promoters, plant species tested, and their biological outcomes. Experiments described consist of overexpression unless otherwise stated.

Manipulation	Transgene	Transgene product	Species	Functional description	References
Calvin-Benson-Bassham cycle	*ICTB*	Inorganic carbon transporter B	Arabidopsis and tobacco	Increased rate of CO_2 assimilation under limiting CO_2 concentrations and lower compensation point. Faster growth rate and 23% increase in biomass. Increased water use efficiency.	[101]
			Tobacco	Increased CO_2 fixation by 20%. Increased height by 31% and biomass by 71%.	[100]
			Soybean	Increased net CO_2 assimilation by 10%. Increased total biomass and seed mass by 30%.	[63]
			Rice	Increased CO_2 assimilation by 18 to 38%. Biomass increase by 18%.	[102]
			Rice	Increased photosynthetic rate by 15-20% and lower compensation point. Increased biomass and seed yield.	[228]
	FBPA	Fructose 1,6-bisphosphate aldolase	Arabidopsis	Increased CO_2 assimilation by 31%. Increased biomass by 35-53% and seed yield by 39%.	[59]
			Tobacco	Increased CO_2 assimilation by 20%. Increased biomass 10-30% in ambient CO_2 and 70-120% in high CO_2.	[98]
	SBPase	Sedoheptulose 1,7-bisphosphatase	Tobacco	Increased CO_2 assimilation by 14% and linear electron flux by 21%. Increased biomass by 10% under saturating CO_2.	[58]
			Tobacco	Increased photosynthetic rate in young leaves. Increased biomass by 40%.	[57]
			Arabidopsis	Increased CO_2 assimilation by 37%. Increased biomass by 42% and 53% in seed yield.	[59]
			Tobacco	Increased photosynthetic rate. Increased biomass by 30%.	[100]
	FBPase/ SBPase	Bifunctional fructose 1,6-/ sedoheptulose 1,7-bisphosphatase	Tobacco	Increased photosynthetic activity by 20%. Increased height and biomass by 40 and 50%.	[23, 97]

Table 3.3: Rationale for transgenes, selected from single targeted manipulations of photorespiration, sucrose biosynthesis, and phloem sucrose loading. Details of manipulations are provided, including targeted metabolic pathways, transgene names and products, promoters, plant species tested, and their biological outcomes. Experiments described consist of overexpression unless otherwise stated.

Manipulation	Transgene	Transgene product	Species	Functional description	References
Photorespiration	*GDC-H*	Glycine decarboxylase H-protein	Arabidopsis	Increased electron transport rate and lower compensation point. Increased biomass by 33%.	[112]
			Arabidopsis	Increased CO_2 assimilation by 19%. Increased biomass by 50%.	[59]
			Tobacco	Increased CO_2 assimilation rate and 13-38% increase in biomass.	[71]
Sucrose biosynthesis	*TPT*	Triose-phosphate/ phosphate translocator	Arabidopsis	Increased CO_2 assimilation rate by 20-30%. Increased biomass by 27-40% when overexpressed.	[116]
	cyFBPase	Cytosolic fructose 1,6-bisphosphatase			
	PPase	Cytosolic pyrophosphatase	Tobacco	Three-fold increase in ratio of soluble sugars to starch. Stunted growth due to reduced internode length.	[229]
			Potato	Reduced leaf starch accumulation and double starch yield in tubers when overexpressed with a simultaneous enhancement in sink capacity.	[118]
Phloem sucrose loading	*SWEET11*	Passive sucrose transporter	Arabidopsis	Mutants exhibit slower growth, mild leaf chlorosis, and excess carbohydrate accumulation in leaves.	[119]
	SUC2	Sucrose/H+ importer	Arabidopsis	Enhanced sucrose phloem loading and long distance transport. Diminished growth.	[123]

3.3 Results

3.3.1 Twelve synthetic overexpression constructs were built for their introduction in tobacco

Twelve synthetic overexpression constructs were designed and assembled for the generation of transgenic tobacco plants (Figure 3.2). These carried the selected transgenes under the control of leaf-specific (*pAtRbcS* (TAIR ID: AT5G38420), *pSlRbcS* [230], and *pStcyFBPase* [231]), companion cell-specific (*pCoYMV*, from the commelina yellow mottle virus [232, 233]), or constitutive promoters (*pCaMV35S*, from the cauliflower mosaic virus (CaMV)) in a pUC18 plasmid backbone. Promoters were chosen based on previous studies where the expression of the transgene proved beneficial (i.e. attempting to replicate those results) and availability. Chloroplast transit peptides were included in the N-terminal region of the sequences encoding the Arabidopsis Rieske FeS protein (*AtPetC*), the algal *P. yezoensis* Cyt c_6 (*Pyc6*), and the *S. elongatus* putative bicarbonate transporter (*SeictB*). The rest of transgenes targeted to the chloroplast included the predicted endogenous transit peptide. An additional construct was used, containing the *nptII* gene conferring kanamycin resistance in a pUC119 backbone (Figure 3.2).

Transgenes were either amplified using PCR or artificially synthesised. Restriction sites flanking the coding sequences were introduced for all transgenes and used to introduce them into backbone vectors containing the appropriate promoters via restriction-ligation. The cDNA sequences for *AtFBPA*, *AtTPT*, and *AtcyFBPase* were retrieved from TAIR by keyword search. Specific primers were used to amplify the corresponding DNA fragments via PCR using Arabidopsis cDNA (Figure 3.3). The purified PCR products were subjected to restriction digest with specific enzymes for their subsequent cloning.

The sequences for transgenes *Pyc6*, *AtPetC*, *CaPFLP*, and *SeictB* were retrieved from the National Center for Biotechnology Information nucleotide database and codon-optimised for their expression in tobacco. The modified versions of the genes were artificially synthesised and cloned in the pUC57 plasmid. The corresponding

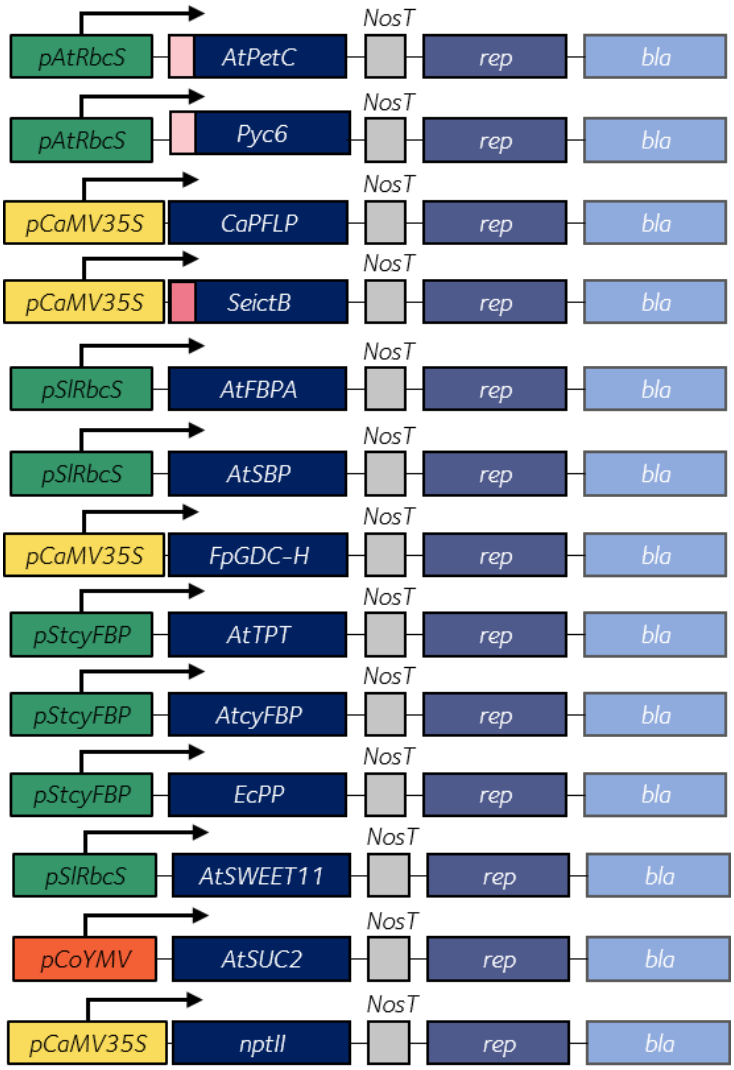

Figure 3.2: Schematic representation of the overexpression constructs introduced in tobacco by biolistic combinatorial co-transformation. **Promoters**: *pAtRbcS*, Arabidopsis RuBisCO small subunit (*RbcS*) promoter; *pCaMV35S*, CaMV 35S promoter; *pSlRbcS*, *S. lycopersicum* (tomato) RbcS promoter; *pStcyFBP*, *S. tuberosum* (potato) cytosolic fructose 1,6-bisphosphatase promoter; *pCoYMV*, commelina yellow mottle virus (*CoYMV*) promoter. Yellow colouring indicates constitutive promoters, green indicates leaf-specific promoters, orange indicates mesophyll-cell specific promoter. **Transit peptides**: tobacco plastocyanin in light pink and *P. sativum* (pea) *RbcS* in pink. **Genes**: Arabidopsis cytochrome b_6f Rieske FeS protein (*AtPetC*); *P. yezoensis* Cytochrome c_6 (*Pyc6*); *C. annuum* (sweet pepper) Ferredoxin-like protein (*CaPFLP*); *S. elongatus* putative bicarbonate transporter (*SeictB*); Arabidopsis fructose 1,6-bisphosphate aldolase (*AtFBPA*); Arabidopsis sedoheptulose 1,7-bisphosphatase (*AtSBP*); *F. pringlei* glycine decarboxylase-H protein (*FpGLDH*); Arabidopsis triose-phosphate/phosphate translocator (*AtTPT*); Arabidopsis cytosolic fructose 1,6-bisphosphatase (*AtcyFBP*); *E. coli* cytosolic pyrophosphatase (*EcPP*); Arabidopsis passive sucrose transporter (*AtSWEET11*); Arabidopsis sucrose/H^+ importer (*AtSUC2*); *E. coli* neomycin phosphotransferase II enzyme (*nptII*). **Terminator**: nopaline synthase terminator (*NosT*), grey colouring. **Other features**: *E. coli* replication gene (*rep*) in dark blue; ampicillin resistance gene (*bla*) in light blue colouring. **Backbones**: *pUC18* and *pUC119*, Addgene plasmids #50004 and #37461.

plasmid DNA was subjected to restriction digest and genes were purified for their subsequent cloning (Figure 3.4).

Plasmid pUC18 vectors were used to place the purified transgenes under the regulation of the corresponding promoters and the *Agrobacterium* nopaline synthase terminator (*Nos*T) via ligation (Figure 3.2). The ligation products were used to transform *E. coli*. Plasmid DNA from the resulting ampicillin-resistant colonies was extracted and digested with the same restriction enzymes used in the cloning steps to confirm the presence of the inserts. The colonies showing the insert were confirmed by sequencing (Appendix B.1). Plasmids of confirmed constructs were purified from *E. coli* via anion-exchange chromatography and used for their biolistic introduction in tobacco.

3.3.2 A transgenic combinatorial library was generated in tobacco by biolistic transformation

The synthetic overexpression constructs were introduced into the tobacco nuclear genome as a cocktail. Young leaves of the tobacco cultivar Petit Havana were subjected to stable co-transformation by particle gun followed by selection for kanamycin resistance. Primary transformants were first grown in tissue culture boxes, then transferred to the greenhouse when two-to-three leaves and roots had been developed. A library of 329 independent transgenic lines overexpressing different transgene combinations was obtained. The phenotype of the T_0 generation was recorded at several developmental stages (Table B.1), with at least one parameter being noted for most lines (60.2%). The rest of the lines (131 lines, 39.8% of the library) did not exhibit any remarkable phenotypic characteristics with respect to the WT.

Half of the combinatorial lines (51.3%) exhibited phenotypic characteristics related to the shape of the leaves. Namely, 14.6% of the lines showed leaf deformations, while others displayed narrow (13.1%) or long (10.3%) leaves. Other shapes were observed to a lesser extent, such as tapered leaves (thinner towards the end, 8.2%), wavy leaves (3.6%), and sickle-shaped leaves (1.5%) (Figure 3.5.A).

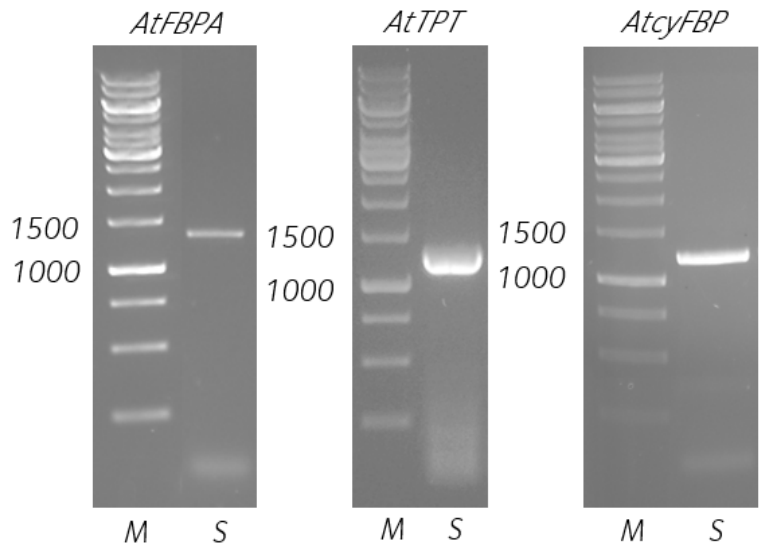

Figure 3.3: PCR amplification of the Arabidopsis genes *AtFBPA*, *AtTPT*, and *AtcyFBPase*. PCR amplification of *AtFBPA* (expected size 1197 bp), *AtTPT* (1248 bp), and *AtcyFBPase* (1026 bp) genes using *A. thaliana* cDNA. Separation of PCR products (S, for samples) according to their molecular weight through DNA electrophoresis (1% agarose TAE gels). Size determination according to molecular size marker (M) GeneRuler™ 1 kb DNA Ladder (Thermo Fisher Scientific, MA, USA); 1000- and 1500-bp markers are indicated.

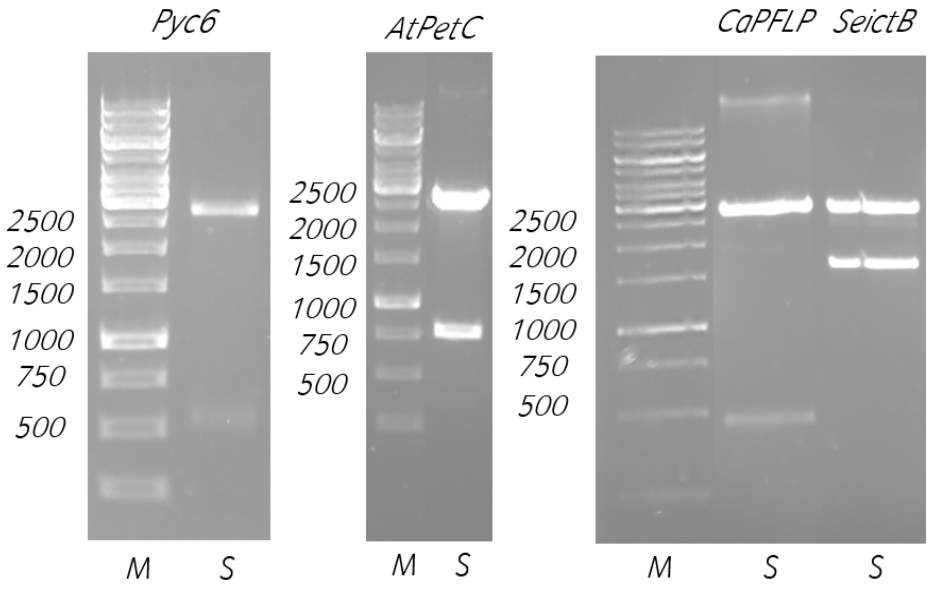

Figure 3.4: Restriction digest of pUC57 vectors (plasmid expected size 2698 bp) holding the synthetic genes *Pyc6* (expected size 546 bp), *AtPetC* (756 bp), *CaPFLP* (447 bp), and *SeictB* (1584 bp). Separation of digest products (S, for samples) according to their molecular weight through DNA electrophoresis (1% agarose TAE gels). Size determination according to molecular size marker (M) GeneRuler™ 1 kb DNA Ladder (Thermo Fisher Scientific, MA, USA); 500-, 750-, 1000-, 1500-, 2000-, and 2500-bp markers are indicated.

About 7% of the lines showed variation in leaf pigmentation, with some 5% of the lines showing brindled leaves, 1.8% showing spots of lighter green, and two lines (0.6%) displaying leaves of a darker green (Figure 3.5.C). Certain variability was found in terms of leaf size, with some lines showing small leaves (2.3%, reduced apparent size with respect to the non-transformed WT control), and only one line showing leaves that could be described as big (0.3%, increased size) (Figure 3.5.B).

Differences in the shape and colour of the flowers could be seen for some lines, mostly with some flowers showing thicker petals and pistils (six lines, 1.8% of the library) (Figure 3.6).

Notably, 45% of the combinatorial lines were identified as male sterile (31%) or putative male sterile (14%) (Figure 3.7.B). This meant that, while 25% of the lines were self-pollinated (Figure 3.7.A), a considerable number of lines had to be manually pollinated using stamens from WT plants. Specifically, a total of 91 lines (27.7% of the library) was rendered unable to self-pollinate (Figure 3.7.A), along with five lines (1.5%) that were considered able to self-pollinate but were still crossed with the WT for precautionary measures (Figure 3.7.A). An extra 25.8% of the lines had a mixture of self-pollinated and WT-pollinated flowers (Figure 3.7.A).

Once flowers were pollinated and started to develop seed capsules, a few of them did not set seed since they dropped down before maturity (2.7%) and some were also empty (0.6%) or full of powder (0.6%, possibly pollen) (Figure 3.7.C).

At the flowering stage, one of the greenhouse cabins where the combinatorial lines were growing had an aphid infestation, with 13 specific lines being preferentially infected over other tobacco plants growing in the same cabin. The affected parts were mostly stems and immature seed capsules (Figure 3.8.A).

Overall, 6.7% of the lines (22) were considered small or dwarf plants (Figure 3.8.B).

Based on the phenotyping of the T_0 generation, a total of 56 lines from the combinatorial library were selected for further analyses. The parameters that were used to select these lines were mainly leaf shape and aphid infestation. Table 3.4 illustrates the frequencies of each phenotypic characteristic in the combinatorial

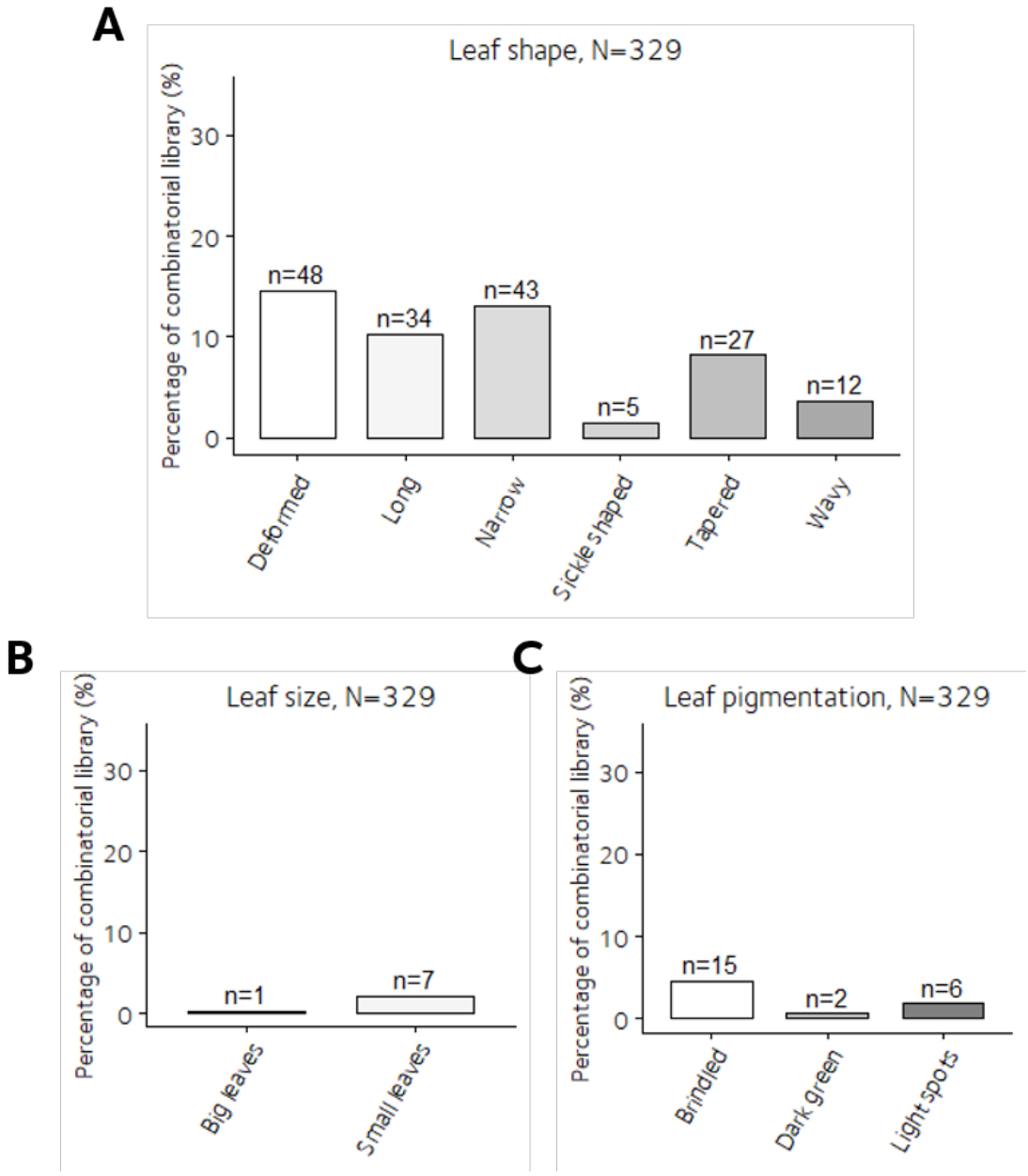

Figure 3.5: Phenotypic characteristics of combinatorial library - Leaves. Combinatorial lines from the T_0 generation were annotated for leaf shape **A**, leaf size **B**, and leaf pigmentation **C**. Plots indicate percentage of combinatorial lines in the library (N=329) displaying the given phenotypic characteristic, with the number of lines (n) indicated on top of the corresponding bar.

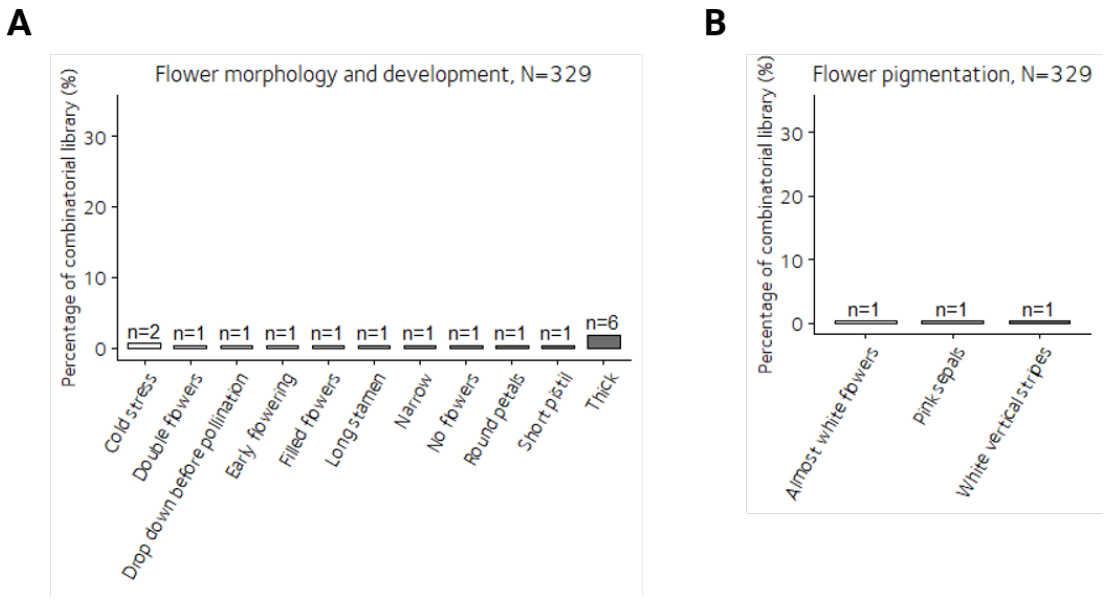

Figure 3.6: Phenotypic characteristics of combinatorial library - Flowers. Combinatorial lines from the T_0 generation were annotated for flower morphology and development (**A**), and flower pigmentation (**C**). Plots indicate percentage of combinatorial lines in the library (N=329) displaying the given phenotypic characteristic, with the number of lines (n) indicated on top of the corresponding bar.

library and for the lines analysed in the primary screen. Longer leaves were considered a desirable parameter as it would represent an increased area of tissue that is photosynthetically active. Aphids preferring these plants against other lines of the same species that were growing nearby was considered a potential indicator of photosynthate-rich phloem sap. Other parameters were chosen incidentally, such as one line having been selected for its long leaves, but also displaying narrow or tapered leaves.

With respect to sexual crosses, lines that were able to self-pollinate were selected against plants that were unable to self-pollinate. Once those lines had been exhausted, lines that were identified as able to self-pollinate but that had nonetheless been crossed with the WT were selected. In instances where seeds had been collected from capsules that resulted both from self-pollination and crosses with the WT, preference was given to the seeds resulting from self-pollination, which explains why most lines resulted from self-pollinated flowers in the screen (Table 3.4).

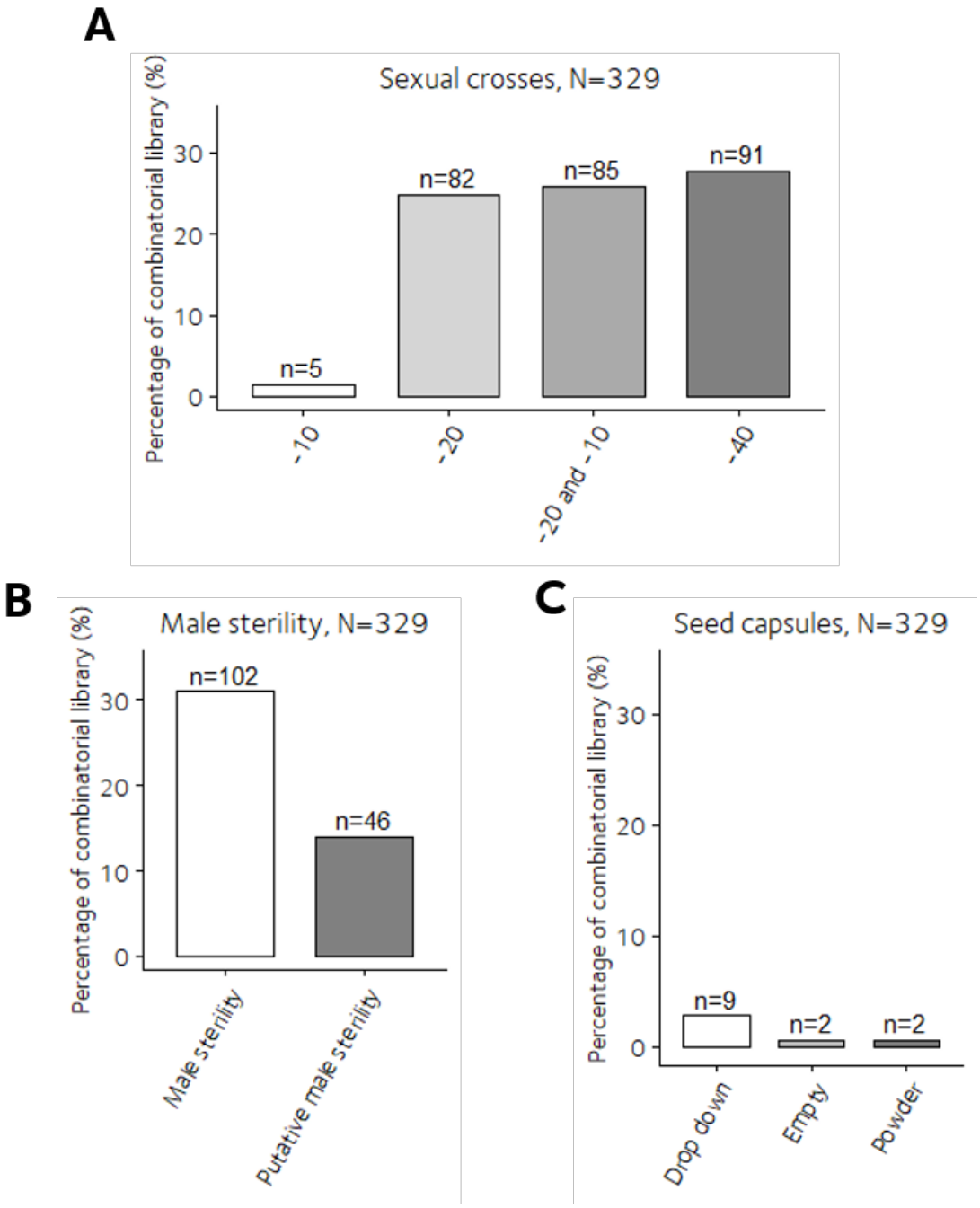

Figure 3.7: Phenotypic characteristics of combinatorial library - sexual crosses. Combinatorial lines from the T_0 generation were annotated for their sexual crosses (**A**), observed male sterility (**B**), and abnormalities in seed capsules (**C**). Sexual crosses are abbreviated as -10 (able to self-pollinate, but crossed with WT), -20 (self-pollinated), -20 and -10 (mix of self-pollinated flowers and flowers crossed with WT), and -40 (unable to self-pollinate, crossed with WT). Plots indicate percentage of combinatorial lines in the library (N=329) displaying the given phenotypic characteristic, with the number of lines (n) indicated on top of the corresponding bar.

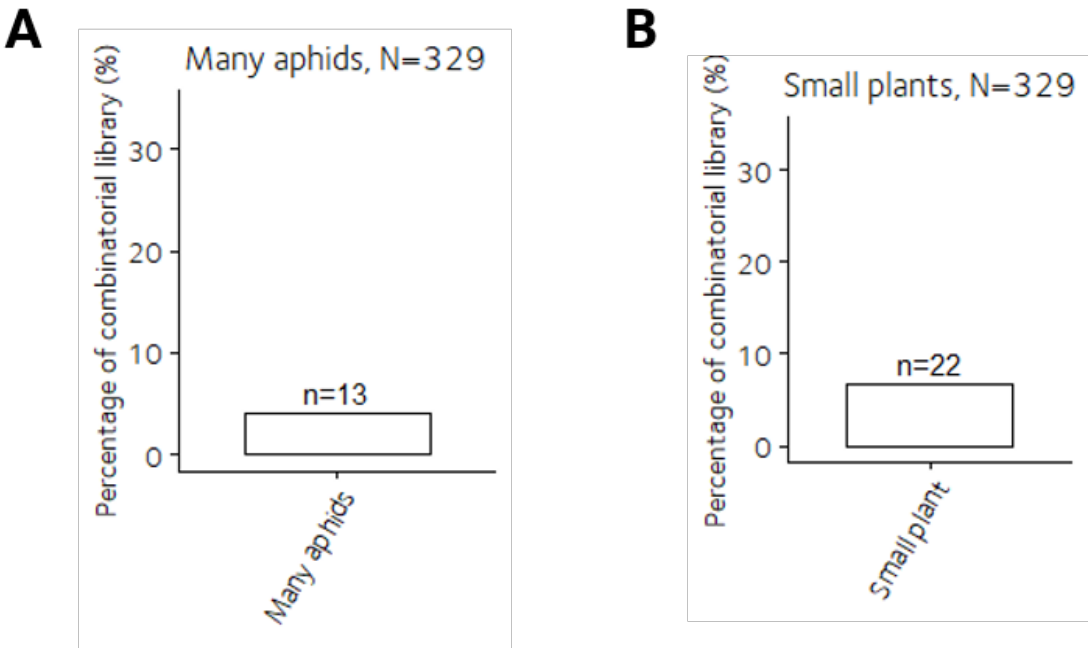

Figure 3.8: Phenotypic characteristics of combinatorial library - Other characteristics. Combinatorial lines from the T_0 generation were annotated for preferential infestation by aphids (**A**) and small plant size (**C**). Plots indicate percentage of combinatorial lines in the library (N=329) displaying the given phenotypic characteristic, with the number of lines (n) indicated on top of the corresponding bar.

3.3.3 Screening the tobacco combinatorial library for increased photosynthetic capacity and growth in high light conditions

The T_1 progeny of pre-selected lines were used to perform a primary screen. Fifty-six lines were analysed for photosynthetic capacity and yield in four subsequent batches with 14 lines each. Plants were germinated on kanamycin-selection plates. After two weeks, antibiotic-resistant seedlings were transferred to small pots and grown in low light conditions ("nursery") for another two weeks. At that point, plants were transferred to bigger pots and, three days after, they were transferred to high light conditions (600 µmol m^{-2} s^{-1}). These growth conditions were chosen in an attempt to reach light intensities close to saturation in tobacco (see light-saturating curves at [234] Figure 1 and [235] Figure 8), commensurate with the photosynthetic machinery not being limited by light. This would allow the measurement of any increases in photosynthetic capacity brought about by the overexpression of the

Table 3.4: Frequencies of phenotypic characteristics observed during the generation of the combinatorial library (T_0 generation) and used to select lines for the primary screen. The number of lines (n) and the percentage it represents in the library (N=329) and the primary screen (N=56) are indicated.

	Combinatorial library		**Primary screen**	
Physiological parameters	n	%	n	%
		Leaves		
Leaf shape	169	51.3	13	23.0
Leaf size	8	2.3	0	0.0
Leaf pigmentation	23	7.0	1	2.0
		Flowers and capsules		
Flower morphology and development	17	5.1	0	0.0
Flower pigmentation	3	0.9	0	0.0
Male sterility	148	45.0	25	45.0
Immature seed capsules	13	3.9	0	0.0
		Sexual crosses		
Able to self-pollinate, crossed with WT (-10)	5	1.5	19	34.0
Self-pollinated (-20)	82	24.9	28	50.0
Self-pollinated (-20) and crossed with WT (-10)	85	25.8	0	0.0
Unable to self-pollinate, crossed with WT (-40)	91	27.7	9	16.0
		General		
Aphid infestation	13	4.0	3	5.4
Small plants	22	6.7	0	0.0

chosen transgenes. The screen was performed 18 days after the transfer to high light, culminating with the harvest of the plants' fresh biomass. The complete screen data set and plots for each parameter can be found in Appendix B.3.

Five combinatorial lines showed an increased chlorophyll content under high light conditions

Five lines were identified that showed a significant increase in chlorophyll content with respect to the control. The increases were observed in total chlorophyll as well as in chlorophyll *a* and *b*, with no alteration in the ratio of chlorophyll *a* to chlorophyll *b* (Table 3.5). Percentage increases in chlorophyll *a*, *b*, and total chlorophyll ranged from 13% in line 82_2B-20 to 28% in line 22A-10. No other significant changes were observed in these lines, except from line 166A-20, where increases in chlorophyll were of 25% with respect to the control, but a decreased biomass content in the leaves (13%) could be perceived (Figure B.4).

Five combinatorial lines showed a stem growth phenotype under high light conditions

Five lines were identified that displayed an elongated stem and increased stem weight (Table 3.6). Percentage increases in height with respect to the WT control were 18% (line 35A-20), 23% (line 142A-10), 26% (line 253A-10), 34% (line 111A-10), and peaked at 45% (line 287A-40). This was accompanied by a significant increase in the fresh weight biomass of the stem, ranging from 28% (line 142A-10) to 57% (line 287A-40) (Figure 3.9). The biomass of the leaves remained unchanged with respect to the control. This meant that the increment in stem biomass was not translated into a significantly increased aerial biomass.

Other changes associated with these lines were related to chlorophyll accumulation. Line 253A-10 showed significant decreases in chlorophyll *b* content, which led to an overall percentage decrease in chlorophyll content of 13% when compared against the control. The ratio of chlorophyll *a* to *b* was also significantly increased (by 10%) in this line. However, no significant changes were observed when performing a chlorophyll fluorescence light response curve in this line's youngest fully expanded leaves, although F_0 and F_m were reduced by 12% and 13% with respect to the WT (Table B.4). Line 111A-10 showed a significant increase in the chlorophyll a/b ratio (Table B.5), but not any other significant changes.

Table 3.5: Chlorophyll quantification data for combinatorial lines showing increased chlorophyll (chl) content. Chlorophyll content was determined in the youngest fully expanded leaf from six-weeks-old WT and combinatorial lines. The values of the transgenic combinatorial lines show significant differences from the WT control. Means with asterisks denote statistical significance (P <0.05 Welch Two sample T-Test). Means of four plants ± SE.

Line	Batch	Chl *a* (mg m^{-2})	Chl *b* (mg m^{-2})	Total chl (mg m^{-2})	Ratio chl *a*/*b*
1_1A-20	1	8.47 ± 0.19**	1.66 ± 0.04**	10.1 ± 0.21**	5.1 ± 0.14
22A-10	1	8.98 ± 0.56*	1.78 ± 0.11*	10.7 ± 0.67*	5.02 ± 0.06
80B-20	1	8.04 ± 0.15**	1.59 ± 0.05*	9.62 ± 0.20**	5.05 ± 0.08
82_2B-20	1	7.93 ± 0.17**	1.59 ± 0.04*	9.52 ± 0.22*	4.99 ± 0.06
166A-20	1	8.78 ± 0.34*	1.74 ± 0.04***	10.5 ± 0.36**	5.02 ± 0.16
WT	1	7.01 ± 0.08	1.40 ± 0.02	8.42 ± 0.09	

Table 3.6: Height and biomass data for combinatorial lines showing a stem growth phenotype. Height and fresh weight biomass were determined in six-weeks-old WT and combinatorial lines. The values of the transgenic combinatorial lines show significant differences from the corresponding WT control for height and stem biomass. Means with asterisks denote statistical significance (P <0.05 Welch Two sample T-Test). Means of four plants ± SE.

Line	Batch	Height (mm)	Leaf biomass (g)	Stem biomass (g)	Total biomass (g)
111A-10	1	644.50 ± 20.58**	111.30 ± 2.50	83.35 ± 4.46*	193.64 ± 6.28
253A-10	1	605.75 ± 17.81*	116.66 ± 6.48	80.68 ± 3.10*	197.35 ± 9.37
142A-10	1	590.00 ± 15.85*	107.45 ± 3.71	79.07 ± 1.98*	186.52 ± 4.40
WT 1	1	480.00 ± 29.81	115.82 ± 3.08	61.87 ± 4.37	177.69 ± 7.02
35A-20	2	698.00 ± 32.75*	125.42 ± 7.26	100.67 ± 8.52*	226.09 ± 14.53
WT 2	2	590.25 ± 12.09	117.49 ± 4.58	74.28 ± 4.70	191.77 ± 9.22
263A-40	4	618.25 ± 33.28*	112.51 ± 2.18	85.62 ± 5.98	198.12 ± 7.95
287A-40	4	709.00 ± 22.07***	116.95 ± 8.49	112.36 ± 12.00*	229.31 ± 20.06
WT 4	4	489.25 ± 26.29	117.38 ± 6.82	71.60 ± 6.55	188.98 ± 12.65

Along with the stem growth observation, a significant reduction in the maximum electron transport rate of line 35A-20 was found in its light curve (Table B.4).

Although the biomass of the leaves was not increased in line 287A-40, a remarkable and significant increase of 56% in the leaf count was observed for this line (Figure B.5). This was the result of an increased number of young leaves growing from lateral shoots.

An extra line, 263A-40, included in Table 3.6, displayed a significantly increased height (26%) although its associated increase in stem biomass (20%) was not statistically significant. This line showed an unusual and significant increase (39%) in the total number of leaves. As a result, although not as pronounced as the other five lines, line 263A-40 also showed a stem growth phenotype, most similar to that of line 287A-40.

Other combinatorial lines of potential interest were found

Nine lines showed a tendency for increased chlorophyll, with the content of chlorophyll *b* being significantly increased in certain lines, along with a subsequent reduction in the ratio of chlorophyll *a* / chlorophyll *b* (Table 3.7). Contrary to the lines shown in Table 3.5, these lines also showed reductions in leaf and/or stem biomass, which led to decreases in overall biomass (Table 3.7).

Additionally, four lines showed significant increases in their total number of leaves (Table 3.8). In general, the rest of the parameters remained unchanged in these lines, although reductions in the efficiency of photosynthesis were detected for lines 128_1B-10 and 156B-20.

Table 3.7: Chlorophyll quantification and biomass data for combinatorial lines showing an increased chlorophyll content and reduced biomass. Chlorophyll content (abbreviated as chl) was determined in the youngest fully expanded leaf from six-weeks-old WT and combinatorial lines. Means with asterisks denote statistical significance (P <0.05 Welch Two sample T-Test). Means of four plants ± SE.

Line	Batch	Chl *a* (mg m^{-2})	Chl *b* (mg m^{-2})	Total chl (mg m^{-2})	Ratio chl *a*/*b*
98B-20	2	7.12 ± 0.27	1.43 ± 0.06	8.55 ± 0.33	4.98 ± 0.07
262A-20	2	8.74 ± 1.22	1.75 ± 0.26	10.5 ± 1.48	5.02 ± 0.08
WT 2	2	7.25 ± 0.53	1.43 ± 0.13	8.69 ± 0.67	5.07 ± 0.12
29A-40	3	8.73 ± 0.70	1.94 ± 0.15*	10.6 ± 0.85	4.49 ± 0.04*
59B-40	3	9.09 ± 0.72	1.94 ± 0.18*	11.0 ± 0.90	4.67 ± 0.08
77_2A-10	3	8.55 ± 0.77	1.71 ± 0.17	10.2 ± 0.94	5.00 ± 0.09
WT 3	3	6.71 ± 0.69	1.34 ± 0.14	8.05 ± 0.83	4.99 ± 0.11
224A-40	4	8.81 ± 0.80	1.87 ± 0.21	10.6 ± 1.02	4.75 ± 0.11*
279A-20	4	8.54 ± 1.00	1.69 ± 0.26	10.2 ± 1.26	5.09 ± 0.15
329A-40	4	9.43 ± 0.21	1.98 ± 0.11*	11.4 ± 0.33	4.77 ± 0.18
345A-10	4	9.51 ± 1.03	2.13 ± 0.26	11.6 ± 1.29	4.48 ± 0.10**
WT 4	4	7.20 ± 0.82	1.38 ± 0.18	8.59 ± 1.00	5.25 ± 0.13

Line	Batch	Leaf biomass (g)	Stem biomass (g)	Total biomass (g)
98B-20	2	87.84 ± 9.99	58.34 ± 11.50	146.18 ± 21.07
262A-20	2	100.88 ± 7.77	42.91 ± 2.50**	143.79 ± 9.62*
WT 2	2	117.49 ± 4.51	74.28 ± 4.70	191.77 ± 9.22
29A-40	3	72.85 ± 6.95**	39.98 ± 7.89*	112.84 ± 14.67**
59B-40	3	123.41 ± 6.85	60.11 ± 7.14	183.50 ± 13.83
77_2A-10	3	86.84 ± 4.88**	60.31 ± 9.06	147.15 ± 12.93*
WT 3	3	130.32 ± 8.01	77.86 ± 7.03	208.18 ± 14.61
224A-40	4	122.96 ± 1.84	60.25 ± 3.65	183.21 ± 3.01
279A-20	4	104.65 ± 1.81	54.94 ± 3.48	159.51 ± 5.29
329A-40	4	116.14 ± 9.45	49.85 ± 4.51*	165.98 ± 13.72
345A-10	4	100.32 ± 2.70	63.06 ± 7.75	163.38 ± 8.37
WT 4	4	117.38 ± 6.82	71.60 ± 6.51	188.98 ± 12.65

Table 3.8: Leaf number and chlorophyll fluorescence data for combinatorial lines showing an increased number of leaves. Total leaf number included all leaves (including young ones). Chlorophyll fluorescence was determined via a light response curve in the youngest fully expanded leaf (dark adapted) from six-weeks-old WT and combinatorial lines using Pulse-amplitude modulated chlorophyll fluorometry. Parameters shown are total number of leaves; F_0, minumum fluorescence; F_m, maximum fluorescence; F_v/F_m, maximum quantum yield of primary PS II photochemistry; ETRmax, maximum relative electron transport rate; and Ik, minimum saturating irradiance. Means with asterisks denote statistical significance (P <0.05 Welch Two sample T-Test). Means of four plants ± SE.

Line	Batch	Leaf number	F_0	F_m	F_v/F_m	ETRmax
128_1B-10	2	40.50 ± 3.48*	0.81 ± 0.04	3.47 ± 0.07*	0.77 ± 0.01*	85.51 ± 8.44
156B-20	2	32.50 ± 2.18*	0.77 ± 0.01	3.50 ± 0.02*	0.78 ± 0.00	78.50 ± 3.51*
WT 2	2	25.50 ± 1.19	0.77 ± 0.00	3.74 ± 0.04	0.79 ± 0.00	94.93 ± 1.50
94_2A-40	3	33.75 ± 0.75*	0.78 ± 0.01	3.48 ± 0.11	0.78 ± 0.00	96.80 ± 3.38
105A-10	3	33.25 ± 1.03*	0.75 ± 0.02	3.31 ± 0.16	0.78 ± 0.01	103.10 ± 4.50
WT 3	3	29.75 ± 0.85	0.76 ± 0.03	3.42 ± 0.08	0.78 ± 0.01	103.30 ± 7.45

3.4 Discussion

3.4.1 Combinatorial library - generation and phenotyping

In this chapter, the use of biolistic combinatorial co-transformation was described for the generation of a tobacco combinatorial library for increased photosynthetic efficiency. Individual synthetic constructs were built and delivered to the nuclear genome of tobacco using biolistic combinatorial co-transformation.

In a combinatorial experiment, the number of lines to be generated should be decided based on the number of transgenes needed to observe a phenotype, the expression level for each transgene, and the balance of expression between transgenes [137]. A total of 329 independent transgenic lines were recovered after selection on kanamycin. With almost every target gene producing an individual phenotype when overexpressed on its own, this was considered an appropriate number of transgenic lines to identify combinations that lead to enhanced productivity. This consideration also included the effort to recover and maintain this number of lines. Undoubtedly, an increased number of lines, with the increased exploration of the combinatorial space that it carries, would be ideal to find the best possible combination.

A high proportion of combinatorial lines were found to show developmental differences with respect to the non-transformed controls, some of which were considered undesired (e.g. deformed leaves, spots of lighter pigmentation in leaves, deformed flowers, etc.). Most morphological abnormalities were found in the same few lines (see Table B.1 for phenotypic characteristics per line). Previous experiments using a comparable number of transgenes did not report any phenotypic observations or the transgenic lines remained unchanged when the phenotype was compared to the controls. However, the chosen transgenes were very different, comprising genomic sequences containing markers for restriction fragment length polymorphisms [145], or genes coding for viral and fluorescent proteins [146].

Other parameters, such as long and big leaves, and darker pigmentation, were considered to be positive attributes considering the chosen transgenes and their expected effect when overexpressed. These were used to pre-select the lines that

would be analysed in the combinatorial screen. Leaf size has been questioned as a positive attribute for increased yield since it has been established that the current leaf area is supraoptimal in soybean [236], leading to increased shading that reduces overall photosynthesis. However, increased leaf area has commonly been considered indicative of improved yield [57, 59, 100]. On the other hand, chlorophyll content is closely linked to light absorption and photosynthetic activity and is considered a positive attribute for improved photosynthetic capacity and yield [76].

Male sterility in plants is commonly linked to modifications in mitochondrial DNA, where the TCA cycle activity is unable to meet the energy demand that pollen development carries [237]. Almost half of the lines in the library were identified as male sterile. Hadi *et al.* also reported reduced fertility, but attributed it to the prolonged tissue culture phase associated with the process of transformant regeneration and not the introduction of foreign DNA *per se* [145]. While no correlation between sterility and number of genes was found by Chen *et al.* when transforming with 14 genes [146], it is common to find complex, high-copy-number transgenic loci when using the biolistic delivery process [137, 147, 238]. This is likely to be exacerbated as the number of transgenes increases and could explain problems of fertility. Indeed, all regenerated lines carrying the maximum number of integrated transgenes (13) were sterile in [146].

Male sterility was linked to abnormal segregation patterns by Maqbool and Christou [239]. However, to ensure that viable seed was obtained from all primary transformants, lines identified as male sterile were manually pollinated with WT flowers. Therefore, the expected Mendelian segregation should occur upon germination of the T_1 generation seed.

3.4.2 Primary screen of the combinatorial library

The primary screen of the combinatorial library under high light conditions led to the identification of a variety of phenotypes. The most marked were groups of lines with significant increases in chlorophyll content and lines displaying a stem growth phenotype. Another two groups were identified, with lines showing a

tendency towards increases in chlorophyll content (although not significant) but reduced biomass, and lines with significant increases in leaf number. The phenotypic differences in the rest of the lines were more varied and complex.

Since batches of combinatorial lines were grown subsequently, each batch of lines was compared against the corresponding WT line that was grown with them. To ensure that the differences that were picked up were not a result of some WT lines behaving differently between batches, the different WT lines were compared to each other for all the analysed parameters (Table B.6). Significant differences ($P < 0.05$) could be observed in height (WT 2 was significantly different to the rest), leaf length (WT 2 and WT 3 were different to each other but not to the rest), and F_0 and F_m (WT 1 was different to the rest). Height was significantly higher in WT 2 and this could have masked some lines with increased height in batch 2, but apart from this, the choice of lines was not impacted by these differences.

The phenotype that was being sought was perhaps a more pronounced observation of the effects found when introducing single targets (Tables 3.1, 3.2, and 3.3) as reported in [23, 59, 100] where combinations of transgenes involved in the photosynthetic electron transport chain, the CBB cycle, and/or photorespiration were introduced in Arabidopsis and tobacco. Nevertheless, the number of lines that were screened with respect to the size of the library was modest (18%), which can explain the lack of more remarkable phenotypes. This is particularly important given the large combinatorial space that arises from the combination of 13 transgenes (circa 1.3 billion combinations including the possibility of no transgenes being present). However, it is worth considering that the selection and regeneration process of the primary transgenic lines favours potentially positive or neutral combinations, while negative combinations are not selected for if they affect plant development. This, along with the germination of seeds in antibiotic-containing media, reduces the chances of obtaining negative combinations or lines without any transgene present.

Another plausible explanation is that plants were limited by the size of the pot. Studies by Poorter have highlighted differences in biomass for plants grown in pots

and soil [240, 241] showing that doubling the pot size could lead to increases in biomass of 43% [240].

Regarding the lines with increased chlorophyll content, increases were associated to both chlorophyll *a* and chlorophyll *b*. Despite the increased chlorophyll accumulation, no changes were detected in chlorophyll fluorescence for these or any of the screened combinatorial lines. Most of the transformed genes had been previously reported to improve photosynthetic capacity when expressed ectopically, so assuming that the transgenes were present and expressed in the combinatorial lines, the lack of changes in chlorophyll fluorescence may have had to do with the reduced number of replicates used in the experiment (Tables 3.1, 3.2, 3.3).

The most striking phenotype was that of lines 35A-20, 111A-10, 142A-10, 253A-10, and 287A-40, that, belonging to different batches, displayed significant increases in height and stem fresh weight biomass (Figure 3.9).

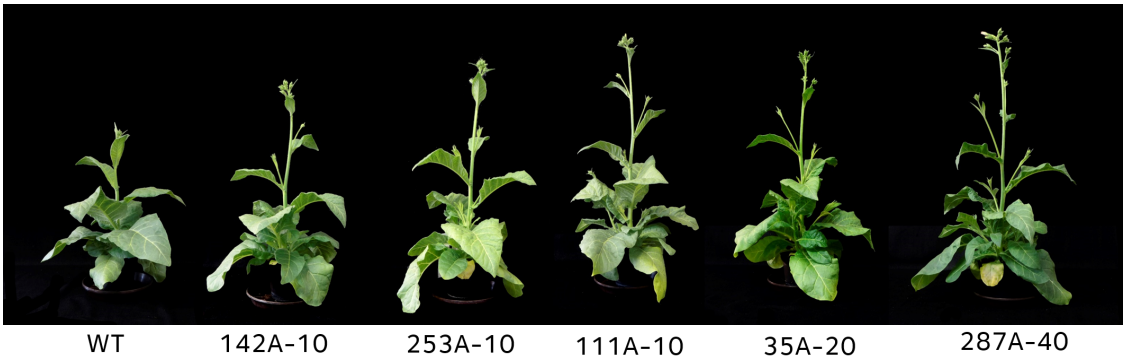

Figure 3.9: Stem growth phenotype in the primary screen of combinatorial library. Photographs of six-week-old combinatorial and WT lines grown in controlled conditions (16h light/8h dark, 600 µmol m^{-2} s^{-1}).

3.4.3 Hypotheses for stem growth phenotype

In herbaceous plants, stem growth takes place mainly through the elongation of internodes and is regulated by auxins and gibberellins. Rapidly dividing cells in the shoot apical meristem lead to shoot growth, followed by subsequent cell elongation. Different hypotheses could explain an increased stem growth in this set of combinatorial lines.

A first hypothesis is that increased stem growth could have been caused by an improved photosynthetic capacity. There have been other reports of improved photosynthetic capacity that described increased stem biomass. Overexpression of *SeictB* led to increases in stem biomass (dry weight) in tobacco, either alone (90%) or with *SBPase* (110%) and *FBPase* (124%) [100]. Similarly, the same transgene led to increases in stem biomass of 47% in soybean [63]. The overexpression of *SBPase* in tobacco led to an increased stem dry weight biomass of 40% [57]. South *et al.* reported a significant increase in stem biomass (dry weight) of 44% when introducing a synthetic photorespiratory bypass in tobacco [24]. Yet, these increases in biomass were always accompanied by a comparable increase in leaf and total biomass, as well as seed biomass (Table 3.2). No consistent differences were detected in these lines in terms of chlorophyll fluorescence. As a result, no improvements were detected in the photosynthetic activity that could explain this phenotype.

A second hypothesis is that a stimulation of sucrose synthesis via the overexpression of *AtTPT*, *AtcyFBPase* or *EcPPase* and/or of sucrose phloem loading via overexpression of *AtSUC2* and *AtSWEET11* in the mesophyll of mature leaves could have led to an increased stem elongation. This would be expected to increase the amount of photosynthate being transported from source leaves through the phloem and, in turn, increase sink biomass. Despite the sharp increases in stem biomass, neither leaf biomass nor total aerial biomass were significantly increased in these lines. However, it is possible that transport capacity and/or sink strength could not match the increased photosynthate production. This could have led to the establishment of the stem as a sink, which makes it reasonable that the stem was elongated and perhaps thicker due to an increased accumulation of sugars in the phloem. This hypothesis is somewhat supported by a previous study where sugar accumulation in source leaves led to stunted growth due to reduced internode length [229]. These arguments raise the issue of source and sink relationships in the context of increasing crop yield. It has been argued that both source and sink capacities must be enhanced for increased yield, and that sink limitation and feedback inhibition could decrease the benefits of improved photosynthesis [5, 44, 242].

An additional third hypothesis is that the proximity of the plants within the high light growth chamber would have led to some specific plants elongating their stem in an attempt to seek light. This theory is supported by the fact that stem elongation is also a feature of shade avoidance. It seems unlikely that shade avoidance led to the observed phenotype. Given that the plants were randomised for growth, it follows that it would seem unlikely that only a few specific lines displayed the stem growth phenotype. The size of the seedlings after two weeks of kanamycin selection was not particularly different to other lines or the WT (data not shown), but all these lines were classified as big in size already in the nursery, before transfer to high light conditions (data not shown). Early flowering is also considered an escape mechanism linked to stem elongation and shade avoidance [243], as it shortens generation time, which could explain the observed increases in biomass.

Because of the remarkable increases in stem growth in these lines, it was decided to carry these lines for further characterisation to understand the genetic, biochemical, and metabolic changes underpinning this phenotype. These would assist in confirming which of these hypotheses can explain the stem growth phenotype. An increased stem biomass phenotype could be of interest in the development of high yielding crop varieties for food and fuel in the coming decades.

In the next chapter, a detailed characterisation of the five lines showing an increased stem length and stem biomass is described.

3.5 Conclusions

This chapter describes the successful generation of a combinatorial library in tobacco for improved photosynthetic capacity and photosynthesis and evaluates the screening performed to identify lines of potential interest. From these, it can be concluded that:

1. The introduction of an array of 12 transgenes involved in the photosynthetic electron transport chain, the CBB cycle, photorespiration, leaf sucrose biosynthesis, and sucrose export into the phloem using biolistic co-transformation allows the generation of nuclear combinatorial transformants in tobacco.

2. Despite a high incidence of developmental abnormalities in leaf morphology and male sterility, seeds were collected from the majority of the tobacco combinatorial lines.

3. The seed of at least 56 of the combinatorial lines was viable and produced transgenic, antibiotic-resistant progeny.

4. The primary screen of these 56 lines in high light conditions led to the identification of a variety of metabolic phenotypes. Namely, lines with increased chlorophyll content and lines displaying a stem growth phenotype were identified. Other groups with less remarkable differences could be found, such as lines with certain increases in chlorophyll content but a tendency to show reduced biomass, and lines with an increased number of leaves.

5. Five lines displaying a stem elongation and increased stem biomass were selected for further analyses.

Chapter 4

Characterisation of selected tobacco combinatorial transgenic lines

Contents

4.1 Aims and objectives

In Chapter 3, a library of transgenic combinatorial tobacco lines was generated and screened in high light conditions for increased photosynthetic capacity and biomass content. In this chapter, five lines displaying an increased stem elongation and biomass were characterised in detail. The aim of the work described in this chapter was:

1. To confirm the growth phenotype of the selected combinatorial transgenic lines in different growth conditions (two glasshouse locations and an outdoor polytunnel).

2. To determine the genetic, photochemical, biochemical, and metabolic characteristics underlying the observed growth phenotype in the selected combinatorial transgenic lines via:

   (a) Determination of the transgene complement and expression levels.

   (b) Determination of photosynthetic capacity, sugar content, and metabolite profiles.

4.2 Introduction and rationale

This chapter presents a characterisation of the combinatorial transgenic lines selected in the high light primary screen of the combinatorial library (see Chapter 3). The first key aspect was to attempt to reproduce the stem growth phenotype in different conditions and locations. Therefore, two glasshouse growth experiments were performed, followed by a subsequent growth experiment in an outdoor polytunnel.

In metabolic engineering, particularly in a combinatorial experiment, the metabolic phenotype of the primary transformants is considered more valuable than knowing which transgenes are present or absent, to what level they are being expressed, or whether single or multiple transgene insertions have been obtained [137]. As such, the primary screen of 59 combinatorial transgenic lines described in the previous chapter allowed a rapid analysis of the library to identify promising lines displaying increases in photosynthetic capacity and/or growth. This meant that at the start of the characterisation, the combination of transgenes present in each of the selected combinatorial transgenic lines was unknown. Accordingly, the next experiments focused on determining the transgene combination present in the selected transgenic lines and the transgene expression levels, measured as transcript abundance.

Evaluation of chlorophyll fluorescence-based parameters was done using a MultispeQ [212] in one of the glasshouse experiments to understand the effect of the introduced transgene combinations on the photosynthetic capacity of the combinatorial transgenic plants. To explore further changes in the combinatorial transgenic lines at the metabolite level, a metabolite profiling experiment was performed by GC-MS.

A hypothesis of the effect of the transgenes on the phenotype of the combinatorial tobacco transgenic plants is proposed based on the results of these experiments.

4.3 Results

4.3.1 The stem growth phenotype could not be reproduced under low or high light conditions

Height and biomass remained unchanged in two glasshouse experiments

Transgenic combinatorial transgenic lines selected based on the high light primary screen (600 µmol m^{-2} s^{-1}) described in Chapter 3 were grown in glasshouse conditions at two locations. The first experiment was performed at the Department of Plant Sciences, University of Oxford, Oxford (UK) and the second at the Max Planck Institute of Molecular Plant Physiology, Potsdam-Golm (Germany). Both glasshouse compartments received natural light and were supplemented to provide illumination which reached 150 and 350 µmol m^{-2} s^{-1} in Oxford and Golm, respectively. Plant growth was assessed at the same developmental stage as in the primary screen, when the first plants were starting to flower, to confirm the growth phenotype. This was six and four weeks after transfer to the soil in Oxford and Golm, respectively. Height and fresh weight biomass were recorded (Figure 4.1 and Table C.1).

Significant changes in plant height were observed in both locations (one-way ANOVA, P = 0.002, Table C.1). However, none of the combinatorial transgenic lines showed significant differences with respect to the WT control in either location. Regarding fresh weight biomass, significant differences were observed between lines in Oxford but not in Golm. However, the combinatorial transgenic lines did not show an increase in biomass in either location (Figure 4.1 and Table C.1), contrary to what was observed in the initial high light primary screen. In fact, one of the lines, 111A-10, showed a significantly reduced leaf and total biomass compared to the control in the Oxford experiment (Figure 4.1.A). This was not the case in the Golm experiment, where the number of replicates was higher (n = 6–10 in Oxford and n = 15 in Golm).

The total number of leaves was measured in the Oxford experiment. While lines 111A-10 and 142A-10 showed a significant reduction in the number of leaves with

respect to the control, line 287A-40 showed a significant increase (Figure C.1), as had been observed in the high light experiment (Table B.2).

There were differences between locations in the height and biomass of the lines. The desired developmental stage (start of blossom) was achieved two weeks later in Oxford. Nevertheless, the plants were taller and yielded more fresh biomass in Golm (Table C.1). The height recorded for each line was on average 131 mm higher in the Golm experiment, with the smallest difference in height having been recorded for line 287A-40 (24 mm) and the biggest for line 142A-10 (276 mm). Similarly, the total biomass was on average 61.5 g (fresh weight) higher in the Golm experiment. The biggest difference in total biomass (82 g) between the two locations was observed for line 111A-10, whose leaf and total biomass were significantly reduced compared to the WT in the Oxford experiment but showed no differences in Golm.

The differences observed between locations may be a result of the light conditions to which the plants were exposed. The light intensities could be considered low for tobacco, where light saturation starts at about 500 m^{-2} s^{-1} [234, 235], especially those achieved in Oxford (150 m^{-2} s^{-1}). Sustained exposure to more intense light conditions could have meant more growth at every developmental stage in the Golm experiment, leading to increased height and biomass at the time of measurement. Another possible explanation for the difference in plant size could have had to do with differences in the pots that the plants were grown in. While the pot shape was the same between experiments (round), differences in the diameter of the pot (15 cm in Oxford, 18 cm in Golm) could have meant more space and nutrient availability for root growth in Golm, resulting in increased plant growth. Depending on the height of the pots and assuming that the pots were cylindrical, the difference in total volume could be of up to 70%.

The combinatorial transgenic lines selected for increased height and stem biomass did not show significant increases in height or biomass when grown in two replicated glasshouse experiments. Therefore, the stem growth phenotype could not be reproduced under glasshouse conditions.

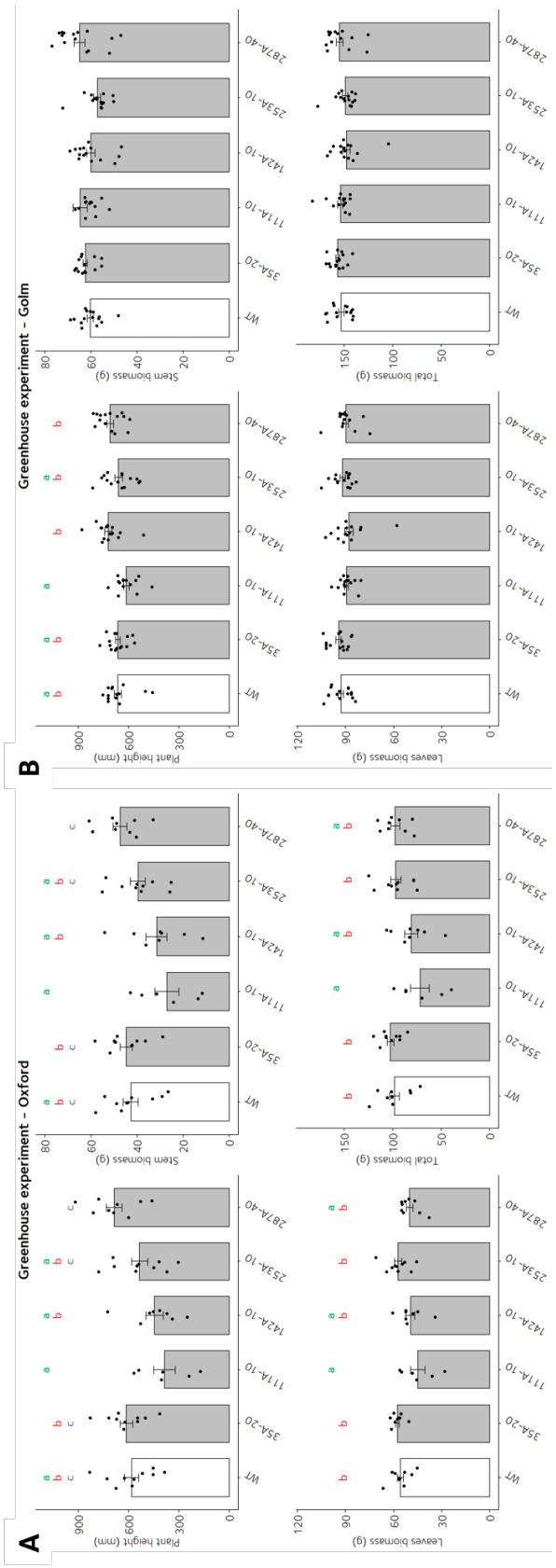

Figure 4.1: Height and biomass of selected combinatorial transgenic lines in replicated glasshouse experiments. combinatorial transgenic lines were grown in glasshouse conditions during the summer of 2019 in Oxford, UK (**A**) and Golm, Germany (**B**). Plants (T_1 generation) were germinated on selection plates and transferred to soil after two weeks. Measurements of plant height, stem, leaf, and total biomass were taken just before flowering, 6 (**A**) and 4 (**B**) weeks after transfer to soil. Data are mean ± SE; n = 6–10 (**A**) n = 15 (**B**). One-way ANOVA was used followed by post hoc Tukey multiple pairwise comparisons test. Different letters indicate significant differences between plant lines (P <0.05).

Growth phenotype in polytunnel experiment

An additional experiment was carried out in an outdoor polytunnel in Golm, with light intensities reaching even higher levels to those provided in the high light primary screen (>1200 m^{-2} s^{-1} vs. 600 m^{-2} s^{-1} in the high light screen). This would help determine if the phenotype could only be observed under high light conditions, close to saturation levels, where photosynthetic capacity was not limited by light. This was part of a larger experiment run by the Max Planck Institute of Molecular Plant Physiology team in Golm to screen an even larger population of the combinatorial transgenic lines for visual phenotypes. This time, the combinatorial transgenic lines were evaluated close to the end of their life cycle, when they were starting to set seed and leaves were starting to senesce. This allowed observation of final plant growth, which would help determine if the increased growth phenotype was linked to a specific developmental stage and not carried over to the final harvested yield of the plants. This was the case when Chida and coworkers introduced the Cyt c_6 in Arabidopsis, where increased height in the transgenic plants was increased during growth but final height remained unchanged with respect to the WT [76].

The appearance of the plants was captured by photography (Figure 4.2.A) and final plant height recorded (Figure 4.2.B, Table C.2). No major morphological changes were observed in the combinatorial transgenic lines compared to the WT control. Note that the difference in colour for line 253A-10 in Figure 4.2.A is purely a result of that photograph having been taken on a different day than the rest, because of the large number of plants that were being photographed. A quantitative comparison of the height of the plants showed that there were no significant changes between lines (one-way ANOVA, $P = 0.151$). However, for logistic reasons, stem elongation was only evaluated at the end of growth in this experiment. Therefore, as stated in the previous paragraph, it is possible that the stem elongation observed in the initial high light screen was linked to early stem growth and not carried over to final stem growth.

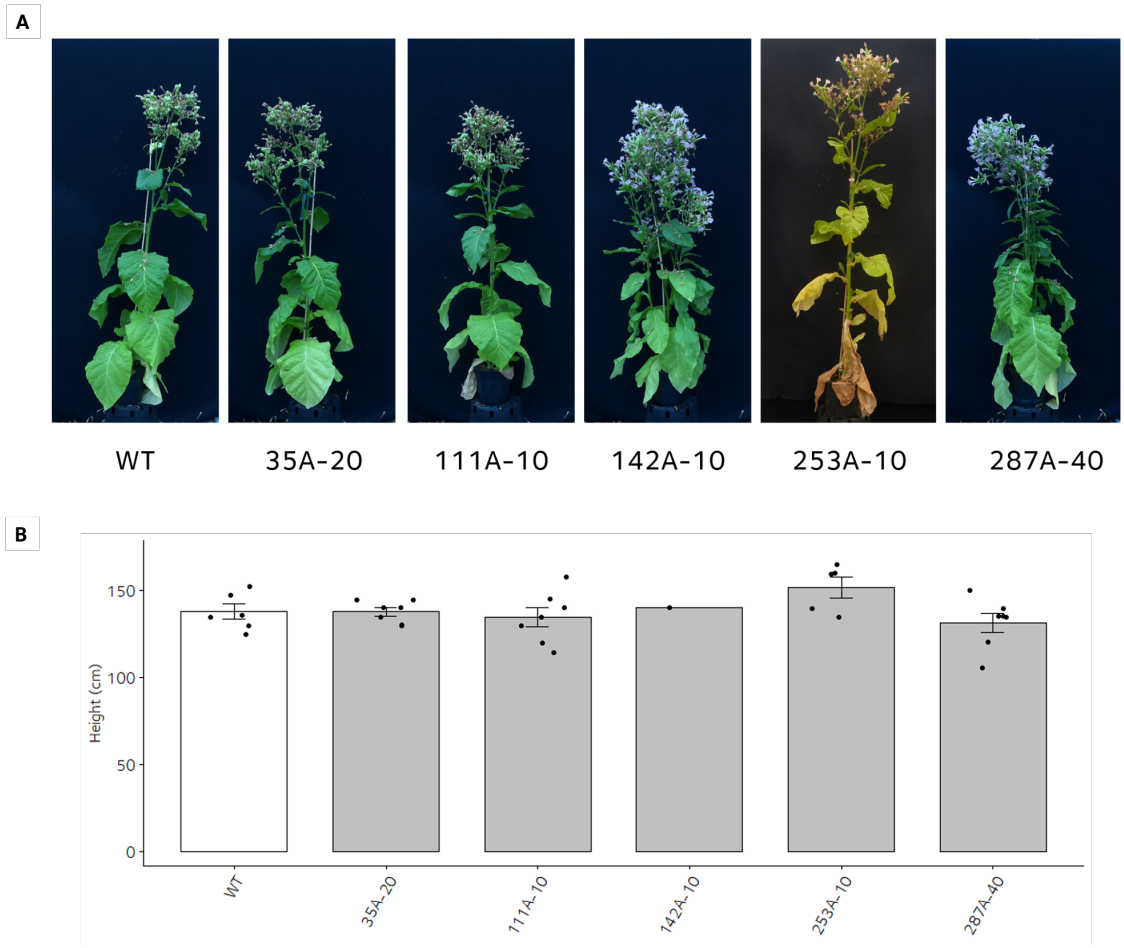

Figure 4.2: Plant phenotype and height of selected combinatorial transgenic lines in an outdoor polytunnel growth experiment. **A**. Photographs of selected combinatorial transgenic lines and WT control at the time of harvest. **B**. Height of selected combinatorial transgenic lines and WT control at the time of harvest. Plants were grown in an outdoor polytunnel during the summer of 2019 in Golm (Potsdam), Germany. Plants were germinated in selection plates and transferred to soil after two weeks. Plant height was determined at the time of harvest. Data are mean ± SE (n = 5-6, except for line 142A-10 where n = 1). One-way ANOVA was used and no significant differences were found between groups (P = 0.151).

Both the glasshouse and polytunnel experiments showed that the initial stem growth phenotype could not be reproduced under low (glasshouse) or high light conditions (polytunnel) (Figures 4.1 and 4.2). The inability to reproduce the phenotype in these settings raised questions about the link between the stem growth phenotype and the presence of the transgenes, which is discussed in the following section.

4.3.2 The observed stem growth phenotype could not be linked to the presence of the transgenes

Genomic PCR amplification with specific primers (Table A.6) was used to determine transgene presence in the selected combinatorial transgenic lines (Figures C.2 and C.3). It was found that the selected lines displaying a stem growth phenotype in the high light primary screen varied in terms of the identity and the number of integrated transgenes (Table 4.1). Nine transgenes were detected in two of the lines (35A-20 and 287A-40), which had six transgenes in common. Lines 111A-10 and 142A-10 contained four and five transgenes, respectively. Strikingly, line 253A-10 did not contain any transgene apart from the selection marker *nptII*, and hence it was a pseudo-WT line.

No conclusions could be drawn on the distribution of integrated transgenes in the combinatorial library, as only these five transgenic lines were characterised from the library of 329 lines. However, from this sample, it could be observed that all but one of the plasmids, carrying the Arabidopsis gene *FBPA* under the control of the potato *RbcS* promoter, could be detected by genomic PCR amplification in at least one of the transgenic combinatorial lines. This is in accordance with previous reports that analysed transgene presence after combinatorial co-transformation, with all transgenes being detected [145, 146, 148, 244]. These studies further reported that the different plasmids were integrated with equal frequencies in the nuclear genome, with no preferential uptake of any of the plasmids [145, 146, 244]. These could be the case for my transgenic combinatorial lines, although the structure of the genomic integrons was not determined in this study.

As there were no transgenes in common across all lines, apart from *nptII*, and line 253A-10 did not contain any of the targets, there was no evidence that the stem growth phenotype was linked to the presence of the transgenes.

Line 253A-10 was treated as a pseudo-WT for the rest of the experiments. Indeed, this line could be considered a control, more reliable than the WT as, similar to an empty vector control, it had also gone through the transformation and tissue culture process like the rest of the combinatorial transgenic lines.

Transgene	Line				
	35A -20	111A -10	142A -10	253A -10	287A -40
AtPetC					
Pyc6					
CaPFLP					
SictB					
AtFBPA					
AtSBPase					
FpGDC-H					
AtTPT					
AtcyFBPase					
EcPPase					
AtSWEET11					
AtSUC2					
nptII - KanR					
Number of transgenes	9	4	5	1	9

Transgene presence Transgene absence

Table 4.1: Summary of genomic PCR results for selected combinatorial transgenic lines. Transgene presence or absence is indicated for each combinatorial line, along with the total number of transgenes present in each line. Abbreviations: *AtcyFBPase*, cytosolic fructose 1,6-bisphosphatase; *AtFBPA*, fructose 1,6-bisphosphate aldolase; *AtPetC*, cytochrome b6f Rieske FeS protein; *AtSBPase*, sedoheptulose 1,7-bisphosphatase; *AtSUC2*, sucrose/H^+ importer; *AtSWEET11*, passive sucrose transporter; *AtTPT*, triose-P/phosphate translocator; *CaPFLP*, ferredoxin-like protein; *EcPPase*, cytosolic pyrophosphatase; *FpGDC-H*, glycine decarboxylase-H protein; *nptII*, *E. coli* neomycin phosphotransferase II; *Pyc6*, cytochrome c6; *SeictB*, putative HCO_3^- transporter.

As a result of this finding, the initial changes observed in the primary screen when comparing against the WT were compared against the pseudo-WT (Table 4.2). Compared to the pseudo-WT, lines 287A-40, 35A-20, and 111A-10 displayed increases in height of 17%, 15%, and 6%, respectively, but none of them were statistically significant. In contrast, line 142A-10 showed a reduction of the height of 3% with respect to the pseudo-WT. Similarly, in terms of fresh weight stem biomass, the increases were of 39% for line 287A-40, 25% for line 35A-20, and 3% for line 111A-10. Again, line 142A-10 showed a 2% decrease in stem biomass.

Table 4.2: Height and biomass data for combinatorial transgenic lines showing a stem growth phenotype. Height and fresh weight biomass were determined in six-weeks-old WT and combinatorial transgenic lines. Data are mean ± SE; n = 4. One-way ANOVA was used followed by post hoc Tukey multiple pairwise comparisons test. Different letters indicate significant differences between plant lines (P <0.05).

Line	Batch	Height (mm)	Stem biomass (g)
111A-10	1	644.50 ± 20.58^{cd}	83.35 ± 4.46^{abc}
253A-10	1	605.75 ± 17.81^{cd}	80.68 ± 3.10^{ab}
142A-10	1	590.00 ± 15.85^{bc}	79.07 ± 1.98^{ab}
WT 1	1	480.00 ± 29.81^{a}	61.87 ± 4.37^{a}
35A-20	2	698.00 ± 32.75^{cd}	100.67 ± 8.52^{bc}
WT 2	2	590.25 ± 12.09^{bc}	74.28 ± 4.70^{ab}
287A-40	4	709.00 ± 22.07^{d}	112.36 ± 12.00^{c}
WT 4	4	489.25 ± 26.29^{ab}	71.60 ± 6.55^{ab}

Line 287A-40 was the only one showing a significantly increased stem biomass when compared against the pseudo-WT. However, despite this increase in biomass being significant with respect to the pseudo-WT, it could not be reproduced in the glasshouse or polytunnel experiments. As Figure 4.1 shows, the comparisons for height and biomass in the glasshouse and polytunnel experiments were done between all lines, and changes were not significant with respect to either the WT or the pseudo-WT.

Having declared line 253A-10 a pseudo-WT, it could be observed that the transgene *Pyc6* was common to the combinatorial transgenic lines 35A-20, 142A-10, and 287A-40.

4.3.3 The selected combinatorial transgenic lines showed varied transcript abundance

Relative transcript abundance patterns, determined via qRT-PCR, were in accordance with the results obtained for transgene presence (i.e. transgenes that were amplified via genomic PCR were found to be expressed in the qRT-PCR analysis; Tables 4.3 and C.3).

Four out of the five selected combinatorial transgenic lines contained between four and nine transgene targets, most of them showing a high relative transcript abundance. In line 35A-20, the transgenes showing the highest relative transcript abundance were *CaPFLP*, *AtSBPase*, and *AtcyFBPase*, followed by *Pyc6* and

SeictB (Table 4.3). This would mean that an increased rate of photosynthetic electron transport in chloroplasts was to be expected, along with an increased RuBP regeneration due to an increased flux through the CBB cycle and stimulation of sucrose biosynthesis. The relative transcript abundance levels were comparable in line 287A-40, where the highest level was found for *FpGDC-H*, followed by *AtTPT*, *AtcyFBPase*, and *Pyc6* (Table 4.3). Similar to the previous line, increased photosynthetic electron transport rate and photorespiratory flux, and stimulated export of triose-phosphates and sucrose biosynthesis would be expected if the transcript levels were reflected by corresponding increases in functionally active versions of the encoded proteins. In line 111A-10, *Pyc6* and *AtPetC* showed high relative transcript abundance (Table 4.3), which would link to an stimulation of photosynthetic electron transport. The relative transcript abundance for the transgenes in line 142A-10 was not as high and the transgenes showing the highest transcript abundance were *AtSUC2*, *Pyc6*, and *EcPPase* (Table 4.3). In this line, an increased sucrose biosynthesis and phloem loading were to be expected.

Transgene expression levels were considerably variable when comparing between transgenes and between lines carrying the same transgene (Table 4.3). Some of the variation was expected due to the different strength of promoters used with the different transgenes. For example the highest expression levels were found for transgenes *CaPFLP* (line 35A-20) and *FpGDC-H* (line 287A-40) (Table 4.3), both under the control of the *CaMV35S* promoter, the strongest of all the introduced promoters [144]. This does not explain the variation of expression of the same transgene in different lines. For example, the Arabidopsis cytosolic *FBPase* ranged from a fold-change compared to the WT of 37 in line 287A-40 to 391 in line 142A-10 to 2383 in line 35A-20 (Table 4.3). This represents a variation of 10- to 64-fold between lines.

Table 4.3: Relative transgene transcript levels in selected combinatorial transgenic lines. Relative transgene transcript levels, represented as fold-change ($2^{-\Delta\Delta Ct}$), were determined by quantitative real-time PCR (qRT-PCR) in leaves, relative to the transcript levels of the housekeeping genes *L25* and *EF-1α*. Fold-change was calculated as per [205], as $2^{-\Delta\Delta Ct} = 2^{Ct_x - Ct_y}/2^{Ct_a - Ct_b}$, where Ct_x is the cycle threshold (Ct) of the transgene in the WT, Ct_y is the Ct of the transgene in the corresponding combinatorial line, Ct_a is the average Ct of the housekeeping genes in the WT, and Ct_b is the average Ct of the housekeeping genes in the corresponding combinatorial line.Three biological replicates (BR, each involving a pool of three independent plants) were used per line. Expression in each biological replicate, mean, and SE are given, along with the simplified results from the genomic PCR for each transgene and line, where the plus (+) symbol indicates transgene presence and the minus (-) symbol indicates transgene absence.

		Line				
Transgene	\textbf{Analysis}	253A-10 (pseudo-WT)	35A-20	111A-10	142A-10	287A-40
AtPetC	qRT-PCR	1.79 ± 0.32	18.15 ± 12.01	588.69 ± 203.83	1.5 ± 0.59	401.31 ± 154.03
	gPCR	-	+	+	-	+
Pyc6	qRT-PCR	2.3 ± 0.59	976.93 ± 690.29	1328.99 ± 778.07	532.84 ± 263.68	3452.72 ± 1580.19
	gPCR	-	+	+	+	+
CaPFLP	qRT-PCR	1.58 ± 0.63	30343.52 ± 17323.91	0.48 ± 0.15	0.57 ± 0.21	45.83 ± 12.22
	gPCR	-	+	-	-	-
SeictB	qRT-PCR	1.91 ± 0.91	290.8 ± 49.18	2.59 ± 2	1.22 ± 0.22	2.22 ± 0.91
	gPCR	-	+	-	+	+
AtFBPA	qRT-PCR	1.24 ± 0.23	2.63 ± 0.36	0.87 ± 0.11	0.6 ± 0.16	180.92 ± 57.22
	gPCR	-	-	-	-	-
AtSBPase	qRT-PCR	5.74 ± 2.33	20281.47 ± 11508.29	53.56 ± 17.08	1.17 ± 0.11	5.93 ± 2.68
	gPCR	-	+	-	-	-
FpGDC-H	qRT-PCR	1.98 ± 0.44	6.86 ± 4.23	0.98 ± 0.17	9.57 ± 5.81	49411.03 ± 9734.06
	gPCR	-	+	-	-	+
AtTPT	qRT-PCR	6.73 ± 5.1	5.06 ± 2.96	3.01 ± 1.12	3.31 ± 1.22	12434.2 ± 4794.3
	gPCR	-	-	-	-	+
AtcyFBPase	qRT-PCR	1.09 ± 0.07	2383.17 ± 690.84	0.49 ± 0.12	391.11 ± 122.31	36.78 ± 11.74
	gPCR	-	+	-	+	+
EcPPase	qRT-PCR	27.57 ± 22.24	20101.82 ± 16091.99	9.36 ± 7.41	4.14 ± 3.15	7120.33 ± 5589.54
	gPCR	-	+	-	-	+
AtSWEET11	qRT-PCR	1.48 ± 0.43	7.56 ± 2.39	1.54 ± 0.88	0.54 ± 0.08	217.46 ± 44.88
	gPCR	-	-	-	-	+
AtSUC2	qRT-PCR	7.91 ± 5.63	1.46 ± 0.61	3.39 ± 1.97	736.67 ± 289.62	92.57 ± 74.5
	gPCR	-	-	+	+	-

Heterogeneity in expression is a common feature of transgenic lines derived from a single transformation event and has been linked to position effects (chromatin structure and regulatory elements at the site of integration), dosage effects (transgene copy number), and DNA rearrangements during or before transgene integration [239, 245]. These three factors can contribute to the level and stability of transgene expression.

Position effects likely contributed to variation between lines as it is established that there is no preferential integration of transgenes in terms of chromosomal region [155]. Different positions of integration in the genome in different lines could have led to different regulatory effects in the expression of the same gene.

The number of copies of the integrated transgenes could explain variability in transgene expression between lines. Differences in copy number between transgenic lines have been reported widely in previous biolistic co-transformation experiments. As an example, Hadi *et al.* used biolistic co-transformation to introduce 12 different plasmids in soybean and quantified transgene copy number via Southern hybridisation [145]. They described the presence of concatemeric loci which contained several copies of the introduced plasmids, classifying the lines as low (1-4 copies), intermediate (4-14), and high copy number clones (6-14) [145]. This implied that lines with high copies for one plasmid tended to have high copies for the rest of the plasmids too, which was later confirmed by Agrawal *et al.* [238].

The link between transgene dosage and expression levels has been subject to debate. It was long argued that high transgene copy number could be linked to lower expression levels and/or silencing and that the generation of plants with single-copy integration events was desirable [245, 246]. Nevertheless, this was later debunked as high copy number can lead to high expression levels as was observed in the case of Golden Rice, where a high copy number led to high expression levels and a subsequent increase in β-carotene accumulation [246, 247].

Transgene rearrangements are common in transgenic plants generated via direct gene transfer [245, 246, 248]. As an example, in an analysis of seven maize lines showing multiple transgene copies, rearrangements of at least one copy of the transgenes were found in all lines [249]. Variations in transgene integration can be

caused by differences in either the length (full-length or truncated versions, caused by deletions or the presence of filler DNA) or the orientation of the expression cassettes (inversions). This variation is decisive for the integrity of the transgenes and is key for transgene expression, probably even more so than copy number. In rice transformed with three plasmids via particle bombardment, the expression of the transgenes was comparable in transformants containing one or up to five copies [250]. Instead, the integrity of the transgenes had a major effect in terms of transgene expression and co-suppression. It is established that the presence of truncated copies can lead to silencing of intact, adjacent copies [250]. In terms of transgene orientation, what seems to matter is that different cassettes are assembled in a head-to-tail or tail-to-head orientation, so that promoter or terminator sequences are not facing each other [245]. The effect of the orientation of different transgenes with respect to each other should be less pronounced in plasmid-mediated transformations than in backbone-free transformation with minimal cassettes, as the plasmid backbones may create enough separation between expression cassettes that the regulatory elements of a transgene do not affect adjacent transgenes [145].

Transgenes were found to be expressed. The only transgene that was confirmed to be present in the genomic PCR and later found to be expressed to a low level was *SecitB* in line 142A-10, with a 20% increase above background.

Even if the presence and transcript abundance of these transgenes could not explain the stem growth phenotype, some of the expressed transgenes had previously been shown to improve photosynthetic capacity and plant productivity on their own. It follows that some of these combinatorial transgenic lines would then be expected to show an improved photosynthetic capacity, despite them not showing an increased biomass production.

4.3.4 The selected combinatorial transgenic lines did not show improvements in photosynthetic capacity

Photosynthetic parameters were assessed in the selected combinatorial transgenic lines by measuring chlorophyll fluorescence using a MultispeQ during the Oxford glasshouse experiment described in Section 4.3.1 above.

Chlorophyll fluorescence-derived parameters

Saturation pulse chlorophyll fluorescence yield parameters were determined in light-adapted leaves using pulse amplitude modulation. Maximum variable fluorescence at steady-state conditions (F_m') was increased in line 287A-40 when compared to both the WT and the pseudo-WT control. In line 142A-10, the value of F_m' was not significantly different from that of line 287A-40. However, its increase in F_m' was not significant when compared against the WT either. In contrast, line 111A-10 showed a significant reduction in F_m' compared to all the other lines, both the transgenics and the controls. An increase was also observed in the minimum variable fluorescence during dark phase after steady-state (F_0') for lines 287A-40 and 142A-10 with respect to both controls (Table 4.4 and Figure C.4).

The maximum operating efficiency of PS II (F_v'/F_m') was determined based on F_0' and F_m', where $F_v' = F_m' - F_0'$. While no changes were found in F_v/F_m (dark-adapted) in the high light experiment, the combinatorial transgenic lines 35A-20, 111A-10, and 287A-40 showed a significantly reduced F_v'/F_m' ratio (light-adapted) with respect to both the WT and the pseudo-WT controls in the glasshouse experiment (Figure C.4). In this case, the pseudo-WT showed a significant increase in F_v'/F_m' with respect to the rest of the lines (Table 4.4 and Figure C.4).

Changes in F_v'/F_m' are related to fluorescence quenching. Both photochemical quenching, estimated as the fraction of PS II centres which are in the open state (qL), and the estimated NPQ (NPQt, which denotes NPQ in light-adapted leaves) were measured. No differences between lines were observed for qL ($P = 0.957$). However, NPQt was significantly increased in lines 35A-20, 111A-10, and 287A-40 with respect to the WT and the pseudo-WT controls (Figure C.4). In contrast,

the pseudo-WT line showed a significant increase in F_v'/F_m' (Table 4.4 and Figure C.4) and a significant reduction in NPQt when compared against all the other lines (Table 4.4 and Figure C.4). Both F_v'/F_m' and NPQt remained unchanged in line 142A-10 with respect to the WT.

Therefore, three of the transgenic lines (35A-20, 111A-10, and 287A-40) showed reductions in F_v'/F_m' and increases in NPQt, which could be indicative of photoinhibition [251].

Ratios of allocation of incoming light

The relative rates of photochemical and non-photochemical quenching were estimated as ΦPSII, the ratio of incoming light that goes towards NPQ (ΦNPQ), and the ratio of incoming light that is dissipated via non-regulated processes (ΦNO). Albeit with small differences between the lines, about 59% of the flux of excitation energy was allocated towards ΦPSII, 29% towards ΦNO and 12% towards ΦNPQ in all lines (Table 4.4 and Figure C.5).

The efficiency of PS II, ΦPSII, which shows a strong linear relationship with the efficiency of carbon fixation [48], remained unchanged in the combinatorial transgenic lines ($P = 0.403$). No differences were observed between lines for ΦNO ($P = 0.412$). It was found that the pseudo-WT line showed a reduction in ΦNPQ with respect to the rest of the lines, but this is unlikely to have biological relevance. Line 287A-40 was not different to the rest of the combinatorial transgenic lines in terms of ΦPSII and ΦNO but it showed a significant increase in ΦNPQ compared to both the WT and the pseudo-WT. The rest of lines, 35A-20, 111A-10, and 142A-10, did not show any changes with respect to the WT in these parameters (Table 4.4 and Figure C.5).

No changes between lines were observed in linear electron flow ($P = 0.138$) (Table 4.4 and Figure C.5).

Proton accumulation and flow

The rate of electrochromic shift (ECSt), which indicates the lifetime of steady-state proton translocation through the chloroplast ATP synthase, was unchanged between

lines, as was the rate of proton flux through the ATP synthase (vH^+). Proton conductivity of the chloroplast ATP synthase (gH^+) was increased in line 287A-40 with respect to the pseudo-WT but not to the WT (Table 4.4 and Figure C.6).

Absorbance-based parameters

Relative chlorophyll, otherwise known as Soil Plant Analysis Development (SPAD), was measured as leaf absorbance between 650 nm (red measuring light) and 940 nm (infrared light) as an estimate of chlorophyll content [212]. This parameter was significantly increased in line 287A-40 with respect to the WT control, but not when compared against the pseudo-WT line, 253A-10 (Table 4.4 and Figure C.6).

Other parameters

Leaf thickness was measured by the Hall Effect sensor embedded in the clamp of the MultispeQ instrument. This parameter was found to be very variable between measurements and no differences were observed between lines ($P = 0.118$) (Table 4.4 and Figure C.6).

Table 4.4: Photosynthetic capacity in selected combinatorial transgenic lines. Photosynthetic capacity was evaluated six weeks after transfer to soil under steady-state growth light conditions (50-150 µmol m^{-2} s^{-1}) using the Leaf Photosynthesis MultispeQ V1.0 protocol with a MultispeQ instrument (PhotosynQ, MI, USA). Parameters are as follows: maximum variable fluorescence (F_m'), minimum variable fluorescence (F_0'), maximum efficiency of PS II (F_v'/F_m'), fraction of PS II centres in open state (qL), estimated NPQ (NPQt), quantum yield of PS II (ΦPSII), ratio of incoming light towards non-regulated processes (ΦNO), ratio of incoming light towards NPQ (ΦNPQ), linear electron flow (LEF, µmol electrons m^{-2} s^{-1}), rate of electrochromic shift (ECSt), rate of proton flux through ATP synthase (vH^+), proton conductivity of ATP synthase (gH^+, s^{-1}), relative chlorophyll content (RC), leaf thickness (µm). Data are mean ± SE; n = 6–10. One-way ANOVA was used followed by post hoc Tukey multiple pairwise comparisons test. Different letters indicate significant differences between plant lines ($P < 0.05$). Non-parametric Kruskal-Wallis test was used when the raw data displayed an abnormal distribution.

Line	F_m'	F_0'	F_v'/F_m'	qL	NPQt
WT	17597.19 ± 196.73^{ac}	3952.00 ± 45^{a}	0.78 ± 0.00^{a}	0.43 ± 0.01	0.41 ± 0.01^{a}
35A-20	17199.42 ± 105.26^{b}	3915.00 ± 26^{a}	0.77 ± 0.00^{b}	0.43 ± 0.01	0.44 ± 0.01^{b}
111A-10	16559.51 ± 128.24^{b}	3779.00 ± 34^{b}	0.77 ± 0.00^{b}	0.42 ± 0.01	0.44 ± 0.01^{b}
142A-10	17730.92 ± 181.54^{ab}	4036.00 ± 48^{c}	0.77 ± 0.00^{ab}	0.42 ± 0.01	0.44 ± 0.01^{ab}
253A-10	17237.55 ± 130.21^{c}	3796.00 ± 30^{b}	0.78 ± 0.00^{c}	0.42 ± 0.01	0.38 ± 0.01^{c}
287A-40	18205.90 ± 149.59^{b}	4155.00 ± 41^{c}	0.77 ± 0.00^{b}	0.42 ± 0.01	0.44 ± 0.01^{b}

Line	ΦPSII	ΦNO	ΦNPQ	LEF
WT	0.59 ± 0.00	0.29 ± 0.00	0.12 ± 0.00^{a}	68.39 ± 1.12
35A-20	0.59 ± 0.00	0.29 ± 0.00	0.13 ± 0.00^{ab}	71.13 ± 0.73
111A-10	0.59 ± 0.01	0.29 ± 0.00	0.13 ± 0.00^{ab}	67.36 ± 1.17
142A-10	0.58 ± 0.01	0.29 ± 0.00	0.13 ± 0.00^{ab}	69.46 ± 0.99
253A-10	0.59 ± 0.00	0.29 ± 0.00	0.11 ± 0.00^{c}	70.17 ± 1.04
287A-40	0.58 ± 0.00	0.29 ± 0.00	0.13 ± 0.00^{b}	68.29 ± 1.28

Line	ECSt	vH^+	gH^+	RC	Thickness
WT	0.0010 ± 0.00^{ab}	0.00013 ± 0.00001^{ab}	8.55 ± 0.82^{ab}	45.53 ± 0.44^{a}	0.61 ± 0.03
35A-20	0.0011 ± 0.00^{a}	0.00015 ± 0.00001^{b}	8.24 ± 0.38^{ab}	45.66 ± 0.46^{a}	0.72 ± 0.05
111A-10	0.0011 ± 0.00^{a}	0.00012 ± 0.00001^{ab}	9.51 ± 0.62^{a}	44.11 ± 0.89^{a}	0.68 ± 0.05
142A-10	0.0010 ± 0.00^{ab}	0.00013 ± 0.00001^{ab}	8.37 ± 0.50^{ab}	46.45 ± 0.51^{ab}	0.57 ± 0.04
253A-10	0.0009 ± 0.00^{b}	0.00012 ± 0.00001^{ab}	7.33 ± 0.40^{b}	46.33 ± 0.55^{ab}	0.73 ± 0.04
287A-40	0.0010 ± 0.00^{ab}	0.00011 ± 0.00001^{a}	9.42 ± 0.52^{a}	48.14 ± 0.62^{b}	0.70 ± 0.06

4.3.5 The metabolite profile of the selected combinatorial transgenic lines reveals variation in amino acid content and increased content of photorespiratory intermediates

Metabolite profiling was performed to understand the changes associated with the observed transgene combinations at the metabolite level. Leaf samples from the selected combinatorial transgenic lines, taken during the high light primary screen, were subjected to metabolite extraction and derivatisation, followed by gas chromatography and mass spectrometry. Relative abundances were calculated from chromatographic peak areas and normalised to the internal standard ribitol. Figures C.7 to C.14 in the appendices depict the GC-MS results for each metabolite and line. Figures 4.5 to 4.8 show a simplified map of metabolic pathways that indicate the statistically significant changes ($P < 0.05$) observed in each line with respect to both the pseudo-WT and the WT controls. The complete dataset can be found in Table C.4.

Significant changes between lines were found for most metabolites, except for chlorogenic acid (Figure C.10), glycerol (Figure C.12), and sucrose (Figure C.13), that remained unchanged between lines. Several metabolites were found to show a significant difference in each combinatorial line compared to both controls. These metabolites are represented as the fold-change with respect to both controls in the combinatorial transgenic lines (Figure 4.3). Lines 35A-20 and 111A-10 showed mostly reductions in metabolites, while lines 142A-10 and 287A-40 showed mainly increases in metabolites compared to both controls.

For line 35A-20, the biggest reductions were found in asparagine (0.5-fold), followed by β-alanine, glucose 6-phosphate, and the glutamate derivatives arginine, and urea, whose reductions were 0.6-fold that of the controls (Figure 4.3.A). Significant increases with respect to both controls were found for xylose, a monosaccharide linked to the cell wall, and glycine, which were increased by 1.6- and 1.5-fold, respectively (Figure 4.3.A).

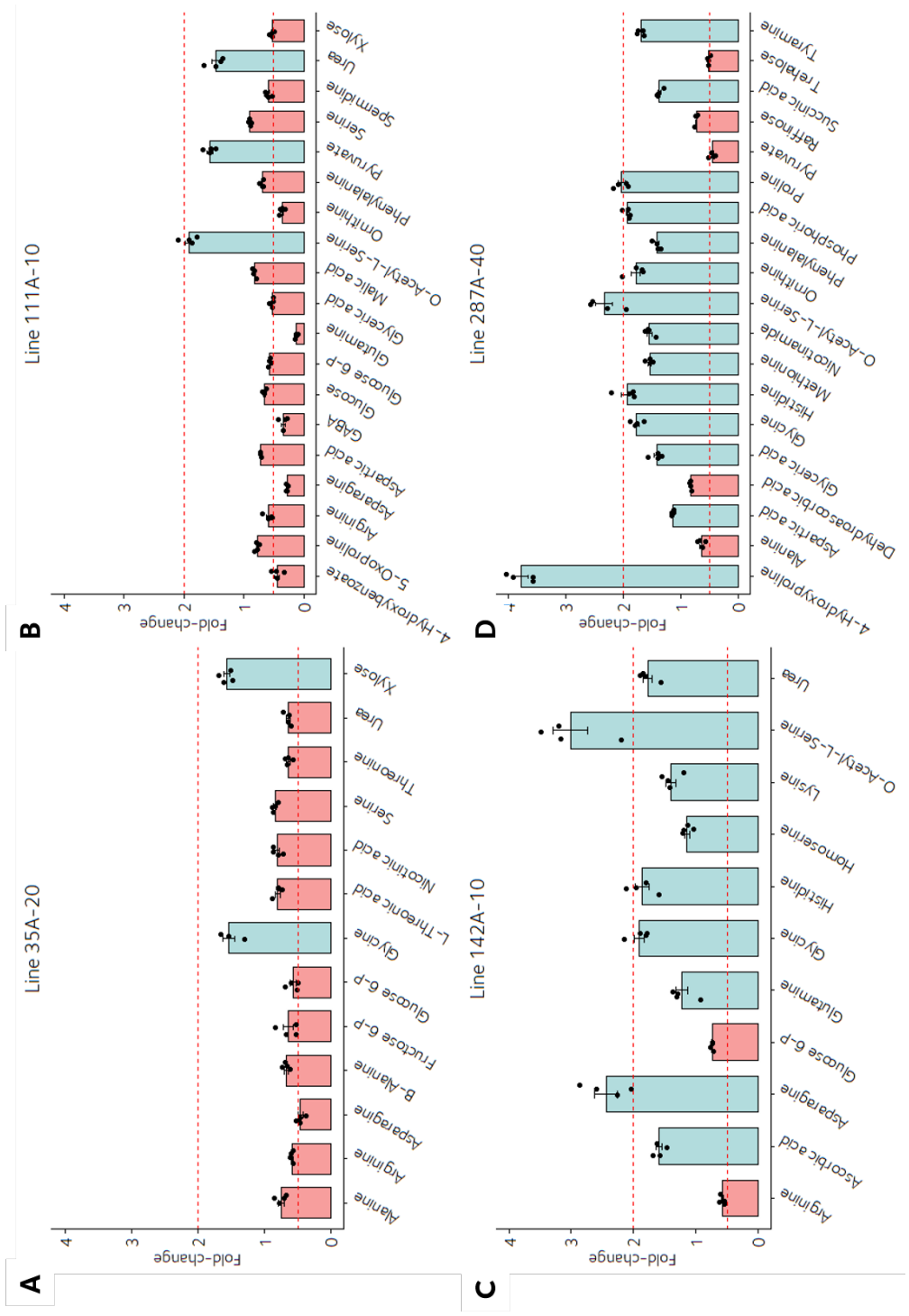

Figure 4.3: Metabolite profiling of selected combinatorial transgenic lines — fold change variations. Metabolite profiling by GC-MS was performed in leaves of the selected combinatorial transgenic lines, six weeks after transfer to soil: **A**, line 35A-20; **B**, line 111A-10; **C**, line 142A-10; **D**, line 287A-40. Data represent the fold-change with respect to the average of the controls (pseudo-WT and WT) in the indicated lines for metabolites that were significantly different with respect to both controls, with increases represented by blue bars and decreases represented by red bars. Significant changes were identified by one-way ANOVA, followed by post hoc Tukey multiple pairwise comparisons test; n = 4.

In line 111A-10, several amino acids and amino acid derivatives were significantly reduced, with the most considerable decreases being found in glutamine (0.1-fold), asparagine (0.3-fold), γ-aminobutyric acid (0.3-fold)), ornithine (0.4-fold), and 4-hydroxybenzoate (0.5-fold). On the other hand, significant increases were found for O-acetyl-L-serine (1.9-fold), pyruvate (1.6-fold), and urea (1.5-fold) (Figure 4.3.B).

For line 142A-10, only arginine and glucose 6-phosphate were significantly reduced, by 0.7- and 0.6-fold, respectively. Substantial increases were found in the amino acids o-acetyl-L-serine (3-fold) and asparagine (2.4-fold). The other three top metabolites showing an increase in this line were glycine (1.9-fold), histidine (1.9-fold), and urea (1.8-fold) (Figure 4.3.C).

A sharp increase in hydroxyproline was found in line 287A-40, with a 3.7-fold increase with respect to the controls. As in line 142A-10, O-acetyl-serine was substantially increased, by 2.3-fold. Proline (2-fold), histidine (1.9-fold), phosphoric acid (1.9-fold), and glycine (1.8-fold) were among the topmost increased metabolites for this line. As for decreases in metabolites, significant changes were found in the product of glycolysis, pyruvate (0.5-fold), and in trehalose (0.5-fold), alanine (0.7-fold), raffinose (0.7-fold), and dehydroascorbate (0.8-fold) (Figure 4.3.D).

As some of the most substantial metabolite changes were found to be in glycine and the L-serine derivative o-acetyl-L-serine, the ratio of glycine to serine (Gly/Ser) was calculated as an indicator of flux through the photorespiratory pathway [252]. The Gly/Ser ratio was found to be significantly different between the combinatorial transgenic lines (P = 2.99e-12) (Figure 4.4). Indeed, the ratio was significantly higher in lines 35A-20, 142A-10, and 287A-40 compared to both controls, which indicates increased accumulation of glycine in these combinatorial transgenic lines.

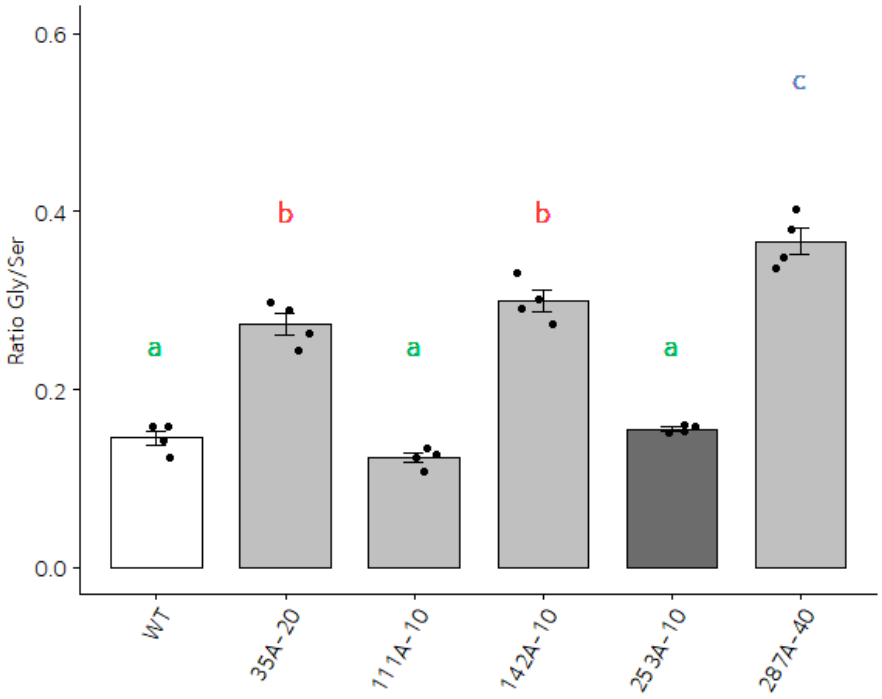

Figure 4.4: Glycine to serine (Gly/Ser) ratio in selected combinatorial transgenic lines. Metabolite profiling by GC-MS was performed in the selected combinatorial transgenic lines, six weeks after transfer to soil. The pseudo-WT is coloured in dark grey. Data are mean ± SE of the relative ratio of glycine to serine in the indicated lines; n = 4. One-way ANOVA was used followed by post hoc Tukey multiple pairwise comparisons test. Different letters indicate significant differences between plant lines ($P < 0.05$).

Overall, the metabolite profiles were unexpected based on the presence and expression levels of the transgenes in the combinatorial transgenic lines. For instance, levels of sugars and sugar alcohols would have been expected to change in lines 35A-20 and 287A-40, where transcripts levels of *AtSBPase*, *AtcyFBPase*, and/or *AtTPT* increased. However, no changes in glucose, fructose, or sucrose were found in these lines with respect to the controls (Figures C.12 and C.13). Instead, significant variations were found in the concentration of amino acids: some were significantly increased in some lines, especially o-acetyl-L-serine, hydroxyproline, and asparagine, while others were reduced, such as glutamine and asparagine in some cases (Figure 4.3). There was no clear link between the changes to amino acids and transcript levels, although they could be indicative of a shift in the carbon to nitrogen ratios.

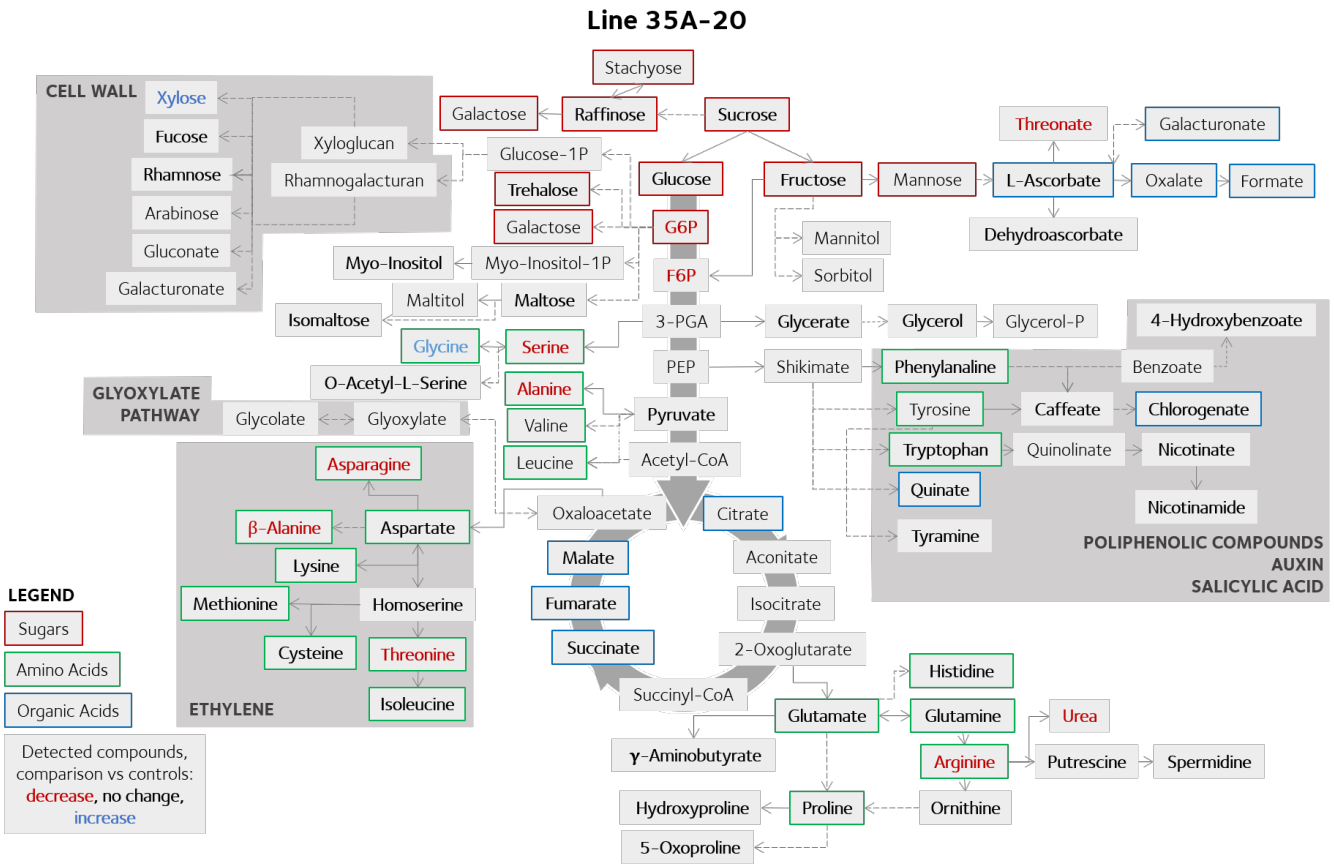

Figure 4.5: Metabolite profiling of line 35A-20 in a simplified map of plant metabolism. Significant changes in metabolite content with respect to the pseudo-WT and WT controls are indicated in red (decrease in combinatorial transgenic line with respect to both controls) or blue font (increase). Detected compounds are indicated in bold, unchanged in combinatorial line with respect to both controls). One-way ANOVA, followed by post hoc Tukey multiple pairwise comparisons test, was used to identify changes between the combinatorial line and the controls. As indicated in the legend, sugars, amino acids, and organic acids are labelled with red, green, and blue boxes, respectively.

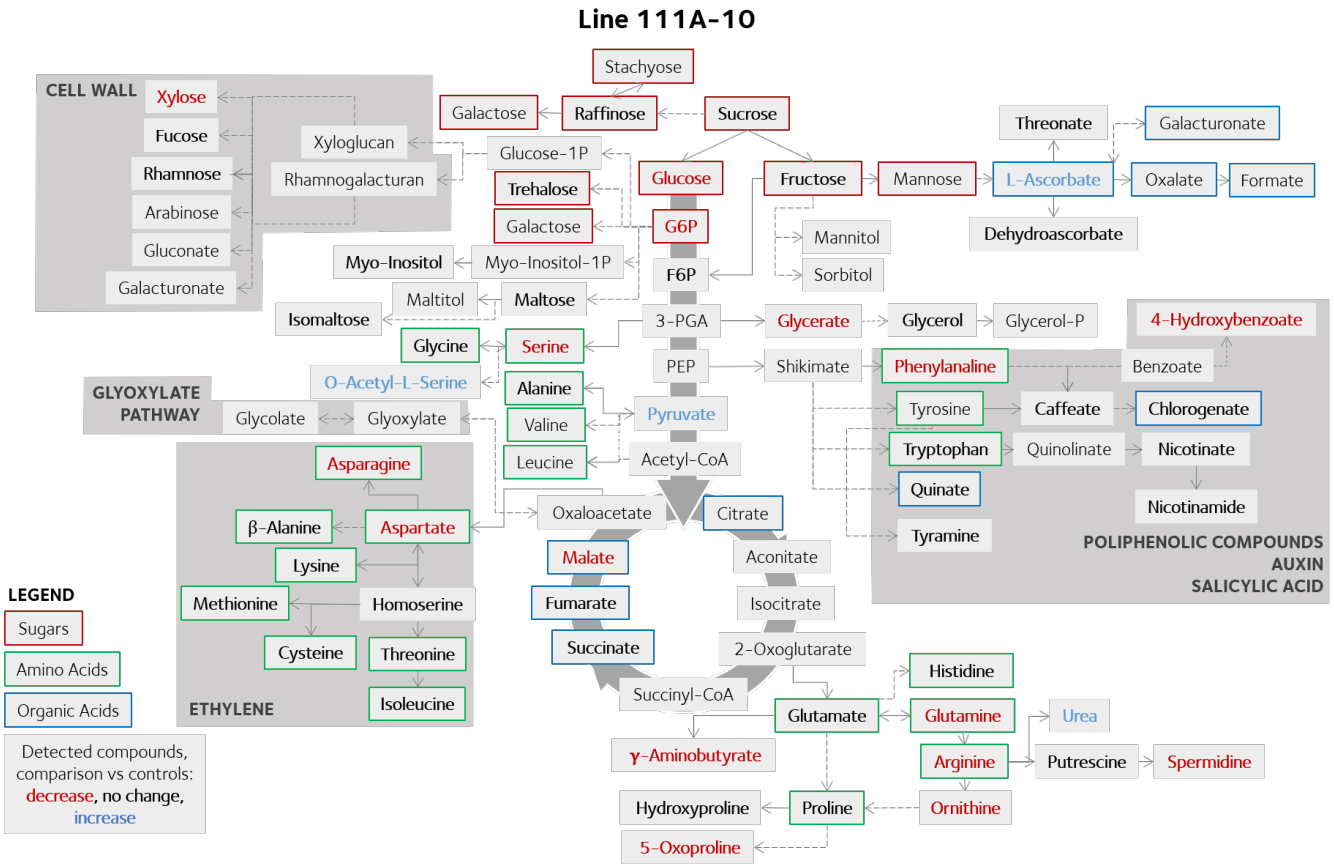

Figure 4.6: Metabolite profiling of line 111A-10 in a simplified map of plant metabolism. Significant changes in metabolite content with respect to the pseudo-WT and WT controls are indicated in red (decrease in combinatorial transgenic line with respect to both controls) or blue font (increase). Detected compounds are indicated in bold, unchanged in combinatorial line with respect to both controls). One-way ANOVA, followed by post hoc Tukey multiple pairwise comparisons test, was used to identify changes between the combinatorial line and the controls. As indicated in the legend, sugars, amino acids, and organic acids are labelled with red, green, and blue boxes, respectively.

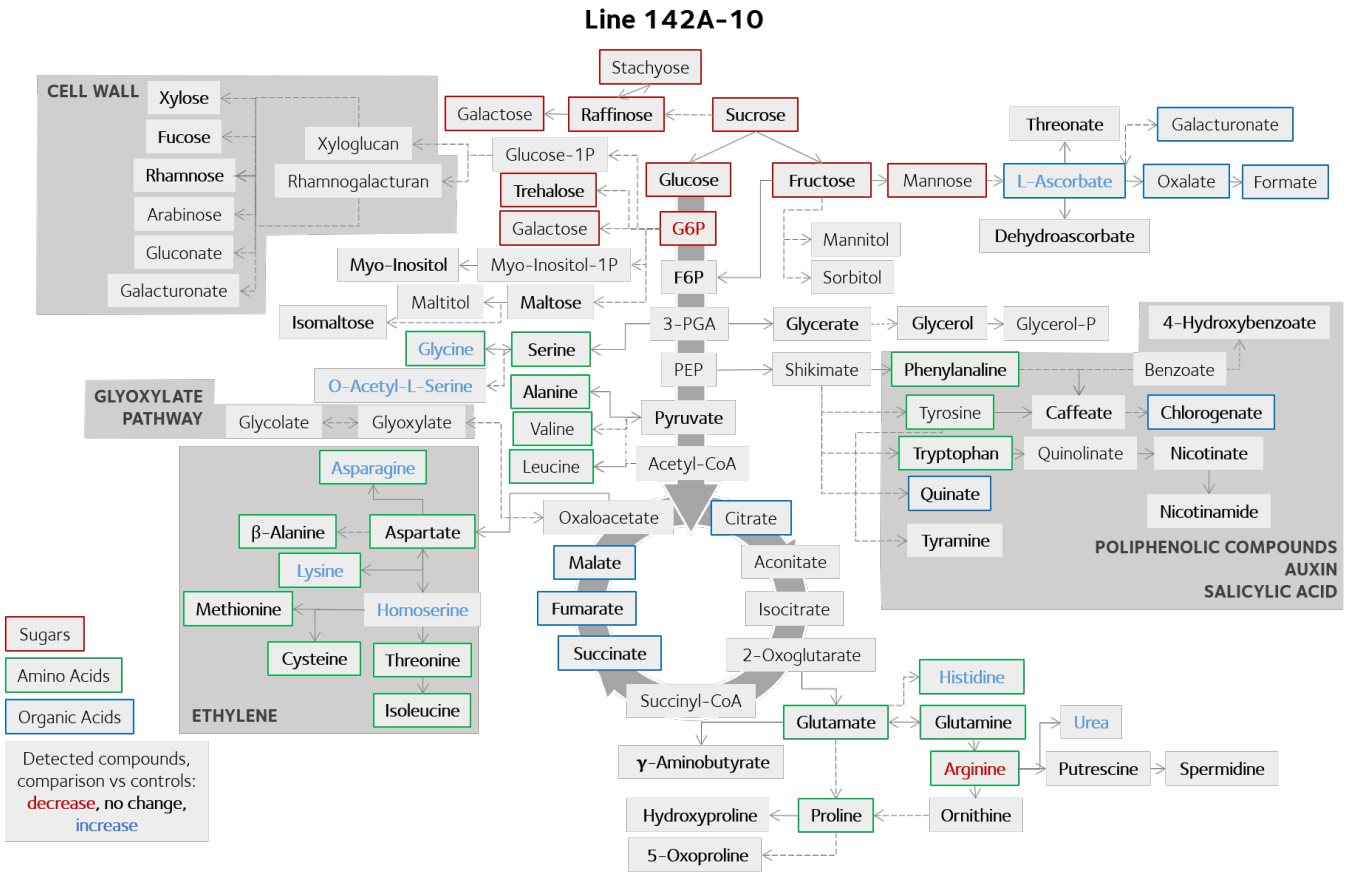

Figure 4.7: Metabolite profiling of line 142A-10 in a simplified map of plant metabolism. Significant changes in metabolite content with respect to the pseudo-WT and WT controls are indicated in red (decrease in combinatorial transgenic line with respect to both controls) or blue font (increase). Detected compounds are indicated in bold, unchanged in combinatorial line with respect to both controls). One-way ANOVA, followed by post hoc Tukey multiple pairwise comparisons test, was used to identify changes between the combinatorial line and the controls. As indicated in the legend, sugars, amino acids, and organic acids are labelled with red, green, and blue boxes, respectively.

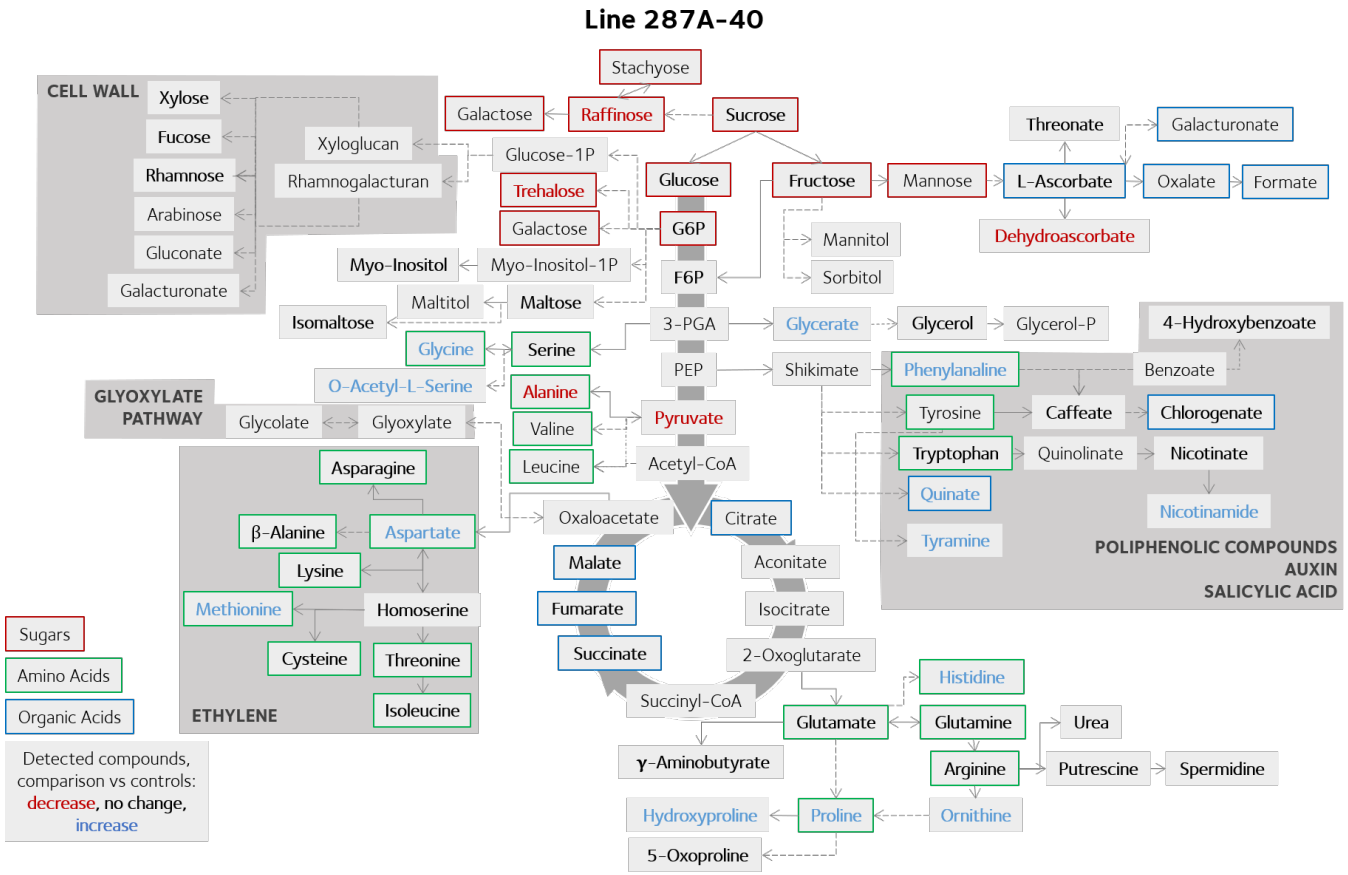

Figure 4.8: Metabolite profiling of line 287A-40 in a simplified map of plant metabolism. Significant changes in metabolite content with respect to the pseudo-WT and WT controls are indicated in red (decrease in combinatorial transgenic line with respect to both controls) or blue font (increase). Detected compounds are indicated in bold, unchanged in combinatorial line with respect to both controls). One-way ANOVA, followed by post hoc Tukey multiple pairwise comparisons test, was used to identify changes between the combinatorial line and the controls. As indicated in the legend, sugars, amino acids, and organic acids are labelled with red, green, and blue boxes, respectively.

4.4 Discussion

4.4.1 The reproducibility of the stem growth phenotype

In this chapter, a detailed analysis of five selected combinatorial transgenic lines has been described. Lines 35A-20, 111A-10, 142A-10, 253A-10, and 287A-40 were chosen as they demonstrated a fast stem growth phenotype when grown in high light conditions in a controlled growth chamber, as described in Chapter 3. Despite the distinct phenotype observed then, it was not possible to reproduce the phenotype in two replicated glasshouse experiments performed at two locations. The light intensity was lower in the glasshouse experiments than that of the high light growth chamber where the phenotype was initially observed. However, the combinatorial transgenic lines did not show differences with respect to the WT control in an additional polytunnel experiment where the light was not limiting photosynthetic capacity.

Contrary to what would have been expected given the common phenotype observed in these combinatorial transgenic lines, they did not show any transgene in common. More importantly, line 253A-10 only contained the *nptII* gene, conferring kanamycin resistance. In a combinatorial co-transformation experiment with 14 constructs in rice, Chen *et al.* analysed 125 lines and observed that this was a relatively rare instance, with only 6% of the lines containing solely the selectable marker [146]. If the tobacco combinatorial library followed that same frequency, 20 lines out of the 329 would be carrying the *nptII* gene only, but a different ratio would likely be found in this set of transgenic plants because of the nature of the transgenes and the plant species used.

The fact that line 253A-10 only carried the *nptII* selectable marker gene, along with the inability to reproduce the phenotype, was the definitive proof that the stem growth phenotype was not caused by the presence of the transgenes. It follows that the observation of the stem growth phenotype in the high light primary screen is more likely explained by the growth conditions or some other experimental variable. From the hypotheses presented in the Discussion section in Chapter 3, the third hypothesis, proposing that the proximity of the plants would have led to stem

elongation towards the light, would be the most appropriate to explain the observed phenotype. Plant proximity was an issue caused by the limited space available in the high light growth chamber that would have led to a manifestation of the shade avoidance syndrome. In shade avoidance, stem elongation, accompanied by early flowering, could lead to increased biomass accumulation.

The phenotype was only observed in the few selected lines in the initial high light experiment despite the randomised planting design and analyses. As discussed in Chapter 3, early germination or faster growth at early stages of development in these specific lines could have played a role in them showing significant increases in height. Although the size of the seedlings was not different upon transfer to soil, these lines, including the pseudo-WT line 253A-10, were classified as particularly big compared to other combinatorial lines in the nursery, before their transfer to the high light chamber. This could have been particularly relevant in the height measurements performed in the primary screen when the plants were six weeks old.

Taken together, the results of the growth experiments in the combinatorial transgenic lines suggest that the stem growth phenotype was unreliable and that an increased number of replicates, as was used in the subsequent glasshouse and outdoor experiments, would have deemed the differences to be non-significant with respect to the controls.

4.4.2 Why the observed transgene combinations fail to improve photosynthetic efficiency

It was concluded that the phenotype observed in the selected combinatorial transgenic lines was not related to the presence of the transgenes and could have instead been caused by the experimental conditions. Nonetheless, apart from the pseudo-WT, the other four lines, 35A-20, 111A-10, 142A-10, and 287A-40, did contain various combinations of the introduced transgenes and had one transgene in common, *Pyc6* (Figure C.2). This transgene codes for the red algal Cyt c_6, a soluble electron carrier which mediates electron transfer from Cyt b_6f to PS I, and overexpression of this gene was shown to enhance growth and photosynthesis in transgenic Arabidopsis

[76]. Expression levels in my combinatorial transgenic tobacco lines, determined as relative transcript abundance, were moderate to high with respect to the WT control for most transgenes and, in the case of *Pyc6* transcript abundance was remarkably high in the selected lines. This was the only transgene with such high transcript accumulation (Figure 4.3).

However, the correlation between transcript abundance and protein concentration and activity is not straightforward. Gene expression is not only regulated at the transcriptional level but also the translational and post-translational level. Therefore, translational rates, protein degradation and turnover rate, as well as the movement of the protein between organelles, particularly in proteins that were targeted to chloroplasts or mitochondria, could have affected the functionality of the transgene products. Protein accumulation and subsequent enzyme/transport activity assays were not performed because antibodies were not available for most of the transgene-encoded proteins and because of time constraints. Nevertheless, the transgene expression cassettes were constructed following previous publications in terms of promoter choice and transgene sequence. Those previous studies showed that transgene overexpression was followed by increased protein accumulation and activity. For example, Chida *et al.* showed that overexpression of *Pyc6* under the *CaMV35S* promoter led to the accumulation of Cyt c_6 in the chloroplast of Arabidopsis [76]. The *Pyc6* transgene sequence that I used to build the expression cassette for my work was based on that detailed in Chida *et al.* [76]. However, the *Pyc6* coding sequence was codon optimised for plant expression, and the transit peptide from tobacco plastocyanin was included. Therefore, it is possible that issues arose around protein stability and targeting at the subcellular level. Nonetheless, an important point in support of the functionality of the transgene products is that metabolite changes with respect to both the WT and the pseudo-WT controls were seen in all combinatorial lines, which are indicative of protein activity. It cannot be ruled out that these changes are not caused by insertional mutation during the integration of the transgenes into the genome.

Considering that each transgene alone resulted in improved photosynthetic performance and/or plant growth in previous studies (Tables 3.1, 3.2, and 3.3), it would have been expected that their combination would have led to at least the same improvement as previously reported and more likely an increase above and beyond previous reports. Indeed, it has been shown that combining transgenes whose products take part in photosynthetic electron transport, the CBB cycle, and photorespiration is an effective strategy to produced large increases in photosynthetic performance and growth [23, 59, 100]. Yet none of my selected lines showed improvements in photosynthetic capacity in two separate experiments, tracking a variety of photosynthetic parameters derived from chlorophyll fluorescence measurements.

Pyc6 could have had unexpected interactions with the rest of the transgenes present in the same locus [253], negating their effects. Additionally, transcript abundance was only determined for the introduced transgenes and not for any of the native genes that could interact with or be affected by them. For example, overexpresion of *AtPetC*, encoding the Rieske FeS protein from Cyt b_6f, led to concomitant increases in Cyt f (*PetA*), Cyt b_6 (*PetB*), the PS I type I chlorophyll a/b-binding protein (*LhcaI*), the core PS I protein (*PsaA*), the D1 (*PsbA*) and D2 (*PsbD*) proteins from the PS II reaction centre, and subunit D (*AtpD*) from the ATP synthase in Arabidopsis [22]. Therefore, it cannot be discounted that interactions between the transgenes and endogenous genes could have led to pleiotropic effects that compensated for or even cancelled out the potential benefits of the transgenes. Nevertheless, a study where the gene coding for Cyt c_6 from the red alga *Porphyra umbilicalis* was overexpressed in tobacco along with the genes coding for the plant SBPase or the cyanobacterial bifunctional FBPase/SBPase demonstrated improvements in the rate of net CO_2 assimilation and growth under glasshouse and field conditions [23]. In my study, line 35A-20 showed high transcript levels for *Pyc6*, *AtSBPase*, and the cytosolic *AtFBPase* and, along with *CaPFLP*, they were the transgenes with the highest transcript abundance. Therefore, the pattern was similar to that of López-Calcagno *et al.* [23]. As a result, it seems unlikely that *Pyc6* was incompatible with other transgenes in improving photosynthetic

capacity and biomass accumulation since a very similar combination of transgenes proved beneficial [23]. It is therefore unclear why this very similar combination of transgenes did not work in the tobacco combinatorial experiment.

For line 287A-40, the highest transcript levels were found for transgene *FpGDC-H*, followed by *AtTPT*, *AtcyFBPase*, and *Pyc6*. In a previous report, the gene coding for the Arabidopsis H-protein of GDC (*AtGDC-H*) was introduced in tobacco under the control of the leaf-specific promoter *St-LS1* or the constitutive promoter *CaMV35S* [71]. The *St-LS1::AtGDC-H* overexpressors showed improved carbon assimilation and increased height, leaf area, and dry weight biomass in glasshouse and field conditions. In contrast, the constitutive overexpression of *AtGDC-H* was detrimental for growth and was associated with decreased leaf area, and reduced growth rates [71]. The authors hypothesised that large amounts of AtGDC-H were affecting plant growth due to an increased allocation of carbon towards starch accumulation in leaves. This is based on the fact that a negative correlation between biomass and starch levels has been found in Arabidopsis, with accessions investing less in starch having fastest growth [254]. Also, slow growth mutants accumulate transitory starch as they are unable to degrade it completely at night [255, 256]. In the combinatorial transgenic lines, *FpGDC-H* was placed under the control of the *CaMV35S* promoter. Therefore, although line 287A-40 did not show growth reductions, this transgene could have impacted negatively on the potential benefit of the other transgenes in this line.

Lines 111A-10 and 142A-10 had abundant transcript levels for transgenes *AtPetC* and *Pyc6*, and *Pyc6*, *EcPP*, and *AtSUC2*, respectively. As was the case in line 287A-40, it is not evident why these transgene combinations did not lead to improvements in photosynthetic capacity or plant growth.

Three lines, 35A-20, 111A-10, and 287A-40, rather than showing improved photosynthetic capacity, instead showed signs of photoinhibition, as indicated by significant reductions in F_v'/F_m' and increases in NPQt. One hypothesis that could explain this is that photoinhibition occurred in response to an increased source activity in the combinatorial transgenic plants, mediated by the presence of excess

Cyt c_6 in the electron transport chain. It is possible that large amounts of Cyt c_6 are detrimental for photosynthetic capacity. For example, a reduction in plant growth was observed when *AtGDC-H* was constitutively overexpressed in tobacco [71],

4.4.3 A hypothesis for the photoinhibitory symptoms observed in the tobacco combinatorial transgenic lines

Photoinhibition is the term that describes the reduction in the efficiency of PS II in response to extended exposure to high light in photosynthetic organisms. It is generally associated with damage to the reaction centres of PS II, particularly subunit D1, and the subsequent photoprotective mechanisms that mediate their repair, such as the compensatory increase in thermal energy dissipation. The light conditions that the plants were exposed to in the experiment that photoinhibition was detected (up to 150 µmol m^{-2} s^{-1}) make it very unlikely that this was due to a stress response in response to strong light intensities, so the cause of photoinhibition must have been a different one. However, it is possible that the photoinhibition signs that the combinatorial lines showed were related to another sort of experimental variable.

Assuming that the transgenes were active and that they were responsible for the photoinhibitory effect, in this section I explore a hypothesis that could explain this response. One possibility is that the increased source activity mediated by the transgenes was not matched by transport and sink capacity. The link between photoinhibition and source-to-sink relationships was proposed by Adams *et al.* [257]. It is generally believed that photoinhibition leads to reductions in plant growth but photoinhibition was considered from a different point of view in this review. It was proposed that a reduction in the efficiency of PS II occurs as a consequence of limited plant productivity and not vice versa. A model of the source, export/transport, and sink continuum was presented in two different scenarios: (i) where the export of photoassimilates and their transport through the phloem is sufficient to meet source activity, and sinks can fully utilise them (balanced situation); and (ii) where source activity exceeds the capacities for transport and sink utilisation [257]. The second scenario would correspond to conditions where light or CO_2 are in excess. In that

situation, there is an insufficient sink activity that is unable to meet an elevated source activity. This has been shown to lead to the accumulation of carbohydrates in the leaf and downregulation of photosynthetic efficiency through a decrease in the activation state of RuBisCO [258]. This response can be reproduced by actively removing sinks (e.g. fruits), transferring plants from low to high light conditions, or feeding sugars through the stomatal apertures [257, 259]. Just like a sustained exposure to high light leads to a reduction of photosynthetic efficiency, a reduction in sink capacity can lead to the same response [259]. In line with the mechanism proposed by Adams *et al.* [257], an elevated source capacity in the combinatorial transgenic lines could have led to a down-regulation of photosynthetic efficiency, manifested by a photoinhibitory response, due to an insufficient transport or sink capacity. This mechanism would likely be mediated by a shift towards increased carbohydrate pools, which can cause feedback inhibition of photosynthesis [161].

The increased source capacity could potentially have been mediated by high levels of the algal Cyt c_6, which could have negatively affected the chloroplast electron transport chain and led to a photoprotective response. The overexpression of a Cyt c_6 did not lead to photoinhibition in the original work where *Pyc6* was introduced in Arabidopsis [76]. In that case, both F_v/F_m and F_v'/F_m' remained unchanged in the transgenic plants with respect to the controls [76]. Nevertheless, the combinatorial transgenic lines showed expression levels that, if correlated with increased content of the functional protein, would be higher than those of the Arabidopsis plants, where the protein content of Cyt c_6 was reported to be about 1.2 fold relative to that of plastocyanin. Line 142A-10 did not show these symptoms of photoinhibition, even though *Pyc6* was present at the genomic and transcript levels. A plausible explanation for this, in line with photoinhibition having been caused by an increased source activity, is that the transcript levels of *Pyc6* (533-fold with respect to the WT) were matched by those of the phloem-localised sucrose/H^+ importer *AtSUC2* (737-fold). It follows that, assuming that the expression levels of these transgenes were matched by the presence of functional, active proteins, the increase in source activity was matched by an increased transport capacity

mediated by a stimulation of sucrose phloem loading. Line 287A-40 was positive for the presence and expression of the passive sucrose transporter *AtSWEET11*, but its transcript abundance was much lower than that of *Pyc6* (218-fold with respect to the WT against 3453-fold, respectively). However, this is an entirely speculative proposal, and it remains unclear why line 142A-10 did not show the same signs of photoinhibition that the other combinatorial transgenic lines showed.

It would be expected that, if photoinhibition originated via an increased source activity that exceeded transport or sink capacity, carbohydrates would accumulate in the leaves. This was not the case in the combinatorial transgenic lines when metabolite accumulation was assessed using samples from the high light primary screen, where soluble sugars and sugar alcohols remained unchanged or were reduced with respect to the controls (Figure 4.3). Nevertheless, no signs of photoinhibition were detected in that experiment. A shift in the carbon and nitrogen ratios seemed to have occurred in some lines, which seems reasonable given the close relationship between photorespiration and nitrogen assimilation [260]. It is also possible that sugars were accumulating elsewhere in the plant, such as in the stem, as suggested in Chapter 3, or that a different form of carbohydrates that were not detected in the GC-MS was accumulated in the leaves, such as starch. Increased starch content would be in accordance with the accumulation of the algal Cyt c_6 [76], and the excessive accumulation of GDC-H [71].

The combinatorial transgenic lines were found to show signs of increased photorespiratory activity along with photoinhibition. Both glycine and the Gly/Ser ratio were found to be significantly increased in those three combinatorial transgenic lines, 35A-20, 142A-10, and 287A-40, with respect to both controls. The photorespiratory intermediate glycerate was significantly increased in line 287A-40. An increased concentration of photorespiratory metabolites, such as glycine and glycerate, and an increased Gly/Ser ratio, are indicative of increased flux through the photorespiratory pathway. The link between photorespiration and photoinhibition was made early on in photosynthesis research, placing photorespiration at the core of photoprotection

for its role in the dissipation of excess excitation energy [261]. Thus, photorespiration is considered a mechanism to prevent and mitigate photoinhibition.

Having explored the possibility that the photoinhibitory response was related to the transgenes and to a lack of transport or sink capacity, it is important to stress that this is just a hypothesis and the cause for photoinhibition in the combinatorial transgenic lines remains unclear.

4.4.4 Improving source and/or sink capacity

It is well established that manipulations of both source and sink strength on their own can lead to improvements in yield. The case for improving source capacity has been stated throughout Chapters 1 and 3 of this thesis. Despite the selected transgenic combinatorial lines not having shown improvements in photosynthetic capacity or growth despite the individual transgenes having been shown to be beneficial on their own, there is ample evidence that improving source capacity via improved photosynthesis can improve yield. I argue that the difference between this and previous studies lies in the transformation technique. Most of the latest efforts to improve photosynthetic efficiency rely on *Agrobacterium*-mediated transformation as the preferred transgene delivery method for the generation of plants with low copy number [24, 262, 263]. In contrast, biolistic transformation naturally generates plants with complex genetic loci. Although the structure of the transgenic loci was not assessed in the combinatorial transgenic lines, previous reports involving biolistic transformation frequently show high transgene copy numbers and transgene rearrangements (see section 4.3.3. above). Compared to *Agrobacterium*-mediated transformation, biolistic transformation leads to an increased prevalence of transgenes with higher copy number and a reduced proportion of intact genes [264]. As detailed in section 4.3.3., and argued in [245, 246], this complexity is not necessarily negative. The use of combinatorial co-transformation has been highly successful in generating plants that accumulate secondary metabolites in recent years [147, 148], where the accumulation of the metabolite of interest in large quantities was sought after. In contrast, it is possible that, in this work, the use of

combinatorial co-transformation for the manipulation of central metabolism, which is inherently reluctant to manipulation [125], resulted in transgene interference effects, possibly mediated by *Pyc6*. This does not strictly mean that the introduced combinations would not potentially be successful, but that a different approach should be undertaken to test them, perhaps using conventional transgene stacking.

Regarding sink utilisation, numerous studies have shown its crucial role in determining crop yield, as reviewed in [39, 161]. However, a growing body of literature suggests that the greatest increases in yield will be achieved by optimising source-sink interactions and stacking the benefits achieved in both increased source capacity and sink utilisation [5, 39, 43, 161, 265]. This becomes apparent by considering the plant source-sink system with an analogy to metabolic control theory [128]. Increasing metabolic flux in the sources is likely to shift the balance towards a limitation in sink capacity, and vice versa, as sources and sinks co-limit yield. In fact, it has been suggested that it is sink strength that limits source activity [266]. This can be exemplified with long-term CO_2 enrichment experiments, which have demonstrated how photosynthesis is down-regulated as the growing season progresses, leading to increases in yield that are lower than expected from theoretical approaches and observations made in closed environments [4]. In this context, the usefulness of CO_2 enrichment experiments has been two-fold. Firstly, they have shown that source capacity is partially limiting under the current atmospheric CO_2 concentrations. Secondly, they have highlighted that the improvement of photosynthesis and its translation into yield are limited by sink strength. Yield increases linearly with increasing CO_2 concentrations, but eventually reaches a plateau, which corresponds to limitations in the capacity of the sinks to utilise the photoassimilates and nutrient uptake, usually nitrogen [267]. This was demonstrated through the use of two varieties of different sink strength in a tobacco field experiment with varying CO_2 concentrations. The Mammoth variety, which is characterised by a high sink capacity, outperformed Petite Havana in terms of biomass, which in Mammoth was three-fold that of Petite Havana. More importantly, the down-regulation of photosynthesis that is observed at the end of

the growing season in Petite Havana was minimised in the Mammoth cultivar and was ameliorated by the application of nitrogen-rich fertiliser [267].

Another line of evidence in support of efforts to manipulate source and sink tissues simultaneously was provided by a push-pull intervention in potato. Initially, sink strength was enhanced by overexpressing two chloroplast transporters in tubers, a glucose 6-phosphate/phosphate and an adenylate transporter [118]. Source activity was then stimulated by super-transforming these lines with an overexpression construct for the cytosolic *EcPPase* in the mesophyll (using the same construct and promoter combination introduced in the combinatorial transgenic lines) or downregulating the leaf *AGPase*. Both strategies resulted in increased sucrose export from the leaves and a doubling of starch accumulation in tubers [118].

The issue of cultivar choice was considered at the time of performing the tobacco biolistic combinatorial co-transformation. The use of the Mammoth cultivar was contemplated, but it was then dismissed due to the lack of evidence for its successful use in biolistic transformation and the subsequent tissue culture stages. The Samsun cultivar was considered, but compared to Petit Havana it has a longer generation time (4–6 weeks longer). As a result, Petit Havana was chosen to avoid potential issues with self-shading in Samsun and because of the time constraints of the project. The use of Petit Havana is strongly supported by previous experiments where the increase of source capacity from this cultivar led to increases in yield [23, 24, 71]. However, a cultivar with a higher sink strength could be considered for future experiments.

Pot size has an influence in sink strength, with larger pots having been shown to lead to increased growth, as it represents increased nutrient availability [240]. Therefore, independent of the tobacco cultivar, the size of the pot could have negated the increased source capacity induced by the presence of the transgenes.

4.5 Conclusions

The use of biolistic combinatorial co-transformation was invaluable for the generation of a combinatorial library with a range of metabolic phenotypes. The selected combinatorial transgenic lines showed a variety of transgene combinations. It is unclear why these combinations failed to improve photosynthetic efficiency, but it is possible that transgene interference effects mediated by *Pyc6* negated the potential benefits of the different transgenes. In addition, some of the selected combinatorial transgenic lines showed certain signs of increased photorespiratory activity and photoinhibition, which could potentially be related to a lack of sufficient transport and/or sink capacity. However, this is just a hypothesis that assumes that the transgenes were related to the photoinhibitory response, but it remains unclear why this occurred. To test this hypothesis, it would be important to (i) perform a determination of sugar content, including soluble sugars and starch, in the leaves of the combinatorial transgenic lines, grown in conditions where photoinhibition is shown; (ii) determine transgene copy number and the structure of the genetic locus in each of the lines. In the longer term, a growth experiment with an increased pot size would help determine if insufficient sink strength could have been the cause for the combinations of transgenes not being successful. Likewise, super-transformation of the selected combinatorial lines with transgenes related to phloem unloading and photoassimilate utilisation in sink tissues would be useful, or the same transgene combinations could be tested in a tobacco cultivar with higher sink strength.

Chapter 5

In silico-guided metabolic engineering of photosynthetic efficiency

Contents

5.1 Aims and objectives

This chapter explores the implementation of computational predictions for increased photosynthetic efficiency in tobacco. The objectives of the work described in this chapter were:

1. To identify potential transgene targets suitable for inducing changes in the fluxes of energy and reducing equivalents through chloroplasts and mitochondria *in planta*, based on the modelling by [182].

2. To characterise Arabidopsis transgenic plants overexpressing one of the selected targets, the mitochondrial fission regulator FIS1A, in terms of mitochondrial volume and respiratory capacity.

3. To generate tobacco plants carrying a multigene construct comprising the selected transgene targets from Objective 1 above.

4. To characterise the multigene transgenic tobacco plants in terms of relative transcript levels of the target genes, the status of the redox couple $NADH/NAD^+$ in the cytosol, respiratory and photosynthetic capacity, and plant growth.

5.2 Introduction and rationale

The previous two chapters have focused on a combinatorial multigene engineering approach for improved plant productivity using empirical targets. In this chapter, computationally-predicted targets were introduced in tobacco as part of a Golden Gate multigene construct.

A stoichiometric model of primary metabolism in leaves was constructed containing 647 reactions and including subcellular compartments and transport processes [182], as described in Section 1.2.11 in Chapter 1. This model explored metabolic and energetic interactions between chloroplasts and mitochondria. It was used to identify system-level metabolic engineering targets whose manipulation could lead to an improved overall leaf performance (measured as export of sugars and amino acids to the phloem) through an enhanced energy balance.

Based on the Shameer model [182], a metabolic engineering strategy was designed to result in: (i) the suppression of the mitochondrial malate dehydrogenase (mMDH) to prevent NADH from being used in the interconversion of malate and oxaloacetate, (ii) an increased capacity for mitochondrial ATP synthesis to fully utilise the increased NADH availability, (iii) an increased chloroplast malate valve NAD(P) shuttle capacity, and (iv) the suppression of GAPC, which is a key chloroplast source of ATP in the cytosol. Subsequently, transgene targets were identified for the implementation of the computational predictions *in planta*. Figure 5.1 shows a schematic representation of the targets selected to induce these changes in a mesophyll cell. Table 5.1 elaborates on the rationale behind the choice of targets.

Suppressed export of reducing equivalents from mitochondria

The mMDH catalyses the last step of the TCA cycle: the interconversion of malate to oxaloacetate, accompanied by the reduction of NAD^+ to NADH. During the reduction of oxaloacetate to malate, mMDH supplies GDC with NAD^+ for the conversion of glycine to serine in photorespiration. Besides, mMDH contributes to the shuttling of reducing power out of mitochondria to support photorespiratory flux as part of the malate/oxaloacetate shuttle [187, 268].

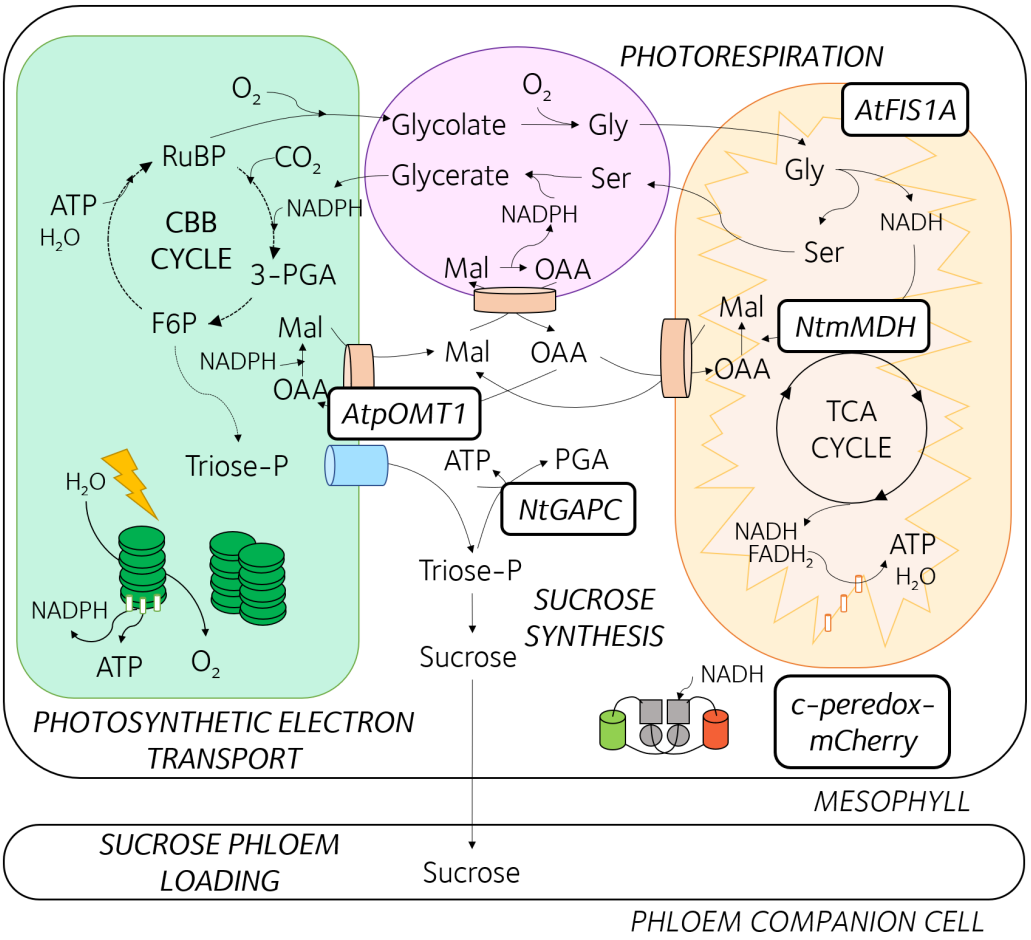

Figure 5.1: Selected transgene targets and metabolic pathways for the implementation of modelling predictions in tobacco Schematic representation of a mesophyll cell and a phloem companion cell, depicting selected transgene targets and related metabolic pathways. Abbreviations: *AtFIS1A*, mitochondrial fission regulator; *AtpOMT1*, plastidic 2-oxoglutarate/malate transporter; *c-Peredox-mCherry*: cytosolic fluorescent sensor of NADH/NAD^+ ratio; *NtGAPC*, cytosolic glyceraldehyde 3-phosphate dehydrogenase; *NtmMDH*, mitochondrial malate dehydrogenase.

Analyses of antisense tomato mutants in mMDH under long-day conditions showed reduced flux through the TCA cycle and decreased respiratory rate, while photosynthesis was improved and aerial growth increased [269]. The authors hypothesised that the improvement in photosynthesis was a compensation for the reduction in ATP production through photosynthesis, with ascorbate playing an important regulatory role. Further investigation of these mutants showed that the phenotype of the tomato mutants under short-day conditions was different, with

plants displaying dwarfism [270]. This suggested that the reduction of the light period meant that the plants were not able to compensate for the reduction in TCA cycle activity through increased photosynthetic activity.

In Arabidopsis, two genes code for mitochondrial isoforms of the NAD-dependent mMDH, termed as *mMDH1* (AT1G53240) and *mMDH2* (AT3G15020). The phenotype in the double knockout mutant *mmdh1mmdh2* showed increased respiratory rates, lower photorespiratory flux, lower net CO_2 assimilation, and slower growth [268]. The altered photorespiratory phenotype was confirmed in [187], where the mutants showed a significant growth reduction under photorespiratory conditions and reduced shuttling of NADH between mitochondria and peroxisomes. More recently, an Arabidopsis *mMDH* mutant was found to show a reduced plant size [271].

Despite the contrasting phenotypes of the range of mMDH mutants, these studies highlight the role of mMDH as a major regulator of respiration in plants and as an important link between respiration, photorespiration, and photosynthesis. The Shameer model [182] predicted that mitochondria using all of the NADH generated in the photorespiratory steps to generate ATP in the respiratory chain was more efficient than other routes to generate ATP such as cyclic phosphorylation, as it has a higher yield of ATP per NAD(P). In this scenario, mitochondrial photorespiratory NADH would no longer be exported to support the peroxisomal steps of photorespiration and the model predicted an increased activity of the chloroplast malate valve instead. A way of preventing export of NADH from mitochondria would be the suppression of mMDH. In this thesis, the genes encoding mMDH in tobacco were targeted via antisense silencing.

Increased mitochondrial accumulation

Given the difficulty of engineering the mitochondrial oxidative phosphorylation pathway due to the high complexity of the components, promoting an increased mitochondrial number via the overexpression of regulators of mitochondrial fission in leaves was conceived as a more feasible approach of bringing about an increased respiratory capacity.

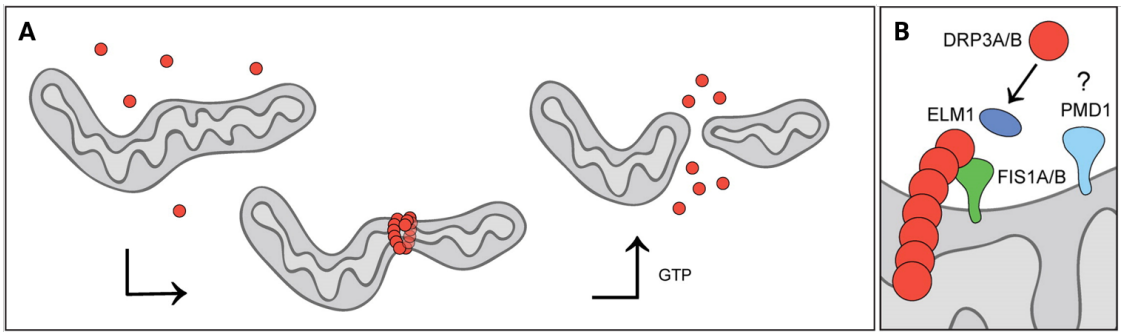

Figure 5.2: Mitochondrial fission in plants as per [277]. **A**. Oligomerisation of the master mediator DYNAMIN-RELATED PROTEIN3 (DRP3) into spirals around mitochondrial fission sites. **B**. Detail of accessory proteins involved in plant mitochondrial fission in the outer mitochondrial membrane: FISSION1 A and B (FIS1A/B), ELONGATED MITOCHONDRIA1 (ELM1) and PEROXISOMAL AND MITOCHONDRIAL DIVISION1 (PMD1).
Modified by permission from Elsevier (`https://www.sciencedirect.com/journal/biochimica-et-biophysica-acta-bba-molecular-cell-research`): Elsevier, Biochimica et Biophysica Acta (BBA) - Molecular Cell Research, (*Recent advances into the understanding of mitochondrial fission*, Kirstin Elgass, Julian Pakay, Michael T. Ryan, Catherine S. Palmer), Copyright © 2013 Elsevier.

New mitochondria arise from the division of pre-existing ones through fission. In plants, the GTPase mechanoenzymes termed DYNAMIN-RELATED PROTEIN3 A and B (DRP3A/B) [272, 273] are the main regulators of mitochondrial fission. They oligomerise around mitochondria and constrict the organelle until two daughter organelles are formed (Figure 5.2). DYNAMIN-RELATED PROTEINs are regulated by their interaction with accessory proteins (Figure 5.2). Specifically, DYNAMIN-RELATED PROTEIN 3 associates with the outer mitochondrial membrane anchor proteins FISSION1 A (FIS1A, also known as BIGYIN) and FISSION1 B (FIS1B) [273, 274]. ELONGATED MITOCHONDRIA1 (ELM1) regulates this interaction, allowing a correct localisation of DYNAMIN-RELATED PROTEINs to fission sites [275]. Besides, PEROXISOMAL AND MITOCHONDRIAL DIVISION1 (PMD1) has been postulated to have a role in fission independent of the above elements [276].

Studies in which the genes coding for DYNAMIN-RELATED PROTEIN3 A and B [272], FIS1A/B [274] or PEROXISOMAL AND MITOCHONDRIAL DIVISION1 [275] were ectopically expressed reported an increased mitochondrial abundance, suggesting that the frequency of mitochondrial fission depends on the abundance of

these regulators. In contrast to the results for DYNAMIN-RELATED PROTEIN3 A and B [272] and PEROXISOMAL AND MITOCHONDRIAL DIVISION1 [275], in which mitochondrial number increased to such an extent that the organelles accumulated in large aggregates of abnormal morphology, the overexpression of FIS1A [274] led to a significant increase in mitochondrial number with normal appearance spread across the cytosol. Additionally, the FIS1A/B overexpression lines did not show any differences in the growth phenotype with respect to the wild type, as opposed to the dwarfism reported for PEROXISOMAL AND MITOCHONDRIAL DIVISION1 [275]. Importantly, the use of the red-fluorescent dye MitoTracker Red [274], which stains mitochondria in live cells and whose accumulation is dependent on membrane potential, suggested the presence of an active mitochondrial electron transport chain in the additional mitochondria. As opposed to FIS1A, FIS1B was shown to be involved in cell cycle-associated replication of peroxisomes in Arabidopsis [278]. Besides, peroxisomal aggregation was reported to be more apparent in *FIS1B*-overexpressors when analysing *FIS1A*- and *FIS1B*-overexpressing plants [274], which suggests that fission is more complete in *FIS1A*- than in *FIS1B*-overexpressors. For these reasons, the Arabidopsis gene coding for FIS1A (AT3G57090) was chosen to be included in the multigene construct for this thesis.

Increased chloroplast malate valve capacity

Malate/oxaloacetate shuttles allow the indirect transport of reducing power between compartments. In chloroplasts, the malate valve is key to maintaining the redox balance as an exporter of excess reductant from the chloroplast [185, 279]. This redox shuttle consists of a chloroplast inner envelope malate/oxaloacetate transporter, and chloroplast and cytosolic isoforms of malate dehydrogenase [280]. The chloroplast envelope transporter responsible for malate/oxaloacetate and 2-oxoglutarate/malate exchange was identified as pOMT (OMT1/DiT1 in Arabidopsis, AT5G12860) [188, 190]. Arabidopsis mutants deficient in this transporter showed symptoms of photoinhibition and impaired growth due to the accumulation of reactive oxygen species in the chloroplast under high light conditions, which inhibit the repair of the

D1 protein at PS II [188]. Severe reductions in plant size were observed in T-DNA insertion mutants of pOMT, the *som787-2* Arabidopsis mutant of programmed cell death [271]. Under high light conditions, Arabidopsis mutants showed increased accumulation of reactive oxygen species and photoinhibition [280].

In this work, the Arabidopsis pOMT was overexpressed to increase the capacity for the chloroplast malate valve NAD(P) shuttle.

Suppressed export of ATP from chloroplasts into the cytosol

The cytosolic phosphorylating GAPC catalyses the production of 3-phosphoglycerate, ATP and NADH from triose-phosphates [190]. Knock-out and antisense Arabidopsis mutants in GAPC1 show reduced growth and respiratory capacity [281]. In contrast, no phenotypic differences were observed in constitutive antisense GAPC mutants in potato [282]. The analysis of Arabidopsis GAPC double mutants, where both the cytosolic and plastidic versions of GAPC were knocked-out, showed root defects and dwarfism [283]. Surprisingly, a different set of Arabidopsis double mutant T-DNA insertion lines did not display phenotypic changes, except for stomatal alterations that made the double mutants less responsive to water deficits, and that were related to GAPC's moonlight role, where GAPC interacts with phospholipase D in the transduction of reactive oxygen species signals [284].

GAPC has been identified as the main source of cytosolic ATP in conditions with high ATP/ADP ratios in the chloroplast [285, 286]. In this work, in an attempt to trap the ATP that is produced in the photosynthetic electron transport chain, for its use in the CBB cycle, GAPC was knocked-down using an antisense construct.

Ratiometric monitoring of cytosolic redox state

In addition to the cited genes, a genetically-encoded metabolite sensor was included to monitor the metabolic status of the transgenic plants. The ratiometric sensor c-Peredox-mCherry reports the status of the redox couple NADH/NAD^+ in the cytosol [198]. This genetically encoded fluorescent biosensor is based on a circularly permuted fluorescent protein, the blue-green fluorescent protein T-Sapphire (Ts),

and a bacterial NADH and NAD^+-binding protein, T-Rex. When the biosensor interacts with NADH, the conformational coupling between fluorescence and binding takes place, with an increase in the fluorescence of Ts, while the binding of NAD^+ has no impact on the fluorescence emission intensity. The sensor includes an additional fluorescent protein, mCherry (mC), which allows for internal fluorescence normalisation. Therefore, the ratio of fluorescence emission of Ts over mC provides a relative, ratiometric measurement of the concentration of NADH to NAD^+ in the cytosol.

The cytosolic localisation of c-Peredox-mCherry allows for the integration of the metabolic redox dynamics and the visualisation of NAD coupling between cell compartments. c-Peredox-mCherry has been used to determine dynamic changes in NADH/NAD^+ in different cells and tissues in Arabidopsis in response to light, inhibitors of mitochondrial respiration, sugar supply, and elicitors [221]. The introduction of this sensor allowed monitoring of the redox state of the transgenic plants, integrating the intended changes in fluxes of reducing equivalents brought about by the different transgenes.

Table 5.1: Rationale for selected transgenes used for *Agrobacterium* transformation of tobacco. Details of manipulations are provided, including target manipulations, strategy (OE, overexpression; KD, knock-down), transgene names and products, plant species, and their biological function.

Manipulation	Strategy	Transgene	Transgene product	Species	Functional description	References
Plastidic ATP export	KD	*GAPC*	Glyceraldehyde 3-phosphate dehydrogenase	Tobacco	Cytosolic glyceraldehyde phosphate dehydrogenase, involved in the production of 3-phosphoglycerate, ATP, and NADH from triose-phosphates.	[285, 286]
Mitochondrial NADH export	KD	*mMDH1*	Mitochondrial malate dehydrogenase	Tobacco	Mitochondrial malate dehydrogenase, catalyses the oxidation of malate to oxaloacetate, coupled to the generation of NADH	[188]
Mitochondrial number	OE	*FIS1A*	Fission 1A	Arabidopsis	Outer mitochondrial membrane anchor protein, involved in mitochondrial biogenesis	[274]
Redox biosensor	OE	*c-Peredox-mCherry*	c-Peredox-mCherry	-	Fluorescence reporter of cytosolic NADH/NAD^+ ratio	[198]
Plastidic malate valve capacity	OE	*pOMT1*	Dual oxaloacetate and 2-oxoglutarate/malate transporter	Arabidopsis	Plastidic bifunctional transporter: malate/oxaloacetate transporter and 2-oxoglutarate/malate transporter, as part of the malate valve.	[190, 280]

5.3 Results

5.3.1 Generation of Arabidopsis transgenic plants overexpressing the fission regulator *AtFIS1A*

Although it has been previously shown that the overexpression of *FIS1A* leads to increased mitochondrial number in Arabidopsis [274], research to date has not yet determined whether this leads to an overall increase in total respiratory capacity. This study, therefore, set out to assess the effect of *FIS1A* overexpression in respiratory capacity. Transgenic Arabidopsis plants overexpressing the gene coding for the outer mitochondrial membrane FIS1A protein were generated.

The *AtFIS1A* gene was amplified by PCR using specific primers on Arabidopsis cDNA (Figure 5.3). The purified DNA was cloned into a Gateway entry vector pCR8/GW/TOPO using TA cloning and then placed under the control of the constitutive promoter *CaMV35S* in a pK7WG2 backbone vector [202] using Gateway recombination (Figure 5.4.A). Selected colonies were confirmed via colony PCR and subsequently subjected to Sanger sequencing. The confirmed construct *pK7WG2-AtFIS1A* was transformed into *Agrobacterium* and then into Arabidopsis (Col-0 accession) using the floral dip method [210]. Sequencing results for *pCR8/GW/TOPO-AtFIS1A* and *pK7WG2-AtFIS1A* are provided in Appendix E.

The resulting T_1 seed was germinated on kanamycin-containing medium and conventional PCR was used on genomic DNA to identify successfully transformed progeny. Two sets of primers were used to distinguish between the endogenous version and the introduced version of *AtFIS1A*. In the first pair, primers were specific to the *CaMV35S* promoter region (forward primer) and the insert *AtFIS1A* (reverse primer), with an expected size of amplification of 937 bp (Figure 5.4.A). Both primers were specific to the *AtFIS1A* coding sequence in the second pair.

Amplification with the first pair of primers produced a band of the expected size in all transgenic lines, and no amplification in the non-transformed control (Figure 5.4.B). As predicted, the second pair led to amplification in both the transgenic and the control plants (Figure 5.4.C). The size of the band in the Col-0 control was

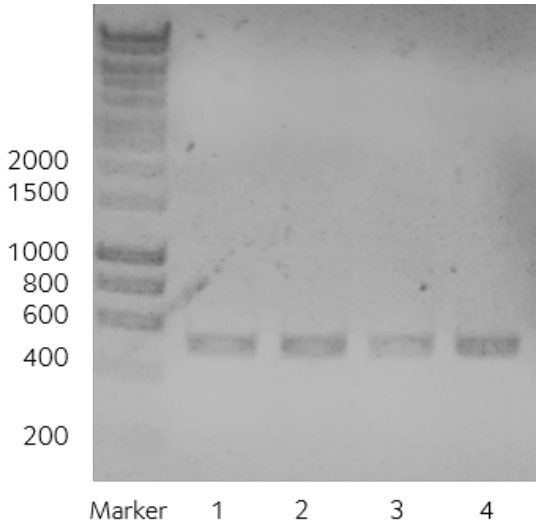

Figure 5.3: PCR amplification of the Arabidopsis gene *AtFIS1A*. PCR amplification of the *AtFIS1A* (expected size 513 bp) gene using *A. thaliana* cDNA. Separation of PCR products (1-4) according to their molecular weight through DNA electrophoresis (1% agarose TAE gels). Size determination according to molecular size marker Hyperladder 1kb (Bioline, London, UK); 200-, 400-, 600-, 800-, 1000-, 1500, and 2000-bp markers are indicated.

bigger than that of the transgenic plants in terms of molecular weight, which can be explained by the presence of introns in the native version of *AtFIS1A*. In the transgenic plants, the strongest band was that of the exogenous version of *AtFIS1A*, and a smeared, weak band could be seen for the endogenous amplicon. Transgenic lines, confirmed for the presence of the *pK7WG2-AtFIS1A* construct, were allowed to self-pollinate and the resulting T_2 seed was used to perform further analyses.

5.3.2 No changes to mitochondrial accumulation or dark respiration could be detected in the Arabidopsis *AtFIS1A* overexpressors

Mitochondrial number was assessed in Arabidopsis plants overexpressing *AtFIS1A* using confocal laser scanning microscopy. The cationic fluorophore tetramethylrhodamine methyl ester (TMRM) and the green-fluorescent dye MitoTracker Green were used to label mature leaves from WT and transgenic lines. TMRM is a membrane potential-dependent probe of functioning mitochondria. As a positively charged molecule, it accumulates within mitochondria in inverse proportion to

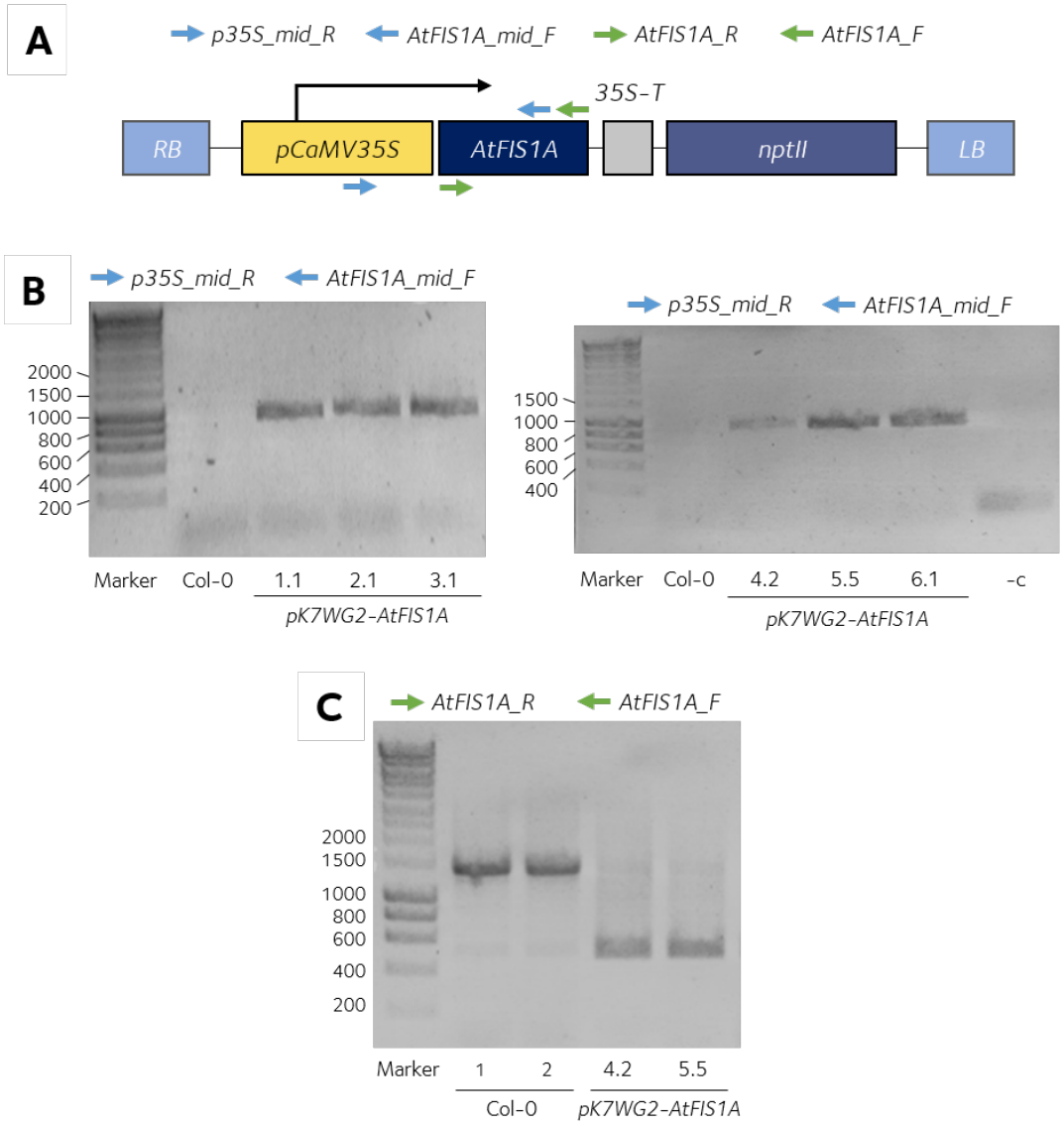

Figure 5.4: Introduction of the *pK7WG2-AtFIS1A* overexpression construct in Arabidopsis. A. Schematic representation of the T-DNA part of the overexpression construct *pK7WG2-AtFIS1A*. The *AtFIS1A* transgene was placed under the control of the constitutive promoter *CaMV35S* and the *CaMV35S* terminator in a pK7WG2 plasmid backbone. The *nptII* gene, conferring kanamycin resistance, was included as a plant selectable marker. The left (LB) and right (RB) borders for *Agrobacterium*-mediated T-DNA transfer are indicated. Primers used to confirm positive Arabidopsis transformants are indicated with blue and green arrows. **B, C.** Confirmation of Arabidopsis transformants carrying the *pK7WG2-AtFIS1A* construct via PCR amplification. Amplifications were done using genomic DNA from four-week-old control (Col-0) and transformed (*pK7WG2-AtFIS1A*) Arabidopsis plants, using (**B**) primers specific to the *CaMV35S* promoter (*p35S_mid_R*) and the *AtFIS1A* gene (*AtFIS1A_mid_F*, expected amplicon size 937 bp) and (**C**) primers specific to the *AtFIS1A* gene (*AtFIS1A_F* and *AtFIS1A_R*, expected amplicon size 513 bp). Different numbers indicate independent lines. Separation of PCR products according to their molecular weight through DNA electrophoresis (1% agarose TAE gels). Size determination according to molecular size marker (ladder) HyperLadder 1kb (Bioline, London, UK).

mitochondrial membrane potential according to the Nernst equation. MitoTracker Green possesses a reactive chloromethyl group that forms a covalent attachment with free thiol groups of cysteine residues in the matrix of active mitochondria.

Fluorescent dye accumulation was determined optically by confocal microscopy in the T_2 generation. The confocal microscopy images showed co-localisation of TMRM and MitoTracker Green. No changes to mitochondrial accumulation of the dyes could be observed in the *35S::AtFIS1A* overexpression plants with respect to the non-transformed plants. The mitochondrial morphology was similar to that reported previously, with an increased number of regular-sized mitochondria being spread across the cytosol [274]. Figure 5.5 shows a representative example of the images captured for transformed and control plants. Given that TMRM is a membrane potential-dependent fluorescent dye and that MitoTracker binds to active mitochondria only, their accumulation in both the non-transformed and the *35S::AtFIS1A plants* suggests that these were functional mitochondria.

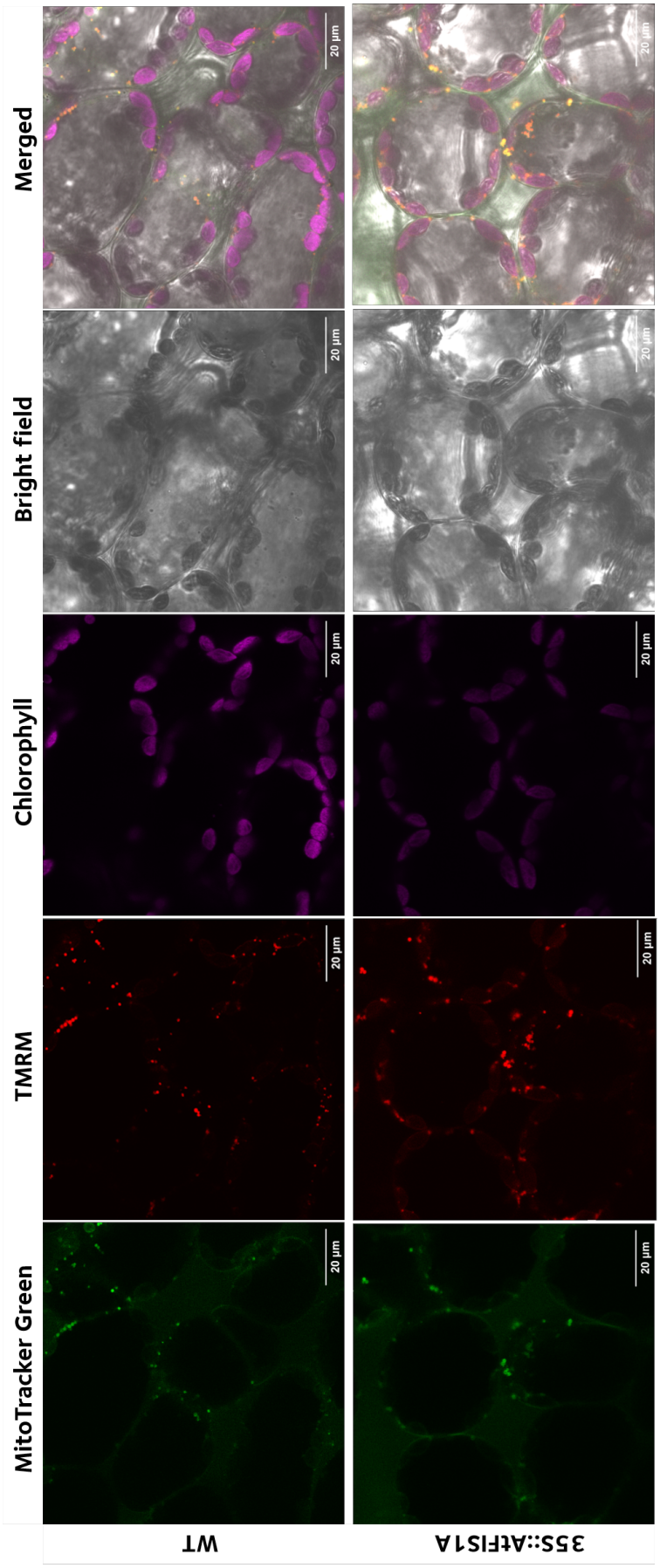

Figure 5.5: Confocal laser scanning microscopic images of leaf mesophyll cells from Arabidopsis WT and *pK7WG2-AtFIS1A* overexpression lines in the T_2 generation. Mature leaves from four-week-old plants were infiltrated with MitoTracker Green and TMRM and incubated for a minimum of three hours before imaging. Transgenic (*35S::AtFIS1A*, line 3.1) and WT lines are represented. Images are representative of eight transgenic ($n = 8$) and two control lines analysed in triplicate.

Dark leaf respiration was evaluated to analyse the mitochondrial respiratory capacity of the Arabidopsis *AtFIS1A* overexpression lines in the T_2 generation. Oxygen consumption rates of leaf discs from mature leaves of *AtFIS1A* transformants and non-transformed controls were measured 3-4 h into the dark phase of the photoperiod using a liquid phase Clarke-type oxygen electrode system. To avoid restrictions in respiration rate due to oxygen consumption being coupled to oxidative phosphorylation of ADP to ATP by the mitochondrial ATP synthase (known as adenylate control of respiration), the mitochondrial uncoupler FCCP was supplied exogenously. The addition of FCCP disturbs the proton gradient at the inner mitochondrial membrane by transferring protons into the mitochondrial matrix in an ATP synthase independent manner, disrupting the membrane potential. This releases the capacity of electron flow and maximises oxygen consumption by complex IV in the mitochondrial electron transport chain, which leads to an increase in OCR. The uncoupled leaf respiration rate demonstrated by the transgenic Arabidopsis lines did not differ from the WT ($P = 0.82$, one-way ANOVA, Table 5.2).

It is possible that the pooling of samples from different biological replicates (in this case, different plants of the same line) reduced the likelihood of detecting differences in OCR between lines, as argued in [219], since the different plants of each line could have been homozygous or heterozygous. It is also possible that despite mitochondria in the *AtFIS1A* overexpressing plants being functional, their overall rate of respiration was compensated for at a cellular level, in the absence of an obvious need to increase ATP production. From this, it followed that the introduction of additional manipulations in the multigene tobacco plants that were subsequently generated would potentially lead to significant changes in respiratory capacity.

Table 5.2: Uncoupled leaf dark respiration analysis of 4-week-old leaves of Arabidopsis WT and *pK7WG2-AtFIS1A* overexpression lines. Oxygen consumption rate (OCR, represented as nmol O_2 m^2 s^{-1}) measurements were performed in the Clark-type polarographic oxygen electrode DW1/AD Oxygraph Plus system (Hansatech Instruments, Norfolk, UK). Rates were determined using three leaf discs per plant, 10 minutes after the addition of the uncoupler of mitochondrial oxidative phosphorylation FCCP at a final concentration of 10 µM. Data are mean ± SE; $n = 4$ for the transgenic lines and $n = 8$ for the WT. One-way ANOVA was used followed by post hoc Tukey multiple pairwise comparisons test, $P = 0.82$.

Line		OCR (nmol O_2 m^2 s^{-1})
pK7WG2-AtFIS1A	1.1	7.34 ± 0.97
	1.9	7.54 ± 1.71
	1.11	9.11 ± 1.09
	2.1	9.02 ± 1.25
	2.2	8.52 ± 1.43
	3.1	6.75 ± 1.72
	3.3	7.04 ± 0.30
	4.2	8.34 ± 1.70
	4.7	8.80 ± 1.27
	5.2	9.36 ± 0.95
	5.5	6.76 ± 1.55
	6.1	8.31 ± 1.08
WT		8.79 ± 0.83

5.3.3 A multigene construct was designed to implement changes in the energetic and redox status of tobacco leaves

A multigene construct was designed and built based on the model predictions, carrying overexpression cassettes for *AtpOMT1*, *AtFIS1A*, and *c-Peredox-mCherry* and antisense, silencing cassettes for *NtmMDH* and *NtGAPC*. Golden Gate technology [142] and the MoClo Plant Parts Kit [144] were used to assemble the five independent transcription modules in a plant binary vector pAGM4723.

Transgenes were either amplified using PCR or artificially synthesised. Specific primers were designed to amplify antisense fragments of the tobacco genes *mMDH* and *GAPC* using the sequences *mRNA_92827_cds* and *mRNA_81739_cds*, respectively, retrieved from the Sol Genomics Network database. Two pairs of primers were designed for each gene and combined to amplify four distinct fragments of different sizes (Figure 5.6). The purified DNA amplicons 2 and 4 in the case of *NtmMDH*, and 1 and 2 in the case of *NtGAPC* (Figure 5.6), were used to build the level 0 Golden Gate modules. Transgenes *AtpOMT1*, *AtFIS1A*, and *c-Peredox-mCherry*

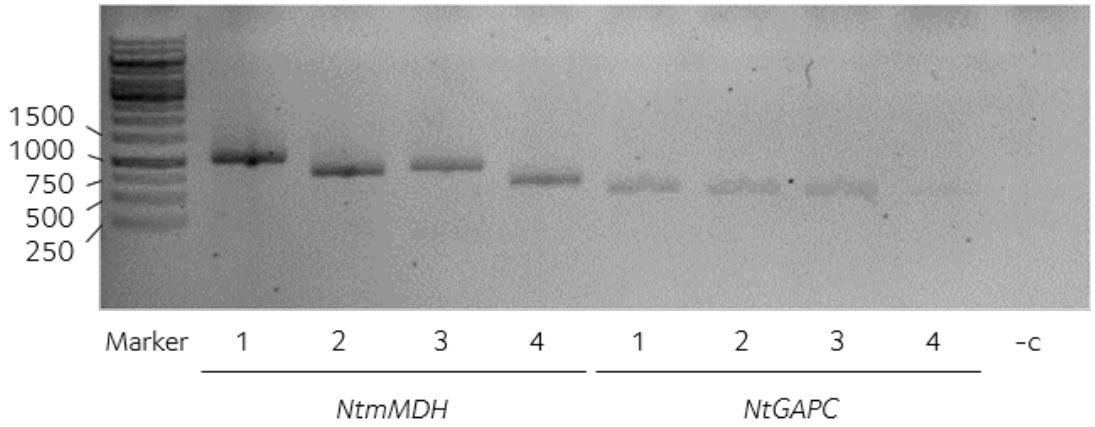

Figure 5.6: PCR amplification of fragments of the tobacco genes *NtmMDH* and *NtGAPC*. PCR amplification of fragments of *NtmMDH* and *NtGAPC* genes using tobacco cDNA. Expected sizes were as follows: *NtmMDH* fragment 1, 1064 bp; *NtmMDH* fragment 2, 838 bp; *NtmMDH* fragment 3, 899 bp; *NtmMDH* fragment 4, 673 bp; *NtGAPC* fragment 1, 571 bp; *NtGAPC* fragment 2, 525 bp; *NtGAPC* fragment 3, 502 bp; *NtGAPC* fragment 4, 456 bp. Separation of PCR products according to their molecular weight through DNA electrophoresis (1% agarose TAE gels). Size determination according to molecular size marker (Thermo Fisher Scientific, MA, USA); 250-, 500-, 750-, 1000-, and 1500-bp markers are indicated.

were synthesised in the pUC57 plasmid. Therefore, level 0 modules consisted of the purified antisense fragments for *NtGAPC* and *NtmMDH*, and synthesised versions of *AtpOMT1*, *AtFIS1A*, and *c-Peredox-mCherry*.

The level 0 modules were combined with specific promoters and terminators from the MoClo library for the Golden Gate assembly of the level 1 modules using the one-step one-pot protocol [141]. Each level 1 plasmid carried the antisense or intact coding sequence for the genes of interest under the control of constitutive or photosynthetic-specific promoters. These were combined to assemble the level 2 modules, carrying the six different transcriptional units in a single plasmid.

The multigene level 2 construct contained a total of six transcription cassettes (Figure 5.7), in the following order: *hygromycin-B* coding for hygromycin phosphotransferase, *NtGAPC* antisense, *NtmMDH* antisense, *AtpOMT1*, *AtFIS1A*, and *c-Peredox-mCherry*. The first five modules were introduced in reverse orientation, in ascending order of promoter strength, while the biosensor *c-Peredox-mCherry* was placed in forward orientation to prevent its high-strength promoter (double-enhancer *CaMV35S*) from affecting the transcriptional level of the other transgenes. An extra

level 2 construct was generated, containing *c-Peredox-mCherry* only, under the control of the *CaM35S* promoter, for the generation of tobacco plants that would have baseline fluorescence levels for the biosensor. Correct clones were identified via colony PCR after each assembly step. The sequence of all level 1 plasmids was confirmed by Sanger sequencing before proceeding to assemble the multigene, level 2 constructs. Sequencing results for level 2 plasmids are provided in Appendix E.

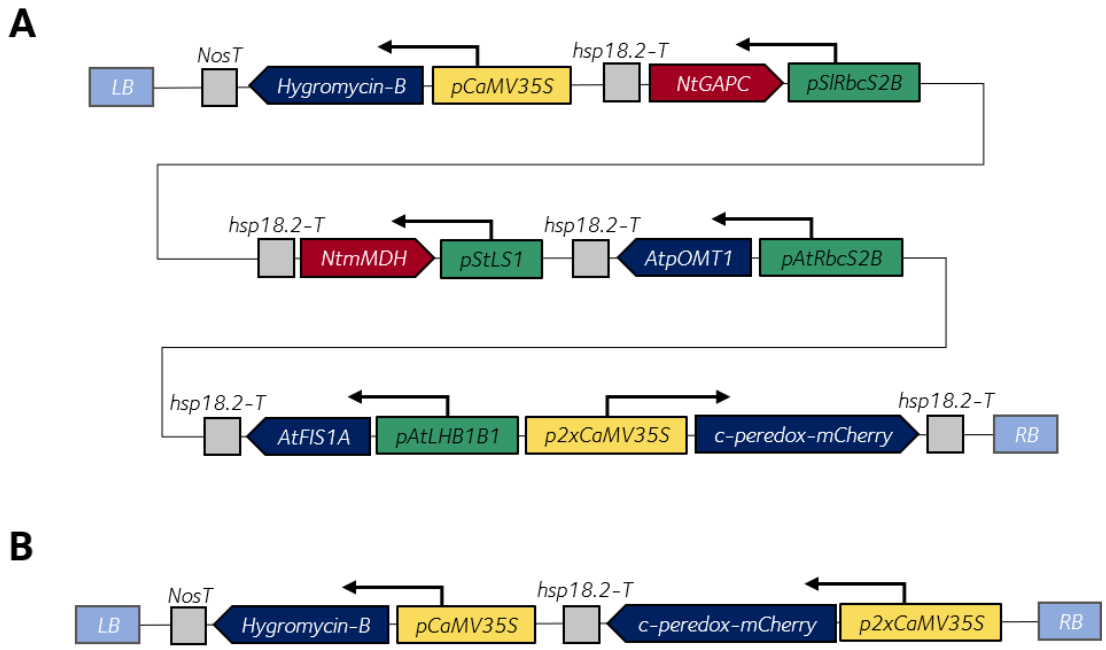

Figure 5.7: Schematic representation of the T-DNA part of the multigene constructs LS0201 and LS0207 introduced in tobacco via *Agrobacterium* transformation. A. Construct LS0201. **B.** Construct LS0207. **Promoters**: *pAtLHB1B1*, Arabidopsis light-harvesting chlorophyll-protein complex II subunit B1 promoter; *pAtRbcS2B*, Arabidopsis RuBisCO small subunit (*RbcS*) promoter 2B; *pCaMV35S*, CaMV 35S promoter; *p2xCaMV35S*, double-enhancer CaMV 35S promoter; *pSlRbcS2*, *S. lycopersicum* (tomato) RbcS2 promoter; *pStLS1*, *S. tuberosum* (potato) leaf and stem-specific promoter; Yellow colouring indicates constitutive promoters, green indicates photosynthetic-specific promoters. **Genes/fragments**: Arabidopsis fission regulator 1A (*AtFIS1A*); Arabidopsis plastidic 2-oxoglutarate/malate transporter (*AtpOMT1*); antisense fragment for the tobacco cytosolic NAD-dependent glyceraldehyde 3-phosphate dehydrogenase (*NtGAPC*); antisense fragment for the tobacco mitochondrial malate dehydrogenase (*NtmMDH*); hygromycin phosphotransferase (*Hygromycin-B*); Blue colouring indicates sense orientation, red indicates antisense orientation. **Terminators, grey colouring**: Arabidopsis heat shock protein 18.2 terminator (*hsp18.2-T)*; nopaline synthase terminator (*NosT*). **Other features**: the left (LB) and right (RB) borders for *Agrobacterium*-mediated T-DNA transfer are indicated in light blue colouring. **Backbone**: Golden Gate level 2 terminal acceptor, plant binary vector *pAGM4723*.

5.3.4 Tobacco plants carrying a multigene construct were generated via *Agrobacterium*-mediated leaf disc transformation

The recombinant plasmids LS0201 and LS0207 were introduced into tobacco using *Agrobacterium* via leaf-disc transformation [227]. Shoots were regenerated and hygromycin-resistant primary transformants (T_0 generation) with established root systems were transferred to soil and allowed to self-fertilise. Fifty-one lines were generated carrying the multigene construct LS0201 and 53 carrying LS0207 containing the biosensor only. No phenotypic differences were observed between the multigene and the biosensor-only lines during the regeneration of the primary transformants. Most lines were able to set seed normally, while a few produced empty capsules. The frequencies for sterility were four out of 51 lines (8%) with the multigene LS0201 construct and three out of 53 lines (6%) with the biosensor LS0207 construct. The progeny of the 47 multigene lines (LS0201) that produced viable seed was fully characterised.

5.3.5 The multigene tobacco lines did not show changes in respiration, physiology, or photosynthetic capacity

The T_1 progeny of the primary transformants, a mix of homo- and heterozygous plants, were used to unravel the effects of the multigene approach in tobacco. The 47 lines carrying the multigene construct LS0201 were analysed in three subsequent batches, each including 16 lines. Another four lines, carrying the construct LS0207, containing the redox biosensor c-Peredox-mCherry only, were grown alongside the multigene transgenic lines and used as transformed controls. Plants were germinated on hygromycin-selection plates. After two weeks, antibiotic-resistant seedlings were transferred to pots and grown in a glasshouse at the Department of Plant Sciences, University of Oxford, Oxford (UK) under low light conditions (50-150 µmol m^{-2} s^{-1}).

Expression, measured as relative transcript levels, was determined for the endogenous genes *NtGAPC* and *NtmMDH* and the transgenes *AtFIS1A* and *AtpOMT1* using qRT-PCR in all multigene lines. Lines were classified into expression

groups based on the transcript levels of the different transgenes (Figure 5.8), with lines carrying the desired transcript levels for all gene targets being labelled as 'GFOM', where *NtGAPC* and *NtmMDH* were silenced and *AtFIS1A* and *AtpOMT1* were overexpressed. Table D.1 shows the relative transcript levels per line.

Group	Silencing NtGAPC (G)	Overexpression AtFIS1A (F)	Overexpression AtpOMT (O)	Silencing NtmMDH (M)	Number of lines
FO					9
FOM					9
GFO					2
GFOM*					18
GM					4
GO					1
GOM					1
M					2
PseudoWT					1

Figure 5.8: Group classification of multigene tobacco lines carrying the construct LS0201 based on transgene expression. Lines were classified into groups based on the desired changes in expression, determined as relative transcript levels via qRT-PCR in the T_1 generation. Green indicates desired change in transcript level and red indicates that the desired change was not obtained in that group of lines. The number of lines of each group is indicated. Abbreviations are as follows: G, silencing of *NtGAPC*; F, overexpression of *AtFIS1A*; O, overexpression of *AtpOMT1*; M, silencing of *NtmMDH*. The asterisk (*) in the group 'GFOM' indicates that this group is the one in which the intended changes in expression were observed for the genes of interest.

The multigene transgenic tobacco lines were analysed in terms of respiratory and photosynthetic capacity, physiology, and the NAD(H) redox status. Mitochondrial respiration was evaluated by measuring leaf disc oxygen consumption rates in a multi-well microplate using a Seahorse XFe24 Extracellular Flux Analyser, adapting the protocol by Sew, Millar, and Stroehe [218]. No changes were observed between expression groups when measuring leaf disc respiration (Figure 5.9.A). While the expression groups showed significant differences in terms of plant height and

total aerial biomass (Figure 5.9.B and C), the multigene lines did not differ from the 'Peredox' or WT controls. In particular, the lines in the 'GFOM' group showed reduced height with respect to the 'Peredox' controls, but not with respect to the WT.

Photosynthetic capacity was evaluated using an OJIP chlorophyll fluorescence transient in the youngest fully expanded leaf, five weeks after transfer to soil, using a PAR-FluorPen FP 110. The quantum yield of PS II (F_v/F_m) and the performance index on an absorption basis did not differ between the 'GFOM' and the control groups (Figure 5.10.A and B).

The dark *in vivo* redox status of NADH/NAD^+ was evaluated in leaf discs using a plate reader fluorimetry assay [220, 221]. Fluorescence emission was collected from Ts and mC and used as a proxy for the ratio of NADH to NAD^+ in the cytosol. The ratio values of Ts/mC were $\log_{10}$ transformed to accurately represent the ratio variance and to restore the symmetry of the ratio data. A spectral profile for the biosensor is included in Figure D.1. The 'Peredox' control lines showed low NADH/NAD^+ ratios (-0.18 on average), in line with previous analyses of the *in vivo* redox status of c-Peredox-mCherry in Arabidopsis leaves [221]. The redox status showed certain variability within expression groups and within lines of the same group (Figure 5.10.C). While most lines had NADH/NAD^+ ratios close to those of the 'Peredox' lines, some lines showed substantial increases. In particular, groups 'GM', 'GO', 'GOM', and 'M' showed significant increases in the average NADH/NAD^+ ratios with respect to the 'Peredox' and other multigene lines, including the 'GFOM' lines. It is important to note that these data represent the NADH/NAD^+ ratios in the dark, due to the difficulty of monitoring sensor fluorescence while illuminating the leaf discs.

Additional parameters that were measured during the characterisation of the multigene lines are included in Appendix D (Tables D.2 to D.8).

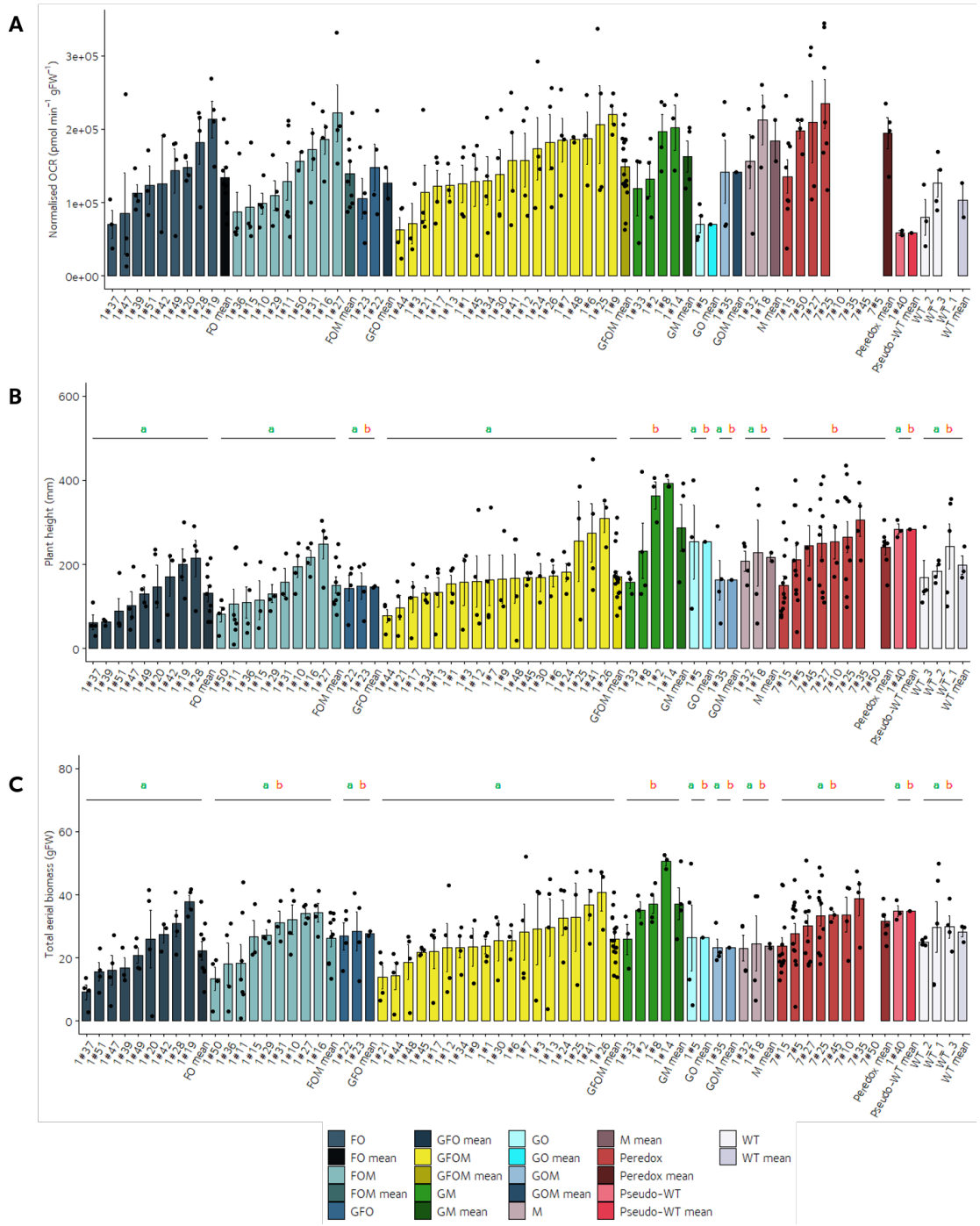

Figure 5.9: Analysis of multigene transgenic tobacco plants (I). Respiratory capacity (**A**) was determined as leaf disc oxygen consumption rates (OCR) using a Seahorse XFe24 Extracellular Flux Analyser (Seahorse Bioscience, MA, USA) on four-week-old plants. Plant height (**B**) and total aerial biomass (**C**) were measured on six-week-old plants. Multigene lines carrying the construct LS0201 are labelled as '1#n' and Peredox lines (LS0207) '7#n', where n represents the line number. Data represent means of four plants ± SE. Colouring represents groups based on transcript levels, as per Figure 5.8. Significant changes between groups were identified by the Kruskal-Wallis rank sum test, followed by post hoc Tukey multiple pairwise comparisons test. P-values are as follows: OCR, 0.016; height, 3.19E-5; biomass, 0.005.

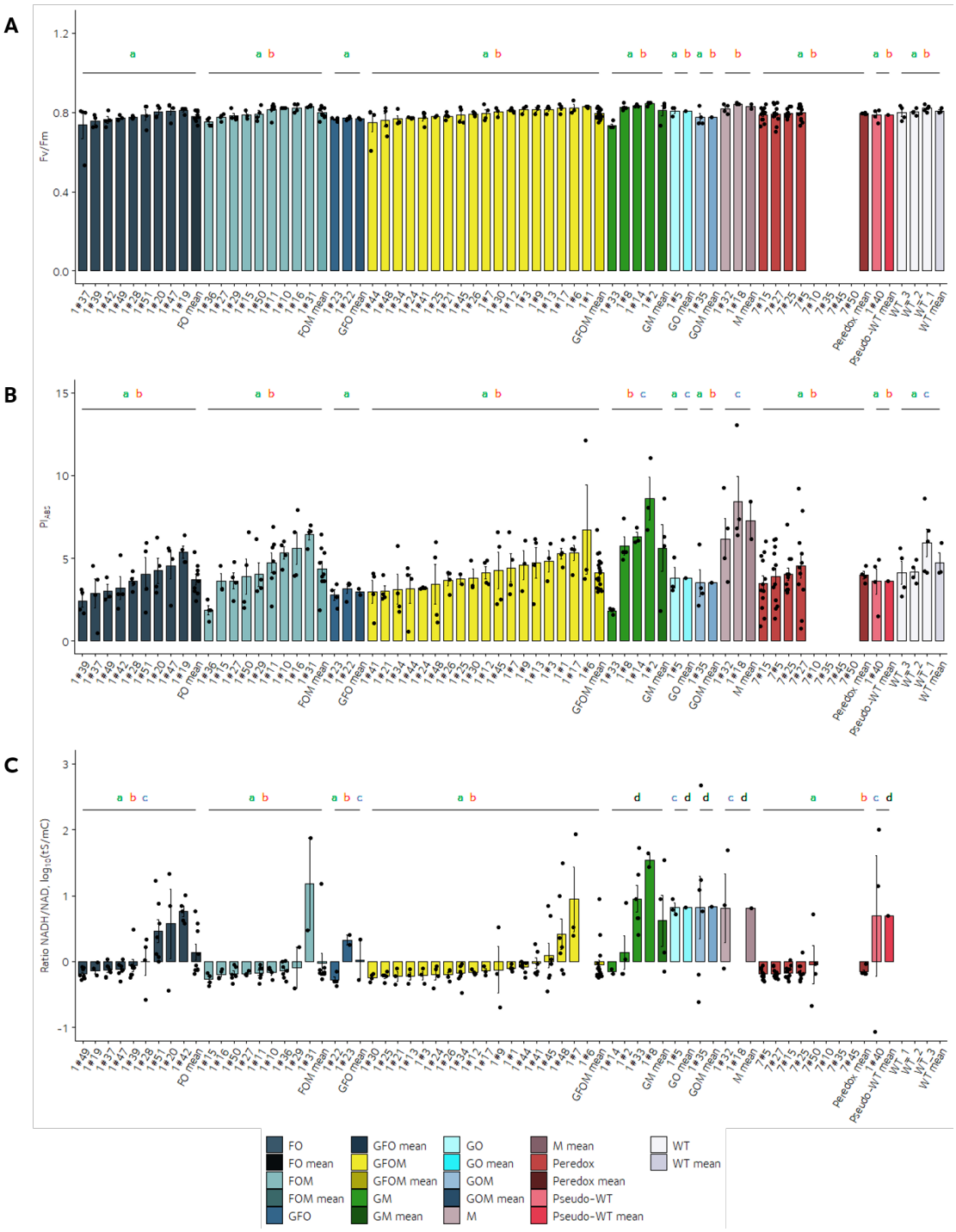

Figure 5.10: Analysis of multigene transgenic tobacco plants (II). Photosynthetic quantum yield (F_v/F_m, **A**) and performance index on absorption basis (PI_{ABS}, **B**) were determined with a PAR-FluorPen FP 110 (Photon Systems Instruments, Drasov, Czech Republic) on five-week-old plants. The ratio of NADH/NAD^+ was determined based on the fluorescence of the biosensor c-Peredox-mCherry on three-week-old plants ($\log_{10}$(tS/mC), **C**). Multigene lines carrying the construct LS0201 are labelled as '1#n' and Peredox lines (LS0207) '7#n', where n represents the line number. Data represent means of four plants ± SE. Colouring represents groups based on transcript levels, as per Figure 5.8. Significant changes between groups were identified by the Kruskal-Wallis rank sum test, followed by post hoc Tukey multiple pairwise comparisons test. P-values are as follows: F_v/F_m, 0.002; PI_{ABS}, 0.002; ratio NADH/NAD^+, 1.94E-06.

5.3.6 Transcript levels in the multigene tobacco lines were negatively correlated with growth and photosynthesis

The expression groups used above were established manually, based on the desired transcript levels for each transgene (Figure 5.8). Next, to investigate if variations in transcript levels of the transgenes or silenced genes were linked to variations in the parameters measured, two types of analysis were done, independent of the expression group of each line.

First, PCA was used as a multivariate analysis in an attempt to reduce the dimensions of the data set while retaining as much variation as possible. For this analysis, the data set containing the measured values for a total of 40 parameters in the 47 multigene lines, seven Peredox lines, and three WT controls was used. Five principal components (PC) explained 81% of the variance (Figure 5.11.A). The top variables (measured parameters) and individuals (transgenic and control lines) contributing to each PC can be found in Table D.9, with the top parameters contributing to a certain PC expected to increase together. Figures 5.11.B and 5.11.C show the graphs for individuals and variables across PC1 and PC2, and Figure D.2 shows a combined plot (biplot) for the individuals and variables across PC1 and PC2.

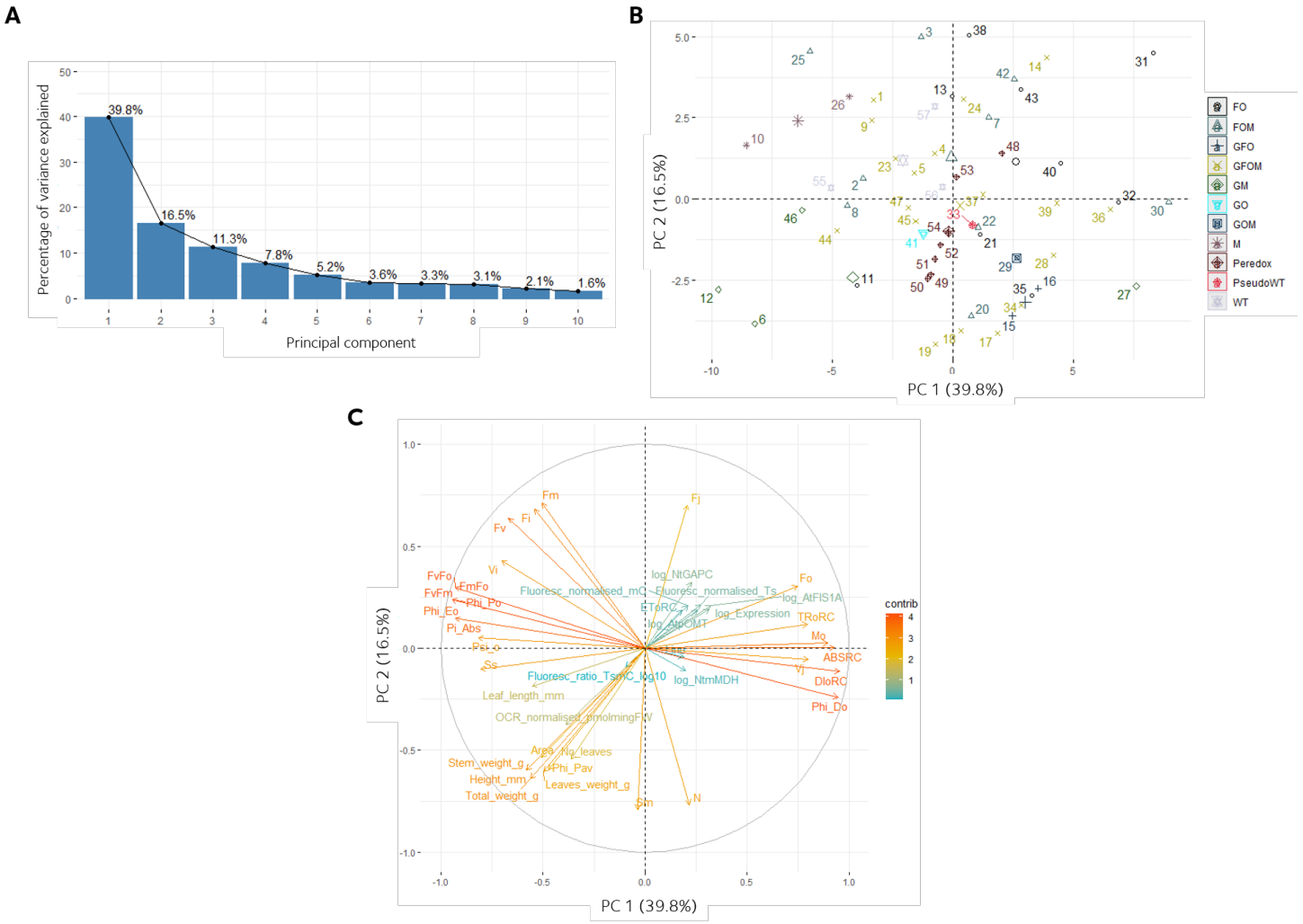

Figure 5.11: Principal component analysis of the parameters measured in the multigene transgenic tobacco lines. A. Scree plot showing the percentage of variance explained by each principal component (PC). **B**. Individuals scatter plot across PC1 and PC2. Lines are colour-coded based on the expression groups defined in Figure 5.8. **C**. Variables graph across PC1 and PC2. The colour palette indicates the contribution of each parameter to each PC.

The first PC (PC1, 39.7% of variance explained) had large positive associations with several chlorophyll-fluorescence parameters, including F_v/F_m and the performance index on absorption basis (Table D.9). The second PC (PC2, 16.5% of variance explained) primarily measured chlorophyll-fluorescence parameters - normalised area between the OJIP curve and F_m (S_m), quinone turnover number (N), and fluorescence intensity at 50 μs (F_0), 2 ms (F_j), 30 ms (F_i), and at the peak of the curve (F_m) - and growth-related parameters, including stem, leaves, and total biomass, and total number of leaves (Table D.9). The third PC (PC3, 11.3% of variance explained) increased with the transcript levels of the overexpressed genes *AtFIS1A* and *AtpOMT1* and the ratio of NADH/NAD^+ (Table D.9). PC4 (7.8% of variance explained) had large positive associations with the fluorescence of c-Peredox-mCherry (Ts and mC) (Table D.9). PC5 (5.2% of variance explained) was associated with certain chlorophyll-fluorescence parameters and the transcript levels of the overexpressed genes (Table D.9). Finally, PC6 (3.6% of variance explained) was primarily associated with the expression of the silenced genes *NtGAPC* and *NtmMDH* (Table D.9).

When exploring the contributions of each individual to the different PCs (Table D.9), it could be seen that the different expression groups were largely widespread among the different PCs. In particular, lines carrying the expected changes in transcript levels, labelled as 'GFOM', were spread among the different PCs (Table D.9). This can also be inferred from the biplot in Figure D.2 and it is consistent with the transgenic expression groups behaving similarly with respect to each other and the control groups in the Kruskal-Wallis test shown in Figures 5.9 and 5.10. The top contributors to PC1 were some of the multigene transgenic lines, from groups 'GM', 'FOM', 'M', and 'FO'. This suggests that lines across the expression range (measured as transcript level) had varied levels of photosynthetic capacity, meaning that increased/decreased levels of chlorophyll fluorescence could not be linked to specific expression groups. It was revealed from PC2 that the top contributors were lines with high expression levels for transgenes *AtFIS1A* and *AtpOMT1* (groups 'FO', 'FOM', and 'GFOM'), which implies a correlation between transcript levels

and certain chlorophyll-fluorescence parameters and plant growth. Unexpectedly, the top lines contributing to PC3, where the top contributing variables were linked to transcript levels, belonged to the control groups Peredox and WT.

Next, correlations between transgene expression and the redox status, respiratory, physiological, and photosynthetic parameters were explored using a Spearman correlation test. Transcript levels for each transgene were converted to $\log_{10}$ values and averaged. Figure D.3 shows the scatter plots for a selection of parameters and Table 5.3 summarises the correlation coefficients and significance for each correlation test. Moderate but significant negative correlations were observed between transgene expression (measured as average transcript levels) and the NADH/NAD$^+$ ratio ($R = -0.31$), plant height ($R = -0.34$), and stem biomass ($R = -0.28$). No correlation was found between transcript levels and oxygen consumption rates ($R = -0.09$) (Table 5.3).

Several chlorophyll fluorescence parameters, extracted from the OJIP transient, showed significant correlations with transcript levels (Table 5.3). A moderate negative correlation was observed between transcript levels and overall photosynthetic capacity, particularly with the quantum yield of PS II ($R = -0.39$), the quantum yield of electron transport from quinone to the plastoquinone pool ($R = -0.32$) and the performance index of PS II ($R = -0.35$). On the other hand, a moderately positive correlation was found with photosynthetic parameters related to specific energy fluxes through the electron transport chain, i.e. apparent antenna size per active PS II ($R = 0.32$), maximum trapped exciton flux per active PS II ($R = 0.28$), and the flux of energy dissipated in processes other than trapping per active PS II ($R = 0.36$). This suggests that active PS II reaction centres could carry more electron flux but there were less active centres overall as transgene expression increased, which led to an overall decrease in photosynthetic capacity as expression increased.

Table 5.3: Correlation coefficients of measured parameters with relative transcript levels in multigene transgenic tobacco lines. Correlations between each parameter and the average relative transcript level for genes *NtGAPC*, *NtmMDH*, *AtFIS1A*, and *AtpOMT1* were tested using a Spearman rank-order correlation test. Data represent 47 independent transgenic lines, with four plants measured per line ($n = 188$). Asterisks indicate significance levels: "***" for P-value<0.0001, "**" for P-value<0.001, or "*" for P-value<0.05..

Parameter	Spearman correlation coefficient
c-Peredox-mCherry fluorescence	
Normalised fluorescence T-Sapphire (Ts)	0.24**
Normalised fluorescence mCherry (mC)	0.20*
Ratio $NADH/NAD^+$ - $\log_{10}$(Ts/mC)	-0.31**
Mitochondrial respiration	
Oxygen consumption rate	-0.09
Plant physiology	
Plant height	-0.34**
Leaf length	-0.10
Total number of leaves	-0.16
Leaf biomass - fresh weight	-0.08
Stem biomass - fresh weight	-0.28**
Total aerial biomass - fresh weight	-0.18
Chlorophyll fluorescence - OJIP curve	
F_0 - Fluorescence intensity at 50 μs	0.31**
F_j - Fluorescence intensity at 2 ms (J-level)	0.07
F_i - Fluorescence intensity at 30 ms (I-level)	-0.14
F_m - Fluorescence intensity at the peak of OJIP curve	-0.10
F_v - Maximum variable fluorescence	-0.18
V_j - Shape of fluorescence kinetics at intermediate step J	0.23*
V_i - Shape of fluorescence kinetics at intermediate step I	-0.28**
F_m/F_0 - Ratio of the extrema	-0.39***
F_v/F_0 - Quantum yield of PS II efficiency	-0.39***
F_v/F_m - Quantum yield of PS II efficiency	-0.39***
M_0 - Normalised value of initial slope of the O-J fluorescence rise	0.31**
Area - Area between fluorescence curve and F_m	-0.27**
S_m - Normalised area between the OJIP curve and the F_m line	-0.14
S_s - Single quinone turnover	-0.28**
N - quinone turnover number (S_m/S_s)	-0.05
ΦP_0 or TR_0/ABS - F_v/F_m	-0.39***
Ψ_0	-0.25*
ΦE_0 or ET_0/ABS - Quantum yield of electron transport from quinone to plastoquinone	-0.32**
ΦD_0	0.39***
ΦPav - Time to reach F_m	-0.22*
PI_{ABS} - Performance index on absorption basis	-0.35***
ABS/RC - Apparent antenna size of active PS II	0.32**
TR_0/RC - Maximum trapped exciton flux per active PS II	0.28**
ET_0/RC - Flux of electrons transferred from quinone to plastoquinone per active PS II	0.14
DI_0/RC - Flux of energy dissipated in processes other than trapping per active PS II	0.36***

5.4 Discussion

Computational models are a key tool for testing and directing metabolic engineering strategies [179, 181, 182, 287]. In their model, Shameer *et al.* [182] provided predictions of metabolic fluxes that could lead to a more energy-efficient cell status. This chapter describes the generation and characterisation of transgenic tobacco lines carrying a multigene construct that could induce the predicted changes.

The transcript presence and lack thereof for the target genes was confirmed in the 47 multigene lines, with 18 lines, referred to as 'GFOM', showing the intended changes in transcript levels. Contrary to expectations, this study did not find a significant difference between the 'GFOM' lines and the rest of the multigene lines or the Peredox and WT control lines in terms of respiratory and photosynthetic capacity, physiology, and the NADH/NAD^+ redox status in the dark (Figures 5.9 and 5.10).

An important finding was that 'GM', 'GO', 'GOM', and 'M' lines had increased NADH/NAD^+ ratios (measured in dark-adapted leaf discs) with respect to the 'Peredox', 'GFOM', and 'FOM' lines. The increased reduction of the cytosolic NAD pool in the multigene lines where *NtGAPC* and/or *NtmMDH* are suppressed is a surprising finding because the pathways in which they take part are considered to operate in the light (see Section 1.2.10 in Chapter 1). It suggests high importance for the mitochondrial malate valve and the chloroplast TPT in the export of reducing equivalents and energy in the dark and the presence of alternative shuttles that compensate for their suppression. This is consistent with recent findings where c-Peredox-mCherry was introduced in the Arabidopsis mutants *mmdh1*, *mmdh2*, and *NADP-mdh* (involved in the chloroplast malate valve). These mutants showed an increased NADH/NAD^+ ratio in the dark with respect to the Peredox control [288]. The magnitude of the change was markedly higher in the multigene tobacco transgenic lines than in the Arabidopsis mutants, but there was less variability in the Arabidopsis data. The fact that this metabolic phenotype is not observed in lines where *AtFIS1A* is overexpressed suggests that increasing the mitochondrial number compensates for the lack of mMDH activity in groups 'GFOM' and 'FOM'.

Analyses of the correlations between $\log_{10}$-converted average transcript levels and the rest of the parameters provided further insight into the effect of the introduced genetic changes, and the effectiveness of the modelling predictions. These revealed a negative correlation between transcript levels and plant height, stem biomass, photosynthetic capacity, and the ratio of NADH/NAD^+, while mitochondrial respiratory capacity did not correlate with transcript levels (Table 5.3). The correlations between transcript levels and certain photosynthetic parameters and plant growth were also inferred in the PCA analysis, where the top individuals contributing to PC2 (primarily measuring chlorophyll-fluorescence parameters) belonged to the expression groups showing the highest transcript levels (Table D.9).

Overexpression and suppression of genes will typically have an asymmetric quantitative contribution when expressed as a $\log_{10}$ ratio relative to the WT transcript abundance. This is because overexpression often results in several hundredfold increases in transcript abundance (as demonstrated in the results here, Table D.1) while antisense suppression typically leads to at most a 75% decrease in transcript abundance (Table D.1). Therefore, when correlating the average transgene expression with the measured phenotypes, the overexpressed genes are likely to have a disproportionate influence on any statistical correlation. As a result, the observed correlations would be better explained as a result of *AtFIS1A* on mitochondrial biogenesis and *AtpOMT1* as part of the malate valve, whose possible effects in reducing plant height, photosynthetic capacity, and the redox status of the cytosolic NAD pool are discussed in the next paragraphs.

The overexpression of *AtFIS1A* did not affect respiratory capacity. This was the case for Arabidopsis (Table 5.2) and the multigene tobacco plants (Figure 5.9) overexpressing the fission regulator. Fluorescent dye accumulation was determined optically by confocal microscopy in the Arabidopsis transgenic lines. MitoTracker Green contains a reactive chloromethyl group which forms a covalent bond with mitochondria, regardless of their membrane potential. However, mitochondrial staining with TMRM in both the non-transformed and the *35S::AtFIS1A* Arabidopsis plants suggested the presence of functional mitochondria, since TMRM binding

is dependent upon mitochondrial membrane potential (Figure 5.5). Mitochondrial capacity was further studied by measuring OCR in leaf discs. In the Arabidopsis OCR measurements, taken with the Clarke oxygen electrode, FCCP was used to uncouple mitochondrial respiration and oxidative phosphorylation. The final concentration of FCCP in the chamber was 10 µM, which is higher than that of a previous study, where the maximum concentration of FCCP was 4 µM [217]. However, the volume of the chamber in [217] was 850 µl compared to 2 ml in the Clarke-type electrode, so it is reasonable that a higher concentration of uncoupler was needed to elicit a response. Maximum dark respiration remained unaltered in the Arabidopsis *AtFIS1A* overexpressing lines with respect to the WT. For the measurements of dark respiration in the multigene transgenic tobacco lines, a higher-throughput method was used, adapting the measurements to a 24-well plate with 1 ml of respiration buffer per well [218]. Dark respiratory capacity did not change in the multigene lines either, despite the induced changes in the system that were designed to lead to an increase in mitochondrial ATP production. With no changes to dark respiratory capacity in the Arabidopsis and tobacco transgenic lines, it follows that the stimulation of mitochondrial biogenesis in *AtFIS1A* overexpressing plants leads to the accumulation of functional mitochondria but not to a higher mitochondrial respiratory capacity.

With respect to plant growth and photosynthetic capacity, it seems unlikely that these were affected by the overexpression of *AtFIS1A*. The Arabidopsis *AtFIS1A* overexpressing lines did not show any phenotypic differences with respect to the WT in this study, in accordance with previous reports [274].

In photosynthetic cells, changes in the redox dynamics of cytosolic NADH/NAD^+ are likely caused by changes in the chloroplast or the mitochondria [288]. The dark cytosolic NADH/NAD^+ ratio correlated negatively with average transcript levels. This is in accordance with what would have been expected of an increased dark respiratory capacity [221]. However, the lack of changes in dark respiratory capacity in the multigene lines with respect to the controls and the lack of correlation between transcript levels and respiratory capacity suggest that the negative correlation

between transcript levels and the reduction status of the cytosolic NAD pool is better explained by the manipulation of the chloroplast malate valve.

An increased activity of the chloroplast malate valve, mediated by the pOMT transporter, would lead to increased export of reducing equivalents from the chloroplast, which would have been expected to increase the ratio of NADH/NAD^+ in the cytosol. Strikingly, the cytosolic NADH/NAD^+ ratio showed a negative correlation with average transcript levels and a decrease in all lines overexpressing the *AtpOMT1* transgene which is somewhat counterintuitive. Arabidopsis mutants in *AtpOMT1* showed increased photoinhibition (increased rate of F_v/F_m decrease after exposure to high light in mutants vs WT) due to reducing equivalents accumulating in the stroma, and impaired growth [188]. The multigene lines did not show phenotypic changes in plant growth but the negative correlation between average transcript levels and F_v/F_m, stem biomass, and height suggests certain similarities between the *AtpOMT1* mutant phenotype and the overexpression of *AtpOMT1* in the multigene lines. On the other hand, it has been established that photosynthetic activity increases the cytosolic NADH/NAD^+ ratio [288]. Therefore, a reduction in the cytosolic NADH/NAD^+ ratio is in accordance with decreased photosynthetic capacity as per Steinbeck *et al.* [221]. A reduction in photosynthetic capacity as transcript levels increase could be explained by an increased accumulation of reducing equivalents in the stroma mediated by a reduced GAPC activity, although this would in principle be compensated for by the increased malate/oxaloacetate exchange mediated by pOMT.

The negative correlation between transcript levels and photosynthetic capacity may be explained by the fact that the malate valve is light-regulated via the ferredoxin/thioredoxin system. Chloroplasts of higher plants contain a non-redox regulated NAD-MDH and a redox-sensitive NADP-MDH. The NADP-MDH is regulated by the ferredoxin/thioredoxin system and activates only when NADPH accumulates because it is not being consumed by the CBB cycle [185]. Assuming that the increased levels of *AtpOMT1* transcripts lead to increased activity of the chloroplast envelope membrane transporter pOMT, this does not necessarily

mean that the malate dehydrogenase in the malate valve will be more active. It is possible, therefore, that increasing the activity of the chloroplast envelope membrane transporter pOMT leads to a deregulation of the plastidic malate dehydrogenases, which may be unable to cope with the increased activity of the transporter. This could, in turn, down-regulate photosynthesis. In other words, changing the transport and utilisation of reducing equivalents can have an effect on its production by the photosynthetic electron transport chain, leading to an overall reduced photosynthetic capacity. With no changes to respiratory capacity, increased export of reducing equivalents from the chloroplast may not have been beneficial for the system.

Interestingly, a recent study has shown how alterations in NAD(H) transport, through the silencing of the NAD^+ transporter NDT leads to reductions in stomatal density and conductivity [289]. Although net CO_2 assimilation was not determined in the mutant lines, it supports the fact that altering the movement of reducing equivalents between organelles can have important implications for photosynthesis.

It is worth noting that, as mentioned for the combinatorial co-transformation approach in Chapters 3 and 4, the presence or absence of transcripts does not imply increases or decreases in enzymatic or transporter activity. Besides, the correlations between the different parameters and the average transcript levels discussed in this section must be interpreted with caution because they refer, to a great extent, to transgenes and *AtFIS1A* and *AtpOMT1*. Some lines where increased transcript levels of *AtFIS1A* and/or *AtpOMT1* were not detected had significant changes in the cytosolic NADH/NAD^+ ratios. This suggests that the silencing of *NtmMDH* and *NtGAPC* had a considerable effect, which was difficult to account for when looking at correlations between average transcript levels and the rest of the parameters.

This study has been unable to demonstrate an alteration of the energetic coupling between organelles or improvements in photosynthetic capacity and productivity *in planta*, as implied from the modelling predictions in [182]. This discrepancy could be attributed to the choice of gene targets, which may not have produced the desired changes in flux. The evidence for this can be clearly seen in the case of *AtFIS1A*, which despite having been chosen for its ability to increase mitochondrial

volume when overexpressed by Zhang *et al.* [274], it failed to lead to increases in respiratory capacity. Alternative genes that could replace *AtFIS1A* in future attempts to increase mitochondrial respiration in plants would be *HAP4* and *SAK1*. Hap4 is the catalytic subunit of the Hap complex, a transcription factor that regulates mitochondrial biogenesis in response to carbon [290]. Sak1 kinase is part of the Snf1/AMP kinase signalling pathway, also involved in the regulation of mitochondrial biogenesis [290]. The overexpression of both *HAP4* and *SAK1* has been shown to increase the levels of mitochondrial ETC proteins and OCR in yeast [290]. Also, in the case of *mMDH*, the antisense fragment was designed based on the coding and protein sequences *AtmMDH1*, which is expressed at higher levels than *AtmMDH2* [291, 292]. However, it was not possible to distinguish between the different orthologues of *mMDH* in tobacco, so it is possible that the antisense fragment only led to the silencing of specific isoforms, which were compensated for by other versions of mMDH. Another clear reason for the lack of a strong phenotype in the multigene transgenic tobacco plants could be the variation caused by having a mixture of homozygous and hemizygous lines in the screened T_1 generation. Time permitting, it would have been valuable to determine copy number in at least the 'GFOM' lines.

It would be appropriate to check the behaviour of the multigene lines in the light with the system developed by Elsässer *et al.* [288] since here it could only be assessed in the dark. Elsässer *et al.* described a custom microscope set up that allows illumination of the leaf discs with actinic light while simultaneously monitoring fluorescence [288]. This would enable monitoring of the redox status of the cytosolic NAD pool in the light, as well as during light-dark transitions, and would be a better system to test the model predictions.

The presented results are significant in at least four major respects. First, the role of the fission regulator *FIS1A* in inducing changes in mitochondrial metabolism, outside mitochondrial biogenesis, has been investigated in Arabidopsis and tobacco. My analyses did not show any changes in OCR in the Arabidopsis and tobacco lines overexpressing *AtFIS1A*, which suggests that the overexpression of *AtFIS1A* does

not increase mitochondrial respiratory capacity. Second, a multigene engineering strategy involving long-studied gene targets has been implemented in tobacco, demonstrating a lack of phenotypic effects when changing the transcript levels of the four of them simultaneously. Third, the functionality of the genetically encoded biosensor c-Peredox-mCherry has been tested in tobacco for the first time in a plate reader fluorimetry assay. Fourth, this study reflects the complexity of plant metabolic engineering strategies in (i) our ability to implement modelling predictions, in terms of the choice of gene targets, and (ii) the suitability of the introduced genes to lead to changes in protein function and metabolic flux.

5.5 Conclusions

This chapter describes the generation and analysis of transgenic Arabidopsis lines overexpressing the mitochondrial fission regulator *AtFIS1A* and transgenic tobacco lines carrying a multigene construct for the implementation of *in silico* predictions for improved leaf performance. From these, it can be concluded that:

1. The overexpression of a *35S::AtFIS1A* construct in Arabidopsis, coding for the outer mitochondrial membrane anchor protein FISSION1A, leads to an increased volume of mitochondria in mesophyll cells, as shown in [274], which does not lead to an increased capacity of mitochondrial dark respiration.

2. The stable transformation of the multigene construct LS0201 in tobacco leads to varying expression levels of the target genes *AtFIS1A*, *AtpOMT1*, *NtGAPC*, and *NtmMDH*. High transcript levels were found for the Arabidopsis transgenes, while the antisense constructs for the tobacco genes led to low to moderate silencing levels.

3. The multigene transgenic tobacco lines carrying the intended changes in transcript levels, named 'GFOM', did not show significant changes with respect to control lines in terms of mitochondrial respiration in the dark, total aerial biomass and other plant growth parameters, photosynthetic capacity, and the cytosolic ratio of NADH/NAD^+.

4. A negative correlation between average transcript levels and plant height, stem biomass, photosynthetic capacity, and the ratio NADH/NAD^+ was observed for the multigene transgenic tobacco lines. This was most likely related to alterations of the chloroplast malate valve, via changes in the transporter pOMT.

5. The genetic changes introduced in the multigene transgenic tobacco lines were not able to induce the improvements in plant growth or plant photosynthetic capacity that the organelle coupling described in [182] predicted.

Chapter 6

General Discussion

Contents

6.1 Summary of main findings

In this thesis, two strategies for multigene metabolic engineering have been explored in tobacco, involving different cloning and plant transformation techniques, with the aim of improving photosynthetic capacity and plant growth.

Combinatorial co-transformation was chosen as a strategy that allows the simultaneous introduction of multiple transgenes, each from a separate plasmid, and produces combinatorial variety in the resulting transgenic lines. The work presented in Chapters 3 and 4 is the first instance in which combinatorial co-transformation has been used in an attempt to engineer photosynthesis, with a focus on improving source capacity. It was expected that combining existing targets that have individually shown to be effective in increasing plant growth and/or photosynthetic capacity would lead to improvements above and beyond those achieved with individual targets. However, this was not found to be the case. Further analyses of selected tobacco combinatorial transgenic lines suggested possible transgene interference effects and the need to test these transgene combinations with a different cloning method to test their potential to improve photosynthetic capacity and growth.

In the second strategy, described in Chapter 5, conventional transgene stacking involving a single multigene construct was used to implement a novel, computationally-predicted approach for improved leaf-energy efficiency and photosynthetic capacity. A diel FBA model of primary metabolism in Arabidopsis leaves, developed by Shameer *et al.* [182], suggested that an optimal leaf energy balance under low light conditions could be achieved by increasing mitochondrial ATP production and altering the activity of the chloroplast shuttles that transfer reducing equivalents and ATP to the cytosol. Contrary to the model predictions, average transcript levels of the target genes in the multigene tobacco transgenic lines were found to correlate negatively with plant growth and chlorophyll fluorescence parameters. One possible explanation for the lack of improvement of photosynthetic capacity and growth suggested by the data could be the increased transcript levels of the chloroplast inner envelope transporter pOMT. Increased activity of the chloroplast malate valve

may have affected the redox-sensitive NADP-MDH, leading to downregulation of photosynthesis. Besides, an increased reduction of the cytosolic NAD pool was observed in lines where *NtmMDH* and/or *NtGAPC* were suppressed, which suggests an important role for the mitochondrial malate valve and the chloroplast TPT in the export of reducing equivalents in the dark.

6.2 Limitations of this study

6.2.1 Experimental limitations

In this study, more than 100 transgenic tobacco lines were screened for increased plant growth and other parameters linked to photosynthesis, mitochondrial respiration, and the cytosolic status of the redox couple NADH-NAD^+. While the transcript level for the target genes was analysed in around 50 lines, the main limitation of this study was that there was not sufficient time or resources (e.g. lack of available antibodies) to analyse the change in amount and activity of the transgene-encoded proteins. This means that the observed phenotypic changes could not always be linked directly to the introduced transgenes. For this, detection of protein presence by Western blot and, ideally, quantification of the protein and/or enzyme/transport activity would be key.

Analyses of the zygosity of the transgenic lines using digital droplet PCR would have been valuable to find homozygous transgenic lines, ideally with single copies of the transgenic cassettes [262, 293]. This would be more straightforward in the multigene transgenic tobacco lines than in the combinatorial ones since it would be difficult to differentiate between homozygous plants with several transgene copies and heterozygous plants with multiple insertions at a single locus. An alternative to digital droplet PCR would be an antibiotic selection test. Because the single-locus transgene cassette in the combinatorial lines should follow Mendelian inheritance, one in four seedlings in the progeny of T_2 plants would be homozygous, resulting in 100% resistance to the antibiotic [294].

In the case of the selected tobacco combinatorial lines, quantitation of sugars and starch content in leaves at several time points in the light period would have been informative. It would have confirmed the hypothesis that an excessive source activity, not matched by transport and sink strength and accompanied by sugar and/or starch accumulation in the leaves, leads to photoinhibition in these transgenic lines. Unfortunately, there was not sufficient time to complete these measurements due to restricted access to laboratory facilities during the COVID-19 pandemic.

6.2.2 Choice of metabolic engineering targets

Although I endeavoured to undertake extensive multigene manipulation of photosynthetic metabolism, the metabolic engineering strategies implemented in this research were limited by the number and choice of target genes.

In the context of the tobacco combinatorial transgenic lines, this study focused exclusively on targeting source capacity. My rationale was that as a large-leafed plant, tobacco has a large leaf sink and that this should have provided sufficient sink capacity to utilise the enhanced photosynthesis. However, as inferred from the results in Chapter 4, increasing sink strength and phloem unloading capacity could have been decisive for the success of the strategy in improving photosynthetic capacity and yield. This is supported by the only two push-pull strategies to date in which simultaneous manipulations of source and sink targets led to significant yield improvements. Enhanced source activity and sink strength led to a doubling of starch content and tuber yield in potato [118]. Recently, simultaneous enhancement of phloem loading in source and unloading in sink by overexpressing a SUC transporter with tissue-specific promoters for the leaf phloem and the cotyledon epidermal cells increased sucrose phloem loading and carbon movement from source to sink, also improving photosynthetic rates [295].

This could also have been done by choosing a different tobacco cultivar other than Petite Havana, such as Mammoth, which has a higher sink strength [267]. The manipulation of regulators of sugar signalling, such as trehalose 6-phosphate,

which regulates sucrose levels, may pose an effective avenue for improved source-sink communication and carbon assimilation [296, 297].

Similarly, in the multigene transgenic tobacco lines, apart from the intrinsic limitations of the modelling predictions, the success of the study was restricted by the choice of target genes. The introduced genetic changes were successful in altering the flux of reducing equivalents between cell compartments in specific lines, as evidenced by alterations in the redox status of the cytosolic NAD pool, and the correlations between transcript levels and the measured parameters. However, no changes to dark respiration were observed in the multigene transgenic lines. As a result, the increased mitochondrial ATP production that the model predicted would improve the overall energy balance of the leaf was not realised in the multigene transgenic tobacco lines.

6.2.3 Combinatorial co-transformation

The use of combinatorial co-transformation carries several limitations. Firstly, depending on the number of transgenes introduced, it is necessary to screen a large number of lines to identify candidate lines. This can be challenging for certain plant species and may not always be possible depending on the desired outcome of the intervention. In this study, it meant that only a modest proportion of the combinatorial library was screened (59 lines out of a library of 329). In a recent study where combinatorial tomato lines were produced using 21 transgenes, only 18 lines were fully characterised [159]. Easing the screening process would be crucial to identify promising lines. For example, when combinatorial co-transformation was used to engineer the carotenoid pathway in maize [147, 160], candidate lines with increased carotenoid accumulation could be identified visually from the colour of the kernel. When engineering for improved photosynthetic capacity, the use of chlorophyll fluorescence imaging at the whole-plant scale would have been one way to generate improved throughput for a more extensive screen. In tobacco, this could be done at early developmental stages.

Secondly, it is difficult to reproduce the effects found in specific lines. Even if a specific transgene combination led to big increases in photosynthetic capacity and/or

plant biomass, the improvements could be associated with specific rearrangements within the transgenic locus or dosage effects. Even when transforming with a single multigene construct, as in Chapter 5, the variability in transcript levels in the target genes was considerable, which stresses the need for replicates of the same transgene combination.

Thirdly, the nature of the biolistic delivery process means that complex genetic loci are commonly generated. High copy number and transgene rearrangements can be beneficial, for example, for the accumulation of secondary metabolites [147, 148]. However, my view is that in light of the work presented in this thesis, in the quest for improved photosynthetic capacity, greater control of transgene integron and structure might be needed for the fine-tuning of transgene expression.

6.3 Engineering central metabolism in plants

The results of this research denote the difficulty of altering fluxes through central metabolism, particularly when combining multiple transgenes. Shared flux control among pathway enzymes implies that significant changes in flux would most likely be obtained by multigene manipulations [128, 298]. However, it is challenging to predict how transgenes will behave when combined. Sweetlove, Nielsen and Fernie discussed the main reasons why central metabolism can be recalcitrant to engineering and how this makes it difficult to predict the effect of engineering interventions [125]. Central metabolism has multiple layers of regulation of enzymes and transporters. Besides, it is highly interconnected, with many metabolites participating in a large number of reactions. These features make it very difficult to design metabolic engineering strategies because any flux changes will inevitably have an effect somewhere else in the system, leading to the so-called pleiotropic effects.

The use of combinatorial co-transformation and computational models to guide metabolic interventions have both been identified as key tools for engineering central metabolism [125]. In particular, combinatorial co-transformation allows the generation of plants carrying multiple gene combinations in a single experiment, and modelling can be useful to identify the most promising targets to manipulate

in plants while overcoming the bias towards the choice of genes. Combinatorial co-transformation has been used successfully as a multigene engineering strategy for secondary metabolism [147, 148, 244]. However, the results of this research question its suitability for engineering central metabolism, unless some of the limitations identified in Section 6.2.3 could be overcome. Recently, a study where combinatorial co-transformation was used to manipulate source and sink targets simultaneously in tomato showed increases in fruit yield up to 23% [159]. As with my combinatorial approach, the authors expected yield increases greater than those obtained with individual targets. While the yield increase they achieved was significant, it was not comparatively higher than that achieved with single targets. Taken together, this combination of findings provides strong evidence that combining genes from central metabolism can lead to unexpected outcomes. This could be explained by the reasons provided by Sweetlove, Nielsen and Fernie [125]. The highly regulated and interconnected nature of central metabolism means that any alteration of its components could lead to unforeseen interactions or imbalances. Any imbalances of metabolite levels could affect gene expression across the transcriptome due to metabolic feedback regulation. Sugars are known to regulate gene expression, particularly in the context of photosynthesis [299]. For example, the small subunit of RuBisCO is known to be repressed by the short-term accumulation of carbohydrates [300].

The findings of this research highlight the difficulty of engineering central metabolism, with important implications for the field of photosynthetic improvement.

6.4 Future directions in plant metabolic engineering

6.4.1 Openings for further research resulting from this research

The work presented in this thesis has provided a deeper insight into the design and implementation of multigene metabolic engineering strategies in plants. The study contributes to our understanding of manipulations of central metabolism and organelle communication for improved photosynthesis and the insights gained from this study will be of interest to the wider field of photosynthetic improvement.

The implementation of a combinatorial co-transformation experiment for improved photosynthetic capacity and growth in tobacco is unprecedented and may provide a basis for future experiments. The generated tobacco combinatorial library, of which only a limited proportion of lines have been analysed, holds the potential for further phenotypic variability. The remaining lines could be analysed extensively: (i) further characterising the group of lines with increased chlorophyll content described in Chapter 3 which could have an increased photosynthetic capacity, (ii) performing a high throughput screen with young seedlings of the remaining uncharacterised lines to identify lines with improved photosynthetic capacity, (iii) further resolving the features of combinatorial co-transformation by analysing transgene presence and absence, copy number, the structure of the transgenic loci, and transgene expression in the combinatorial lines, (iv) analysing the response of the combinatorial lines to (a)biotic stresses, etc. The existing lines could also be crossed sexually with other lines carrying different transgenes or transgene combinations or super-transformed with additional transgenes of interest to achieve greater growth improvements. The same individual-transgene constructs built in this study could be combined in smaller groups to analyse their effects at a smaller scale, or introduced in a different species in which the screenings are more straightforward to perform, such as Arabidopsis. Another avenue for research arising from this thesis could be the use of combinatorial co-transformation with a small number of transgenes known to boost

photosynthetic efficiency when overexpressed simultaneously (such as the single multigene construct containing SBPase, FBPA, and GDC-H [71]), which could lead to greater metabolic variability than that achieved with a single multigene construct.

With respect to the computationally-predicted, multigene strategy, this study constitutes one of the first attempts to implement the predictions from a metabolic modelling approach in plants. The findings from this thesis enhance our understanding of the energy and redox communication between organelles, suggesting an important role for the export of reducing equivalents in the dark and for pOMT in maintaining the activity of the chloroplast malate valve, and lay the groundwork for future research. The energy and redox dynamics of the multigene transgenic lines could be further explored using chemical inhibitors of photosynthesis or mitochondrial respiration, or by super-transforming the plants with other genetically-encoded biosensors, such as iNAP for NADPH [301] or ATeam1.03-nD/nA for $MgATP^{2-}$ sensing [302]. Having tested the specific transgene combination in construct LS0201, new targets could be identified and combined to further test the energy rebalancing predictions described by Shameer *et al.* [182], or a different suppression strategy could be used to achieve higher silencing levels.

6.4.2 Improving photosynthetic efficiency

A range of targets for improved photosynthetic efficiency is being developed and implemented, as detailed in Chapter 1. Major research consortia are underway for crop improvement with a focus on photosynthesis, including the C_4 Rice Consortium (https://c4rice.com/), Realizing Increased Photosynthetic Efficiency (RIPE, https://ripe.illinois.edu/), and the Cassava Source-Sink Project (CASS, https://cass-research.org/), whose contribution will be invaluable to the field. The results of this thesis add to this rapidly expanding field and constitute one of the first studies where multigene strategies are explored. Increasingly, evidence points towards the need to improve multiple strategies simultaneously, with only modest improvements to yield being achieved with individual targets [3, 303]. For example, a recent model calculating the impacts of leaf photosynthesis on field

crop performance showed that a 20% increase in the rate of electron transport would only result in yield increases of 7-8% in irrigated wheat and sorghum [3]. Only combined efforts will succeed in achieving the required increases in yield. The findings from the strategies described in this thesis highlight the need for further scrutiny of network behaviour and the complexity of the effects of combining transgenes in plants, which will prove useful when multiple approaches for improved photosynthesis are combined in coming years.

In addition, the design of novel synthetic pathways will be key to the implementation of many of the current strategies for photosynthetic improvement, such as the assembly of carboxysomes in chloroplasts [64], or the implementation of more efficient photorespiratory bypasses [17, 25]. In this sense, computational modelling will remain key to direct which targets to prioritise in a fast and affordable manner, such as the Zhu, de Sturler and Long model [95] which identified SBPase and FBPA as targets for improved photosynthesis.

Also, with most traits having been tested only in tobacco, and controversies arising around field studies [296], these strategies must be gradually implemented into food crops to ensure that increases in biomass translate into increases in harvest yield.

6.4.3 Enabling technologies

New technologies are emerging that will significantly ease the implementation of future metabolic engineering strategies in plants in the coming years, from fine-tuning gene expression to accelerating the transformation process.

Traditionally, the promoters used in transgenic cassettes contain *cis* regulatory motifs that respond to endogenous plant transcription factors. Plant transcription factors belong to large gene families and respond to a variety of environmental cues, such as light, (a)biotic stresses, hormones, chemicals, etc. This confers plants with higher metabolic plasticity but also means that transcription factors can be quite promiscuous and the levels of transcription for transgenes introduced with native promoters can be difficult to predict. The development of synthetic promoters that contain minimal modules and respond to specific environmental stimuli or

synthetic transcription factors could ensure a defined relationship between promoter activation and output gene expression, which would be paramount to fine-tune the expression levels of the different transgenes [304–306]. The use of nuclease-dead Cas9 coupled to transcriptional regulators can help mediate gene activation or repression in endogenous targets of interest [307].

Another important factor that affects gene expression is the location of the inserted transgenes in the genome, which is relatively random with the current DNA delivery methods. Targeted delivery on landing pads using homologous recombination or site-specific recombinases, and the use of artificial chromosomes altogether promise to be an important enabling technology for metabolic engineering [305].

The emergence of methods that solve major bottlenecks in the plant transformation process will considerably speed up the generation of transgenic plants with novel metabolic engineering targets. Recently, novel approaches that circumvent the tissue culture stage of the transformation processes have been described. This would be beneficial not only to accelerate the speed with which existing species are transformed but also to obtain transgenic plants from species that are recalcitrant to regeneration in tissue culture. Maher *et al.* described a fast-treated *Agrobacterium* co-culture (Fast-TrACC) method that has the potential to revolutionise plant transformation by drastically reducing the time needed to regenerate transformants and minimising somaclonal variation, reaching the seed stage after only 12 weeks. Fast-TrACC utilises developmental regulators that induce *de novo* development of meristems that will develop into shoots, with *Wus2* (from maize) with either *STM* (from Arabidopsis) or *ipt* (from *Agrobacterium*) having proved the most effective [308]. The developmental regulators are delivered with viral replicons using *Agrobacterium* and can include transgenes or guide RNAs for gene editing. This method was initially applied to seedlings developed through tissue culture in sterile conditions but was shown to be applicable to cut apices of soil-grown plants, including *Nicotiana benthamiana*, potato, tomato, and grape [308]. A betalain-reporter *RUBY* has been developed that allows monitoring of positive transformants from the tissue culture to the whole-plant stage [309].

Besides, it has been shown that grafting facilitates horizontal gene transfer and the transfer of whole organelles between the scion and the rootstock [310]. This can ease the transformation of recalcitrant plant species, particularly for chloroplast transformation, which could be highly beneficial for redesigning photosynthesis. The development of transient, *Agrobacterium*-mediated transformation in plant species other than tobacco and *N. benthamiana* will help to evaluate the effect of transgenes, or transgene combinations, more rapidly. The analysis of gene expression, protein subcellular localisation, and protein-protein interactions in agro-infiltrated Arabidopsis, potato, pepper, and various species of the Brassicaceae family has been recently described [311].

6.5 Closing remarks

The translation of successful plant metabolic engineering strategies into crop breeding programs will take more than a decade [297]. With an increasing demand for food and fuel, aggravated by the current climate crises, there is definitely no time to lose. This thesis set out to use innovative multigene metabolic engineering strategies to accelerate current efforts to improve crop yield. While these strategies were expected to realise improvements in photosynthetic capacity and plant growth, the results of this thesis have highlighted the complexity of the plant metabolic network and the need to start testing the effects of simultaneous manipulations for improved yield to ensure food availability in the coming decades. Important lessons have been learnt around the design and analyses of multigene transgenic plants, which I sincerely hope will contribute to shaping future plant metabolic engineering strategies for improved crop productivity and food security.

Appendices

Appendix A

Supplementary materials - Chapter 2

Tables

Table A.1: Plasmids used as backbones for restriction-ligation cloning for the generation of a tobacco combinatorial library. Details include plasmid name, revelant characteristics, and source. When the source indicates 'Bock, R', plasmids were provided by Prof. Ralph Bock from the Max Planck Institute of Molecular Plant Physiology in Potsdam-Golm (Germany). Ap: ampicillin.

Plasmid	**Relevant characteristics**	**Source**
pUC18::AtRbcS-MCS-NosT	Cloning vector containing the leaf-specific promoter from the RuBisCO small subunit (*RbcS*) gene of Arabidopsis, XhoI and SacI restriction sites, and the nopaline synthase terminator (*NosT*) in the pUC18 plasmid backbone; ApR	This work
pUC18::CaMV35S-MCS-NosT	Cloning vector containing the constitutive promoter *CaMV35S*, XbaI and XhoI restriction sites, and the *NosT* in the pUC18 plasmid backbone; ApR	Bock, R
pUC18::SlRbcS-MCS-NosT	Cloning vector containing the leaf-specific promoter from the RuBisCO small subunit gene (*RbcS*) of tomato (*S.lycopersicum*), XbaI and SpeI restriction sites, and the *NosT* terminator in the pUC18 plasmid backbone; ApR	Bock, R
pUC18::StcyFBP-MCS-NosT	Cloning vector containing the leaf-specific promoter of the cytosolic fructose 1,6-bisphosphatase (*cyFBPase*) from potato (*S. tuberosum*), XbaI and BamHI restriction sites, and the *NosT* terminator in the pUC18 plasmid backbone; ApR	Bock, R
pUC57::Pyc6	Cloning vector containing the *Pyc6* gene in the pUC57 plasmid backbone; ApR	Synthetic, Biomatik Co., Ontario, CA
pUC57::AtPetC	Cloning vector containing the *AtPetC* gene in the pUC57 plasmid backbone; ApR	Synthetic, Biomatik Co., Ontario, CA
pUC57::CaPFLP	Cloning vector containing the *CaPFLP* gene in the pUC57 plasmid backbone; ApR	Synthetic, Biomatik Co., Ontario, CA
pUC57::SeictB	Cloning vector containing the *SeictB* gene in the pUC57 plasmid backbone; ApR	Synthetic, Biomatik Co., Ontario, CA

Table A.2: Plasmids used for plant biolistic combinatorial co-transformation. Details include plasmid name, relevant characteristics, and source. When the source indicates 'Bock, R', plasmids were provided by Prof. Ralph Bock from the Max Planck Institute of Molecular Plant Physiology in Potsdam-Golm (Germany). Ap: ampicillin.

Plasmid	Relevant characteristics	Source
pUC18::AtRbcS-AtPetC-NosT	Transformation vector containing the gene coding for the Rieske Fe-S protein (*PetC*) from Arabidopsis under the control of the Arabidopsis *RbcS* promoter (light inducible, leaf specific) and the *NosT* terminator; ApR	This work
pUC18::AtRbcS-Pyc6-NosT	Transformation vector containing the cytochrome c6 (*Pyc6*) gene from *P. yezoensis* under the control of the Arabidopsis *RbcS* promoter (light inducible, leaf specific) and the *NosT* terminator; ApR	This work
pUC18::CaMV35S-CaPFLP-NosT	Transformation vector containing the gene coding for the ferredoxin-like protein (*PFLP*) from sweet pepper (*C. annuum*) under the control of the *CaMV35S* promoter (constitutive) and the *NosT* terminator; ApR	This work
pUC18::CaMV35S-SeictB-NosT	Transformation vector containing the gene coding for the putative inorganic transporter ictB (*ictB*) from *Synechococcus* under the control of the *CaMV35S* promoter (constitutive) and the *NosT* terminator; ApR	This work
pUC18::CaMV35S-FpGDC-H-NosT	Transformation vector containing the gene coding for the H-protein of the glycine decarboxylase enzyme (*GDC-H*) from *F. pringlei* under the control of the *CaMV35S* promoter (constitutive) and the *NosT* terminator; ApR	Bock, R
pUC18::SlRbcS-AtFBPA-NosT	Transformation vector containing the gene coding for the Arabidopsis fructose 1,6-bisphosphate aldolase (*FBPA*) under the control of the tomato *RbcS* promoter (light inducible, leaf specific) and the *NosT* terminator; ApR	This work
pUC18::SlRbcS-AtSBP-NosT	Transformation vector containing the gene coding the Arabidopsis sedoheptulose 1,7-bisphosphate (*SBP*) under the control of the tomato *RbcS* promoter (light inducible, leaf specific) and the *NosT* terminator; ApR	Bock, R
pUC18::SlRbcS-AtSWEET11-NosT	Transformation vector containing the gene coding for the Arabidopsis phloem sucrose loading transporter SWEET11 (*SWEET11*) under the control of the tomato *RbcS* promoter (light inducible, leaf specific) and the *NosT* terminator; ApR	Bock, R
pUC18::StcyFBP-AtTPT-NosT	Transformation vector containing the gene coding for the Arabidopsis fructose 1,6-bisphosphate aldolase (*FBPA*) under the control of the potato *cyFBPase* promoter (mesophyll specific) and the *NosT* terminator; ApR	This work
pUC18::StcyFBP-AtcyFBP-NosT	Transformation vector containing the gene coding for the Arabidopsis *cyFBPase* under the control of the potato *cyFBPase* promoter (mesophyll specific) and the *NosT* terminator; ApR	This work
pUC18::StcyFBP-EcPP-NosT	Transformation vector containing the gene coding for the *E. coli* inorganic pyrophosphatase (*PPase*) under the control of the potato *cyFBPase* promoter (mesophyll specific) and the *NosT* terminator; ApR	Bock, R
pUC18::CoYMV-AtSUC2-NosT	Transformation vector containing the gene coding for the Arabidopsis phloem sucrose loading transporter SUC2 (*SUC2*) under the control of the *CoYMV* promoter (phloem companion-cell specific) and the *NosT* terminator; ApR	Bock, R

Table A.3: Plasmids used for *Agrobacterium*-mediated transformation of Arabidopsis. Details include plasmid name, revelant characteristics, and source. Kn: kanamycin, Sp: spectinomycin.

Plasmid	**Relevant characteristics**	**Source**
pCR8/GW/TOPO	Gateway TOPO TA cloning vector, entry plasmid; SpR	Thermo Fisher Scientific, MA, USA
pCR8/GW/TOPO-AtFIS1A	Gateway TOPO TA entry vector containing the Arabidopsis gene coding for the fission 1A regulator (FIS1A); SpR	This work
pK7WG2	Gateway binary vector for *Agrobacterium* plant transformation, containing the *CaMV35S* promoter and terminator; SpR in bacteria, KnR in plants	[202]
pK7WG2-AtFIS1A	Gateway binary vector for *Agrobacterium* plant transformation, containing the Arabidopsis gene FIS1A under the control of the *CaMV35S* promoter and terminator; SpR in bacteria, KnR in plants	This work

Table A.4: Golden Gate level 1 plasmids used in modular cloning for the generation of multigene constructs. Details include plasmid name, relevant characteristics, and source. When the source indicates 'Raines, C', plasmids were provided by Prof. Christine Raines from the School of Life Sciences at the University of Essex in Colchester (UK). Ap: ampicillin.

Plasmid	**Relevant characteristics**	**Source**
EC15030 - pL1M-R1-p35S-HYG-tNOS	Golden Gate level 1 plasmid (position 1, reverse) containing the gene hygromycin-B coding for hygromycin phosphotransferase under the control of the *CaMV35S* promoter (constitutive) and the *NOS* terminator; ApR	Raines, C
LS0113 - pL1M-R2-pSlRbcS2-uSlRbcS2-(AS)GAPC2-tHSP	Golden Gate level 1 plasmid (position 2, reverse) containing an antisense fragment of the tobacco glyceraldehyde 3-phosphate dehydrogenase (GAPC) under the control of the tomato RuBisCO small subunit (RbcS) promoter (light inducible, leaf specific) and the *HSP* terminator; ApR	This work
LS0106 - pL1M-R3-pStLS1-(AS)mMDH3-tHSP	Golden Gate level 1 plasmid (position 3, reverse) containing an antisense fragment of the tobacco mitochondrial malate dehydrogenase (mMDH) under the control of the potato leaf and stem-specific (LS1) promoter and the *HSP* terminator; ApR	This work
LS0119 - pL1M-R4-pAtRbcS2-pOMT1-tHSP	Golden Gate level 1 plasmid (position 4, reverse) containing the Arabidopsis gene coding for the plastidic 2-oxoglutarate/malate transporter (pOMT) under the control of the Arabidopsis RbcS (light inducible, leaf specific) promoter and the *HSP* terminator; ApR	This work
LS0124 - pL1M-R5-pAtLhb1B1-FIS1A-tHSP	Golden Gate level 1 plasmid (position 5, reverse) containing the Arabidopsis gene coding for the fission regulator 1A (FIS1A) under the control of the Arabidopsis light-harvesting chlorophyll-protein complex II subunit B1 (Lhb1B1) promoter (light inducible, leaf specific) and the *HSP* terminator; ApR	This work
LS0125 - pL1M-F6-p2xCaMV35S-peredox-tHSP	Golden Gate level 1 plasmid (position 6, forward) containing the gene coding for the cytosolic NADH:NAD+ biosensor c-Peredox-mCherry under the control of the double-enhancer *CaMV35S* promoter (constitutive, high strength) and the *HSP* terminator; ApR	This work
LS0127 - pL1M-R2-p2xCaMV35S-peredox-tHSP	Golden Gate level 1 plasmid (position 2, reverse) containing the gene coding for the cytosolic NADH:NAD+ biosensor c-Peredox-mCherry under the control of the double-enhancer *CaMV35S* promoter (constitutive, high strength) and the *HSP* terminator; ApR	This work

Table A.5: Golden Gate level 2 multigene plasmids used for *Agrobacterium*-mediated transformation of tobacco. Details include plasmid name, relevant characteristics, and source. Kn: kanamycin, Hyg: hygromycin.

Plasmid	**Relevant characteristics**	**Source**
LS0201 - pL2V-p35S-Hyg-pSlRbcS2-ASGAPC2-pStLS1-ASmMDH4-pAtRbcS2-pOMT1-pAtLHB-FIS1A-p35S-peredox	Golden Gate level 2 plasmid (multigene construct) made up of level 1 plasmids EC15030, LS0113, LS0106, LS0119, LS0124, and LS0125; KnR in bacteria, HygR in plants	This work
LS0207 - pL2V-35S-Hyg-p35S-peredox	Golden Gate level 2 plasmid (multigene construct) made up of level 1 plasmids EC15030 and LS0127; KnR in bacteria, HygR in plants	This work

Table A.6: List of primers used in the generation and analysis of the tobacco combinatorial library. Details include primer name, sequence (5'-3'), and usage.

Primer name	Forward sequence (5'-3')	Reverse sequence (5'-3')	Usage
AtcyFBPase	GCGCTCTAGAATGGATCACGCAGCAGA TGCTCA	GCGCGGATCCTTAGTTCTTCTTTTCCTC CTCAGCATAGA	Cloning
AtTPT	GCGCTCTAGAATGGAGTCACGCGTGCT GTTAC	GCGCGGATCCTCAGCTGCTTTCTATGCT TTCTTTCCTTG	
AtFBPA	GCGCTCTAGAATGGCATCAACCTCACT CCTCAAGG	GCGCACTAGTTCAATAGGTGTACCCTTT GACGAACATGC	
EcPPase	GCGCACTAGATGAGCTTACTCAACGTC CCTGCG	GCGCGGATCCTTATTTATTCTTTGCGCG CTCGAAGGAGG	
AtPetC	CTCGAGATGGCTTCTGTTACTTCAGC	TGCTCCATGGTGGTCTTAAGAGCTC	
Pyc6	CTCGAGATGGCTTCTGTTACTTCAGCTG	GAGCTCTTACCATCCCTTTTCAGATTG	
M13	GTAAAACGACGGCCAG	GTCATAGCTGTTTCCTG	Sequencing
SEQ_SlRbcS	GAGTGTGTAATTTCAGAGG	-	
SEQ_StcyFBP	GTTAACAGAATGACGAATTGG	-	
SEQ_AtRbcS	GAAGAAGAGAAACAACAA	-	
SEQ_35S	CCACGTCTTCAAAGCAAG	-	
SEQ_NosT	TGCGGGACTCTAATCATAAAAACCC	-	
SEQ_StcyFBP_2	GCATCACTCTGCTCTTTCCACG	-	
pExBMG3-AtPetC	CGTAAGTGCAATTGCGTTGTGC	CGGGACCATGAGTCTTAAGCCA	Plant genomic PCR
pExBMG4-Pyc6	CGTAAGTGCAATTGCGTTGTGC	AGCAACAACAACAGCACCAACA	
pExBMG1-CaPFLP	CTTCGTCAACATGGTGGAGCAC	AAGATGAGCAAGAACCTGCCCT	
pExBMG2-SeictB	AGGTGGCTCCTACAAATGCCAT	TCTCCAAACACCGATAGCAGCA	
pExBMG5-AtFBPA	ACAGCCTAAATGGGAGGAGACA	TTGCCTCAGTGTTCTCTAGCCC	
pExBMG7-TPT	TGCTTTCGCCGTCCATTGTAAC	TAGCACTGATGAAACCGAGCCA	
pSKJ10-EcPP	TGCTTTCGCCGTCCATTGTAAC	GCATGGATAGAACATCGCGGTG	
pSKJ24-SWEET11	ACAGCCTAAATGGGAGGAGACA	AAGCACATTCGGGAAAGCAACA	
pSKJ5-SUC2	CAGCGTTAGTGGCACTGAAAGG	AGCTCTGCAGGGTCCTTGTAAG	
pSKJ43-nptII	GACTGGGCACAACAGACAATCG	TCCAGAAAAGCGGCCATTTTCC	
pSKJ1-GDC-H	CTGCAGGTCCCCAGATTAGCCT	GCAAGACCGGCAACAGGATTCA	
pSKJ1-GDC-H_2	AGGCTTGCTTCACAAACCAAGG	TCGGGGAAATTCGAGCTCCTAC	
pSKJ14-SBPase	TTTGGCACAAGCAACTCCTGAC	GCCACTTCAAACAACAGCCTCA	
pSKJ14-SBPase_2	CCACATCCTCCAGCTTCAAGCGT	TGGTCTTGTCAAGCACGGACTTGT	
pExBMG6-cyFBP	TCCACGTGGCATCCTCTGACGT	TGACCTCCGGCTTGCTCCATCA	
pExBMG6-cyFBP_2	GCAGCAGATGCTCACCGTACGG	TCCCGTAAAGGCCTGACCTCCG	

Table A.7: List of primers used in the generation of plasmids pK7WG2-AtFIS1A, LS0201, and LS0207. Details include primer name, sequence (5'-3'), and usage.

Primer name	Forward sequence (5'-3')	Reverse sequence (5'-3')	Usage
AtFIS1A	ATGGATGCTAAGATCGGACAATTC	TCATTTCTTGCGAGACATCGCTG	Cloning
NtmMDH_1	CACTCTGTGGTCTCAAATGTTAATTG TCATTAGCGAATTTGATTCCCTTCTC	CACTTCGTGGTCTCAAAGCATGTT GAGATCTATCGCCCGCAGAACCT	
NtmMDH_2	CACTCTGTGGTCTCAAATGTGTCAC AGTTGACTGCACGAATGAACACTC	CACTTCGTGGTCTCAAAGCACACC AGATCTCAGGTTTCTGGGTTTGC	
NtGAPC_1	CACTCTGTGGTCTCAAATGCCCTCC ACAATTCCAAACCT	CACTTCGTGGTCTCAAAGCATGGC ATCTGACAAGAAGATCAAGATCGG	
NtGAPC_2	CACTCTGTGGTCTCAAATGGCATTG GAGACAATGTCATACTCTGG	CACTTCGTGGTCTCAAAGCGGATT GGTCGTTTGGTGGCAAGAGTT	
TDNA_LB	TTTGCCGGATCAAGAGCTACCA	CGCGCGGTGTCATCTATGTTAC	Colony PCR level 2 constructs
R1_HYG	TGCCGTCAACCAAGCTCTGATA	GTAGGAGGGCGTGGATATGTCC	
R2_ASGAPC	GAAGGATTGGTCGTTTGGTGGC	CCTCTTCCTACCCCCATCTTGG	
R2_ASGAPC_2	ACTAGTTGCAGTGAACGACCCA	CTTAGCCAAAGGTGCAAGGCAG	
R3_FIS1A	ACTAGAATTCGAGCTCAGCGAG	ATCTGATGCCAGCTCGACAAGA	
R4_OMT	TTCCATCCCCAACGTTACTCCC	GGCCCCTTTGATCATTAGGGCT	
R4_OMT_2	-	CCAGTCTCTTTACGCCGGAGAT	
R5_ASMDH	CTCCCTCCCAGAGAATTCGCAT	TCAAGGGACCATGCAAAGTGAA	
R5_ASMDH4_2	TAAGACAGGCTTTGGAGGGAGC	CCCTTCAAGCAAGCATCAGCAA	
F6_peredox	ACGGCCACAAATTCAGCGTTAG	GAACCCATCATTTCTTCGCGCC	
SEQ_p35S	-	CTATCCTTCGCAAGACCCTTC	Sequencing pK7WG2-AtFIS1A
SEQ_T35S	TCTGGGAACTACTCACAC	-	
SEQ_pL1M-R	CGGATAAACCTTTTCACGCCC	GTACTGGGGTGGATGCAGTG	Sequencing multigene constructs
SEQ_scr-pL2B_2	CGAGTGGTGATTTTGTGCCG	-	
SEQ_OMT1mid	-	TAGCGATCGAAGCGAGAAGAGG	
SEQ_peredoxmid_1	GCTACACTGTACCGGTCCTCAA	-	
SEQ_peredoxmid_2	TCAAGATCCGCCACAACATCGA	-	
SEQ_peredoxmid_3	CAGCACGACTTCTTCAAGAGCG	-	
SEQ_peredoxmid_4	TGGTGAATCTTTCGAACTGCGC	-	
SEQ_peredoxmid_5	GGAGTTCATGCGCTTCAAGGTG	-	

Table A.8: List of primers used for qRT-PCR. Details include primer name, sequence, target gene, and final concentration used.

Name	Sequence (5'-3')	Target	Concentration
qPCR_F_EF1a	TGAGATGCACCACGAAGCTC	Internal reference EF1-a	0.313 µM
qPCR_R_EF1a	CCAACATTGTCACCAGGAAGTG	Internal reference EF1-a	
qPCR_F_L25	CCCCTCACCACAGAGTCTGC	Internal reference L25 ribosomal protein	0.078 µM
qPCR_R_L25	AAGGGTGTTGTTGTCCTCAATCTT	Internal reference L25 ribosomal protein	
qPCR_F_AtPetC	CGGAGGTGGAGGTGGTGGTACT	pExBMG3-AtPetC	0.2 µM
qPCR_R_AtPetC	GGTCAAGGTTCGGTCACCGGGA	pExBMG3-AtPetC	
qPCR_F_Pyc6	TGTGCTGCTTGTCATGCTGGAGG	pExBMG4-Pyc6	
qPCR_R_Pyc6	CCTCCGAAAGCAGGCATAGCGT	pExBMG4-Pyc6	
qPCR_F_CaPFLP	GGTGGCAAAGTCACTTGCATGGC	pExBMG1-CaPFLP	
qPCR_R_CaPFLP	ACCTGCCCTGCACGAATAAGGA	pExBMG1-CaPFLP	
qPCR_F_SeictB_2	TGCTGTTGAGGGTGGATTGCTTGG	pExBMG6-cyFBP	
qPCR_R_SeictB_2	CCAGCAAGTCCAGCAAGAGAAGCC	pExBMG6-cyFBP	
qPCR_F_AtFBPA	TGAAAACATGGGGCGGCAGACC	pExBMG5-AtFBPA	
qPCR_R_AtFBPA	CTTCGGACTCACCCTCACCGGT	pExBMG5-AtFBPA	
qPCR_F_SBP	GGAGGTCCAGTGGAAGGTGGGT	pSKJ14-SBPase	
qPCR_R_SBP	TGTCTCCAGGCCAAACACCGAA	pSKJ14-SBPase	
qPCR_F_GDC-H	GCCACCAGTGACGTTAACTCCCC	pSKJ1-GDC-H	
qPCR_R_GDC-H	GAATCCAGCTCCGACGGGTTGC	pSKJ1-GDC-H	
qPCR_F_TPT	GCTTGATCAGCTGGTCCGTGGG	pExBMG7-TPT	
qPCR_R_TPT	GCCTAAGGCGTGACAGACTGCG	pExBMG7-TPT	
qPCR_F_cyFBP_2	ACGTTGGACCACACTGATGAGCC	pExBMG6-cyFBP	
qPCR_R_cyFBP_2	ATCCGTGGACACCGGTTCCAGT	pExBMG6-cyFBP	
qPCR_F_EcPP	TTGACCGCTTCATGTCCACCGC	pSKJ10-EcPP	
qPCR_R_EcPP	CGGGTACGGAGTTGGGACCAGT	pSKJ10-EcPP	
qPCR_F_SWEET11	TCTTCAGTGCGACGCTTTGGCT	pSKJ24-SWEET11	
qPCR_R_SWEET11	CTGGCTTGGGAGCGTAGGCAAG	pSKJ24-SWEET11	
qPCR_F_SUC2_2	TTCGCCATCCTCGGTATCCCCC	pSKJ5-SUC2	
qPCR_R_SUC2_2	TAGGGAAAGTCCTTGGCCGGCA	pSKJ5-SUC2	
qPCR_F_AtFIS1A	TCGATACAGCGGTCCACGAGCT	pLS0201-AtFIS1A	
qPCR_R_AtFIS1A	TCTGGAAAGCAGTGCCCCTCCA	pLS0201-AtFIS1A	
qPCR_F_AtpOMT1	GTTGCGAGTGACACCTTCGGGG	pLS0201-AtpOMT1	
qPCR_R_AtpOMT1	GTTCCAGCTCCGGTTCCATGGC	pLS0201-AtpOMT1	
qPCR_F_NtmMDH_2	AGAACCTCGACCACCGGTGCAT	pLS0201-mMDH	
qPCR_R_NtmMDH_2	AGAGGCTGTCCGATCCCACCAG	pLS0201-mMDH	
qPCR_F_NtGAPC_3	TGCACTCCCTTACTGCCACCCA	pLS0201-GAPC	
qPCR_R_NtGAPC_3	TTCCAACAGCCTTGGCAGCACC	pLS0201-GAPC	

Appendix B

Supplementary materials - Chapter 3

Figures

Tables

Table B.1: Details of tobacco combinatorial library, T_0 generation. Line name; phenotype: leaf shape and size, leaf pigmentation, flower morphology and development, flower pigmentation, aphid infestation, and plant size; male sterility: confirmed (x) or putative ((x)); sexual crosses: able to self-pollinate and crossed with WT (-10), self-pollinated (-20), unable to self-pollinate and crossed with WT (-40); and use of progeny in primary screen (Yes/No).

Line	Phenotype	Male sterility	Cross	Screen
1_1A_Pr	NA	NA	-20	Yes
1_1B_Pr	NA	NA	-20	No
1_2A_Pr	NA	x	-20, -10	No
5_2A_Pr	Sickle shaped leaves, Deformed leaves	x	-40	No
7A_Pr	NA	x	-40	No
7B_Pr	NA	x	-40	No
9A_Pr	NA	NA	-20	Yes
9B_Pr	NA	NA	-20	No
11A_Pr	Many aphids	(x)	-20, -10	No
11A_1Rr	NA	NA	-20	No
12_2A_Pr	NA	NA	NA	No
13A_Pr	NA	NA	-20	Yes
16_1A_Pr	NA	NA	-20	Yes
16_2A_Pr	Narrow leaves, Long leaves	NA	NA	No
19_1A_Pr	Deformed leaves	x	-40	No
19_1B_Pr	NA	x	-40	No
22A_Pr	NA	(x)	-20, -10	Yes
23A_Pr	NA	x	-20, -10	No
23B_Pr	NA	NA	-20	Yes
24A_Pr	NA	NA	-20	No
24B_Pr	NA	NA	-20	Yes
25A_Pr	NA	NA	-20	No
27A_Pr	NA	NA	-20	No
27B_1Rr	NA	NA	-20	Yes
28A_Pr	NA	NA	-20	No
28B_Pr	NA	NA	-20, -10	No
29A_1Rr	Narrow leaves, Very long leaves,Tapered leaves	(x)	-40	Yes
29B_1Rr	Narrow leaves, Very long leaves, White vertical striped flowers	x	-20, -10	No
31A_Pr	Small plant, Early flowering	NA	-20, -10	No
34A_Pr	NA	NA	-20	No
34B_Pr	NA	NA	-20	No
35A_Pr	NA	NA	-20	Yes
36A_Pr	NA	NA	-20	Yes
36B_Pr	Deformed leaves	x	-20, -10	No
38A_Pr	NA	NA	-20	No
38B_Pr	NA	NA	-20	No
40_1A_1Rr	NA	NA	NA	No
40_1B_1Rr	Light spots	x	-20, -10	No
40_2A_Pr	Brindled leaves, Narrow leaves	NA	-40	No
41A_Pr	NA	NA	-20	Yes
41B_Pr	NA	NA	-20	No
42A_Pr	NA	NA	-20	No
42B_Pr	NA	NA	-20	Yes

Continued on next page

Line	Phenotype	Male sterility	Cross	Screen
43A_Pr	NA	NA	-20	Yes
43B_Pr	NA	NA	-20	No
45A_Pr	NA	NA	-20	NA
45B_Pr	NA	NA	-20	No
46A_Pr	NA	NA	-20	Yes
47A_Pr	NA	NA	-20	Yes
47B_Pr	NA	NA	-20	No
48A_Pr	NA	NA	-20	Yes
48B_Pr	NA	NA	-20	No
50A_Pr	NA	x	-20, -10	No
54_1A_Pr	Bridled leaves, Narrow leaves, Very long leaves, Almost white flowers	NA	NA	No
54_2A_Pr	Narrow leaves, small plant	NA	NA	No
56_1A_Pr	NA	NA	-20	No
56_1B_Pr	NA	NA	-20	No
56_2A_Pr	White spots, Deformed leaves	x	-40	No
57_1A_Pr	NA	NA	-20	No
57_2A_Pr	NA	NA	-20	No
57_2B_Pr	NA	NA	-20	No
59A_1Rr	NA	NA	-40	No
59B_1Rr	NA	x	-40	Yes
62A_Pr	NA	NA	NA	No
62B_Pr	NA	NA	-40	No
63A_Pr	NA	NA	-20	No
64A_Pr	NA	NA	NA	No
65_1A_Pr	Deformed leaves, Brindled leaves, Narrow leaves, Long leaves, Tapered leaves, Small plant	NA	-10	No
67A_Pr	NA	(x)	-20, -10	Yes
70A_Pr	Lighter green, Brindled leaves	(x)	-40	No
71A_Pr	NA	NA	-20	No
71B_Pr	Many aphids, Deformed leaves, Long leaves, Tapered leaves	x	-20, -10	No
72A_Pr	Sickle shaped leaves, Deformed leaves, Small plant	x	-20	No
74A_Pr	NA	x	-20, -10	No
75A_Pr	Wavy leaves	x	-20, -10	No
75B_Pr	NA	NA	-20	No
77_2A_Pr	NA	NA	-20, -10	Yes
77_2B_Pr	NA	NA	-20	No
80A_Pr	NA	NA	-20	No
80B_Pr	NA	NA	-20	Yes
81A_Pr	Deformed leaves, Narrow leaves, Long leaves, Tapered leaves, Cold stress flowers	(x)	-20, -10	No
81B_Pr	Narrow leaves, Long leaves, Cold stress flowers, Powder capsules	(x)	-40	No
82_1A_Pr	NA	NA	-20	No
82_2A_Pr	NA	NA	-20, -10	No
82_2B_Pr	NA	NA	-20	Yes
83A_Pr	NA	x	-20, -10	No
84A_Pr	NA	x	-20, -10	No
84B_Pr	NA	NA	NA	No

Continued on next page

Line	Phenotype	Male sterility	Cross	Screen
89A_Pr	NA	NA	NA	No
89B_Pr	NA	NA	NA	No
94_2A_Pr	NA	(x)	-20, -10	Yes
97A_Pr	NA	NA	-20	No
98A_1Rr	NA	NA	-20	No
98B_1Rr	NA	NA	-20	Yes
99A_Pr	NA	NA	-20	Yes
100A_Pr	NA	NA	-20	Yes
101A_Pr	NA	NA	-20	Yes
103A_Pr	NA	NA	-20	No
103B_Pr	NA	NA	-20	No
104A_Pr	Narrow leaves, Long leaves	NA	NA	No
104B_Pr	Narrow leaves, Long leaves	NA	-20, -10	No
105A_Pr	NA	(x)	-20, -10	Yes
109_1A_1Rr	Brindled leaves	NA	-20, -10	No
109_1B_1Rr	Brindled leaves	NA	-20, -10	No
109_3A_Pr	NA	(x)	-20, -10	No
110A_Pr	Deformed leaves	x	-40	No
110B_Pr	Deformed leaves	(x)	-20, -10	No
111A_Pr	Many aphids , Wavy laves	x	-20, -10	Yes
112A_Pr	NA	NA	-20	No
112B_Pr	NA	(x)	-20, -10	No
113A_Pr	Many aphids , Marbled, Narrow leaves, Tapered leaves, Drop down capsules	x	-40	No
113B_Pr	NA	(x)	-40	No
114A_Pr	Many aphids, Deformed leaves, Small leaves, Drop down, immature capsules	x	-40	No
114B_Pr	Narrow leaves, Small leaves, Tapered leaves	(x)	-40	No
116A_Pr	Tapered leaves, Small plant, Drop down capsules	x	NA	No
118A_Pr	NA	NA	-20	No
118B_Pr	NA	NA	-20	No
120A_Pr	NA	NA	-20	No
120B_Pr	NA	NA	-20	No
121A_Pr	Deformed leaves, Small plant	x	-40	No
122A_Pr	Deformed leaves	(x)	-20, -10	No
122B_Pr	NA	x	-40	No
123A_Pr	NA	NA	-20	No
123B_Pr	NA	NA	-20	No
124A_Pr	Narrow leaves, Long leaves	NA	NA	No
125A_Pr	Many aphids, Deformed leaves, Tapered leaves, Empty capsules	x	-40	No
126A_Pr	NA	(x)	-20, -10	No
126B_Pr	NA	NA	-20	Yes
128_1A_Pr	Narrow leaves, Narrow	x	-40	No
128_1B_Pr	NA	(x)	-20, -10	Yes
128_2A_Pr	Deformed leaves	(x)	-40	No
129A_Pr	Narrow leaves, Long leaves	NA	NA	No
134A_Pr	Narrow leaves, Tapered leaves, Small plant	x	-20, -10	No
135A_Pr	Deformed leaves, Small leaves, Wavy leaves, Drop down capsules	x	-40?	No
135B_Pr	Many aphids, Powder capsules	x	-40?	No

Continued on next page

Line	Phenotype	Male sterility	Cross	Screen
136A_Pr	NA	NA	-20, -10	No
137A_Pr	NA	(x)	-20, -10	Yes
137B_Pr	NA	NA	-20	No
138A_Pr	Deformed leaves	x	-40	No
138B_Pr	NA	(x)	-20, -10	No
139A_Pr	NA	NA	-40	No
140_1A_Pr	NA	NA	-20	No
140_2A_Pr	Sickle shaped leaves, Deformed leaves	x	-40	No
141A_Pr	NA	NA	-20	Yes
142A_Pr	Many aphids, Narrow leaves, Very long leaves	x	-20, -10	Yes
143A_Pr	NA	NA	-10	No
143B_Pr	Brindled leaves, Narrow leaves, Small leaves, Small plant	x	-40	No
144A_Pr	Wavy leaves, Tapered leaves	x	-40	No
144B_Pr	NA	(x)	-20, -10	No
146A_Pr	Deformed leaves, Wavy leaves	x	-20, -10	No
149A_Pr	Deformed leaves	x	-40	No
149B_Pr	NA	NA	-40	No
151A_Pr	NA	NA	-40	No
153A_Pr	Long leaves	NA	NA	No
155A_Pr	Light spots, Deformed leaves, Narrow leaves, Wavy leaves	x	-20, -10	No
155B_Pr	NA	NA	-40	No
156A_Pr	NA	NA	-20	No
156B_Pr	Many aphids	(x)	-20, -10	Yes
157A_Pr	NA	NA	-20	Yes
158A_Pr	NA	NA	NA	No
158B_Pr	NA	x	-20, -10	No
159A_Pr	Double flowers	x	-20, -10	No
159B_Pr	NA	x	-20, -10	No
163A_Pr	NA	(x)	-20, -10	Yes
163B_Pr	NA	NA	-40	No
164A_Pr	Deformed leaves, Tapered leaves, Deformed, filled flowers	x	-40	No
166A_Pr	NA	NA	-20	Yes
166B_Pr	NA	NA	-20	No
167A_Pr	No flowers, Small plant	NA	-20, -10	No
167B_Pr	Flowers rop down before pollination, Small plant	x	-20, -10	No
169A_Pr	NA	NA	-20	No
169B_Pr	NA	NA	-20	No
170A_Pr	NA	NA	-20	No
170B_Pr	NA	NA	-20, -10	No
171A_Pr	NA	NA	-40	No
172A_Pr	NA	x	-20, -10	No
173A_1A_Pr	Many aphids	x	-40	No
173_2A_Pr	Narrow leaves, Very long leaves, Tapered leaves	x	-40	No
173_2B_Pr	Narrow leaves	NA	-40	No
174A_Pr	Sickle shaped leaves, Deformed leaves	(x)	-20, -10	No
174B_Pr	Many aphids, Small leaves, Wavy leaves	x	-40	No
175A_Pr	Many aphids, Deformed leaves, Narrow leaves, Long leaves	x	-40	No

Continued on next page

Line	Phenotype	Male sterility	Cross	Screen
176A_Pr	Small plant	x	NA	No
177A_Pr	Wavy leaves	x	-20, -10	Yes
178A_Pr	Long leaves	NA	NA	No
182A_Pr	Long leaves	x	-40	No
182B_Pr	Long leaves	x	-40	No
183A_Pr	NA	x	-40	No
184A_Pr	Big leaves, Wavy leaves	x	-20, -10	No
185A_Pr	NA	NA	-40	No
186A_1Rr	Deformed leaves, Long leaves	NA	-40	No
187A_Pr	NA	NA	-20	No
188A_Pr	Deformed leaves, Narrow leaves, Tapered leaves, Small plant	x	-40	No
189A_Pr	Dark green, Deformed leaves	x	-40	No
191A_Pr	Thick flowers	NA	NA	No
192A_Pr	Deformed leaves, Small leaves, Tapered leaves	(x)	-20, -10	No
192B_Pr	Narrow leaves, Tapered leaves	(x)	-20, -10	No
193A_Pr	Deformed leaves	x	-40	No
193B_Pr	NA	x	-40	No
195A_Pr	Narrow leaves, Tapered leaves	x	-40	No
195B_Pr	Narrow leaves, Tapered leaves	x	-20, -10	No
197A_Pr	Very small capsules	x	-20, -10	No
197B_Pr	Wavy leaves	(x)	-20, -10	No
198A_Pr	NA	(x)	-20, -10	No
198B_Pr	NA	NA	-20	No
199A_Pr	Pink sepals	x	-40	No
201A_Pr	Thick	x	-40	No
202A_Pr	NA	NA	-20	No
203A_Pr	Thick, deformed flowers , Thick, empty capsules	x	NA	No
204A_Pr	Tapered leaves, Small plant	x	NA	No
205A_Pr	NA	x	-20, -10	No
205B_Pr	NA	(x)	-20, -10	No
206A_Pr	NA	(x)	-20, -10	No
206B_Pr	NA	x	-40	No
209A_Pr	NA	x	-40	No
209B_Pr	Deformed leaves, Brindled leaves	x	-40	No
210A_Pr	NA	NA	NA	No
211A_Pr	NA	NA	NA	No
211B_Pr	NA	NA	NA	No
214A_Pr	NA	NA	NA	No
215A_Pr	NA	NA	-20, -10	No
216A_Pr	Long leaves	NA	NA	No
216B_Pr	NA	NA	NA	No
217A_Pr	Tapered leaves	x	-20, -10	No
218A_Pr	NA	NA	NA	No
220A_Pr	Tapered leaves, Small plant	x	NA	No
222A_Pr	Sickle shaped leaves	NA	-20, -10	No
224A_Pr	NA	NA	-40	Yes
226A_Pr	NA	NA	-20, -10	No
226B_Pr	NA	NA	NA	No
227A_Pr	NA	NA	-20	No
227B_Pr	NA	NA	-20	No

Continued on next page

Line	Phenotype	Male sterility	Cross	Screen
228A_Pr	NA	NA	-20, -10	No
229A_Pr	Deformed leaves	NA	-40	No
230A_Pr	Narrow leaves, Long leaves	NA	-10	No
230B_Pr	Narrow leaves, Long leaves	x	-10	No
231A_Pr	NA	NA	-20	No
231B_Pr	NA	NA	-20	No
235A_Pr	Narrow leaves, Long leaves	NA	NA	No
236A_Pr	Deformed leaves	(x)	-40	No
237A_Pr	Brindled leaves, Narrow leaves, Long leaves, Tapered leaves	x	-40	No
237B_Pr	Narrow leaves, Long leaves	x	-40	No
239A_Pr	Deformed leaves	NA	-20, -10	No
239B_Pr	Deformed leaves	NA	-20, -10	No
240A_1Rr	NA	(x)	-40	No
240B_1Rr	NA	(x)	-40	No
242A_Pr	NA	(x)	-10	Yes
242B_Pr	NA	NA	NA	No
243A_Pr	Deformed leaves	x	-40	No
243B_Pr	Narrow leaves, Long leaves	NA	NA	No
244A_Pr	Narrow leaves	NA	-20, -10	No
244B_Pr	NA	NA	NA	No
246A_Pr	Thick	x	-40	No
249A_Pr	NA	NA	NA	No
250A_Pr	Deformed leaves	(x)	-40	No
252A_Pr	NA	(x)	-20, -10	No
252B_Pr	NA	(x)	-20, -10	Yes
253A_Pr	Wavy leaves	(x)	-20, -10	Yes
254A_Pr	NA	NA	-40	No
255A_Pr	Long leaves	x	-40	Yes
255B_Pr	Brindled leaves, Narrow leaves, Very long leaves, Tapered leaves	x	-20, -10	No
256A_Pr	Drop down	x	-40	No
258A_Pr	Deformed leaves, Brindled leaves	NA	NA	No
260A_Pr	Deformed leaves	NA	-40	No
261A_Pr	NA	NA	NA	No
261B_Pr	NA	NA	NA	No
262A_Pr	NA	NA	-20	Yes
263A_Pr	Long leaves	x	-40	Yes
263B_Pr	Long leaves	x	-40	No
264A_Pr	Long leaves, Small leaves	x	NA	No
265A_Pr	Deformed leaves	NA	NA	No
265B_Pr	NA	NA	NA	No
267A_Pr	NA	NA	-20, -10	Yes
270A_Pr	Many aphids, Deformed leaves, Wavy leaves, Tapered leaves, Drop down capsules	x	-40	No
272A_Pr	NA	x	-40	No
272B_Pr	NA	x	-40	No
275A_Pr	Narrow leaves, Long stamen, Small plant, Drop down capsules	x	NA	No
276A_Pr	NA	x	-20, -10	Yes
279A_Pr	Narrow leaves	NA	-20	Yes

Continued on next page

Line	Phenotype	Male sterility	Cross	Screen
279B_Pr	Long leaves	NA	NA	No
280A_Pr	Narrow leaves, Short pistil, Small plant	x	NA	No
281A_Pr	NA	NA	-20, -10	No
282A_Pr	Narrow leaves, Small plant, Drop down capsules	x	NA	No
283A_Pr	Narrow leaves	NA	-40	No
285A_1Rr	Deformed leaves	NA	-40	No
285B_1Rr	NA	NA	NA	No
287A_Pr	NA	x	-40	Yes
287B_Pr	Drop down	x	-40	No
289A_Pr	NA	NA	-40	No
291A_Pr	Frayed flowers, Small plant	NA	NA	No
292A_Pr	NA	NA	-40	No
293A_Pr	NA	NA	-40	No
296A_Pr	Tapered leaves	(x)	-40	No
296B_Pr	Tapered leaves	(x)	-40	No
297A_Pr	Deformed leaves, Brindled leaves, Small plant	NA	NA	No
300A_Pr	Dark green	NA	NA	No
300B_Pr	NA	NA	NA	No
301A_Pr	Tapered leaves	(x)	-20, -10	No
302A_Pr	Lighter and darker parts, Deformed leaves	NA	-40	No
303A_Pr	NA	x	-20, -10	No
303B_Pr	NA	(x)	NA	No
304A_Pr	Deformed leaves, Brindled leaves	x	NA	No
305A_Pr	Narrow leaves, Long leaves	(x)	-20, -10	Yes
305B_Pr	Narrow leaves, Tapered leaves	NA	-40	No
306A_Pr	Deformed leaves	(x)	-20, -10	No
306B_Pr	Deformed leaves	NA	-20, -10	No
309A_Pr	NA	x	-40	No
311A_Pr	Deformed leaves	x	-40	No
311B_Pr	Deformed leaves	(x)	-40	No
312A_Pr	NA	x	-20, -10	Yes
319A_Pr	NA	(x)	-20, -10	Yes
323A_Pr	Lighter spots	NA	-20, -10	Yes
325A_Pr	NA	NA	NA	No
327A_Pr	NA	NA	NA	No
328A_Pr	NA	NA	-20?	No
328B_Pr	NA	NA	-40	No
329A_Pr	NA	x	-40	Yes
330A_Pr	Thick flowers	NA	-40	No
334A_Pr	Narrow leaves, Round petals, Small plant	NA	NA	No
340A_Pr	NA	x	-20, -10	No
342A_Pr	Thick, deformed flowers	x	NA	No
345A_Pr	NA	x	-20, -10	Yes
348A_Pr	NA	x	NA	No
352_2A_Pr	NA	NA	-20, -10	No
359A_Pr	NA	NA	NA	No
368A_Pr	NA	NA	NA	No
369A_Pr	Small plant	NA	NA	No
372A_Pr	Small plant	NA	NA	No

Table B.2: Primary screen of the combinatorial library — Physiology. Details of batch, line, height (mm), leaf length (mm), and total number of leaves are shown. Means with asterisks denote statistical significance against WT control from the corresponding batch (P <0.05 Welch Two sample T-Test). Significance is reported as "***" for P-value<0.001, "**" for P-value<0.01, or "*" for P-value<0.05. Means of four plants ± SE.

Batch	Line	Height	Leaf length	Leaf number
1	**1_1A-20**	498.25 ± 41.41	174.00 ± 9.37	23.75 ± 1.65
1	**13A-20**	476.00 ± 44.27	200.25 ± 8.22	23.00 ± 1.63
1	**22A-10**	565.75 ± 24.30	200.75 ± 4.15	22.25 ± 2.06
1	**24B-20**	537.00 ± 34.85	185.25 ± 11.31	22.25 ± 1.75
1	**42B-20**	**586.25 ± 13.42***	188.00 ± 10.28	20.25 ± 1.84
1	**80B-20**	547.25 ± 34.35	188.25 ± 13.02	20.25 ± 1.18
1	**82_2B-20**	511.25 ± 18.65	187.00 ± 5.00	19.50 ± 1.66
1	**111A-10**	**644.50 ± 20.51****	179.50 ± 5.14	23.25 ± 1.38
1	**137A-10**	550.25 ± 24.70	205.25 ± 4.49	28.50 ± 2.10
1	**142A-10**	**590.00 ± 15.85***	186.75 ± 12.00	23.75 ± 0.85
1	**166A-20**	424.75 ± 29.12	191.50 ± 15.24	20.00 ± 0.71
1	**177A-10**	514.75 ± 22.24	196.75 ± 21.31	28.25 ± 2.01
1	**253A-10**	**605.75 ± 17.81***	187.25 ± 2.49	25.00 ± 1.41
1	**276A-10**	529.75 ± 25.69	212.00 ± 15.50	19.50 ± 2.50
1	**WT 1**	480.00 ± 29.81	208.50 ± 15.64	22.25 ± 2.87
2	**16_1A-20**	586.75 ± 41.502	177.25 ± 12.24	31.75 ± 3.04
2	**23B-20**	623.50 ± 34.77	180.50 ± 17.96	32.75 ± 2.93
2	**27B-20**	531.00 ± 29.72	**165.50 ± 6.38***	28.25 ± 1.03
2	**35A-20**	**698.00 ± 32.75***	173.25 ± 4.71	30.00 ± 1.51
2	**46A-20**	546.50 ± 21.509	192.00 ± 6.39	28.00 ± 1.47
2	**47A-20**	593.00 ± 21.99	179.25 ± 6.64	29.25 ± 1.38
2	**67A-10**	596.75 ± 39.67	180.75 ± 9.03	35.00 ± 3.29
2	**98B-20**	537.00 ± 60.26	**159.25 ± 7.04***	26.25 ± 2.17
2	**100A-20**	565.25 ± 27.08	180.25 ± 10.94	29.50 ± 2.02
2	**128_1B-10**	633.25 ± 51.14	170.25 ± 12.16	**40.50 ± 3.48***
2	**141A-20**	**520.00 ± 21.89***	182.50 ± 10.36	23.75 ± 4.40
2	**156B-20**	561.500 ± 18.00	**166.50 ± 7.13***	**32.50 ± 2.18***
2	**163A-40**	569.25 ± 15.40	187.75 ± 12.93	27.00 ± 1.22
2	**262A-20**	**346.500 ± 21.29*****	188.50 ± 14.63	25.00 ± 1.68
2	**WT 2**	590.25 ± 12.08	189.00 ± 5.23	25.50 ± 1.19
3	**9A-20**	484.00 ± 63.27	173.00 ± 6.15	24.75 ± 2.50
3	**29A-40**	388.75 ± 62.05	167.50 ± 4.05	26.25 ± 3.20
3	**36A-20**	464.25 ± 18.502	175.50 ± 10.08	28.00 ± 1.22
3	**41A-20**	469.75 ± 23.17	170.50 ± 10.18	29.25 ± 1.44
3	**43A-20**	474.75 ± 30.98	177.25 ± 12.13	29.75 ± 3.06
3	**48A-20**	448.75 ± 17.46	151.25 ± 0.95	28.75 ± 1.49
3	**59B-40**	448.75 ± 29.06	187.00 ± 14.50	25.75 ± 1.44
3	**77_2A-10**	539.500 ± 49.72	166.75 ± 7.22	27.50 ± 2.18
3	**94_2A-40**	487.50 ± 24.06	166.50 ± 5.87	**33.75 ± 0.75***
3	**99A-20**	378.50 ± 86.98	170.25 ± 11.34	24.50 ± 3.51
3	**101A-20**	569.75 ± 32.12	185.00 ± 10.24	31.00 ± 0.91
3	**105A-10**	587.25 ± 27.12	177.50 ± 6.22	**33.25 ± 1.03***
3	**126B-20**	420.50 ± 43.87	165.75 ± 11.78	27.75 ± 2.32
3	**157A-20**	490.75 ± 55.39	181.00 ± 11.68	28.50 ± 2.02
3	**WT 3**	537.50 ± 32.14	169.75 ± 11.50	29.75 ± 0.85
4	**224A-40**	**401.50 ± 20.02***	166.50 ± 12.82	22.50 ± 0.29
4	**242A-10**	**392.50 ± 14.45***	178.75 ± 11.88	26.00 ± 0.41
4	**252B-10**	485.25 ± 48.503	156.00 ± 3.19	25.75 ± 1.18
4	**255A-40**	478.75 ± 24.28	167.00 ± 5.90	27.00 ± 1.35
4	**263A-40**	**618.25 ± 33.28***	177.50 ± 5.74	**36.75 ± 2.66***
4	**267A-10**	495.00 ± 21.76	169.50 ± 5.81	21.75 ± 0.75
4	**279A-20**	**395.50 ± 22.30***	170.25 ± 10.76	28.00 ± 0.91
4	**287A-40**	**709.00 ± 22.07*****	180.50 ± 12.07	**41.25 ± 2.95****
4	**305A-10**	520.75 ± 66.504	175.50 ± 8.503	28.50 ± 0.50
4	**312A-10**	559.75 ± 14.16	175.00 ± 9.42	27.50 ± 2.22
4	**319A-10**	451.75 ± 20.01	165.50 ± 5.07	22.75 ± 0.63
4	**323A-10**	400.75 ± 29.502	181.25 ± 12.98	22.00 ± 2.16
4	**329A-40**	**342.50 ± 22.62****	172.25 ± 8.39	22.50 ± 1.89
4	**345A-10**	508.00 ± 73.93	179.75 ± 8.68	27.25 ± 4.33
4	**WT 4**	489.25 ± 26.29	172.00 ± 7.15	26.50 ± 1.66

Table B.3: Primary screen of the combinatorial library — Fresh weight biomass. Details of batch, line, leaves biomass (g), stem biomass (g), and total aerial biomass (g) are shown. Means with asterisks denote statistical significance against WT control from the corresponding batch (P <0.05 Welch Two sample T-Test). Significance is reported as "***" for P-value<0.001, "**" for P-value<0.01, or "*" for P-value<0.05. Means of four plants ± SE.

Batch	Line	Leaves biomass	Stem biomass	Total biomass
1	**1_1A-20**	109.13 ± 3.72	70.14 ± 5.85	179.26 ± 7.24
1	**13A-20**	112.46 ± 1.40	63.18 ± 3.89	175.63 ± 4.71
1	**22A-10**	110.78 ± 3.05	72.90 ± 2.47	183.67 ± 3.30
1	**24B-20**	110.38 ± 3.28	72.03 ± 3.31	182.41 ± 6.48
1	**42B-20**	106.34 ± 7.97	67.343 ± 4.37	173.68 ± 12.23
1	**80B-20**	108.95 ± 3.85	70.75 ± 3.01	179.70 ± 6.70
1	**82_2B-20**	104.07 ± 4.18	64.00 ± 2.41	168.07 ± 6.27
1	**111A-10**	110.30 ± 2.50	**83.35 ± 4.46***	193.64 ± 6.28
1	**137A-10**	121.26 ± 4.90	74.11 ± 8.67	195.37 ± 13.49
1	**142A-10**	107.45 ± 3.71	**79.07 ± 1.98***	186.50 ± 4.40
1	**166A-20**	**102.20 ± 3.82***	53.40 ± 5.28	155.51 ± 7.50
1	**177A-10**	118.32 ± 8.87	67.48 ± 6.51	168.93 ± 13.37
1	**253A-10**	116.66 ± 6.48	**80.68 ± 3.10***	197.35 ± 9.37
1	**276A-10**	105.97 ± 7.67	64.17 ± 3.07	170.14 ± 8.51
1	**WT 1**	115.82 ± 3.08	61.87 ± 4.37	177.69 ± 7.02
2	**16_1A-20**	109.88 ± 3.84	72.01 ± 8.41	181.88 ± 11.50
2	**23B-20**	**98.72 ± 2.51***	73.42 ± 4.42	172.13 ± 6.02
2	**27B-20**	103.84 ± 4.07	63.39 ± 5.719	167.24 ± 9.77
2	**35A-20**	125.42 ± 7.26	**100.67 ± 8.50***	226.09 ± 14.50
2	**46A-20**	117.67 ± 4.13	74.63 ± 5.67	192.30 ± 7.47
2	**47A-20**	114.09 ± 4.03	78.29 ± 1.80	192.38 ± 5.13
2	**67A-10**	120.49 ± 9.17	80.23 ± 9.43	200.72 ± 18.51
2	**98B-20**	87.84 ± 9.99	58.34 ± 11.50	146.18 ± 21.07
2	**100A-20**	114.26 ± 6.51	73.40 ± 4.30	187.66 ± 10.41
2	**128_1B-10**	**79.26 ± 6.30****	69.51 ± 8.76	148.85 ± 14.92
2	**141A-20**	**97.66 ± 5.98***	65.42 ± 4.65	163.08 ± 10.51
2	**156B-20**	117.43 ± 4.89	78.00 ± 1.35	195.43 ± 5.78
2	**163A-40**	132.85 ± 5.28	71.34 ± 1.68	204.19 ± 6.77
2	**262A-20**	100.88 ± 7.77	**42.91 ± 2.50****	**143.79 ± 9.62***
2	**WT 2**	117.49 ± 4.51	74.28 ± 4.70	191.77 ± 9.22
3	**9A-20**	113.26 ± 6.51	61.71 ± 8.26	174.97 ± 14.31
3	**29A-40**	**72.85 ± 6.95****	**39.98 ± 7.89***	**112.84 ± 14.67****
3	**36A-20**	117.89 ± 5.66	62.19 ± 4.39	180.08 ± 9.89
3	**41A-20**	112.50 ± 4.04	60.13 ± 4.67	172.67 ± 8.09
3	**43A-20**	117.20 ± 0.85	61.49 ± 4.10	178.69 ± 4.51
3	**48A-20**	107.14 ± 5.03	**55.95 ± 3.80***	**163.09 ± 8.09***
3	**59B-40**	123.41 ± 6.85	60.11 ± 7.14	183.50 ± 13.83
3	**77_2A-10**	**86.84 ± 4.88****	60.31 ± 9.06	**147.15 ± 12.93***
3	**94_2A-40**	123.70 ± 12.20	61.81 ± 5.08	185.50 ± 16.37
3	**99A-20**	104.03 ± 8.09	46.08 ± 14.20	150.11 ± 22.05
3	**101A-20**	114.50 ± 3.13	77.71 ± 5.17	192.24 ± 8.01
3	**105A-10**	119.79 ± 7.75	80.10 ± 7.50	199.89 ± 15.11
3	**126B-20**	108.76 ± 4.05	56.49 ± 9.19	165.25 ± 13.17
3	**157A-20**	115.93 ± 5.30	66.09 ± 10.99	182.01 ± 15.99
3	**WT 3**	130.32 ± 8.01	77.86 ± 7.03	208.18 ± 14.61
4	**224A-40**	122.96 ± 1.84	60.25 ± 3.65	183.21 ± 3.01
4	**242A-10**	107.96 ± 4.32	**51.36 ± 1.98***	159.32 ± 4.22
4	**252B-10**	131.91 ± 3.33	80.63 ± 4.99	212.50 ± 1.75
4	**255A-40**	115.41 ± 5.21	72.09 ± 3.71	187.50 ± 8.51
4	**263A-40**	112.50 ± 2.18	85.62 ± 5.98	198.12 ± 7.95
4	**267A-10**	132.32 ± 4.51	80.67 ± 6.34	212.99 ± 10.49
4	**279A-20**	104.65 ± 1.81	54.94 ± 3.48	159.51 ± 5.29
4	**287A-40**	116.95 ± 8.49	**112.36 ± 12.00***	229.31 ± 20.06
4	**305A-10**	122.88 ± 2.44	74.49 ± 9.12	197.37 ± 8.76
4	**312A-10**	126.29 ± 1.06	84.42 ± 2.73	210.71 ± 3.71
4	**319A-10**	126.28 ± 1.66	73.31 ± 3.28	199.51 ± 4.72
4	**323A-10**	124.98 ± 6.66	64.87 ± 6.70	189.85 ± 12.78
4	**329A-40**	116.14 ± 9.45	**49.85 ± 4.51***	165.98 ± 13.72
4	**345A-10**	100.32 ± 2.70	63.06 ± 7.75	163.38 ± 8.37
4	**WT 4**	117.38 ± 6.82	71.60 ± 6.51	188.98 ± 12.65

Table B.4: Primary screen of the combinatorial library — Light response curve of chlorophyll fluorescence. Details of batch, line, F_0 (minumum fluorescence), F_m (maximum fluorescence), F_v/F_m (maximum quantum yield of primary photosystem II photochemistry), ETRmax (maximum relative electron transport rate), and Ik (minimum saturating irradiance) are shown. The youngest fully expanded leaf (dark adapted) was used to perform a light response curve using PAM fluorometry. Means with asterisks denote statistical significance against WT control from the corresponding batch (P <0.05 Welch Two sample T-Test). Significance is reported as "***" for P-value<0.001, "**" for P-value<0.01, or "*" for P-value<0.05. Means of four plants ± SE.

Batch	Line	Fo	F_m	F_v/F_m	ETRmax	Ik
1	**1__1A-20**	1.06 ± 0.07	5.16 ± 0.45	0.80 ± 0.01	118.50 ± 10.21	303.10 ± 31.02
1	**13A-20**	1.12 ± 0.11	5.26 ± 0.50	0.79 ± 0.00	117.50 ± 10.34	298.68 ± 26.87
1	**22A-10**	1.19 ± 0.04	5.51 ± 0.28	0.79 ± 0.02	119.25 ± 8.24	294.23 ± 21.09
1	**24B-20**	0.97 ± 0.10	4.63 ± 0.50	0.79 ± 0.00	107.33 ± 5.21	268.65 ± 15.61
1	**42B-20**	1.12 ± 0.15	5.39 ± 0.69	0.79 ± 0.00	106.63 ± 5.84	261.95 ± 18.27
1	**80B-20**	1.25 ± 0.11	5.78 ± 0.36	0.79 ± 0.01	121.23 ± 7.39	307.60 ± 21.46
1	**82__2B-20**	1.12 ± 0.11	4.91 ± 0.50	0.78 ± 0.01	118.50 ± 5.507	306.25 ± 12.67
1	**111A-10**	1.14 ± 0.12	4.98 ± 0.33	0.78 ± 0.01	109.25 ± 7.88	280.85 ± 25.45
1	**137A-10**	1.12 ± 0.10	4.99 ± 0.37	0.78 ± 0.01	95.43 ± 6.10	235.13 ± 13.66
1	**142A-10**	1.15 ± 0.01	5.51 ± 0.16	0.79 ± 0.00	119.50 ± 3.80	302.68 ± 13.09
1	**166A-20**	1.14 ± 0.18	4.84 ± 0.44	0.77 ± 0.02	111.05 ± 8.78	276.28 ± 23.41
1	**177A-10**	1.14 ± 0.01	5.36 ± 0.14	0.79 ± 0.00	108.18 ± 7.89	266.85 ± 21.20
1	**253A-10**	1.02 ± 0.11	4.67 ± 0.34	0.79 ± 0.01	117.43 ± 11.22	290.35 ± 31.97
1	**276A-10**	1.15 ± 0.13	4.98 ± 0.44	0.77 ± 0.01	105.25 ± 7.50	263.78 ± 25.13
1	**WT 1**	1.16 ± 0.02	5.38 ± 0.13	0.79 ± 0.00	116.08 ± 12.39	293.05 ± 29.28
2	**16__1A-20**	0.79 ± 0.02	3.69 ± 0.07	0.79 ± 0.01	85.90 ± 4.48	210.33 ± 10.82
2	**23B-20**	0.79 ± 0.03	3.51 ± 0.07	0.78 ± 0.01	85.25 ± 3.98	203.63 ± 15.32
2	**27B-20**	0.79 ± 0.01	3.69 ± 0.03	0.79 ± 0.00	87.90 ± 3.91	210.75 ± 11.36
2	**35A-20**	0.8 ± 0.03	3.63 ± 0.06	0.78 ± 0.01	**81.90 ± 3.75***	**201.35 ± 10.83***
2	**46A-20**	0.81 ± 0.03	3.82 ± 0.11	0.79 ± 0.00	99.70 ± 3.29	248.15 ± 6.91
2	**47A-20**	0.78 ± 0.02	3.69 ± 0.09	0.79 ± 0.00	96.50 ± 9.08	241.88 ± 25.67
2	**67A-10**	0.78 ± 0.00	3.62 ± 0.04	0.79 ± 0.00	96.50 ± 4.77	244.23 ± 13.09
2	**98B-20**	0.77 ± 0.02	3.50 ± 0.07*	0.78 ± 0.01	93.28 ± 4.66	218.51 ± 13.49
2	**100A-20**	0.77 ± 0.01	3.60 ± 0.06	0.79 ± 0.00	88.85 ± 7.22	216.28 ± 19.25
2	**128__1B-10**	0.81 ± 0.04	**3.47 ± 0.07***	**0.77 ± 0.01***	85.51 ± 8.44	205.65 ± 26.22
2	**141A-20**	0.79 ± 0.03	3.70 ± 0.05	0.79 ± 0.01	90.88 ± 3.85	211.40 ± 12.60
2	**156B-20**	0.77 ± 0.01	**3.50 ± 0.02***	0.78 ± 0.00	**78.50 ± 3.51***	**180.80 ± 9.35****
2	**163A-40**	0.79 ± 0.02	3.71 ± 0.07	0.79 ± 0.00	90.70 ± 4.68	220.73 ± 13.32
2	**262A-20**	0.74 ± 0.02	3.61 ± 0.11	0.80 ± 0.01	97.73 ± 7.17	234.20 ± 15.50
2	**WT 2**	0.77 ± 0.00	3.74 ± 0.04	0.79 ± 0.00	94.93 ± 1.50	238.40 ± 2.50
3	**9A-20**	0.75 ± 0.02	3.33 ± 0.10	0.78 ± 0.00	92.75 ± 9.19	225.73 ± 25.69
3	**29A-40**	**0.89 ± 0.03***	3.50 ± 0.17	0.75 ± 0.01	114.25 ± 2.80	306.35 ± 4.78
3	**36A-20**	0.77 ± 0.00	3.51 ± 0.08	0.79 ± 0.00	96.65 ± 4.91	234.50 ± 10.51
3	**41A-20**	0.79 ± 0.02	3.46 ± 0.10	0.77 ± 0.01	96.35 ± 9.67	235.23 ± 23.31
3	**43A-20**	0.76 ± 0.02	3.43 ± 0.10	0.78 ± 0.00	97.85 ± 9.04	245.93 ± 28.13
3	**48A-20**	0.75 ± 0.01	3.42 ± 0.04	0.78 ± 0.00	93.35 ± 5.61	224.45 ± 16.16
3	**59B-40**	0.75 ± 0.02	3.49 ± 0.08	0.79 ± 0.01	108.23 ± 13.50	270.40 ± 37.25
3	**77__2A-10**	0.75 ± 0.01	3.32 ± 0.22	0.77 ± 0.01	101.85 ± 9.95	262.63 ± 26.33
3	**94__2A-40**	0.78 ± 0.01	3.48 ± 0.11	0.78 ± 0.00	96.80 ± 3.38	237.28 ± 7.03
3	**99A-20**	0.78 ± 0.02	3.49 ± 0.12	0.78 ± 0.00	91.10 ± 4.28	227.08 ± 14.96
3	**101A-20**	0.78 ± 0.02	3.62 ± 0.03	0.79 ± 0.00	93.15 ± 5.09	244.85 ± 33.08
3	**105A-10**	0.75 ± 0.02	3.31 ± 0.16	0.78 ± 0.01	103.10 ± 4.50	261.48 ± 16.08
3	**126B-20**	0.74 ± 0.02	3.39 ± 0.08	0.78 ± 0.00	110.05 ± 8.66	277.25 ± 27.99
3	**157A-20**	0.77 ± 0.01	3.49 ± 0.07	0.78 ± 0.01	101.00 ± 5.11	252.00 ± 15.86
3	**WT 3**	0.76 ± 0.03	3.42 ± 0.08	0.78 ± 0.01	103.30 ± 7.45	260.75 ± 19.07
4	**224A-40**	0.71 ± 0.01	3.43 ± 0.09	0.80 ± 0.00	108.08 ± 4.93	269.40 ± 14.51
4	**242A-10**	0.71 ± 0.02	3.34 ± 0.08	0.79 ± 0.01	117.30 ± 6.73	293.70 ± 22.66
4	**252B-10**	0.75 ± 0.02	3.50 ± 0.09	0.79 ± 0.00	113.78 ± 8.39	285.95 ± 28.60
4	**255A-40**	0.71 ± 0.03	3.41 ± 0.13	0.79 ± 0.00	100.93 ± 6.23	245.03 ± 15.42
4	**263A-40**	0.71 ± 0.01	3.43 ± 0.11	0.79 ± 0.00	101.13 ± 1.99	246.25 ± 9.35
4	**267A-10**	0.73 ± 0.03	3.47 ± 0.14	0.79 ± 0.00	112.88 ± 6.94	278.95 ± 19.20
4	**279A-20**	0.74 ± 0.02	3.50 ± 0.02	0.79 ± 0.00	101.83 ± 5.41	238.73 ± 13.38
4	**287A-40**	0.71 ± 0.01	3.51 ± 0.13	0.80 ± 0.00	113.95 ± 7.49	281.80 ± 19.24
4	**305A-10**	0.73 ± 0.02	3.38 ± 0.05	0.79 ± 0.01	97.10 ± 6.72	241.51 ± 20.87
4	**312A-10**	0.75 ± 0.02	3.47 ± 0.10	0.79 ± 0.01	98.20 ± 3.71	246.50 ± 13.29
4	**319A-10**	0.74 ± 0.01	3.64 ± 0.05	0.80 ± 0.00	110.83 ± 5.14	272.43 ± 18.44
4	**323A-10**	0.77 ± 0.01	3.51 ± 0.07	0.79 ± 0.00	110.25 ± 7.11	273.23 ± 20.42
4	**329A-40**	0.74 ± 0.02	3.47 ± 0.11	0.79 ± 0.00	115.35 ± 11.67	285.35 ± 29.13
4	**345A-10**	0.81 ± 0.04	3.51 ± 0.15	0.77 ± 0.01	102.95 ± 11.77	250.05 ± 27.80
4	**WT 4**	0.73 ± 0.01	3.47 ± 0.12	0.79 ± 0.00	98.08 ± 4.50	252.23 ± 23.41

Table B.5: Primary screen of the combinatorial library — Chlorophyll content. Details of batch, line, chlorophyll *a* (mg m^{-2}), chlorophyll *b* (mg m^{-2}), total chlorophyll (mg m^{-2}), and the ratio of chlorophyll *a* to chlorophyll *b* are shown. Chlorophyll was extracted from the youngest fully expanded leaf. Means with asterisks denote statistical significance against WT control from the corresponding batch (P <0.05 Welch Two sample T-Test). Significance is reported as "***" for P-value<0.001, "**" for P-value<0.01, or "*" for P-value<0.05. Means of four plants ± SE.

Batch	Line	Chlorophyll a	Chlorophyll b	Total chlorophyll	Ratio chlorophyll
1	**1__1A-20**	**8.47 ± 0.19****	**1.66 ± 0.04****	**10.1 ± 0.21****	5.10 ± 0.14
1	**13A-20**	6.87 ± 0.35	1.35 ± 0.08	8.22 ± 0.44	5.11 ± 0.11
1	**22A-10**	**8.98 ± 0.56***	**1.78 ± 0.11***	**10.7 ± 0.67***	5.02 ± 0.06
1	**24B-20**	8.08 ± 0.65	1.56 ± 0.13	9.64 ± 0.78	**5.17 ± 0.03***
1	**42B-20**	8.04 ± 0.49	1.54 ± 0.12	9.59 ± 0.61	5.21 ± 0.12
1	**80B-20**	**8.04 ± 0.15****	**1.59 ± 0.05***	**9.62 ± 0.20****	5.05 ± 0.08
1	**82__2B-20**	**7.93 ± 0.17****	**1.59 ± 0.04***	**9.52 ± 0.22***	4.99 ± 0.06
1	**111A-10**	6.75 ± 0.40	1.28 ± 0.07	8.03 ± 0.47	**5.23 ± 0.07***
1	**137A-10**	6.85 ± 0.36	1.37 ± 0.08	8.23 ± 0.44	4.95 ± 0.09
1	**142A-10**	7.79 ± 0.46	1.63 ± 0.12	9.43 ± 0.58	4.78 ± 0.15
1	**166A-20**	**8.78 ± 0.34***	**1.74 ± 0.04*****	**10.5 ± 0.36****	5.02 ± 0.16
1	**177A-10**	6.94 ± 0.22	1.38 ± 0.05	8.33 ± 0.28	4.99 ± 0.04
1	**253A-10**	6.19 ± 0.29	**1.12 ± 0.06***	**7.32 ± 0.35***	**5.51 ± 0.07****
1	**276A-10**	7.56 ± 0.72	1.53 ± 0.16	9.10 ± 0.89	4.94 ± 0.08
1	**WT 1**	7.01 ± 0.08	1.40 ± 0.02	8.42 ± 0.09	5.00 ± 0.04
2	**16__1A-20**	6.45 ± 0.30	1.31 ± 0.04	7.77 ± 0.34	4.89 ± 0.09
2	**23B-20**	7.52 ± 0.58	1.58 ± 0.13	9.11 ± 0.71	4.74 ± 0.03
2	**27B-20**	7.15 ± 0.75	1.44 ± 0.18	8.59 ± 0.93	5.00 ± 0.13
2	**35A-20**	6.30 ± 0.39	1.22 ± 0.12	7.53 ± 0.51	5.17 ± 0.20
2	**46A-20**	7.33 ± 0.18	1.49 ± 0.05	8.82 ± 0.24	4.93 ± 0.05
2	**47A-20**	6.83 ± 0.86	1.38 ± 0.17	8.21 ± 1.03	4.95 ± 0.10
2	**67A-10**	6.93 ± 0.35	1.36 ± 0.06	8.30 ± 0.41	5.07 ± 0.05
2	**98B-20**	7.12 ± 0.27	1.43 ± 0.06	8.55 ± 0.33	4.98 ± 0.07
2	**100A-20**	7.04 ± 0.27	1.43 ± 0.07	8.47 ± 0.34	4.92 ± 0.07
2	**128__1B-10**	7.65 ± 0.91	1.58 ± 0.18	9.23 ± 1.10	4.84 ± 0.01
2	**141A-20**	6.80 ± 0.75	1.38 ± 0.18	8.18 ± 0.93	4.94 ± 0.13
2	**156B-20**	6.86 ± 0.35	1.33 ± 0.05	8.20 ± 0.40	5.14 ± 0.11
2	**163A-40**	6.74 ± 0.34	1.30 ± 0.06	8.04 ± 0.40	5.15 ± 0.07
2	**262A-20**	8.74 ± 1.22	1.75 ± 0.26	10.5 ± 1.48	5.02 ± 0.08
2	**WT 2**	7.25 ± 0.53	1.43 ± 0.13	8.69 ± 0.67	5.07 ± 0.12
3	**9A-20**	6.61 ± 0.59	1.41 ± 0.14	8.02 ± 0.73	4.70 ± 0.07
3	**29A-40**	8.73 ± 0.70	**1.94 ± 0.15***	10.6 ± 0.85	**4.49 ± 0.04***
3	**36A-20**	5.96 ± 0.16	1.15 ± 0.02	7.12 ± 0.18	5.17 ± 0.06
3	**41A-20**	6.39 ± 0.51	1.28 ± 0.10	7.67 ± 0.60	5.02 ± 0.22
3	**43A-20**	6.63 ± 0.24	1.29 ± 0.06	7.92 ± 0.30	5.16 ± 0.07
3	**48A-20**	7.38 ± 0.32	1.49 ± 0.04	8.88 ± 0.36	4.93 ± 0.06
3	**59B-40**	9.09 ± 0.72	**1.94 ± 0.18***	11.0 ± 0.90	4.67 ± 0.08
3	**77__2A-10**	8.55 ± 0.77	1.71 ± 0.17	10.2 ± 0.94	5.00 ± 0.09
3	**94__2A-40**	6.15 ± 0.31	1.32 ± 0.06	7.47 ± 0.35	4.66 ± 0.19
3	**99A-20**	6.47 ± 0.22	1.36 ± 0.07	7.84 ± 0.29	4.75 ± 0.11
3	**101A-20**	7.05 ± 0.24	1.39 ± 0.06	8.45 ± 0.31	5.07 ± 0.10
3	**105A-10**	6.36 ± 0.31	1.29 ± 0.07	7.66 ± 0.38	4.92 ± 0.10
3	**126B-20**	8.26 ± 0.50	1.72 ± 0.10	9.99 ± 0.60	4.8 ± 0.06
3	**157A-20**	7.02 ± 0.33	1.45 ± 0.06	8.47 ± 0.39	4.82 ± 0.03
3	**WT 3**	6.71 ± 0.69	1.34 ± 0.14	8.05 ± 0.83	4.99 ± 0.11
4	**224A-40**	8.81 ± 0.80	1.87 ± 0.21	10.6 ± 1.02	**4.75 ± 0.11***
4	**242A-10**	7.30 ± 0.35	1.40 ± 0.09	8.71 ± 0.45	5.19 ± 0.08
4	**252B-10**	8.51 ± 0.24	1.76 ± 0.08	10.2 ± 0.32	4.83 ± 0.11
4	**255A-40**	7.49 ± 0.63	1.50 ± 0.14	8.99 ± 0.77	5.01 ± 0.12
4	**263A-40**	7.98 ± 0.65	1.58 ± 0.14	9.56 ± 0.80	5.06 ± 0.07
4	**267A-10**	8.73 ± 0.32	1.83 ± 0.06	10.5 ± 0.38	**4.77 ± 0.06***
4	**279A-20**	8.54 ± 1.00	1.69 ± 0.26	10.2 ± 1.26	5.09 ± 0.15
4	**287A-40**	8.50 ± 0.47	1.67 ± 0.10	10.1 ± 0.57	5.08 ± 0.06
4	**305A-10**	7.64 ± 1.54	1.49 ± 0.32	9.13 ± 1.87	5.18 ± 0.16
4	**312A-10**	6.76 ± 0.38	1.31 ± 0.10	8.08 ± 0.49	5.2 ± 0.15
4	**319A-10**	8.75 ± 0.42	1.77 ± 0.08	10.5 ± 0.51	4.95 ± 0.04
4	**323A-10**	8.94 ± 0.93	1.84 ± 0.17	10.7 ± 1.10	4.84 ± 0.04
4	**329A-40**	9.43 ± 0.21	**1.98 ± 0.11***	11.4 ± 0.33	4.77 ± 0.18
4	**345A-10**	9.51 ± 1.03	2.13 ± 0.26	11.6 ± 1.29	**4.48 ± 0.10****
4	**WT 4**	7.20 ± 0.82	1.38 ± 0.18	8.59 ± 1.00	5.25 ± 0.13

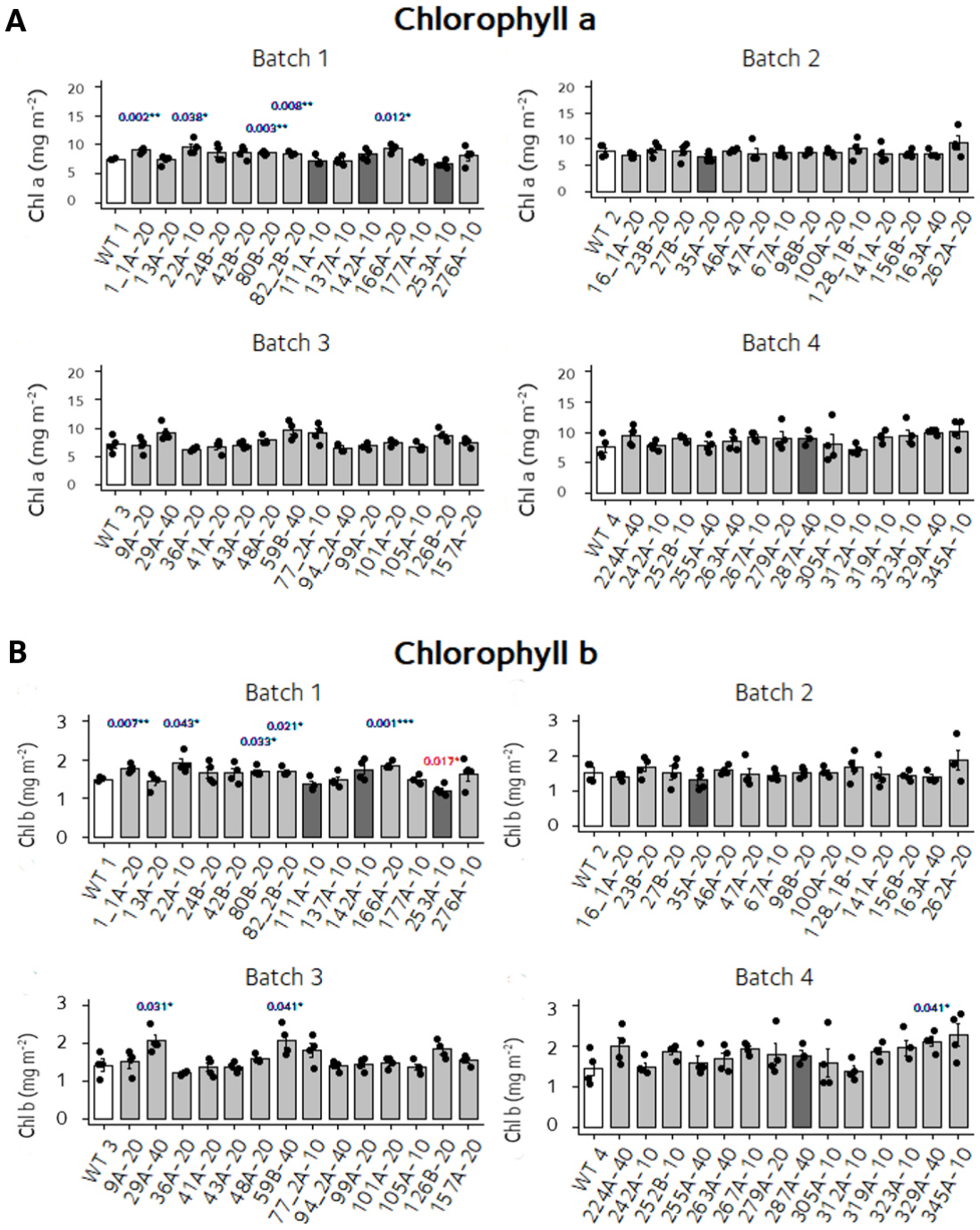

Figure B.1: Primary screen of the combinatorial library — Chlorophyll *a* and *b* content. Chlorophyll was extracted from the youngest fully expanded leaf. Chlorophyll *a* (**A**) and chlorophyll *b* (**B**) content are given for batches 1-4 in the primary screen. P-values are indicated for significant changes with respect to the corresponding WT (P <0.05 Welch Two sample T-Test). Significant increases are indicated in blue and decreases in red. Significance is reported as "***" for P-value<0.001, "**" for P-value<0.01, or "*" for P-value<0.05. Dark grey bars represent lines showing a stem growth phenotype, selected for further characterisation.

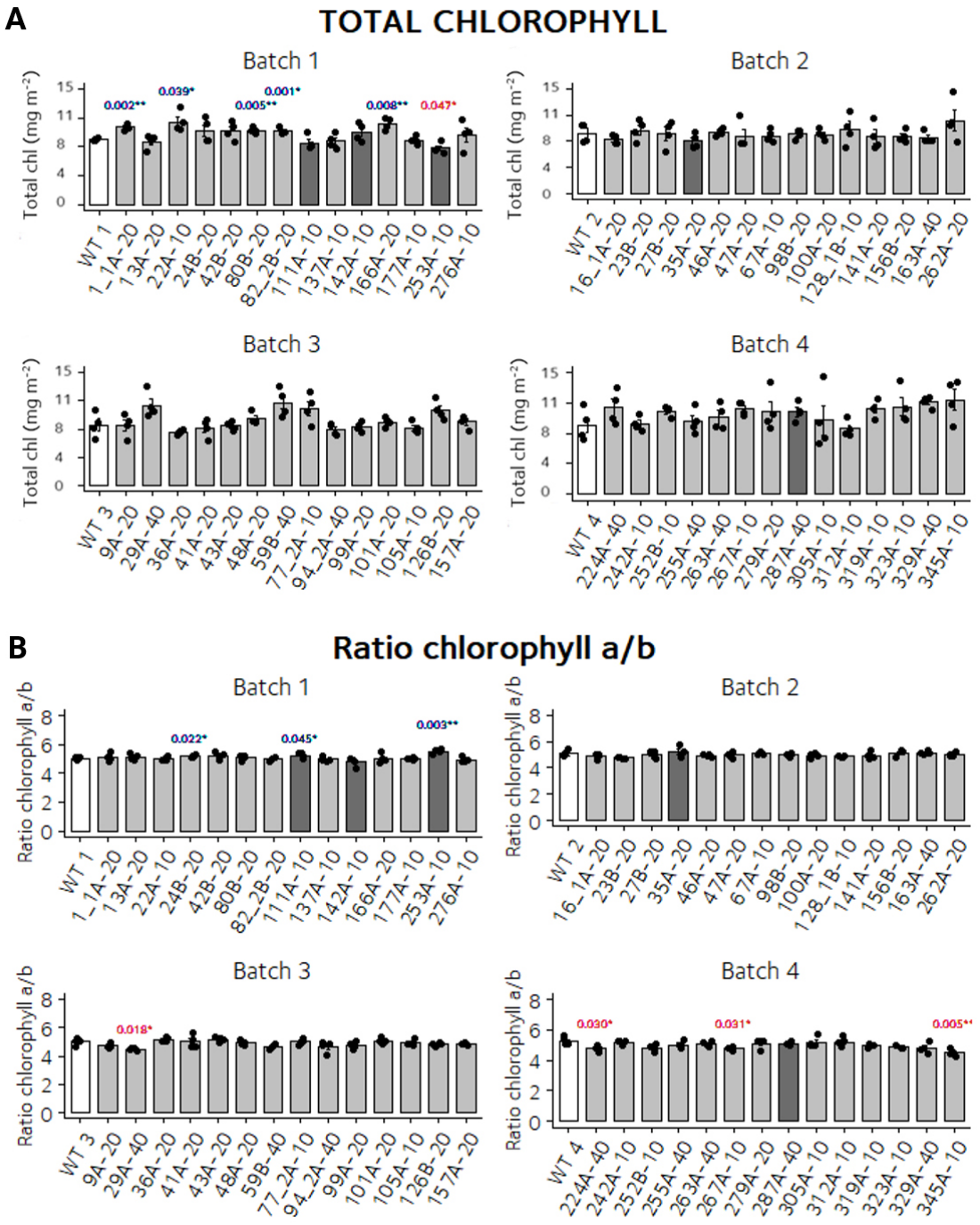

Figure B.2: Primary screen of the combinatorial library — Total chlorophyll content and ratio chlorophyll *a* to chlorophyll *b*. Chlorophyll was extracted from the youngest fully expanded leaf. Total chlorophyll content (**A**) and ratio chlorophyll *a* to chlorophyll *b* (**B**) are given for batches 1-4 in the primary screen. P-values are indicated for significant changes with respect to the corresponding WT (P <0.05 Welch Two sample T-Test). Significant increases are indicated in blue and decreases in red. Significance is reported as "***" for P-value<0.001, "**" for P-value<0.01, or "*" for P-value<0.05. Dark grey bars represent lines showing a stem growth phenotype, selected for further characterisation.

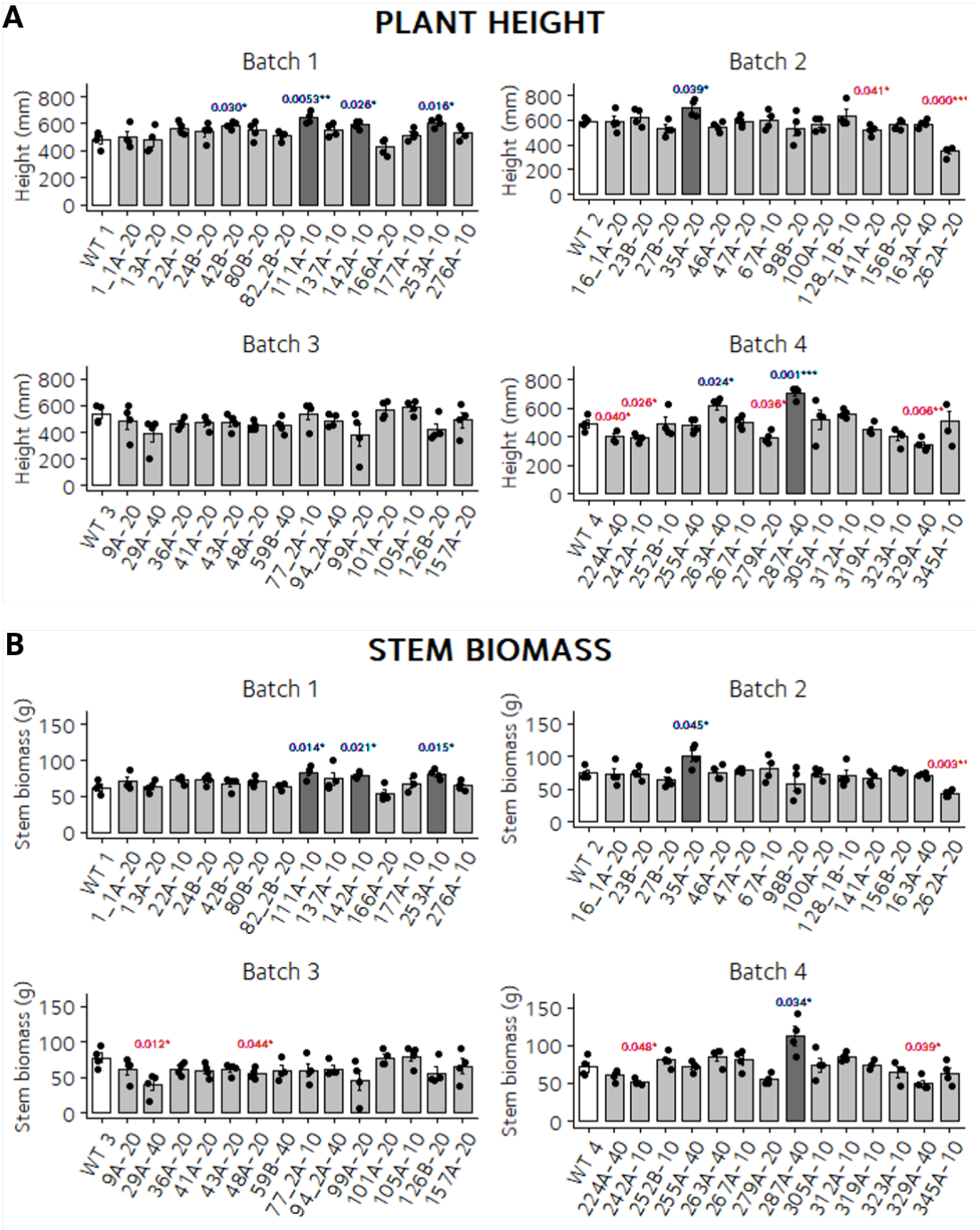

Figure B.3: Primary screen of the combinatorial library — Plant height and stem biomass. Plant height and stem biomass (fresh weight) are given for batches 1-4 in the primary screen. P-values are indicated for significant changes with respect to the corresponding WT (P <0.05 Welch Two sample T-Test). Significant increases are indicated in blue and decreases in red. Significance is reported as "***" for P-value<0.001, "**" for P-value<0.01, or "*" for P-value<0.05. Dark grey bars represent lines showing a stem growth phenotype, selected for further characterisation.

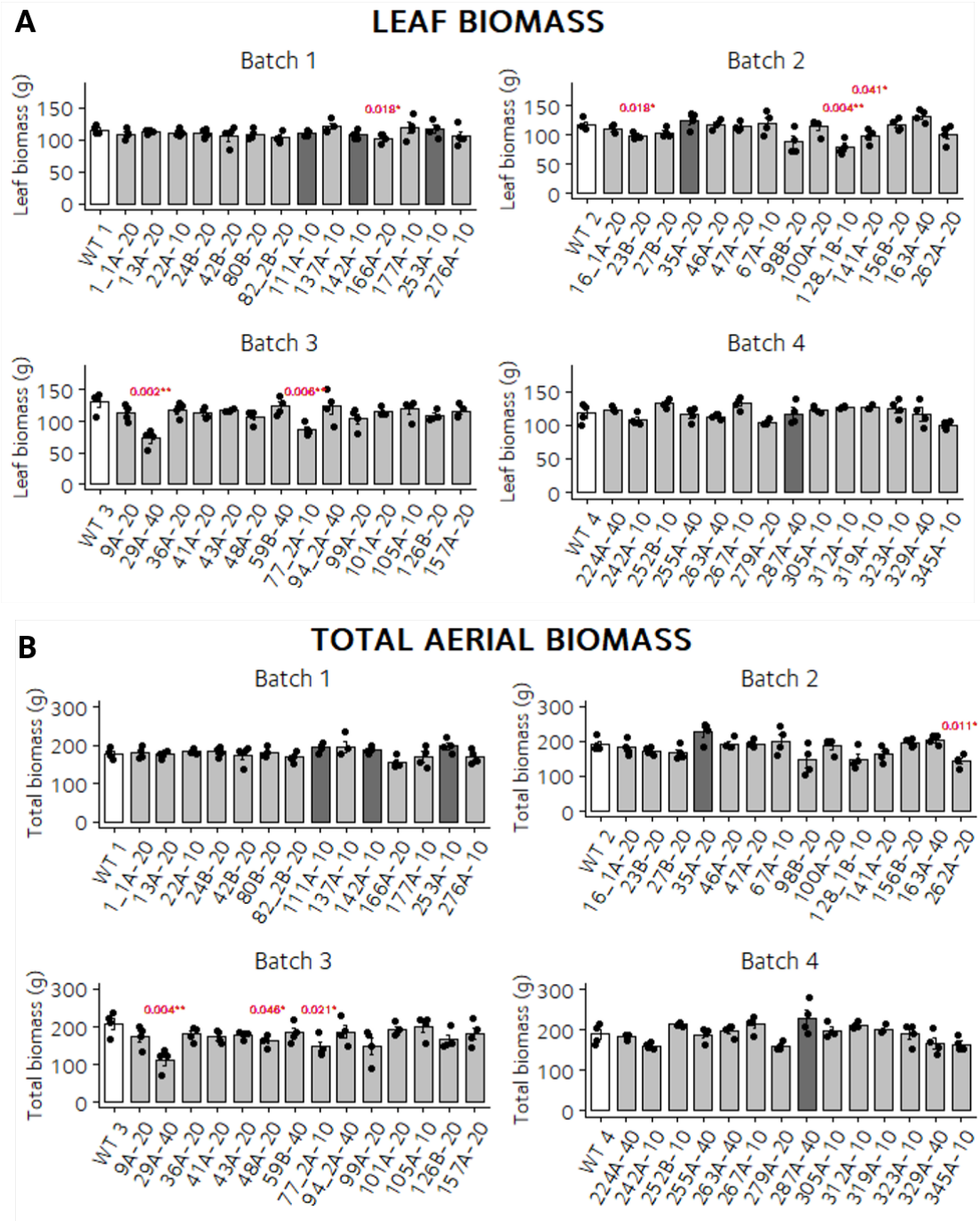

Figure B.4: Primary screen of the combinatorial library — Leaf and total biomass. Leaf and total biomass (fresh weight) are given for batches 1-4 in the primary screen. P-values are indicated for significant changes with respect to the corresponding WT ($P < 0.05$ Welch Two sample T-Test). Significant increases are indicated in blue and decreases in red. Significance is reported as "***" for P-value<0.001, "**" for P-value<0.01, or "*" for P-value<0.05. Dark grey bars represent lines showing a stem growth phenotype, selected for further characterisation.

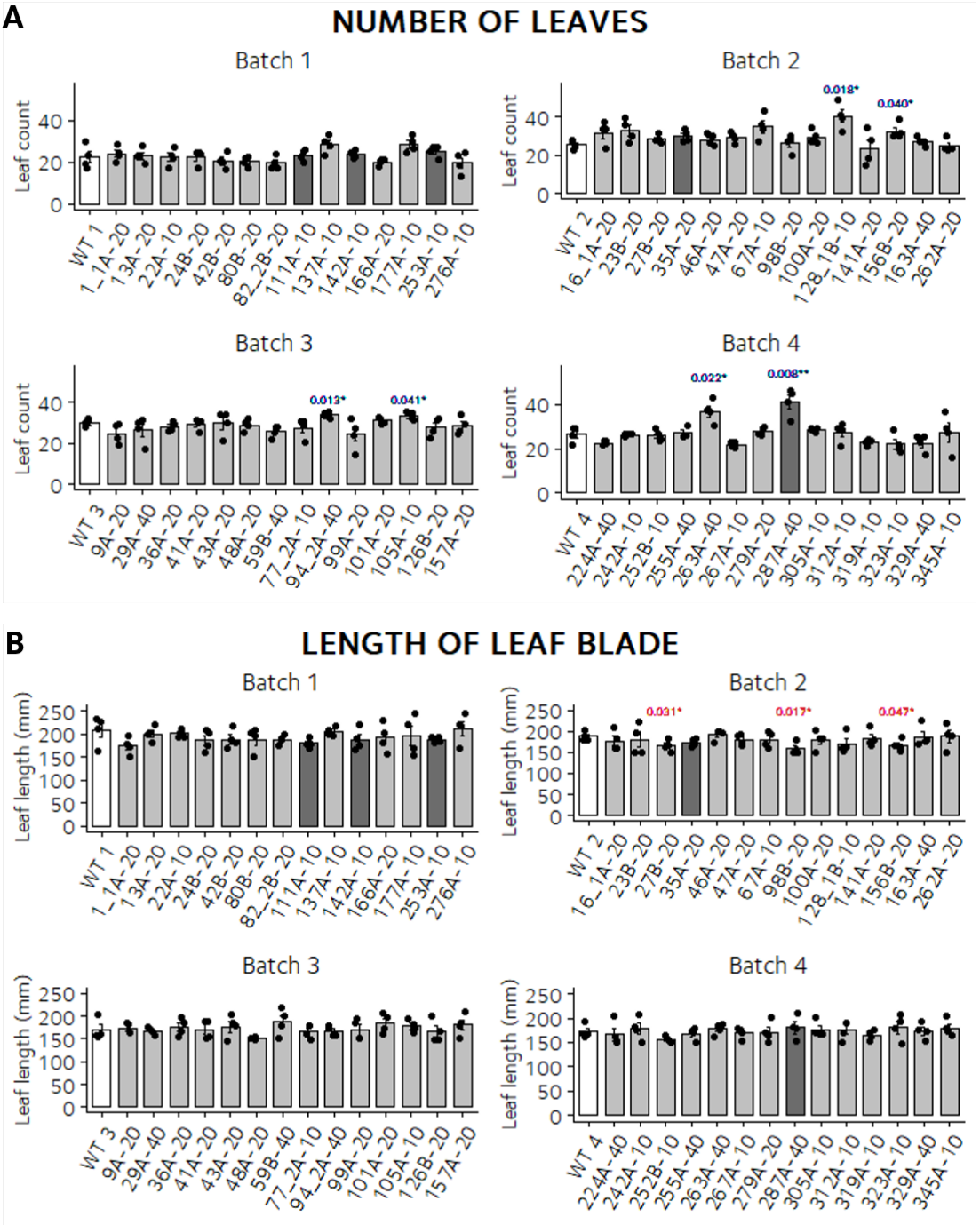

Figure B.5: Primary screen of the combinatorial library — Number of leaves and leaf length. Total number of leaves and length of leaf blade (youngest fully expanded leaf) are given for batches 1-4 in the primary screen. P-values are indicated for significant changes with respect to the corresponding WT (P <0.05 Welch Two sample T-Test). Significant increases are indicated in blue and decreases in red. Significance is reported as "***" for P-value<0.001, "**" for P-value<0.01, or "*" for P-value<0.05. Dark grey bars represent lines showing a stem growth phenotype, selected for further characterisation.

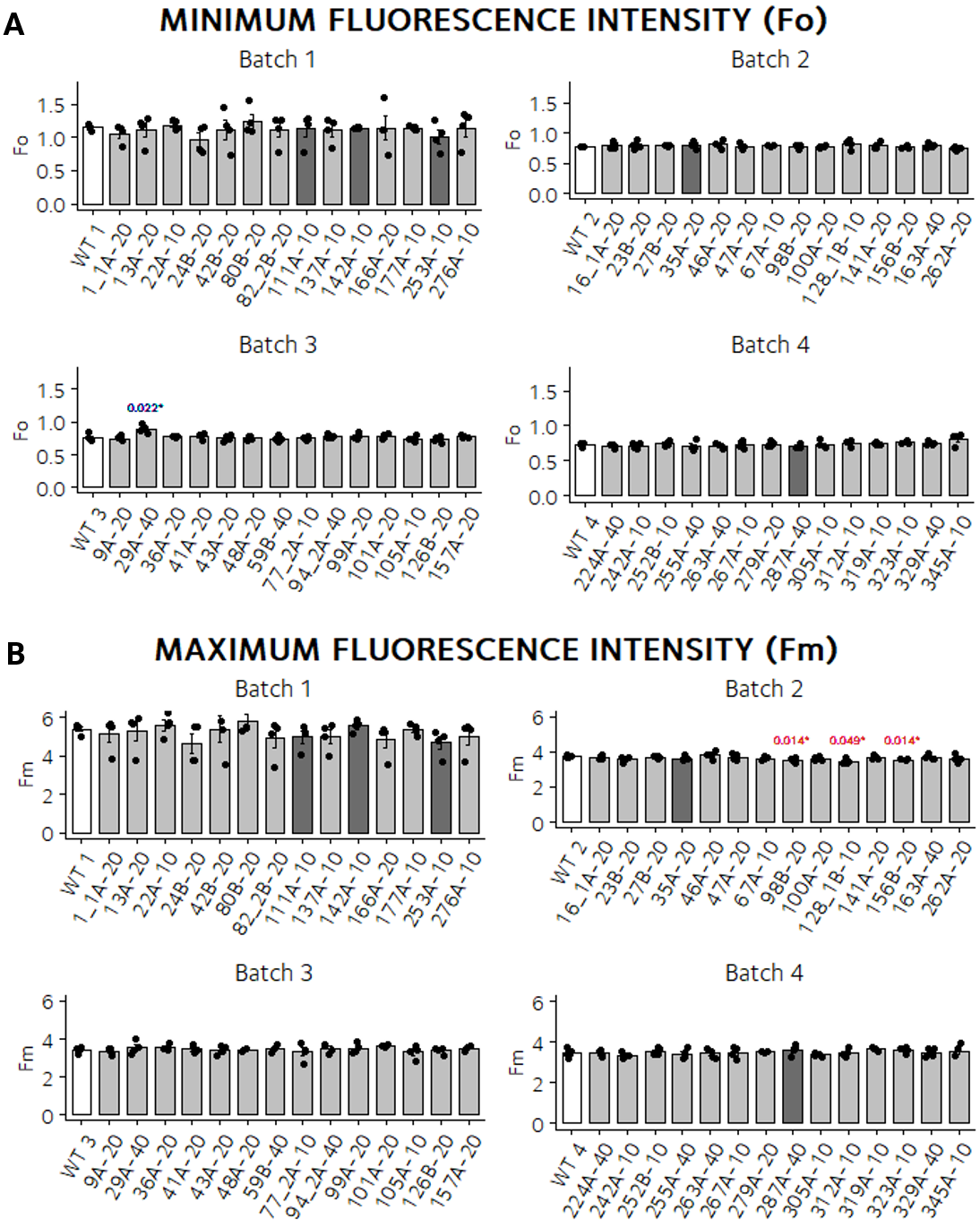

Figure B.6: Primary screen of the combinatorial library — Minimum (F_0) and maximum (F_m) fluorescence intensity. Minimum and maximum fluorescence intensity were determined using a light response curve of chlorophyll fluorescence with a PAM fluorometer. Batches 1-4 from the primary screen are represented. P-values are indicated for significant changes with respect to the corresponding WT (P <0.05 Welch Two sample T-Test). Significant increases are indicated in blue and decreases in red. Significance is reported as "***" for P-value<0.001, "**" for P-value<0.01, or "*" for P-value<0.05. Dark grey bars represent lines showing a stem growth phenotype, selected for further characterisation.

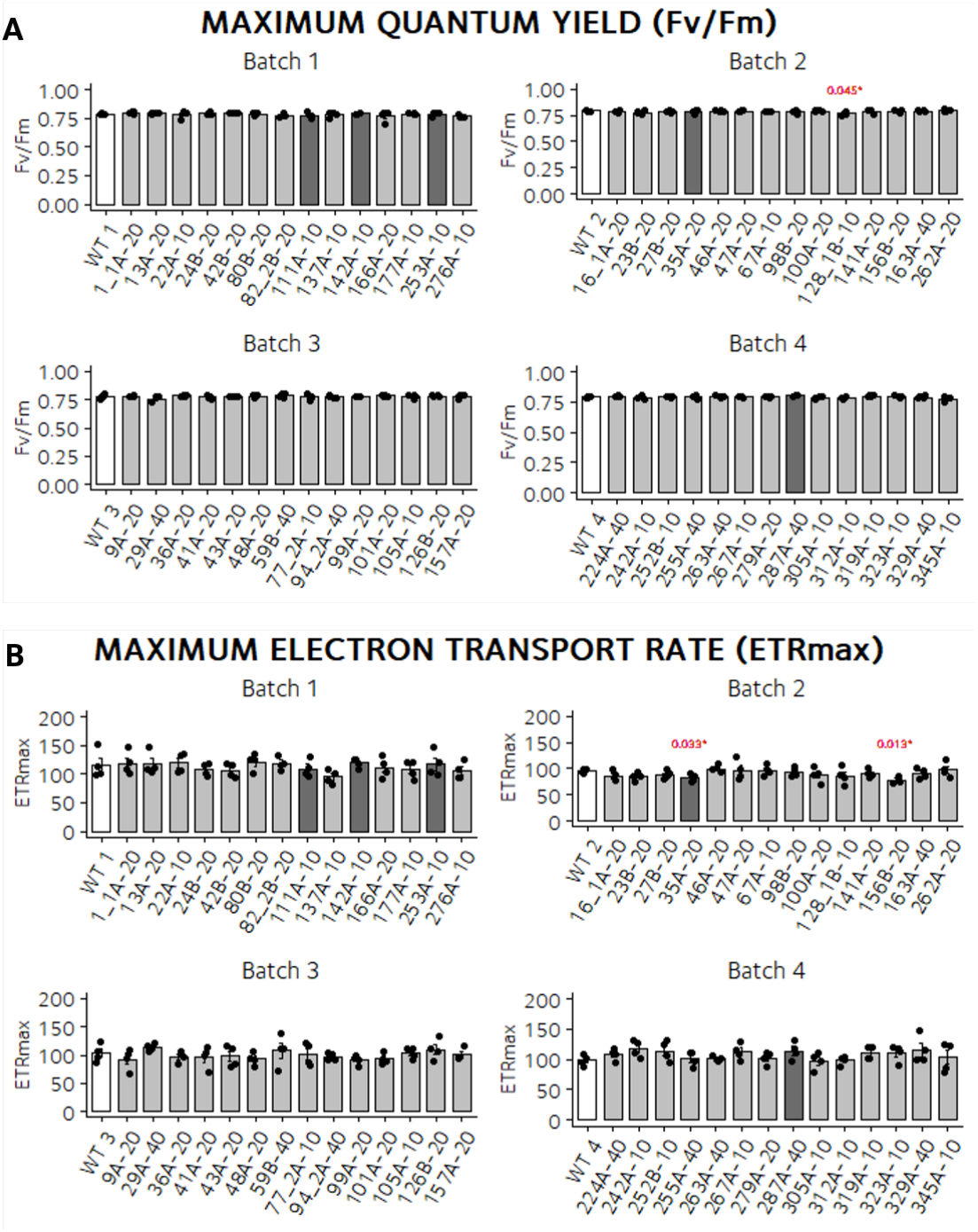

Figure B.7: Primary screen of the combinatorial library — Maximum quantum yield of photosystem II (F_v/F_m) and maximum relative electron transport rate (ETRmax). Maximum quantum yield of photosystem II and maximum electron transport rate were determined using a light response curve of chlorophyll fluorescence with a PAM fluorometer. Batches 1-4 from the primary screen are represented. P-values are indicated for significant changes with respect to the corresponding WT ($P < 0.05$ Welch Two sample T-Test). Significant increases are indicated in blue and decreases in red. Significance is reported as "***" for P-value<0.001, "**" for P-value<0.01, or "*" for P-value<0.05. Dark grey bars represent lines showing a stem growth phenotype, selected for further characterisation.

Table B.6: Comparison between control lines for the parameters analysed in the combinatorial screen. Units are as follows: height, mm; leaf length, mm; biomass, g; chlorophyll, µg/ml. P-values are represented, and asterisks denote statistical significance (P <0.05 Welch Two sample T-Test). Significance is reported as "***" for P-value<0.001, "**" for P-value<0.01, or "*" for P-value<0.05. Means of four plants ± SE.

	P-value							
Comparison	**Height**	**Leaf length**	**Leaf number**	**F_0**	**F_m**	**F_v/F_m**	**ETRmax**	**Ik**
WT_1 vs WT_2	**0.027***	0.308	0.354	**0.000*****	**0.000*****	0.128	0.187	0.159
WT_1 vs WT_3	0.238	0.097	0.075	**0.000*****	**0.000*****	0.386	0.421	0.396
WT_1 vs WT_4	0.824	0.098	0.258	**0.000*****	**0.000*****	0.522	0.249	0.320
WT_2 vs WT_1	**0.027***	0.308	0.354	**0.000*****	**0.000*****	0.128	0.187	0.159
WT_2 vs WT_3	0.202	0.200	**0.031***	0.832	0.017*	0.117	0.346	0.327
WT_2 vs WT_4	**0.023***	0.108	0.643	0.053	0.110	0.392	0.547	0.598
WT_3 vs WT_1	0.238	0.097	0.075	**0.000*****	**0.000*****	0.386	0.421	0.396
WT_3 vs WT_2	0.202	0.200	**0.031***	0.832	**0.017***	0.117	0.346	0.327
WT_3 vs WT_4	0.291	0.875	0.149	0.291	0.756	0.226	0.575	0.788
WT_4 vs WT_1	0.824	0.098	0.258	**0.000*****	**0.000*****	0.522	0.249	0.320
WT_4 vs WT_2	**0.023***	0.108	0.643	0.053	0.110	0.392	0.547	0.598
WT_4 vs WT_3	0.291	0.875	0.149	0.291	0.756	0.226	0.575	0.788

	P-value						
Comparison	**Leaf biomass**	**Stem biomass**	**Total biomass**	**Chl *a***	**Chl *b***	**Total chl**	**Ratio chl *a*/*b***
WT_1 vs WT_2	0.774	0.101	0.273	0.688	0.806	0.710	0.624
WT_1 vs WT_3	0.169	0.111	0.128	0.687	0.723	0.692	0.958
WT_1 vs WT_4	0.845	0.269	0.473	0.835	0.933	0.878	0.164
WT_2 vs WT_1	0.774	0.101	0.273	0.688	0.806	0.710	0.624
WT_2 vs WT_3	0.226	0.689	0.385	0.556	0.654	0.572	0.672
WT_2 vs WT_4	0.990	0.752	0.865	0.959	0.826	0.933	0.363
WT_3 vs WT_1	0.169	0.111	0.128	0.687	0.723	0.692	0.958
WT_3 vs WT_2	0.226	0.689	0.385	0.556	0.654	0.572	0.672
WT_3 vs WT_4	0.266	0.539	0.360	0.661	0.875	0.698	0.208
WT_4 vs WT_1	0.845	0.269	0.473	0.835	0.933	0.878	0.164
WT_4 vs WT_2	0.990	0.752	0.865	0.959	0.826	0.933	0.363
WT_4 vs WT_3	0.266	0.539	0.360	0.661	0.875	0.698	0.208

Appendix C

Supplementary materials - Chapter 4

Figures

Tables

Table C.1: Height and fresh weight biomass of selected combinatorial lines in replicated greenhouse experiments. Selected combinatorial lines were grown in greenhouse conditions during the summer of 2019 in Oxford, UK and Golm (Potsdam), Germany. Plants were germinated in selection plates and transferred to soil after two weeks. Measurements of plant height, stem biomass, leaf biomass, and total biomass were taken just before flowering, 6 and 4 weeks after transfer to soil in Oxford and Golm, respectively. Data are mean ± SE; n=6–10 (A) n=15 (B). One-way ANOVA was used followed by post hoc Tukey multiple pairwise comparisons test. Different letters indicate significant differences between plant lines (P <0.05). Non-parametric Kruskal-Wallis test was used when the raw data displayed an abnormal distribution.

	Height (mm)		**Leaves biomass (g)**		**Stem biomass (g)**		**Total biomass (g)**	
Line	Oxford (P=0.002)	Golm (P=0.002)	Oxford (P=0.002)	Golm (P=0.124)	Oxford (P=0.003)	Golm (P=0.051)	Oxford (P=0.005)	Golm (P=0.259)
WT	583.00 ± 44.00^{abc}	663.80 ± 21.27^{ab}	55.70 ± 1.90^{b}	92.87 ± 1.69	42.80 ± 3.30^{abc}	60.30 ± 1.35	98.40 ± 50^{b}	153.17 ± 2.76
35A-20	614.00 ± 37.00^{bc}	665.93 ± 15.05^{ab}	57.60 ± 1.00^{b}	94.41 ± 1.59	44.80 ± 2.70^{bc}	62.53 ± 1.01	102.40 ± 3.40^{b}	156.94 ± 2.01
111A-10	387.00 ± 65.00^{a}	614.00 ± 17.00^{a}	44.90 ± 4.50^{a}	89.36 ± 1.21	27.00 ± 5.20^{a}	64.72 ± 3.07	71.90 ± 9.50^{a}	154.08 ± 2.68
142A-10	445.00 ± 50.00^{ab}	721.20 ± 20.74^{b}	49.50 ± 2.70^{ab}	87.94 ± 2.65	31.60 ± 4.60^{ab}	60.08 ± 1.80	81.10 ± 6.80^{ab}	148.02 ± 3.78
253A-10	535.00 ± 48.00^{abc}	660.20 ± 22.11^{ab}	57.30 ± 2.30^{b}	91.90 ± 1.56	39.60 ± 3.20^{abc}	57.31 ± 1.38	96.90 ± 5.30^{b}	149.21 ± 2.60
287A-40	686.00 ± 48.00^{c}	710.07 ± 18.71^{b}	50.00 ± 2.00^{ab}	89.93 ± 1.81	47.40 ± 30^{c}	64.95 ± 2.35	97.40 ± 4.60^{ab}	154.89 ± 3.64

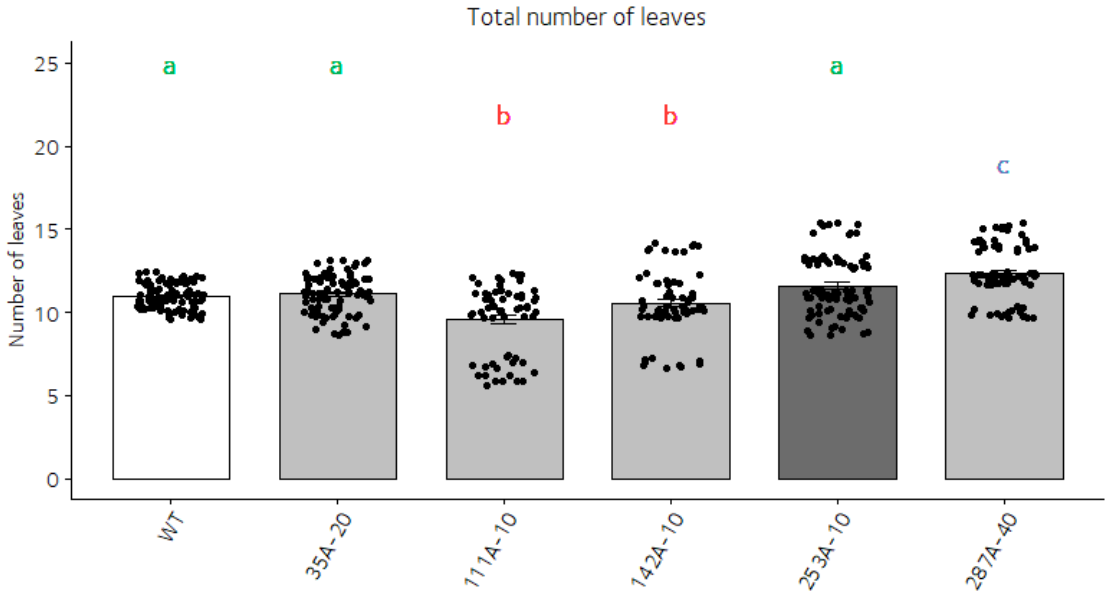

Figure C.1: Total number of leaves for selected combinatorial lines in greenhouse experiment. Selected combinatorial lines were grown in greenhouse conditions during the summer of 2019 in Oxford, UK. Plants (T_1 generation) were germinated in selection plates and transferred to soil after two weeks. Total leaf count was performed just before flowering, 6 weeks after transfer to soil. Pseudo-WT is represented in dark grey. Data are mean ± SE; n=6-10. One-way ANOVA was used followed by post hoc Tukey multiple pairwise comparisons test. Different letters indicate significant differences between plant lines ($P < 0.05$). Non-parametric Kruskal-Wallis test was used when the raw data displayed an abnormal distribution.

Table C.2: Height of selected combinatorial lines in an outdoor polytunnel experiment. Selected combinatorial lines were grown in an outdoor polytunnel during the summer of 2019 in Golm (Potsdam), Germany. Plants were germinated in selection plates and transferred to soil after two weeks. Plant height was determined at the time of harvest. Data are mean ± SE One-way ANOVA was used and no significant differences were found between groups (P = 0.151).

Line	**Heigth**	***n***
WT	138 ± 4	6
35A-20	138 ± 2	7
111A-10	135 ± 6	7
142A-10	140	1
253A-10	152 ± 6	5
287A-40	131 ± 6	7

Table C.3: Transgene expression for selected combinatorial lines. Transgene expression, represented as fold-change ($2^{-\Delta\Delta Ct}$) was determined by quantitative real-time PCR (qRT-PCR) in leaves and normalised to the housekeeping genes *L25* and *EF-1α*. Three biological replicates (BR, samples from independent plants) were used per line. Expression in each biological replicate, mean, and SE are given, along with the simplified results from the genomic PCR for each transgene and line, where the plus (+) symbol indicates transgene presence and the minus (-) symbol indicates transgene absence.

AtPetC						
Line	BR1 ($2^{-\Delta\Delta Ct}$)	BR2 ($2^{-\Delta\Delta Ct}$)	BR3 ($2^{-\Delta\Delta Ct}$)	**Mean**	SE	gPCR result
35A-20	3.08	47.55	3.81	**18.15**	12.01	+
111A-10	104.19	726.56	935.33	**588.69**	203.83	+
142A-10	0.64	0.94	2.94	**1.5**	0.59	-
253A-10	1.14	1.77	2.48	**1.79**	0.32	-
287A-40	55.28	704.53	444.13	**401.31**	154.03	+

Pyc6						
Line	BR1 ($2^{-\Delta\Delta Ct}$)	BR2 ($2^{-\Delta\Delta Ct}$)	BR3 ($2^{-\Delta\Delta Ct}$)	**Mean**	SE	gPCR result
35A-20	71.24	2666.31	193.25	**976.93**	690.29	+
111A-10	63.32	3195.87	727.78	**1328.99**	778.07	+
142A-10	58.74	1149.74	390.04	**532.84**	263.68	+
253A-10	3.36	2.62	0.91	**2.3**	0.59	-
287A-40	532.55	7113.03	2712.56	**3452.72**	1580.19	+

CaPFLP						
Line	BR1 ($2^{-\Delta\Delta Ct}$)	BR2 ($2^{-\Delta\Delta Ct}$)	BR3 ($2^{-\Delta\Delta Ct}$)	**Mean**	SE	gPCR result
35A-20	10946.64	72727.61	7356.31	**30343.52**	17323.91	+
111A-10	0.84	0.3	0.28	**0.48**	0.15	-
142A-10	1.04	0.53	0.13	**0.57**	0.21	-
253A-10	2.95	1.5	0.3	**1.58**	0.63	-
287A-40	31.83	75.74	29.92	**45.83**	12.22	-

SeictB						
Line	BR1 ($2^{-\Delta\Delta Ct}$)	BR2 ($2^{-\Delta\Delta Ct}$)	BR3 ($2^{-\Delta\Delta Ct}$)	**Mean**	SE	gPCR result
35A-20	188.96	397.44	285.99	290.8	49.18	+
111A-10	0.29	0	7.49	2.59	2	-
142A-10	0.84	1.07	1.74	1.22	0.22	+
253A-10	0.39	1.25	4.09	1.91	0.91	-
287A-40	1.01	1.2	4.44	2.22	0.91	+

AtFBPA						
Line	BR1 ($2^{-\Delta\Delta Ct}$)	BR2 ($2^{-\Delta\Delta Ct}$)	BR3 ($2^{-\Delta\Delta Ct}$)	**Mean**	SE	gPCR result
35A-20	3.11	3.03	1.74	2.63	0.36	-
111A-10	0.92	1.09	0.61	0.87	0.11	-
142A-10	0.79	0.8	0.22	0.6	0.16	-
253A-10	1.66	1.36	0.71	1.24	0.23	-
287A-40	76.6	314.16	151.99	180.92	57.22	-

AtSBPase						
Line	BR1 ($2^{-\Delta\Delta Ct}$)	BR2 ($2^{-\Delta\Delta Ct}$)	BR3 ($2^{-\Delta\Delta Ct}$)	**Mean**	SE	gPCR result
35A-20	4346.2	48386.97	8111.24	20281.47	11508.29	+
111A-10	14.07	85.29	61.31	53.56	17.08	-
142A-10	1.43	1.01	1.06	1.17	0.11	-
253A-10	6.39	10.32	0.51	5.74	2.33	-
287A-40	0.91	12.11	4.77	5.93	2.68	-

FpGDC-H						
Line	BR1 ($2^{-\Delta\Delta Ct}$)	BR2 ($2^{-\Delta\Delta Ct}$)	BR3 ($2^{-\Delta\Delta Ct}$)	**Mean**	SE	gPCR result
35A-20	3.17	17.09	0.31	6.86	4.23	+
111A-10	1.3	0.58	1.05	0.98	0.17	-
142A-10	4.96	23.53	0.22	9.57	5.81	-
253A-10	2.74	0.92	2.27	1.98	0.44	-
287A-40	34580.8	40657.29	72995.01	49411.03	9734.06	+

AtTPT						
Line	BR1 ($2^{-\Delta\Delta Ct}$)	BR2 ($2^{-\Delta\Delta Ct}$)	BR3 ($2^{-\Delta\Delta Ct}$)	**Mean**	SE	gPCR result
35A-20	0.71	12.26	2.22	5.06	2.96	-
111A-10	0.57	3.13	5.33	3.01	1.12	-
142A-10	0.91	6.05	2.98	3.31	1.22	-
253A-10	0.57	19.24	0.39	6.73	5.1	-
287A-40	697.17	17962.89	18642.54	12434.2	4794.3	+

EcPPase						
Line	BR1 ($2^{-\Delta\Delta Ct}$)	BR2 ($2^{-\Delta\Delta Ct}$)	BR3 ($2^{-\Delta\Delta Ct}$)	**Mean**	SE	gPCR result
35A-20	2946.29	3483.59	719.64	2383.17	690.84	+
111A-10	0.38	0.78	0.31	0.49	0.12	-
142A-10	672.95	338.2	162.18	391.11	122.31	+
253A-10	0.92	1.22	1.12	1.09	0.07	-
287A-40	59.76	40.27	10.31	36.78	11.74	+

AtcyFBPase						
Line	BR1 ($2^{-\Delta\Delta Ct}$)	BR2 ($2^{-\Delta\Delta Ct}$)	BR3 ($2^{-\Delta\Delta Ct}$)	**Mean**	SE	gPCR result
35A-20	766.61	59516.64	22.2	20101.82	16091.99	+
111A-10	0.3	27.51	0.29	9.36	7.41	-
142A-10	0.48	11.86	0.08	4.14	3.15	-
253A-10	0.38	82.04	0.29	27.57	22.24	-
287A-40	438.06	20810.56	112.36	7120.33	5589.54	+

AtSWEET11						
Line	BR1 ($2^{-\Delta\Delta Ct}$)	BR2 ($2^{-\Delta\Delta Ct}$)	BR3 ($2^{-\Delta\Delta Ct}$)	**Mean**	SE	gPCR result
35A-20	5.09	13.4	4.19	7.56	2.39	-
111A-10	0.38	3.7	0.53	1.54	0.88	-
142A-10	0.73	0.47	0.43	0.54	0.08	-
253A-10	1.3	2.47	0.67	1.48	0.43	-
287A-40	199.52	320.36	132.49	217.46	44.88	+

AtSUC2						
Line	BR1 ($2^{-\Delta\Delta Ct}$)	BR2 ($2^{-\Delta\Delta Ct}$)	BR3 ($2^{-\Delta\Delta Ct}$)	**Mean**	SE	gPCR result
35A-20	0.82	0.62	2.94	1.46	0.61	-
111A-10	0.82	1.13	8.22	3.39	1.97	+
142A-10	122.96	1351.73	735.32	736.67	289.62	+
253A-10	0.75	21.7	1.28	7.91	5.63	-
287A-40	1.13	1.53	275.05	92.57	74.5	-

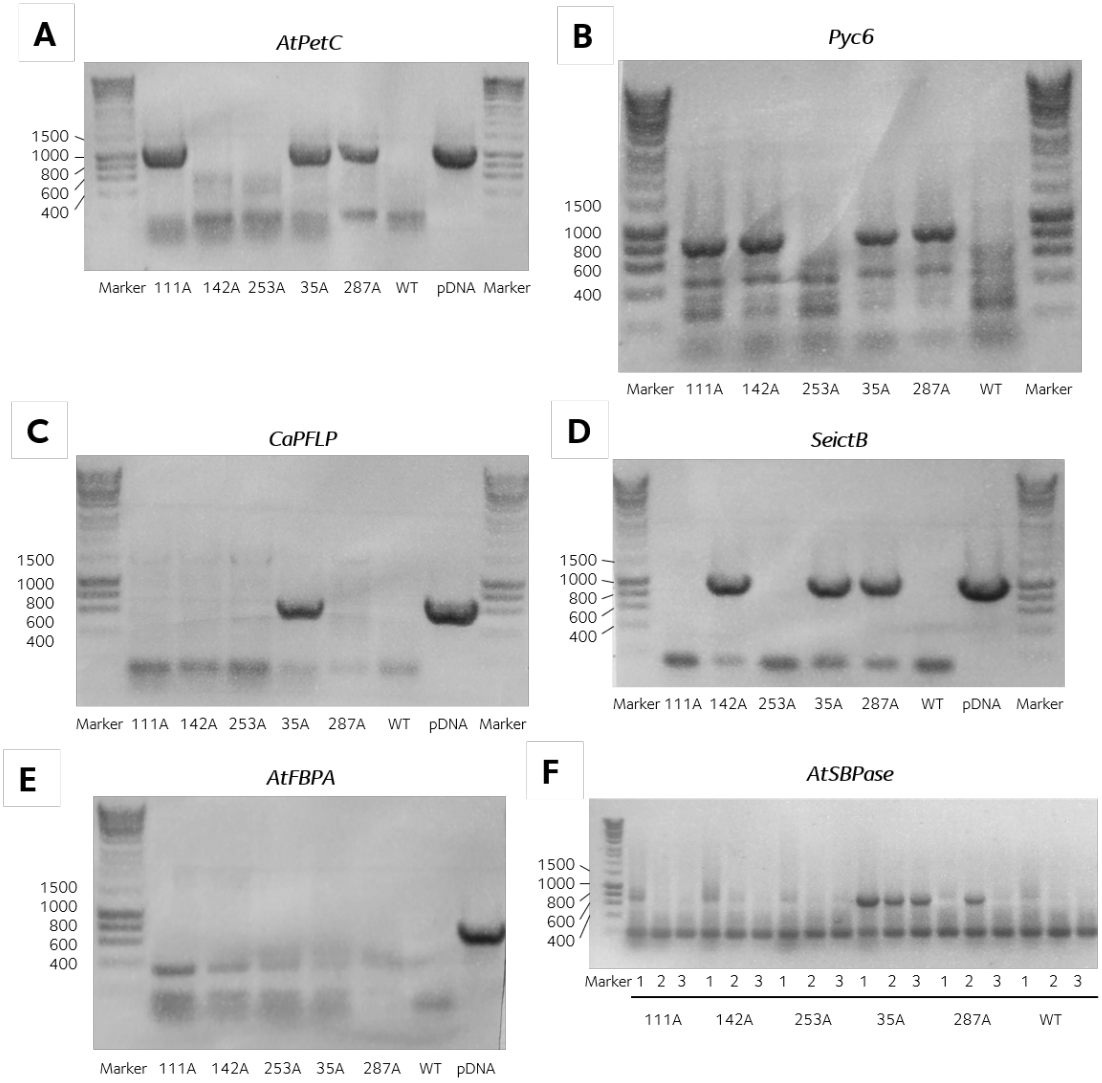

Figure C.2: PCR amplification of transgenes in selected combinatorial lines (1). PCR amplification of transgenes *AtPetC* (**A**, expected band size 1195 bp), *Pyc6* (**B**, 933 bp), *CaPFLP* (**C**, 721 bp), *SeictB* (**D**, 1089 bp), *AtFBPA* (**E**, 883 bp), and *AtSBPase* (**F**, 738 bp). Amplification was performed on genomic DNA extracted from leaves of three biological replicates (each consisting of an individual plant) per line. Results are representative from an individual replicate per line, with all replicates shown in pannel F. Separation of PCR products according to their molecular weight through DNA electrophoresis (1% agarose TAE gels). Size determination according to molecular size marker (Marker) Hyperladder I (Bioline, London, UK); 400-, 600-, 800-, 1000-, and 1500-bp markers are indicated. Line names are abbreviated as follows: 35A-20 (35A), 111A-10 (111A), 142A-10 (142A), 253A-10 (253A), and 287A-40 (287A). Plasmid DNA for each corresponding construct was used as positive control (+c) for amplification; distilled water was used as negative control (-c).

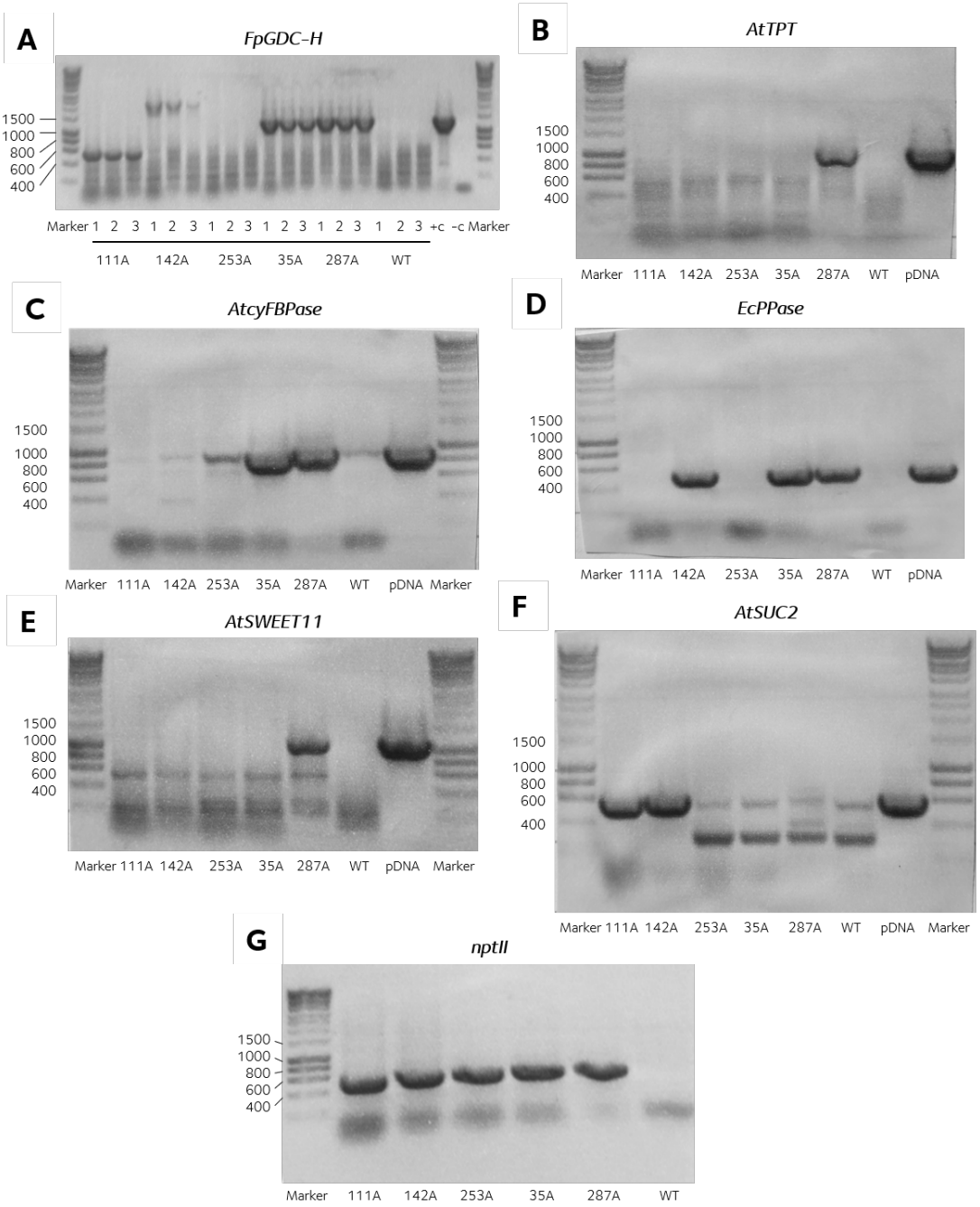

Figure C.3: PCR amplification of transgenes in selected combinatorial lines (2). PCR amplification of transgenes *FpGDC-H* (**A**, expected band size 1447 bp), *AtTPT* (**B**, 1162 bp), *AtcyFBPase* (**C**, 974 bp), *EcPPase* (**D**, 558 bp), *AtSWEET11* (**E**, 1200 bp), *AtSUC2* (**F**, 650 bp), and *nptII* (**G**, 549 bp). Amplification was performed on genomic DNA extracted from leaves of three biological replicates (each consisting of an individual plant) per line. Results are representative from an individual replicate per line, with all replicates shown in pannel F. Separation of PCR products according to their molecular weight through DNA electrophoresis (1% agarose TAE gels). Size determination according to molecular size marker (Marker) BiolineTM Hyperladder I (Bioline, London, UK); 400-, 600-, 800-, 1000-, and 1500-bp markers are indicated. Line names are abbreviated as follows: 35A-20 (35A), 111A-10 (111A), 142A-10 (142A), 253A-10 (253A), and 287A-40 (287A). Plasmid DNA for each corresponding construct was used as positive control (+c) for amplification.

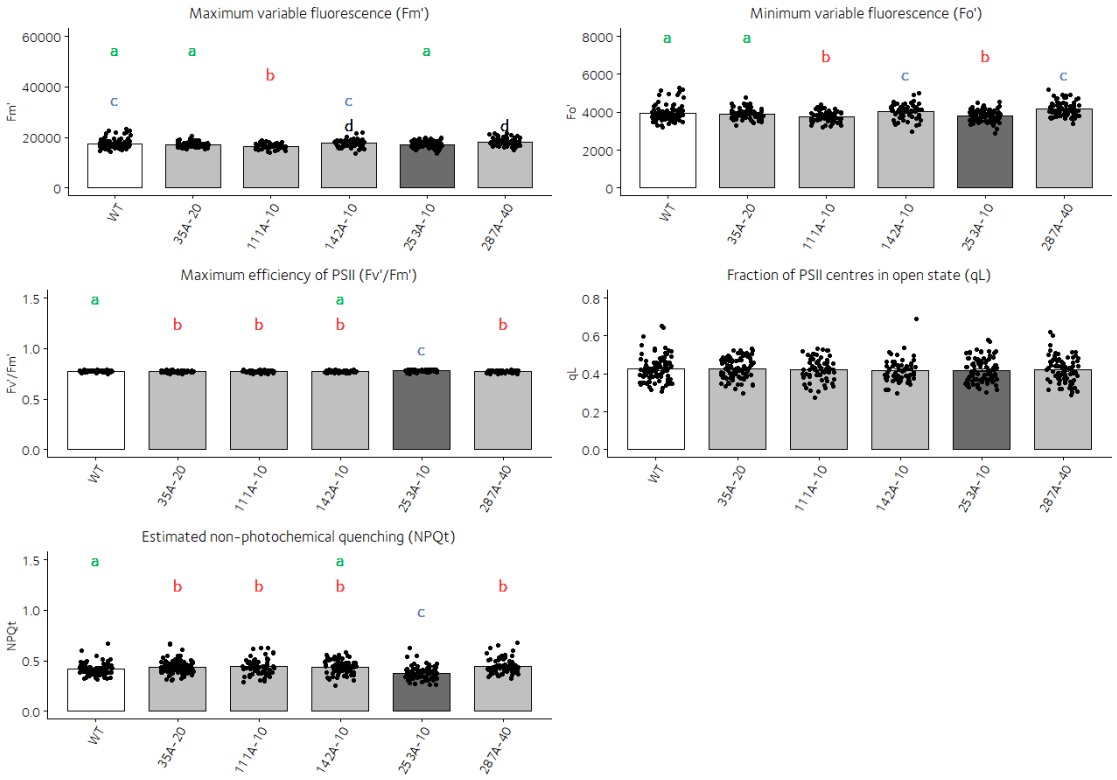

Figure C.4: Photosynthetic capacity in selected combinatorial lines — Chlorophyll fluorescence-derived parameters. Photosynthetic capacity was evaluated six weeks after transfer to soil under steady-state growth light conditions (50-150 µmol m^{-2} s^{-1}) using the Leaf Photosynthesis MultispeQ V1.0 protocol with a MultispeQ instrument (PhotosynQ, MI, USA). Data are mean ± SE; n = 6-10. One-way ANOVA was used followed by post hoc Tukey multiple pairwise comparisons test. Different letters indicate significant differences between plant lines (P <0.05). Non-parametric Kruskal-Wallis test was used when the raw data displayed an abnormal distribution.

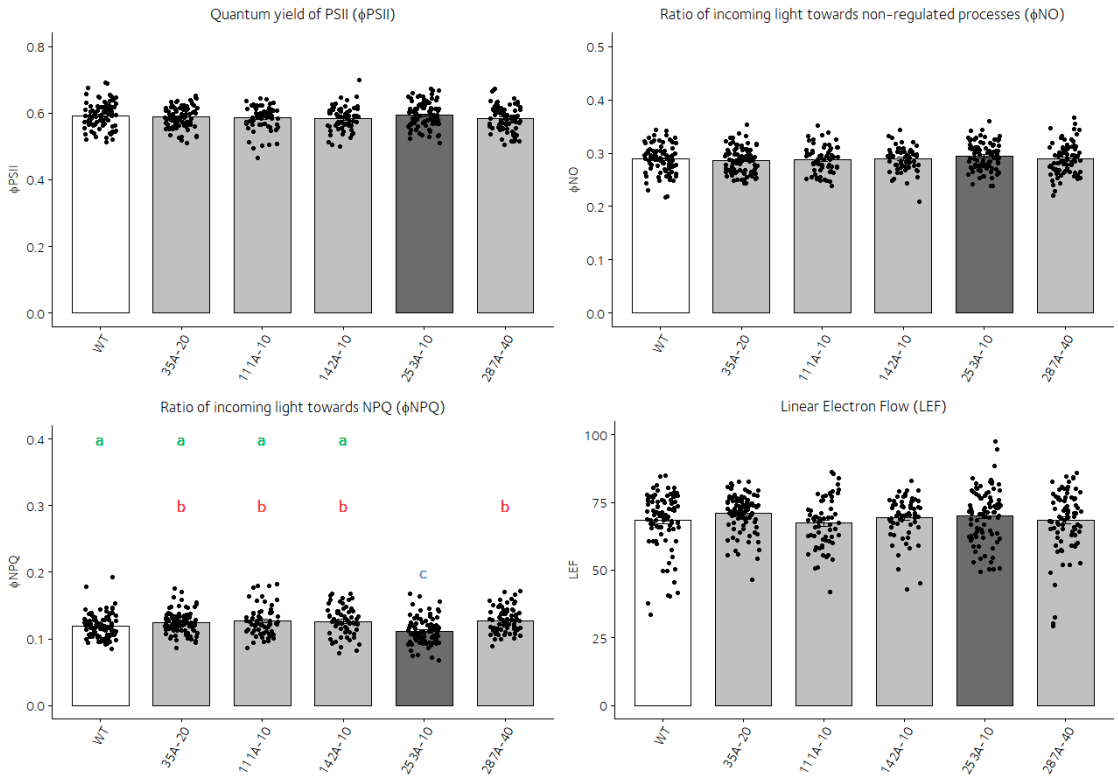

Figure C.5: Photosynthetic capacity in selected combinatorial lines — Ratios of allocation of incoming light. Linear electron flow (LEF) is represented in µmol electrons m^{-2} s^{-1}. Photosynthetic capacity was evaluated six weeks after transfer to soil under steady-state growth light conditions (50-150 µmol m^{-2} s^{-1}) using the Leaf Photosynthesis MultispeQ V1.0 protocol with a MultispeQ instrument (PhotosynQ, MI, USA). Data are mean ± SE; n = 6-10. One-way ANOVA was used followed by post hoc Tukey multiple pairwise comparisons test. Different letters indicate significant differences between plant lines ($P < 0.05$). Non-parametric Kruskal-Wallis test was used when the raw data displayed an abnormal distribution.

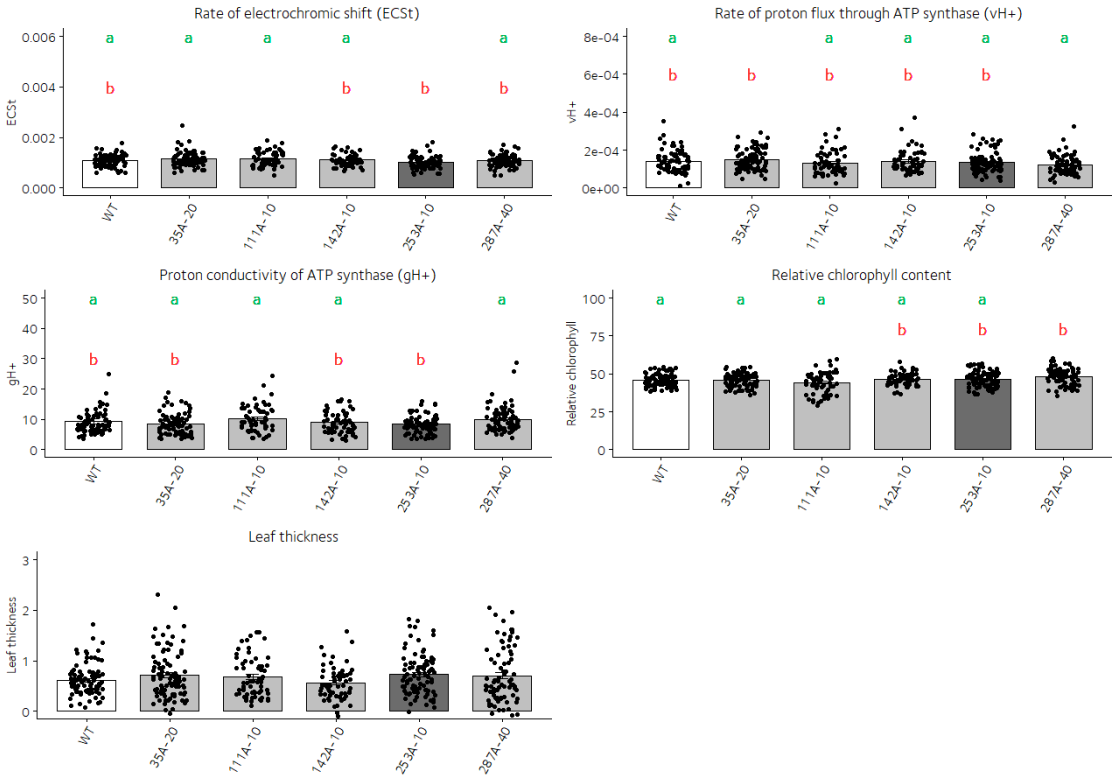

Figure C.6: Photosynthetic capacity in selected combinatorial lines — Proton accumulation and flow, and absorbance-based parameters. Proton conductivity of ATP synhtase (gH+) is represented in s^{-1}) and leaf thickness in µm. Photosynthetic capacity was evaluated six weeks after transfer to soil under steady-state growth light conditions (50-150 µmol m^{-2} s^{-1}) using the Leaf Photosynthesis MultispeQ V1.0 protocol with a MultispeQ instrument (PhotosynQ, MI, USA). Data are mean ± SE; n = 6-10. One-way ANOVA was used followed by post hoc Tukey multiple pairwise comparisons test. Different letters indicate significant differences between plant lines ($P < 0.05$). Non-parametric Kruskal-Wallis test was used when the raw data displayed an abnormal distribution.

Table C.4: Metabolite profiling of combinatorial lines. Metabolite profiling by GC-MS was performed in the selected combinatorial lines, six weeks after transfer to soil. Metabolites are classified into acids, amino acids and amino acid derivatives, and sugars, sugar alcohols and other metabolites. γ-Aminobutyric acid is abbreviated as GABA. Data are mean ± SE; n = 4. One-way ANOVA was used followed by post hoc Tukey multiple pairwise comparisons test. Different letters indicate significant differences between plant lines (P <0.05). Non-parametric Kruskal-Wallis test was used when the raw data displayed an abnormal distribution.

Acids						
Compound	**Line**					
	WT	**35A-20**	**111A-10**	**142A-10**	**253A-10**	**287A-40**
Chlorogenic acid	67.22 ± 0.69	70.96 ± 2.18	72.88 ± 1.12	72.31 ± 1.81	73.34 ± 1.02	67.93 ± 2.06
4-Hydroxybenzoate	0.39 ± 0.04^{b}	0.32 ± 0.04^{b}	0.17 ± 0.02^{a}	0.27 ± 0.02^{ab}	0.37 ± 0.04^{b}	0.38 ± 0.02^{b}
Ascorbic acid	3.09 ± 0.22^{a}	2.53 ± 0.06^{a}	4.2 ± 0.08^{b}	4.68 ± 0.14^{b}	2.79 ± 0.23^{a}	3.01 ± 0.31^{a}
Dehydroascorbic acid	19.83 ± 0.37^{bcd}	18.9 ± 0.79^{abc}	17.94 ± 0.70^{ab}	21.83 ± 0.55^{d}	20.85 ± 0.89^{cd}	16.87 ± 0.15^{a}
Fumaric acid	4.20 ± 0.25^{c}	3.35 ± 0.14^{bc}	1.65 ± 0.02^{a}	2.85 ± 0.12^{b}	2.79 ± 0.34^{abd}	3.73 ± 0.11^{cd}
GABA	32.96 ± 1.15^{bc}	26.88 ± 2.15^{b}	11.58 ± 1.12^{a}	29.81 ± 2.78^{bc}	35.46 ± 2.17^{bc}	36.78 ± 1.65^{c}
Glyceric acid	95.67 ± 1.51^{b}	102.39 ± 4.52^{b}	48.66 ± 1.16^{a}	105.4 ± 6.84^{b}	86.98 ± 5.12^{b}	129.7 ± 4.58^{c}
Malic acid	46.55 ± 1.52^{a}	46.56 ± 1.04^{a}	38.57 ± 0.68^{b}	48.77 ± 2.04^{a}	46.76 ± 1.12^{a}	50.66 ± 2.61^{a}
Phosphoric acid	11.66 ± 0.76^{b}	7.79 ± 0.53^{a}	11.83 ± 0.72^{b}	13.8 ± 0.20^{b}	6.59 ± 0.13^{a}	17.56 ± 0.28^{c}
Pyruvic acid	76.32 ± 2.18^{b}	55.34 ± 2.22^{c}	101.99 ± 2.96^{a}	58.83 ± 2.74^{c}	53.84 ± 1.86^{c}	29.8 ± 1.83^{d}
Quinic acid	53.32 ± 1.50^{abc}	52.75 ± 1.34^{abc}	46.75 ± 1.76^{a}	51.09 ± 0.90^{ab}	58.79 ± 1.95^{c}	54.45 ± 1.6^{bc}
Succinic acid	5.35 ± 0.35^{a}	6.25 ± 0.45^{a}	5.21 ± 0.14^{a}	6.39 ± 0.13^{a}	6.07 ± 0.32^{a}	7.86 ± 0.16^{b}
L-Threonic acid	58.98 ± 1.14^{bc}	47.37 ± 1.91^{a}	50.54 ± 1.72^{ab}	60.08 ± 4.21^{bc}	59.46 ± 1.58^{bc}	63.86 ± 0.96^{c}
trans-Caffeic acid	2.59 ± 0.17^{b}	2.00 ± 0.15^{ab}	1.46 ± 0.21^{a}	1.65 ± 0.15^{a}	2.09 ± 0.06^{ab}	2.65 ± 0.19^{b}
Urea	0.88 ± 0.06^{b}	0.6 ± 0.02^{a}	1.37 ± 0.06^{c}	1.66 ± 0.07^{d}	0.99 ± 0.07^{b}	1.07 ± 0.06^{b}

Amino acids and amino acid derivatives						
Compound	**Line**					
	WT	**35A-20**	**111A-10**	**142A-10**	**253A-10**	**287A-40**
4-Hydroxyproline	1.15 ± 0.13^{ab}	1.37 ± 0.17^{b}	0.68 ± 0.02^{a}	1.71 ± 0.1^{b}	1.38 ± 0.14^{b}	4.77 ± 0.15^{c}
Alanine	56.12 ± 1.98^{a}	40.77 ± 2.16^{c}	48.62 ± 0.68^{b}	53.12 ± 1.2^{ab}	52.89 ± 1.15^{ab}	35.19 ± 1.66^{c}
Arginine	4.62 ± 0.25^{b}	3.35 ± 0.06^{a}	3.34 ± 0.21^{a}	3.3 ± 0.11^{a}	6.82 ± 0.21^{c}	6.77 ± 0.29^{c}
Asparagine	1.09 ± 0.05^{a}	0.51 ± 0.04^{b}	0.31 ± 0.00^{c}	2.75 ± 0.21^{d}	1.16 ± 0.13^{a}	1.46 ± 0.12^{a}
Aspartic acid	47.19 ± 1.07^{ac}	43.02 ± 1.39^{c}	34.41 ± 0.2^{b}	51.73 ± 2.34^{ad}	48.89 ± 0.73^{a}	54.91 ± 0.54^{d}
Beta-Alanine	2.68 ± 0.16^{ab}	1.65 ± 0.06^{d}	1.76 ± 0.08^{cd}	2.16 ± 0.14^{bcd}	2.24 ± 0.16^{bc}	2.97 ± 0.09^{a}
Cysteine	1.25 ± 0.04^{ab}	1.4 ± 0.17^{ab}	0.94 ± 0.05^{a}	1.36 ± 0.17^{ab}	1.49 ± 0.11^{b}	1.62 ± 0.07^{b}
Glutamic acid	83.39 ± 4.01^{ab}	70.84 ± 1.62^{a}	80.56 ± 3.05^{ab}	81.29 ± 4.57^{ab}	91.98 ± 3.31^{bc}	104.13 ± 4.66^{c}
Glutamine	1.63 ± 0.11^{ab}	0.45 ± 0.02^{c}	0.12 ± 0.01^{d}	1.27 ± 0.10^{b}	0.44 ± 0.02^{c}	1.67 ± 0.02^{a}
Glycine	10.65 ± 0.55^{ab}	16.98 ± 0.94^{c}	8.14 ± 0.36^{a}	21.13 ± 0.94^{d}	11.48 ± 0.35^{b}	19.58 ± 0.55^{cd}
Histidine	0.5 ± 0.05^{a}	0.52 ± 0.01^{a}	0.5 ± 0.03^{a}	0.99 ± 0.06^{b}	0.56 ± 0.03^{a}	1.03 ± 0.05^{b}
Homoserine	0.61 ± 0.01^{a}	0.3 ± 0.00^{b}	0.23 ± 0.01^{d}	0.51 ± 0.02^{c}	0.29 ± 0.00^{b}	0.77 ± 0.03^{a}
Isoleucine	3.29 ± 0.07^{ab}	3.42 ± 0.13^{abc}	3.01 ± 0.10^{a}	4.05 ± 0.24^{c}	3.92 ± 0.11^{bc}	3.97 ± 0.15^{c}
Lysine	1.10 ± 0.06^{ab}	0.84 ± 0.06^{a}	0.94 ± 0.02^{a}	1.67 ± 0.09^{c}	1.28 ± 0.08^{b}	0.91 ± 0.03^{a}
Methionine	2.44 ± 0.18^{a}	2.2 ± 0.23^{a}	1.35 ± 0.14^{b}	1.97 ± 0.13^{ab}	1.88 ± 0.04^{ab}	3.34 ± 0.06^{c}
O-Acetyl-L-Serine	0.59 ± 0.02^{a}	0.59 ± 0.01^{a}	1.02 ± 0.03^{b}	1.61 ± 0.15^{c}	0.47 ± 0.02^{d}	1.24 ± 0.08^{bc}
Ornithine	0.54 ± 0.03^{a}	0.46 ± 0.01^{c}	0.19 ± 0.01^{b}	0.60 ± 0.03^{a}	0.5 ± 0.03^{ac}	0.93 ± 0.04^{d}
Phenylalanine	13.12 ± 0.42^{a}	13.4 ± 0.64^{a}	8.64 ± 0.19^{b}	13.75 ± 0.57^{a}	11.67 ± 0.83^{a}	17.51 ± 0.42^{c}
Proline	116.14 ± 7.81^{ab}	127.43 ± 5.89^{ab}	96.6 ± 2.89^{a}	137.27 ± 9.77^{b}	140.9 ± 5.27^{b}	260.88 ± 7.77^{c}
5-Oxoproline	108.76 ± 4.40^{ac}	91.30 ± 0.87^{ab}	85.88 ± 1.80^{b}	116.67 ± 5.10^{cd}	111.75 ± 7.22^{cd}	130.28 ± 4.19^{d}
Serine	73.34 ± 1.65^{a}	61.97 ± 1.21^{b}	66.07 ± 0.83^{bc}	70.77 ± 1.73^{ac}	73.76 ± 1.81^{a}	53.53 ± 0.91^{d}
Threonine	29.42 ± 1.28^{ab}	19.35 ± 0.83^{c}	26.6 ± 0.99^{b}	28.02 ± 0.80^{ab}	31.32 ± 0.62^{a}	32.12 ± 1.07^{a}
Trytpophan	2.21 ± 0.22^{ab}	2.14 ± 0.26^{ab}	1.64 ± 0.08^{b}	2.3 ± 0.17^{ab}	2.29 ± 0.20^{ab}	2.92 ± 0.06^{a}
Tyramine	11.10 ± 0.66^{ac}	22.01 ± 1.11^{bc}	24.4 ± 0.67^{bc}	25.25 ± 1.52^{c}	13.14 ± 0.6^{a}	20.58 ± 0.36^{b}

Sugars, sugar alcohols, and other metabolites						
Compound	**Line**					
	WT	**35A-20**	**111A-10**	**142A-10**	**253A-10**	**287A-40**
1-O-Methyl-Mannopyranoside	1.31 ± 0.05^{a}	1.41 ± 0.03^{ab}	1.52 ± 0.05^{b}	1.51 ± 0.04^{b}	1.52 ± 0.03^{ab}	1.24 ± 0.03^{a}
Fructose	13.69 ± 0.29^{ab}	11.84 ± 0.40^{a}	11.75 ± 0.64^{a}	12.25 ± 1.14^{a}	15.84 ± 0.53^{b}	14.29 ± 0.29^{ab}
Fructose-6-phosphate	0.29 ± 0.01^{a}	0.17 ± 0.02^{c}	0.20 ± 0.01^{bc}	0.19 ± 0.01^{bc}	0.24 ± 0.02^{ab}	0.21 ± 0.00^{bc}
Fucose	3.65 ± 0.13^{ab}	4.01 ± 0.22^{bc}	3.1 ± 0.21^{a}	4.45 ± 0.15^{c}	4.26 ± 0.16^{bc}	4.44 ± 0.17^{bc}
D-Galactono-1,4-Lactone	5.76 ± 0.24^{a}	3.58 ± 0.16^{b}	5.4 ± 0.18^{a}	5.29 ± 0.24^{a}	3.71 ± 0.19^{b}	6.19 ± 0.40^{a}
Glucose	717.54 ± 6.30^{a}	718.88 ± 23.72^{a}	515.11 ± 9.94^{b}	774.35 ± 25.68^{ac}	840.64 ± 24.73^{c}	790.65 ± 20.17^{ac}
Glucose-6-P	0.78 ± 0.04^{a}	0.48 ± 0.04^{b}	0.47 ± 0.01^{b}	0.62 ± 0.01^{c}	0.89 ± 0.03^{a}	0.92 ± 0.06^{a}
Glycerol	4.54 ± 0.17	4.75 ± 0.26	4.99 ± 0.34	5.1 ± 0.24	5.1 ± 0.11	4.68 ± 0.05
Isomaltose	0.29 ± 0.03^{a}	0.25 ± 0.01^{a}	0.28 ± 0.02^{a}	0.38 ± 0.01^{b}	0.39 ± 0.02^{b}	0.42 ± 0.02^{b}
Maltose	6.49 ± 0.2^{a}	5.85 ± 0.34^{a}	5.68 ± 0.04^{a}	6.27 ± 0.16^{a}	8.98 ± 0.46^{b}	6.22 ± 0.29^{a}
Maltotriose	0.14 ± 0.02^{a}	0.18 ± 0.01^{ab}	0.28 ± 0.02^{c}	0.25 ± 0.01^{c}	0.23 ± 0.01^{bc}	0.13 ± 0.02^{a}
Myo-Inositol	62.70 ± 2.26^{a}	64.95 ± 2.49^{a}	71.94 ± 0.77^{ab}	76.66 ± 1.39^{b}	71.11 ± 3.13^{ab}	67.52 ± 1.44^{ab}
Raffinose	0.48 ± 0.02^{ab}	0.53 ± 0.03^{ab}	0.45 ± 0.02^{bc}	0.54 ± 0.02^{ab}	0.56 ± 0.02^{a}	0.38 ± 0.01^{c}
Rhamnose	4.51 ± 0.17^{a}	7.39 ± 0.28^{bc}	7.6 ± 0.25^{bc}	7.76 ± 0.51^{bc}	8.33 ± 0.18^{b}	6.74 ± 0.09^{c}
Sucrose	503.69 ± 24.29	465.29 ± 16.11	480.47 ± 15.37	504.52 ± 23.88	538.72 ± 8.31	491.97 ± 35.67
Trehalose	13.35 ± 0.71^{a}	9.61 ± 1.03^{a}	10.89 ± 0.19^{a}	10.97 ± 0.63^{a}	11.32 ± 0.39^{a}	6.36 ± 0.15^{b}
Xylose	15.39 ± 0.48^{a}	25.65 ± 0.74^{b}	8.66 ± 0.29^{c}	18.28 ± 1.32^{a}	17.31 ± 1.12^{a}	18.12 ± 0.89^{a}
Nicotinamide	0.59 ± 0.02^{a}	0.53 ± 0.03^{ab}	0.48 ± 0.03^{b}	0.51 ± 0.01^{ab}	0.53 ± 0.02^{ab}	0.86 ± 0.02^{c}
Nicotinic acid	7.18 ± 0.37^{ab}	5.86 ± 0.26^{b}	6.11 ± 0.27^{ab}	6.5 ± 0.16^{ab}	7.3 ± 0.2^{a}	6.81 ± 0.43^{ab}
Putrescine	12.95 ± 1.19^{ab}	12.9 ± 0.40^{ab}	13.67 ± 0.93^{ab}	12.35 ± 0.68^{ab}	12.1 ± 0.85^{b}	16.61 ± 1.48^{a}
Spermidine	0.76 ± 0.02^{a}	0.71 ± 0.03^{a}	0.37 ± 0.01^{b}	0.55 ± 0.03^{cd}	0.48 ± 0.02^{d}	0.59 ± 0.01^{c}

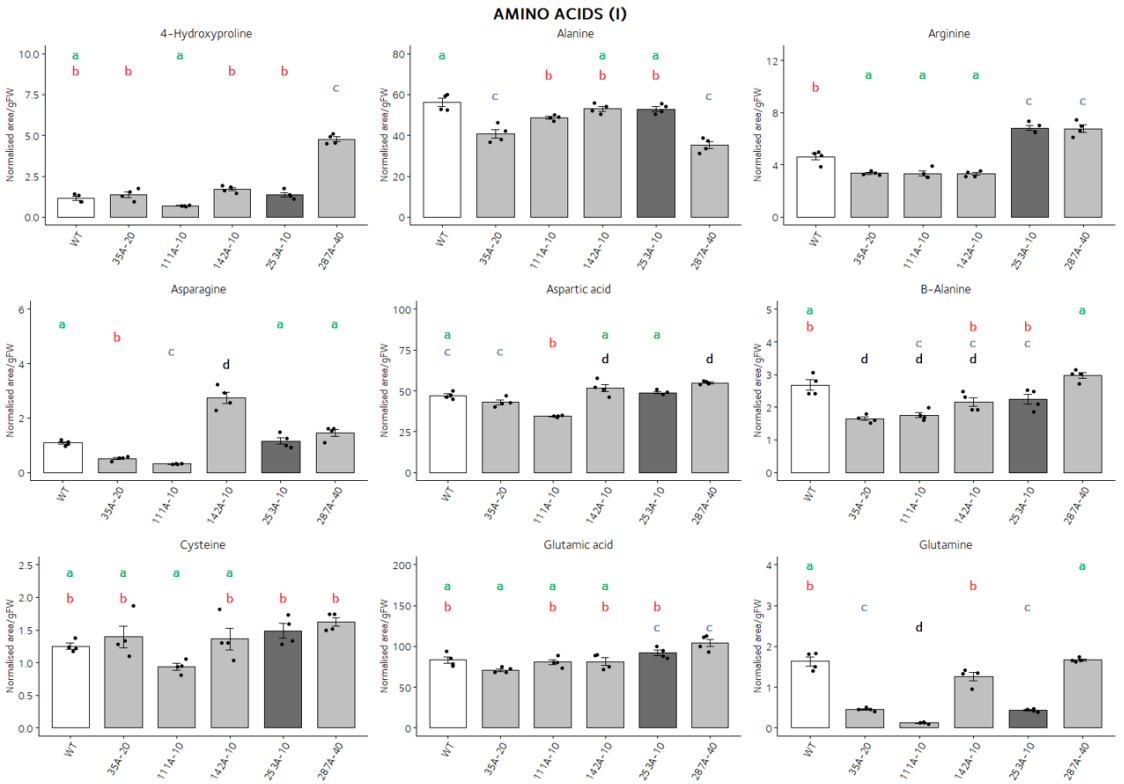

Figure C.7: Metabolite profiling of selected combinatorial lines — Amino acids (I). Metabolite profiling by GC-MS was performed in the selected combinatorial lines, six weeks after transfer to soil. Data are mean ± SE; n = 4. One-way ANOVA was used followed by post hoc Tukey multiple pairwise comparisons test. Different letters indicate significant differences between plant lines (P <0.05). Non-parametric Kruskal-Wallis test was used when the raw data displayed an abnormal distribution.

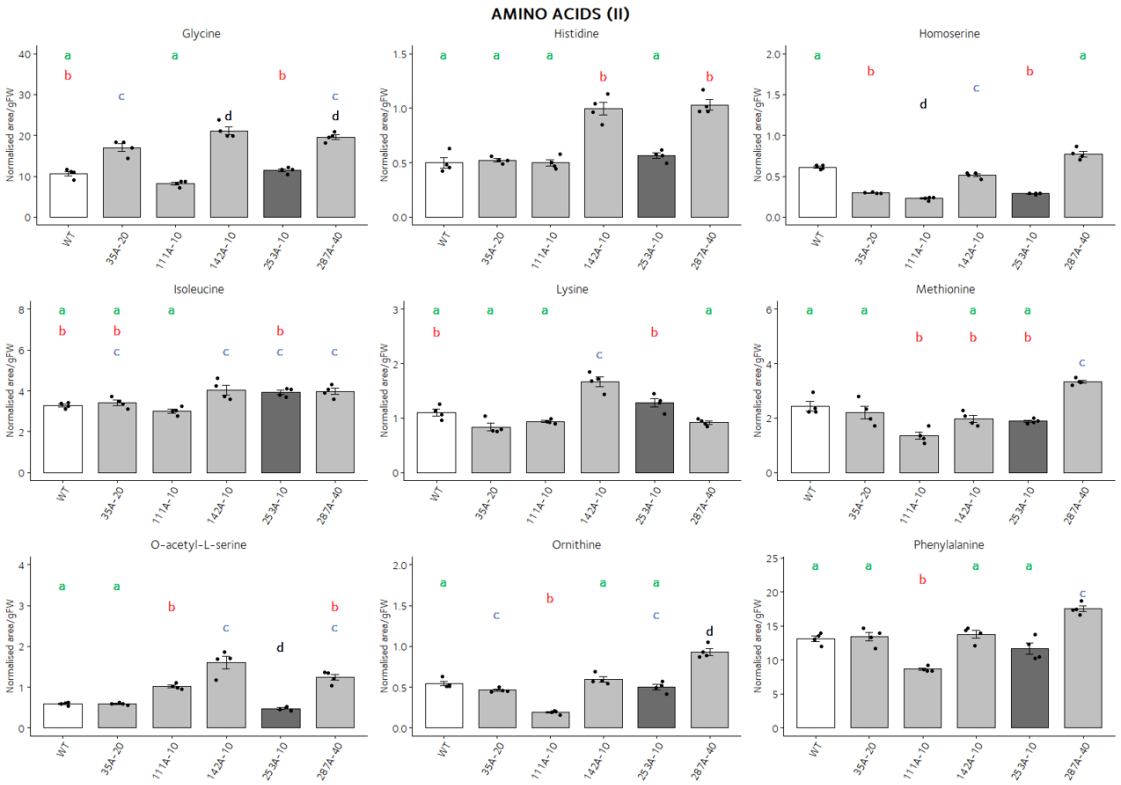

Figure C.8: Metabolite profiling of selected combinatorial lines — Amino acids (II). Metabolite profiling by GC-MS was performed in the selected combinatorial lines, six weeks after transfer to soil. Data are mean ± SE; n = 4. One-way ANOVA was used followed by post hoc Tukey multiple pairwise comparisons test. Different letters indicate significant differences between plant lines (P <0.05). Non-parametric Kruskal-Wallis test was used when the raw data displayed an abnormal distribution.

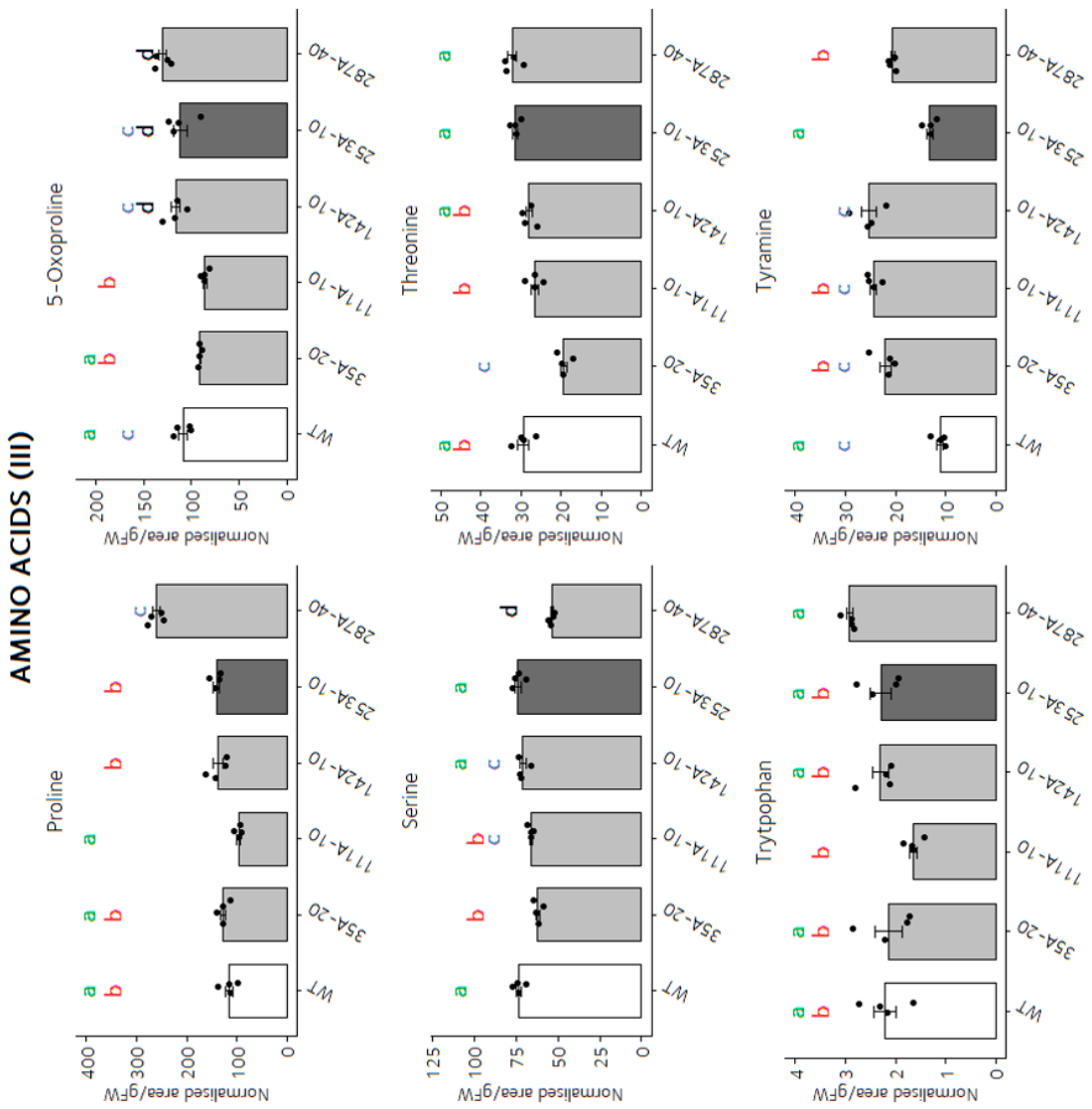

Figure C.9: Metabolite profiling of selected combinatorial lines — Amino acids (III). Metabolite profiling by GC-MS was performed in the selected combinatorial lines, six weeks after transfer to soil. Data are mean ± SE; n = 4. One-way ANOVA was used followed by post hoc Tukey multiple pairwise comparisons test. Different letters indicate significant differences between plant lines (P <0.05). Non-parametric Kruskal-Wallis test was used when the raw data displayed an abnormal distribution.

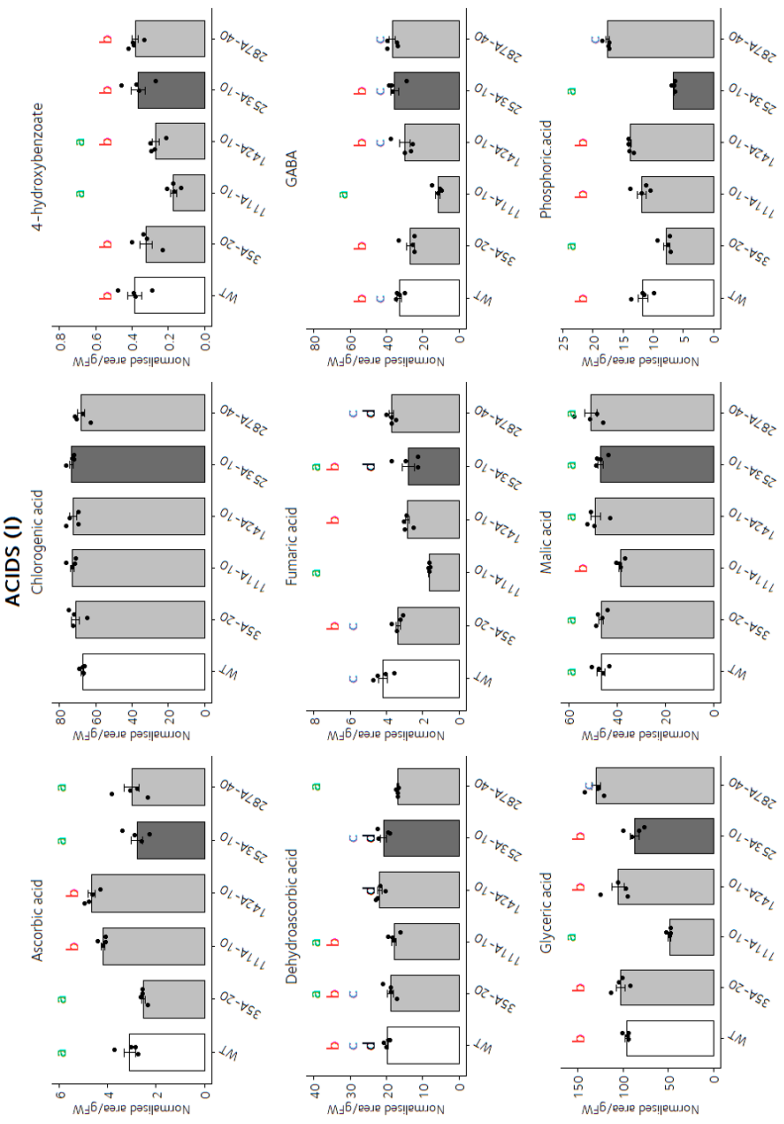

Figure C.10: Metabolite profiling of selected combinatorial lines — Acids (I). Metabolite profiling by GC-MS was performed in the selected combinatorial lines, six weeks after transfer to soil. Data are mean ± SE; n = 4. One-way ANOVA was used followed by post hoc Tukey multiple pairwise comparisons test. Different letters indicate significant differences between plant lines (P <0.05). Non-parametric Kruskal-Wallis test was used when the raw data displayed an abnormal distribution.

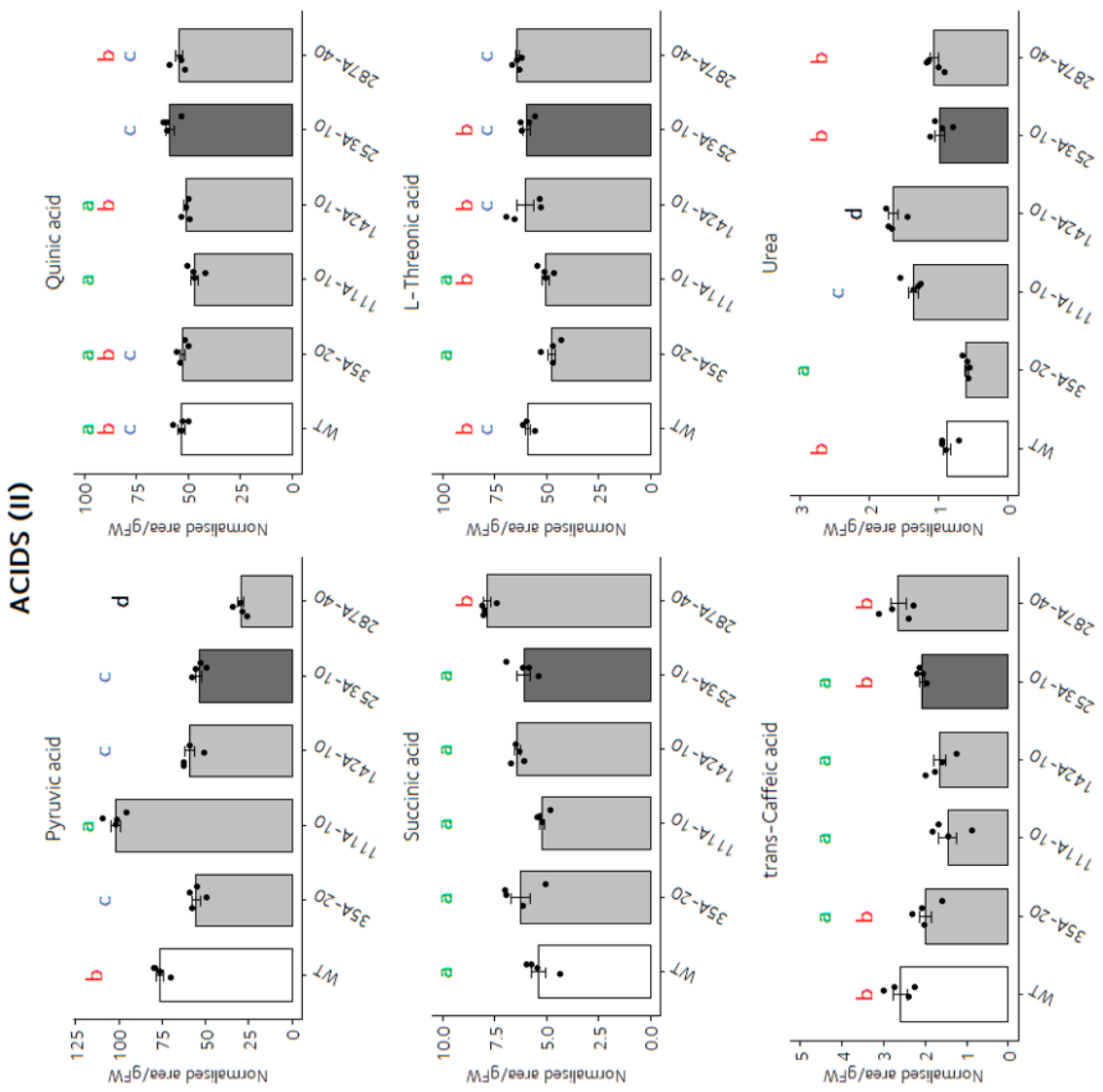

Figure C.11: Metabolite profiling of selected combinatorial lines — Acids (II). Metabolite profiling by GC-MS was performed in the selected combinatorial lines, six weeks after transfer to soil. Data are mean ± SE; n = 4. One-way ANOVA was used followed by post hoc Tukey multiple pairwise comparisons test. Different letters indicate significant differences between plant lines (P <0.05). Non-parametric Kruskal-Wallis test was used when the raw data displayed an abnormal distribution.

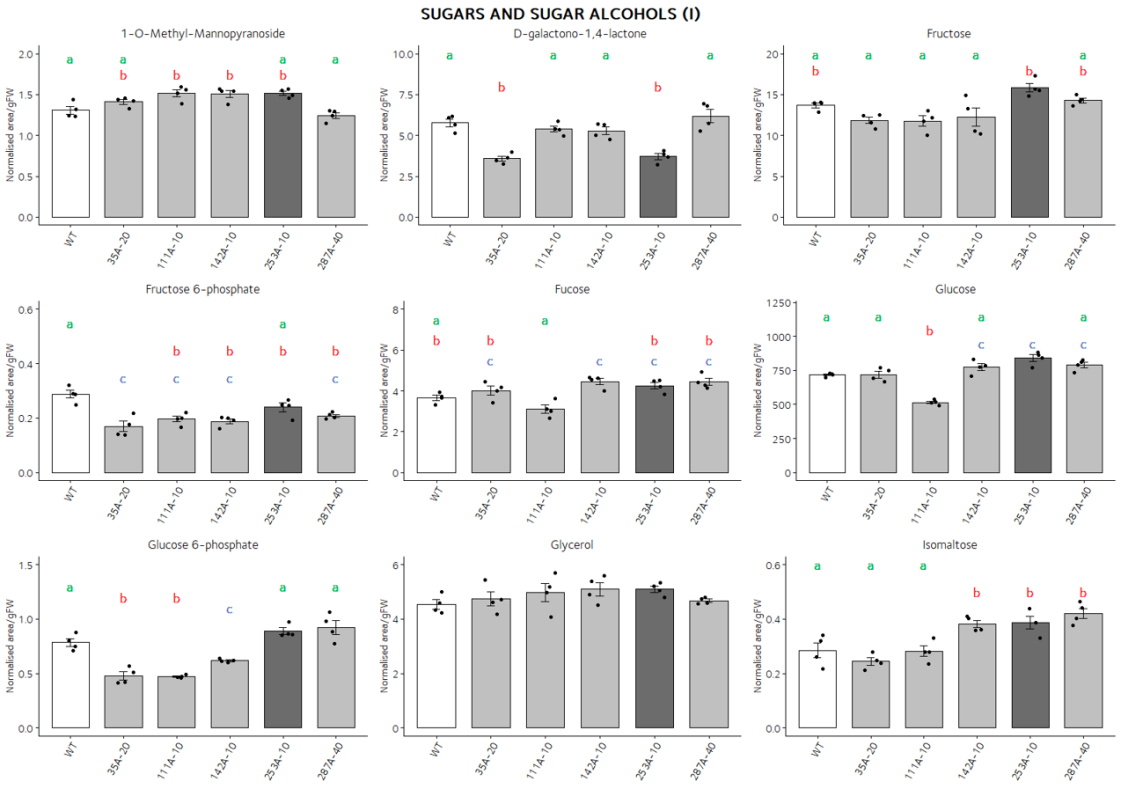

Figure C.12: Metabolite profiling of selected combinatorial lines — Sugars (I). Metabolite profiling by GC-MS was performed in the selected combinatorial lines, six weeks after transfer to soil. Data are mean ± SE; n = 4. One-way ANOVA was used followed by post hoc Tukey multiple pairwise comparisons test. Different letters indicate significant differences between plant lines (P <0.05). Non-parametric Kruskal-Wallis test was used when the raw data displayed an abnormal distribution.

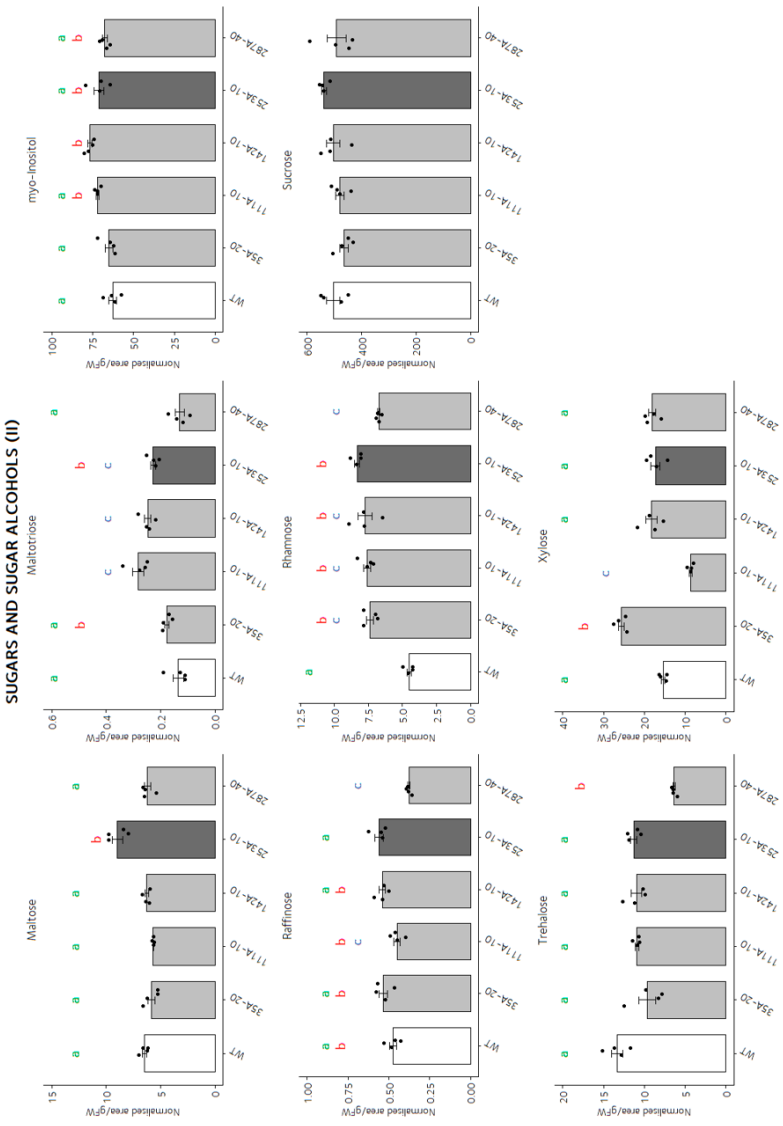

Figure C.13: Metabolite profiling of selected combinatorial lines — Sugars (II). Metabolite profiling by GC-MS was performed in the selected combinatorial lines, six weeks after transfer to soil. Data are mean ± SE; n = 4. One-way ANOVA was used followed by post hoc Tukey multiple pairwise comparisons test. Different letters indicate significant differences between plant lines (P <0.05). Non-parametric Kruskal-Wallis test was used when the raw data displayed an abnormal distribution.

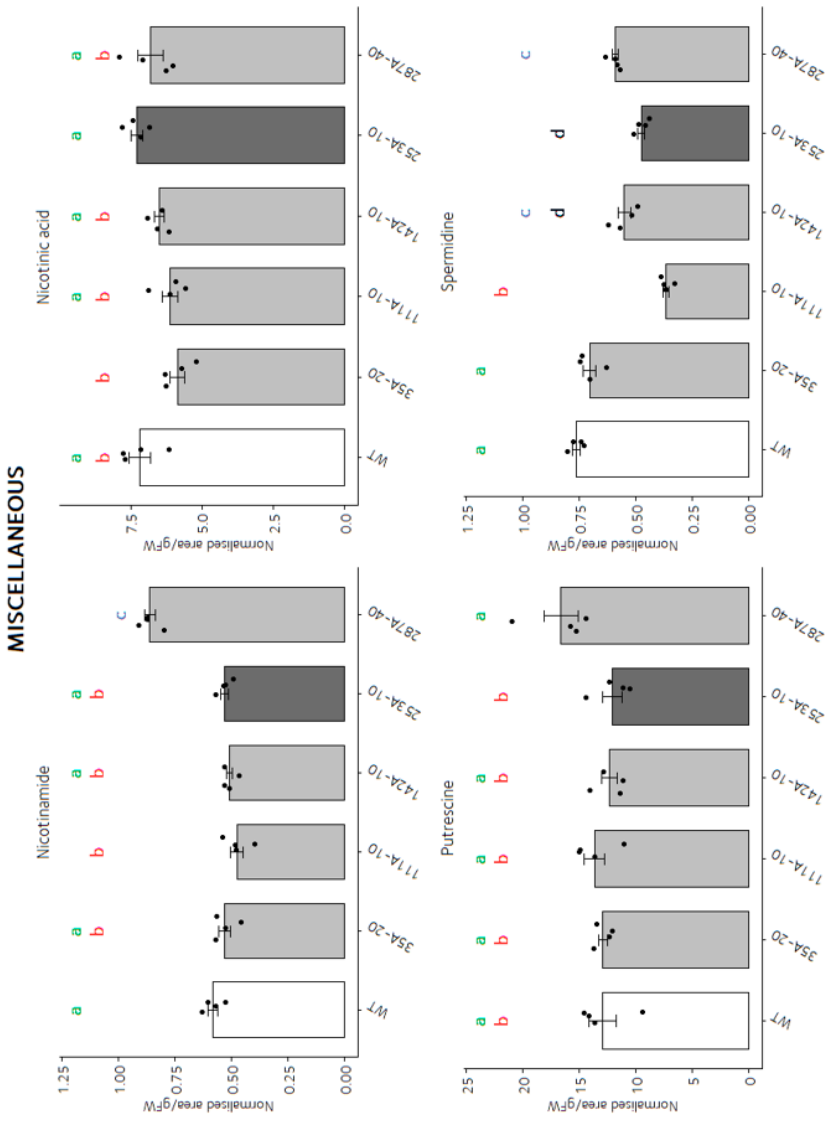

Figure C.14: Metabolite profiling of selected combinatorial lines — Other metabolites. Metabolite profiling by GC-MS was performed in the selected combinatorial lines, six weeks after transfer to soil. Data are mean ± SE; n = 4. One-way ANOVA was used followed by post hoc Tukey multiple pairwise comparisons test. Different letters indicate significant differences between plant lines (P <0.05). Non-parametric Kruskal-Wallis test was used when the raw data displayed an abnormal distribution.

Appendix D

Supplementary materials - Chapter 5

Figures

Tables

Table D.1: Relative transcript levels in multigene lines carrying the LS0201 construct. Relative transcript levels, represented as fold-change ($2^{-\Delta\Delta Ct}$), were determined by quantitative real-time PCR (qRT-PCR) in leaves, relative to the transcript levels of the housekeeping genes *L25* and *EF-1α*. Fold-change was calculated as per [205], as $2^{-\Delta\Delta Ct} = 2^{Ct_x - Ct_y}/2^{Ct_a - Ct_b}$, where Ct_x is the cycle threshold (Ct) of the transgene in the WT, Ct_y is the Ct of the transgene in the corresponding combinatorial line, Ct_a is the average Ct of the housekeeping genes in the WT, and Ct_b is the average Ct of the housekeeping genes in the corresponding combinatorial line. Three biological replicates (each involving one independent plant) were used per line. Average transcript levels and SE are given, along with a group classification based on the transcript levels of each transgene, as per Figure 5.8.

Line	NtGAPC	AtFIS1A	AtpOMT	NtmMDH	Group
1#1	0.92 ± 0.15	7442.28 ± 4943.04	12542.76 ± 15030.53	0.77 ± 0.09	GFOM
1#10	1.3 ± 0.25	10723.15 ± 7921.13	34537.01 ± 41896.97	0.97 ± 0.26	FOM
1#11	1.21 ± 0.49	24138.1 ± 28953.56	31704.83 ± 26962.77	0.81 ± 0.06	FOM
1#12	0.83 ± 0.04	60026.37 ± 96553.56	124841.51 ± 211492.17	0.72 ± 0.11	GFOM
1#13	0.92 ± 0.13	30142.07 ± 49289.51	39409.18 ± 62963.95	0.93 ± 0.23	GFOM
1#14	0.95 ± 0.18	0.7 ± 0.31	0.85 ± 0.7	0.83 ± 0.44	GM
1#15	1.09 ± 0.48	16286.91 ± 13383.98	11402.28 ± 974.63	0.88 ± 0.34	FOM
1#16	1.03 ± 0.58	15861.22 ± 21603.23	24805.93 ± 38968.31	0.82 ± 0.16	FOM
1#17	0.8 ± 0.31	3043.02 ± 1953.49	5697.2 ± 5646.8	0.66 ± 0.25	GFOM
1#18	1.23 ± 0.23	2.27 ± 3	2.19 ± 1.41	0.77 ± 0.14	M
1#19	1.51 ± 0.26	12685.08 ± 1230.11	18662.63 ± 3894.82	1.07 ± 0.29	FO
1#2	0.54 ± 0.2	0.75 ± 0.66	3.41 ± 3.7	0.86 ± 0.35	GM
1#20	1.35 ± 0.04	34249.03 ± 22692.54	7636.7 ± 2924.94	1.07 ± 0.16	FO
1#21	0.95 ± 0.56	9003.95 ± 2551.76	13740.77 ± 9793.33	0.68 ± 0.41	GFOM
1#22	0.96 ± 0.07	10161.63 ± 8201.7	17692.38 ± 12190.72	1.15 ± 0.31	GFO
1#23	0.88 ± 0.47	14840.78 ± 9599.85	5923.98 ± 7056.91	1.12 ± 0.76	GFO
1#24	0.87 ± 0.2	7915.5 ± 3108.18	8817.38 ± 5931.44	0.87 ± 0.29	GFOM
1#25	0.8 ± 0.24	7449.65 ± 1914.75	13940.05 ± 12770.92	0.95 ± 0.15	GFOM
1#26	0.85 ± 0.2	5267.27 ± 1914.12	5863.82 ± 2171.32	0.79 ± 0.23	GFOM
1#27	1.07 ± 0.18	10394.54 ± 3242.41	8327.13 ± 4709.33	0.86 ± 0.02	FOM
1#28	1.3 ± 0.39	19264.59 ± 9266.19	1.82 ± 0.55	1.01 ± 0.11	FO
1#29	1.07 ± 0.52	13138.97 ± 6339.89	4.08 ± 0.9	0.85 ± 0.51	FOM
1#3	0.49 ± 0.16	13202.14 ± 8738.45	25201.07 ± 30646.42	0.41 ± 0.07	GFOM
1#30	0.85 ± 0.17	7399.58 ± 2728.6	8436.12 ± 4251.54	0.64 ± 0.36	GFOM
1#31	1.27 ± 0.29	12900.15 ± 11989.25	2535.88 ± 1828.93	0.7 ± 0.27	FOM
1#32	0.99 ± 0.24	3.73 ± 0.56	10.39 ± 9.53	0.5 ± 0.25	M
1#33	0.97 ± 0.39	2.34 ± 1.58	2.96 ± 3.08	0.78 ± 0.19	GM
1#34	0.43 ± 0.19	20410.63 ± 25730.36	24977.09 ± 27343.3	0.44 ± 0	GFOM
1#35	0.78 ± 0.4	1.62 ± 2.12	1257.07 ± 2175	0.76 ± 0.35	GOM
1#36	1.37 ± 0.46	9049.09 ± 3112.73	7252.26 ± 5379.77	0.97 ± 0.45	FOM
1#37	1.42 ± 0.39	14556.44 ± 2270.1	8039.62 ± 3666.08	1.05 ± 0.15	FO
1#39	1.21 ± 0.17	10131.76 ± 4550.44	2874.23 ± 876.68	0.99 ± 0.11	FO
1#40	1.38 ± 0.58	1.36 ± 0.2	3.14 ± 3.54	1.25 ± 0.31	PseudoWT
1#41	0.99 ± 0.38	3719.75 ± 1769.92	2993.67 ± 4468.32	0.86 ± 0.22	GFOM
1#42	1.32 ± 0.42	5498.4 ± 5816.12	2219.9 ± 3121.84	0.99 ± 0.06	FO
1#44	0.86 ± 0.25	8938.16 ± 7512.01	4308.24 ± 3373.85	0.87 ± 0.11	GFOM
1#45	0.84 ± 0.34	9549.33 ± 6455.8	2117.12 ± 1098.48	0.67 ± 0.28	GFOM
1#47	1.74 ± 0.58	8073.17 ± 6838.27	3432.6 ± 1892.56	1.36 ± 0.57	FO
1#48	0.79 ± 0	7309.11 ± 0	443.33 ± 0	0.86 ± 0	GFOM
1#49	1.49 ± 0.64	8842.69 ± 2518.3	5498.79 ± 3479.32	1.11 ± 0.01	FO
1#5	0.86 ± 0.12	0.55 ± 0.18	2.06 ± 1.49	0.95 ± 0.11	GO
1#50	1.23 ± 0.3	15235.26 ± 6778.01	9537.55 ± 2577.5	0.77 ± 0.03	FOM
1#51	1.65 ± 0.71	24592.81 ± 17176.85	2970.93 ± 2324.41	1.3 ± 0.15	FO
1#6	0.55 ± 0.17	2855.74 ± 2033.42	8421.3 ± 9619.93	0.62 ± 0.35	GFOM
1#7	0.74 ± 0.23	17005.09 ± 24666.12	14016.14 ± 19608.84	0.87 ± 0.33	GFOM
1#8	0.69 ± 0.2	0.69 ± 0.59	0.67 ± 0.26	0.86 ± 0.25	GM
1#9	0.98 ± 0.13	44468.08 ± 61560.86	27639.26 ± 32179.45	0.97 ± 0.15	GFOM
WT	1 ± 0	0 ± 0	0 ± 0	1 ± 0	WT

Table D.2: Characterisation of multigene transgenic tobacco lines — c-Peredox-mCherry fluorescence and dark respiration. Details of line, normalised fluorescence T-Sapphire (Ts), normalised fluorescence mCherry (mC), ratio Ts/mC, and the $\log_{10}$-converted ratio Ts/mC (representing the cytosolic ratio of NADH/NAD^+), are shown. Means of four plants ± SE.

Line	Fluorescence Ts	Fluorescence mC	$\log_{10}$-ratio Ts/mC	OCR (pmol min^{-1} gFW^{-1})
1#1	16466.5 ± 3216.11	20498.25 ± 2099.18	-0.1 ± 0.05	125624.5 ± 50187.44
1#10	14883.75 ± 1929.9	21347.75 ± 1570.28	-0.16 ± 0.09	98719.5 ± 29095.81
1#11	5909.87 ± 8696.49	7235.15 ± 10112.22	-0.17 ± 0.11	129166.4 ± 67199.42
1#12	18210.25 ± 5673	26829 ± 9583.34	-0.16 ± 0.04	157981 ± 72660.08
1#13	11624.33 ± 1902.88	19364.67 ± 3411.75	-0.22 ± 0.11	123765.67 ± 26401.07
1#14	2878 ± 6126.32	5999.75 ± 7421.01	-0.15 ± 0.05	201884.33 ± 53115.35
1#15	734.72 ± 939.6	514.69 ± 524.8	-0.27 ± 0.09	93663.56 ± 59319.03
1#16	12254 ± 4347.93	18436.75 ± 3776.08	-0.19 ± 0.07	186165 ± 41247.25
1#17	14484 ± 1977.15	20174.67 ± 1412.8	-0.14 ± 0.07	122289.25 ± 43376.79
1#18	-1607.67 ± 714.78	166.67 ± 116.6	-	212812.33 ± 58351.44
1#19	1120.21 ± 1616.25	719.69 ± 680.86	-0.13 ± 0.1	213478.11 ± 49615.18
1#2	14871.75 ± 9727.36	17284.25 ± 18328.43	0.14 ± 0.51	132284.5 ± 47812.58
1#20	371.17 ± 190.8	115.73 ± 88.44	0.58 ± 0.91	148190.37 ± 17208.49
1#21	704.99 ± 673.29	126.3 ± 76.18	-0.22 ± 0.13	113524.4 ± 75587.72
1#22	338.61 ± 373.29	544.1 ± 508.48	-0.28 ± 0.09	148089.01 ± 63077.59
1#23	496.69 ± 510.66	80.79 ± 86.54	0.33 ± 0.11	105029.16 ± 55108.92
1#24	938.47 ± 378.03	682.29 ± 656.22	-0.2 ± 0.15	173296.38 ± 84461.12
1#25	713.44 ± 487.55	892.25 ± 877.14	-0.22 ± 0.07	206054.07 ± 106189.92
1#26	795.71 ± 1026.72	736.29 ± 642.71	-0.2 ± 0.08	182113.89 ± 75065.31
1#27	647.04 ± 282.05	740.82 ± 341	-0.18 ± 0.03	221768.15 ± 76862.31
1#28	183.07 ± 191.8	124.53 ± 72.94	0 ± 0.41	182122.52 ± 60097.85
1#29	225.44 ± 205.41	97.28 ± 80.53	-0.09 ± 0.44	109747.71 ± 41285.93
1#3	15997 ± 9113.54	25431.33 ± 13587.06	-0.21 ± 0.11	71233.33 ± 47917.99
1#30	486.14 ± 507.19	899.97 ± 893.21	-0.24 ± 0.06	138281.95 ± 68919.95
1#31	419.85 ± 274.68	43.19 ± 34.45	1.18 ± 0.98	172302.82 ± 57461.23
1#32	238.42 ± 172.67	72.99 ± 44.94	0.81 ± 0.9	156064.7 ± 73185.1
1#33	2518.67 ± 2655.35	325.6 ± 669.18	0.95 ± 0.49	118997 ± 63860.05
1#34	17208.2 ± 7400.63	23643.82 ± 5867.64	-0.18 ± 0.14	130001.75 ± 65481.45
1#35	-32.7 ± 1430.43	405.95 ± 836.43	0.83 ± 1.16	141935.75 ± 85631.63
1#36	22874.77 ± 13882.34	28160.23 ± 11710.69	-0.13 ± 0.12	87038 ± 53202.87
1#37	23269.43 ± 8792.34	30779.2 ± 11590.71	-0.13 ± 0.1	70656.67 ± 33276.72
1#39	9679.6 ± 7161.62	13554.88 ± 8507.77	-0.06 ± 0.25	112425 ± 24516.95
1#40	-622.47 ± 2550.81	170.93 ± 476.99	0.69 ± 1.58	58936.5 ± 4652.06
1#41	9092.28 ± 11236.51	11960.63 ± 15320.85	-0.02 ± 0.19	157623.75 ± 80525.76
1#42	-70.68 ± 2917.55	255.69 ± 390.68	0.76 ± 0.17	125954 ± 92780.89
1#44	25906.86 ± 10408.22	29999.51 ± 9495.09	-0.08 ± 0.09	63372.25 ± 34254.72

Line	**Fluorescence Ts**	**Fluorescence mC**	**log_{10}-ratio Ts/mC**	**OCR (pmol min^{-1} gFW^{-1})**
1#45	11101 ± 10863.85	11833.5 ± 12351.08	0.09 ± 0.49	128971 ± 68271.17
1#47	16742.93 ± 6109.71	21083.48 ± 5021.15	-0.12 ± 0.1	85320.75 ± 109596.94
1#48	3645.17 ± 6283.91	4730.89 ± 9678.95	0.41 ± 0.61	185664.5 ± 5625.03
1#49	14549.13 ± 7779.24	21472.12 ± 9510.21	-0.19 ± 0.08	143402 ± 60053.72
1#5	2042 ± 2793.85	417.75 ± 164.91	0.82 ± 0.12	70744 ± 23318.08
1#50	14701.93 ± 3711.86	22505.83 ± 5080.71	-0.19 ± 0.11	155995 ± 17943.54
1#51	10919.34 ± 12758.37	9167.89 ± 11359.24	0.46 ± 0.46	123860.67 ± 44538.49
1#6	-1197 ± 1415.58	1001.67 ± 902.63	-	187415.33 ± 61495.93
1#7	190.75 ± 1200.01	397 ± 376.52	0.95 ± 0.85	185370.5 ± 59289.15
1#8	-2363.75 ± 1136.41	1102 ± 1752.06	1.54 ± 0.15	197024.25 ± 45425.17
1#9	4302.5 ± 7046.29	6560 ± 11051.37	-0.12 ± 0.61	220009.75 ± 25240.74
7#10	-	-	-	-
7#15	17027.53 ± 14559.58	23179.09 ± 19620.03	-0.18 ± 0.09	135685.08 ± 65070.84
7#25	12914.46 ± 11763.81	15474.26 ± 13918.11	-0.17 ± 0.13	234697.65 ± 88724.36
7#27	12202.16 ± 10302.02	18410.17 ± 14931.85	-0.19 ± 0.07	209893.93 ± 111398.81
7#35	-	-	-	-
7#45	-	-	-	-
7#5	14818.47 ± 14076.38	20627.66 ± 19008.67	-0.19 ± 0.08	-
7#50	15596.75 ± 22136.29	22970.5 ± 23966.2	-0.04 ± 0.58	197992.25 ± 22071.71
WT_1	-	-	-	-
WT_2	-	-	-	80201.67 ± 42358.92
WT_3	-	-	-	126329.71 ± 36741.12

Table D.3: Characterisation of multigene transgenic tobacco lines - Plant growth parameters. Details of line, height (mm), leaf length (mm), and total number of leaves are shown. Means of four plants ± SE.

Line	Height (mm)	Leaf length (mm)	Number of leaves
1#1	154 ± 40	196 ± 21	9 ± 1
1#10	195 ± 52	191 ± 33	10 ± 1
1#11	106 ± 94	157 ± 46	9 ± 3
1#12	160 ± 123	169 ± 30	9 ± 2
1#13	134 ± 71	170 ± 55	10 ± 2
1#14	393 ± 14	197 ± 31	12 ± 0
1#15	115 ± 80	141 ± 16	10 ± 2
1#16	216 ± 36	214 ± 5	11 ± 1
1#17	123 ± 73	169 ± 36	10 ± 3
1#18	228 ± 156	165 ± 32	9 ± 2
1#19	200 ± 76	179 ± 8	12 ± 1
1#2	363 ± 56	188 ± 28	11 ± 0
1#20	148 ± 102	152 ± 73	11 ± 3
1#21	98 ± 57	159 ± 48	9 ± 1
1#22	144 ± 60	177 ± 7	12 ± 1
1#23	149 ± 63	157 ± 15	10 ± 2
1#24	182 ± 43	201 ± 14	11 ± 1
1#25	255 ± 165	150 ± 18	11 ± 2
1#26	310 ± 59	170 ± 5	13 ± 0
1#27	248 ± 71	189 ± 12	11 ± 1
1#28	214 ± 86	193 ± 29	11 ± 1
1#29	131 ± 42	203 ± 20	10 ± 1
1#3	158 ± 98	187 ± 67	10 ± 2
1#30	169 ± 58	202 ± 3	11 ± 2
1#31	158 ± 58	194 ± 4	12 ± 1
1#32	207 ± 48	189 ± 13	11 ± 2
1#33	158 ± 26	133 ± 3	10 ± 1
1#34	131 ± 27	157 ± 18	10 ± 1
1#35	163 ± 96	177 ± 16	11 ± 1
1#36	110 ± 75	143 ± 32	10 ± 1
1#37	63 ± 34	139 ± 53	8 ± 1
1#39	63 ± 8	150 ± 56	9 ± 1
1#40	284 ± 21	171 ± 5	12 ± 1
1#41	275 ± 139	157 ± 19	11 ± 1
1#42	170 ± 78	195 ± 22	11 ± 1
1#44	78 ± 32	152 ± 51	9 ± 1
1#45	169 ± 14	185 ± 35	9 ± 1
1#47	103 ± 65	167 ± 50	10 ± 2

Line	**Height (mm)**	**Leaf length (mm)**	**Number of leaves**
1#48	166 ± 116	136 ± 44	9 ± 1
1#49	131 ± 33	180 ± 26	9 ± 1
1#5	253 ± 153	188 ± 11	11 ± 6
1#50	81 ± 36	151 ± 27	9 ± 1
1#51	89 ± 61	135 ± 21	8 ± 1
1#6	173 ± 43	172 ± 19	10 ± 2
1#7	163 ± 121	181 ± 10	10 ± 2
1#8	233 ± 132	180 ± 12	12 ± 1
1#9	165 ± 100	188 ± 16	11 ± 1
7#10	254 ± 82	189 ± 25	11 ± 1
7#15	150 ± 74	185 ± 16	10 ± 1
7#25	265 ± 121	181 ± 26	11 ± 2
7#27	250 ± 111	164 ± 18	11 ± 2
7#35	306 ± 80	198 ± 17	10 ± 2
7#45	245 ± 83	212 ± 13	11 ± 1
7#5	211 ± 111	177 ± 39	10 ± 2
7#50	-	-	-
WT_1	243 ± 119	202 ± 33	9 ± 1
WT_2	184 ± 25	179 ± 25	10 ± 0
WT_3	169 ± 82	185 ± 15	10 ± 1

Table D.4: Characterisation of multigene transgenic tobacco lines — Biomass. Details of line, leaf biomass (gFW), stem biomass (gFW), and total aerial biomass (gFW) are shown. Means of four plants ± SE.

Line	Leaf biomass (gFW)	Stem biomass (gFW)	Total biomass (gFW)
1#1	18.82 ± 3.12	4.83 ± 1.42	23.64 ± 4.52
1#10	24.73 ± 6.15	7.46 ± 3.24	32.19 ± 9.38
1#11	14.73 ± 11.3	4.34 ± 4.26	18.45 ± 15.42
1#12	17.06 ± 9.94	6.22 ± 5.23	23.28 ± 15.12
1#13	23.02 ± 14.19	6.65 ± 4.27	29.66 ± 18.44
1#14	32.22 ± 2.05	18.33 ± 0.73	50.56 ± 2.34
1#15	22.07 ± 4.83	4.62 ± 4.37	26.7 ± 9.04
1#16	26.35 ± 4.41	8.02 ± 1.81	34.37 ± 6.1
1#17	17.92 ± 8.6	4.12 ± 2.69	22.04 ± 10.85
1#18	17.05 ± 10.74	7.56 ± 6.77	24.61 ± 17.46
1#19	30.07 ± 2.56	7.64 ± 3.11	37.71 ± 4.16
1#2	22.18 ± 2.56	13.01 ± 2.94	35.19 ± 4.43
1#20	19.82 ± 13.55	6.17 ± 4.76	25.99 ± 18.24
1#21	11.37 ± 5.42	2.59 ± 1.92	13.96 ± 7.33
1#22	21.1 ± 6.61	5.79 ± 2.89	26.89 ± 8.55
1#23	22.53 ± 8.96	5.94 ± 3.49	28.47 ± 12.42
1#24	25.56 ± 8.64	7.12 ± 2.86	32.67 ± 11.05
1#25	22.9 ± 12.23	10 ± 6.71	32.9 ± 18.93
1#26	27.73 ± 7.12	12.93 ± 3.04	40.65 ± 10.13
1#27	25.35 ± 1.41	8.86 ± 2.97	34.2 ± 2.94
1#28	23.62 ± 4.83	7.32 ± 3.67	30.94 ± 8.31
1#29	22.87 ± 2.42	4.46 ± 1.26	27.33 ± 3.03
1#3	22.11 ± 14.37	7.17 ± 5.5	29.28 ± 19.83
1#30	19.48 ± 8.36	5.95 ± 2.71	25.42 ± 10.98
1#31	25.31 ± 4.14	5.81 ± 2.42	31.12 ± 6.51
1#32	16.93 ± 5.56	6.1 ± 2.6	23.03 ± 8.1
1#33	20.16 ± 6.68	5.72 ± 1.76	25.88 ± 8.4
1#34	19.18 ± 5.39	4.16 ± 1.37	23.34 ± 6.6
1#35	17.28 ± 2.12	5.93 ± 3.92	23.21 ± 5.38
1#36	14.24 ± 9.98	3.79 ± 3.58	18.02 ± 13.24
1#37	7.92 ± 3.72	1.21 ± 0.96	9.12 ± 4.58
1#39	15.2 ± 5.25	1.69 ± 0.34	16.89 ± 5.53
1#40	24.78 ± 1.54	10.09 ± 1.6	34.87 ± 3.12
1#41	25.72 ± 4.43	11.08 ± 5.67	36.79 ± 9.96
1#42	21.91 ± 2.03	5.47 ± 2.65	27.39 ± 4.66
1#44	12.33 ± 7.4	1.98 ± 1.34	14.32 ± 8.51
1#45	17.27 ± 1.33	4.62 ± 0.56	21.89 ± 1.22
1#47	13.44 ± 7.2	2.63 ± 2.39	16.07 ± 9.38

Line	**Leaf biomass (gFW)**	**Stem biomass (gFW)**	**Total biomass (gFW)**
1#48	14.26 ± 7.97	4.34 ± 3.48	18.6 ± 11.11
1#49	17.05 ± 3.65	3.69 ± 1.24	20.74 ± 4.88
1#5	18.23 ± 12.61	10.86 ± 7.67	26.38 ± 20.84
1#50	11.66 ± 6.37	1.67 ± 1.09	13.33 ± 7.38
1#51	13.54 ± 4.22	2.05 ± 1.75	15.6 ± 5.76
1#6	19.69 ± 5.03	5.85 ± 1.03	25.53 ± 5.59
1#7	21.46 ± 10.73	6.72 ± 7.52	28.18 ± 17.91
1#8	25.01 ± 2.17	11.95 ± 5.18	36.96 ± 5.81
1#9	17.43 ± 7.28	6.02 ± 4.16	23.45 ± 10.39
7#10	23.86 ± 7.91	9.84 ± 3.82	33.7 ± 10.93
7#15	18.11 ± 6.18	5.58 ± 4.13	23.69 ± 9.96
7#25	23.16 ± 5.66	10.17 ± 5.22	33.33 ± 10.64
7#27	20.98 ± 6.56	9.3 ± 5.33	30.28 ± 10.99
7#35	25.21 ± 6.68	13.52 ± 4.95	38.73 ± 10.73
7#45	23.39 ± 2.54	10.14 ± 2.84	33.53 ± 2.1
7#5	20.06 ± 7.15	7.7 ± 4.95	27.76 ± 11.22
7#50	-	-	-
WT_1	20.31 ± 11.22	9.44 ± 6.74	29.74 ± 17.92
WT_2	19.31 ± 0.99	5.76 ± 0.72	25.07 ± 1.15
WT_3	23.47 ± 4.46	6.34 ± 3.52	29.81 ± 6.95

Table D.5: Characterisation of multigene transgenic tobacco lines — Chlorophyll fluorescence (I). Details of line, fluorescence intensity at 50 μs (F_0), fluorescence intensity at 2 ms (J-level, F_j), fluorescence intensity at 30 ms (I-level, F_i), fluorescence intensity at the peak of OJIP curve (F_m), maximum variable fluorescence (F_v), shape of fluorescence kinetics at intermediate step J (V_j), and shape of fluorescence kinetics at intermediate step I (V_i) are shown. Means of four plants ± SE.

Line	F_0	F_j	F_i	F_m	F_v	V_j	V_i
1#1	4391.8 ± 425	12472.5 ± 2044.5	19679 ± 3246	25040 ± 3215	20648 ± 2791.9	0.39 ± 0.0294	0.74 ± 0.037
1#10	4312 ± 304	11799.8 ± 1018.6	18629 ± 1824	23816 ± 1881	19504.3 ± 1584.8	0.3825 ± 0.0222	0.73 ± 0.022
1#11	5110.6 ± 864.6	14057 ± 1889.7	22092 ± 2709	27700 ± 3005	22589.9 ± 2670.7	0.397 ± 0.0365	0.751 ± 0.034
1#12	4628.8 ± 529.7	12649.5 ± 2012.1	19100 ± 2693	24140 ± 2692	19511.5 ± 2225.6	0.4075 ± 0.034	0.742 ± 0.03
1#13	4377 ± 444.6	12260.8 ± 1571.4	18702 ± 1469	23804 ± 1089	19426.5 ± 956.9	0.4075 ± 0.0525	0.738 ± 0.033
1#14	4128 ± 112.7	11562 ± 317	19229 ± 848	24603 ± 375	20474.7 ± 421.7	0.3633 ± 0.0115	0.74 ± 0.036
1#15	5207.7 ± 157.7	12891.3 ± 1068.6	19103 ± 2853	24629 ± 3171	19421.7 ± 3020.8	0.3973 ± 0.0261	0.712 ± 0.029
1#16	4192.8 ± 509.3	11702.8 ± 1154.6	18397 ± 1951	23686 ± 2011	19493.5 ± 1850.9	0.3875 ± 0.0222	0.727 ± 0.022
1#17	4329.5 ± 453.4	12091.3 ± 1284.1	19355 ± 2347	24222 ± 2529	19892.8 ± 2388.7	0.3925 ± 0.0171	0.755 ± 0.019
1#18	3943.3 ± 548.9	11455.5 ± 2374.2	19716 ± 3565	25025 ± 3269	21081.8 ± 2727.3	0.35 ± 0.051	0.742 ± 0.051
1#19	4653.8 ± 347	11769.8 ± 1651.6	19041 ± 2984	24636 ± 3034	19982 ± 2739.9	0.3545 ± 0.0196	0.716 ± 0.041
1#2	3692.3 ± 369.2	10276 ± 1028.6	17750 ± 1048	23194 ± 1265	19501.7 ± 932.6	0.3367 ± 0.0153	0.72 ± 0
1#20	5177 ± 525.6	13260.3 ± 1173.2	20479 ± 2750	26436 ± 3463	21258.8 ± 3367.7	0.3835 ± 0.0329	0.719 ± 0.013
1#21	5378.3 ± 575.8	13427 ± 1589.5	19171 ± 3126	24684 ± 3573	19305.8 ± 3079.4	0.419 ± 0.0283	0.712 ± 0.024
1#22	4880.3 ± 434	11470.5 ± 1132.7	15611 ± 1464	21264 ± 1791	16383.3 ± 1402.1	0.4023 ± 0.0314	0.654 ± 0.01
1#23	5142.3 ± 565.7	12275.8 ± 1658.5	16559 ± 1332	21823 ± 1606	16680.3 ± 1057.6	0.426 ± 0.0401	0.684 ± 0.021
1#24	4805.5 ± 141.7	11253.8 ± 167.9	15551 ± 279	21116 ± 439	16310.8 ± 314.1	0.3955 ± 0.007	0.659 ± 0.007
1#25	4606 ± 0	10772.5 ± 641.3	15254 ± 437	20773 ± 501	16167 ± 500.6	0.381 ± 0.0283	0.659 ± 0.006
1#26	4506.5 ± 88.5	11396 ± 344.7	16197 ± 1077	21688 ± 1350	17181 ± 1288.6	0.4027 ± 0.0359	0.68 ± 0.026
1#27	4720.8 ± 371.3	11004.8 ± 1536.4	15653 ± 2203	21121 ± 2322	16400.5 ± 2073.8	0.3818 ± 0.0375	0.664 ± 0.033
1#28	5269 ± 229.9	11926.8 ± 559.6	17331 ± 857	23325 ± 830	18055.8 ± 691.1	0.369 ± 0.0214	0.668 ± 0.025
1#29	4733.3 ± 378.6	11034.3 ± 678.2	15760 ± 825	21874 ± 1475	17141 ± 1648	0.37 ± 0.0371	0.644 ± 0.01
1#3	4413.3 ± 602	12043.7 ± 750.7	18518 ± 494	23739 ± 371	19325.7 ± 272.4	0.3967 ± 0.0115	0.73 ± 0
1#30	5174.7 ± 518.5	13439.7 ± 2351.3	20515 ± 4616	26357 ± 4936	21182.7 ± 4497.6	0.39 ± 0.0236	0.717 ± 0.052
1#31	4778.3 ± 91.3	13125.5 ± 644.5	22393 ± 656	28235 ± 382	23457 ± 374.4	0.3557 ± 0.0217	0.751 ± 0.017
1#32	4900.5 ± 442.6	12427.8 ± 399.1	21244 ± 1513	27099 ± 1260	22198.3 ± 1602.1	0.3403 ± 0.0264	0.735 ± 0.036
1#33	5448.8 ± 809.7	12348.3 ± 1365.4	15245 ± 1967	20429 ± 2212	14979.8 ± 1458.5	0.4608 ± 0.0383	0.653 ± 0.019
1#34	5002.8 ± 353.9	11759.8 ± 965.1	16022 ± 1540	21583 ± 2005	16579.8 ± 2352.4	0.412 ± 0.074	0.663 ± 0.032
1#35	4925.8 ± 322.9	11552.8 ± 1242.9	16264 ± 3578	22457 ± 4451	17531.5 ± 4518.3	0.3825 ± 0.0362	0.641 ± 0.044
1#36	5055 ± 333.5	12457.8 ± 1402.8	15282 ± 1878	20381 ± 2206	15326.3 ± 2015.1	0.4845 ± 0.0596	0.666 ± 0.027
1#37	6585.8 ± 3290.9	14429 ± 2399.6	19269 ± 1407	24918 ± 771	18332.3 ± 3542.2	0.4318 ± 0.049	0.696 ± 0.03
1#39	4937.8 ± 250.5	11595.3 ± 1249.1	15125 ± 2767	20429 ± 3480	15491 ± 3240.4	0.4343 ± 0.0342	0.654 ± 0.034
1#40	4920.3 ± 213.3	12393 ± 780.3	17692 ± 2088	23208 ± 2527	18287.5 ± 2687.8	0.4158 ± 0.0772	0.696 ± 0.023
1#41	4832.8 ± 342.3	12071.3 ± 805.7	16127 ± 1295	21523 ± 2210	16690 ± 2293.4	0.444 ± 0.0996	0.678 ± 0.02
1#42	4481.8 ± 50.2	10329 ± 823.5	14262 ± 2492	19245 ± 3048	14762.8 ± 3053.1	0.4003 ± 0.0284	0.658 ± 0.031

Line	F_0	F_j	F_i	F_m	F_v	V_j	V_i
1#44	5432.1 ± 1682.6	12405.1 ± 2027.8	16724 ± 1130	22042 ± 1590	16610.1 ± 2945.2	0.4376 ± 0.1137	0.688 ± 0.064
1#45	4529 ± 277.4	10994.8 ± 285.8	15743 ± 1821	21486 ± 2736	16956.5 ± 3011	0.3883 ± 0.054	0.661 ± 0.009
1#47	4858 ± 339.7	13011 ± 2138.6	19983 ± 5427	26336 ± 6305	21478 ± 6010.2	0.386 ± 0.034	0.693 ± 0.055
1#48	5263.3 ± 1867.9	12240.3 ± 2802.5	16586 ± 3489	21999 ± 3960	16735.3 ± 3349.4	0.4278 ± 0.0852	0.675 ± 0.036
1#49	4981.7 ± 503.3	11811 ± 1097.5	16298 ± 1059	21931 ± 1040	16949.3 ± 598.5	0.4023 ± 0.0237	0.667 ± 0.012
1#5	4682.7 ± 533.3	12751.7 ± 1376.4	19053 ± 1066	23951 ± 933	19268.7 ± 990.7	0.42 ± 0.0436	0.747 ± 0.021
1#50	4895 ± 876.7	12703.8 ± 2274.6	17970 ± 3652	23853 ± 4434	18957.5 ± 4025.9	0.4178 ± 0.0653	0.686 ± 0.028
1#51	4880.3 ± 521.5	12231 ± 2130.3	17996 ± 4615	24023 ± 5862	19142.5 ± 5669.1	0.3905 ± 0.0334	0.677 ± 0.038
1#6	4031.3 ± 1127.8	11037.3 ± 2777.7	17215 ± 3115	22379 ± 2914	18348 ± 1786.5	0.3767 ± 0.0577	0.717 ± 0.042
1#7	4963 ± 744.1	12291 ± 819.5	19025 ± 1425	24148 ± 1978	19185 ± 2169.2	0.385 ± 0.0265	0.735 ± 0.03
1#8	4608.8 ± 391.9	12537.5 ± 766.2	20937 ± 1668	26109 ± 1786	21500.3 ± 1728.6	0.37 ± 0.0141	0.76 ± 0.02
1#9	4592.7 ± 659.4	12449.3 ± 1104.1	18933 ± 1070	24427 ± 1451	19834 ± 1235.1	0.4 ± 0.0265	0.723 ± 0.012
7#10	-	-	-	-	-	-	-
7#15	5325.3 ± 938.7	13726.3 ± 2190.5	19895 ± 3320	25292 ± 3412	19967 ± 2990.3	0.4267 ± 0.0777	0.725 ± 0.038
7#25	4695 ± 556	11747.5 ± 1586.4	17412 ± 2523	22905 ± 2773	18209.7 ± 2480.6	0.3866 ± 0.0236	0.695 ± 0.027
7#27	4577.5 ± 538.7	11749.5 ± 1077.7	17460 ± 2904	22562 ± 3472	17984.6 ± 3644.2	0.4126 ± 0.0965	0.713 ± 0.038
7#35	-	-	-	-	-	-	-
7#45	-	-	-	-	-	-	-
7#5	5067.3 ± 369.1	13293.5 ± 711.3	19860 ± 2903	25375 ± 3147	20308.2 ± 3363.4	0.4113 ± 0.0526	0.724 ± 0.04
7#50	-	-	-	-	-	-	-
WT_1	4470.8 ± 839.3	12034 ± 2541.3	19583 ± 3684	24806 ± 3621	20334.8 ± 2863	0.37 ± 0.0374	0.74 ± 0.041
WT_2	4606 ± 245.9	11817 ± 1046	17448 ± 2732	23298 ± 2950	18691.5 ± 2735.5	0.387 ± 0.0152	0.684 ± 0.035
WT_3	5256.8 ± 225.6	13581.8 ± 1984.5	21134 ± 5207	26800 ± 5584	21542.8 ± 5443.8	0.389 ± 0.0151	0.728 ± 0.054

Table D.6: Characterisation of multigene transgenic tobacco lines — Chlorophyll fluorescence (II). Details of line, ratio of the extrema (F_m/F_0), quantum yield of PS II efficiency (F_v/F_0 and F_v/F_m), normalised value of initial slope of the O-J fluorescence rise (M_0), area between fluorescence curve and F_m (Area), normalised area between the OJIP curve and the F_m line (S_m), single Q_A turnover (S_s), and Q_A turnover number (N or S_m/S_s) are shown. Means of four plants ± SE.

Line	F_m/F_0	F_v/F_0	F_v/F_m	M_0	Area	S_m	S_s	N
1#1	5.6875 ± 0.1981	4.6875 ± 0.1981	0.827 ± 0.005	0.455 ± 0.058	7306018 ± 575134	361.845 ± 79.202	0.865 ± 0.066	414.7025 ± 61.3461
1#10	5.52 ± 0.0942	4.52 ± 0.0942	0.82 ± 0	0.435 ± 0.0443	7989659 ± 461028	411.765 ± 43.623	0.893 ± 0.038	461.9875 ± 32.8576
1#11	5.5056 ± 0.712	4.5056 ± 0.712	0.815 ± 0.03	0.4927 ± 0.0663	7970734 ± 4639057	375.318 ± 277.921	0.814 ± 0.06	450.9506 ± 304.2965
1#12	5.22 ± 0.2406	4.22 ± 0.2406	0.81 ± 0.008	0.495 ± 0.0614	8414303 ± 1664497	442.243 ± 136.697	0.83 ± 0.037	530.9525 ± 146.6787
1#13	5.47 ± 0.4621	4.47 ± 0.4621	0.815 ± 0.017	0.505 ± 0.142	8154425 ± 548215	419.8 ± 20.743	0.828 ± 0.1	510.7525 ± 51.4271
1#14	5.9633 ± 0.212	4.9633 ± 0.212	0.833 ± 0.006	0.42 ± 0.02	10103343 ± 2550290	495.267 ± 135.657	0.87 ± 0.061	576.5167 ± 185.9314
1#15	4.7207 ± 0.4729	3.7207 ± 0.4729	0.787 ± 0.021	0.4947 ± 0.0234	5933923 ± 309873	308.915 ± 33.019	0.803 ± 0.019	384.1187 ± 32.1083
1#16	5.6925 ± 0.6573	4.6925 ± 0.6573	0.823 ± 0.021	0.4425 ± 0.0655	7900500 ± 1634780	413.855 ± 128.1	0.88 ± 0.084	478.6625 ± 178.3477
1#17	5.6225 ± 0.5992	4.6225 ± 0.5992	0.82 ± 0.022	0.44 ± 0.0346	7410809 ± 446376	375.792 ± 42.436	0.89 ± 0.039	420.1175 ± 29.6222
1#18	6.355 ± 0.1429	5.355 ± 0.1429	0.842 ± 0.005	0.37 ± 0.0757	7990865 ± 1168364	380.695 ± 47.031	0.97 ± 0.089	395.32 ± 52.8732
1#19	5.2848 ± 0.3804	4.2848 ± 0.3804	0.81 ± 0.015	0.4205 ± 0.0426	11294736 ± 9898803	621.605 ± 640.682	0.846 ± 0.048	736.689 ± 762.6887
1#2	6.3 ± 0.3236	5.3 ± 0.3236	0.843 ± 0.012	0.3533 ± 0.0569	9917005 ± 363569	509.773 ± 41.072	0.967 ± 0.108	529.48 ± 17.0374
1#20	5.1348 ± 0.7517	4.1348 ± 0.7517	0.802 ± 0.029	0.499 ± 0.0537	6685695 ± 831899	316.159 ± 20.909	0.773 ± 0.078	410.1425 ± 18.1951
1#21	4.582 ± 0.3433	3.582 ± 0.3433	0.781 ± 0.016	0.5475 ± 0.0359	5141508 ± 365669	269.586 ± 29.758	0.766 ± 0.033	351.836 ± 30.2643
1#22	4.3605 ± 0.1531	3.3605 ± 0.1531	0.771 ± 0.008	0.4955 ± 0.052	9145650 ± 5152319	567.025 ± 337.48	0.814 ± 0.034	687.8315 ± 384.3244
1#23	4.256 ± 0.163	3.256 ± 0.163	0.765 ± 0.009	0.5265 ± 0.0633	9495948 ± 7919888	549.572 ± 415.536	0.811 ± 0.026	687.4923 ± 541.1869
1#24	4.3953 ± 0.0593	3.3953 ± 0.0593	0.773 ± 0.003	0.4945 ± 0.0101	9133828 ± 5604020	564.771 ± 359.452	0.8 ± 0.008	706.5127 ± 450.6696
1#25	4.51 ± 0.1089	3.51 ± 0.1089	0.778 ± 0.006	0.4545 ± 0.0474	7674524 ± 1372861	476.246 ± 99.665	0.84 ± 0.025	565.569 ± 101.508
1#26	4.8108 ± 0.2414	3.8108 ± 0.2414	0.792 ± 0.01	0.4953 ± 0.0307	8144521 ± 1710667	474.45 ± 94.898	0.813 ± 0.032	587.0152 ± 135.9933
1#27	4.475 ± 0.3297	3.475 ± 0.3297	0.776 ± 0.017	0.4733 ± 0.0716	7348032 ± 1520108	456.42 ± 129.561	0.812 ± 0.049	568.0405 ± 190.493
1#28	4.4298 ± 0.1464	3.4298 ± 0.1464	0.774 ± 0.007	0.468 ± 0.0342	6893900 ± 1335552	380.793 ± 62.619	0.79 ± 0.032	484.747 ± 96.6506
1#29	4.6528 ± 0.6092	3.6528 ± 0.6092	0.783 ± 0.026	0.4623 ± 0.0409	6609700 ± 637537	385.646 ± 4.601	0.801 ± 0.041	482.66 ± 20.8912
1#3	5.4367 ± 0.6307	4.4367 ± 0.6307	0.813 ± 0.021	0.4633 ± 0.0252	7379892 ± 1281847	381.457 ± 62.645	0.863 ± 0.023	441.9833 ± 60.8608
1#30	5.0707 ± 0.6101	4.0707 ± 0.6101	0.801 ± 0.024	0.5273 ± 0.057	6545048 ± 615020	317.737 ± 66.454	0.742 ± 0.044	425.702 ± 63.3405
1#31	5.9105 ± 0.1239	4.9105 ± 0.1239	0.831 ± 0.004	0.4103 ± 0.0235	5888900 ± 384196	251.054 ± 15.939	0.868 ± 0.026	289.8805 ± 25.5391
1#32	5.5752 ± 0.6961	4.5752 ± 0.6961	0.818 ± 0.023	0.4278 ± 0.0856	7083676 ± 868189	318.324 ± 16.277	0.811 ± 0.108	397.153 ± 52.4133
1#33	3.7703 ± 0.2394	2.7703 ± 0.2394	0.734 ± 0.016	0.5955 ± 0.0318	6343021 ± 379761	426.681 ± 50.792	0.774 ± 0.046	551.1348 ± 55.5442
1#34	4.3538 ± 0.7576	3.3538 ± 0.7576	0.766 ± 0.035	0.5333 ± 0.0985	8071609 ± 1579434	500.672 ± 145.329	0.774 ± 0.037	654.474 ± 218.1965
1#35	4.5805 ± 0.998	3.5805 ± 0.998	0.775 ± 0.042	0.5098 ± 0.051	7922914 ± 1942282	486.232 ± 188.802	0.751 ± 0.032	650.4525 ± 263.0473
1#36	4.0325 ± 0.3344	3.0325 ± 0.3344	0.751 ± 0.02	0.6547 ± 0.0928	5859625 ± 1003287	384.888 ± 71.461	0.744 ± 0.066	518.2275 ± 86.6163
1#37	4.3345 ± 1.4696	3.3345 ± 1.4696	0.735 ± 0.135	0.5595 ± 0.0915	5967367 ± 889807	345.456 ± 139.362	0.777 ± 0.048	452.6693 ± 211.7528
1#39	4.1192 ± 0.5079	3.1192 ± 0.5079	0.755 ± 0.03	0.5635 ± 0.0317	5912083 ± 1187572	404.461 ± 155.83	0.77 ± 0.017	523.7078 ± 197.1149
1#40	4.7353 ± 0.6661	3.7353 ± 0.6661	0.786 ± 0.032	0.519 ± 0.1103	5993631 ± 448155	335.773 ± 75.27	0.804 ± 0.02	419.0763 ± 102.9177
1#41	4.475 ± 0.5972	3.475 ± 0.5972	0.773 ± 0.033	0.5585 ± 0.1164	7396482 ± 2720999	439.302 ± 132.205	0.794 ± 0.034	558.5823 ± 185.0075
1#42	4.2947 ± 0.6818	3.2948 ± 0.6818	0.763 ± 0.035	0.4968 ± 0.0561	6025082 ± 698739	425.715 ± 116.384	0.809 ± 0.048	533.482 ± 167.2706

Line	F_m/F_0	F_v/F_0	F_v/F_m	M_0	Area	S_m	S_s	N
1#44	4.3254 ± 1.183	3.3254 ± 1.183	0.749 ± 0.095	0.5591 ± 0.1641	8041036 ± 3174748	553.7 ± 388.115	0.787 ± 0.029	713.2191 ± 524.1256
1#45	4.7853 ± 0.8977	3.7853 ± 0.8977	0.786 ± 0.04	0.4713 ± 0.0856	6090574 ± 1386544	371.237 ± 126.619	0.829 ± 0.037	453.5865 ± 177.9256
1#47	5.3815 ± 1.0181	4.3815 ± 1.0181	0.808 ± 0.044	0.4978 ± 0.0415	6286964 ± 1046039	312.262 ± 105.291	0.775 ± 0.017	402.8635 ± 135.2892
1#48	4.4075 ± 1.1542	3.4075 ± 1.1542	0.76 ± 0.066	0.5265 ± 0.1273	6367093 ± 715376	397.414 ± 116.98	0.819 ± 0.053	487.8333 ± 147.2003
1#49	4.4203 ± 0.2714	3.4203 ± 0.2714	0.773 ± 0.014	0.532 ± 0.0511	5880463 ± 424682	347.255 ± 28.047	0.758 ± 0.034	459.216 ± 50.3172
1#5	5.1567 ± 0.5532	4.1567 ± 0.5532	0.807 ± 0.023	0.5233 ± 0.0874	8886821 ± 2623464	457.43 ± 110.165	0.8 ± 0.046	573.7767 ± 162.8383
1#50	4.9175 ± 0.9036	3.9175 ± 0.9036	0.792 ± 0.036	0.5153 ± 0.0997	5742473 ± 416985	313.481 ± 69.364	0.816 ± 0.048	383.5545 ± 78.1373
1#51	4.9238 ± 1.1553	3.9238 ± 1.1553	0.787 ± 0.057	0.4993 ± 0.0597	6016744 ± 386490	348.161 ± 155.106	0.784 ± 0.031	446.8035 ± 209.2312
1#6	5.7467 ± 1.0515	4.7467 ± 1.0515	0.823 ± 0.032	0.42 ± 0.1153	8405458 ± 1620776	467.013 ± 139.997	0.927 ± 0.146	500.13 ± 78.8806
1#7	4.95 ± 0.8994	3.95 ± 0.8994	0.795 ± 0.037	0.4525 ± 0.0359	8846316 ± 390110	464.66 ± 44.866	0.847 ± 0.021	548.3175 ± 60.8228
1#8	5.6925 ± 0.5639	4.6925 ± 0.5639	0.825 ± 0.017	0.425 ± 0.0265	8402221 ± 487052	392.058 ± 28.008	0.868 ± 0.041	452.705 ± 39.1443
1#9	5.3733 ± 0.6258	4.3733 ± 0.6258	0.813 ± 0.021	0.4867 ± 0.0737	9665149 ± 1063067	488.5 ± 61.191	0.827 ± 0.078	590.8767 ± 21.4694
7#10	-	-	-	-	-	-	-	-
7#15	4.8295 ± 0.735	3.8295 ± 0.735	0.789 ± 0.034	0.5651 ± 0.1226	7869960 ± 3196096	403.315 ± 168.011	0.761 ± 0.056	522.6449 ± 192.841
7#25	4.9081 ± 0.5346	3.9081 ± 0.5346	0.795 ± 0.023	0.4851 ± 0.0523	7775543 ± 1597457	434.593 ± 109.835	0.801 ± 0.053	539.8163 ± 113.8523
7#27	5.0253 ± 1.1274	4.0253 ± 1.1274	0.792 ± 0.048	0.4897 ± 0.1285	8158435 ± 2625200	460.039 ± 127.277	0.852 ± 0.064	540.2265 ± 140.4305
7#35	-	-	-	-	-	-	-	-
7#45	-	-	-	-	-	-	-	-
7#5	5.0567 ± 0.8761	4.0567 ± 0.8761	0.797 ± 0.038	0.5323 ± 0.0839	7966744 ± 2229815	394.473 ± 92.024	0.778 ± 0.056	509.1818 ± 115.7876
7#50	-	-	-	-	-	-	-	-
WT_1	5.592 ± 0.4348	4.592 ± 0.4348	0.82 ± 0.016	0.42 ± 0.0671	8261265 ± 1203818	415.362 ± 94.896	0.888 ± 0.059	467.374 ± 102.7048
WT_2	5.0467 ± 0.4091	4.0467 ± 0.4091	0.801 ± 0.016	0.4788 ± 0.0253	6692222 ± 1260691	359.733 ± 62.864	0.809 ± 0.03	445.7108 ± 83.7822
WT_3	5.083 ± 0.927	4.083 ± 0.927	0.798 ± 0.037	0.4923 ± 0.0275	6164230 ± 883803	298.126 ± 73.653	0.791 ± 0.035	379.8478 ± 104.2466

Table D.7: Characterisation of multigene transgenic tobacco lines — Chlorophyll fluorescence (III). Details of line, quantum yield of PS II efficiency (ΦP_0 or TR_0/ABS), Ψ_0, quantum yield of electron transport from Q_A to PQ (ΦE_0 or ET_0/ABS), ΦD_0, and time to reach F_m (ΦPav) are shown. Means of four plants ± SE.

Line	**ΦP_0**	**Ψ_0**	**ΦE_0**	**ΦD_0**	**ΦPav**
1#1	0.827 ± 0.005	0.6125 ± 0.025	0.505 ± 0.0173	0.178 ± 0.01	918.2475 ± 4.1757
1#10	0.82 ± 0	0.6175 ± 0.0222	0.505 ± 0.0191	0.183 ± 0.005	926.005 ± 6.7601
1#11	0.815 ± 0.03	0.603 ± 0.0365	0.4937 ± 0.046	0.185 ± 0.03	918.2486 ± 19.5655
1#12	0.81 ± 0.008	0.5925 ± 0.034	0.4775 ± 0.0263	0.19 ± 0.008	928.8675 ± 8.5594
1#13	0.815 ± 0.017	0.5975 ± 0.0574	0.485 ± 0.0545	0.185 ± 0.017	928.815 ± 2.7933
1#14	0.833 ± 0.006	0.64 ± 0.01	0.5333 ± 0.0058	0.167 ± 0.006	937.5767 ± 9.663
1#15	0.787 ± 0.021	0.6027 ± 0.0261	0.474 ± 0.0305	0.213 ± 0.021	915.4213 ± 4.9919
1#16	0.823 ± 0.021	0.615 ± 0.0238	0.505 ± 0.03	0.178 ± 0.021	922.035 ± 13.3583
1#17	0.82 ± 0.022	0.6125 ± 0.0189	0.5025 ± 0.0171	0.18 ± 0.022	921.85 ± 8.5841
1#18	0.842 ± 0.005	0.65 ± 0.051	0.545 ± 0.0465	0.158 ± 0.005	925.035 ± 9.5491
1#19	0.81 ± 0.015	0.6455 ± 0.0196	0.5228 ± 0.0135	0.19 ± 0.015	924.3838 ± 12.7249
1#2	0.843 ± 0.012	0.6667 ± 0.0208	0.5567 ± 0.0208	0.16 ± 0.01	935.8867 ± 0.7049
1#20	0.802 ± 0.029	0.6165 ± 0.0329	0.4953 ± 0.0433	0.198 ± 0.029	916.4073 ± 4.6155
1#21	0.781 ± 0.016	0.581 ± 0.0283	0.454 ± 0.0301	0.219 ± 0.016	907.5693 ± 3.6854
1#22	0.771 ± 0.008	0.5978 ± 0.0314	0.4608 ± 0.0267	0.23 ± 0.008	921.4943 ± 8.5386
1#23	0.765 ± 0.009	0.574 ± 0.0401	0.4393 ± 0.0358	0.235 ± 0.009	920.9953 ± 9.6189
1#24	0.773 ± 0.003	0.6045 ± 0.007	0.4673 ± 0.0038	0.228 ± 0.003	918.0318 ± 8.5433
1#25	0.778 ± 0.006	0.619 ± 0.0283	0.482 ± 0.0184	0.222 ± 0.006	933.1645 ± 6.1299
1#26	0.792 ± 0.01	0.5973 ± 0.0359	0.473 ± 0.0333	0.208 ± 0.01	933.9458 ± 7.8326
1#27	0.776 ± 0.017	0.6183 ± 0.0375	0.4795 ± 0.0337	0.224 ± 0.017	928.0418 ± 10.3821
1#28	0.774 ± 0.007	0.631 ± 0.0214	0.4885 ± 0.02	0.226 ± 0.007	921.6428 ± 15.474
1#29	0.783 ± 0.026	0.63 ± 0.0371	0.494 ± 0.0455	0.218 ± 0.026	917.266 ± 7.352
1#3	0.813 ± 0.021	0.6033 ± 0.0115	0.4933 ± 0.0208	0.187 ± 0.021	919.6033 ± 10.554
1#30	0.801 ± 0.024	0.61 ± 0.0236	0.4887 ± 0.0272	0.199 ± 0.024	911.0177 ± 3.0427
1#31	0.831 ± 0.004	0.6443 ± 0.0217	0.535 ± 0.0186	0.169 ± 0.003	909.9348 ± 6.0694
1#32	0.818 ± 0.023	0.6598 ± 0.0264	0.54 ± 0.0349	0.182 ± 0.023	917.3708 ± 8.0583
1#33	0.734 ± 0.016	0.5393 ± 0.0383	0.3955 ± 0.0219	0.266 ± 0.016	917.0713 ± 7.0881
1#34	0.766 ± 0.035	0.588 ± 0.074	0.451 ± 0.0709	0.234 ± 0.035	922.5373 ± 12.5835
1#35	0.775 ± 0.042	0.6175 ± 0.0362	0.479 ± 0.0482	0.225 ± 0.042	912.9115 ± 25.0155
1#36	0.751 ± 0.02	0.5155 ± 0.0596	0.3878 ± 0.0503	0.249 ± 0.02	918.932 ± 6.7897
1#37	0.735 ± 0.135	0.5683 ± 0.049	0.4208 ± 0.0994	0.265 ± 0.135	914.3715 ± 20.9243
1#39	0.755 ± 0.03	0.5658 ± 0.0342	0.4275 ± 0.0406	0.246 ± 0.03	912.5168 ± 20.6008
1#40	0.786 ± 0.032	0.5842 ± 0.0772	0.4605 ± 0.0759	0.215 ± 0.032	912.5085 ± 12.2566
1#41	0.773 ± 0.033	0.556 ± 0.0996	0.4323 ± 0.0924	0.227 ± 0.033	931.217 ± 16.0428
1#42	0.763 ± 0.035	0.5998 ± 0.0284	0.4585 ± 0.042	0.237 ± 0.035	913.9088 ± 9.1694
1#44	0.749 ± 0.095	0.5624 ± 0.1137	0.4304 ± 0.1254	0.251 ± 0.095	921.8151 ± 24.7531

Line	**ΦP$_0$**	**Ψ$_0$**	**ΦE$_0$**	**ΦD$_0$**	**ΦPav**
1#45	0.786 ± 0.04	0.6118 ± 0.054	0.4823 ± 0.0665	0.215 ± 0.04	909.5803 ± 12.7514
1#47	0.808 ± 0.044	0.614 ± 0.034	0.497 ± 0.0527	0.192 ± 0.044	907.2463 ± 10.8041
1#48	0.76 ± 0.066	0.5723 ± 0.0852	0.439 ± 0.0995	0.24 ± 0.066	914.835 ± 15.0406
1#49	0.773 ± 0.014	0.5977 ± 0.0237	0.462 ± 0.0252	0.227 ± 0.014	909.7837 ± 6.5881
1#5	0.807 ± 0.023	0.5867 ± 0.0493	0.4667 ± 0.0351	0.193 ± 0.023	932.49 ± 11.3265
1#50	0.792 ± 0.036	0.5823 ± 0.0653	0.4625 ± 0.0705	0.208 ± 0.036	909.4595 ± 7.2954
1#51	0.787 ± 0.057	0.6095 ± 0.0334	0.4813 ± 0.0595	0.213 ± 0.057	907.325 ± 12.8655
1#6	0.823 ± 0.032	0.6233 ± 0.0577	0.5133 ± 0.0666	0.177 ± 0.032	930.33 ± 8.3128
1#7	0.795 ± 0.037	0.62 ± 0.0216	0.49 ± 0.0365	0.205 ± 0.037	933.185 ± 7.2784
1#8	0.825 ± 0.017	0.6325 ± 0.0126	0.52 ± 0.02	0.175 ± 0.017	929.85 ± 6.3731
1#9	0.813 ± 0.021	0.6033 ± 0.0252	0.4933 ± 0.0351	0.19 ± 0.02	934.16 ± 9.5519
7#10	-	-	-	-	-
7#15	0.789 ± 0.034	0.5733 ± 0.0777	0.4544 ± 0.0762	0.211 ± 0.034	922.804 ± 18.033
7#25	0.795 ± 0.023	0.6143 ± 0.0233	0.4881 ± 0.0268	0.206 ± 0.022	927.1585 ± 14.2472
7#27	0.792 ± 0.048	0.5883 ± 0.0968	0.469 ± 0.0962	0.208 ± 0.048	932.8274 ± 16.943
7#35	-	-	-	-	-
7#45	-	-	-	-	-
7#5	0.797 ± 0.038	0.5887 ± 0.0526	0.4699 ± 0.0599	0.204 ± 0.037	925.8371 ± 14.4769
7#50	-	-	-	-	-
WT_1	0.82 ± 0.016	0.632 ± 0.0342	0.52 ± 0.0361	0.182 ± 0.013	926.554 ± 6.3509
WT_2	0.801 ± 0.016	0.613 ± 0.0152	0.4913 ± 0.0195	0.199 ± 0.016	916.4868 ± 7.7093
WT_3	0.798 ± 0.037	0.611 ± 0.0151	0.4883 ± 0.0333	0.202 ± 0.037	910.7585 ± 7.0015

Table D.8: Characterisation of multigene transgenic tobacco lines — Chlorophyll fluorescence (IV). Details of line, performance index on absorption basis (PI_{ABS}), apparent antenna size of active PS II (ABS/RC), maximum trapped exciton flux per active PS II (TR_0/RC), flux of electrons transferred from Q_A to PQ per active PS II (ET_0/RC), and flux of energy dissipated in processes other than trapping per active PS II (DI_0/RC) are shown. Means of four plants ± SE.

Line	PI_{ABS}	ABS/RC	TR_0/RC	ET_0/RC	DI_0/RC
1#1	5.285 ± 0.6665	1.405 ± 0.09	1.158 ± 0.083	0.7075 ± 0.033	0.25 ± 0.008
1#10	5.33 ± 0.7588	1.375 ± 0.054	1.125 ± 0.042	0.695 ± 0.0129	0.25 ± 0.014
1#11	4.7434 ± 1.582	1.519 ± 0.135	1.235 ± 0.093	0.745 ± 0.0571	0.282 ± 0.062
1#12	4.135 ± 0.7647	1.5 ± 0.071	1.213 ± 0.059	0.715 ± 0.0129	0.29 ± 0.022
1#13	4.7325 ± 1.8056	1.5 ± 0.231	1.223 ± 0.161	0.72 ± 0.0316	0.278 ± 0.07
1#14	6.3033 ± 0.4772	1.387 ± 0.101	1.153 ± 0.072	0.7367 ± 0.0586	0.233 ± 0.021
1#15	3.604 ± 0.8172	1.583 ± 0.011	1.245 ± 0.031	0.751 ± 0.0497	0.338 ± 0.034
1#16	5.6125 ± 1.9752	1.393 ± 0.161	1.145 ± 0.107	0.7 ± 0.0383	0.25 ± 0.058
1#17	5.3275 ± 0.9558	1.368 ± 0.067	1.122 ± 0.051	0.6825 ± 0.0287	0.245 ± 0.037
1#18	8.41 ± 3.1253	1.235 ± 0.107	1.043 ± 0.092	0.6725 ± 0.034	0.198 ± 0.019
1#19	5.371 ± 0.7669	1.463 ± 0.084	1.185 ± 0.065	0.7643 ± 0.0312	0.278 ± 0.031
1#2	8.6133 ± 2.229	1.243 ± 0.136	1.043 ± 0.108	0.69 ± 0.0529	0.2 ± 0.03
1#20	4.2483 ± 1.5022	1.626 ± 0.168	1.304 ± 0.141	0.8052 ± 0.1122	0.322 ± 0.057
1#21	3.0073 ± 0.6666	1.676 ± 0.069	1.308 ± 0.057	0.7608 ± 0.0571	0.368 ± 0.033
1#22	3.1678 ± 0.5338	1.598 ± 0.076	1.231 ± 0.051	0.7353 ± 0.0389	0.367 ± 0.028
1#23	2.7798 ± 0.6457	1.614 ± 0.064	1.234 ± 0.04	0.7075 ± 0.0378	0.38 ± 0.028
1#24	3.2065 ± 0.0379	1.619 ± 0.015	1.251 ± 0.013	0.7563 ± 0.0116	0.368 ± 0.006
1#25	3.7395 ± 0.4137	1.531 ± 0.036	1.192 ± 0.036	0.737 ± 0.0113	0.34 ± 0.001
1#26	3.6795 ± 0.6308	1.557 ± 0.056	1.232 ± 0.049	0.7373 ± 0.0703	0.324 ± 0.019
1#27	3.6373 ± 0.9743	1.594 ± 0.125	1.235 ± 0.074	0.762 ± 0.0247	0.359 ± 0.054
1#28	3.609 ± 0.5091	1.639 ± 0.07	1.269 ± 0.053	0.8005 ± 0.0418	0.37 ± 0.021
1#29	4.0298 ± 1.4421	1.6 ± 0.062	1.252 ± 0.06	0.7897 ± 0.0739	0.348 ± 0.043
1#3	4.8267 ± 1.1461	1.43 ± 0.075	1.163 ± 0.029	0.7033 ± 0.0153	0.27 ± 0.046
1#30	3.8173 ± 0.9026	1.686 ± 0.078	1.351 ± 0.08	0.8233 ± 0.0405	0.336 ± 0.04
1#31	6.438 ± 0.6287	1.388 ± 0.043	1.153 ± 0.034	0.7433 ± 0.0393	0.235 ± 0.011
1#32	6.1708 ± 2.4611	1.533 ± 0.271	1.251 ± 0.186	0.823 ± 0.1069	0.283 ± 0.086
1#33	1.8403 ± 0.1644	1.767 ± 0.134	1.295 ± 0.073	0.7 ± 0.0821	0.472 ± 0.061
1#34	3.1222 ± 1.7967	1.694 ± 0.145	1.294 ± 0.062	0.7605 ± 0.1025	0.4 ± 0.087
1#35	3.521 ± 1.6219	1.726 ± 0.135	1.334 ± 0.055	0.8238 ± 0.0634	0.392 ± 0.099
1#36	1.8523 ± 0.5459	1.801 ± 0.145	1.353 ± 0.129	0.6985 ± 0.107	0.448 ± 0.039
1#37	2.893 ± 1.7586	1.829 ± 0.526	1.291 ± 0.08	0.732 ± 0.0425	0.538 ± 0.457
1#39	2.4205 ± 0.7188	1.724 ± 0.048	1.3 ± 0.028	0.7363 ± 0.0594	0.424 ± 0.062
1#40	3.6138 ± 1.5301	1.587 ± 0.097	1.245 ± 0.031	0.7255 ± 0.0825	0.343 ± 0.073
1#41	2.9783 ± 1.3815	1.634 ± 0.09	1.262 ± 0.055	0.7033 ± 0.1369	0.372 ± 0.07
1#42	3.1993 ± 1.3876	1.63 ± 0.156	1.24 ± 0.07	0.7428 ± 0.0356	0.39 ± 0.09

Line	**PI_{ABS}**	**ABS/RC**	**TR_0/RC**	**ET_0/RC**	**DI_0/RC**
1#44	3.1746 ± 1.7619	1.728 ± 0.31	1.272 ± 0.046	0.7126 ± 0.1288	0.456 ± 0.272
1#45	4.26 ± 2.2134	1.543 ± 0.142	1.208 ± 0.055	0.737 ± 0.0391	0.336 ± 0.091
1#47	4.55 ± 1.6129	1.6 ± 0.086	1.29 ± 0.028	0.7923 ± 0.0517	0.31 ± 0.089
1#48	3.4413 ± 2.4361	1.626 ± 0.25	1.224 ± 0.082	0.6975 ± 0.084	0.401 ± 0.172
1#49	3.0237 ± 0.722	1.71 ± 0.107	1.321 ± 0.059	0.7887 ± 0.0227	0.389 ± 0.048
1#5	3.82 ± 1.0714	1.553 ± 0.107	1.247 ± 0.071	0.7233 ± 0.0351	0.307 ± 0.05
1#50	3.8925 ± 2.1294	1.556 ± 0.144	1.229 ± 0.076	0.7135 ± 0.0673	0.327 ± 0.079
1#51	4.0563 ± 1.9641	1.631 ± 0.174	1.277 ± 0.05	0.7773 ± 0.0242	0.355 ± 0.135
1#6	6.7367 ± 4.6869	1.343 ± 0.237	1.1 ± 0.164	0.6767 ± 0.0503	0.243 ± 0.074
1#7	4.4275 ± 1.6857	1.488 ± 0.105	1.18 ± 0.029	0.7275 ± 0.0126	0.31 ± 0.074
1#8	5.7625 ± 1.1116	1.405 ± 0.07	1.155 ± 0.057	0.7275 ± 0.0359	0.25 ± 0.029
1#9	4.5933 ± 1.5273	1.503 ± 0.18	1.22 ± 0.115	0.7333 ± 0.0569	0.287 ± 0.064
7#10	-	-	-	-	-
7#15	3.465 ± 1.6335	1.682 ± 0.181	1.321 ± 0.102	0.7557 ± 0.0966	0.36 ± 0.092
7#25	4.0552 ± 1.2207	1.581 ± 0.129	1.254 ± 0.081	0.7683 ± 0.0403	0.327 ± 0.056
7#27	4.5505 ± 2.5311	1.5 ± 0.175	1.181 ± 0.085	0.692 ± 0.114	0.32 ± 0.107
7#35	-	-	-	-	-
7#45	-	-	-	-	-
7#5	3.8971 ± 1.707	1.629 ± 0.162	1.292 ± 0.086	0.759 ± 0.076	0.336 ± 0.091
7#50	-	-	-	-	-
WT_1	5.928 ± 1.8624	1.378 ± 0.118	1.13 ± 0.075	0.712 ± 0.0228	0.25 ± 0.041
WT_2	4.1718 ± 0.6296	1.545 ± 0.043	1.237 ± 0.045	0.758 ± 0.0347	0.308 ± 0.025
WT_3	4.1488 ± 1.3951	1.59 ± 0.12	1.266 ± 0.054	0.774 ± 0.04	0.324 ± 0.081

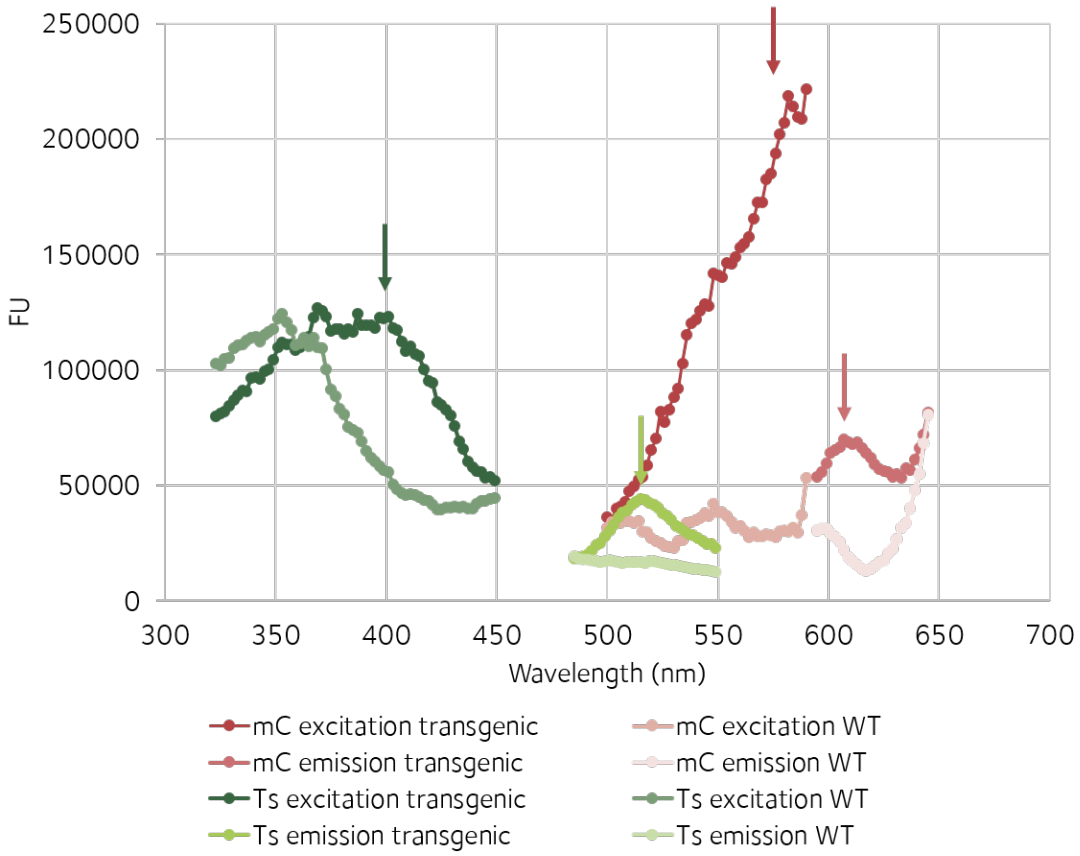

Figure D.1: Spectral profile for the fluorescent biosensor c-Peredox-mCherry. Leaf discs of three-week-old transgenic plants carrying the c-Peredox-mCherry sensor (construct LS0207) and WT control plants were used to assess the spectral profile of the biosensor. The fluorophores T-Sapphire (Ts) and mCherry (mC) were excited at 400 ± 9 nm and 570 ± 9 nm, respectively, and emission collected at 520 ± 20 nm and 610 ± 20 nm. Fluorescence peaks are indicated with arrows.

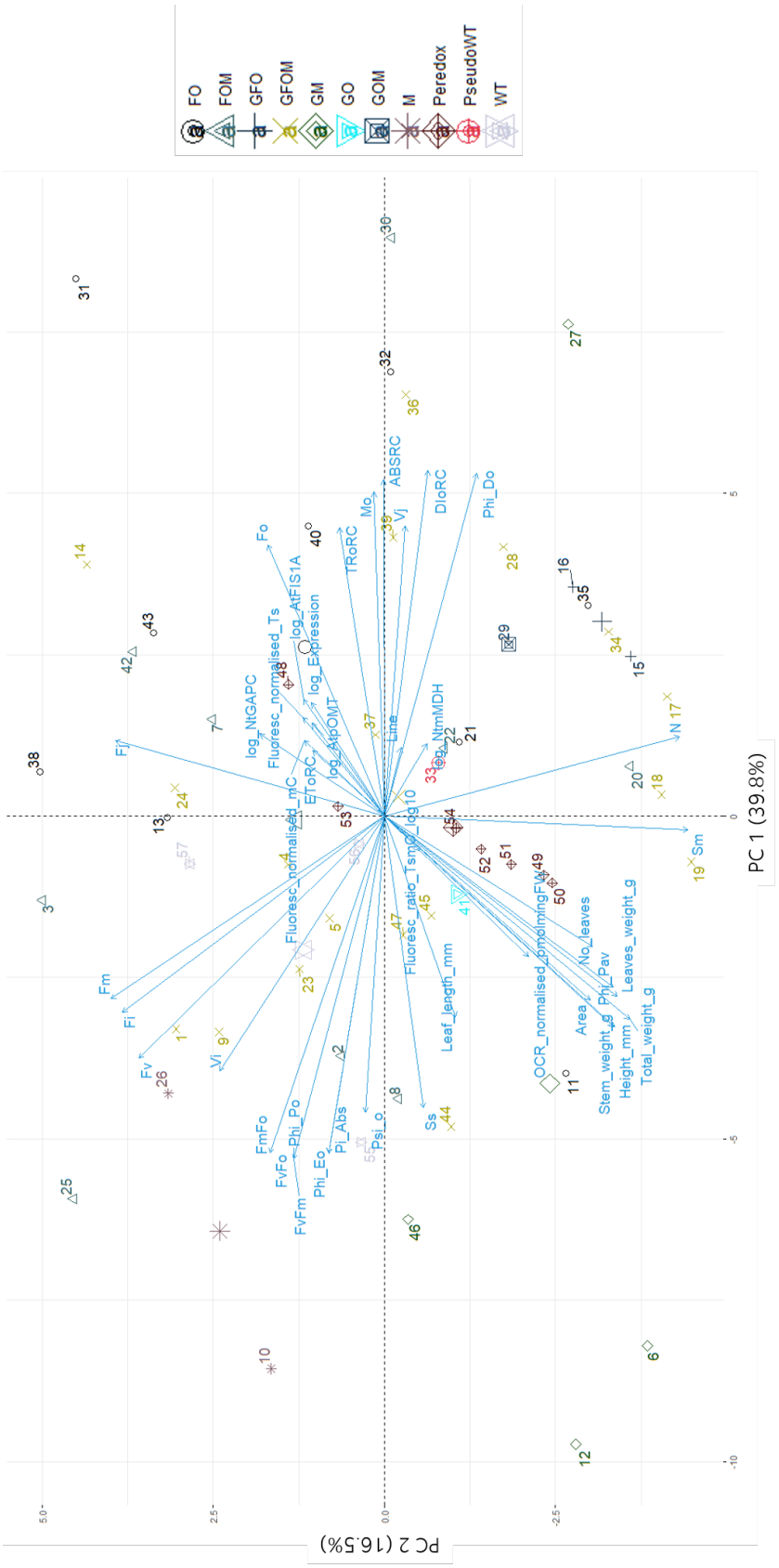

Figure D.2: Principal component analysis of the parameters measured in the multigene transgenic tobacco lines - biplot of individuals and variables across PC1 and PC2. Lines are colour-coded based on the expression groups defined in Figure 5.8.

Table D.9: Contributions of variables and individuals to each PC in the PCA analysis of the multigene transgenic tobacco lines. Top contributors are represented, with threshold set at contribution $\geq$ 4. The column "Number (in plot)" refers to the numbers represented in Figure D.2, and "Group" to Figure 5.8. .

PC1 - 39.8% of variance explained					
Variable		**Individual**			
Parameter	**Contribution**	**Number (in plot)**	**Line**	**Group**	**Contribution**
DI_0/RC	5.59	12	1#2	GM	10.19
F_v/F_m	5.49	30	1#36	FOM	8.63
ΦP_0	5.49	10	1#18	M	7.88
ΦD_0	5.49	31	1#37	FO	7.46
ΦE_0	5.32	6	1#14	GM	7.25
PI_{ABS}	5.30	27	1#33	GM	6.24
F_v/F_0	5.30	32	1#39	FO	5.10
F_m/F_0	5.30	36	1#44	GFOM	4.59
ABS/RC	5.29	46	1#8	GM	4.20
M_0	4.91				
Ψ_0	4.09				

PC2 - 16.5% of variance explained					
Variable		**Individual**			
Parameter	**Contribution**	**Number (in plot)**	**Line**	**Group**	**Contribution**
S_m	9.25	38	1#47	FO	6.58
N	8.72	3	1#11	FOM	6.48
F_m	7.49	25	1#31	FOM	5.36
F_j	7.26	31	1#37	FO	5.27
F_i	6.87	19	1#26	GFOM	5.21
Total biomass	6.04	14	1#21	GFOM	4.91
Fv	6.03	17	1#24	GFOM	4.44
Leaves biomass	5.44	18	1#25	GFOM	4.25
Plant height	5.30				
Stem biomass	5.26				
ΦPav	5.25				
Number of leaves	4.35				
Area	4.24				

PC3 - 11.3% of variance explained					
Variable		**Individual**			
Parameter	**Contribution**	**Number (in plot)**	**Line**	**Group**	**Contribution**
AtpOMT - log-transcript	13.44	57	WT_3	WT	5.99
Average - log-transcript	13.02	54	7#50	Peredox	5.77
AtFIS1A - log-transcript	12.24	51	7#35	Peredox	5.62
Ratio $NADH/NAD^+$	10.23	53	7#5	Peredox	5.14
Line	8.04	48	7#15	Peredox	5.13
		52	7#45	Peredox	4.98
		44	1#6	GFOM	4.43
		33	1#40	PseudoWT	4.29
		46	1#8	GM	4.20

PC4 - 7.8% of variance explained					
Variable		**Individual**			
Parameter	**Contribution**	**Number (in plot)**	**Line**	**Group**	**Contribution**
Fluorescence mCherry	16.51	21	1#28	FO	6.78
Fluorescence t-Sapphire	15.66	22	1#29	FOM	5.96
ET_0/RC	14.88	36	1#44	GFOM	5.66
Vj	6.80	24	1#30	GFOM	4.47
Ψ_0	6.20	13	1#20	FO	4.20
ΦPav	5.06	30	1#36	FOM	4.20
		50	7#27	Peredox	4.13

PC5 - 5.2% of variance explained					
Variable		**Individual**			
Parameter	**Contribution**	**Number (in plot)**	**Line**	**Group**	**Contribution**
Area	10.09	11	1#19	FO	10.1
Fj	8.96	10	1#18	M	8.5
N	6.58	37	1#45	GFOM	6.3
AtpOMT - log-transcript	6.09	56	WT_2	WT	5.9
Fi	5.16	35	1#42	FO	5.2
F_m	4.85	3	1#11	FOM	4.8
Average - log-transcript	4.54				
S_m	4.31				
Line	4.23				
Number of leaves	4.19				

PC6 - 3.6% of variance explained					
Variable		**Individual**			
Parameter	**Contribution**	**Number (in plot)**	**Line**	**Group**	**Contribution**
NtmMDH - log-transcript	45.17	28	1#34	GFOM	18.90
NtGAPC - log-transcript	42.07	23	1#3	GFOM	9.69
		26	1#32	M	8.81
		29	1#35	GOM	6.27
		2	1#10	FOM	5.77
		38	1#47	FO	5.69
		24	1#30	GFOM	5.50
		43	1#51	FO	4.09

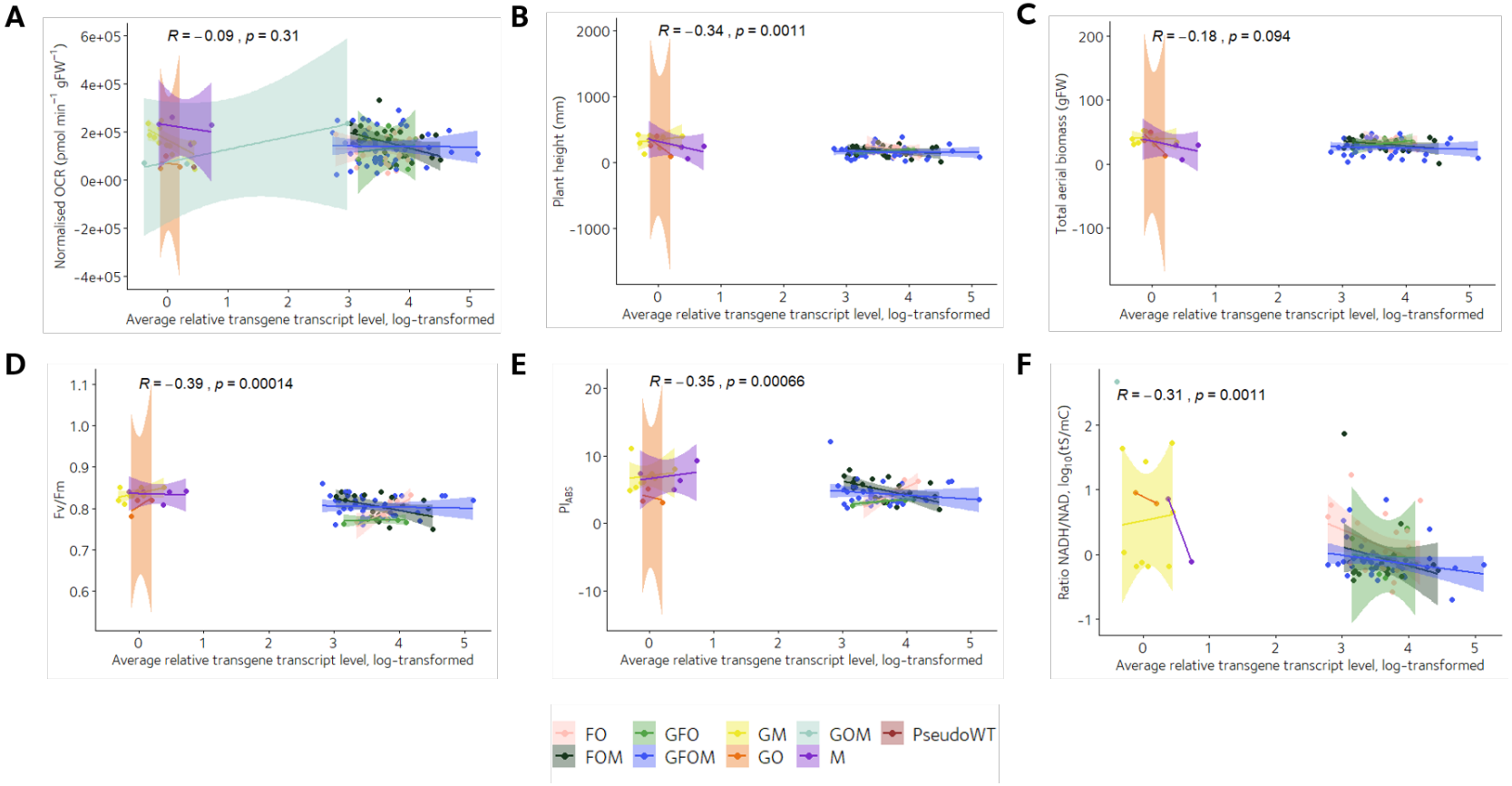

Figure D.3: Scatter plots of selected parameters and transcript levels in the multigene transgenic tobacco lines. Correlations between the selected parameters and the log-transformed, average transcript level of *NtGAPC*, *NtmMDH*, *AtFIS1A*, and *AtpOMT* was evaluated for the 47 multigene transgenic tobacco lines, with four plants measured per line, using a Spearman rank-order correlation test ($n = 188$). **A**. Mitochondrial respiration, measured as leaf disc oxygen consumption rates (OCR). **B**. Plant height. **C**. Total aerial biomass. **D**. Quantum yield of PS II (F_v/F_m). *E*. Performance index on an absorption basis (PI_{ABS}). *F*. Cytosolic ratio of NADH/NAD$^+$. Correlation coefficients (R) and p-values (p) are indicated. Different colours represent different expression groups as per Figure 5.8.

Appendix E

Supplementary materials - Sequencing results

Table E.1: Sequencing results of plasmids used for plant transformation - table of contents. Details of plasmids, experiment in which they were used, and location of sequencing results within this appendix.

pExBMG3 – pUC18-AtRbcS-AtPetC-NosT

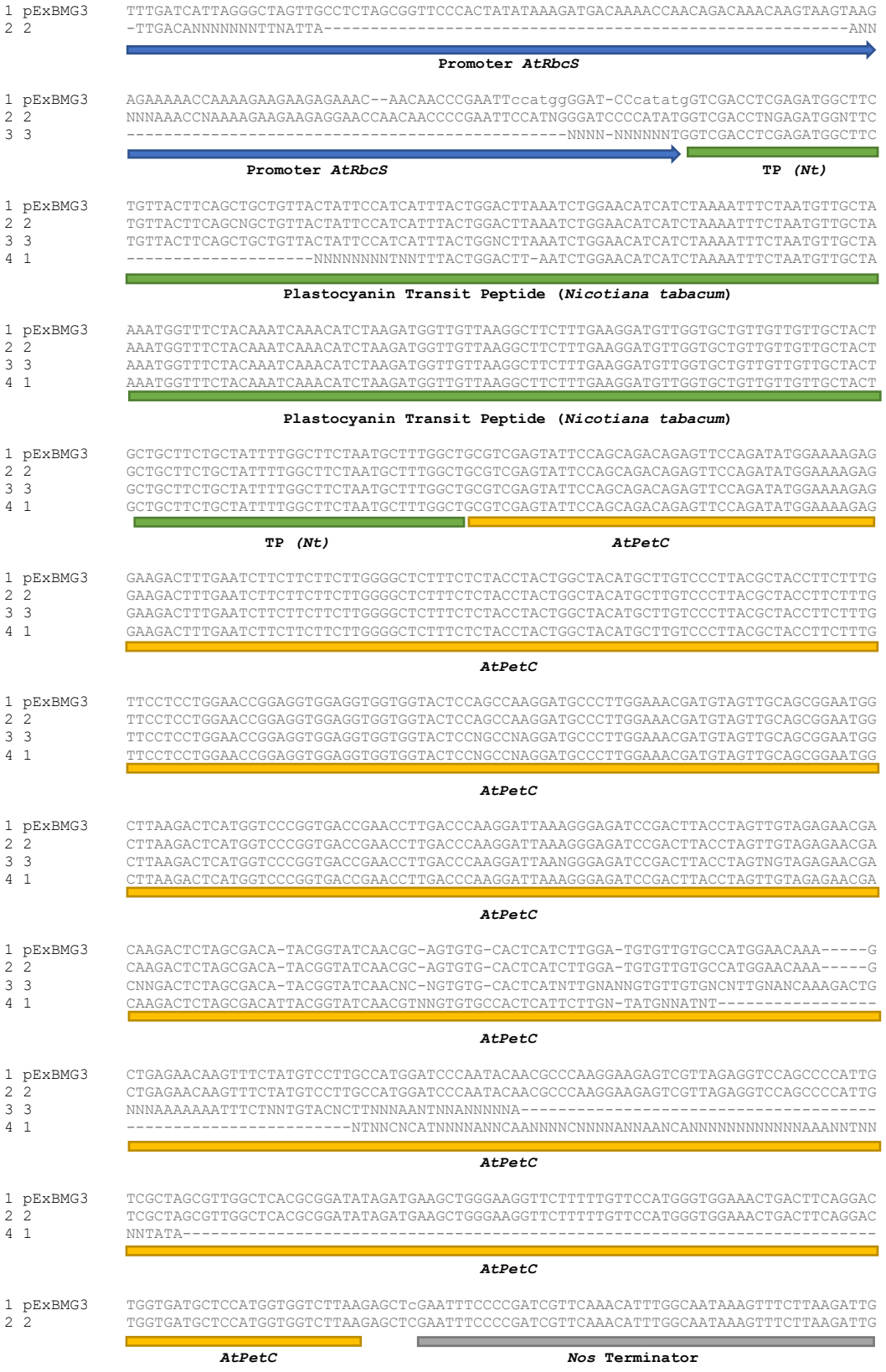

```
1 pExBMG3     AATCCTGTTGCCGGTCTTGCGATGATTATCATATAATTTCTGTTGAATTACGTTAAGCATGTAATAATTAACATGTAATG
2 2           AATCCTGTTGCCGGTCTTGCGATGATTATCATATAATTTCTGTTGAATTACGTTAAGCATGTAATAATTAACATGTAANN
```


***Nos* Terminator**

pExBMG4 – pUC18-AtRbcS-Pyc6-NosT

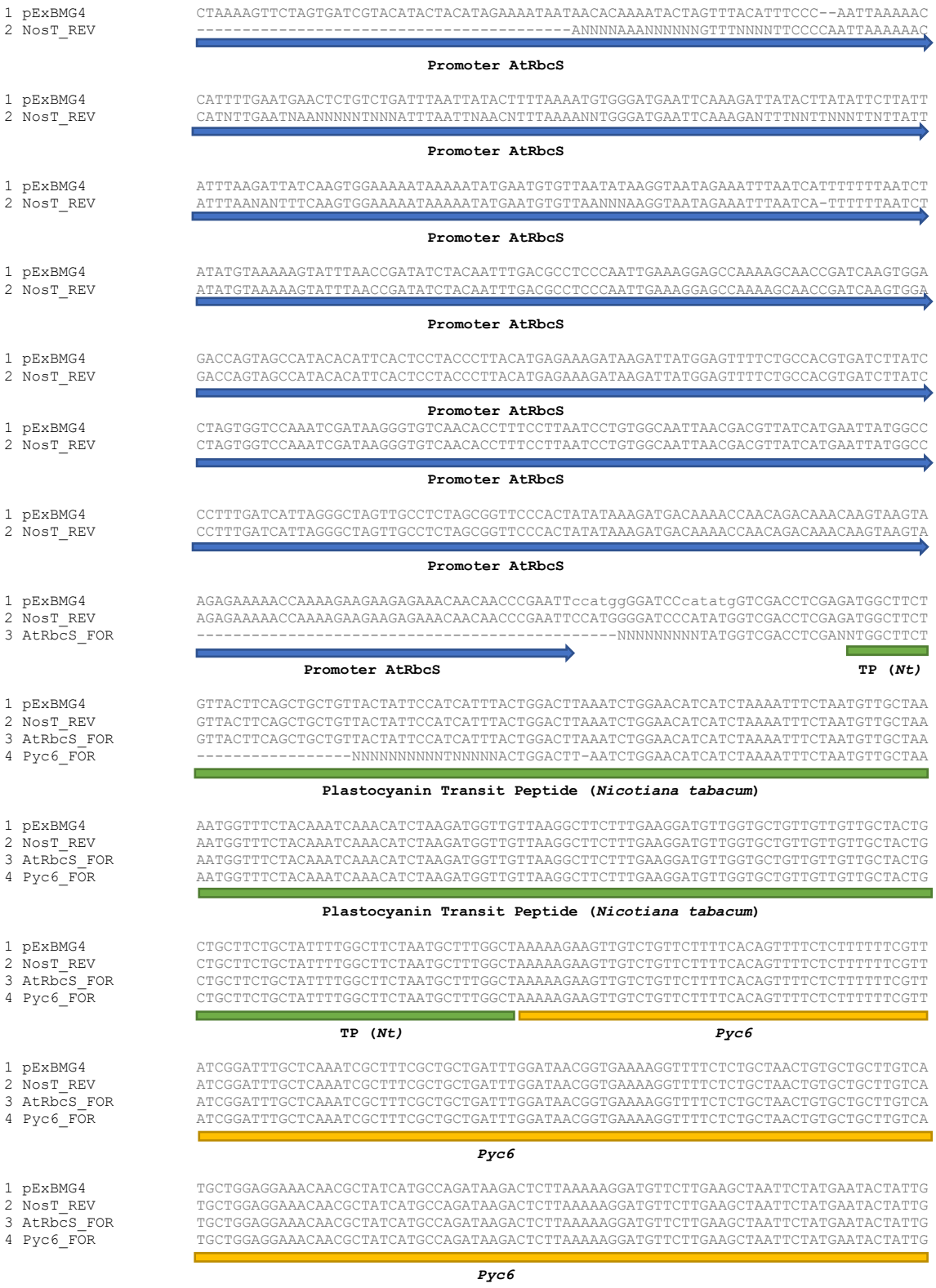

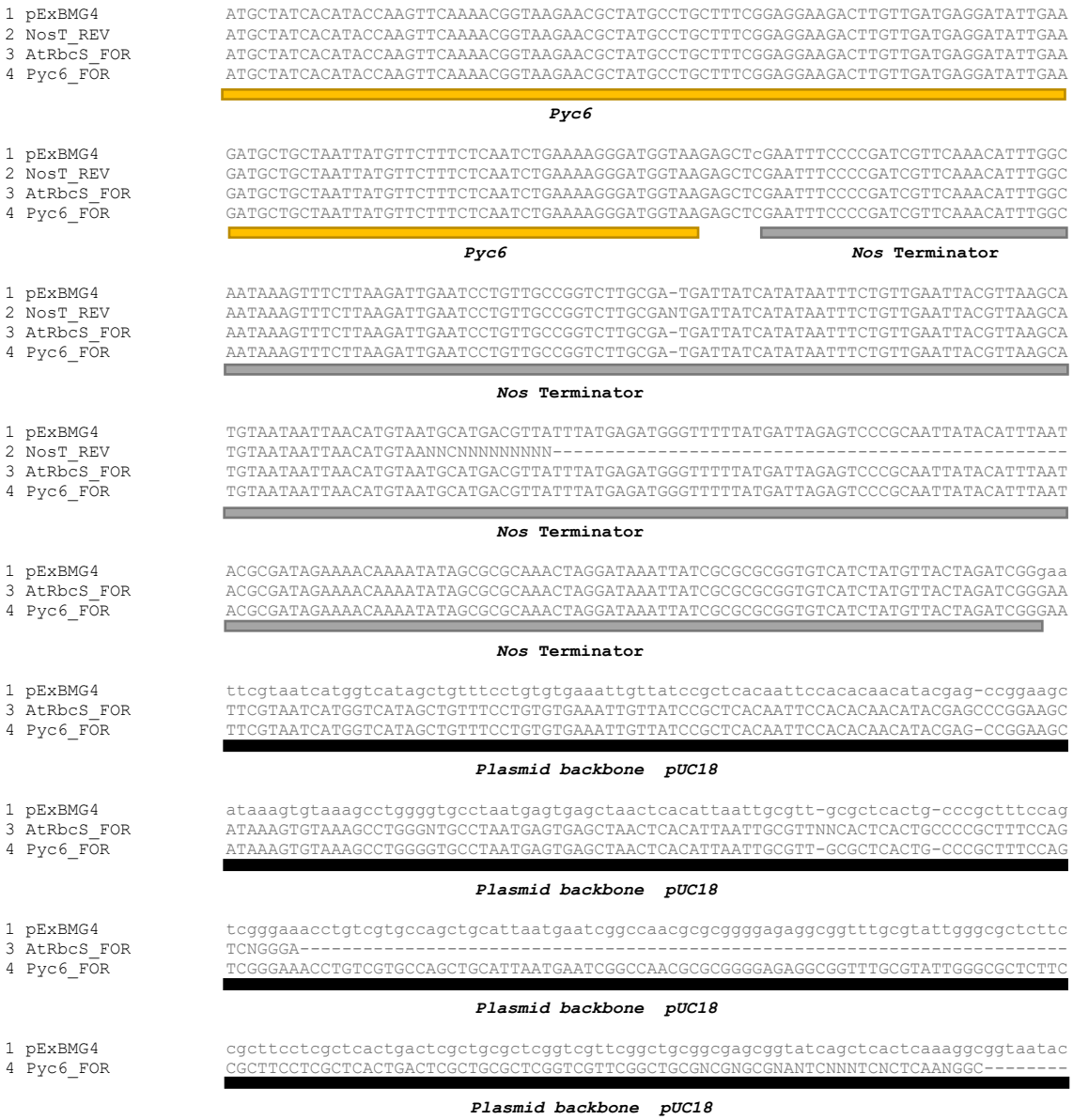
1 pExBMG4 ATGCTATCACATACCAAGTTCAAAACGGTAAGAACGCTATGCCTGCTTTCGGAGGAAGACTTGTTGATGAGGATATTGAA
2 NosT_REV ATGCTATCACATACCAAGTTCAAAACGGTAAGAACGCTATGCCTGCTTTCGGAGGAAGACTTGTTGATGAGGATATTGAA
3 AtRbcS_FOR ATGCTATCACATACCAAGTTCAAAACGGTAAGAACGCTATGCCTGCTTTCGGAGGAAGACTTGTTGATGAGGATATTGAA
4 Pyc6_FOR ATGCTATCACATACCAAGTTCAAAACGGTAAGAACGCTATGCCTGCTTTCGGAGGAAGACTTGTTGATGAGGATATTGAA
Pyc6
1 pExBMG4 GATGCTGCTAATTATGTTCTTTCTCAATCTGAAAAGGGATGGTAAGAGCTcGAATTTCCCCGATCGTTCAAACATTTGGC
2 NosT_REV GATGCTGCTAATTATGTTCTTTCTCAATCTGAAAAGGGATGGTAAGAGCTCGAATTTCCCCGATCGTTCAAACATTTGGC
3 AtRbcS_FOR GATGCTGCTAATTATGTTCTTTCTCAATCTGAAAAGGGATGGTAAGAGCTCGAATTTCCCCGATCGTTCAAACATTTGGC
4 Pyc6_FOR GATGCTGCTAATTATGTTCTTTCTCAATCTGAAAAGGGATGGTAAGAGCTCGAATTTCCCCGATCGTTCAAACATTTGGC
Pyc6
Nos Terminator
1 pExBMG4 AATAAAGTTTCTTAAGATTGAATCCTGTTGCCGGTCTTGCGA-TGATTATCATATAATTTCTGTTGAATTACGTTAAGCA
2 NosT_REV AATAAAGTTTCTTAAGATTGAATCCTGTTGCCGGTCTTGCGANTGATTATCATATAATTTCTGTTGAATTACGTTAAGCA
3 AtRbcS_FOR AATAAAGTTTCTTAAGATTGAATCCTGTTGCCGGTCTTGCGA-TGATTATCATATAATTTCTGTTGAATTACGTTAAGCA
4 Pyc6_FOR AATAAAGTTTCTTAAGATTGAATCCTGTTGCCGGTCTTGCGA-TGATTATCATATAATTTCTGTTGAATTACGTTAAGCA
Nos Terminator
1 pExBMG4 TGTAATAATTAACATGTAATGCATGACGTTATTTATGAGATGGGTTTTTATGATTAGAGTCCCGCAATTATACATTTAAT
2 NosT_REV TGTAATAATTAACATGTAANNCNNNNNNNNN----------
3 AtRbcS_FOR TGTAATAATTAACATGTAATGCATGACGTTATTTATGAGATGGGTTTTTATGATTAGAGTCCCGCAATTATACATTTAAT
4 Pyc6_FOR TGTAATAATTAACATGTAATGCATGACGTTATTTATGAGATGGGTTTTTATGATTAGAGTCCCGCAATTATACATTTAAT
Nos Terminator
1 pExBMG4 ACGCGATAGAAAACAAAATATAGCGCGCAAACTAGGATAAATTATCGCGCGCGGTGTCATCTATGTTACTAGATCGGgaa
3 AtRbcS_FOR ACGCGATAGAAAACAAAATATAGCGCGCAAACTAGGATAAATTATCGCGCGCGGTGTCATCTATGTTACTAGATCGGGAA
4 Pyc6_FOR ACGCGATAGAAAACAAAATATAGCGCGCAAACTAGGATAAATTATCGCGCGCGGTGTCATCTATGTTACTAGATCGGGAA
Nos Terminator
1 pExBMG4 ttcgtaatcatggtcatagctgtttcctgtgtgaaattgttatccgctcacaattccacacaacatacgag-ccggaagc
3 AtRbcS_FOR TTCGTAATCATGGTCATAGCTGTTTCCTGTGTGAAATTGTTATCCGCTCACAATTCCACACAACATACGAGCCCGGAAGC
4 Pyc6_FOR TTCGTAATCATGGTCATAGCTGTTTCCTGTGTGAAATTGTTATCCGCTCACAATTCCACACAACATACGAG-CCGGAAGC
Plasmid backbone pUC18
1 pExBMG4 ataaagtgtaaagcctggggtgcctaatgagtgagctaactcacattaattgcgtt-gcgctcactg-cccgctttccag
3 AtRbcS_FOR ATAAAGTGTAAAGCCTGGGNTGCCTAATGAGTGAGCTAACTCACATTAATTGCGTTNNCACTCACTGCCCCGCTTTCCAG
4 Pyc6_FOR ATAAAGTGTAAAGCCTGGGGTGCCTAATGAGTGAGCTAACTCACATTAATTGCGTT-GCGCTCACTG-CCCGCTTTCCAG
Plasmid backbone pUC18
1 pExBMG4 tcgggaaacctgtcgtgccagctgcattaatgaatcggccaacgcgcggggagaggcggtttgcgtattgggcgctcttc
3 AtRbcS_FOR TCNGGGA----------
4 Pyc6_FOR TCGGGAAACCTGTCGTGCCAGCTGCATTAATGAATCGGCCAACGCGCGGGGAGAGGCGGTTTGCGTATTGGGCGCTCTTC
Plasmid backbone pUC18
1 pExBMG4 cgcttcctcgctcactgactcgctgcgctcggtcgttcggctgcggcgagcggtatcagctcactcaaaggcggtaatac
4 Pyc6_FOR CGCTTCCTCGCTCACTGACTCGCTGCGCTCGGTCGTTCGGCTGCGNCGNGCGNANTCNNNTCNCTCAANGGC--------
Plasmid backbone pUC18

pExBMG1 - pUC18-35S-CaPFLP-NosT

```
1 pExBMG1        GGATGTGCTGCAAGGCGATTAAGTTGGGTAACGCCAGGGTTTTCCCAGTCACGACGTTGTAAAACGACGGCCAGTGCCaa
2 35SCaPFLP_F    ------------------------------------------------------------------------GTG-CCA
```

Plasmid backbone pUC18

```
1 pExBMG1        gcttGCATGCCTGCAGGTCCCCAGATTAGCCTTTTCAATTTCAGAAAGAATGCTAACCCACAGATGGTTAGAGAGGCTTA
2 35SCaPFLP_F    GCTTGCATGCCTGCAGGTCCCCAGATTAGCCTTTTCAATTTCAGAAAGAATGCTAACCCACAGATGGTTAGAGAGGCTTA
```

Promoter *CaMV35S*

```
1 pExBMG1        CGCAGCAGGTCTCATCAAGACGATCTACCCGAGCAATAATCTCCAGGAAATCAAATACCTTCCCAAGAAGGTTAAAGATG
2 35SCaPFLP_F    CGCAGCAGGTCTCATCAAGACGATCTACCCGAGCAATAATCTCCAGGAAATCAAATACCTTCCCAAGAAGGTTAAAGATG
```

Promoter *CaMV35S*

```
1 pExBMG1        CAGTCAAAAGATTCAGGACTAACTGCATCAAGAACACAGAGAAAGATATATTTCTCAAGATCAGAAGTACTATTCCAGTA
2 35SCaPFLP_F    CAGTCAAAAGATTCAGGACTAACTGCATCAAGAACACAGAGAAAGATATATTTCTCAAGATCAGAAGTACTATTCCAGTA
```

Promoter *CaMV35S*

```
1 pExBMG1        TGGACGATTCAAGGCTTGCTTCACAAACCAAGGCAAGTAATAGAGATTGGAGTCTCTAAAAAGGTAGTTCCCACTGAATC
2 35SCaPFLP_F    TGGACGATTCAAGGCTTGCTTCACAAACCAAGGCAAGTAATAGAGATTGGAGTCTCTAAAAAGGTAGTTCCCACTGAATC
```

Promoter *CaMV35S*

```
1 pExBMG1        AAAGGCCATGGAGTCAAAGATTCAAATAGAGGACCTAACAGAACTCGCCGTAAAGACTGGCGAACAGTTCATACAGAGTC
2 35SCaPFLP_F    AAAGGCCATGGAGTCAAAGATTCAAATAGAGGACCTAACAGAACTCGCCGTAAAGACTGGCGAACAGTTCATACAGAGTC
3 35SCaPFLP_R    ------------------------------------------------------------------------ACACAGGTTC
```

Promoter *CaMV35S*

```
1 pExBMG1        TCTTAC-GACTCAATGACAAGAAGAAAA---TCTTCGTCAACATGGTGGAGC----ACGACACACTTGTCTACTCCAAAA
2 35SCaPFLP_F    TCTTAC-GACTCAATGACAAGAAGAAAA---TCTTCGTCAACATGGTGGAGC----ACGACACACTTGTCTACTCCAAAA
3 35SCaPFLP_R    TCTTTCGGATCTAATGGCACAGAAGAAAATTCTTTTCTCAACATGGTGGAGCCACGACACCATTTGTTTTATTCCAAAAA
```

Promoter *CaMV35S*

```
1 pExBMG1        ATATC-AAAGATACAGTCTCAGAAGA--CCAAAGGGCAATTGAGACTTTTCAACAAA-GGGTAATATCCGGAAACCTCC-
2 35SCaPFLP_F    ATATC-AAAGATACAGTCTCAGAAGA--CCAAAGGGCAATTGAGACTTTTCAACAAA-GGGTAATATCCGGAAACCTCC-
3 35SCaPFLP_R    ATATCAAAAGATACAGTCTCAGGAAGACCAAAGGGGCAATTGAGACTTTTCAACAAAGGGGTAATATCCGGAAACCTCCT
```

Promoter *CaMV35S*

```
1 pExBMG1        TCGGATTCCATTGCCCAGCTATCTGTCACTTTATTGTGAAGATAGTGGAAAAGGAAGGTGGCTCCTACAAATGCCATCAT
2 35SCaPFLP_F    TCGGATTCCATTGCCCAGCTATCTGTCACTTTATTGTGAAGATAGTGGAAAAGGAAGGTGGCTCCTACAAATGCCATCAT
3 35SCaPFLP_R    TCGGATTCCATTGCCCAGCTATCTGTCACTTTATTGTGAAGATAGTGGAAAAGGAAGGTGGCTCCTACAAATGCCATCAT
```

Promoter *CaMV35S*

```
1 pExBMG1        TGCGATAAAGGAAAGGCCATCGTTGAAGATGCCTCTGCCGACAGTGGTCCCAAAGATGGACCCCCACCCACGAGGAGCAT
2 35SCaPFLP_F    TGCGATAAAGGAAAGGCCATCGTTGAAGATGCCTCTGCCGACAGTGGTCCCAAAGATGGACCCCCACCCACGAGGAGCAT
3 35SCaPFLP_R    TGCGATAAAGGAAAGGCCATCGTTGAAGATGCCTCTGCCGACAGTGGTCCCAAAGATGGACCCCCACCCACGAGGAGCAT
```

Promoter *CaMV35S*

```
1 pExBMG1        CGTGGAAAAAGAAGACGTTCCAACCACGTCTTCAAAGCAAGTGGATTGATGTGATATCTCCACTGACGTAAGGGATGACG
2 35SCaPFLP_F    CGTGGAAAAAGAAGACGTTCCAACCACGTCTTCAAAGCAAGTGGATTGATGTGATATCTCCACTGACGTAAGGGATGACG
3 35SCaPFLP_R    CGTGGAAAAAGAAGACGTTCCAACCACGTCTTCAAAGCAAGTGGATTGATGTGATATCTCCACTGACGTAAGGGATGACG
```

Promoter *CaMV35S*

```
1 pExBMG1        CACAATCCCACTATCCTTCGCAAGACCCTTCCTCTATATAAGGAAGTTCATTTCATTTGGAGAGAACACGGGGGACtcta
2 35SCaPFLP_F    CACAATCCCACTATCCTTCGCAAGACCCTTCCTCTATATAAGGAAGTTCATTTCATTTGGAGAGAACACGGGGGACTCTA
3 35SCaPFLP_R    CACAATCCCACTATCCTTCGCAAGACCCTTCCTCTATATAAGGAAGTTCATTTCATTTGGAGAGAACACGGGGGACTCTA
```

Promoter *CaMV35S*

```
1 pExBMG1        gaATGGCTAGTGTCTCAGCTACCATGATTAGTACCTCCTTCATGCCAAGAAAACCAGCTGTGACAAGCCTTAAACCCATC
2 35SCaPFLP_F    GAATGGCTAGTGTCTCAGCTACCATGATTAGTACCTCCTTCATGCCAAGAAAACCAGCTGTGACAAGCCTTAAACCCATC
3 35SCaPFLP_R    GAATGGCTAGTGTCTCAGCTACCATGATTAGTACCTCCTTCATGCCAAGAAAACCAGCTGTGACAAGCCTTAAACCCATC
```

CaFPLP

```
1 pExBMG1        CCAAACGTTGGGGAAGCACTGTTTGGGCTTAAATCAGCAAATGGTGGCAAAGTCACTTGCATGGCTTCATACAAAGTGAA
2 35SCaPFLP_F    CCAAACGTTGGGGAAGCACTGTTTGGGCTTAAATCAGCAAATGGTGGCAAAGTCACTTGCATGGCTTCATACAAAGTGAA
3 35SCaPFLP_R    CCAAACGTTGGGGAAGCACTGTTTGGGCTTAAATCAGCAAATGGTGGCAAAGTCACTTGCATGGCTTCATACAAAGTGAA
```

CaFPLP

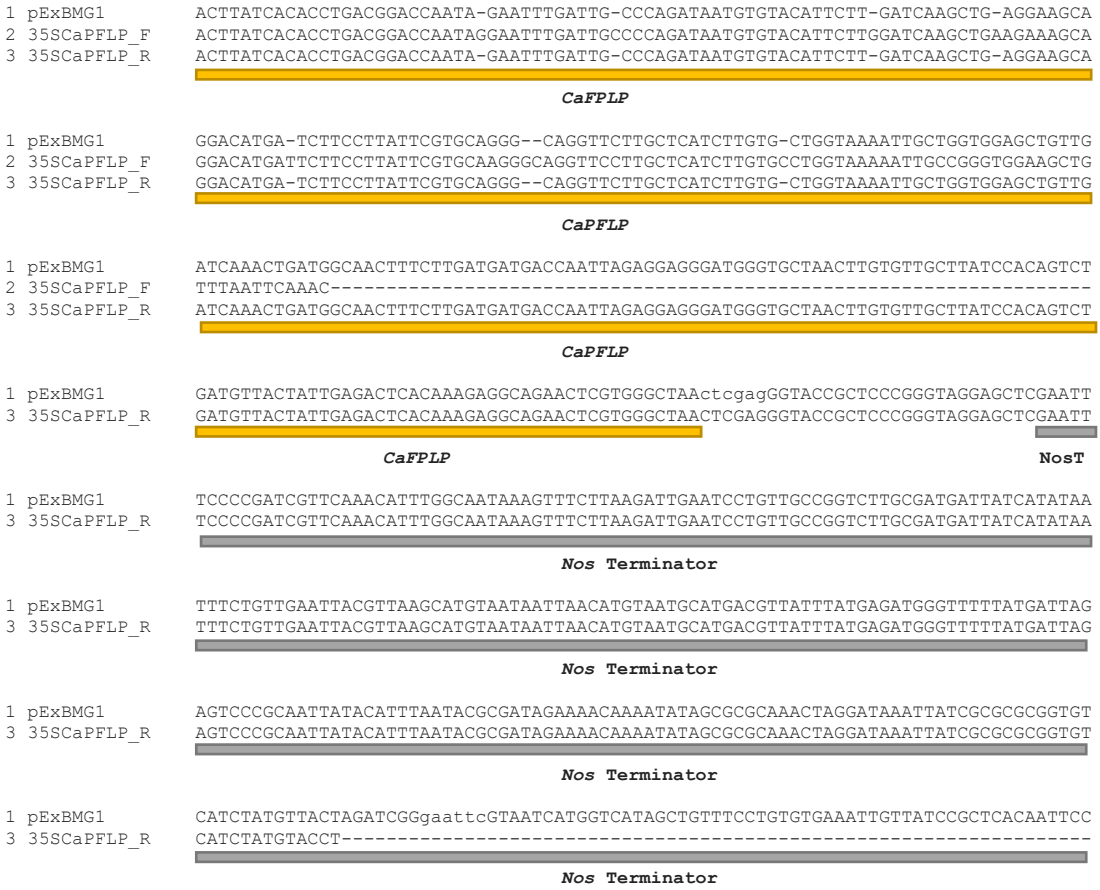
1 pExBMG1 ACTTATCACACCTGACGGACCAATA-GAATTTGATTG-CCCAGATAATGTGTACATTCTT-GATCAAGCTG-AGGAAGCA
2 35SCaPFLP_F ACTTATCACACCTGACGGACCAATAGGAATTTGATTGCCCCAGATAATGTGTACATTCTTGGATCAAGCTGAAGAAAGCA
3 35SCaPFLP_R ACTTATCACACCTGACGGACCAATA-GAATTTGATTG-CCCAGATAATGTGTACATTCTT-GATCAAGCTG-AGGAAGCA
CaFPLP
1 pExBMG1 GGACATGA-TCTTCCTTATTCGTGCAGGG--CAGGTTCTTGCTCATCTTGTG-CTGGTAAAATTGCTGGTGGAGCTGTTG
2 35SCaPFLP_F GGACATGATTCTTCCTTATTCGTGCAAGGGCAGGTTCCTTGCTCATCTTGTGCCTGGTAAAAATTGCCGGGTGGAAGCTG
3 35SCaPFLP_R GGACATGA-TCTTCCTTATTCGTGCAGGG--CAGGTTCTTGCTCATCTTGTG-CTGGTAAAATTGCTGGTGGAGCTGTTG
CaPFLP
1 pExBMG1 ATCAAACTGATGGCAACTTTCTTGATGATGACCAATTAGAGGAGGGATGGGTGCTAACTTGTGTTGCTTATCCACAGTCT
2 35SCaPFLP_F TTTAATTCAAAC----------
3 35SCaPFLP_R ATCAAACTGATGGCAACTTTCTTGATGATGACCAATTAGAGGAGGGATGGGTGCTAACTTGTGTTGCTTATCCACAGTCT
CaPFLP
1 pExBMG1 GATGTTACTATTGAGACTCACAAAGAGGCAGAACTCGTGGGCTAActcgagGGTACCGCTCCCGGGTAGGAGCTCGAATT
3 35SCaPFLP_R GATGTTACTATTGAGACTCACAAAGAGGCAGAACTCGTGGGCTAACTCGAGGGTACCGCTCCCGGGTAGGAGCTCGAATT
CaFPLP
NosT
1 pExBMG1 TCCCCGATCGTTCAAACATTTGGCAATAAAGTTTCTTAAGATTGAATCCTGTTGCCGGTCTTGCGATGATTATCATATAA
3 35SCaPFLP_R TCCCCGATCGTTCAAACATTTGGCAATAAAGTTTCTTAAGATTGAATCCTGTTGCCGGTCTTGCGATGATTATCATATAA
Nos Terminator
1 pExBMG1 TTTCTGTTGAATTACGTTAAGCATGTAATAATTAACATGTAATGCATGACGTTATTTATGAGATGGGTTTTTATGATTAG
3 35SCaPFLP_R TTTCTGTTGAATTACGTTAAGCATGTAATAATTAACATGTAATGCATGACGTTATTTATGAGATGGGTTTTTATGATTAG
Nos Terminator
1 pExBMG1 AGTCCCGCAATTATACATTTAATACGCGATAGAAAACAAAATATAGCGCGCAAACTAGGATAAATTATCGCGCGCGGTGT
3 35SCaPFLP_R AGTCCCGCAATTATACATTTAATACGCGATAGAAAACAAAATATAGCGCGCAAACTAGGATAAATTATCGCGCGCGGTGT
Nos Terminator
1 pExBMG1 CATCTATGTTACTAGATCGGgaattcGTAATCATGGTCATAGCTGTTTCCTGTGTGAAATTGTTATCCGCTCACAATTCC
3 35SCaPFLP_R CATCTATGTACCT----------
Nos Terminator

pExBMG2 - pUC18-35S-SictB-NosT

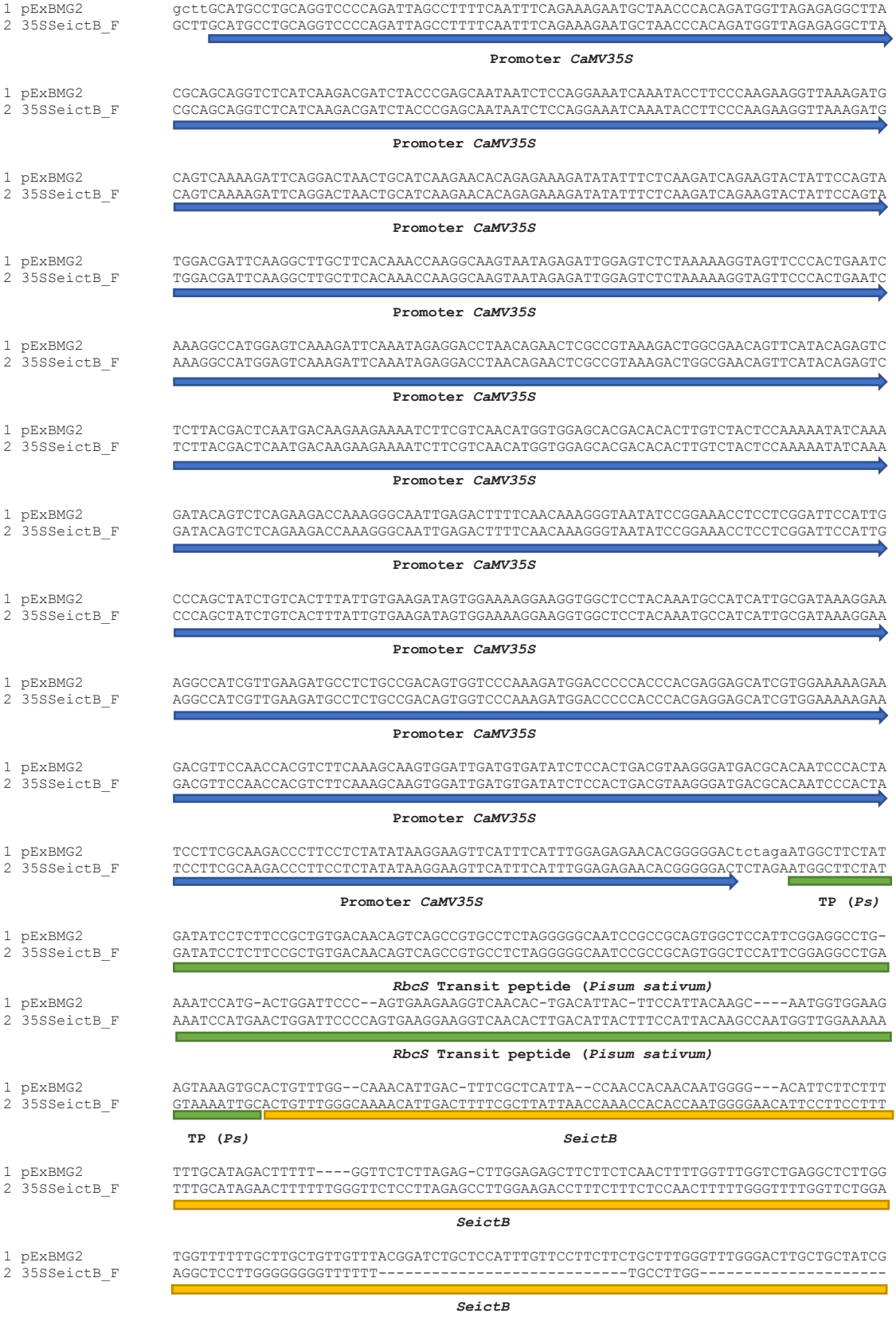

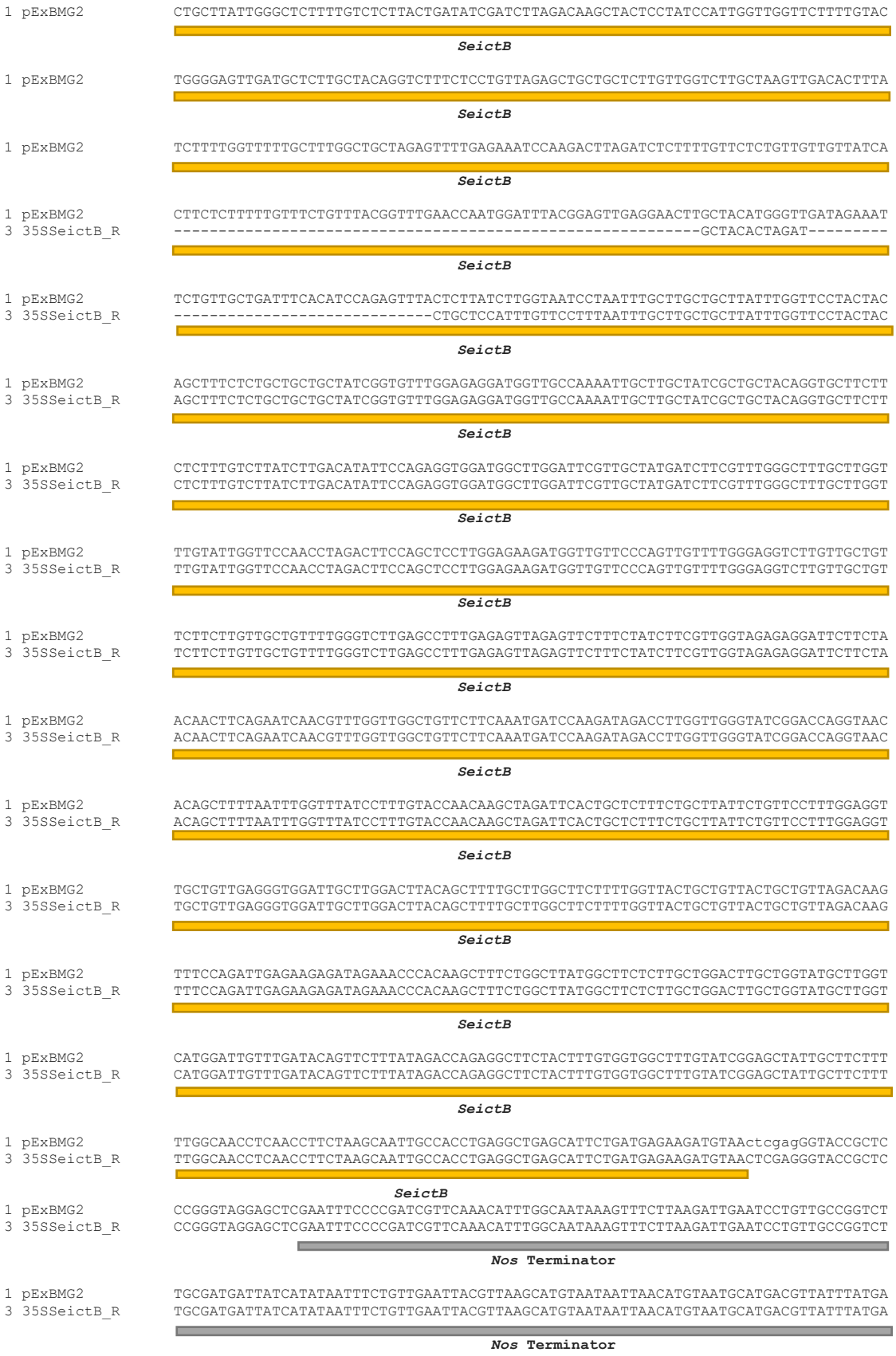
1 pExBMG2 CTGCTTATTGGGCTCTTTTGTCTCTTACTGATATCGATCTTAGACAAGCTACTCCTATCCATTGGTTGGTTCTTTTGTAC
SeictB
1 pExBMG2 TGGGGAGTTGATGCTCTTGCTACAGGTCTTTCTCCTGTTAGAGCTGCTGCTCTTGTTGGTCTTGCTAAGTTGACACTTTA
SeictB
1 pExBMG2 TCTTTTGGTTTTTGCTTTGGCTGCTAGAGTTTTGAGAAATCCAAGACTTAGATCTCTTTTGTTCTCTGTTGTTGTTATCA
SeictB
1 pExBMG2 CTTCTCTTTTTGTTTCTGTTTACGGTTTGAACCAATGGATTTACGGAGTTGAGGAACTTGCTACATGGGTTGATAGAAAT
3 35SSeictB_R ----------GCTACACTAGAT---------
SeictB
1 pExBMG2 TCTGTTGCTGATTTCACATCCAGAGTTTACTCTTATCTTGGTAATCCTAATTTGCTTGCTGCTTATTTGGTTCCTACTAC
3 35SSeictB_R ----------CTGCTCCATTTGTTCCTTTAATTTGCTTGCTGCTTATTTGGTTCCTACTAC
SeictB
1 pExBMG2 AGCTTTCTCTGCTGCTGCTATCGGTGTTTGGAGAGGATGGTTGCCAAAATTGCTTGCTATCGCTGCTACAGGTGCTTCTT
3 35SSeictB_R AGCTTTCTCTGCTGCTGCTATCGGTGTTTGGAGAGGATGGTTGCCAAAATTGCTTGCTATCGCTGCTACAGGTGCTTCTT
SeictB
1 pExBMG2 CTCTTTGTCTTATCTTGACATATTCCAGAGGTGGATGGCTTGGATTCGTTGCTATGATCTTCGTTTGGGCTTTGCTTGGT
3 35SSeictB_R CTCTTTGTCTTATCTTGACATATTCCAGAGGTGGATGGCTTGGATTCGTTGCTATGATCTTCGTTTGGGCTTTGCTTGGT
SeictB
1 pExBMG2 TTGTATTGGTTCCAACCTAGACTTCCAGCTCCTTGGAGAAGATGGTTGTTCCCAGTTGTTTTGGGAGGTCTTGTTGCTGT
3 35SSeictB_R TTGTATTGGTTCCAACCTAGACTTCCAGCTCCTTGGAGAAGATGGTTGTTCCCAGTTGTTTTGGGAGGTCTTGTTGCTGT
SeictB
1 pExBMG2 TCTTCTTGTTGCTGTTTTGGGTCTTGAGCCTTTGAGAGTTAGAGTTCTTTCTATCTTCGTTGGTAGAGAGGATTCTTCTA
3 35SSeictB_R TCTTCTTGTTGCTGTTTTGGGTCTTGAGCCTTTGAGAGTTAGAGTTCTTTCTATCTTCGTTGGTAGAGAGGATTCTTCTA
SeictB
1 pExBMG2 ACAACTTCAGAATCAACGTTTGGTTGGCTGTTCTTCAAATGATCCAAGATAGACCTTGGTTGGGTATCGGACCAGGTAAC
3 35SSeictB_R ACAACTTCAGAATCAACGTTTGGTTGGCTGTTCTTCAAATGATCCAAGATAGACCTTGGTTGGGTATCGGACCAGGTAAC
SeictB
1 pExBMG2 ACAGCTTTTAATTTGGTTTATCCTTTGTACCAACAAGCTAGATTCACTGCTCTTTCTGCTTATTCTGTTCCTTTGGAGGT
3 35SSeictB_R ACAGCTTTTAATTTGGTTTATCCTTTGTACCAACAAGCTAGATTCACTGCTCTTTCTGCTTATTCTGTTCCTTTGGAGGT
SeictB
1 pExBMG2 TGCTGTTGAGGGTGGATTGCTTGGACTTACAGCTTTTGCTTGGCTTCTTTTGGTTACTGCTGTTACTGCTGTTAGACAAG
3 35SSeictB_R TGCTGTTGAGGGTGGATTGCTTGGACTTACAGCTTTTGCTTGGCTTCTTTTGGTTACTGCTGTTACTGCTGTTAGACAAG
SeictB
1 pExBMG2 TTTCCAGATTGAGAAGAGATAGAAACCCACAAGCTTTCTGGCTTATGGCTTCTCTTGCTGGACTTGCTGGTATGCTTGGT
3 35SSeictB_R TTTCCAGATTGAGAAGAGATAGAAACCCACAAGCTTTCTGGCTTATGGCTTCTCTTGCTGGACTTGCTGGTATGCTTGGT
SeictB
1 pExBMG2 CATGGATTGTTTGATACAGTTCTTTATAGACCAGAGGCTTCTACTTTGTGGTGGCTTTGTATCGGAGCTATTGCTTCTTT
3 35SSeictB_R CATGGATTGTTTGATACAGTTCTTTATAGACCAGAGGCTTCTACTTTGTGGTGGCTTTGTATCGGAGCTATTGCTTCTTT
SeictB
1 pExBMG2 TTGGCAACCTCAACCTTCTAAGCAATTGCCACCTGAGGCTGAGCATTCTGATGAGAAGATGTAActcgagGGTACCGCTC
3 35SSeictB_R TTGGCAACCTCAACCTTCTAAGCAATTGCCACCTGAGGCTGAGCATTCTGATGAGAAGATGTAACTCGAGGGTACCGCTC
SeictB
1 pExBMG2 CCGGGTAGGAGCTCGAATTTCCCCGATCGTTCAAACATTTGGCAATAAAGTTTCTTAAGATTGAATCCTGTTGCCGGTCT
3 35SSeictB_R CCGGGTAGGAGCTCGAATTTCCCCGATCGTTCAAACATTTGGCAATAAAGTTTCTTAAGATTGAATCCTGTTGCCGGTCT
Nos Terminator
1 pExBMG2 TGCGATGATTATCATATAATTTCTGTTGAATTACGTTAAGCATGTAATAATTAACATGTAATGCATGACGTTATTTATGA
3 35SSeictB_R TGCGATGATTATCATATAATTTCTGTTGAATTACGTTAAGCATGTAATAATTAACATGTAATGCATGACGTTATTTATGA
Nos Terminator

```
1 pExBMG2          GATGGGTTTTTATGATTAGAGTCCCGCAATTATACATTTAATACGCGATAGAAAACAAAATATAGCGCGCAAACTAGGAT
3 35SSeictB_R      GATGGGTTTTTATGATTAGAGTCCCGCAATTATACATTTAATACGCGATAGAAAACAAAATATAGCGCGCAAACTAGGAT
```

***Nos* Terminator**

```
1 pExBMG2          AAATTATCGCGCGCGGTGTCATCTATGTTACTAGATCGGgaattcGTAATCATGGTCATAGCTGTTTCCTGTGTGAAATT
3 35SSeictB_R      AAATTATCGCGCGCGGTGTCATCTATGTTACTAGATCGGGAATTCTT---------------------------------
```

***Nos* Terminator**

pExBMG5 – pUC18-SlRbcS-AtFBPA-NosT

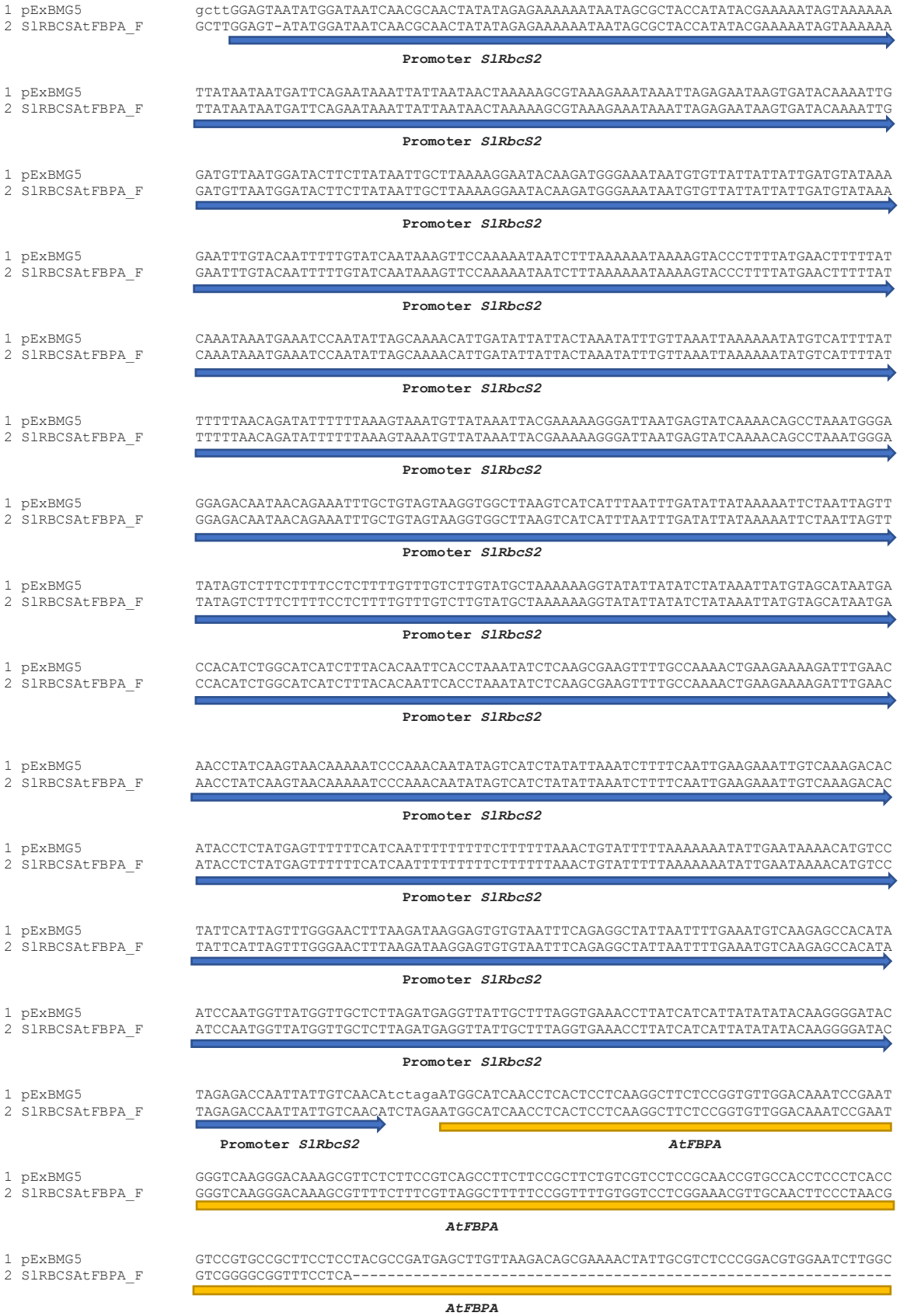

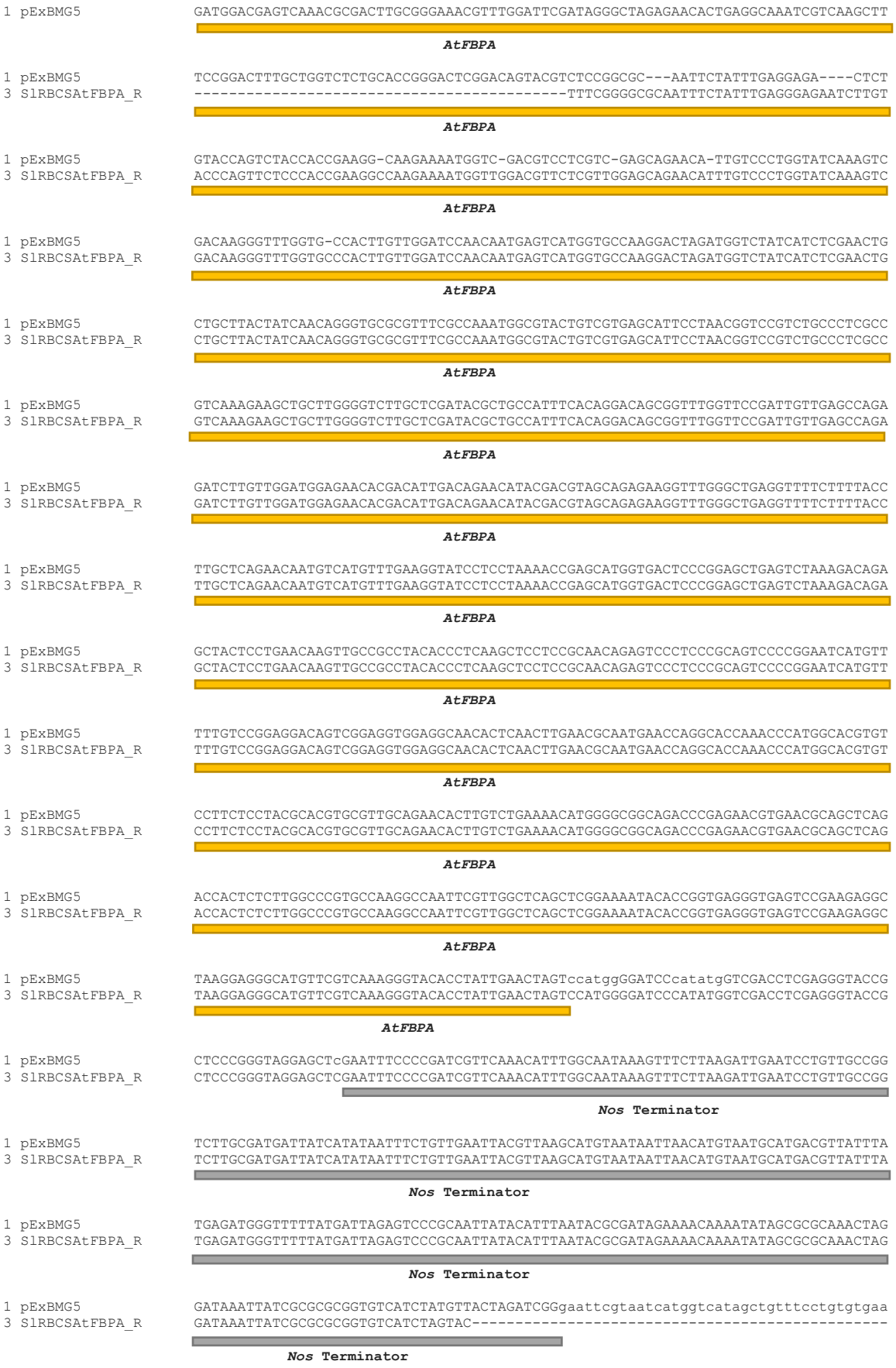
1 pExBMG5 GATGGACGAGTCAAACGCGACTTGCGGGAAACGTTTGGATTCGATAGGGCTAGAGAACACTGAGGCAAATCGTCAAGCTT
AtFBPA
1 pExBMG5 TCCGGACTTTGCTGGTCTCTGCACCGGGACTCGGACAGTACGTCTCCGGCGC---AATTCTATTTGAGGAGA----CTCT
3 SlRBCSAtFBPA_R ----------TTTCGGGGCGCAATTTCTATTTGAGGGAGAATCTTGT
AtFBPA
1 pExBMG5 GTACCAGTCTACCACCGAAGG-CAAGAAAATGGTC-GACGTCCTCGTC-GAGCAGAACA-TTGTCCCTGGTATCAAAGTC
3 SlRBCSAtFBPA_R ACCCAGTTCTCCCACCGAAGGCCAAGAAAATGGTTGGACGTTCTCGTTGGAGCAGAACATTTGTCCCTGGTATCAAAGTC
AtFBPA
1 pExBMG5 GACAAGGGTTTGGTG-CCACTTGTTGGATCCAACAATGAGTCATGGTGCCAAGGACTAGATGGTCTATCATCTCGAACTG
3 SlRBCSAtFBPA_R GACAAGGGTTTGGTGCCCACTTGTTGGATCCAACAATGAGTCATGGTGCCAAGGACTAGATGGTCTATCATCTCGAACTG
AtFBPA
1 pExBMG5 CTGCTTACTATCAACAGGGTGCGCGTTTCGCCAAATGGCGTACTGTCGTGAGCATTCCTAACGGTCCGTCTGCCCTCGCC
3 SlRBCSAtFBPA_R CTGCTTACTATCAACAGGGTGCGCGTTTCGCCAAATGGCGTACTGTCGTGAGCATTCCTAACGGTCCGTCTGCCCTCGCC
AtFBPA
1 pExBMG5 GTCAAAGAAGCTGCTTGGGGTCTTGCTCGATACGCTGCCATTTCACAGGACAGCGGTTTGGTTCCGATTGTTGAGCCAGA
3 SlRBCSAtFBPA_R GTCAAAGAAGCTGCTTGGGGTCTTGCTCGATACGCTGCCATTTCACAGGACAGCGGTTTGGTTCCGATTGTTGAGCCAGA
AtFBPA
1 pExBMG5 GATCTTGTTGGATGGAGAACACGACATTGACAGAACATACGACGTAGCAGAGAAGGTTTGGGCTGAGGTTTTCTTTTACC
3 SlRBCSAtFBPA_R GATCTTGTTGGATGGAGAACACGACATTGACAGAACATACGACGTAGCAGAGAAGGTTTGGGCTGAGGTTTTCTTTTACC
AtFBPA
1 pExBMG5 TTGCTCAGAACAATGTCATGTTTGAAGGTATCCTCCTAAAACCGAGCATGGTGACTCCCGGAGCTGAGTCTAAAGACAGA
3 SlRBCSAtFBPA_R TTGCTCAGAACAATGTCATGTTTGAAGGTATCCTCCTAAAACCGAGCATGGTGACTCCCGGAGCTGAGTCTAAAGACAGA
AtFBPA
1 pExBMG5 GCTACTCCTGAACAAGTTGCCGCCTACACCCTCAAGCTCCTCCGCAACAGAGTCCCTCCCGCAGTCCCCGGAATCATGTT
3 SlRBCSAtFBPA_R GCTACTCCTGAACAAGTTGCCGCCTACACCCTCAAGCTCCTCCGCAACAGAGTCCCTCCCGCAGTCCCCGGAATCATGTT
AtFBPA
1 pExBMG5 TTTGTCCGGAGGACAGTCGGAGGTGGAGGCAACACTCAACTTGAACGCAATGAACCAGGCACCAAACCCATGGCACGTGT
3 SlRBCSAtFBPA_R TTTGTCCGGAGGACAGTCGGAGGTGGAGGCAACACTCAACTTGAACGCAATGAACCAGGCACCAAACCCATGGCACGTGT
AtFBPA
1 pExBMG5 CCTTCTCCTACGCACGTGCGTTGCAGAACACTTGTCTGAAAACATGGGGCGGCAGACCCGAGAACGTGAACGCAGCTCAG
3 SlRBCSAtFBPA_R CCTTCTCCTACGCACGTGCGTTGCAGAACACTTGTCTGAAAACATGGGGCGGCAGACCCGAGAACGTGAACGCAGCTCAG
AtFBPA
1 pExBMG5 ACCACTCTCTTGGCCCGTGCCAAGGCCAATTCGTTGGCTCAGCTCGGAAAATACACCGGTGAGGGTGAGTCCGAAGAGGC
3 SlRBCSAtFBPA_R ACCACTCTCTTGGCCCGTGCCAAGGCCAATTCGTTGGCTCAGCTCGGAAAATACACCGGTGAGGGTGAGTCCGAAGAGGC
AtFBPA
1 pExBMG5 TAAGGAGGGCATGTTCGTCAAAGGGTACACCTATTGAACTAGTccatggGGATCCcatatgGTCGACCTCGAGGGTACCG
3 SlRBCSAtFBPA_R TAAGGAGGGCATGTTCGTCAAAGGGTACACCTATTGAACTAGTCCATGGGGATCCCATATGGTCGACCTCGAGGGTACCG
AtFBPA
1 pExBMG5 CTCCCGGGTAGGAGCTcGAATTTCCCCGATCGTTCAAACATTTGGCAATAAAGTTTCTTAAGATTGAATCCTGTTGCCGG
3 SlRBCSAtFBPA_R CTCCCGGGTAGGAGCTCGAATTTCCCCGATCGTTCAAACATTTGGCAATAAAGTTTCTTAAGATTGAATCCTGTTGCCGG
Nos Terminator
1 pExBMG5 TCTTGCGATGATTATCATATAATTTCTGTTGAATTACGTTAAGCATGTAATAATTAACATGTAATGCATGACGTTATTTA
3 SlRBCSAtFBPA_R TCTTGCGATGATTATCATATAATTTCTGTTGAATTACGTTAAGCATGTAATAATTAACATGTAATGCATGACGTTATTTA
Nos Terminator
1 pExBMG5 TGAGATGGGTTTTTATGATTAGAGTCCCGCAATTATACATTTAATACGCGATAGAAAACAAAATATAGCGCGCAAACTAG
3 SlRBCSAtFBPA_R TGAGATGGGTTTTTATGATTAGAGTCCCGCAATTATACATTTAATACGCGATAGAAAACAAAATATAGCGCGCAAACTAG
Nos Terminator
1 pExBMG5 GATAAATTATCGCGCGCGGTGTCATCTATGTTACTAGATCGGgaattcgtaatcatggtcatagctgtttcctgtgtgaa
3 SlRBCSAtFBPA_R GATAAATTATCGCGCGCGGTGTCATCTAGTAC----------
Nos Terminator

pSKJ14 – pUC18-SlRbcS-AtSBP-NosT

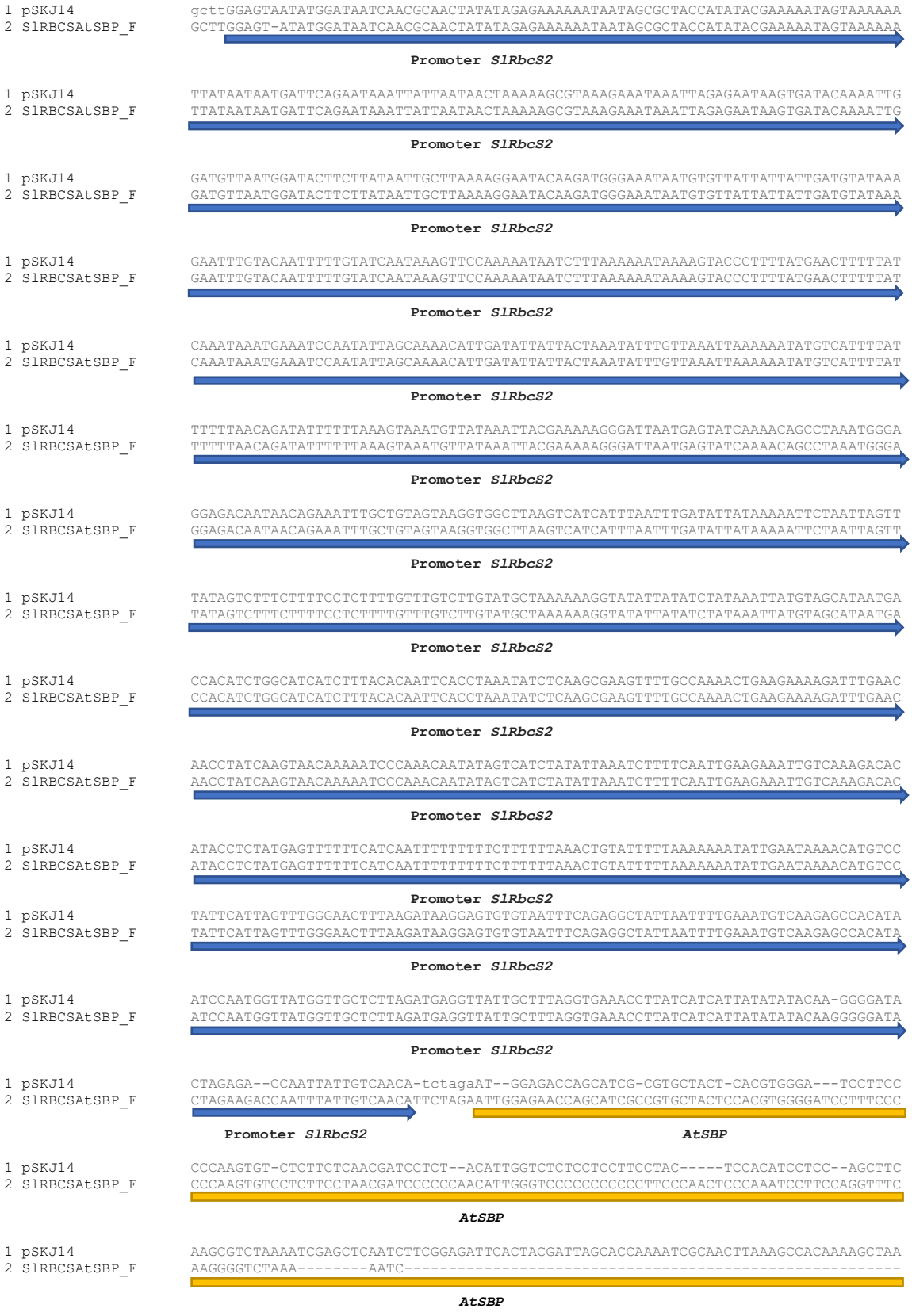

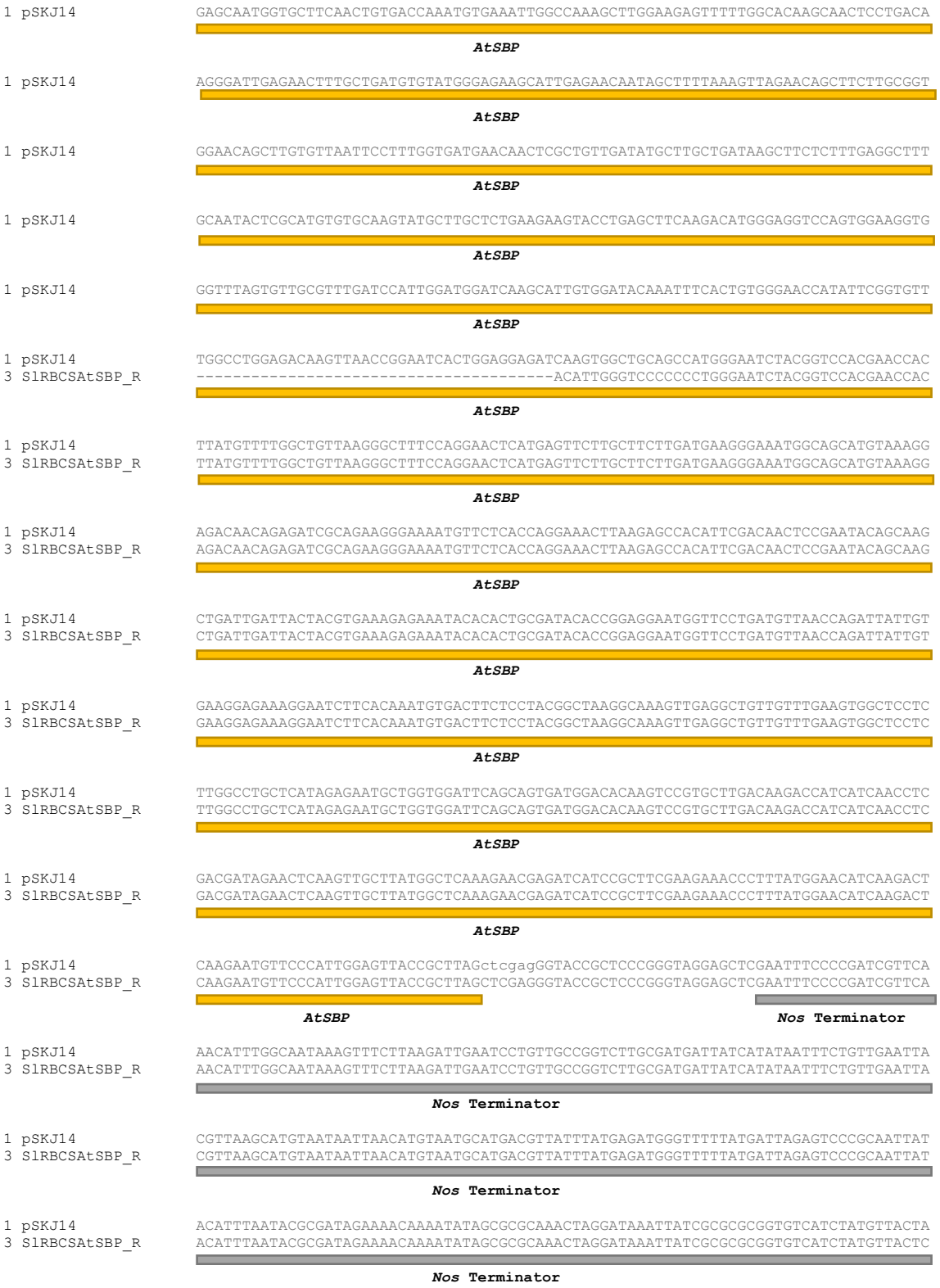
1 pSKJ14 GAGCAATGGTGCTTCAACTGTGACCAAATGTGAAATTGGCCAAAGCTTGGAAGAGTTTTTGGCACAAGCAACTCCTGACA
AtSBP
1 pSKJ14 AGGGATTGAGAACTTTGCTGATGTGTATGGGAGAAGCATTGAGAACAATAGCTTTTAAAGTTAGAACAGCTTCTTGCGGT
AtSBP
1 pSKJ14 GGAACAGCTTGTGTTAATTCCTTTGGTGATGAACAACTCGCTGTTGATATGCTTGCTGATAAGCTTCTCTTTGAGGCTTT
AtSBP
1 pSKJ14 GCAATACTCGCATGTGTGCAAGTATGCTTGCTCTGAAGAAGTACCTGAGCTTCAAGACATGGGAGGTCCAGTGGAAGGTG
AtSBP
1 pSKJ14 GGTTTAGTGTTGCGTTTGATCCATTGGATGGATCAAGCATTGTGGATACAAATTTCACTGTGGGAACCATATTCGGTGTT
AtSBP
1 pSKJ14 TGGCCTGGAGACAAGTTAACCGGAATCACTGGAGGAGATCAAGTGGCTGCAGCCATGGGAATCTACGGTCCACGAACCAC
3 SlRBCSAtSBP_R ----------ACATTGGGTCCCCCCCTGGGAATCTACGGTCCACGAACCAC
AtSBP
1 pSKJ14 TTATGTTTTGGCTGTTAAGGGCTTTCCAGGAACTCATGAGTTCTTGCTTCTTGATGAAGGGAAATGGCAGCATGTAAAGG
3 SlRBCSAtSBP_R TTATGTTTTGGCTGTTAAGGGCTTTCCAGGAACTCATGAGTTCTTGCTTCTTGATGAAGGGAAATGGCAGCATGTAAAGG
AtSBP
1 pSKJ14 AGACAACAGAGATCGCAGAAGGGAAAATGTTCTCACCAGGAAACTTAAGAGCCACATTCGACAACTCCGAATACAGCAAG
3 SlRBCSAtSBP_R AGACAACAGAGATCGCAGAAGGGAAAATGTTCTCACCAGGAAACTTAAGAGCCACATTCGACAACTCCGAATACAGCAAG
AtSBP
1 pSKJ14 CTGATTGATTACTACGTGAAAGAGAAATACACACTGCGATACACCGGAGGAATGGTTCCTGATGTTAACCAGATTATTGT
3 SlRBCSAtSBP_R CTGATTGATTACTACGTGAAAGAGAAATACACACTGCGATACACCGGAGGAATGGTTCCTGATGTTAACCAGATTATTGT
AtSBP
1 pSKJ14 GAAGGAGAAAGGAATCTTCACAAATGTGACTTCTCCTACGGCTAAGGCAAAGTTGAGGCTGTTGTTTGAAGTGGCTCCTC
3 SlRBCSAtSBP_R GAAGGAGAAAGGAATCTTCACAAATGTGACTTCTCCTACGGCTAAGGCAAAGTTGAGGCTGTTGTTTGAAGTGGCTCCTC
AtSBP
1 pSKJ14 TTGGCCTGCTCATAGAGAATGCTGGTGGATTCAGCAGTGATGGACACAAGTCCGTGCTTGACAAGACCATCATCAACCTC
3 SlRBCSAtSBP_R TTGGCCTGCTCATAGAGAATGCTGGTGGATTCAGCAGTGATGGACACAAGTCCGTGCTTGACAAGACCATCATCAACCTC
AtSBP
1 pSKJ14 GACGATAGAACTCAAGTTGCTTATGGCTCAAAGAACGAGATCATCCGCTTCGAAGAAACCCTTTATGGAACATCAAGACT
3 SlRBCSAtSBP_R GACGATAGAACTCAAGTTGCTTATGGCTCAAAGAACGAGATCATCCGCTTCGAAGAAACCCTTTATGGAACATCAAGACT
AtSBP
1 pSKJ14 CAAGAATGTTCCCATTGGAGTTACCGCTTAGctcgagGGTACCGCTCCCGGGTAGGAGCTCGAATTTCCCCGATCGTTCA
3 SlRBCSAtSBP_R CAAGAATGTTCCCATTGGAGTTACCGCTTAGCTCGAGGGTACCGCTCCCGGGTAGGAGCTCGAATTTCCCCGATCGTTCA
AtSBP
Nos Terminator
1 pSKJ14 AACATTTGGCAATAAAGTTTCTTAAGATTGAATCCTGTTGCCGGTCTTGCGATGATTATCATATAATTTCTGTTGAAATTA
3 SlRBCSAtSBP_R AACATTTGGCAATAAAGTTTCTTAAGATTGAATCCTGTTGCCGGTCTTGCGATGATTATCATATAATTTCTGTTGAATTA
Nos Terminator
1 pSKJ14 CGTTAAGCATGTAATAATTAACATGTAATGCATGACGTTATTTATGAGATGGGTTTTTATGATTAGAGTCCCGCAATTAT
3 SlRBCSAtSBP_R CGTTAAGCATGTAATAATTAACATGTAATGCATGACGTTATTTATGAGATGGGTTTTTATGATTAGAGTCCCGCAATTAT
Nos Terminator
1 pSKJ14 ACATTTAATACGCGATAGAAAACAAAATATAGCGCGCAAACTAGGATAAATTATCGCGCGCGGTGTCATCTATGTTACTA
3 SlRBCSAtSBP_R ACATTTAATACGCGATAGAAAACAAAATATAGCGCGCAAACTAGGATAAATTATCGCGCGCGGTGTCATCTATGTTACTC
Nos Terminator

pSKJ1 – pUC18-35S-GDCH-NosT

```
1 pSKJ1          gcttGCATGCCTGCAGGTCCCCAGATTAGCCTTTTCAATTTCAGAAAGAATGCTAACCCACAGATGGTTAGAGAGGCTTA
2 35SGDCH_F      TGCTGCATGCCTGCAGGTCCCCAGATTAGCCTTTTCAATTTCAGAAAGAATGCTAACCCACAGATGGTTAGAGAGGCTTA
```


```
1 pSKJ1          CGCAGCAGGTCTCATCAAGACGATCTACCCGAGCAATAATCTCCAGGAAATCAAATACCTTCCCAAGAAGGTTAAAGATG
2 35SGDCH_F      CGCAGCAGGTCTCATCAAGACGATCTACCCGAGCAATAATCTCCAGGAAATCAAATACCTTCCCAAGAAGGTTAAAGATG
```



```
1 pSKJ1          CAGTCAAAAGATTCAGGACTAACTGCATCAAGAACACAGAGAAAGATATATTTCTCAAGATCAGAAGTACTATTCCAGTA
2 35SGDCH_F      CAGTCAAAAGATTCAGGACTAACTGCATCAAGAACACAGAGAAAGATATATTTCTCAAGATCAGAAGTACTATTCCAGTA
```


```
1 pSKJ1          TGGACGATTCAAGGCTTGCTTCACAAACCAAGGCAAGTAATAGAGATTGGAGTCTCTAAAAAGGTAGTTCCCACTGAATC
2 35SGDCH_F      TGGACGATTCAAGGCTTGCTTCACAAACCAAGGCAAGTAATAGAGATTGGAGTCTCTAAAAAGGTAGTTCCCACTGAATC
```

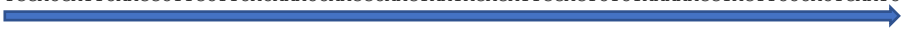


```
1 pSKJ1          AAAGGCCATGGAGTCAAAGATTCAAATAGAGGACCTAACAGAACTCGCCGTAAAGACTGGCGAACAGTTCATACAGAGTC
2 35SGDCH_F      AAAGGCCATGGAGTCAAAGATTCAAATAGAGGACCTAACAGAACTCGCCGTAAAGACTGGCGAACAGTTCATACAGAGTC
3 35SGDCH_R      ------------------------------------------------CCCTTTTGGTT-------------TTCGGGGCG
```


```
1 pSKJ1          TCTTACGACTCAATGACAAGAAGAAAATCTTCGTCAACATGGTGGAGCACGACACACTTGTCTACTCCAAAAATATCAAA
2 35SGDCH_F      TCTTACGACTCAATGACAAGAAGAAAATCTTCGTCAACATGGTGGAGCACGACACACTTGTCTACTCCAAAAATATCAAA
3 35SGDCH_R      TTTTCGGGTGATGGACGGTGGAAAACCTTCTTGACAACATGCCGGCTCCCCGGAGAACGGTCAACAGC--TTTTTCTGTT
```


```
1 pSKJ1          GATACAGTCTCAGAAGACCAAAGGGCAATTGAGACTTTTCAACAAAGGGTAATATCCGGAAACCTCCTCGGATTCCATTG
2 35SGDCH_F      GATACAGTCTCAGAAGACCAAAGGGCAATTGAGACTTTTCAACAAAGGGTAATATCCGGAAACCTCCTCGGATTCCATTG
3 35SGDCH_R      AAGCCAGTCTCAGAAGACCAAAGGGCAATTGAGACTTTTCAACAAAGGGTAATATCCGGAAACCTCCTCGGATTCCATTG
```


```
1 pSKJ1          CCCAGCTATCTGTCACTTTATTGTGAAGATAGTGGAAAAGGAAGGTGGCTCCTACAAATGCCATCATTGCGATAAAGGAA
2 35SGDCH_F      CCCAGCTATCTGTCACTTTATTGTGAAGATAGTGGAAAAGGAAGGTGGCTCCTACAAATGCCATCATTGCGATAAAGGAA
3 35SGDCH_R      CCCAGCTATCTGTCACTTTATTGTGAAGATAGTGGAAAAGGAAGGTGGCTCCTACAAATGCCATCATTGCGATAAAGGAA
```


```
1 pSKJ1          AGGCCATCGTTGAAGATGCCTCTGCCGACAGTGGTCCCAAAGATGGACCCCCACCCACGAGGAGCATCGTGGAAAAAGAA
2 35SGDCH_F      AGGCCATCGTTGAAGATGCCTCTGCCGACAGTGGTCCCAAAGATGGACCCCCACCCACGAGGAGCATCGTGGAAAAAGAA
3 35SGDCH_R      AGGCCATCGTTGAAGATGCCTCTGCCGACAGTGGTCCCAAAGATGGACCCCCACCCACGAGGAGCATCGTGGAAAAAGAA
```

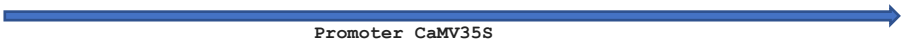


```
1 pSKJ1          GACGTTCCAACCACGTCTTCAAAGCAAGTGGATTGATGTGATATCTCCACTGACGTAAGGGATGACGCACAATCCCACTA
2 35SGDCH_F      GACGTTCCAACCACGTCTTCAAAGCAAGTGGATTGATGTGATATCTCCACTGACGTAAGGGATGACGCACAATCCCACTA
3 35SGDCH_R      GACGTTCCAACCACGTCTTCAAAGCAAGTGGATTGATGTGATATCTCCACTGACGTAAGGGATGACGCACAATCCCACTA
```


```
1 pSKJ1          TCCTTCGCAAGACCCTTCCTCTATATAAGGAAGTTCATTTCATTTGGAGAGAACACGGGGGACtctagaATGGCTCTTAG
2 35SGDCH_F      TCCTTCGCAAGACCCTTCCTCTATATAAGGAAGTTCATTTCATTTGGAGAGAACACGGGGGACTCTAGAATGGCTCTTAG
3 35SGDCH_R      TCCTTCGCAAGACCCTTCCTCTATATAAGGAAGTTCATTTCATTTGGAGAGAACACGGGGGACTCTAGAATGGCTCTTAG
```


```
1 pSKJ1          AATCTGGGCTTCTTCCACAGCCAATGCTCTAAGGCTATCCTCTGCTACTAGACCTCATTTCTCACCTCTTTCCAGATGCT
2 35SGDCH_F      AATCTGGGCTTCTTCCACAGCCAATGCTCTAAGGCTATCCTCTGCTACTAGACCTCATTTCTCACCTCTTTCCAGATGCT
3 35SGDCH_R      AATCTGGGCTTCTTCCACAGCCAATGCTCTAAGGCTATCCTCTGCTACTAGACCTCATTTCTCACCTCTTTCCAGATGCT
```

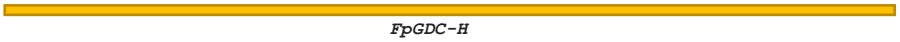


```
1 pSKJ1          TCTCTTCAGTTTTGGATGGATTGAAGTATGCAAATTCACATGAGTGGGTGAAGCATGAAGGTTCTGTTGCTACTATTGGT
2 35SGDCH_F      TCTCTTCAGTTTTGGATGGATTGAAGTATGCAAATTCACATGAGTGGGTGAAGCATGAAGGTTCTGTTGCTACTATTGGT
3 35SGDCH_R      TCTCTTCAGTTTTGGATGGATTGAAGTATGCAAATTCACATGAGTGGGTGAAGCATGAAGGTTCTGTTGCTACTATTGGT
```

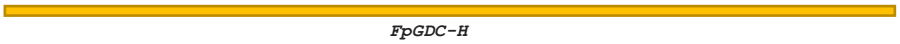


```
1 pSKJ1          ATCACTGACCATGCTCAGGATCATCTTGGGGAGGTGGTGTTTGTGGATTTACCAGAAGCCGGTGGCTCTGTGACCAAAGC
2 35SGDCH_F      ATCACTGACCATGCTCAGGATCATCTTGGGGAGGTGGTGTTTGTGGATTTACCAGAAGCCGGTGGCTCTGTGACCAAAGC
3 35SGDCH_R      ATCACTGACCATGCTCAGGATCATCTTGGGGAGGTGGTGTTTGTGGATTTACCAGAAGCCGGTGGCTCTGTGACCAAAGC
```

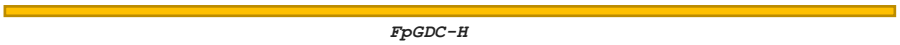

```
1 pSKJ1          CACCGGCTTTGGTGCAGTAGAAAGTGTCAAAGCCACCAGTGACGTTAACTCCCCGATCTCTGGAGAGATCGTTGAGGTGA
2 35SGDCH_F      CACCGGCTTTGGTGCAGTAGAAAGTGTCAAAGCCACCAGTGACGTTAACTCCCCGATCTCTGGAGAGATCGTTGAGGTGA
3 35SGDCH_R      CACCGGCTTTGGTGCAGTAGAAAGTGTCAAAGCCACCAGTGACGTTAACTCCCCGATCTCTGGAGAGATCGTTGAGGTGA
```


FpGDC-H

```
1 pSKJ1          ACTCGAAGTTGTCTGAGACTCCTGGTTTGATCAATTCGAGCCCGTATGAAGATGGATGGATGATTAAGGTGAAGCCAAGC
2 35SGDCH_F      --------TTATTGGGGCACTCTTGCCG------------------------------------------------------
3 35SGDCH_R      ACTCGAAGTTGTCTGAGACTCCTGGTTTGATCAATTCGAGCCCGTATGAAGATGGATGGATGATTAAGGTGAAGCCAAGC
```


FpGDC-H

```
1 pSKJ1          AACCCGTCGGAGCTGGATTCTTTAATGGGTGCAAAAGAGTACACAAAGTTCTGCGAAGAAGAAGATTCTGCTCACTAGct
3 35SGDCH_R      AACCCGTCGGAGCTGGATTCTTTAATGGGTGCAAAAGAGTACACAAAGTTCTGCGAAGAAGAAGATTCTGCTCACTAGCT
```


FpGDC-H

```
1 pSKJ1          cgagGGTACCGCTCCCGGGTAGGAGCTCGAATTTCCCCGATCGTTCAAACATTTGGCAATAAAGTTTCTTAAGATTGAAT
3 35SGDCH_R      CGAGGGTACCGCTCCCGGGTAGGAGCTCGAATTTCCCCGATCGTTCAAACATTTGGCAATAAAGTTTCTTAAGATTGAAT
```


***Nos* Terminator**

```
1 pSKJ1          CCTGTTGCCGGTCTTGCGATGATTATCATATAATTTCTGTTGAATTACGTTAAGCATGTAATAATTAACATGTAATGCAT
3 35SGDCH_R      CCTGTTGCCGGTCTTGCGATGATTATCATATAATTTCTGTTGAATTACGTTAAGCATGTAATAATTAACATGTAATGCAT
```


***Nos* Terminator**

```
1 pSKJ1          GACGTTATTTATGAGATGGGTTTTTATGATTAGAGTCCCGCAATTATACATTTAATACGCGATAGAAAACAAAATATAGC
3 35SGDCH_R      GACGTTATTTATGAGATGGGTTTTTATGATTAGAGTCCCGCAATTATACATTTAATACGCGATAGAAAACAAAATATAGC
```


***Nos* Terminator**

```
1 pSKJ1          GCGCAAACTAGGATAAATTATCGCGCGCGGTGTCATCTATGTTACTAGATCGGgaattcGTAATCATGGTCATAGCTGTT
3 35SGDCH_R      GCGCAAACTAGGATAAATTATCGCGCGCGGTGTCATCTAT----------------------------------------
```


***Nos* Terminator**

pExBMG7 – pUC18-StcyFBP-AtTPT-NosT

```
1 pExBMG7          CCAGCTAATGCTGCTCTTGTCACTCAAAATGATGGTATCCCTCTCGTCATCCAGTGTTTGTCAAGTCCTGTTAGGAACAC
2 StcyFBPAtTPT_F   CCAGCTAATGCTGCTCTTGTCACTCAAAATGATGGTATCCCTCTCGTCATCCAGTGTTTGTCAAGTCCTGTTAGGAACAC
```

Promoter *StcyFBP*

```
1 pExBMG7          AGTAAGGATATAAACAAACATTTTGTGGTCTTCTTGGTTATTGAGTGCTTGCTGTTCACTTGTTAAAATTGCACATATAC
2 StcyFBPAtTPT_F   AGTAAGGATATAAACAAACATTTTGTGGTCTTCTTGGTTATTGAGTGCTTGCTGTTCACTTGTTAAAATTGCACATATAC
```

Promoter *StcyFBP*

```
1 pExBMG7          GTAGTGAGAAACTCAACTGTTGAGTACCATTGATCCGTCAATCTTGTCGATAACTTTGATAAGGATATTTCAGGCATCAG
2 StcyFBPAtTPT_F   GTAGTGAGAAACTCAACTGTTGAGTACCATTGATCCGTCAATCTTGTCGATAACTTTGATAAGGATATTTCAGGCATCAG
```

Promoter *StcyFBP*

```
1 pExBMG7          ACATGTCACCTCTATAGAACTTGGTCTTTTTTTTTAAAAATAAAAATAAAAATGTTTGGCATCATACGAACTTCTGTTAC
2 StcyFBPAtTPT_F   ACATGTCACCTCTATAGAACTTGGTCTTTTTTTTTAAAAATAAAAATAAAAATGTTTGGCATCATACGAACTTCTGTTAC
```

Promoter *StcyFBP*

```
1 pExBMG7          TTTAGGCTGTATCCAGAATAAAATGTTGTTTCCTCATTCTGGAATTAGTTGTTTTGCACACGGAAGACTTTCGAAATTTA
2 StcyFBPAtTPT_F   TTTAGGCTGTATCCAGAATAAAATGTTGTTTCCTCATTCTGGAATTAGTTGTTTTGCACACGGAAGACTTTCGAAATTTA
```

Promoter *StcyFBP*

```
1 pExBMG7          CTAATTGTGTTCGTCCGTCTCAAACTGGCTCACACTTTGGTGGTCAATTTTACTTCTCAAGGTAAGCAATTACAGAATAT
2 StcyFBPAtTPT_F   CTAATTGTGTTCGTCCGTCTCAAACTGGCTCACACTTTGGTGGTCAATTTTACTTCTCAAGGTAAGCAATTACAGAATAT
```

Promoter *StcyFBP*

```
1 pExBMG7          GAATGTCGCTCTCCTCATATTTATCCGAACAATAAAAAATGATATCTGTTTGCATATGCATGTAGATCACACACCCCCCC
2 StcyFBPAtTPT_F   GAATGTCGCTCTCCTCATATTTATCCGAACAATAAAAAATGATATCTGTTTGCATATGCATGTAGATCACACACCCCCCC
```

Promoter *StcyFBP*

```
1 pExBMG7          CCCCCCCGCCCCTAGATTCCCTCGATTTAGATTAAATATAATCATCTACAAGAATTCCGTTGGGCTTCATTATGTGTTTT
2 StcyFBPAtTPT_F   CCCCCCCGCCCCTAGATTCCCTCGATTTAGATTAAATATAATCATCTACAAGAATTCCGTTGGGCTTCATTATGTGTTTT
```

Promoter *StcyFBP*

```
1 pExBMG7          TACATATTCGTTTCTGAACCACCCCCACCCCGGTGAAAAACATTGCTCTGCCACTGGCTCAATGTATTGACACAAATGAA
2 StcyFBPAtTPT_F   TACATATTCGTTTCTGAACCACCCCCACCCCGGTGAAAAACATTGCTCTGCCACTGGCTCAATGTATTGACACAAATGAA
```

Promoter *StcyFBP*

```
1 pExBMG7          CTTCAAACTGGGCAGGTGAATTATGCTCTAGGAGCATTGTATTATCTATGCAATGCATCAAACAAGGAAGAGATCTTAAA
2 StcyFBPAtTPT_F   CTTCAAACTGGGCAGGTGAATTATGCTCTAGGAGCATTGTATTATCTATGCAATGCATCAAACAAGGAAGAGATCTTAAA
```

Promoter *StcyFBP*

```
1 pExBMG7          GCCAGAAGTAATTGATGCAATCAAAAGTTATGCAGCTGCAGGTGGAGTTAGTACAAGCTTCAGTAATTTGGCTCAGGCTT
2 StcyFBPAtTPT_F   GCCAGAAGTAATTGATGCAATCAAAAGTTATGCAGCTGCAGGTGGAGTTAGTACAAGCTTCAGTAATTTGGCTCAGGCTT
```

Promoter *StcyFBP*

```
1 pExBMG7          TCTTAGATCAACATGTTCCTCAGCTTAATTAAAATGGAGGAAACCAAAGATTATGTTGTAAAATCATTTTCTATCCTAGA
2 StcyFBPAtTPT_F   TCTTAGATCAACATGTTCCTCAGCTTAATTAAAATGGAGGAAACCAAAGATTATGTTGTAAAATCATTTTCTATCCTAGA
```

Promoter *StcyFBP*

```
1 pExBMG7          TGGTCTATCGGAAACAATTTATTTATTACTCCTATCCAATTCATTATATTTTCAAAAGTTATGAAGTCCACGAAATATGT
2 StcyFBPAtTPT_F   TGGTCTATCGGAAACAATTTATTTATTACTCCTATCCAATTCATTATATTTTCAAAAGTTATGAAGTCCACGAAATGGAT
```

Promoter *StcyFBP*

```
1 pExBMG7          GACGTGGGTAAAGAAGACCCATGCCAAGCCAGTGGGATATAGAAACAAAACATGTAATAAAGAGAACAAATAATGAGTTT
2 StcyFBPAtTPT_F   -ACTAGAAGACCAATTAATTGTCAACATCTAGAGGGGCCCAGGGCCACCTAGTATGAAG----------------------
```

Promoter *StcyFBP*

```
1 pExBMG7          CGAAAAGAACAGAAGTTAGCATAAGGACGAGAATCACATTATCTTAGGTGCCAACCACTAATCCTATGTATCATTCTCCT
2 StcyFBPAtTPT_F   ------------------------------------------------------------------------------CTT
```

Promoter *StcyFBP*

```
1 pExBMG7          CTTTCCACGTGTCATCCTACACTTCCTTTGCCATCAGATTAGATAGCCCGGTTAGTACCTACACTGTATATCAAAAAATA
2 StcyFBPAtTPT_F   ACTTCAACGTCCC-----------------------------------------------------------------
```

Promoter *StcyFBP*

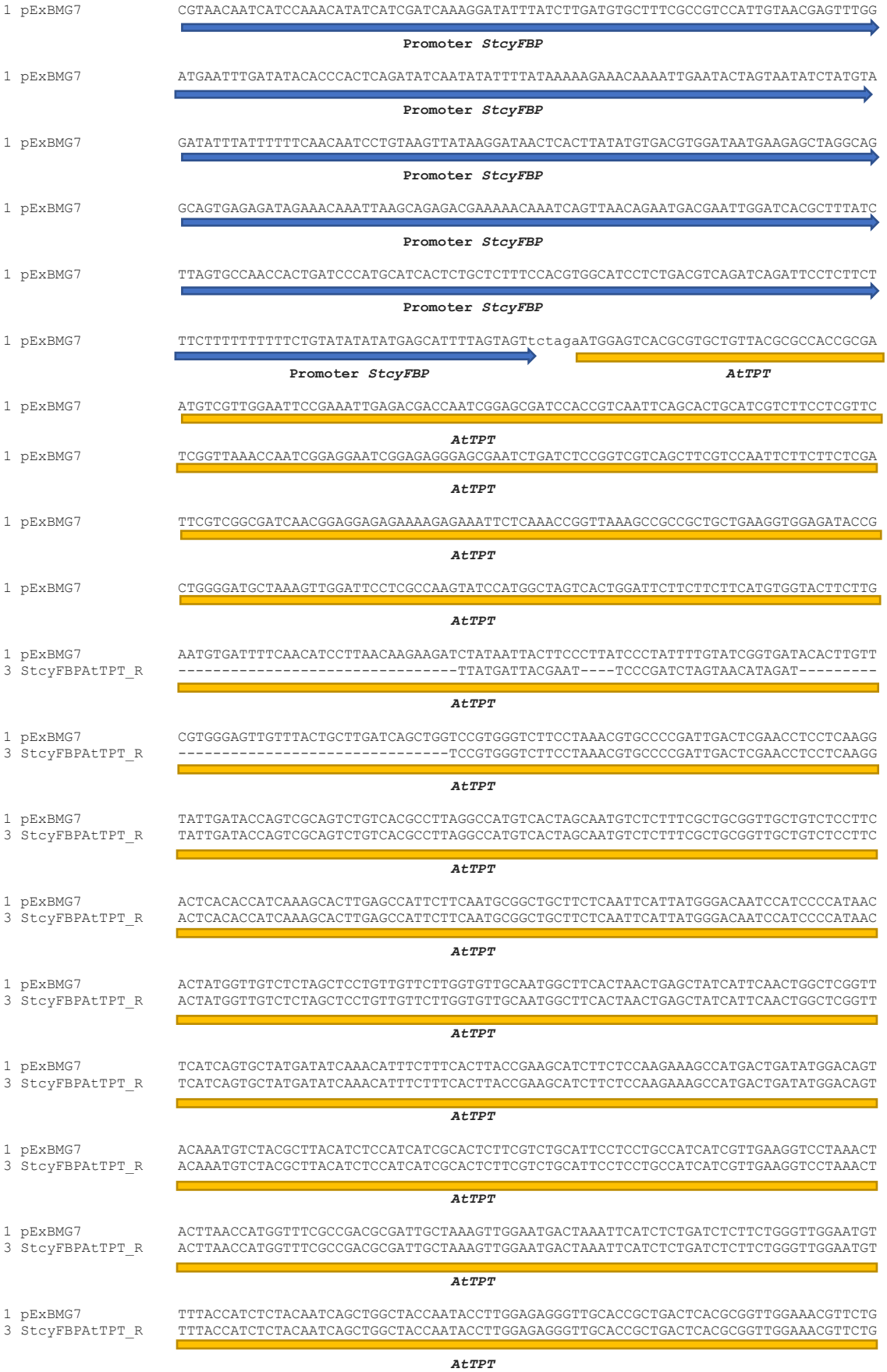
1 pExBMG7 CGTAACAATCATCCAAACATATCATCGATCAAAGGATATTTATCTTGATGTGCTTTCGCCGTCCATTGTAACGAGTTTGG
Promoter StcyFBP
1 pExBMG7 ATGAATTTGATATACACCCACTCAGATATCAATATATTTTATAAAAAGAAACAAAATTGAATACTAGTAATATCTATGTA
Promoter StcyFBP
1 pExBMG7 GATATTTATTTTTTCAACAATCCTGTAAGTTATAAGGATAACTCACTTATATGTGACGTGGATAATGAAGAGCTAGGCAG
Promoter StcyFBP
1 pExBMG7 GCAGTGAGAGATAGAAACAAATTAAGCAGAGACGAAAAACAAATCAGTTAACAGAATGACGAATTGGATCACGCTTTATC
Promoter StcyFBP
1 pExBMG7 TTAGTGCCAACCACTGATCCCATGCATCACTCTGCTCTTTCCACGTGGCATCCTCTGACGTCAGATCAGATTCCTCTTCT
Promoter StcyFBP
1 pExBMG7 TTCTTTTTTTTTTTCTGTATATATATGAGCATTTTAGTAGTtctagaATGGAGTCACGCGTGCTGTTACGCGCCACCGCGA
Promoter StcyFBP
AtTPT
1 pExBMG7 ATGTCGTTGGAATTCCGAAATTGAGACGACCAATCGGAGCGATCCACCGTCAATTCAGCACTGCATCGTCTTCCTCGTTC
AtTPT
1 pExBMG7 TCGGTTAAACCAATCGGAGGAATCGGAGAGGGAGCGAATCTGATCTCCGGTCGTCAGCTTCGTCCAATTCTTCTTCTCGA
AtTPT
1 pExBMG7 TTCGTCGGCGATCAACGGAGGAGAGAAAAGAGAAATTCTCAAACCGGTTAAAGCCGCCGCTGCTGAAGGTGGAGATACCG
AtTPT
1 pExBMG7 CTGGGGATGCTAAAGTTGGATTCCTCGCCAAGTATCCATGGCTAGTCACTGGATTCTTCTTCTTCATGTGGTACTTCTTG
AtTPT
1 pExBMG7 AATGTGATTTTCAACATCCTTAACAAGAAGATCTATAATTACTTCCCTTATCCCTATTTTGTATCGGTGATACACTTGTT
3 StcyFBPAtTPT_R ----------TTATGATTACGAAT----TCCCGATCTAGTAACATAGAT---------
AtTPT
1 pExBMG7 CGTGGGAGTTGTTTACTGCTTGATCAGCTGGTCCGTGGGTCTTCCTAAACGTGCCCCGATTGACTCGAACCTCCTCAAGG
3 StcyFBPAtTPT_R ----------TCCGTGGGTCTTCCTAAACGTGCCCCGATTGACTCGAACCTCCTCAAGG
AtTPT
1 pExBMG7 TATTGATACCAGTCGCAGTCTGTCACGCCTTAGGCCATGTCACTAGCAATGTCTCTTTCGCTGCGGTTGCTGTCTCCTTC
3 StcyFBPAtTPT_R TATTGATACCAGTCGCAGTCTGTCACGCCTTAGGCCATGTCACTAGCAATGTCTCTTTCGCTGCGGTTGCTGTCTCCTTC
AtTPT
1 pExBMG7 ACTCACACCATCAAAGCACTTGAGCCATTCTTCAATGCGGCTGCTTCTCAATTCATTATGGGACAATCCATCCCCATAAC
3 StcyFBPAtTPT_R ACTCACACCATCAAAGCACTTGAGCCATTCTTCAATGCGGCTGCTTCTCAATTCATTATGGGACAATCCATCCCCATAAC
AtTPT
1 pExBMG7 ACTATGGTTGTCTCTAGCTCCTGTTGTTCTTGGTGTTGCAATGGCTTCACTAACTGAGCTATCATTCAACTGGCTCGGTT
3 StcyFBPAtTPT_R ACTATGGTTGTCTCTAGCTCCTGTTGTTCTTGGTGTTGCAATGGCTTCACTAACTGAGCTATCATTCAACTGGCTCGGTT
AtTPT
1 pExBMG7 TCATCAGTGCTATGATATCAAACATTTCTTTCACTTACCGAAGCATCTTCTCCAAGAAAGCCATGACTGATATGGACAGT
3 StcyFBPAtTPT_R TCATCAGTGCTATGATATCAAACATTTCTTTCACTTACCGAAGCATCTTCTCCAAGAAAGCCATGACTGATATGGACAGT
AtTPT
1 pExBMG7 ACAAATGTCTACGCTTACATCTCCATCATCGCACTCTTCGTCTGCATTCCTCCTGCCATCATCGTTGAAGGTCCTAAACT
3 StcyFBPAtTPT_R ACAAATGTCTACGCTTACATCTCCATCATCGCACTCTTCGTCTGCATTCCTCCTGCCATCATCGTTGAAGGTCCTAAACT
AtTPT
1 pExBMG7 ACTTAACCATGGTTTCGCCGACGCGATTGCTAAAGTTGGAATGACTAAATTCATCTCTGATCTCTTCTGGGTTGGAATGT
3 StcyFBPAtTPT_R ACTTAACCATGGTTTCGCCGACGCGATTGCTAAAGTTGGAATGACTAAATTCATCTCTGATCTCTTCTGGGTTGGAATGT
AtTPT
1 pExBMG7 TTTACCATCTCTACAATCAGCTGGCTACCAATACCTTGGAGAGGGTTGCACCGCTGACTCACGCGGTTGGAAACGTTCTG
3 StcyFBPAtTPT_R TTTACCATCTCTACAATCAGCTGGCTACCAATACCTTGGAGAGGGTTGCACCGCTGACTCACGCGGTTGGAAACGTTCTG
AtTPT


1 pExBMG7 AAACGTGTGTTCGTGATCGGTTTCTCCATCGTTATCTTCGGAAACAAGATATCGACACAGACAGGTATAGGAACAGGAAT
3 StcyFBPAtTPT_R AAACGTGTGTTCGTGATCGGTTTCTCCATCGTTATCTTCGGAAACAAGATATCGACACAGACAGGTATAGGAACAGGAAT
AtTPT
1 pExBMG7 AGCCATTGCTGGAGTTGCAATGTACTCTATCATTAAGGCCAAGATCGAAGAAGAGAAACGGGTCACAAGGAAAGAAAGCA
3 StcyFBPAtTPT_R AGCCATTGCTGGAGTTGCAATGTACTCTATCATTAAGGCCAAGATCGAAGAAGAGAAACGGGTCACAAGGAAAGAAAGCA
AtTPT
1 pExBMG7 TAGAAAGCAGCTGAGGATCCcatatgGTCGACCTCGAGGGTACCGCTCCCGGGTAGGAGCTcGAATTTCCCCGATCGTTC
3 StcyFBPAtTPT_R TAGAAAGCAGCTGAGGATCCCATATGGTCGACCTCGAGGGTACCGCTCCCGGGTAGGAGCTCGAATTTCCCCGATCGTTC
AtTPT
NosT
1 pExBMG7 AAACATTTGGCAATAAAGTTTCTTAAGATTGAATCCTGTTGCCGGTCTTGCGATGATTATCATATAATTTCTGTTGAATT
3 StcyFBPAtTPT_R AAACATTTGGCAATAAAGTTTCTTAAGATTGAATCCTGTTGCCGGTCTTGCGATGATTATCATATAATTTCTGTTGAATT
Nos Terminator
1 pExBMG7 ACGTTAAGCATGTAATAATTAACATGTAATGCATGACGTTATTTATGAGATGGGTTTTTATGATTAGAGTCCCGCAATTA
3 StcyFBPAtTPT_R ACGTTAAGCATGTAATAATTAACATGTAATGCATGACGTTATTTATGAGATGGGTTTTTATGATTAGAGTCCCGCAATTA
Nos Terminator
1 pExBMG7 TACATTTAATACGCGATAGAAAACAAAATATAGCGCGCAAACTAGGATAAATTATCGCGCGCGGTGTCATCTATGTTACT
3 StcyFBPAtTPT_R TACATTTAATACGCGATAGAAAACAAAATATAGCGCGCAAACTAGGATAAATTATCGCGCGCGGTGTCATCTATGTTACT
Nos Terminator
1 pExBMG7 AGATCGGgaattcgtaatcatggtcatagctgtttcctgtgtgaaattgttatccgctcacaattccacacaacatacga
3 StcyFBPAtTPT_R AGATCGGGAATTCGTG----------
NosT

pExBMG6 - pUC18-StcyFBP-AtcyFBP-NosT

```
1 pExBMG6           gcttagtacttctagaCCAGCTAATGCTGCTCTTGTCACTCAAAATGATGGTATCCCTCTCGTCATCCAGTGTTTGTCAA
2 StcyFBPAtcyFBP_F  ----------------CCAGCTAATGCTGCTCTTGTCACTCAAAATGATGGTATCCCTCTCGTCATCCAGTGTTTGTCAA
                                                Promoter StcyFBP

1 pExBMG6           GTCCTGTTAGGAACACAGTAAGGATATAAACAAACATTTTGTGGTCTTCTTGGTTATTGAGTGCTTGCTGTTCACTTGTT
2 StcyFBPAtcyFBP_F  GTCCTGTTAGGAACACAGTAAGGATATAAACAAACATTTTGTGGTCTTCTTGGTTATTGAGTGCTTGCTGTTCACTTGTT
                                       Promoter StcyFBP

1 pExBMG6           AAAATTGCACATATACGTAGTGAGAAACTCAACTGTTGAGTACCATTGATCCGTCAATCTTGTCGATAACTTTGATAAGG
2 StcyFBPAtcyFBP_F  AAAATTGCACATATACGTAGTGAGAAACTCAACTGTTGAGTACCATTGATCCGTCAATCTTGTCGATAACTTTGATAAGG
                                       Promoter StcyFBP

1 pExBMG6           ATATTTCAGGCATCAGACATGTCACCTCTATAGAACTTGGTCTTTTTTTTTAAAAATAAAAATAAAAATGTTTGGCATCA
2 StcyFBPAtcyFBP_F  ATATTTCAGGCATCAGACATGTCACCTCTATAGAACTTGGTCTTTTTTTTTAAAAATAAAAATAAAAATGTTTGGCATCA
                                       Promoter StcyFBP

1 pExBMG6           TACGAACTTCTGTTACTTTAGGCTGTATCCAGAATAAAATGTTGTTTCCTCATTCTGGAATTAGTTGTTTTGCACACGGA
2 StcyFBPAtcyFBP_F  TACGAACTTCTGTTACTTTAGGCTGTATCCAGAATAAAATGTTGTTTCCTCATTCTGGAATTAGTTGTTTTGCACACGGA
                                       Promoter StcyFBP

1 pExBMG6           AGACTTTCGAAATTTACTAATTGTGTTCGTCCGTCTCAAACTGGCTCACACTTTGGTGGTCAATTTTACTTCTCAAGGTA
2 StcyFBPAtcyFBP_F  AGACTTTCGAAATTTACTAATTGTGTTCGTCCGTCTCAAACTGGCTCACACTTTGGTGGTCAATTTTACTTCTCAAGGTA
                                       Promoter StcyFBP

1 pExBMG6           AGCAATTACAGAATATGAATGTCGCTCTCCTCATATTTATCCGAACAATAAAAAATGATATCTGTTTGCATATGCATGTA
2 StcyFBPAtcyFBP_F  AGCAATTACAGAATATGAATGTCGCTCTCCTCATATTTATCCGAACAATAAAAAATGATATCTGTTTGCATATGCATGTA
                                       Promoter StcyFBP

1 pExBMG6           GATCACACACCCCCCCCCCCCCCGCCCCTAGATTCCCTCGATTTAGATTAAATATAATCATCTACAAGAATTCCGTTGGG
2 StcyFBPAtcyFBP_F  GATCACACACCCCCCCCCCCCCCGCCCCTAGATTCCCTCGATTTAGATTAAATATAATCATCTACAAGAATTCCGTTGGG
                                       Promoter StcyFBP

1 pExBMG6           CTTCATTATGTGTTTTTACATATTCGTTTCTGAACCACCCCCACCCCGGTGAAAAACATTGCTCTGCCACTGGCTCAATG
2 StcyFBPAtcyFBP_F  CTTCATTATGTGTTTTTACATATTCGTTTCTGAACCACCCCCACCCCGGTGAAAAACATTGCTCTGCCACTGGCTCAATG
                                       Promoter StcyFBP

1 pExBMG6           TATTGACACAAATGAACTTCAAACTGGGCAGGTGAATTATGCTCTAGGAGCATTGTATTATCTATGCAATGCATCAAACA
2 StcyFBPAtcyFBP_F  TATTGACACAAATGAACTTCAAACTGGGCAGGTGAATTATGCTCTAGGAGCATTGTATTATCTATGCAATGCATCAAACA
                                       Promoter StcyFBP

1 pExBMG6           AGGAAGAGATCTTAAAGCCAGAAGTAATTGATGCAATCAAAAGTTATGCAGCTGCAGGTGGAGTTAGTACAAGCTTCAGT
2 StcyFBPAtcyFBP_F  AGGAAGAGATCTTAAAGCCAGAAGTAATTGATGCAATCAAAAGTTATGCAGCTGCAGGTGGAGTTAGTACAAGCTTCAGT
                                       Promoter StcyFBP

1 pExBMG6           AATTTGGCTCAGGCTTTCTTAGATCAACATGTTCCTCAGCTTAATTAAAATGGAGGAAACCAAAGATTATGTTGTAAAAT
2 StcyFBPAtcyFBP_F  AATTTGGCTCAGGCTTTCTTAGATCAACATGTTCCTCAGCTTAATTAAAATGGAGGAAACCAAAGATTATGTTGTAAAAT
                                       Promoter StcyFBP

1 pExBMG6           CATTTTCTATCCTAGATGGTCTATCGGAAACAATTTATTTATTACTCCTATCCAATTCATTATATTTTCAAAAGTTATGA
2 StcyFBPAtcyFBP_F  CATTTTCTATCCTAGATGGTCTATCGGAAACAATTTATTTATTACTCCTATCCAATTCATTATATTTTCAAAAGTTATGA
                                       Promoter StcyFBP

1 pExBMG6           AGTCCACGAAATATGTGACGTGGGTAAAGAAGACCCATGCCAAGCCAGTGGGATATAGAAACAAAACATGTAATAAAGAG
2 StcyFBPAtcyFBP_F  AGTCCACGAAATATGTGACGTGGGTAAAGAAGACCCATGCCAAGCCAGTGGGATATAGAAACAAAACATGTAATAAAGAG
                                       Promoter StcyFBP

1 pExBMG6           AACAAATAATGAGTTTCGAAAAGAACAGAAGTTAGCATAAGGACGAGAATCACATTATCTTAGGTGCCAACCACTAATCC
2 StcyFBPAtcyFBP_F  AACAAATAATGAGTTTCGAAAAGAACAGAAGTTAGCATAAGGACGAGAATCACATTATCTTAGGTGCCAACCACTAATCC
                                       Promoter StcyFBP

1 pExBMG6           TATGTATCATTCTCCTCTTTCCACGTGTCATCCTACACTTCCTTTGCCATCAGATTAGATAGCCCGGTTAGTACCTACAC
2 StcyFBPAtcyFBP_F  TATGTATCATTCTCCTCTTTCCACGTGTCATCCTACACTTCCTTTGCCATCAGATTAGATAGCTT---------------
                                       Promoter StcyFBP
```

```
1 pExBMG6             TGTATATCAAAAAATACGTAACAATCATCCAAACATATCATCGATCAAAGGATATTTATCTTGATGTGCTTTCGCCGTCC
2 StcyFBPAtcyFBP_F    --------------TCCGTAAGGCCTTTCTTCA------------------------------------------------
```


```
1 pExBMG6             ATTGTAACGAGTTTGGATGAATTTGATATACACCCACTCAGATATCAATATATTTTATAAAAAGAAACAAAATTGAATAC
```


```
1 pExBMG6             TAGTAATATCTATGTAGATATTTATTTTTTCAACAATCCTGTAAGTTATAAGGATAACTCACTTATATGTGACGTGGATA
```

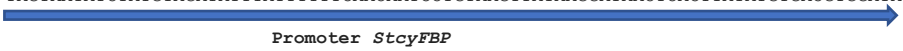


```
1 pExBMG6             ATGAAGAGCTAGGCAGGCAGTGAGAGATAGAAACAAATTAAGCAGAGACGAAAAACAAATCAGTTAACAGAATGACGAAT
```

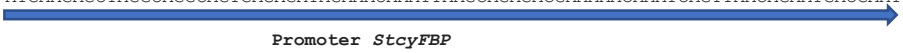


```
1 pExBMG6             TGGATCACGCTTTATCTTAGTGCCAACCACTGATCCCATGCATCACTCTGCTCTTTCCACGTGGCATCCTCTGACGTCAG
```


```
1 pExBMG6             ATCAGATTCCTCTTCTTTCTTTTTTTTTTCTGTATATATATGAGCATTTTAGTAGTccatggGGATCCATGGATCACGCA
3 StcyFBPAtcyFBP_R    ------------------------------------------------------------GGGAATTCCCGATCTAGTA
```


```
1 pExBMG6             GCAGATGCTCACCGTACGGATTTGATGACCATTACAAGATTCGTGTTGAATGAACAATCAAAGTATCCAGAATCTCGTGG
3 StcyFBPAtcyFBP_R    ACA------------------TAGATGAC-----------------------ACCGCTCAAGCTTTCCGGACTTTGCTGG
```


```
1 pExBMG6             TGATTTCACCATTTTGCTTAGTCACATCGTTTTGGGTTGCAAATTCGTTTGCAGTGCTGTTAATAAGGCTGGTTTGGCTA
3 StcyFBPAtcyFBP_R    TCTCTGCACCG--GGACTCGGACAGTACGTCTCCGG-CGCAATTCTATTTGAGGAGAC------------------TCTG
```


```
1 pExBMG6             AGTTAATTGGACTTGCAGGGGAAACAAACATTCAGGGTGAAGAGCAAAAGAAACTTGATGTGCTCTCTAATGATGTCTTT
3 StcyFBPAtcyFBP_R    TACCAGTCTACCACCGAAGGCAAGAAAATGGTCGACGTCCTCGTCGAGCAGAAC-----ATTGTCCCTGGTATCAAAGTC
```


```
1 pExBMG6             GTCAACGCTTTGGTTAGCAGTGGTAGAACT-----TCTGTTCTTGTCTCGGAG----GAAGATGAGGAAGCTACGTTTGT
3 StcyFBPAtcyFBP_R    GACAAGGGTTTGGTGCCACTTGTTGGATCCAACAATGAGTCATGGTGCCAAGGACTAGATGGTCTATCATCTCGAACTGC
```


```
1 pExBMG6             GGAGCCATCCAAGCGTGGAAAGTACTGTGTTGTTTTTGATCCGCTTGATGGATCTTCAAACATTGACTGTGGTGTTTCCA
3 StcyFBPAtcyFBP_R    TGCTTACTATCAACAGGGTGCGCGTTTCGCCAAATGGCGTACTGTCGTGAGCATTCCTAACGGTCCGTCTGCCCTCGCCG
```


```
1 pExBMG6             TTGGCACAATTTTTGGAATTTACACGTTGGACCACACTGATGAGCCAACCACTGCAGATGTTCTGAAACCTGGGAATGAA
3 StcyFBPAtcyFBP_R    TCAAAGAAGCTGCTTGGGGTCTTGCTCGATACGCTGCCATTTCACAGGACAGCGGTTTGGTTCCGATTGTTGAGCCAGAG
```


```
1 pExBMG6             A---TGGTGGCTGCAGGTTATTGTATGTACGGAAGCTCCTGCATGCTTGTGTTGAGCACTGGAACCGGTGTCCACGGATT
3 StcyFBPAtcyFBP_R    ATCTTGTTGGATGGAGAACACGACATTGACAGAACATACGACGTAGCAGAGAAGGTTTGGGCTGAGGTTTTCTTTTACCT
```


```
1 pExBMG6             TACACTGGACCCATCTCTAGGAGAGTTCATTCTAACTCACCCGGACATTAAGATTCCAAATAAGGGAAACATTTATTCGG
3 StcyFBPAtcyFBP_R    TGCTCAGAACAATGTCATGTTTGAAGGTATCCTCCTAAAACCGAGCATGGTGACTCC-----------------------
```


```
1 pExBMG6             TGAATGAAGGCAATGCGCAGAACTGGGATGGTCCAACTACAAAGTATGTAGAGAAATGCAAGTTTCCTAAAGATGGTTCT
3 StcyFBPAtcyFBP_R    ----CGGAGCTGAGTCTAAAGACAGAGCTACTCCTGAACAAGTTGCCGCCTACACCCTCAAGCTCCTCCGCAACAGAGTC
```


```
1 pExBMG6             CCTGCAAAGTCTCTGAGATACGTAGGAAGTATGGTAGCTGATGTTCATCGTACACTACTTTATGGAGGAATCTTCTTGTA
3 StcyFBPAtcyFBP_R    CCTCCCGCAGTCCCCGGAATCAT-------------GTTTTTGTCCGGAGGACAGTCGGAGGTGGAGGCAACACTCAACT
```


```
1 pExBMG6             CCCGGCTGACAAGAAAAGCCCCAATGGAAAATTGCGTGT-CTTGTATGAAGTTTTCCCGATGTCGTTTTTGATGGAGCAA
3 StcyFBPAtcyFBP_R    TGAACGCAATGAACCAGGCACCAAACCCATGGCACGTGTCCTTCTCCTACGCACGTGCGTTGCAGAACACTTGTCTGAAA
```


1 pExBMG6 GCCGGAGGTCAGGCCTTTACGGGAAAGAAAAGGGCGCTAGACCTTGTCCCGGAGAAGATCCATGAGCGTTCTCCGATATT
3 StcyFBPAtcyFBP_R ACATGGGGCGGCAGACCCGAGAACGTGAACGCAGCTCAGACCACTCTCTTGGCCCGTGCCAAGGCCAATTCGTTGGCTCA
AtcyFBP
1 pExBMG6 TCTTGGTAGCTACGATGATGTAGAAGAGATTAAAGCTCTCTATGCTGAGGAGGAAA----------
3 StcyFBPAtcyFBP_R GCTCGGAAAATACACCGGTGAGGGTGAGTCCGAAG------AGGCTAAGGAGGGCATGTTCGTCAAAGGGTACACCTATT
AtcyFBP
1 pExBMG6 ----------AGAAGAACTAACTCGAGGGTACCGCTCCCGGGTAGGAGCTcGAATTTCCCCGATCGTTC
3 StcyFBPAtcyFBP_R GAACTAGTCCATGGGGATCCCATATGGTCGACCTCGAGGGTACCGCTCCCGGGTAGGAGCTCGAATTTCCCCGATCGTTC
AtcyFBP
Nos Terminator
1 pExBMG6 AAACATTTGGCAATAAAGTTTCTTAAGATTGAATCCTGTTGCCGGTCTTGCGATGATTATCATATAATTTCTGTTGAATT
3 StcyFBPAtcyFBP_R AAACATTTGGCAATAAAGTTTCTTAAGATTGAATCCTGTTGCCGGTCTTGCGATGATTATCATATAATTTCTGTTGAATT
Nos Terminator
1 pExBMG6 ACGTTAAGCATGTAATAATTAACATGTAATGCATGACGTTATTTATGAGATGGGTTTTTATGATTAGAGTCCCGCAATTA
3 StcyFBPAtcyFBP_R ACGTTAAGCATGTAATAATTAACATGTAATGCATGACGTTATTTATGAGATGGGTTTTTATGATTAGAGTCCCGCAATTA
Nos Terminator
1 pExBMG6 TACATTTAATACGCGATAGAAAACAAAATATAGCGCGCAAACTAGGATAAATTATCGCGCGCGGTGTCATCTATGTTACT
3 StcyFBPAtcyFBP_R TACATTTAATACGCGATAGAAAACAAAATATAGCGCGCAAACTAGGATAAATTATCGCGCGCGGTGTCATCTATGTTACA
Nos Terminator
1 pExBMG6 AGATCGGgaattcgtaatcatggtcatagctgtttcctgtgtgaaattgttatccgctcacaattccacacaacatacga
3 StcyFBPAtcyFBP_R G----------
NosT

pSKJ10 - pUC18-StcyFBP-EcPP-NosT

```
1 pSKJ10          CCAGCTAATGCTGCTCTTGTCACTCAAAATGATGGTATCCCTCTCGTCATCCAGTGTTTGTCAAGTCCTGTTAGGAACAC
2 StcyFBPEcPP_F   CCAGCTAATGCTGCTCTTGTCACTCAAAATGATGGTATCCCTCTCGTCATCCAGTGTTTGTCAAGTCCTGTTAGGAACAC
```

Promoter *StcyFBP*

```
1 pSKJ10          AGTAAGGATATAAACAAACATTTTGTGGTCTTCTTGGTTATTGAGTGCTTGCTGTTCACTTGTTAAAATTGCACATATAC
2 StcyFBPEcPP_F   AGTAAGGATATAAACAAACATTTTGTGGTCTTCTTGGTTATTGAGTGCTTGCTGTTCACTTGTTAAAATTGCACATATAC
```

Promoter *StcyFBP*

```
1 pSKJ10          GTAGTGAGAAACTCAACTGTTGAGTACCATTGATCCGTCAATCTTGTCGATAACTTTGATAAGGATATTTCAGGCATCAG
2 StcyFBPEcPP_F   GTAGTGAGAAACTCAACTGTTGAGTACCATTGATCCGTCAATCTTGTCGATAACTTTGATAAGGATATTTCAGGCATCAG
```

Promoter *StcyFBP*

```
1 pSKJ10          ACATGTCACCTCTATAGAACTTGGTCTTTTTTTTTTAAAAATAAAAATAAAAATGTTTGGCATCATACGAACTTCTGTTAC
2 StcyFBPEcPP_F   ACATGTCACCTCTATAGAACTTGGTCTTTTTTTTTTAAAAATAAAAATAAAAATGTTTGGCATCATACGAACTTCTGTTAC
```

Promoter *StcyFBP*

```
1 pSKJ10          TTTAGGCTGTATCCAGAATAAAATGTTGTTTCCTCATTCTGGAATTAGTTGTTTTGCACACGGAAGACTTTCGAAATTTA
2 StcyFBPEcPP_F   TTTAGGCTGTATCCAGAATAAAATGTTGTTTCCTCATTCTGGAATTAGTTGTTTTGCACACGGAAGACTTTCGAAATTTA
```

Promoter *StcyFBP*

```
1 pSKJ10          CTAATTGTGTTCGTCCGTCTCAAACTGGCTCACACTTTGGTGGTCAATTTTACTTCTCAAGGTAAGCAATTACAGAATAT
2 StcyFBPEcPP_F   CTAATTGTGTTCGTCCGTCTCAAACTGGCTCACACTTTGGTGGTCAATTTTACTTCTCAAGGTAAGCAATTACAGAATAT
```

Promoter *StcyFBP*

```
1 pSKJ10          GAATGTCGCTCTCCTCATATTTATCCGAACAATAAAAAATGATATCTGTTTGCATATGCATGTAGATCACACACCCCCCC
2 StcyFBPEcPP_F   GAATGTCGCTCTCCTCATATTTATCCGAACAATAAAAAATGATATCTGTTTGCATATGCATGTAGATCACACACCCCCCC
```

Promoter *StcyFBP*

```
1 pSKJ10          CCCCCCCGCCCCTAGATTCCCTCGATTTAGATTAAATATAATCATCTACAAGAATTCCGTTGGGCTTCATTATGTGTTTT
2 StcyFBPEcPP_F   CCCCCCCGCCCCTAGATTCCCTCGATTTAGATTAAATATAATCATCTACAAGAATTCCGTTGGGCTTCATTATGTGTTTT
```

Promoter *StcyFBP*

```
1 pSKJ10          TACATATTCGTTTCTGAACCACCCCCACCCCGGTGAAAAACATTGCTCTGCCACTGGCTCAATGTATTGACACAAATGAA
2 StcyFBPEcPP_F   TACATATTCGTTTCTGAACCACCCCCACCCCGGTGAAAAACATTGCTCTGCCACTGGCTCAATGTATTGACACAAATGAA
```

Promoter *StcyFBP*

```
1 pSKJ10          CTTCAAACTGGGCAGGTGAATTATGCTCTAGGAGCATTGTATTATCTATGCAATGCATCAAACAAGGAAGAGATCTTAAA
2 StcyFBPEcPP_F   CTTCAAACTGGGCAGGTGAATTATGCTCTAGGAGCATTGTATTATCTATGCAATGCATCAAACAAGGAAGAGATCTTAAA
```

Promoter *StcyFBP*

```
1 pSKJ10          GCCAGAAGTAATTGATGCAATCAAAAGTTATGCAGCTGCAGGTGGAGTTAGTACAAGCTTCAGTAATTTGGCTCAGGCTT
2 StcyFBPEcPP_F   GCCAGAAGTAATTGATGCAATCAAAAGTTATGCAGCTGCAGGTGGAGTTAGTACAAGCTTCAGTAATTTGGCTCAGGCTT
```

Promoter *StcyFBP*

```
1 pSKJ10          TCTTAGATCAACATGTTCCTCAGCTTAATTAAAATGGAGGAAACCAAAGATTATGTTGTAAAATCATTTTCTATCCTAGA
2 StcyFBPEcPP_F   TCTTAGATCAACATGTTCCTCAGCTTAATTAAAATGGAGGAAACCAAAGATTATGTTGTAAAATCATTTTCTATCCTAGA
```

Promoter *StcyFBP*

```
1 pSKJ10          TGGTCTATCGGAAACAATTTATTTATTACTCCTATCCAATTCATTATATTTTCAAAAGTTATGAAGTCCACGAAATATGT
2 StcyFBPEcPP_F   TGGTCTATCGGAAACAATTTATTTATTACTCCTATCCAATTCATTATATTTTCAAAAGTTATGAAGTCCACGAAATATGT
```

Promoter *StcyFBP*

```
1 pSKJ10          GACGTGGGTAAAGAAGACCCATGCCAAGCCAGTGGGATATAGAAACAAAACATGTAATAAAGAGAACAAATAATGAGTTT
2 StcyFBPEcPP_F   GACGTGGGTAAAGAAGACCCATGCCAAGCCAGTGGGATATAGAAACAAAACATGTAATAAAGAGAACAAATAATGAGTTT
```

Promoter *StcyFBP*

```
1 pSKJ10          CGAAAAGAACAGAAGTTAGCATAAGGACGAGAATCACATTATCTTAGGTGCCAACCACTAATCCTATGTATCATTCTCCT
2 StcyFBPEcPP_F   CGAAAAGAACAGAAGTTAGCATA--TCCCCAACTCCCGTAACCCCGCTTGCAAGCCGGGGGTTCT--------------
```

Promoter *StcyFBP*

```
1 pSKJ10          CTTTCCACGTGTCATCCTACACTTCCTTTGCCATCAGATTAGATAGCCCGGTTAGTACCTACACTGTATATCAAAAAATA
2 StcyFBPEcPP_F   --------------TGTTGAATCCCGTTTGCC------------CGTCCCGGGTTG-------GCCGTTTCCTGAAAAAT-
```

Promoter *StcyFBP*

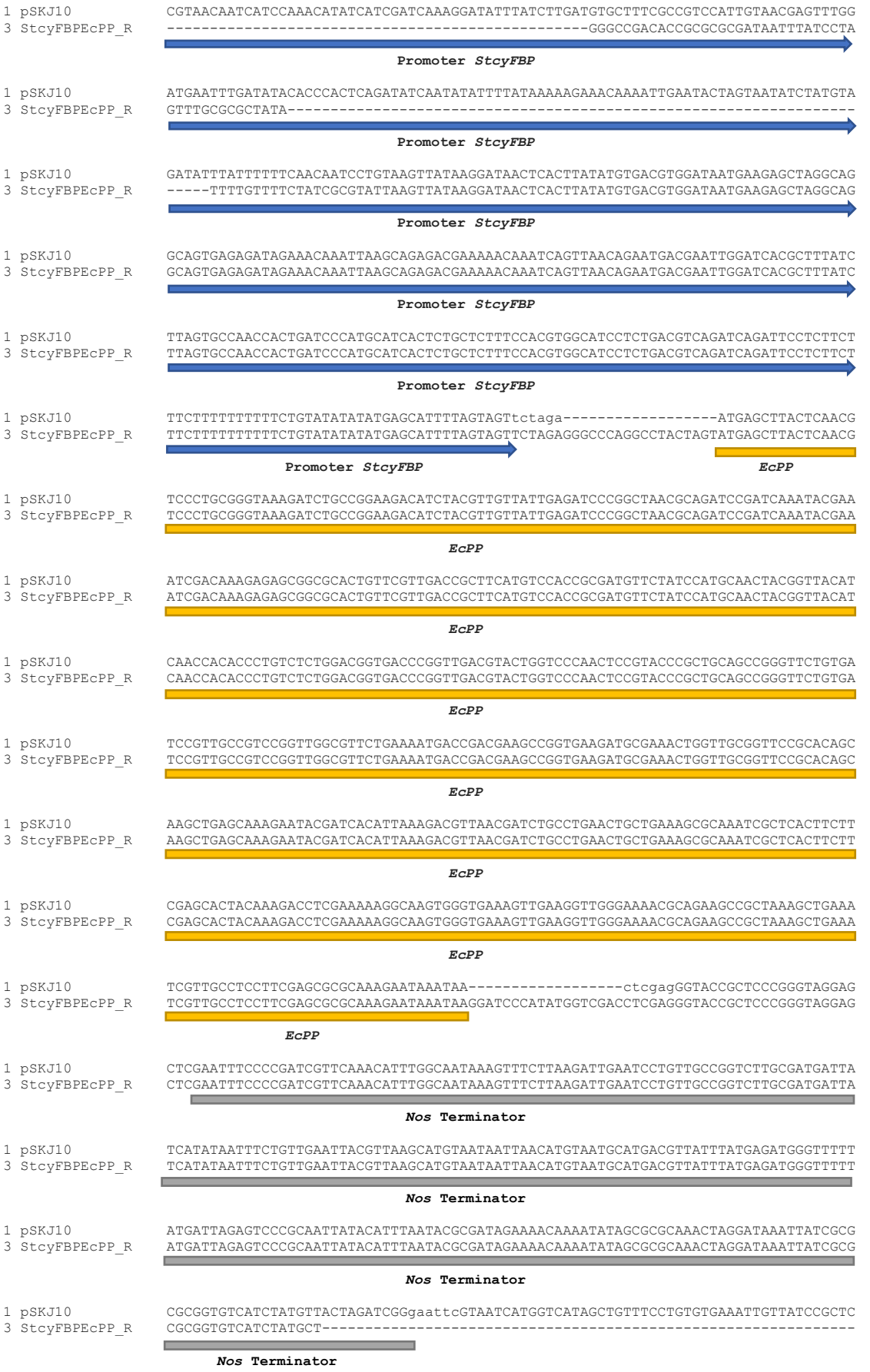
1 pSKJ10 CGTAACAATCATCCAAACATATCATCGATCAAAGGATATTTATCTTGATGTGCTTTCGCCGTCCATTGTAACGAGTTTGG
3 StcyFBPEcPP_R ----------GGGCCGACACCGCGCGCGATAATTTATCCTA
Promoter StcyFBP
1 pSKJ10 ATGAATTTGATATACACCCACTCAGATATCAATATATTTTATAAAAAGAAACAAAATTGAATACTAGTAATATCTATGTA
3 StcyFBPEcPP_R GTTTGCGCGCTATA----------
Promoter StcyFBP
1 pSKJ10 GATATTTATTTTTTCAACAATCCTGTAAGTTATAAGGATAACTCACTTATATGTGACGTGGATAATGAAGAGCTAGGCAG
3 StcyFBPEcPP_R -----TTTTGTTTTCTATCGCGTATTAAGTTATAAGGATAACTCACTTATATGTGACGTGGATAATGAAGAGCTAGGCAG
Promoter StcyFBP
1 pSKJ10 GCAGTGAGAGATAGAAACAAATTAAGCAGAGACGAAAAACAAATCAGTTAACAGAATGACGAATTGGATCACGCTTTATC
3 StcyFBPEcPP_R GCAGTGAGAGATAGAAACAAATTAAGCAGAGACGAAAAACAAATCAGTTAACAGAATGACGAATTGGATCACGCTTTATC
Promoter StcyFBP
1 pSKJ10 TTAGTGCCAACCACTGATCCCATGCATCACTCTGCTCTTTCCACGTGGCATCCTCTGACGTCAGATCAGATTCCTCTTCT
3 StcyFBPEcPP_R TTAGTGCCAACCACTGATCCCATGCATCACTCTGCTCTTTCCACGTGGCATCCTCTGACGTCAGATCAGATTCCTCTTCT
Promoter StcyFBP
1 pSKJ10 TTCTTTTTTTTTTCTGTATATATATGAGCATTTTAGTAGTtctaga----------ATGAGCTTACTCAACG
3 StcyFBPEcPP_R TTCTTTTTTTTTTCTGTATATATATGAGCATTTTAGTAGTTCTAGAGGGCCCAGGCCTACTAGTATGAGCTTACTCAACG
Promoter StcyFBP
EcPP
1 pSKJ10 TCCCTGCGGGTAAAGATCTGCCGGAAGACATCTACGTTGTTATTGAGATCCCGGCTAACGCAGATCCGATCAAATACGAA
3 StcyFBPEcPP_R TCCCTGCGGGTAAAGATCTGCCGGAAGACATCTACGTTGTTATTGAGATCCCGGCTAACGCAGATCCGATCAAATACGAA
EcPP
1 pSKJ10 ATCGACAAAGAGAGCGGCGCACTGTTCGTTGACCGCTTCATGTCCACCGCGATGTTCTATCCATGCAACTACGGTTACAT
3 StcyFBPEcPP_R ATCGACAAAGAGAGCGGCGCACTGTTCGTTGACCGCTTCATGTCCACCGCGATGTTCTATCCATGCAACTACGGTTACAT
EcPP
1 pSKJ10 CAACCACACCCTGTCTCTGGACGGTGACCCGGTTGACGTACTGGTCCCAACTCCGTACCCGCTGCAGCCGGGTTCTGTGA
3 StcyFBPEcPP_R CAACCACACCCTGTCTCTGGACGGTGACCCGGTTGACGTACTGGTCCCAACTCCGTACCCGCTGCAGCCGGGTTCTGTGA
EcPP
1 pSKJ10 TCCGTTGCCGTCCGGTTGGCGTTCTGAAAATGACCGACGAAGCCGGTGAAGATGCGAAACTGGTTGCGGTTCCGCACAGC
3 StcyFBPEcPP_R TCCGTTGCCGTCCGGTTGGCGTTCTGAAAATGACCGACGAAGCCGGTGAAGATGCGAAACTGGTTGCGGTTCCGCACAGC
EcPP
1 pSKJ10 AAGCTGAGCAAAGAATACGATCACATTAAAGACGTTAACGATCTGCCTGAACTGCTGAAAGCGCAAATCGCTCACTTCTT
3 StcyFBPEcPP_R AAGCTGAGCAAAGAATACGATCACATTAAAGACGTTAACGATCTGCCTGAACTGCTGAAAGCGCAAATCGCTCACTTCTT
EcPP
1 pSKJ10 CGAGCACTACAAAGACCTCGAAAAAGGCAAGTGGGTGAAAGTTGAAGGTTGGGAAAACGCAGAAGCCGCTAAAGCTGAAA
3 StcyFBPEcPP_R CGAGCACTACAAAGACCTCGAAAAAGGCAAGTGGGTGAAAGTTGAAGGTTGGGAAAACGCAGAAGCCGCTAAAGCTGAAA
EcPP
1 pSKJ10 TCGTTGCCTCCTTCGAGCGCGCAAAGAATAAATAA----------ctcgagGGTACCGCTCCCGGGTAGGAG
3 StcyFBPEcPP_R TCGTTGCCTCCTTCGAGCGCGCAAAGAATAAATAAGGATCCCATATGGTCGACCTCGAGGGTACCGCTCCCGGGTAGGAG
EcPP
1 pSKJ10 CTCGAATTTCCCCGATCGTTCAAACATTTGGCAATAAAGTTTCTTAAGATTGAATCCTGTTGCCGGTCTTGCGATGATTA
3 StcyFBPEcPP_R CTCGAATTTCCCCGATCGTTCAAACATTTGGCAATAAAGTTTCTTAAGATTGAATCCTGTTGCCGGTCTTGCGATGATTA
Nos Terminator
1 pSKJ10 TCATATAATTTCTGTTGAATTACGTTAAGCATGTAATAATTAACATGTAATGCATGACGTTATTTATGAGATGGGTTTTT
3 StcyFBPEcPP_R TCATATAATTTCTGTTGAATTACGTTAAGCATGTAATAATTAACATGTAATGCATGACGTTATTTATGAGATGGGTTTTT
Nos Terminator
1 pSKJ10 ATGATTAGAGTCCCGCAATTATACATTTAATACGCGATAGAAAACAAAATATAGCGCGCAAACTAGGATAAATTATCGCG
3 StcyFBPEcPP_R ATGATTAGAGTCCCGCAATTATACATTTAATACGCGATAGAAAACAAAATATAGCGCGCAAACTAGGATAAATTATCGCG
Nos Terminator
1 pSKJ10 CGCGGTGTCATCTATGTTACTAGATCGGgaattcGTAATCATGGTCATAGCTGTTTCCTGTGTGAAATTGTTATCCGCTC
3 StcyFBPEcPP_R CGCGGTGTCATCTATGCT----------
Nos Terminator

pSKJ24 – pUC18-SlRbcS-AtSWEET11-NosT

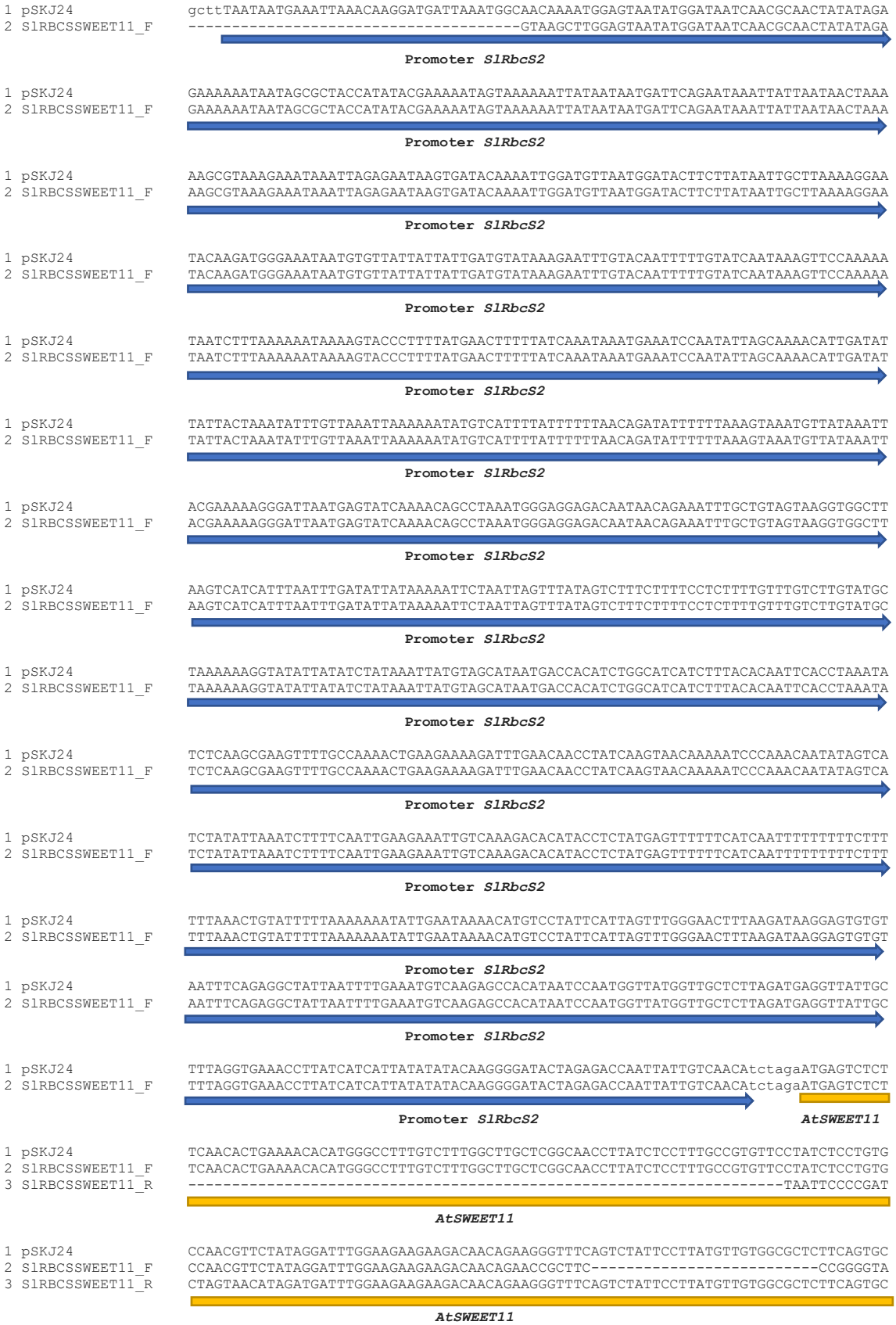

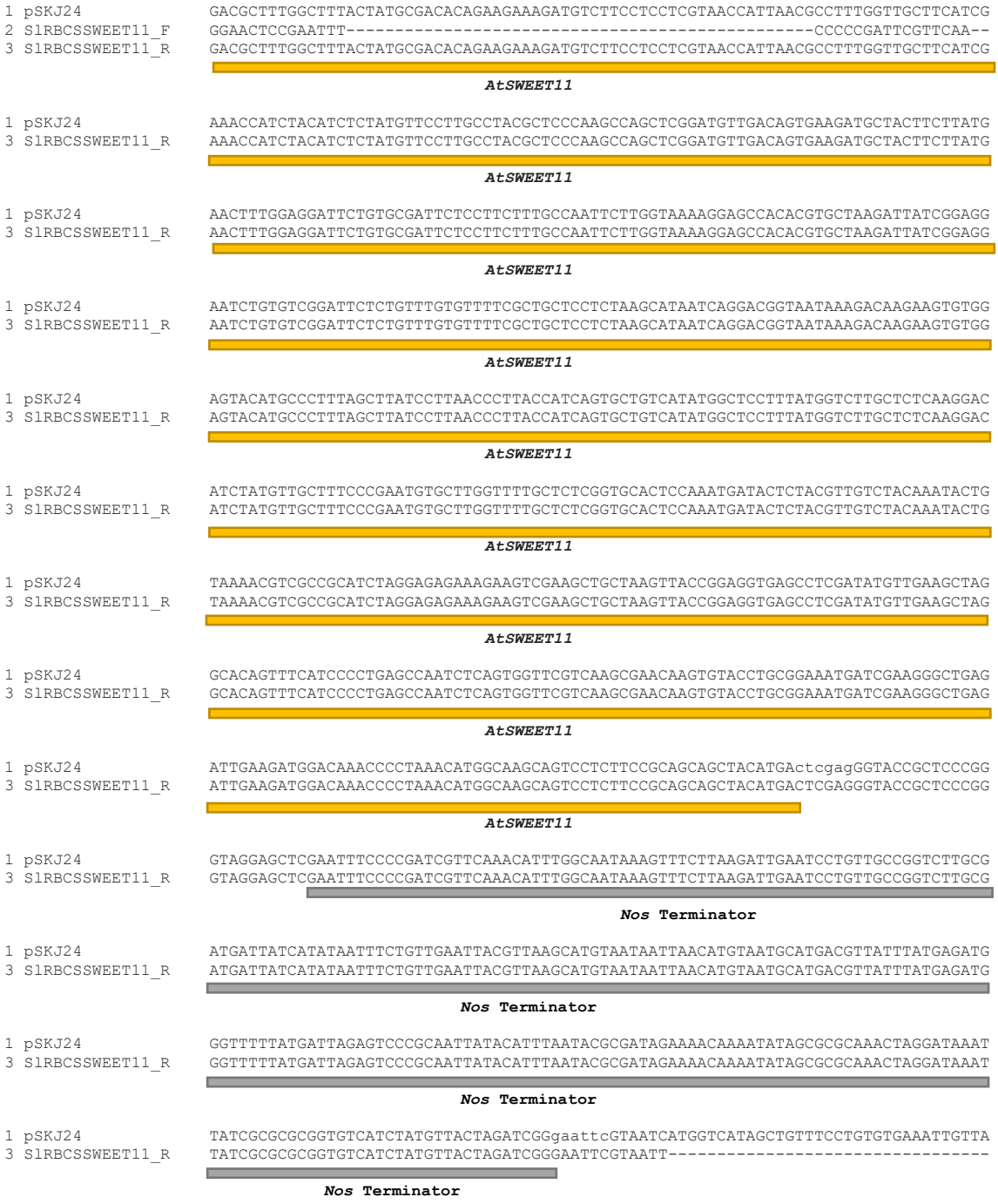
1 pSKJ24 GACGCTTTGGCTTTACTATGCGACACAGAAGAAAGATGTCTTCCTCCTCGTAACCATTAACGCCTTTGGTTGCTTCATCG
2 SlRBCSSWEET11_F GGAACTCCGAATTT----------CCCCCGATTCGTTCAA--
3 SlRBCSSWEET11_R GACGCTTTGGCTTTACTATGCGACACAGAAGAAAGATGTCTTCCTCCTCGTAACCATTAACGCCTTTGGTTGCTTCATCG
AtSWEET11
1 pSKJ24 AAACCATCTACATCTCTATGTTCCTTGCCTACGCTCCCAAGCCAGCTCGGATGTTGACAGTGAAGATGCTACTTCTTATG
3 SlRBCSSWEET11_R AAACCATCTACATCTCTATGTTCCTTGCCTACGCTCCCAAGCCAGCTCGGATGTTGACAGTGAAGATGCTACTTCTTATG
AtSWEET11
1 pSKJ24 AACTTTGGAGGATTCTGTGCGATTCTCCTTCTTTGCCAATTCTTGGTAAAAGGAGCCACACGTGCTAAGATTATCGGAGG
3 SlRBCSSWEET11_R AACTTTGGAGGATTCTGTGCGATTCTCCTTCTTTGCCAATTCTTGGTAAAAGGAGCCACACGTGCTAAGATTATCGGAGG
AtSWEET11
1 pSKJ24 AATCTGTGTCGGATTCTCTGTTTGTGTTTTCGCTGCTCCTCTAAGCATAATCAGGACGGTAATAAAGACAAGAAGTGTGG
3 SlRBCSSWEET11_R AATCTGTGTCGGATTCTCTGTTTGTGTTTTCGCTGCTCCTCTAAGCATAATCAGGACGGTAATAAAGACAAGAAGTGTGG
AtSWEET11
1 pSKJ24 AGTACATGCCCTTTAGCTTATCCTTAACCCTTACCATCAGTGCTGTCATATGGCTCCTTTATGGTCTTGCTCTCAAGGAC
3 SlRBCSSWEET11_R AGTACATGCCCTTTAGCTTATCCTTAACCCTTACCATCAGTGCTGTCATATGGCTCCTTTATGGTCTTGCTCTCAAGGAC
AtSWEET11
1 pSKJ24 ATCTATGTTGCTTTCCCGAATGTGCTTGGTTTTGCTCTCGGTGCACTCCAAATGATACTCTACGTTGTCTACAAATACTG
3 SlRBCSSWEET11_R ATCTATGTTGCTTTCCCGAATGTGCTTGGTTTTGCTCTCGGTGCACTCCAAATGATACTCTACGTTGTCTACAAATACTG
AtSWEET11
1 pSKJ24 TAAAACGTCGCCGCATCTAGGAGAGAAAGAAGTCGAAGCTGCTAAGTTACCGGAGGTGAGCCTCGATATGTTGAAGCTAG
3 SlRBCSSWEET11_R TAAAACGTCGCCGCATCTAGGAGAGAAAGAAGTCGAAGCTGCTAAGTTACCGGAGGTGAGCCTCGATATGTTGAAGCTAG
AtSWEET11
1 pSKJ24 GCACAGTTTCATCCCCTGAGCCAATCTCAGTGGTTCGTCAAGCGAACAAGTGTACCTGCGGAAATGATCGAAGGGCTGAG
3 SlRBCSSWEET11_R GCACAGTTTCATCCCCTGAGCCAATCTCAGTGGTTCGTCAAGCGAACAAGTGTACCTGCGGAAATGATCGAAGGGCTGAG
AtSWEET11
1 pSKJ24 ATTGAAGATGGACAAACCCCTAAACATGGCAAGCAGTCCTCTTCCGCAGCAGCTACATGActcgagGGTACCGCTCCCGG
3 SlRBCSSWEET11_R ATTGAAGATGGACAAACCCCTAAACATGGCAAGCAGTCCTCTTCCGCAGCAGCTACATGACTCGAGGGTACCGCTCCCGG
AtSWEET11
1 pSKJ24 GTAGGAGCTCGAATTTCCCCGATCGTTCAAACATTTGGCAATAAAGTTTCTTAAGATTGAATCCTGTTGCCGGTCTTGCG
3 SlRBCSSWEET11_R GTAGGAGCTCGAATTTCCCCGATCGTTCAAACATTTGGCAATAAAGTTTCTTAAGATTGAATCCTGTTGCCGGTCTTGCG
Nos Terminator
1 pSKJ24 ATGATTATCATATAATTTCTGTTGAATTACGTTAAGCATGTAATAATTAACATGTAATGCATGACGTTATTTATGAGATG
3 SlRBCSSWEET11_R ATGATTATCATATAATTTCTGTTGAATTACGTTAAGCATGTAATAATTAACATGTAATGCATGACGTTATTTATGAGATG
Nos Terminator
1 pSKJ24 GGTTTTTATGATTAGAGTCCCGCAATTATACATTTAATACGCGATAGAAAACAAAATATAGCGCGCAAACTAGGATAAAT
3 SlRBCSSWEET11_R GGTTTTTATGATTAGAGTCCCGCAATTATACATTTAATACGCGATAGAAAACAAAATATAGCGCGCAAACTAGGATAAAT
Nos Terminator
1 pSKJ24 TATCGCGCGCGGTGTCATCTATGTTACTAGATCGGgaattcGTAATCATGGTCATAGCTGTTTCCTGTGTGAAATTGTTA
3 SlRBCSSWEET11_R TATCGCGCGCGGTGTCATCTATGTTACTAGATCGGGAATTCGTAATT----------
Nos Terminator

pSKJ5 – pUC18-CoYMV-AtSUC2-NosT

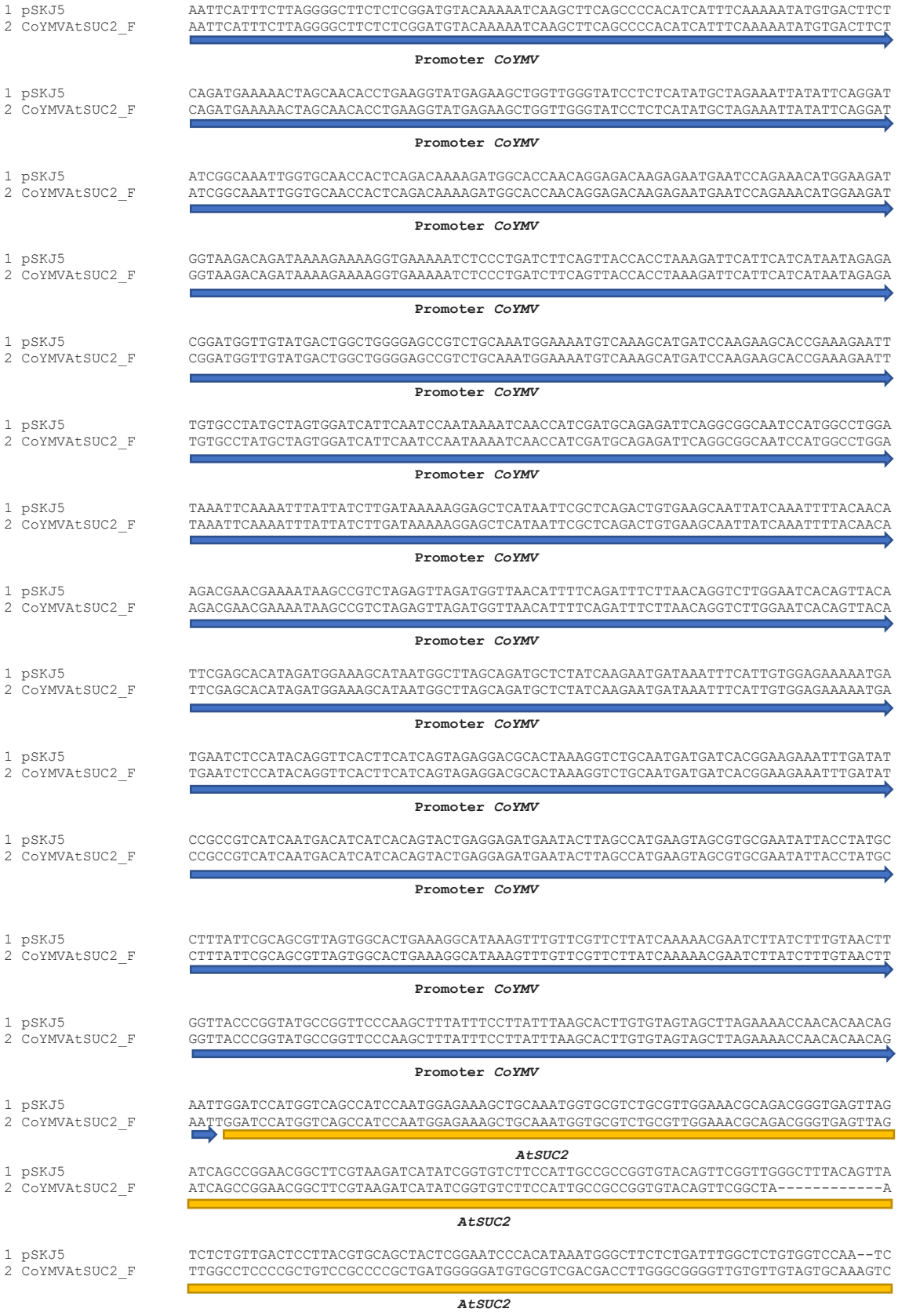


1 pSKJ5 TCCGGTATGCTTGTTCAGCCTATCGTCGGTTACCACAGTGACCGTTGCACCTCAAGATTCGGCCGTCGTCGTCCCTTCAT
2 CoYMVAtSUC2_F ATCTGTATGATGAGTTGAGCCA-----GGTAA----------
AtSUC2
1 pSKJ5 CGTCGCTGGAGCTGGTTTAGTCACCGTTGCTGTTTTCCTTATCGGTTACGCTGCCGATATAGGTCACAGCATGGGCGATC
AtSUC2
1 pSKJ5 AGCTTGACAAACCGCCGAAAACGCGAGCCATCGCGATATTCGCTCTCGGGTTTTGGATTCTTGACGTGGCTAACAACACC
AtSUC2
1 pSKJ5 TTACAAGGACCCTGCAGAGCTTTCTTGGCTGATTTATCAGCAGGGAACGCTAAGAAAACGCGAACCGCAAACGCGTTTTT
AtSUC2
1 pSKJ5 CTCGTTTTTCATGGCGGTTGGAAACGTTTTGGGTTACGCTGCGGGATCTTACAGAAATCTCTACAAAGTTGTGCCTTTCA
AtSUC2
1 pSKJ5 CGATGACTGAGTCATGCGATCTCTACTGCGCAAACCTCAAAA---CGTGTTTTTTCCTATCCATAACGCTTCTCC-TCAT
3 CoYMVAtSUC2_R ----------AAACCTCAAAAACGTGTTTTTTTCCTATCCAAAAACGCTTCTCCTTCAT
AtSUC2
1 pSKJ5 AGTC--ACTTTCGTATCTCTCTGTTACGTGAA-GGAGAAGCCATGGACGCCAGAGCCAACAGCCGATGGAAAAGCC-TCC
3 CoYMVAtSUC2_R AGTCCACTTTCGGAATCTCTCTGTTACGTGAAGGGAGAAGCCATGGACGCCAGAGCCAACAGCCGATGGAAAAGCCTTCC
AtSUC2
1 pSKJ5 AACGTTCCGTTTTTCGGAGAAATCTTCGGAGCTTTCAAGGAACTAAAAAGACCCATGTGGATGCTTCTTATAGTCACTGC
3 CoYMVAtSUC2_R AACGTTCCGTTTTTCGGAGAAATCTTCGGAGCTTTCAAGGAACTAAAAAGACCCATGTGGATGCTTCTTATAGTCACTGC
AtSUC2
1 pSKJ5 ACTAAACTGGATCGCTTGGTTCCCTTTCCTTCTCTTCGACACTGATTGGATGGGCCGTGAGGTGTACGGAGGAAACTCAG
3 CoYMVAtSUC2_R ACTAAACTGGATCGCTTGGTTCCCTTTCCTTCTCTTCGACACTGATTGGATGGGCCGTGAGGTGTACGGAGGAAACTCAG
AtSUC2
1 pSKJ5 ACGCAACCGCAACCGCAGCCTCTAAGAAGCTTTACAACGACGGAGTCAGAGCTGGTGCTTTGGGGCTTATGCTTAACGCT
3 CoYMVAtSUC2_R ACGCAACCGCAACCGCAGCCTCTAAGAAGCTTTACAACGACGGAGTCAGAGCTGGTGCTTTGGGGCTTATGCTTAACGCT
AtSUC2
1 pSKJ5 ATTGTTCTTGGTTTCATGTCTCTTGGTGTTGAATGGATTGGTCGGAAATTGGGAGGAGCTAAAAGGCTTTGGGGTATTGT
3 CoYMVAtSUC2_R ATTGTTCTTGGTTTCATGTCTCTTGGTGTTGAATGGATTGGTCGGAAATTGGGAGGAGCTAAAAGGCTTTGGGGTATTGT
AtSUC2
1 pSKJ5 TAACTTCATCCTCGCCATTTGCTTGGCCATGACGGTTGTGGTTACGAAACAAGCTGAGAATCACCGACGAGATCACGGCG
3 CoYMVAtSUC2_R TAACTTCATCCTCGCCATTTGCTTGGCCATGACGGTTGTGGTTACGAAACAAGCTGAGAATCACCGACGAGATCACGGCG
AtSUC2
1 pSKJ5 GCGCTAAAACAGGTCCACCTGGTAACGTCACAGCTGGTGCTTTAACTCTCTTCGCCATCCTCGGTATCCCCCAAGCCATT
3 CoYMVAtSUC2_R GCGCTAAAACAGGTCCACCTGGTAACGTCACAGCTGGTGCTTTAACTCTCTTCGCCATCCTCGGTATCCCCCAAGCCATT
AtSUC2
1 pSKJ5 ACGTTTAGCATTCCTTTTGCACTAGCTTCCATATTTTCAACCAATTCCGGTGCCGGCCAAGGACTTTCCCTAGGTGTTCT
3 CoYMVAtSUC2_R ACGTTTAGCATTCCTTTTGCACTAGCTTCCATATTTTCAACCAATTCCGGTGCCGGCCAAGGACTTTCCCTAGGTGTTCT
AtSUC2
1 pSKJ5 GAATCTAGCCATTGTCGTCCCTCAGATGGTAATATCTGTGGGAGGTGGACCATTCGACGAACTATTCGGTGGTGGAAACA
3 CoYMVAtSUC2_R GAATCTAGCCATTGTCGTCCCTCAGATGGTAATATCTGTGGGAGGTGGACCATTCGACGAACTATTCGGTGGTGGAAACA
AtSUC2
1 pSKJ5 TTCCAGCATTTGTGTTAGGAGCGATTGCGGCAGCGGTAAGTGGTGTATTGGCGTTGACGGTGTTGCCTTCACCGCCTCCG
3 CoYMVAtSUC2_R TTCCAGCATTTGTGTTAGGAGCGATTGCGGCAGCGGTAAGTGGTGTATTGGCGTTGACGGTGTTGCCTTCACCGCCTCCG
AtSUC2
1 pSKJ5 GATGCTCCTGCCTTCAAAGCTACTATGGGATTTCATGActcgagGGTACCGCTCCCGGGTAGGAGCTCGAATTTCCCCGA
3 CoYMVAtSUC2_R GATGCTCCTGCCTTCAAAGCTACTATGGGATTTCATGACTCGAGGGTACCGCTCCCGGGTAGGAGCTCGAATTTCCCCGA
AtSUC2
Nos Terminator

```
1 pSKJ5              TCGTTCAAACATTTGGCAATAAAGTTTCTTAAGATTGAATCCTGTTGCCGGTCTTGCGATGATTATCATATAATTTCTGT
3 CoYMVAtSUC2_R      TCGTTCAAACATTTGGCAATAAAGTTTCTTAAGATTGAATCCTGTTGCCGGTCTTGCGATGATTATCATATAATTTCTGT
```

***Nos* Terminator**

```
1 pSKJ5              TGAATTACGTTAAGCATGTAATAATTAACATGTAATGCATGACGTTATTTATGAGATGGGTTTTTATGATTAGAGTCCCG
3 CoYMVAtSUC2_R      TGAATTACGTTAAGCATGTAATAATTAACATGTAATGCATGACGTTATTTATGAGATGGGTTTTTATGATTAGAGTCCCG
```

***Nos* Terminator**

```
1 pSKJ5              CAATTATACATTTAATACGCGATAGAAAACAAAATATAGCGCGCAAACTAGGATAAATTATCGCGCGCGGTGTCATCTAT
3 CoYMVAtSUC2_R      CAATTATACATTTAATACGCGATAGAAAACAAAATATAGCGCGCAAACTAGGATAAATTATCGCGCGCGGTGTCATCTAT
```

***Nos* Terminator**

```
1 pSKJ5              GTTACTAGATCGGgaattcGTAATCATGGTCATAGCTGTTTCCTGTGTGAAATTGTTATCCGCTCACAATTCCACACAAC
3 CoYMVAtSUC2_R      GTA-----------------------------------------------------------------------------
```

***Nos*T**

pCR8/GW/TOPO-AtFIS1A

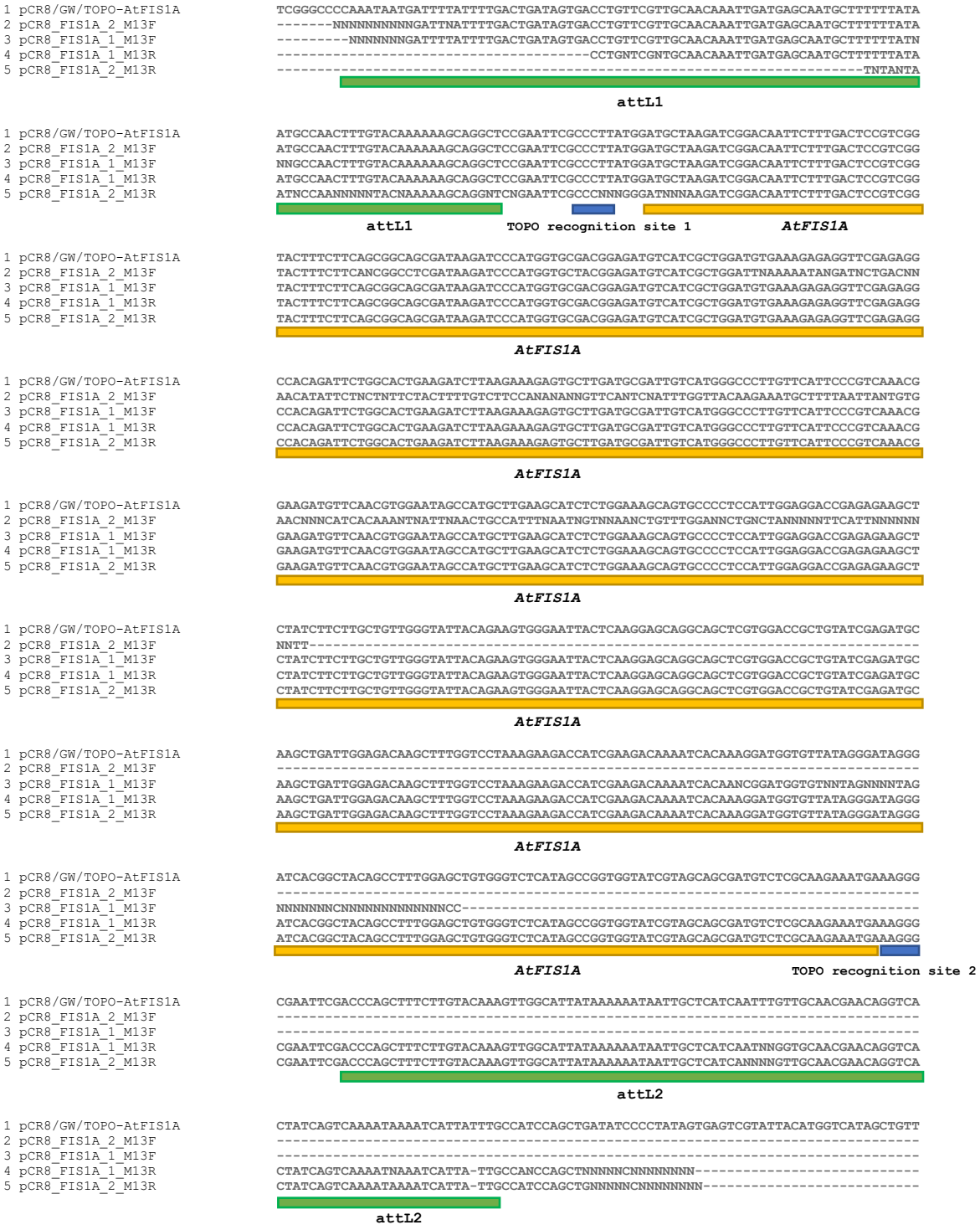

pK7WG2::CaMV35S-AtFIS1A-35ST

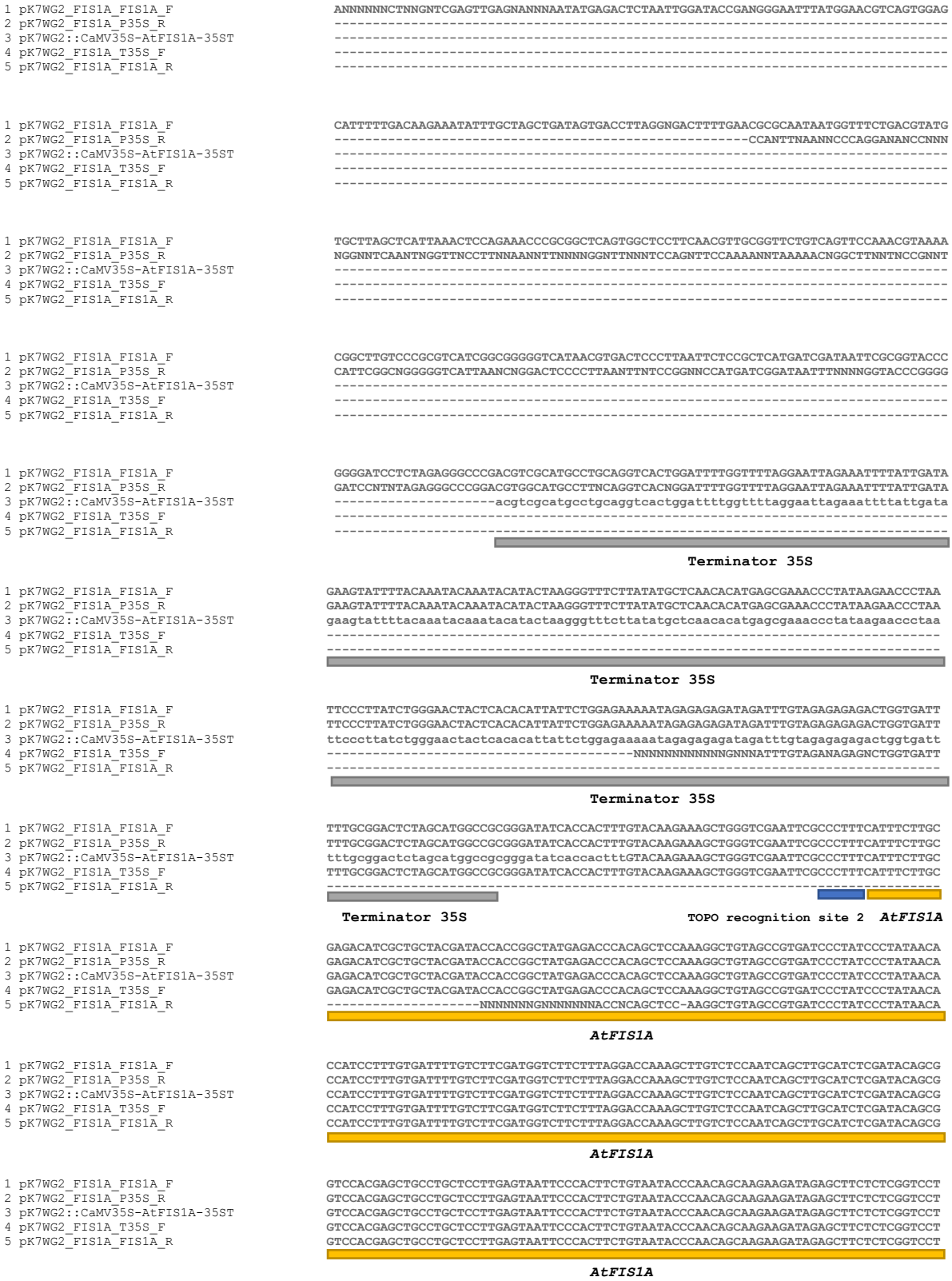

```
1 pK7WG2_FIS1A_FIS1A_F              CCAATGGAGGGGCACTGCTTTCCAGAGATGCTTCAAGCATGGCTATTCCACGTTGAACATCTTCCGTTTGACGGGAATGA
2 pK7WG2_FIS1A_P35S_R               CCAATGGAGGGGCACTGCTTTCCAGAGATGCTTCAAGCATGGCTATTCCACGTTGAACATCTTCCGTTTGACGGGAATGA
3 pK7WG2::CaMV35S-AtFIS1A-35ST      CCAATGGAGGGGCACTGCTTTCCAGAGATGCTTCAAGCATGGCTATTCCACGTTGAACATCTTCCGTTTGACGGGAATGA
4 pK7WG2_FIS1A_T35S_F               CCAATGGAGGGGCACTGCTTTCCAGAGATGCTTCAAGCATGGCTATTCCACGTTGAACATCTTCCGTTTGACGGGAATGA
5 pK7WG2_FIS1A_FIS1A_R              CCAATGGAGGGGCACTGCTTTCCAGAGATGCTTCAAGCATGGCTATTCCACGTTGAACATCTTCCGTTTGACGGGAATGA
                                                                    AtFIS1A
```

```
1 pK7WG2_FIS1A_FIS1A_F              ACAAGGGCCCATGACAATCGCATCAAGCACTCTTTCTTAAGATCTTCAGTGCCAGAATCTGTGGCCTCTCGAACCTCTCT
2 pK7WG2_FIS1A_P35S_R               ACAAGGGCCCATGACAATCGCATCAAGCACTCTTTCTTAAGATCTTCAGTGCCAGAATCTGTGGCCTCTCGAACCTCTCT
3 pK7WG2::CaMV35S-AtFIS1A-35ST      ACAAGGGCCCATGACAATCGCATCAAGCACTCTTTCTTAAGATCTTCAGTGCCAGAATCTGTGGCCTCTCGAACCTCTCT
4 pK7WG2_FIS1A_T35S_F               ACAAGGGCCCATGACAATCGCATCAAGCACTCTTTCTTAAGATCTTCAGTGCCAGAATCTGTGGCCTCTCGAACCTCTCT
5 pK7WG2_FIS1A_FIS1A_R              ACAAGGGCCCATGACAATCGCATCAAGCACTCTTTCTTAAGATCTTCAGTGCCAGAATCTGTGGCCTCTCGAACCTCTCT
                                                                    AtFIS1A
```

```
1 pK7WG2_FIS1A_FIS1A_F              TTCACATCCAGCGATGACATCTCCGTCGCACCATGGGATCTTATCGCTGCCGNGAAGANNNNNNNNNNN-----------
2 pK7WG2_FIS1A_P35S_R               TTCACATCCAGCGATGACATCTCCGTCGCACCATGGGATCTTATCGCTGCCGCTGAAGAAAGTACCGACGGAGTCAAAGA
3 pK7WG2::CaMV35S-AtFIS1A-35ST      TTCACATCCAGCGATGACATCTCCGTCGCACCATGGGATCTTATCGCTGCCGCTGAAGAAAGTACCGACGGAGTCAAAGA
4 pK7WG2_FIS1A_T35S_F               TTCACATCCAGCGATGACATCTCCGTCGCACCATGGGATCTTATCGCTGCCGCTGAAGAAAGTACCGACGGAGTCAAAGA
5 pK7WG2_FIS1A_FIS1A_R              TTCACATCCAGCGATGACATCTCCGTCGCACCATGGGATCTTATCGCTGCCGCTGAAGAAAGTACCGACGGAGTCAAAGA
                                                                    AtFIS1A
```

```
1 pK7WG2_FIS1A_FIS1A_F              --------------------------------------------------------------------------------
2 pK7WG2_FIS1A_P35S_R               ATTGTCCGATCTTAGCATCCATAAGGGCGAATTCGGAGCCTGCTTTTTTGTACAAACTTGTGATATCACTAGTGCGGCCG
3 pK7WG2::CaMV35S-AtFIS1A-35ST      ATTGTCCGATCTTAGCATCCATAAGGGCGAATTCGGAGCCTGCTTTTTTGTACaaacttgtgatatcactagtgcggccg
4 pK7WG2_FIS1A_T35S_F               ATTGTCCGATCTTAGCATCCATAAGGGCGAATTCGGAGCCTGCTTTTTTGTACAAACTTGTGATATCACTAGTGCGGCCG
5 pK7WG2_FIS1A_FIS1A_R              ATTGTCCGATCTTAGCATCCATAAGGGCGAATTCGGAGCCTGCTTTTTTGTACAAACTTGTGATATCACTAGTGCGGCCG
                                            AtFIS1A      TOPO recognition site 1
```

```
1 pK7WG2_FIS1A_FIS1A_F              --------------------------------------------------------------------------------
2 pK7WG2_FIS1A_P35S_R               CCTGCAGGTCGACTAGAATAGTAAATTGTAATGTTGTTTGTTGTTTGTTTTGTTGTGGTAATTGTTGNNAAAATACCGGA
3 pK7WG2::CaMV35S-AtFIS1A-35ST      cctgcaggtcgactagaatagtaaattgtaatgttgtttgttgtttgttttgttgtggtaattgttgtaaaatacggat
4 pK7WG2_FIS1A_T35S_F               CCTGCAGGTCGACTAGAATAGTAAATTGTAATGTTGTTTGTTGTTTGTTTTGTTGTGGTAATTGTTGTAAAAATA-----
5 pK7WG2_FIS1A_FIS1A_R              CCTGCAGGTCGACTAGAATAGTAAATTGTAATGTTGTTTGTTGTTTGTTTTGTTGTGGTAATTGTTGTAAAAATA-----
                                                                    Promoter CaMV35S
```

```
1 pK7WG2_FIS1A_FIS1A_F              --------------------------------------------------------------------------------
2 pK7WG2_FIS1A_P35S_R               GNCCNNTCCAAANNNNNNNNNNN---------------------------------------------------------
3 pK7WG2::CaMV35S-AtFIS1A-35ST      cgtcctgcagtcctctccaaatgaaatgaacttccttatatagaggaagggtcttgcgaaggatagtgggattgtgcgtc
4 pK7WG2_FIS1A_T35S_F               ----CCGGAGTCCTCTCCAAATGAAATGAACTTCCTTATATAGAGGAAGGGTCTTGCGAAGGATAGTGGGATTGTGCGTC
5 pK7WG2_FIS1A_FIS1A_R              ----CCGGAGTCCTCTCCAAATGAAATGAACTTCCTTATATAGAGGAAGGGTCTTGCGAAGGATAGTGGGATTGTGCGTC
                                                                    Promoter CaMV35S
```

```
1 pK7WG2_FIS1A_FIS1A_F              --------------------------------------------------------------------------------
2 pK7WG2_FIS1A_P35S_R               --------------------------------------------------------------------------------
3 pK7WG2::CaMV35S-AtFIS1A-35ST      atcccttacgtcagtggagatatcacatcaatccacttgctttgaagacgtggttggaacgtcttctttttccacgatgc
4 pK7WG2_FIS1A_T35S_F               ATCCCNTACGTCNNNGAANNTATCAANTCANNCC----------------------------------------------
5 pK7WG2_FIS1A_FIS1A_R              ATCCCTTACGTCAGTGGAGATATCACATCAATCCACTTGCTTTGAAGACGTGGTTGGAACGTCTTCTTTTTCCACGATGC
                                                                    Promoter CaMV35S
```

```
1 pK7WG2_FIS1A_FIS1A_F              --------------------------------------------------------------------------------
2 pK7WG2_FIS1A_P35S_R               --------------------------------------------------------------------------------
3 pK7WG2::CaMV35S-AtFIS1A-35ST      tcctcgtgggtgggggtccatctttgggaccactgtcggcagaggcatcttgaacgatagcctttcctttatcgcaatga
4 pK7WG2_FIS1A_T35S_F               -------------------------------------------------------------------------------
5 pK7WG2_FIS1A_FIS1A_R              TCCTCGTGGGTGGGGGTCCATCTTTGGGACNNCTNNNGNCAG--------------------------------------
                                                                    Promoter CaMV35S
```

pLS0201 – Multigene construct

```
1 LS0201_Scr          TTGCGGACGTTTTTAATGTACTGGGGTTGAACACTCTGTGCCGAATTCGGATCCAGCGTCGATCTAGTAACATAGATGAC
2 LS0201              ----------------------------ttgaacactctgtgccgaattcggatccagcgtcgatctagtaacatagatgac
```

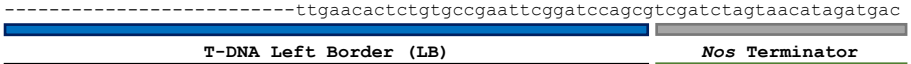

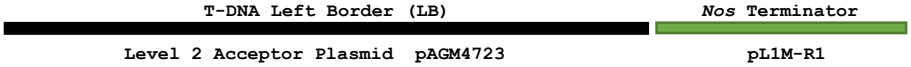


```
1 LS0201_Scr          ACCGCGCGCGATAATTTATCCTAGTTTGCGCGCTATATTTTGTTTTCTATCGCGTATTAAATGTATAATTGCGGGACTCT
2 LS0201              accgcgcgcgataatttatcctagtttgcgcgctatattttgttttctatcgcgtattaaatgtataattgcgggactct
```

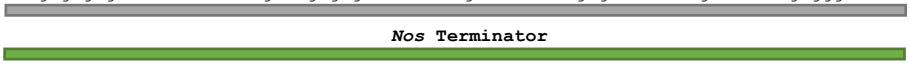


```
1 LS0201_Scr          AATCATAAAAACCCATCTCATAAATAACGTCATGCATTACATGTTAATTATTACATGCTTAACGTAATTCAACAGAAATT
2 LS0201              aatcataaaaacccatctcataaataacgtcatgcattacatgttaattattacatgcttaacgtaattcaacagaaatt
```

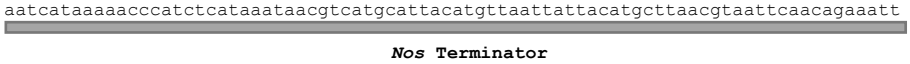


```
1 LS0201_Scr          ATATGATAATCATCGCAAGACCGGCAACAGGATTCAATCTTAAGAAACTTTATTGCCAAATGTTTGAACGATCTGCTTGA
2 LS0201              atatgataatcatcgcaagaccggcaacaggattcaatcttaagaaactttattgccaaatgtttgaacgatctgcttga
```

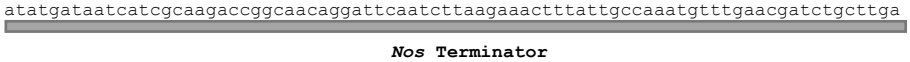


```
1 LS0201_Scr          CAAGCCTATTCCTTTGCCCTCGGACGAGTGCTGGGGCGTCGGTTTCCACTATCGGCGAGTACTTCTACACAGCCATCGGT
2 LS0201              caagcctattcctttgccctcggacgagtgctggggcgtcggtttccactatcggcgagtacttctacacagccatcggt
```

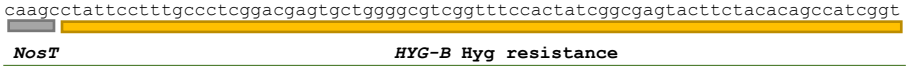


```
1 LS0201_Scr          CCAGACGGCCGCGCTTCTGCGGGCGATTTGTGTACGCCCGACAGTCCCGGCTCCGGATCGGACGATTGCGTCGCATCGAC
2 LS0201              ccagacggccgcgcttctgcgggcgatttgtgtacgcccgacagtcccggctccggatcggacgattgcgtcgcatcgac
```

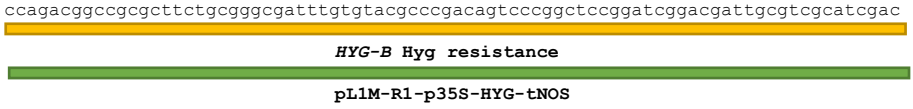


```
1 LS0201_Scr          CCTGCGCCCAAGCTGCATCATCGAAATTGCCGTCAACCAAGCTCTGATAGAGTTGGTCAAGACCAATGCGGAGCATATAC
2 LS0201              cctgcgcccaagctgcatcatcgaaattgccgtcaaccaagctctgatagagttggtcaagaccaatgcggagcatatac
```

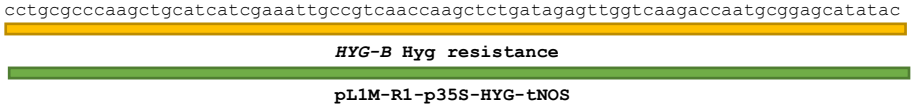


```
1 LS0201_Scr          GCCCGGAGCCGCGGCGATCCTGCAAGCTCCGGATGCCTCCGCTCGAAGTAGCGCGTCTGCTGCTCCATACAAGCCAACCA
2 LS0201              gcccggagccgcggcgatcctgcaagctccggatgcctccgctcgaagtagcgcgtctgctgctccatacaagccaacca
```

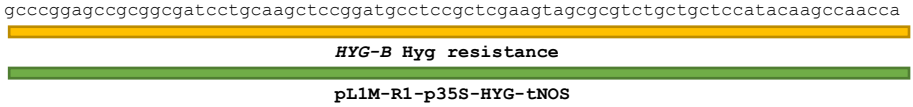


```
1 LS0201_Scr          CGGCCTCCAGAAGAAGATGTTGGCGACCTCGTATTGGGAATCCCCGAACATCGCCTCGCTCCAGTCAATGACCGCTGTTA
2 LS0201              cggcctccagaagaagatgttggcgacctcgtattgggaatccccgaacatcgcctcgctccagtcaatgaccgctgtta
```

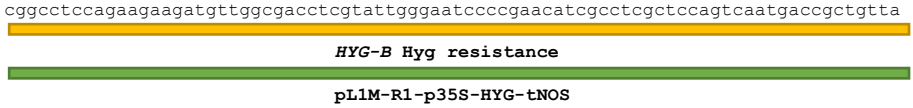


```
1 LS0201_Scr          TGCGGCCATTGTCCGTCAGGACATTGTTGGAGCCGAAATCCGCGTGCACGAGATGCCGGACTTCGGGGCAGTCCTCGGCC
2 LS0201              tgcggccattgtccgtcaggacattgttggagccgaaatccgcgtgcacgagatgccggacttcggggcagtcctcggcc
```

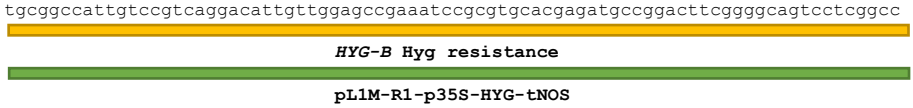


```
1 LS0201_Scr          CAAAGCATCAGCTCATCGAGAGCCTGCGCGACGGACGCACTGACGGTGTCGTCCATCACAGTTTGCCAGTGATACACATG
2 LS0201              caaagcatcagctcatcgagagcctgcgcgacggacgcactgacggtgtcgtccatcacagtttgccagtgatacacatg
3 LS0201_2_B06        ----------------------NNNNNNNNNNNNGNNGCNCTGACGGTGTCGTCCATCACAGTTTGCCAGTGATACACATG
```

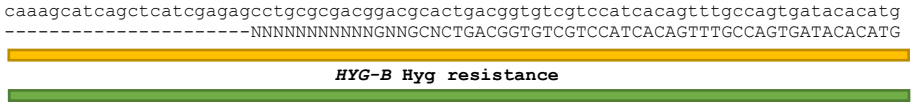

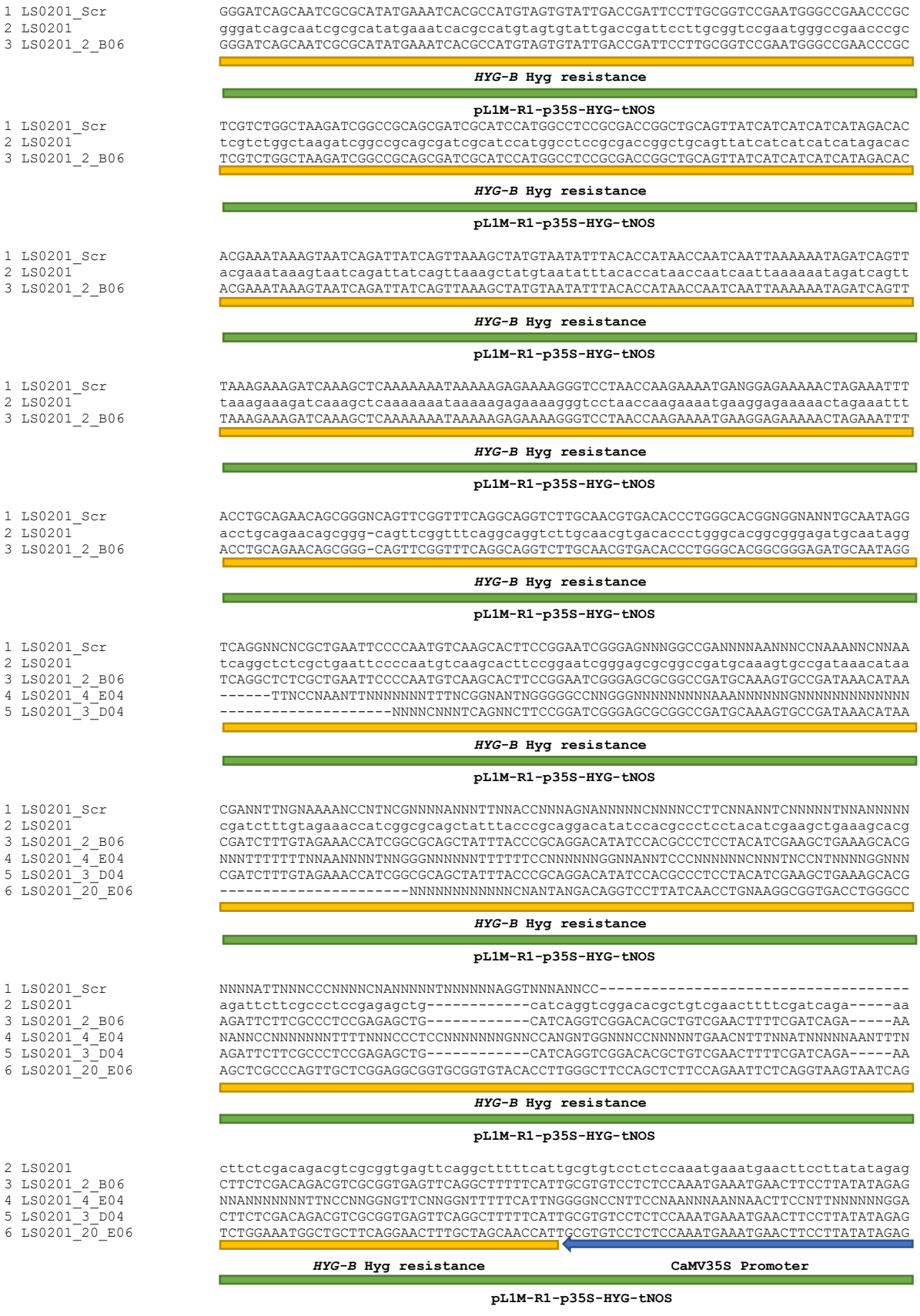
1 LS0201_Scr GGGATCAGCAATCGCGCATATGAAATCACGCCATGTAGTGTATTGACCGATTCCTTGCGGTCCGAATGGGCCGAACCCGC
2 LS0201 gggatcagcaatcgcgcatatgaaatcacgccatgtagtgtattgaccgattccttgcggtccgaatgggccgaacccgc
3 LS0201_2_B06 GGGATCAGCAATCGCGCATATGAAATCACGCCATGTAGTGTATTGACCGATTCCTTGCGGTCCGAATGGGCCGAACCCGC
HYG-B Hyg resistance
pL1M-R1-p35S-HYG-tNOS
1 LS0201_Scr TCGTCTGGCTAAGATCGGCCGCAGCGATCGCATCCATGGCCTCCGCGACCGGCTGCAGTTATCATCATCATCATAGACAC
2 LS0201 tcgtctggctaagatcggccgcagcgatcgcatccatggcctccgcgaccggctgcagttatcatcatcatcatagacac
3 LS0201_2_B06 TCGTCTGGCTAAGATCGGCCGCAGCGATCGCATCCATGGCCTCCGCGACCGGCTGCAGTTATCATCATCATCATAGACAC
HYG-B Hyg resistance
pL1M-R1-p35S-HYG-tNOS
1 LS0201_Scr ACGAAATAAAGTAATCAGATTATCAGTTAAAGCTATGTAATATTTACACCATAACCAATCAATTAAAAAATAGATCAGTT
2 LS0201 acgaaataaagtaatcagattatcagttaaagctatgtaatatttacaccataaccaatcaattaaaaaatagatcagtt
3 LS0201_2_B06 ACGAAATAAAGTAATCAGATTATCAGTTAAAGCTATGTAATATTTACACCATAACCAATCAATTAAAAAATAGATCAGTT
HYG-B Hyg resistance
pL1M-R1-p35S-HYG-tNOS
1 LS0201_Scr TAAAGAAAGATCAAAGCTCAAAAAAATAAAAAGAGAAAAGGGTCCTAACCAAGAAAATGANGGAGAAAAACTAGAAATTT
2 LS0201 taaagaaagatcaaagctcaaaaaaataaaaagagaaaagggtcctaaccaagaaaatgaaggagaaaaactagaaattt
3 LS0201_2_B06 TAAAGAAAGATCAAAGCTCAAAAAAATAAAAAGAGAAAAGGGTCCTAACCAAGAAAATGAAGGAGAAAAACTAGAAATTT
HYG-B Hyg resistance
pL1M-R1-p35S-HYG-tNOS
1 LS0201_Scr ACCTGCAGAACAGCGGGNCAGTTCGGTTTCAGGCAGGTCTTGCAACGTGACACCCTGGGCACGGNGGNANNTGCAATAGG
2 LS0201 acctgcagaacagcggg-cagttcggtttcaggcaggtcttgcaacgtgacaccctgggcacggcgggagatgcaatagg
3 LS0201_2_B06 ACCTGCAGAACAGCGGG-CAGTTCGGTTTCAGGCAGGTCTTGCAACGTGACACCCTGGGCACGGCGGGAGATGCAATAGG
HYG-B Hyg resistance
pL1M-R1-p35S-HYG-tNOS
1 LS0201_Scr TCAGGNNCNCGCTGAATTCCCCAATGTCAAGCACTTCCGGAATCGGGAGNNNGGCCGANNNNAANNNCCNAAANNCNNAA
2 LS0201 tcaggctctcgctgaattccccaatgtcaagcacttccggaatcgggagcgcggccgatgcaaagtgccgataaacataa
3 LS0201_2_B06 TCAGGCTCTCGCTGAATTCCCCAATGTCAAGCACTTCCGGAATCGGGAGCGCGGCCGATGCAAAGTGCCGATAAACATAA
4 LS0201_4_E04 ------TTNCCNAANTTNNNNNNNTTTNCGGNANTNGGGGGCCNNGGGNNNNNNNNNAAANNNNNNGNNNNNNNNNNNN
5 LS0201_3_D04 ----------NNNNCNNNTCAGNNCTTCCGGATCGGGAGCGCGGCCGATGCAAAGTGCCGATAAACATAA
HYG-B Hyg resistance
pL1M-R1-p35S-HYG-tNOS
1 LS0201_Scr CGANNTTNGNAAAANCCNTNCGNNNNANNNTTNNACCNNNAGNANNNNNCNNNNCCTTCNNANNTCNNNNNTNNANNNNN
2 LS0201 cgatctttgtagaaaccatcggcgcagctatttacccgcaggacatatccacgccctcctacatcgaagctgaaagcacg
3 LS0201_2_B06 CGATCTTTGTAGAAACCATCGGCGCAGCTATTTACCCGCAGGACATATCCACGCCCTCCTACATCGAAGCTGAAAGCACG
4 LS0201_4_E04 NNNTTTTTTTNNAANNNNTNNGGGNNNNNNTTTTTTCCNNNNNNGGNNANNTCCCNNNNNNCNNNTNCCNTNNNNGGNNN
5 LS0201_3_D04 CGATCTTTGTAGAAACCATCGGCGCAGCTATTTACCCGCAGGACATATCCACGCCCTCCTACATCGAAGCTGAAAGCACG
6 LS0201_20_E06 ----------NNNNNNNNNNNNCNANTANGACAGGTCCTTATCAACCTGNAAGGCGGTGACCTGGGCC
HYG-B Hyg resistance
pL1M-R1-p35S-HYG-tNOS
1 LS0201_Scr NNNNATTNNNCCCNNNNCNANNNNNTNNNNNNAGGTNNNANNCC----------
2 LS0201 agattcttcgccctccgagagctg----------catcaggtcggacacgctgtcgaacttttcgatcaga-----aa
3 LS0201_2_B06 AGATTCTTCGCCCTCCGAGAGCTG----------CATCAGGTCGGACACGCTGTCGAACTTTTCGATCAGA-----AA
4 LS0201_4_E04 NANNCCNNNNNNNTTTTNNNCCCTCCNNNNNNNGNNCCANGNTGGNNNCCNNNNNTGAACNTTTNNATNNNNNAANTTTN
5 LS0201_3_D04 AGATTCTTCGCCCTCCGAGAGCTG----------CATCAGGTCGGACACGCTGTCGAACTTTTCGATCAGA-----AA
6 LS0201_20_E06 AGCTCGCCCAGTTGCTCGGAGGCGGTGCGGTGTACACCTTGGGCTTCCAGCTCTTCCAGAATTCTCAGGTAAGTAATCAG
HYG-B Hyg resistance
pL1M-R1-p35S-HYG-tNOS
2 LS0201 cttctcgacagacgtcgcggtgagttcaggctttttcattgcgtgtcctctccaaatgaaatgaacttccttatatagag
3 LS0201_2_B06 CTTCTCGACAGACGTCGCGGTGAGTTCAGGCTTTTTCATTGCGTGTCCTCTCCAAATGAAATGAACTTCCTTATATAGAG
4 LS0201_4_E04 NNANNNNNNNTTNCCNNGGNGTTCNNGGNTTTTTCATTNGGGGNCCNTTCCNAANNNAANNAACTTCCNTTNNNNNGGA
5 LS0201_3_D04 CTTCTCGACAGACGTCGCGGTGAGTTCAGGCTTTTTCATTGCGTGTCCTCTCCAAATGAAATGAACTTCCTTATATAGAG
6 LS0201_20_E06 TCTGGAAATGGCTGCTTCAGGAACTTTGCTAGCAACCATTGCGTGTCCTCTCCAAATGAAATGAACTTCCTTATATAGAG
HYG-B Hyg resistance
CaMV35S Promoter
pL1M-R1-p35S-HYG-tNOS

```
2 LS0201          gaagggtcttgcgaaggatagtgggattgtgcgtcatcccttacgtcagtggagatgtcacatcaatccacttgctttgt
3 LS0201_2_B06    GAAGGGTCTTGCGAAGGATAGTGGGATTGTGCGTCATCCCTTACGTCNGTGGAGATGTCANATCAATCCACTTGCTTTGT
4 LS0201_4_E04    ANGGTCNTTNNAAGGATANGGGGATTNGGCGTCATCCCTTANGTCAGTGGAGATGTCACNTCAATCCCACTTGCTTTGTA
5 LS0201_3_D04    GAAGGGTCTTGCGAAGGATAGTGGGATTGTGCGTCATCCCTTACGTCAGTGGAGATGTCACATCAATCCACTTGCTTTGT
6 LS0201_20_E06   GAAGGGTCTTGCGAAGGATAGTGGGATTGTGCGTCATCCCTTACGTCAGTGGAGATGTCACATCAATCCACTTGCTTTGT
```

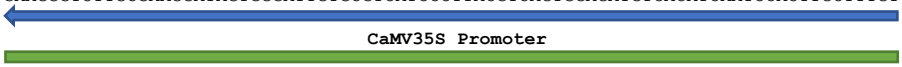


```
2 LS0201          agacgtggttggaacctcttctttttccacgatgctcctcgtgggtgggggtccatctttgggaccactgtcggcagaga
3 LS0201_2_B06    AGACGTGGTTGGAACCTCTTCNTNGTCCACGATGCTCATCGTGNGTGGNNNTCCATNNTTNGAANCNAGNNNNNNCA---
4 LS0201_4_E04    GACGTGGTTGGAACCNTTTNNTTTTNCCACGATGCTCCTCGTGGGTGGGGGTCCATCTTTGGGACCACNNTCGGCAGAGA
5 LS0201_3_D04    AGACGTGGTTGGAACCTCTTCTTTTTCCACGATGCTCCTCGTGGGTGGGGGTCCATCTTTGGGACCACTGTCGGCAGAGA
6 LS0201_20_E06   ANACGTGGTTGGAACCTCTTCTTTTTCCACGATGCTCCTCGTGNNTGGGGNTCCATCTTTGGGACCACTGTCNNCNNANA
```

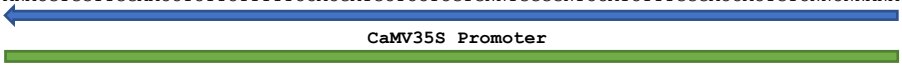


```
2 LS0201          gatcttgaatgatagccttccttttatcgcaatgatggcatttgtaggagccaccttccttttctactgtcctttcgatg
4 LS0201_4_E04    GATCTTGAATGATAGCCTTTCCTTTATCGCAATGATGGCATTTGTAGGAGCCACCTTCCTTTTCTACTGTCCTTTCGATG
5 LS0201_3_D04    GATCTTGAATGATAGCCTTTCCTTTATCGCAATGATGGCATTTGTAGGAGCCACCTTCCTTTTCTACTGTCCTTTCGATG
6 LS0201_20_E06   GATCTTGAATGATAGCCTTTCCTTTATCGCAATGATNNCATTTGTAGGAGCCACCTTCCTTTTCTACTGTCCTTNCGATG
```

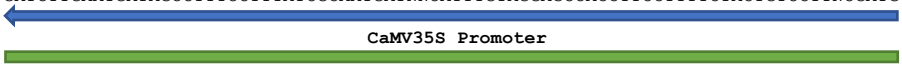


```
2 LS0201          aagtgacagatagctgggcaatggaatccgaggaggtttcccgaaattatcctttgttgaaaagtctcaatagccctttg
4 LS0201_4_E04    AAGTGACAGATAGCTGGGCAATGGAATCCGAGGAGGTTTCCCGAAATTATCCTTTGTTGAAAAGTCTCAATAGCCCTTTG
5 LS0201_3_D04    AAGTGACAGATAGCTGGGCAATGGAATCCGAGGAGGTTTCCCGAAATTATCCTTTGTTGAAAAGTCTCAATAGCCCTTTG
6 LS0201_20_E06   AAGTGACAGATAGCTGGNNAATNNAATCCNNGNAGGTTTCCCGAAATTATCCTNNNTTGAAAAGTCTCAATAGCCCTTTG
```

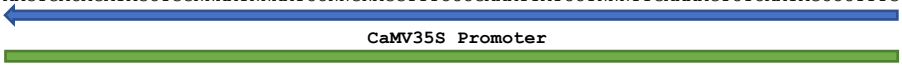


```
2 LS0201          atcttctgagactgtatctttgacatttttggagtagaccagagtgtcgtgctccaccatgttgacctccgcaagaattc
4 LS0201_4_E04    ATCTTCTGAGACTGTATCTTTGACATTTTTGGAGTAGACCAGAGTGTCGTGCTCCACCATGTTGACCTCCGCAAGAATTC
5 LS0201_3_D04    ATCTTCTGAGACTGTATCTTTGACATTTTTGGAGTAGACCAGAGTGTCGTGCTCCACCATGTTGACCTCCGCAAGAATTC
6 LS0201_20_E06   ATCTTCTGAGACTGTATCTTTGACATTTTTGGANTANACCANANNGTCGTGCTCCACCATGTTATCACATCAATCCACTT
```

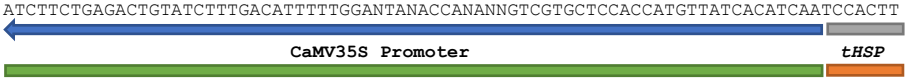


```
2 LS0201          aagcttagcgcttatctttaatcatattccatagtccataccatagcacatacagtagttatatgctgcagaagagatcc
4 LS0201_4_E04    AAGCTTAGCGCTTATCTTTAATCATATTCCATAGTCCATACCATAGCACATACAGTAGTTATATGCTGCAGAAGAGATCC
5 LS0201_3_D04    AAGCTTAGCGCTTATCTTTAATCATATTCCATAGTCCATACCATAGCACATACAGTAGTTATATGCTGCAGAAGAGATCC
6 LS0201_20_E06   GCTTTGTANACGTGGTTGNAACCTCTTCTTTTTCCACGATGCTCCTCGTGGGTGNGNNTCCATCTTTGGGACNACTGTCG
```

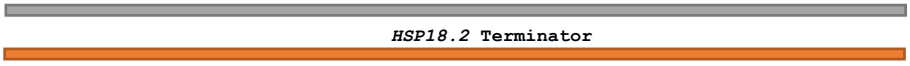


```
2 LS0201          aacaaaacattcacaatggattatagaaacatttgtttattcattataatgagatcttacattcatttaatattagaaaa
4 LS0201_4_E04    AACAAAACATTCACAATGGATTATAGAAACATTTGTTTATTCATTATAATGAGATCTTACATTCATTTAATATTAGAAAA
5 LS0201_3_D04    AACAAAACATTCACAATGGATTATAGAAACATTTGTTTATTCATTATAATGAGATCTTACATTCATTTAATATTAGAAAA
6 LS0201_20_E06   NCANANAGATCTNNAATGATNNCNTTTCCTTTATCACNATGATGGNATTTGTAGNNNCNACCTTCNTTTTCTACTGTCCT
```

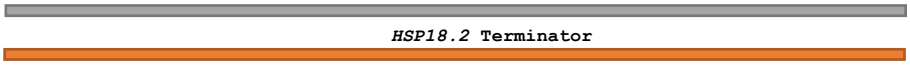


```
2 LS0201          agccacaaattcataacacaacaagccaagaaaaaaacacaaacttaagcacacaagctttttatttgacacaccaaata
4 LS0201_4_E04    AGCCACAAATTCATAACACAACAAGCCAAGAAAAAAACACAAACTTAAGCACACAAGCTTTTTATTTGACACACCAAATA
5 LS0201_3_D04    AGCCACAAATTCATAACACAACAAGCCAAGAAAAAAACACAAACTTAAGCACACAAGCTTTTTATTTGACACACCAAATA
6 LS0201_20_E06   TTNNATGAANTGACAGATAGCTGGGCAATGGAATCCGAGGAGGTTTCCCGAAATTATCCTTTGTTGAAAAGTCTCAANAG
```

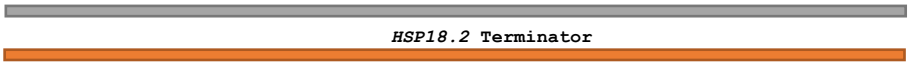


```
2 LS0201          tttcatcttcatcttcatataagcggattggtcgtttggtggcaagagttgctctgcagagagatgatgttgaactagtt
4 LS0201_4_E04    TTTCATCTTCATCTTCATATAAGCGGATTGGTCGTTTGGTGGCAAGAGTTGCTCTGCAGAGAGATGATGTTGAACTAGTT
5 LS0201_3_D04    TTTCATCTTCATCTTCATATAAGCGGATTGGTCGTTTGGTGGCAAGAGTTGCTCTGCAGAGAGATGATGTTGAACTAGTT
6 LS0201_20_E06   CCCTTTGATCTTCTGAGACTGTATCTTTGACATTTTTGNAGNAGACCANAGTGTCGTGCTCCACCATNTTGACCTCCCTC
```

```
2 LS0201          gcagtgaacgacccatttatctctactgattacatgacatacatgtttaagtatgattcGGTTCATGGACAATGGAAACA
4 LS0201_4_E04    GCAGTGAACGACCCATTTATCTCTACTGATTACATGACATACATGTTTAAGTATGATTCGGTTCATGGACAATGGAAACA
5 LS0201_3_D04    GCAGTGAACGACCCATTTATCTCTACTGATTACATGACATACATGTTTAAGTATGATTCGGTTCATGGACAATGGAAACA
6 LS0201_20_E06   GAGGAATTCNACANGANATATGACTNNTAAGTTNNTCTTGNNNNTACGAATTANNNNACATGTCTTTGAAGATGAACTGT
```

***NtGAPC* antisense fragment**

pL1M-R2-pSlRbcS2-AS_NtGAPC-tHSP

```
2 LS0201          CCATGAGCTTAAAGTAaaggatgaaaagacccttctttttggtgagaagtccgtcagagtctttggaaTTAGGAACCCTG
4 LS0201_4_E04    CCATGAGCTTAAAGTAAAGGATGAAAAGACCCTTCTTTTTGGTGAGAAGTCCGTCAGAGTCTTTGGAATTAGGAACCCTG
5 LS0201_3_D04    CCATGAGCTTAAAGTAAAGGATGAAAAGACCCTTCTTTTTGGTGAGAAGTCCGTCAGAGTCTTTGGAATTAGGAACCCTG
6 LS0201_20_E06   ATTTTTTTTTTTACTTTGNTGTCATTTAATGTACTTTCTTATCAGGATTAANTCTTCTGNAATTTANAGTAGTTTTTNAA
```

***NtGAPC* antisense fragment**

pL1M-R2-pSlRbcS2-AS_NtGAPC-tHSP

```
2 LS0201          AGGAAATTCCATGGGCTGAAGCTGGTGCTGATTTCGTTGTGGAATCCACTGGTGTCTTCACTGACaaggacaaggctgct
4 LS0201_4_E04    AGGAAATTCCATGGGCTGAAGCTGGTGCTGATTTCGTTGTGGAATCCACTGGTGTCTTCACTGACAAGGACAAGGCTGCT
5 LS0201_3_D04    AGGAAATTCCATGGGCTGAAGCTGGTGCTGATTNCGTTGTGGAATCCACTGNNGTCTTCACTGACAAGGACAAGGCTGCT
6 LS0201_20_E06   CAAGATAATTAACAAACTTAGAGTAATGAAAATTGAGATGTTCAGTTTTCACTCATATTTCACATTTTGGTGAAANNGTG
```

***NtGAPC* antisense fragment**

pL1M-R2-pSlRbcS2-AS_NtGAPC-tHSP

```
2 LS0201          gctcactt-gaagggtggtgccaagaaggttgtgatctctgctcctagcaaggatgcccccatgtttgttgtgggtgtca
4 LS0201_4_E04    GCTCACTT-GAAGGGTGGTGCCAAGAAGGTTGTGATCTCTGCTCCTAGCAAGGATGCCCCCATGTTTGTTGTGGGTGTCA
5 LS0201_3_D04    GCTCACTTNGAAGGGTGGTGCCAAGAAGGTTGNNATCTCTGCTCCTAGCAAGGATGCCCCCNNGTTTNTNGGGGGNNGTC
6 LS0201_20_E06   GNTAGTATGCAACGTTCTAAGTATGTTTGGACTTTGTATCATGTTGTTTTGATTCTTTGACGACATGTCTATTTGGGAAN
```

***NtGAPC* antisense fragment**

pL1M-R2-pSlRbcS2-AS_NtGAPC-tHSP

```
2 LS0201          acgagaaggaatacaagCCCGAATATgacattgtctccaatgctagttgcactaccaactgccttgcacctttggctaag
4 LS0201_4_E04    ACGAGAAGGAATACAAGCCCGAATATGACATTGTCTCCAATGCTAGTTGCACTACCAACTGCCTTGCACCTTTGGCTAAG
5 LS0201_3_D04    AACNNNAANGGAANNCAANCCNGAANNNGNANTTNNNNTCCAATGCTAGTTGNCCTACCAACTGNCTTGGACCTTTGGNN
6 LS0201_20_E06   NNNCAATGACGTGTACCTTGNNACTGATANNATTCAAAGGGAAAAANNNCNTCAAATTTACAAGTGGNNCCTCTTCAATG
7 LS0201_5_F06    ----------------------NNNNNNNNNNNTGTCNNATGCTAGTTGCACTACCAACTGCCTTGCACCTTTGGCTAAG
8 LS0201_5_F10    ----------------------NNNNNNNNNTTGTCNCATGCTAGTTGCACTACCAACTGCCTTGCACCTTTGGCTAAG
9 LS0201_5_F04    ----------------------NNNNNNNNNTTGTCNNNNGCTAGTTGCACTACCAACTGCCTTGCACCTTTGGCTAAG
```

***NtGAPC* antisense fragment**

pL1M-R2-pSlRbcS2-AS_NtGAPC-tHSP

```
2 LS0201          gtcatcaatg-ataggtttggaattgtggagggcattttgcttcttctctctttttttggttcaatatgaacctttgat
4 LS0201_4_E04    GTCATCAATG-ATAGGTTTGGAATTGTGGAGGGCATTTTGCTTCTTCTCTCTTTTTTTGGTTCAATATGAACCTTTTGAT
5 LS0201_3_D04    AAGGNNNNCAANGNAANGGTTTGGAATTNNGGNNGGGNCATTTNGNNNNNTTNCCCCNTTTTTTNGGGTTCAAAANGAAC
6 LS0201_20_E06   GANANTGGGTATTCCATATGCTAANNTGCTACANNANNNCTAATTNNNNANNNCAANTCATTNCAAACCAAAATCTGATG
7 LS0201_5_F06    GTCATCAATGNNNAGGTTTGGAATTGTGGAGGGCATTTTGCTTCTTCTCTCTTTTTTTGGTTCAATATGAACCTTTTGAT
8 LS0201_5_F10    GTCATCAATG-ATAGGTTTGGAATTGTGGAGGGCATTTTGCTTCTTCTCTCTTTTTTTGGTTCAATATGAACCTTTTGAT
9 LS0201_5_F04    GTCATCAATG-ATAGGTTTGGAATTGTGGAGGGCATTTTGCTTCTTCTCTCTTTTTTTGGTTCAATATGAACCTTTTGAT
```

***NtGAPC* antisense fragment** ***SlRbcS2* Promoter**

pL1M-R2-pSlRbcS2-AS_NtGAPC-tHSP

```
2 LS0201          gtccactatccttttatataatgaaatgataaggtttttgatatgttatgtggttcttgataacattatacaattactta
4 LS0201_4_E04    GTCCACTATCCTTTTATATAATGAAATGATAAGGTTTTTGATATGTTATGTGGTTCTTGATAACATTATACAATTACTTA
5 LS0201_3_D04    NNTTTNNNAAGGCCCNNNNCCCTTTTNNNAANNGGAANNGGAAANGGNTTTTNNNANNNNNNAAGGGGGNTCNNNGGAAN
6 LS0201_20_E06   CNNNNNNAAAANNCAAAAATCCAAGNNNNAAAATGNCANNNCCAATAAANTTCAGGNCNTTNNCAANTTCCNAAANTAGC
7 LS0201_5_F06    GTCCACTATCCTTTTATATAATGAAATGATAAGGTTTTTGATATGTTATGTGGTTCTTGATAACATTATACAATTACTTA
8 LS0201_5_F10    GTCCACTATCCTTTTATATAATGAAATGATAAGGTTTTTGATATGTTATGTGGTTCTTGATAACATTATACAATTACTTA
9 LS0201_5_F04    GTCCACTATCCTTTTATATAATGAAATGATAAGGTTTTTGATATGTTATGTGGTTCTTGATAACATTATACAATTACTTA
```

***SlRbcS2* Promoter**

pL1M-R2-pSlRbcS2-AS_NtGAPC-tHSP

```
2 LS0201          atatctacatatgaaaggttggaatttttttttaagtcaccacaatagaggtgacacgtgtaagcacctcgttaatcttat
4 LS0201_4_E04    ATATCTACATATGAAAGGTTGGAATTTTTTTTAAGTCACCACAATAGAGGTGACACGTGTAAGCACCTCGTTAATCTTAN
5 LS0201_3_D04    NNNTTNAANNAANTTCNTNAANNCNNNNNNNGGAANGGNNGGNNATTTTTTTTNAAANGNNCCCNAAANNANNNNGGNAA
6 LS0201_20_E06   AANTNAANCTTCANTTTNNCAATTCATNGNTCCTTNAANNNCCCNAAAACCCCC----------------------------
7 LS0201_5_F06    ATATCTACATATGAAAGGTTGGAATTTTTTTTAAGTCACCACAATAGAGGTGACACGTGTAAGCACCTCGTTAATCTTAT
8 LS0201_5_F10    ATATCTACATATGAAAGGTTGGAATTTTTTTTAAGTCACCACAATAGAGGTGACACGTGTAAGCACCTCGTTAATCTTAT
9 LS0201_5_F04    ATATCTACATATGAAAGGTTGGAATTTTTTTTAAGTCACCACAATAGAGGTGACACGTGTAAGCACCTCGTTAATCTTAT
```

***SlRbcS2* Promoter**

pL1M-R2-pSlRbcS2-AS_NtGAPC-tHSP

```
2 LS0201                ctcatccaagatgggggtaggaagaggatatgaatgtatgattgaggttggttttgagtttttttttttttttttttga
4 LS0201_4_E04          NTCANCCAANANNNNNN----------------------------------------------------------------
5 LS0201_3_D04          NC------------------------------------------------------------------------------
7 LS0201_5_F06          CTCATCCAAGATGGGGGTAGGAAGAGGATATGAATGTATGATTGAGGTTGGTTTTGAGTTTTTTTTTTTTTTTTTTTTGA
8 LS0201_5_F10          CTCATCCAAGATGGGGGTAGGAAGAGGATATGAATGTATGATTGAGGTTGGTTTTGAGTTTTTTTTTTTTTTTTTTTNN
9 LS0201_5_F04          CTCATCCAAGATGGGGGTAGGAAGAGGATATGAATGTATGATTGAGGTTGGTTTTGAGTTTTTTTTTTTTTTTTTTTGA
```

***SlRbcS2* Promoter**

pL1M-R2-pSlRbcS2-AS_NtGAPC-tHSP

```
2 LS0201                gtccttcaacttgttatttttaatttttttttggtgggggaggaggggggttgaaatatttatcatatagtagtccaaagt
7 LS0201_5_F06          GTCCTTCAACTTGTTATTTTAATTTTTTTTTGGTGGGGGAGGAGGGGGGTTGAAATATTTATCATATAGTAGTCCAAAGT
8 LS0201_5_F10          NTNNTTNNNNNNNTNNTTNNNNTTTTTTTTNNNNNNNNNNNNNNNNNNNNNNNNNNNNTNNNNNNNNNN----------
9 LS0201_5_F04          GTCCTTCAACTTGTTATTTTAATTTTTTTTTGGTGGGGGAGGAGGGGGGTTGNNNNNNNNNNNNNNNNNNNNNNNNNNNN
10 LS0201_6_G04         ------------------------------------------------------------NNNNNNNAGNAGTC---AAG
```

***SlRbcS2* Promoter**

pL1M-R2-pSlRbcS2-AS_NtGAPC-tHSP

```
2 LS0201                aaattgatagctagagtacttgtttgcttgcttatattgtcctcaactttatgtaataccatgattccaacttagacact
7 LS0201_5_F06          AAATTGATAGCTAGAGTACTTGTTTGCTTGCTTATATTGTCCTCAACTTTATGTAATACCATGATTCCAACTTAGACACT
9 LS0201_5_F04          NNNNNNNNNNNNNNNNNNNTNGTTTGNTNNNTNNNTNNGNNNNNNNTTNNNNNNNNTNNTNNNNTNNNNNNNNNNTT
10 LS0201_6_G04         TAATTGATAGCTAGAGTACTTGTTTGCTTGCTTATATTGTCCTCAACTTTATGTAATACCATGATTCCAACTTAGACACT
```

***SlRbcS2* Promoter**

pL1M-R2-pSlRbcS2-AS_NtGAPC-tHSP

```
2 LS0201                cttttaagttgtaattttcattatttttctttttttagagttttatgttgaattcgcataattttcaatcggataatacaa
7 LS0201_5_F06          CTTTTAAGTTGTAATTTTCATTATTTTCTTTTTTTAGAGTTTTATGTTGAATTCGCATAATTTTCAATCGGATAATACAA
9 LS0201_5_F04          TNTTNNNNTNGNNNTTTNTNNNTTNNTTTTTTNNNNNTTNNNGTTNNNNNNNNNNNNTNNNNNNNNNNNNNNNTNN
10 LS0201_6_G04         CTTTTAAGTTGTAATTTTCATTATTTTCTTTTTTTAGAGTTTTATGTTGAATTCGCATAATTTTCAATCGGATAATACAA
```

***SlRbcS2* Promoter**

pL1M-R2-pSlRbcS2-AS_NtGAPC-tHSP

```
2 LS0201                gaaaaataatattttagtataatttttatacatgaaatttcgggaaggtaggatatacggattgtttgtcggatcagagac
7 LS0201_5_F06          GAAAAATAATATTTTAGTATAATTTTATACATGAAATTTCGGGAAGGTAGGATATACGGATTGTTTGTCGGATCAGAGAC
9 LS0201_5_F04          NNNNNNNNTNNNTNNNNNNNTNNNNTTTNNNT-------------------------------------------------
10 LS0201_6_G04         GAAAAATAATATTTTAGTATAATTTTATACATGAAATTTCGGGAAGGTAGGATATACGGATTGTTTGTCGGATCAGAGAC
```

***SlRbcS2* Promoter**

pL1M-R2-pSlRbcS2-AS_NtGAPC-tHSP

```
2 LS0201                tttactcgtacctttgtaactgttgatcccaaatacagatagtgactccagagttatatattatacctatagagactaat
7 LS0201_5_F06          TTTACTCGTACCTTTGTAACTGTTGATCCCAAATACAGATAGTGACTCCAGAGTTATATATTATACCTATAGAGACTAAT
10 LS0201_6_G04         TTTACTCGTACCTTTGTAACTGTTGATCCCAAATACAGATAGTGACTCCAGAGTTATATATTATACCTATAGAGACTAAT
```

***SlRbcS2* Promoter**

pL1M-R2-pSlRbcS2-AS_NtGAPC-tHSP

```
2 LS0201                atgatttagtgttattaaaattagtattactaattaattgtaatgccccatgaattcTCCACTAGAATTCGAGCTCAGCg
7 LS0201_5_F06          ATGATTTAGTGTTATTAAAATTAGTATTACTAATTAATTGTAATGCCCCATGAATTCTCCACTAGAATTCGAGCTCAGCG
10 LS0201_6_G04         ATGATTTAGTGTTATTAAAATTAGTATTACTAATTAATTGTAATGCCCCATGAATTCTCCACTAGAATTCGAGCTCAGCG
```

SlRbcS2* Promoter** ***tHSP

pL1M-R2-pSlRbcS2-AS_NtGAPC-tHSP **pL1M-R3**

```
2 LS0201                cttatctttaatcatattccatagtccataccatagcacatacagtagttatatgctgcagaagagatccaacaaaacat
7 LS0201_5_F06          CTTATCTTTAATCATATTCCATAGTCCATACCATAGCACATACAGTAGTTATATGCTGCAGAAGAGATCCAACAAAACAT
10 LS0201_6_G04         CTTATCTTTAATCATATTCCATAGTCCATACCATAGCACATACAGTAGTTATATGCTGCAGAAGAGATCCAACAAAACAT
```

***HSP18.2* Terminator**

pL1M-R3-pStLS1-AS_NtmMDH-tHSP

```
2 LS0201                tcacaatggattatagaaacatttgtttattcattataatgagatcttacattcatttaatattagaaaaagccacaaat
7 LS0201_5_F06          TCACAATGGATTATAGAAACATTTGTTTATTCATTATAATGAGATCTTACATTCATTTAATATTAGAAAAAGCCACAAAT
10 LS0201_6_G04         TCACAATGGATTATAGAAACATTTGTTTATTCATTATAATGAGATCTTACATTCATTTAATATTAGAAAAAGCCACAAAT
```

***HSP18.2* Terminator**

pL1M-R3-pStLS1-AS_NtmMDH-tHSP


2 LS0201
7 LS0201_5_F06
10 LS0201_6_G04
tcataacacaacaagccaagaaaaaaacacaaacttaagcacacaagctttttatttgacacaccaaatatttcatcttc
TCATAACACAACAAGCCAAGAAAAAAACACAAACTTAAGCACACAAGCTTTTTATTNGACACACCAAATATTTCATCTTC
TCATAACACAACAAGCCAAGAAAAAAACACAAACTTAAGCACACAAGCTTTTTATTTGACACACCAAATATTTCATCTTC
HSP18.2 Terminator
NtmMDH AS
pL1M-R3-pStLS1-AS_NtmMDH-tHSP
2 LS0201
7 LS0201_5_F06
10 LS0201_6_G04
11 LS0201_14_F05
atcttcatataagcacaccagatctcaggtttctgggtttgcaggagatgaacagctAGGACAGGCTTTGGAGGGAGCTG
ATCTTCATATAAGCACACCAGATCTCAGGTTTCTGGGTTTGCAGGANATGAACAGCTAGGACAGGCTTTGGANGGNNCTG
ATCTTCATATAAGCACACCAGATCTCAGGTTTCTGGGTTTGCAGGAGATGAACAGCTAGGACAGGCTTTGGAGGGAGCTG
----------NNNNNNNNNNNCANGGCTTTGGAGGGAGCTG
NtmMDH antisense fragment
pL1M-R3-pStLS1-AS_NtmMDH-tHSP
2 LS0201
7 LS0201_5_F06
10 LS0201_6_G04
11 LS0201_14_F05
ATGTTGTCATCATTCCTGCTGGTGTGCCACGAAAGCCTGGTATGACCCGTGATGATCTGTTCAACATTAACGCTGGTATT
ANNTTNNCANNATTCCCGGCTGGGGGNCCANAAAAGCCTGGTATGACNNGNNATGANNNGTTCAACNTTAACCNNGGNAA
ATGTTGTCATCATTCCTGCTGGTGTGCCACGAAAGCCTGGTATGACCCGTGATGATCTGTTCAACATTAACGCTGGTATT
ANGTTGTCATCATTCCTGCTGGTGTGCCACGAAAGCCTGGTATGACCCGTGATGATCTGTTCAACATTAACGCTGGTATT
NtmMDH antisense fragment
pL1M-R3-pStLS1-AS_NtmMDH-tHSP
2 LS0201
7 LS0201_5_F06
10 LS0201_6_G04
11 LS0201_14_F05
GTTAAATCTCTTTGCACAGCCATCGCAAAGTATTGCCCTCATGCCCTTGTCAATATGATCAGCAACCCTGTGAACTCCAC
TTGTTAAANNNNNTTNGCCNNNNCNNNNNCAAANNNNTTGNCCCCNNNNCCNTTGTCAANTNNNNNNAGNANCCNTNGNN
GTTAAATCTCTTTGCACAGCCATCGCAAAGTATTGCCCTCATGCCCTTGTCAATATGATCAGCAACCCTGTGAACTCCAC
GTTAAATCTCTTTGCACAGCCATCGCAAAGTATTGCCCTCATGCCCTTGTCAATATGATCAGCAACCCTGTGAACTCCAC
NtmMDH antisense fragment
pL1M-R3-pStLS1-AS_NtmMDH-tHSP
2 LS0201
7 LS0201_5_F06
10 LS0201_6_G04
11 LS0201_14_F05
TGTCCCAATTGCCGCTGAGGTGTTCAAGAAGGCTGGAACCTATGATGAAAAGAGACTCTTTGGAGTGACCACACTTGATG
AANCCCCNNTNGTCCCAANNNNCNNNTTAAGNTTTNNAANNNGNNNGNAACCTTNNNNNAAAANNNANNTTTTNNNNNNN
TGTCCCAATTGCCGCTGAGGTGTTCAAGAAGGCTGGAACCTATGATGAAAAGAGACTCTTTGGAGTGACCACACTTGATG
TGTCCCAATTGCCGCTGAGGTGTTCAAGAAGGCTGGAACCTATGATGAAAAGAGACTCTTTGGAGTGACCACACTTGATG
NtmMDH antisense fragment
pL1M-R3-pStLS1-AS_NtmMDH-tHSP
2 LS0201
7 LS0201_5_F06
10 LS0201_6_G04
11 LS0201_14_F05
TTGTTAGGGCAAAGACTTTCTATGCGGGAAAAGCTAAAGTTAATGTTGCTGACGTCATTGTCCCCGTTGTTGGTGGTCAT
NNCCNNNCNTTNANNTTTTTNAGGNNAAAAANCTTTTNNNNNNGGNAAAANCNAAAANNNAAANTTTNCC----------
TTGTTAGGGCAAAGACTTTCTATGCGGGAAAAGCTAAAGTTAATGTTGCTGACGTCATTGTCCCCGTTGTTGGTGGTCAT
TTGTTAGGGCAAAGACTTTCTATGCGGGAAAAGCTAAAGTTAATGTTGCTGACGTCATTGTCCCCGTTGTTGGTGGTCAT
NtmMDH antisense fragment
pL1M-R3-pStLS1-AS_NtmMDH-tHSP
2 LS0201
10 LS0201_6_G04
11 LS0201_14_F05
GCTGGCATAACCATCCTCCCACTATTTTCCCAAGCCACCCCAAAGGCAAATTTGGGAGACGAAGAAATTGAGGCACTCAC
GCTGGCATAACCATCCTCCCACTATTTTCCCAAGCCACCCCAAAGGCAAATTTGGGAGACGAAGAAATTGAGGCACTCAC
GCTGGCATAACCATCCTCCCACTATTTTCCCAAGCCACCCCAAAGGCAAATTTGGGAGACGAAGAAATTGAGGCACTCAC
NtmMDH antisense fragment
pL1M-R3-pStLS1-AS_NtmMDH-tHSP
2 LS0201
10 LS0201_6_G04
11 LS0201_14_F05
CAAGCGAACCCAAGATGGTGGCACTGAAGTTGTGGAGGCCAAGGCTGGAAAGGGTTCAGCAACCCTCTCTATGGCCTATG
CAAGCGAACCCAAGATGGTGGCACTGAAGTTGTGGAGGCCAAGGCTGGAAAGGGTTCAGCAACCCTCTCTATGGCCTATG
CAAGCGAACCCAAGATGGTGGCACTGAAGTTGTGGAGGCCAAGGCTGGAAAGGGTTCAGCAACCCTCTCTATGGCCTATG
NtmMDH antisense fragment
pL1M-R3-pStLS1-AS_NtmMDH-tHSP
2 LS0201
10 LS0201_6_G04
11 LS0201_14_F05
12 LS0201_15_G05
ctggggccatctttgctgatgcttgcttgaaggggctgaatggggttccagatgttgtagagtgttcattcgtgcagtca
CTGGGGCCATCTTTGCTGATGCTTGCTTGAAGGGGCTGAATGGGGTTCCAGATGTTGTAANGNNTTCATTCNTGCAGTCA
CTGGGGCCATCTTTGCTGATGCTTGCTTGAAGGGGCTGAATGGGGTTCCAGATGTTGTAGAGTGTTCATTCGTGCAGTCA
----------NNNNNNNNNNNNTGGNGTNCNGATGTTGTAGAGTGTTCATTCGTGCAGTCA
NtmMDH antisense fragment
pL1M-R3-pStLS1-AS_NtmMDH-tHSP

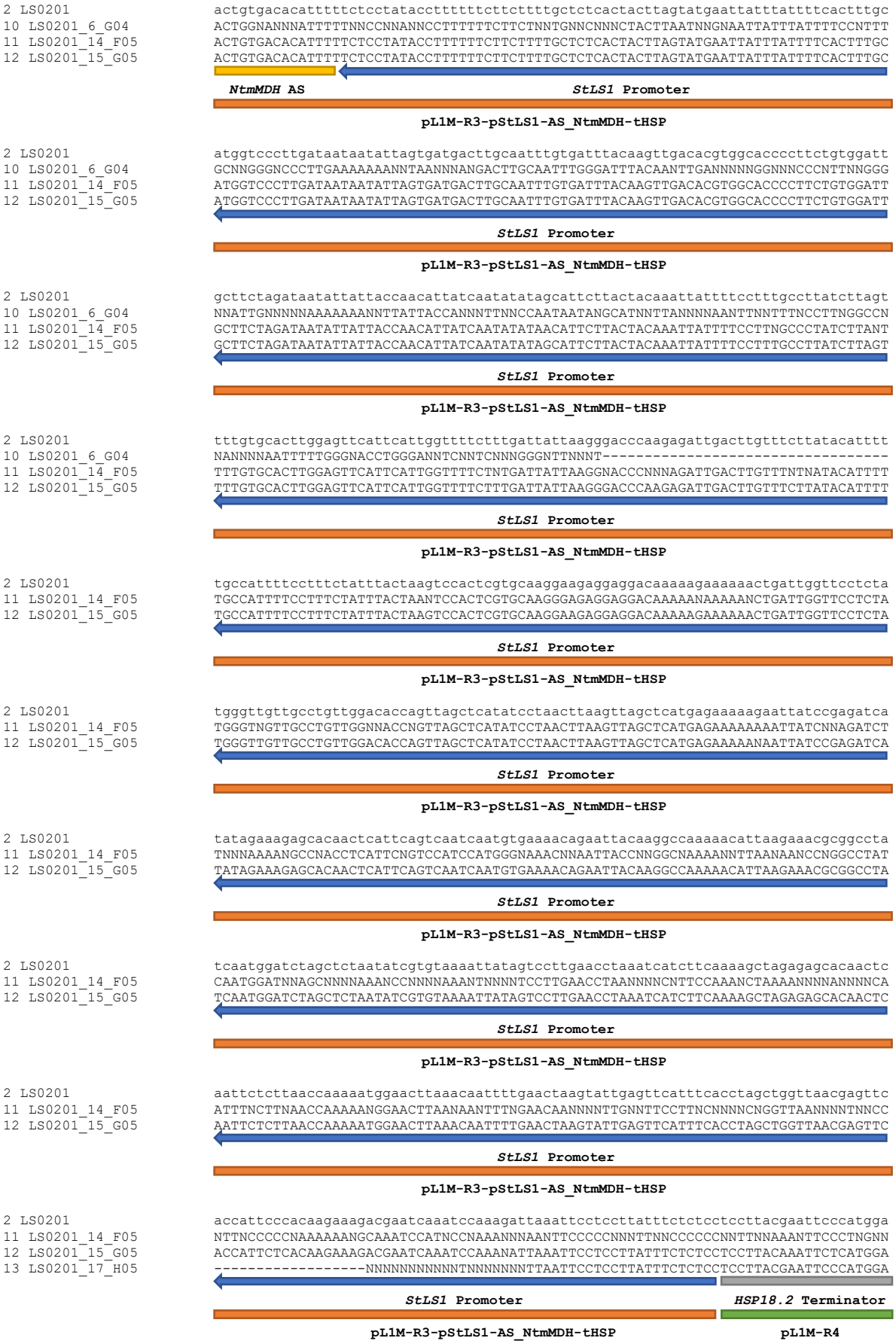
2 LS0201 actgtgacacatttttctcctataccttttttcttcttttgctctcactacttagtatgaattatttatttttcactttgc
10 LS0201_6_G04 ACTGGNANNNATTTTTNNCCNNANNCCTTTTTTCTTCTNNTGNNCNNNCTACTTAATNNGNAATTATTTATTTTCCNTTT
11 LS0201_14_F05 ACTGTGACACATTTTTCTCCTATACCTTTTTTCTTCTTTTGCTCTCACTACTTAGTATGAATTATTTATTTTCACTTTGC
12 LS0201_15_G05 ACTGTGACACATTTTTCTCCTATACCTTTTTTCTTCTTTTGCTCTCACTACTTAGTATGAATTATTTATTTTCACTTTGC
NtmMDH AS
StLS1 Promoter
pL1M-R3-pStLS1-AS_NtmMDH-tHSP
2 LS0201 atggtcccttgataataatattagtgatgacttgcaatttgtgatttacaagttgacacgtggcacccccttctgtggatt
10 LS0201_6_G04 GCNNGGGNCCCTTGAAAAAAANNTAANNNANGACTTGCAATTTGGGATTTACAANTTGANNNNNGGNNNCCCNTTNNGGG
11 LS0201_14_F05 ATGGTCCCTTGATAATAATATTAGTGATGACTTGCAATTTGTGATTTACAAGTTGACACGTGGCACCCCTTCTGTGGATT
12 LS0201_15_G05 ATGGTCCCTTGATAATAATATTAGTGATGACTTGCAATTTGTGATTTACAAGTTGACACGTGGCACCCCTTCTGTGGATT
StLS1 Promoter
pL1M-R3-pStLS1-AS_NtmMDH-tHSP
2 LS0201 gcttctagataatattattaccaacattatcaatatatagcattcttactacaaattatttttcctttgccttatcttagt
10 LS0201_6_G04 NNATTGNNNNNAAAAAAANNTTATTACCANNNTTNNCCAATAATANGCATNNTTANNNNAANTTNNTTTNCCTTNGGCCN
11 LS0201_14_F05 GCTTCTAGATAATATTATTACCAACATTATCAATATATAACATTCTTACTACAAATTATTTTCCTTNGCCCTATCTTANT
12 LS0201_15_G05 GCTTCTAGATAATATTATTACCAACATTATCAATATATAGCATTCTTACTACAAATTATTTTCCTTTGCCTTATCTTAGT
StLS1 Promoter
pL1M-R3-pStLS1-AS_NtmMDH-tHSP
2 LS0201 tttgtgcacttggagttcattcattggttttctttgattattaagggacccaagagattgacttgtttcttatacatttt
10 LS0201_6_G04 NANNNNAATTTTTGGGNACCTGGGANNTCNNTCNNNGGGNTTNNNT----------
11 LS0201_14_F05 TTTGTGCACTTGGAGTTCATTCATTGGTTTTCTNTGATTATTAAGGNACCCNNNAGATTGACTTGTTTNTNATACATTTT
12 LS0201_15_G05 TTTGTGCACTTGGAGTTCATTCATTGGTTTTCTTTGATTATTAAGGGACCCAAGAGATTGACTTGTTTCTTATACATTTT
StLS1 Promoter
pL1M-R3-pStLS1-AS_NtmMDH-tHSP
2 LS0201 tgccattttccttttctatttactaagtccactcgtgcaaggaagaggaggacaaaaagaaaaaactgattggttcctcta
11 LS0201_14_F05 TGCCATTTTCCTTTCTATTTACTAANTCCACTCGTGCAAGGGAGAGGAGGACAAAAANAAAAANCTGATTGGTTCCTCTA
12 LS0201_15_G05 TGCCATTTTCCTTTCTATTTACTAAGTCCACTCGTGCAAGGAAGAGGAGGACAAAAAGAAAAAACTGATTGGTTCCTCTA
StLS1 Promoter
pL1M-R3-pStLS1-AS_NtmMDH-tHSP
2 LS0201 tgggttgttgcctgttggacaccagttagctcatatcctaacttaagttagctcatgagaaaaagaattatccgagatca
11 LS0201_14_F05 TGGGTNGTTGCCTGTTGGNNACCNGTTAGCTCATATCCTAACTTAAGTTAGCTCATGAGAAAAAAAATTATCNNAGATCT
12 LS0201_15_G05 TGGGTTGTTGCCTGTTGGACACCAGTTAGCTCATATCCTAACTTAAGTTAGCTCATGAGAAAAANAATTATCCGAGATCA
StLS1 Promoter
pL1M-R3-pStLS1-AS_NtmMDH-tHSP
2 LS0201 tatagaaagagcacaactcattcagtcaatcaatgtgaaaacagaattacaaggccaaaaacattaagaaacgcggccta
11 LS0201_14_F05 TNNNAAAANGCCNACCTCATTCNGTCCATCCATGGGNAAACNNAATTACCNNGGCNAAAANNTTAANAANCCNGGCCTAT
12 LS0201_15_G05 TATAGAAAGAGCACAACTCATTCAGTCAATCAATGTGAAAACAGAATTACAAGGCCAAAAACATTAAGAAACGCGGCCTA
StLS1 Promoter
pL1M-R3-pStLS1-AS_NtmMDH-tHSP
2 LS0201 tcaatggatctagctctaatatcgtgtaaaattatagtccttgaacctaaatcatcttcaaaagctagagagcacaactc
11 LS0201_14_F05 CAATGGATNNAGCNNNNAAANCCNNNNAAANTNNNNTCCTTGAACCTAANNNNCNTTCCAAANCTAAAANNNNANNNNCA
12 LS0201_15_G05 TCAATGGATCTAGCTCTAATATCGTGTAAAATTATAGTCCTTGAACCTAAATCATCTTCAAAAGCTAGAGAGCACAACTC
StLS1 Promoter
pL1M-R3-pStLS1-AS_NtmMDH-tHSP
2 LS0201 aattctcttaaccaaaaatggaacttaaacaattttgaactaagtattgagttcatttcacctagctggttaacgagttc
11 LS0201_14_F05 ATTTNCTTNAACCAAAAANGGAACTTAANAANTTTNGAACAANNNNTTGNNTTCCTTNCNNNNCNGGTTAANNNNTNNCC
12 LS0201_15_G05 AATTCTCTTAACCAAAAATGGAACTTAAACAATTTTGAACTAAGTATTGAGTTCATTTCACCTAGCTGGTTAACGAGTTC
StLS1 Promoter
pL1M-R3-pStLS1-AS_NtmMDH-tHSP
2 LS0201 accattcccacaagaaagacgaatcaaatccaaagattaaattcctcctttatttctctcctcctcttacgaattcccatgga
11 LS0201_14_F05 NTTNCCCCCNAAAAAANGCAAATCCATNCCNAAANNNAANTTCCCCCNNNTTNNCCCCCCNNTTNNAAANTTCCCTNGNN
12 LS0201_15_G05 ACCATTCTCACAAGAAAGACGAATCAAATCCAAANATTAAATTCCTCCTTATTTCTCTCCTCCTTACAAATTCTCATGGA
13 LS0201_17_H05 ----------NNNNNNNNNNNNTNNNNNNNTTAATTCCTCCTTATTTCTCTCCTCCTTACGAATTCCCATGGA
StLS1 Promoter
HSP18.2 Terminator
pL1M-R3-pStLS1-AS_NtmMDH-tHSP
pL1M-R4

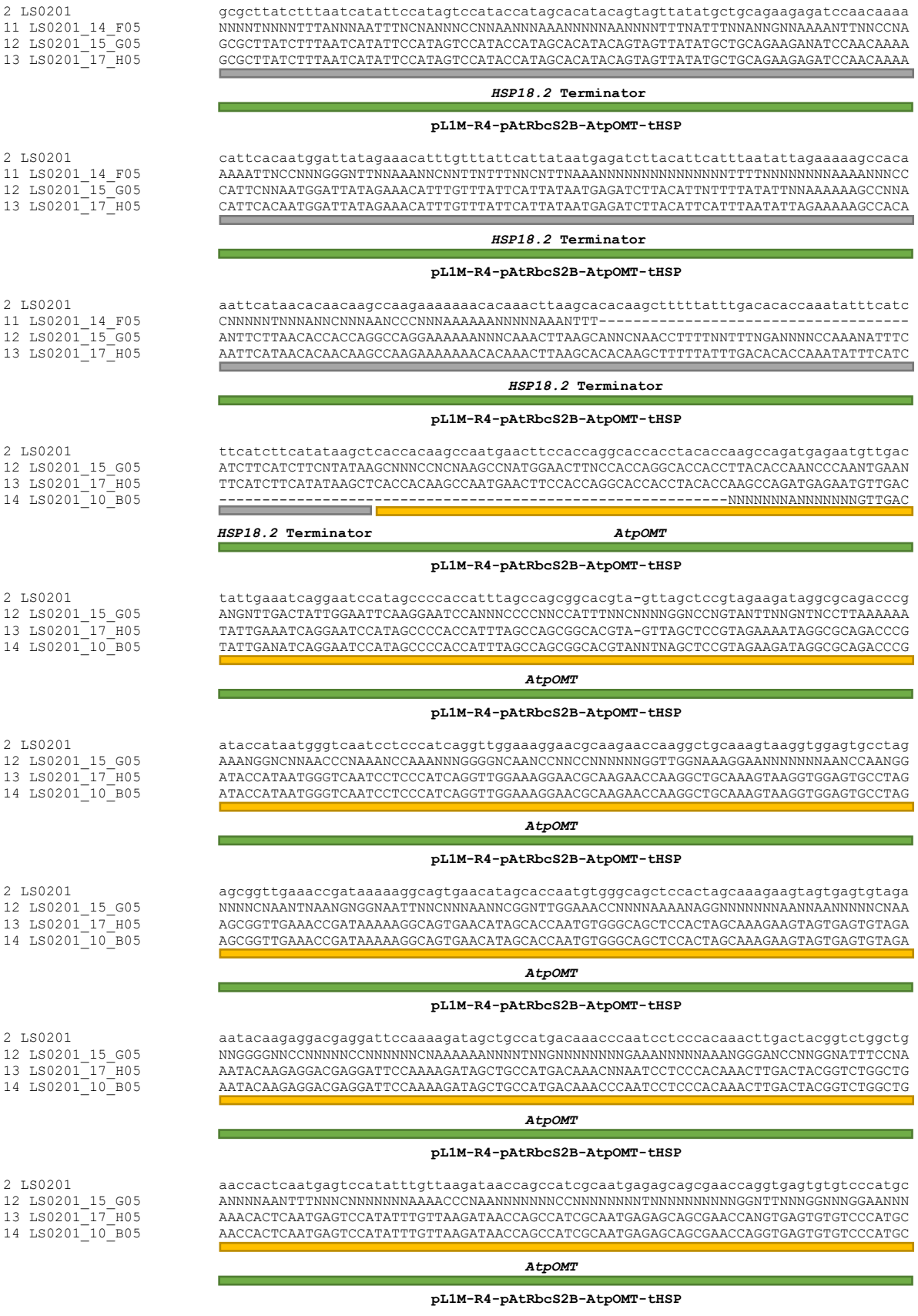
2 LS0201 gcgcttatctttaatcatattccatagtccataccatagcacatacagtagttatatgctgcagaagagatccaacaaaa
11 LS0201_14_F05 NNNNTNNNNTTTANNNAATTTNCNANNNCCNNAANNNAAANNNNNAANNNNTTTNATTTNNANNGNNAAAANTTNNCCNA
12 LS0201_15_G05 GCGCTTATCTTTAATCATATTCCATAGTCCATACCATAGCACATACAGTAGTTATATGCTGCAGAAGANATCCAACAAAA
13 LS0201_17_H05 GCGCTTATCTTTAATCATATTCCATAGTCCATACCATAGCACATACAGTAGTTATATGCTGCAGAAGAGATCCAACAAAA
HSP18.2 Terminator
pL1M-R4-pAtRbcS2B-AtpOMT-tHSP
2 LS0201 cattcacaatggattatagaaacatttgtttattcattataatgagatcttacattcatttaatattagaaaaagccaca
11 LS0201_14_F05 AAAATTNCCNNNGGGNTTNNAAANNCNNTTNTTTNNCNTTNAAANNNNNNNNNNNNNNNNTTTTNNNNNNNNAAAANNNCC
12 LS0201_15_G05 CATTCNNAATGGATTATAGAAACATTTGTTTATTCATTATAATGAGATCTTACATTNTTTTATATTNNAAAAAAGCCNNA
13 LS0201_17_H05 CATTCACAATGGATTATAGAAACATTTGTTTATTCATTATAATGAGATCTTACATTCATTTAATATTAGAAAAAGCCACA
HSP18.2 Terminator
pL1M-R4-pAtRbcS2B-AtpOMT-tHSP
2 LS0201 aattcataacacaacaagccaagaaaaaaacacaaacttaagcacacaagctttttatttgacacaccaaatatttcatc
11 LS0201_14_F05 CNNNNNTNNNANNCNNNAANCCCNNNAAAAAANNNNNAAANTTT----------
12 LS0201_15_G05 ANTTCTTAACACCACCAGGCCAGGAAAAAANNNCAAACTTAAGCANNCNAACCTTTTNNTTTNGANNNNCCAAANATTTC
13 LS0201_17_H05 AATTCATAACACAACAAGCCAAGAAAAAAACACAAACTTAAGCACACAAGCTTTTTATTTGACACACCAAATATTTCATC
HSP18.2 Terminator
pL1M-R4-pAtRbcS2B-AtpOMT-tHSP
2 LS0201 ttcatcttcatataagctcaccacaagccaatgaacttccaccaggcaccacctacaccaagccagatgagaatgttgac
12 LS0201_15_G05 ATCTTCATCTTCNTATAAGCNNNCCNCNAAGCCNATGGAACTTNCCACCAGGCACCACCTTACACCAANCCCAANTGAAN
13 LS0201_17_H05 TTCATCTTCATATAAGCTCACCACAAGCCAATGAACTTCCACCAGGCACCACCTACACCAAGCCAGATGAGAATGTTGAC
14 LS0201_10_B05 ----------NNNNNNNANNNNNNNGTTGAC
HSP18.2 Terminator AtpOMT
pL1M-R4-pAtRbcS2B-AtpOMT-tHSP
2 LS0201 tattgaaatcaggaatccatagccccaccatttagccagcggcacgta-gttagctccgtagaagataggcgcagacccg
12 LS0201_15_G05 ANGNTTGACTATTGGAATTCAAGGAATCCANNNCCCCNNCCATTTNNCNNNNGGNCCNGTANTTNNGNTNCCTTAAAAAA
13 LS0201_17_H05 TATTGAAATCAGGAATCCATAGCCCCACCATTTAGCCAGCGGCACGTA-GTTAGCTCCGTAGAAAATAGGCGCAGACCCG
14 LS0201_10_B05 TATTGANATCAGGAATCCATAGCCCCACCATTTAGCCAGCGGCACGTANNTNAGCTCCGTAGAAGATAGGCGCAGACCCG
AtpOMT
pL1M-R4-pAtRbcS2B-AtpOMT-tHSP
2 LS0201 ataccataatgggtcaatcctcccatcaggttggaaaggaacgcaagaaccaaggctgcaaagtaaggtggagtgcctag
12 LS0201_15_G05 AAANGGNCNNAACCCNAAANCCAAANNNGGGGNCAANCCNNCCNNNNNNGGTTGGNAAAGGAANNNNNNNAANCCAANGG
13 LS0201_17_H05 ATACCATAATGGGTCAATCCTCCCATCAGGTTGGAAAGGAACGCAAGAACCAAGGCTGCAAAGTAAGGTGGAGTGCCTAG
14 LS0201_10_B05 ATACCATAATGGGTCAATCCTCCCATCAGGTTGGAAAGGAACGCAAGAACCAAGGCTGCAAAGTAAGGTGGAGTGCCTAG
AtpOMT
pL1M-R4-pAtRbcS2B-AtpOMT-tHSP
2 LS0201 agcggttgaaaccgataaaaaggcagtgaacatagcaccaatgtgggcagctccactagcaaagaagtagtgagtgtaga
12 LS0201_15_G05 NNNNCNAANTNAANGNGGNAATTNNCNNNAANNCGGNTTGGAAACCNNNNAAAANAGGNNNNNNNAANNAANNNNNCNAA
13 LS0201_17_H05 AGCGGTTGAAACCGATAAAAAGGCAGTGAACATAGCACCAATGTGGGCAGCTCCACTAGCAAAGAAGTAGTGAGTGTAGA
14 LS0201_10_B05 AGCGGTTGAAACCGATAAAAAGGCAGTGAACATAGCACCAATGTGGGCAGCTCCACTAGCAAAGAAGTAGTGAGTGTAGA
AtpOMT
pL1M-R4-pAtRbcS2B-AtpOMT-tHSP
2 LS0201 aatacaagaggacgaggattccaaaagatagctgccatgacaaacccaatcctcccacaaacttgactacggtctggctg
12 LS0201_15_G05 NNGGGGNNCCNNNNNCCNNNNNNCNAAAAAANNNNTNNGNNNNNNNNGAAANNNNNAAANGGGANCCNNGGNATTTCCNA
13 LS0201_17_H05 AATACAAGAGGACGAGGATTCCAAAAGATAGCTGCCATGACAAACNNAATCCTCCCACAAACTTGACTACGGTCTGGCTG
14 LS0201_10_B05 AATACAAGAGGACGAGGATTCCAAAAGATAGCTGCCATGACAAACCCAATCCTCCCACAAACTTGACTACGGTCTGGCTG
AtpOMT
pL1M-R4-pAtRbcS2B-AtpOMT-tHSP
2 LS0201 aaccactcaatgagtccatatttgttaagataaccagccatcgcaatgagagcagcgaaccaggtgagtgtgtcccatgc
12 LS0201_15_G05 ANNNNAANTTTNNNCNNNNNNNAAAACCCNAANNNNNNNCCNNNNNNNNTNNNNNNNNNGGNTTNNNGGNNNGGAANNN
13 LS0201_17_H05 AAACACTCAATGAGTCCATATTTGTTAAGATAACCAGCCATCGCAATGAGAGCAGCGAACCANGTGAGTGTGTCCCATGC
14 LS0201_10_B05 AACCACTCAATGAGTCCATATTTGTTAAGATAACCAGCCATCGCAATGAGAGCAGCGAACCAGGTGAGTGTGTCCCATGC
AtpOMT
pL1M-R4-pAtRbcS2B-AtpOMT-tHSP

```
2 LS0201              gaccgactcagctaagcactctttccatgtcacaacacctgtcacaagaaggactgataatccaagaatggctgcagtca
12 LS0201_15_G05      NCCNAAANNGNNNNCCCNANNTTNNNNNNNAANNNNANNNNNNNNNNTNNCCCNNNNGGGNNAAAANNNNGGNNAANNNN
13 LS0201_17_H05      GACCGACTCAGCTAANCACTCTTTTCATGTCACAACACCTGTCACAAGAAAGACTGATAATCNANGAATGGCTGCAGTCA
14 LS0201_10_B05      GACCGACTCAGCTAAGCACTCTTTCCATGTCACAACACCTGTCACAAGAAGGACTGATAATCCAAGAATGGCTGCAGTCA
```

AtpOMT

pL1M-R4-pAtRbcS2B-AtpOMT-tHSP

```
2 LS0201              cagcatctacacccaacttagctccaaagatccagagtccaaccgtgaggaataaagtggcagccataatcaattcgttc
12 LS0201_15_G05      NGNNNNNNNNNNNNNNNNNNNNNGGGGNNNNNNNAANNNCCCNNNAAAAAANNNNNNTTTTTTNTTT----------
13 LS0201_17_H05      CAGCATCTACACCCAACTTNNCTCCCAAGATCCANAGNCCAACCNNGAGGANTAAANNGGCAGCCCTAATCAATTCGTTC
14 LS0201_10_B05      CAGCATCTACACCCAACTTAGCTCCAAAGATCCAGAGTCCAACCGTGAGGAATAAAGTGGCAGCCATAATCAATTCGTTC
```

AtpOMT

pL1M-R4-pAtRbcS2B-AtpOMT-tHSP

```
2 LS0201              ttagacataggtcccatcttgtcaagcttttcctgagccagcttaggagcatcaggactgctcttcaccgtaggaggata
13 LS0201_17_H05      TTANANAAAGGTCCCATCTTGTCAAGCTTTTNNNGAGCCAGCTTAGGAGCATCAGGACTGCNNTNNNCCTTAGGAGGANA
14 LS0201_10_B05      TTAGACATAGGTCCCATCTTGTCAAGCTTTTCCTGAGCCAGCTTAGGAGCATCAGGACTGCTCTTCACCGTAGGAGGATA
```

AtpOMT

pL1M-R4-pAtRbcS2B-AtpOMT-tHSP

```
2 LS0201              gatgagatacaaaagaaacggaacaacaatcaaagacacaagtcctggtacaatcgcagctttagcccaatcagtccatc
13 LS0201_17_H05      ANTGNNNNNCAAAAAAAACGGNACCACCATNCAAAGACNCAANGTCCTGGTTACAATCNNAACCTTTAATCCAATCAATN
14 LS0201_10_B05      GATGAGATACAAAAGAAACGGAACAACAATCAAAGACACAAGTCCTGGTACAATCGCAGCTTTAGCCCAATCAGTCCATC
```

AtpOMT

pL1M-R4-pAtRbcS2B-AtpOMT-tHSP

```
2 LS0201              caatcgtctgcttaatcgtgttaaacgccaaattagcactcaaaggattcgcagccatagccg-tcaagaacatagaaga
13 LS0201_17_H05      CAATNAATCGGNNTGCTTGATTCNGNTTNAANGNCCNANTTAANNNNTCCAACGGATTNNNNNGNCCNNNCCNGTCCANN
14 LS0201_10_B05      CAATCGTCTGCTTAATCGTGTTAAACGCCANNTTAGCACTCAAAGGATTCGCAGCCATAGCCG-TCAAGAACATAGAAGA
15 LS0201_11_C05      NNNTCGTNNNNCTTATCGTGTT-AACGCCAAATTAGCACTCAAAGGATTCGCAGCCATAGCCGNTCAAGAACATAGAAGA
```

AtpOMT

pL1M-R4-pAtRbcS2B-AtpOMT-tHSP

```
2 LS0201              agagatcacagaagtctggaaacaagtaagcatcaaccacgagccaagacggtgctctgttccatccccaacgttactcc
13 LS0201_17_H05      AANNNNAAAAAAAAAAAANTTNNNNNAANNNNGGGNAACAAGGTANGGNNNNACCCCCNANGCCNAAAAANNGGGNNNNTN
14 LS0201_10_B05      AGAGATCACAGAAGTCTGGAAACAAGTAAGCATCAACCACGAGCCAAGACGGTGCTCTGTTCCATCNCCNACGTTACTCN
15 LS0201_11_C05      AGAGATCACAGAAGTCTGGAAACAAGTAAGCATCAACCACGAGCCAAGACGGTGCTCTGTTCCATCCCCAACGTTACTCC
```

AtpOMT

pL1M-R4-pAtRbcS2B-AtpOMT-tHSP

```
2 LS0201              cacaagcaacacagagagatttcaccaacgggagaaagattccaccggcacgagccgagacagaaggaatcgccggagct
13 LS0201_17_H05      GGTTTCCATTNCCNNNNCNNTTNATTTCCCCNAANCCNAAACCCNAAGNNNNNNTTNNCNNNNCCCNGNNNAANNNNATT
14 LS0201_10_B05      CACAAGCAACACANAGAGATTTCACCACCGNGAGAGAGATTCNACCGNNNCGAGCCGAGACAGAAAGAANCGCCCGAGCT
15 LS0201_11_C05      CACAAGCAACACAGAGAGATTTCACCAACGGGAGAAAGATTCCACCGGCACGAGCCGAGACAGAAGGAATCGCCGGAGCT
```

AtpOMT

pL1M-R4-pAtRbcS2B-AtpOMT-tHSP

```
2 LS0201              aaaagagcttcactgaaaacgagactgtaaccgagtccaagggaggagctaccgaagagtctaacgaactggtaagctac
13 LS0201_17_H05      TNNCCCNGGCCCNNNGCCNGGAANCNNAANGGAAATTNCNCNNGGACTTNAAAAANNNCCTTTCCNTTGTAANCCNGAAC
14 LS0201_10_B05      AAAAAANCTTNNNTGAAAACNANACTGTAACCCAGTCNAAGGGAGGAGCNACCNNAAANNNTAACGAANTGGNAAGCTAC
15 LS0201_11_C05      AAAAGAGCTTCACTGAAAACGAGACTGTAACCGAGTCCAAGGGAGGAGCTACCGAAGAGTCTAACGAACTGGTAAGCTAC
```

AtpOMT

pL1M-R4-pAtRbcS2B-AtpOMT-tHSP

```
2 LS0201              acggttaccgagtccggttttgatgaaaccgcgagcgaagaagaaggcaagagcgatgagccacgggattggatctccga
13 LS0201_17_H05      CCTTGTTANCCNNNTTTNNAANNNNNNNNNNNNNTNNCCCNGNNNAAGGNTNNNAANNAAAACCTTTGGNAANGNTTNNCN
14 LS0201_10_B05      NNNGTTACCNNNTCCCNNTTTTGATGAANCNNCCCAGCGAAAAAAAAANNGCANAANCGATGANNCNCCGGNATTGNATTT
15 LS0201_11_C05      ACGGTTACCGAGTCCGGTTTTGATGAAACCGCGAGCGAAGAAGAAGGCAAGAGCGATGAGCCACGGGATTGGATCTCCGA
```

AtpOMT

pL1M-R4-pAtRbcS2B-AtpOMT-tHSP

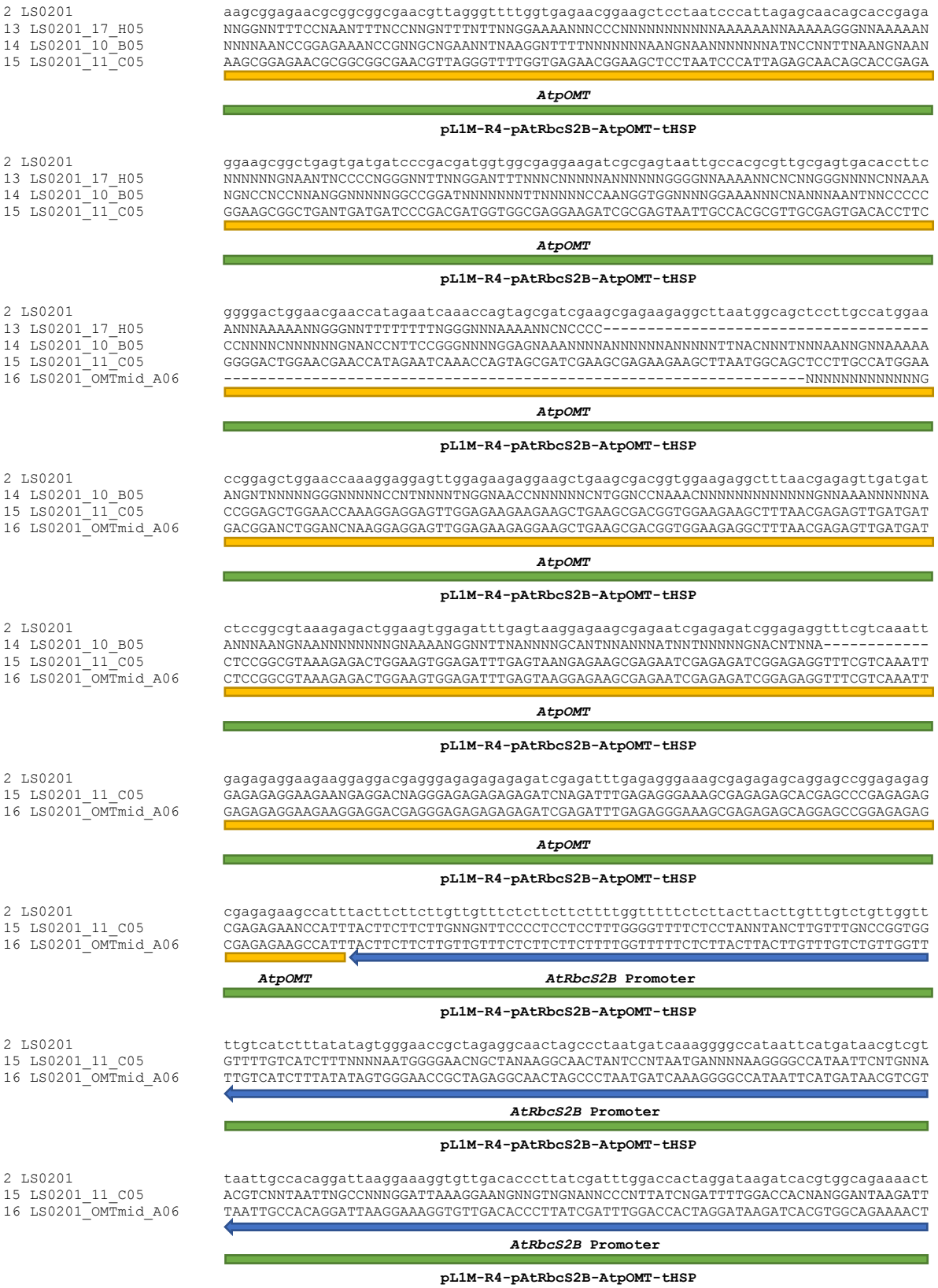
2 LS0201 aagcggagaacgcggcggcgaacgttagggttttggtgagaacggaagctcctaatcccattagagcaacagcaccgaga
13 LS0201_17_H05 NNGGNNTTTCCNAANTTTNCCNNGNTTTNTTNNGGAAAANNNCCCNNNNNNNNNNAAAAAANNAAAAAGGGNNAAAAAN
14 LS0201_10_B05 NNNNAANCCGGAGAAANCCGNNGCNGAANNTNAAGGNTTTTNNNNNNNAANGNAANNNNNNNATNCCNNTTNAANGNAAN
15 LS0201_11_C05 AAGCGGAGAACGCGGCGGCGAACGTTAGGGTTTTGGTGAGAACGGAAGCTCCTAATCCCATTAGAGCAACAGCACCGAGA
AtpOMT
pL1M-R4-pAtRbcS2B-AtpOMT-tHSP
2 LS0201 ggaagcggctgagtgatgatcccgacgatggtggcgaggaagatcgcgagtaattgccacgcgttgcgagtgacaccttc
13 LS0201_17_H05 NNNNNNGNAANTNCCCCNGGGNNTTNNGGANTTTNNNCNNNNNANNNNNNGGGGNNAAAANNCNCNNGGGNNNNCNNAAA
14 LS0201_10_B05 NGNCCNCCNNANGGNNNNNGGCCGGATNNNNNNNTTNNNNNCCAANGGTGGNNNNGGAAANNNCNANNNAANTNNCCCCC
15 LS0201_11_C05 GGAAGCGGCTGANTGATGATCCCGACGATGGTGGCGAGGAAGATCGCGAGTAATTGCCACGCGTTGCGAGTGACACCTTC
AtpOMT
pL1M-R4-pAtRbcS2B-AtpOMT-tHSP
2 LS0201 ggggactggaacgaaccatagaatcaaaccagtagcgatcgaagcgagaagaggcttaatggcagctccttgccatggaa
13 LS0201_17_H05 ANNNAAAAANNGGGNNTTTTTTTTNGGGNNNAAAANNCNCCCC----------
14 LS0201_10_B05 CCNNNNCNNNNNNGNANCCNTTCCGGGNNNNGGAGNAAANNNNANNNNNNANNNNNTTNACNNNTNNNAANNGNNAAAAA
15 LS0201_11_C05 GGGGACTGGAACGAACCATAGAATCAAACCAGTAGCGATCGAAGCGAGAAGAAGCTTAATGGCAGCTCCTTGCCATGGAA
16 LS0201_OMTmid_A06 ----------NNNNNNNNNNNNNG
AtpOMT
pL1M-R4-pAtRbcS2B-AtpOMT-tHSP
2 LS0201 ccggagctggaaccaaaggaggagttggagaagaggaagctgaagcgacggtggaagaggctttaacgagagttgatgat
14 LS0201_10_B05 ANGNTNNNNNGGGNNNNNCCNTNNNNTNGGNAACCNNNNNNCNTGGNCCNAAACNNNNNNNNNNNNNGNNAAANNNNNA
15 LS0201_11_C05 CCGGAGCTGGAACCAAAGGAGGAGTTGGAGAAGAAGAAGCTGAAGCGACGGTGGAAGAAGCTTTAACGAGAGTTGATGAT
16 LS0201_OMTmid_A06 GACGGANCTGGANCNAAGGAGGAGTTGGAGAAGAGGAAGCTGAAGCGACGGTGGAAGAGGCTTTAACGAGAGTTGATGAT
AtpOMT
pL1M-R4-pAtRbcS2B-AtpOMT-tHSP
2 LS0201 ctccggcgtaaagagactggaagtggagatttgagtaaggagaagcgagaatcgagagatcggagaggtttcgtcaaatt
14 LS0201_10_B05 ANNNAANGNAANNNNNNNNGNAAAANGGNNTTNANNNNGCANTNNANNNATNNTNNNNNGNACNTNNA----------
15 LS0201_11_C05 CTCCGGCGTAAAGAGACTGGAAGTGGAGATTTGAGTAANGAGAAGCGAGAATCGAGAGATCGGAGAGGTTTCGTCAAATT
16 LS0201_OMTmid_A06 CTCCGGCGTAAAGAGACTGGAAGTGGAGATTTGAGTAAGGAGAAGCGAGAATCGAGAGATCGGAGAGGTTTCGTCAAATT
AtpOMT
pL1M-R4-pAtRbcS2B-AtpOMT-tHSP
2 LS0201 gagagaggaagaaggaggacgagggagagagagagatcgagatttgagagggaaagcgagagagcaggagccggagagag
15 LS0201_11_C05 GAGAGAGGAAGAANGAGGACNAGGGAGAGAGAGAGATCNAGATTTGAGAGGGAAAGCGAGAGAGCACGAGCCCGAGAGAG
16 LS0201_OMTmid_A06 GAGAGAGGAAGAAGGAGGACGAGGGAGAGAGAGAGATCGAGATTTGAGAGGGAAAGCGAGAGAGCAGGAGCCGGAGAGAG
AtpOMT
pL1M-R4-pAtRbcS2B-AtpOMT-tHSP
2 LS0201 cgagagaagccatttacttcttcttgttgtttctcttcttcttttggtttttctcttacttacttgtttgtctgttggtt
15 LS0201_11_C05 CGAGAGAANCCATTTACTTCTTCTTGNNGNTTCCCCTCCTCCTTTGGGGTTTTCTCCTANNTANCTTGTTTGNCCGGTGG
16 LS0201_OMTmid_A06 CGAGAGAAGCCATTTACTTCTTCTTGTTGTTTCTCTTCTTCTTTTGGTTTTTCTCTTACTTACTTGTTTGTCTGTTGGTT
AtpOMT
AtRbcS2B Promoter
pL1M-R4-pAtRbcS2B-AtpOMT-tHSP
2 LS0201 ttgtcatctttatatagtgggaaccgctagaggcaactagccctaatgatcaaaggggccataattcatgataacgtcgt
15 LS0201_11_C05 GTTTTGTCATCTTTNNNNAATGGGGAACNGCTANAAGGCAACTANTCCNTAATGANNNNAAGGGGCCATAATTCNTGNNA
16 LS0201_OMTmid_A06 TTGTCATCTTTATATAGTGGGAACCGCTAGAGGCAACTAGCCCTAATGATCAAAGGGGCCATAATTCATGATAACGTCGT
AtRbcS2B Promoter
pL1M-R4-pAtRbcS2B-AtpOMT-tHSP
2 LS0201 taattgccacaggattaaggaaaggtgttgacacccttatcgatttggaccactaggataagatcacgtggcagaaaact
15 LS0201_11_C05 ACGTCNNTAATTNGCCNNNGGATTAAAGGAANGNNGTNGNANNCCCNTTATCNGATTTTGGACCACNANGGANTAAGATT
16 LS0201_OMTmid_A06 TAATTGCCACAGGATTAAGGAAAGGTGTTGACACCCTTATCGATTTGGACCACTAGGATAAGATCACGTGGCAGAAAACT
AtRbcS2B Promoter
pL1M-R4-pAtRbcS2B-AtpOMT-tHSP

```
2 LS0201                ccataatcttatctttctcatgtaagggtaggagtgaatgtgtatggctactgctctccacttgatcggttgcttttggc
15 LS0201_11_C05        ANCNNNGNNNAAAANTCCNNNANNCTTNNTCTTTTNCNNGNTAAAGGGTNGGNAANGNAAANGGNNNNNNGGCTNNCCNC
16 LS0201_OMTmid_A06    CCATAATCTTATCTTTCTCATGTAAGGGTAGGAGTGAATGTGTATGGCTACTGCTCTCCACTTGATCGGTTGCTTTTGGC
17 LS0201_12_D05         ----------------------------------------------------------NNNNNNNNNNNNNNNGTTGCTNNTGG-
```

***AtRbcS2B* Promoter**

pL1M-R4-pAtRbcS2B-AtpOMT-tHSP

```
2 LS0201                tcctttcaattgggaggcgtcaaattgtagatatcggttaaatac--tttttacatatagattaaaaaaatgattaaatt
15 LS0201_11_C05        CTNCCCCNNTTNNNNNNGGTNGNTTTTNGGNNCCNTTTNNAATTNGGGANGGGGNNCCAAATTNNNAAAAANTNCCGGTT
16 LS0201_OMTmid_A06    TCCTTTCAATTGGGAGGCGTCAAATTGTAGATATCGGTTAAATAC--TTTTTACATATAGATTAAAAAAATGATTAAATT
17 LS0201_12_D05         -CTCTTTCATTGGGAGGCGTCAAATTGTAGATATCGGTTAAATACTNTNTTTACATATAGATTAAAAAAATGATTAAATT
```

***AtRbcS2B* Promoter**

pL1M-R4-pAtRbcS2B-AtpOMT-tHSP

```
2 LS0201                tctattaccttatattaacacattcatatttttatttttccacttgataatcttaaataataagaatataagtataatct
15 LS0201_11_C05        NAAAAAANNNTTTTTNNCNNNNAAANTTTAAAAAAAAAAGGGTTAAAATTTTCCNTTNAACCNTNNAANTTNAAAANNNN
16 LS0201_OMTmid_A06    TCTATTACCTTATATTAACACATTCATATTTTTATTTTTCCACTTGATAATCTTAAATAATAAGAATATAAGTATAATCT
17 LS0201_12_D05         TCTATTACCTTATATTAACACATTCATATTTTTATTTTTCCACTTGATAATCTTAAATAATAAGAATATAAGTATAATCT
```

***AtRbcS2B* Promoter**

pL1M-R4-pAtRbcS2B-AtpOMT-tHSP

```
2 LS0201                ttgaattcatcccacattttaaaagtataattaaatcagacagagttcattcaaaatggtttttaattgggaaatgtaaa
15 LS0201_11_C05        NTTCCCNAAATTTTTAANTTTTTTTCCCCNTTNGNNAAANNNNNNAANNAAAAAAAAAAAAAAANNNAAANGGNAAAAANC
16 LS0201_OMTmid_A06    TTGAATTCATCCCACATTTTAAAAGTATAATTAAATCAGACAGAGTTCATTCAAAATGGTTTTTAATTGGGAAATGTAAA
17 LS0201_12_D05         TTGAATTCATCCCACATTTTAAAAGTATAATTAAATCAGACAGAGTTCATTCAAAATGGTTTTTAATTGGGAAATGTAAA
```

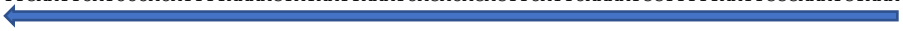

***AtRbcS2B* Promoter**

pL1M-R4-pAtRbcS2B-AtpOMT-tHSP

```
2 LS0201                ctagtattttgtgttattattttctatgtagtatgtacgatcactagaacttttagtcacataatggatattaaattaga
15 LS0201_11_C05        CNTTNNNAATTNNCCCCCCNNNNNNTTTTTNNAAAANNNAAANTTTTNAANTNNCNNNNNNAAANNNNTTTNNNNNNNAA
16 LS0201_OMTmid_A06    CTAGTATTTTGTGTTATTATTTTCTATGTAGTATGTACGATCACTAGAACTTTTAGTCACATAATGGATATTAAATTAGA
17 LS0201_12_D05         CTAGTATTTTGTGTTATTATTTTCTATGTAGTATGTACGATCACTAGAACTTTTAGTCACATAATGGATATTAAATTAGA
```

***AtRbcS2B* Promoter**

pL1M-R4-pAtRbcS2B-AtpOMT-tHSP

```
2 LS0201                aaacaatccaaatgcttgtgaattttcaggttttacggctaattaatatatttctgatgaacaagaggaacccacggcac
15 LS0201_11_C05        AAANGGGGGTTTTNNNAANNNNGGGGNAAAAAANNNGNNAAANNNNNNAANTTTTTNNN----------------------
16 LS0201_OMTmid_A06    AAACAATCCAAATGCTTGTGAATTTTCAGGTTTTACGGCTAATTAATATATTTCTGATGAACAAGAGGAACCCACGGCAC
17 LS0201_12_D05         AAACAATCCAAATGCTTGTGAATTTTCAGGTTTTACGGCTAATTAATATATTTCTGATGAACAAGAGGAACCCACGGCAC
```

***AtRbcS2B* Promoter**

pL1M-R4-pAtRbcS2B-AtpOMT-tHSP

```
2 LS0201                cgttccttttggagcacaacgcaattgcacttacggcccacttaagcacgaatgtggcacctcaagataattcccaccat
16 LS0201_OMTmid_A06    CGTTCCTTTTGGAGCACAACGCAATTGCACTTACGGCCCACTTAAGCACGAATGTGGCACCTCAAGATAATTCCCACCAT
17 LS0201_12_D05         CGTTCCTTTTGGAGCACAACGCAATTGCACTTACGGCCCACTTAAGCACGAATGTGGCACCTCAAGATAATTCCCACCAT
```

***AtRbcS2B* Promoter**

pL1M-R4-pAtRbcS2B-AtpOMT-tHSP

```
2 LS0201                gacaacttaagcacaaaagccatgacggatcatggggaaattttataacacacttcaatggatggtgtggatccgaggga
16 LS0201_OMTmid_A06    GACAACTTAAGCACAAAAGCCATGACGGATCATGGGGAAATTTTATAACACACTTCAATGGATGGTGTGGATCCGAGGGA
17 LS0201_12_D05         GACAACTTAAGCACAAAAGCCATGACGGATCATGGGGAAATTTTATAACACACTTCAATGGATGGTGTGGATCCGAGGGA
```

***AtRbcS2B* Promoter**

pL1M-R4-pAtRbcS2B-AtpOMT-tHSP

```
2 LS0201                agaatccacactctaaggccacatgaagaagctcatatggtcatgggtccacgaataccacgtaaaagctcatatatgcc
16 LS0201_OMTmid_A06    AGAATCCACACTCTAAGGCCACATGAAGAAGCTCATATGGTCATGGGTCCACGAATACCACGTAAAAGCTCATATATGCC
17 LS0201_12_D05         AGAATCCACACTCTAAGGCCACATGAAGAAGCTCATATGGTCATGGGTCCACGAATACCACGTAAAAGCTCATATATGCC
18 LS0201_13_E05         ---------NNNNNNNNNNNNNNCNTNNNGANCTCATATGGTCATGGGTCCACGAATACCACGTAAAAGCTCATATATGCC
```

***AtRbcS2B* Promoter**

pL1M-R4-pAtRbcS2B-AtpOMT-tHSP

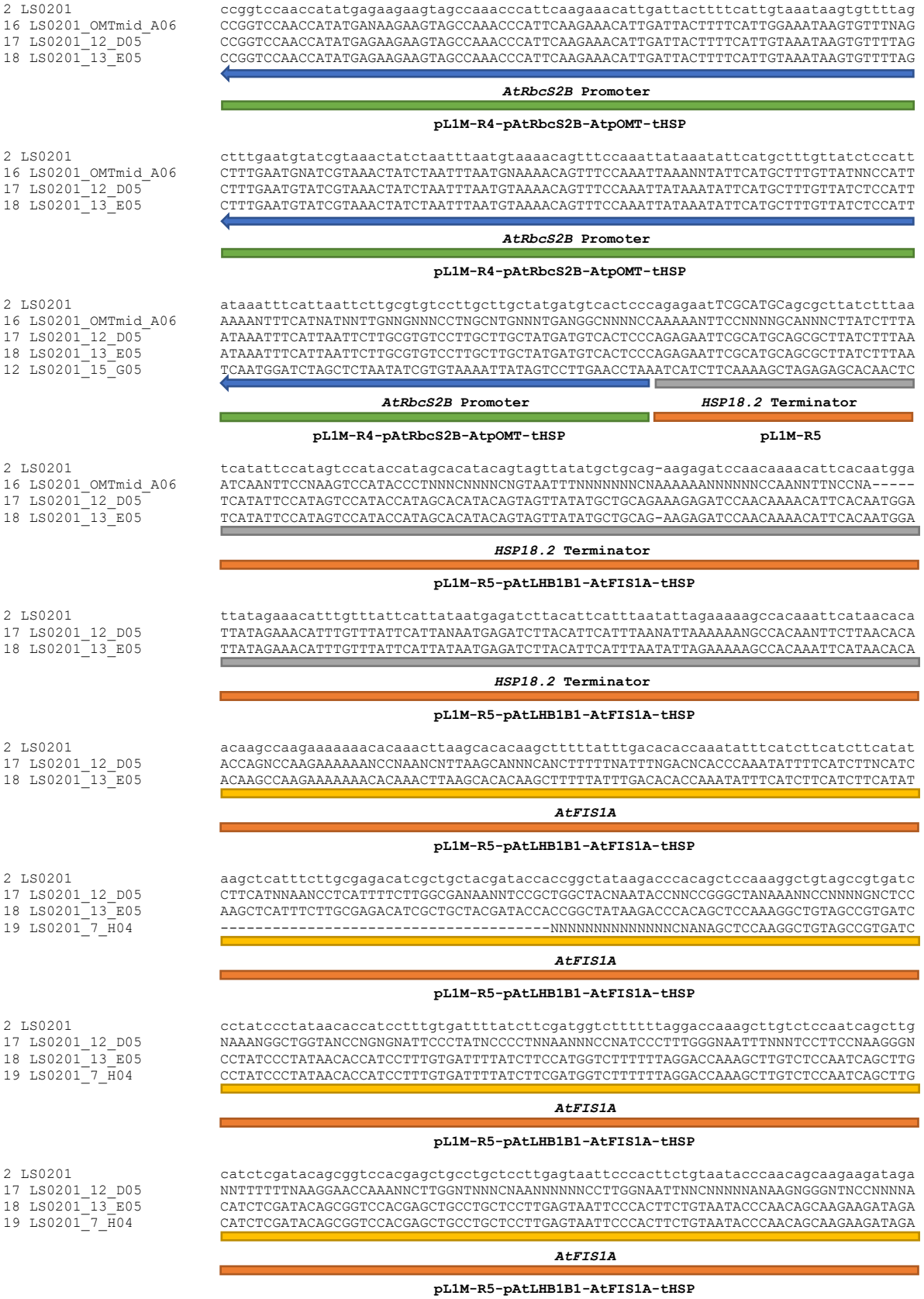
2 LS0201 ccggtccaaccatatgagaagaagtagccaaacccattcaagaaacattgattacttttcattgtaaataagtgttttag
16 LS0201_OMTmid_A06 CCGGTCCAACCATATGANAAGAAGTAGCCAAACCCATTCAAGAAACATTGATTACTTTTCATTGGAAATAAGTGTTTNAG
17 LS0201_12_D05 CCGGTCCAACCATATGAGAAGAAGTAGCCAAACCCATTCAAGAAACATTGATTACTTTTCATTGTAAATAAGTGTTTTAG
18 LS0201_13_E05 CCGGTCCAACCATATGAGAAGAAGTAGCCAAACCCATTCAAGAAACATTGATTACTTTTCATTGTAAATAAGTGTTTTAG
AtRbcS2B Promoter
pL1M-R4-pAtRbcS2B-AtpOMT-tHSP
2 LS0201 ctttgaatgtatcgtaaactatctaatttaatgtaaaacagtttccaaattataaatattcatgctttgttatctccatt
16 LS0201_OMTmid_A06 CTTTGAATGNATCGTAAACTATCTAATTTAATGNAAAACAGTTTCCAAATTAAANNTATTCATGCTTTGTTATNNCCATT
17 LS0201_12_D05 CTTTGAATGTATCGTAAACTATCTAATTTAATGTAAAACAGTTTCCAAATTATAAATATTCATGCTTTGTTATCTCCATT
18 LS0201_13_E05 CTTTGAATGTATCGTAAACTATCTAATTTAATGTAAAACAGTTTCCAAATTATAAATATTCATGCTTTGTTATCTCCATT
AtRbcS2B Promoter
pL1M-R4-pAtRbcS2B-AtpOMT-tHSP
2 LS0201 ataaatttcattaattcttgcgtgtccttgcttgctatgatgtcactcccagagaatTCGCATGCagcgcttatctttaa
16 LS0201_OMTmid_A06 AAAANTTTCATNATNNTTGNNGNNNCCTNGCNTGNNNTGANGGCNNNNCCAAAAANTTCCNNNNGCANNNCTTATCTTTA
17 LS0201_12_D05 ATAAATTTCATTAATTCTTGCGTGTCCTTGCTTGCTATGATGTCACTCCCAGAGAATTCGCATGCAGCGCTTATCTTTAA
18 LS0201_13_E05 ATAAATTTCATTAATTCTTGCGTGTCCTTGCTTGCTATGATGTCACTCCCAGAGAATTCGCATGCAGCGCTTATCTTTAA
12 LS0201_15_G05 TCAATGGATCTAGCTCTAATATCGTGTAAAATTATAGTCCTTGAACCTAAATCATCTTCAAAAGCTAGAGAGCACAACTC
AtRbcS2B Promoter
HSP18.2 Terminator
pL1M-R4-pAtRbcS2B-AtpOMT-tHSP
pL1M-R5
2 LS0201 tcatattccatagtccataccatagcacatacagtagttatatgctgcag-aagagatccaacaaaacattcacaatgga
16 LS0201_OMTmid_A06 ATCAANTTCCNAAGTCCATACCCTNNNCNNNNCNGTAATTTNNNNNNNCNAAAAAANNNNNNCCAANNTTNCCNA-----
17 LS0201_12_D05 TCATATTCCATAGTCCATACCATAGCACATACAGTAGTTATATGCTGCAGAAAGAGATCCAACAAAACATTCACAATGGA
18 LS0201_13_E05 TCATATTCCATAGTCCATACCATAGCACATACAGTAGTTATATGCTGCAG-AAGAGATCCAACAAAACATTCACAATGGA
HSP18.2 Terminator
pL1M-R5-pAtLHB1B1-AtFIS1A-tHSP
2 LS0201 ttatagaaacatttgtttattcattataatgagatcttacattcatttaatattagaaaaagccacaaattcataacaca
17 LS0201_12_D05 TTATAGAAACATTTGTTTATTCATTANAATGAGATCTTACATTCATTTAANATTAAAAAANGCCACAANTTCTTAACACA
18 LS0201_13_E05 TTATAGAAACATTTGTTTATTCATTATAATGAGATCTTACATTCATTTAATATTAGAAAAAGCCACAAATTCATAACACA
HSP18.2 Terminator
pL1M-R5-pAtLHB1B1-AtFIS1A-tHSP
2 LS0201 acaagccaagaaaaaaacacaaacttaagcacacaagctttttatttgacacaccaaatatttcatcttcatcttcatat
17 LS0201_12_D05 ACCAGNCCAAGAAAAAANCCNAANCNTTAAGCANNNCANCTTTTTNATTTNGACNCACCCAAATATTTTCATCTTNCATC
18 LS0201_13_E05 ACAAGCCAAGAAAAAAACACAAACTTAAGCACACAAGCTTTTTATTTGACACACCAAATATTTCATCTTCATCTTCATAT
AtFIS1A
pL1M-R5-pAtLHB1B1-AtFIS1A-tHSP
2 LS0201 aagctcatttcttgcgagacatcgctgctacgataccaccggctataagacccacagctccaaaggctgtagccgtgatc
17 LS0201_12_D05 CTTCATNNAANCCTCATTTTCTTGGCGANAANNTCCGCTGGCTACNAATACCNNCCGGGCTANAAANNCCNNNNGNCTCC
18 LS0201_13_E05 AAGCTCATTTCTTGCGAGACATCGCTGCTACGATACCACCGGCTATAAGACCCACAGCTCCAAAGGCTGTAGCCGTGATC
19 LS0201_7_H04 ----------NNNNNNNNNNNNNNCNANAGCTCCAAGGCTGTAGCCGTGATC
AtFIS1A
pL1M-R5-pAtLHB1B1-AtFIS1A-tHSP
2 LS0201 cctatccctataacaccatcctttgtgattttatcttcgatggtctttttttaggaccaaagcttgtctccaatcagcttg
17 LS0201_12_D05 NAAANGGCTGGTANCCNGNGNATTCCCTATNCCCCTNNAANNNCCNATCCCTTTGGGNAATTTNNNTCCTTCCNAAGGGN
18 LS0201_13_E05 CCTATCCCTATAACACCATCCTTTGTGATTTTATCTTCCATGGTCTTTTTTTAGGACCAAAGCTTGTCTCCAATCAGCTTG
19 LS0201_7_H04 CCTATCCCTATAACACCATCCTTTGTGATTTTATCTTCGATGGTCTTTTTTTAGGACCAAAGCTTGTCTCCAATCAGCTTG
AtFIS1A
pL1M-R5-pAtLHB1B1-AtFIS1A-tHSP
2 LS0201 catctcgatacagcggtccacgagctgcctgctccttgagtaattcccacttctgtaatacccaacagcaagaagatagа
17 LS0201_12_D05 NNTTTTTTNAAGGAACCAAANNCTTGGNTNNNCNAANNNNNNCCTTGGNAATTNNCNNNNNANAAGNGGGNTNCCNNNNA
18 LS0201_13_E05 CATCTCGATACAGCGGTCCACGAGCTGCCTGCTCCTTGAGTAATTCCCACTTCTGTAATACCCAACAGCAAGAAGATAGA
19 LS0201_7_H04 CATCTCGATACAGCGGTCCACGAGCTGCCTGCTCCTTGAGTAATTCCCACTTCTGTAATACCCAACAGCAAGAAGATAGA
AtFIS1A
pL1M-R5-pAtLHB1B1-AtFIS1A-tHSP

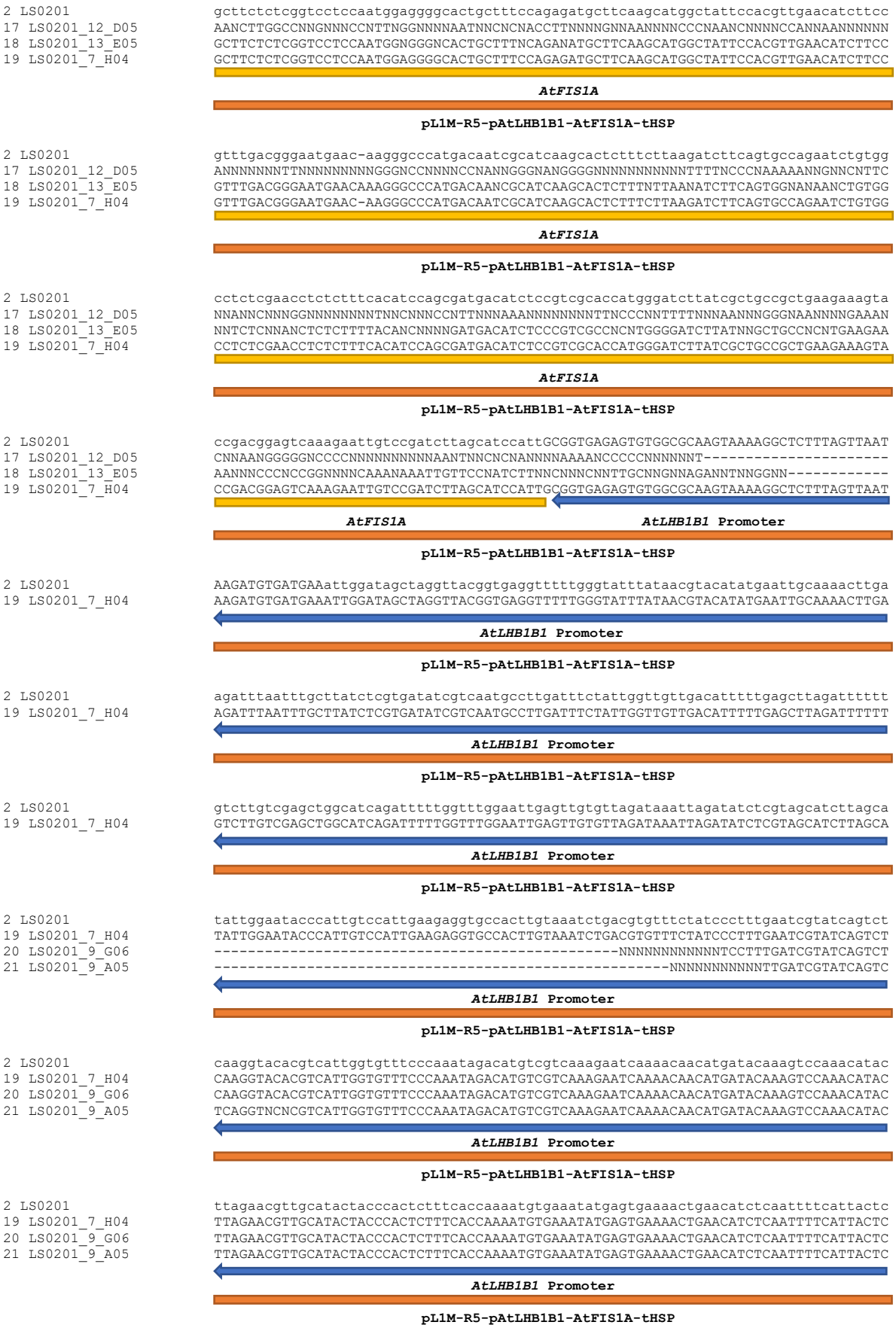
2 LS0201 gcttctctcggtcctccaatggaggggcactgctttccagagatgcttcaagcatggctattccacgttgaacatcttcc
17 LS0201_12_D05 AANCTTGGCCNNGNNNCCNTTNGGNNNNAATNNCNCNACCTTNNNNGNNAANNNNCCCNAANCNNNNCCANNAANNNNNN
18 LS0201_13_E05 GCTTCTCTCGGTCCTCCAATGGNGGGNCACTGCTTTNCAGANATGCTTCAAGCATGGCTATTCCACGTTGAACATCTTCC
19 LS0201_7_H04 GCTTCTCTCGGTCCTCCAATGGAGGGGCACTGCTTTCCAGAGATGCTTCAAGCATGGCTATTCCACGTTGAACATCTTCC
AtFIS1A
pL1M-R5-pAtLHB1B1-AtFIS1A-tHSP
2 LS0201 gtttgacgggaatgaac-aagggcccatgacaatcgcatcaagcactctttcttaagatcttcagtgccagaatctgtgg
17 LS0201_12_D05 ANNNNNNNTTNNNNNNNNGGGNCCNNNNCCNANNGGGNANGGGGNNNNNNNNNNTTTTNCCCNAAAAANNGNNCNTTC
18 LS0201_13_E05 GTTTGACGGGAATGAACAAAGGGCCCATGACAANCGCATCAAGCACTCTTTNTTAANATCTTCAGTGGNANAANCTGTGG
19 LS0201_7_H04 GTTTGACGGGAATGAAC-AAGGGCCCATGACAATCGCATCAAGCACTCTTTCTTAAGATCTTCAGTGCCAGAATCTGTGG
AtFIS1A
pL1M-R5-pAtLHB1B1-AtFIS1A-tHSP
2 LS0201 cctctcgaacctctctttcacatccagcgatgacatctccgtcgcaccatgggatcttatcgctgccgctgaagaaagta
17 LS0201_12_D05 NNANNCNNNGGNNNNNNNNTNNCNNNCCNTTNNNAAANNNNNNNNTTNCCCNNTTTNNNAANNNGGGNAANNNNGAAAN
18 LS0201_13_E05 NNTCTCNNANCTCTCTTTTACANCNNNNGATGACATCTCCCGTCGCCNCNTGGGGATCTTATNNGCTGCCNCNTGAAGAA
19 LS0201_7_H04 CCTCTCGAACCTCTCTTTCACATCCAGCGATGACATCTCCGTCGCACCATGGGATCTTATCGCTGCCGCTGAAGAAAGTA
AtFIS1A
pL1M-R5-pAtLHB1B1-AtFIS1A-tHSP
2 LS0201 ccgacggagtcaaagaattgtccgatcttagcatccattGCGGTGAGAGTGTGGCGCAAGTAAAAGGCTCTTTAGTTAAT
17 LS0201_12_D05 CNNAANGGGGGNCCCCNNNNNNNNNNAANTNNCNCNANNNNAAAANCCCCCNNNNNNT----------
18 LS0201_13_E05 AANNNCCCNCCGGNNNNCAAANAAATTGTTCCNATCTTNNCNNNCNNTTGCNNGNNAGANNTNNGGNN----------
19 LS0201_7_H04 CCGACGGAGTCAAAGAATTGTCCGATCTTAGCATCCATTGCGGTGAGAGTGTGGCGCAAGTAAAAGGCTCTTTAGTTAAT
AtFIS1A
AtLHB1B1 Promoter
pL1M-R5-pAtLHB1B1-AtFIS1A-tHSP
2 LS0201 AAGATGTGATGAAattggatagctaggttacggtgaggtttttgggtatttataacgtacatatgaattgcaaaacttga
19 LS0201_7_H04 AAGATGTGATGAAATTGGATAGCTAGGTTACGGTGAGGTTTTTGGGTATTTATAACGTACATATGAATTGCAAAACTTGA
AtLHB1B1 Promoter
pL1M-R5-pAtLHB1B1-AtFIS1A-tHSP
2 LS0201 agatttaatttgcttatctcgtgatatcgtcaatgccttgatttctattggttgttgacatttttgagcttagatttttt
19 LS0201_7_H04 AGATTTAATTTGCTTATCTCGTGATATCGTCAATGCCTTGATTTCTATTGGTTGTTGACATTTTTGAGCTTAGATTTTTT
AtLHB1B1 Promoter
pL1M-R5-pAtLHB1B1-AtFIS1A-tHSP
2 LS0201 gtcttgtcgagctggcatcagatttttggtttggaattgagttgtgttagataaattagatatctcgtagcatcttagca
19 LS0201_7_H04 GTCTTGTCGAGCTGGCATCAGATTTTTGGTTTGGAATTGAGTTGTGTTAGATAAATTAGATATCTCGTAGCATCTTAGCA
AtLHB1B1 Promoter
pL1M-R5-pAtLHB1B1-AtFIS1A-tHSP
2 LS0201 tattggaatacccattgtccattgaagaggtgccacttgtaaatctgacgtgtttctatccctttgaatcgtatcagtct
19 LS0201_7_H04 TATTGGAATACCCATTGTCCATTGAAGAGGTGCCACTTGTAAATCTGACGTGTTTCTATCCCTTTGAATCGTATCAGTCT
20 LS0201_9_G06 ----------NNNNNNNNNNNNTCCTTTGATCGTATCAGTCT
21 LS0201_9_A05 ----------NNNNNNNNNNTTGATCGTATCAGTC
AtLHB1B1 Promoter
pL1M-R5-pAtLHB1B1-AtFIS1A-tHSP
2 LS0201 caaggtacacgtcattggtgtttcccaaatagacatgtcgtcaaagaatcaaaacaacatgatacaaagtccaaacatac
19 LS0201_7_H04 CAAGGTACACGTCATTGGTGTTTCCCAAATAGACATGTCGTCAAAGAATCAAAACAACATGATACAAAGTCCAAACATAC
20 LS0201_9_G06 CAAGGTACACGTCATTGGTGTTTCCCAAATAGACATGTCGTCAAAGAATCAAAACAACATGATACAAAGTCCAAACATAC
21 LS0201_9_A05 TCAGGTNCNCGTCATTGGTGTTTCCCAAATAGACATGTCGTCAAAGAATCAAAACAACATGATACAAAGTCCAAACATAC
AtLHB1B1 Promoter
pL1M-R5-pAtLHB1B1-AtFIS1A-tHSP
2 LS0201 ttagaacgttgcatactacccactctttcaccaaaatgtgaaatatgagtgaaaactgaacatctcaattttcattactc
19 LS0201_7_H04 TTAGAACGTTGCATACTACCCACTCTTTCACCAAAATGTGAAATATGAGTGAAAACTGAACATCTCAATTTTCATTACTC
20 LS0201_9_G06 TTAGAACGTTGCATACTACCCACTCTTTCACCAAAATGTGAAATATGAGTGAAAACTGAACATCTCAATTTTCATTACTC
21 LS0201_9_A05 TTAGAACGTTGCATACTACCCACTCTTTCACCAAAATGTGAAATATGAGTGAAAACTGAACATCTCAATTTTCATTACTC
AtLHB1B1 Promoter
pL1M-R5-pAtLHB1B1-AtFIS1A-tHSP


2 LS0201 taagtttgttaattatcttgttaaaaaaactactctaaattacagaagatttaatcctgataagaaagtacattaaaatg
19 LS0201_7_H04 TAAGTTTGTTAATTATCTTGTTAAAAAAACTACTCTAAATTACAGAAGATTTAATCCTGATAAGAAAGTACATTAAAATG
20 LS0201_9_G06 TAAGTTTGTTAATTATCTTGTTAAAAAAACTACTCTAAATTACAGAAGATTTAATCCTGATAAGAAAGTACATTAAAATG
21 LS0201_9_A05 TAAGTTTGTTAATTATCTTGTTAAAAAAACTACTCTAAATTACAGAAGATTTAATCCTGATAAGAAAGTACATTAAAATG
AtLHB1B1 Promoter
pL1M-R5-pAtLHB1B1-AtFIS1A-tHSP
2 LS0201 acaacaaagtaaaaaaaaaaaatacagttcatcttcaaagacatgttttctaattcgtattggcaagaaaaacttaccag
19 LS0201_7_H04 ACAACAAAGTAAAAAAAAAAAATACAGTTCATCTTCAAAGACATGTTTTCTAATTCGTATTGGCAAGAAAAACTTACCAG
20 LS0201_9_G06 ACAACAAAGTAAAAAAAAAAAATACAGTTCATCTTCAAAGACATGTTTTCTAATTCGTATTGGCAAGAAAAACTTACCAG
21 LS0201_9_A05 ACAACAAAGTAAAAAAAAAAAATACAGTTCATCTTCAAAGACATGTTTTCTAATTCGTATTGGCAAGAAAAACTTACCAG
AtLHB1B1 Promoter
pL1M-R5-pAtLHB1B1-AtFIS1A-tHSP
2 LS0201 tcatatCTCCTGTGGaattcctcgagggaggtcaacatggtgg-agcacgacactctggtctactccaaaaatgtcaaag
19 LS0201_7_H04 TCATATCTCCTGTGGAATTCCTCGAGGGAGGTCAACATGGTGGNGGNAGCACGACNCTCTGGTCTACTCCAAAAATGTCAAAN
20 LS0201_9_G06 TCATATCTCCTGTGGAATTCCTCGAGGGAGGTCAACATGGTGG-AGCACGACACTCTGGTCTACTCCAAAAATGTCAAAG
21 LS0201_9_A05 TCATATCTCCTGTGGAATTCCTCGAGGGAGGTCAACATGGTGG-AGCACGACACTCTGGTCTACTCCAAAAATGTCAAAG
pAtLHB1B1
2xCaMV35S Promoter
pL1M-R5
pL1M-F6-p2xCaMV35S-c-peredox-mCherry-tHSP
2 LS0201 atacagtctcagaagatcaaagggctattgagacttttcaacaaaggataatttcgggaaacctcctcggattccattgc
19 LS0201_7_H04 ATACAGTCTCNNAANNTCAAAGGGCTATTGANNCTTTTCAACAAAGGATAATTTCGGGAAACCTCCTCGGATTCCATTGC
20 LS0201_9_G06 ATACAGTCTCAGAAGATCAAAGGGCTATTGAGACTTTTCAACAAAGGATAATTTCGGGAAACCTCCTCGGATTCCATTGC
21 LS0201_9_A05 ATACAGTCTCAGAAGATCAAAGGGCTATTGAGACTTTTCAACAAAGGATAATTTCGGGAAACCTCCTCGGATTCCATTGC
2xCaMV35S Promoter
pL1M-F6-p2xCaMV35S-c-peredox-mCherry-tHSP
2 LS0201 ccagctatctgtcacttcatcgaaaggacagtagaaaaggaaggtggctcctacaaatgccatcattgcgataaaggaaa
19 LS0201_7_H04 CCAGCTANCTGTCACTTCATCGAAAGGACAGTAAAAAAGGAAGGNGNCTCCTACAAATGCCATCATTGNNAAANNGGAAA
20 LS0201_9_G06 CCAGCTATCTGTCACTTCATCGAAAGGACAGTAGAAAAGGAAGGTGGCTCCTACAAATGCCATCATTGCGATAAAGGAAA
21 LS0201_9_A05 CCAGCTATCTGTCACTTCATCGAAAGGACAGTAGAAAAGGAAGGTGGCTCCTACAAATGCCATCATTGCGATAAAGGAAA
2xCaMV35S Promoter
pL1M-F6-p2xCaMV35S-c-peredox-mCherry-tHSP
2 LS0201 ggctatcattcaagatctctctgccgacagtggtcccaaagatggacccccacccacgaggagcatcgtggaaaaagaag
19 LS0201_7_H04 GGNNNNNTTNCAANNNNNNNNNGNCCNANNGNGNNCCCNANNANTGGACCCCNNCCNNNNNGGNACNNCNGGNAAAAAAA
20 LS0201_9_G06 GGCTATCATTCAAGATCTCTCTGCCGACAGTGGTCCCAAAGATGGACCCCCACCCACGAGGAGCATCGTGGAAAAAGAAG
21 LS0201_9_A05 GGCTATCATTCAAGATCTCTCTGCCGACAGTGGTCCCAAAGATGGACCCCCACCCACGAGGAGCATCGTGGAAAAAGAAG
2xCaMV35S Promoter
pL1M-F6-p2xCaMV35S-c-peredox-mCherry-tHSP
2 LS0201 aggttccaaccacgtctacaaagcaagtggattgatgtgataacatggtggagcacgacactctggtctactccaaaaat
20 LS0201_9_G06 AGGTTCCAACCACGTCTACAAAGCAAGTGGATTGATGTGATAACATGGTGGAGCACGACACTCTGGTCTACTCCAAAAAT
21 LS0201_9_A05 AGGTTCCAACCACGTCTACAAAGCAAGTGGATTGATGTGATAACATGGTGGAGCACGACACTCTGGTCTACTCCAAAAAT
2xCaMV35S Promoter
pL1M-F6-p2xCaMV35S-c-peredox-mCherry-tHSP
2 LS0201 gtcaaagatacagtctcagaagatcaaagggctattgagacttttcaacaaaggataatttcgggaaacctcctcggatt
19 LS0201_7_H04 CCC----------
20 LS0201_9_G06 GTCAAAGATACAGTCTCAGAAGATCAAAGGGCTATTGAGACTTTTCAACAAAGGATAATTTCGGGAAACCTCCTCGGATT
21 LS0201_9_A05 GTCAAAGATACAGTCTCAGAAGATCAAAGGGCTATTGAGACTTTTCAACAAAGGATAATTTCGGGAAACCTCCTCGGATT
2xCaMV35S Promoter
pL1M-F6-p2xCaMV35S-c-peredox-mCherry-tHSP
2 LS0201 ccattgcccagctatctgtcacttcatcgaaaggacagtagaaaaggaaggtggctcctacaaatgccatcattgcgata
20 LS0201_9_G06 CCATTGCCCAGCTATCTGTCACTTCATCGAAAGGACAGTAGAAAAGGAAGGTGGCTCCTACAAATGCCATCATTGCGATA
21 LS0201_9_A05 CCATTGCCCAGCTATCTGTCACTTCATCGAAAGGACAGTAGAAAAGGAAGGTGGCTCCTACAAATGCCATCATTGCGATA
2xCaMV35S Promoter
pL1M-F6-p2xCaMV35S-c-peredox-mCherry-tHSP

```
2 LS0201                aaggaaaggctatcattcaagatctctctgccgacagtggtcccaaagatggacccccacccacgaggagcatcgtggaa
20 LS0201_9_G06         AAGGAAAGGCTATCATTCAAGATCTCTCTGCCGACAGTGGTCCCAAAGATGGACCCCCACCCACGAGGAGCATCGTGGAA
21 LS0201_9_A05         AAGGAAAGGCTATCATTCAAGATCTCTCTGCCGACAGTGGTCCCAAAGATGGACCCCCACCCACGAGGAGCATCGTGGAA
```

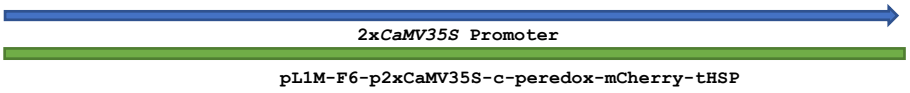


```
2 LS0201                aaagaagaggttccaaccacgtctacaaagcaagtggattgatgtgacatctccactgacgtaagggatgacgcacaatc
20 LS0201_9_G06         AAAGAAGAGGTTCCAACCACGTCTACAAAGCAAGTGGATTGATGTGACATCTCCACTGACGTAAGGGATGACGCACAATC
21 LS0201_9_A05         AAAGAAGAGGTTCCAACCACGTCTACAAAGCAAGTGGATTGATGTGACATCTCCACTGACGTAAGGGATGACGCACAATC
```

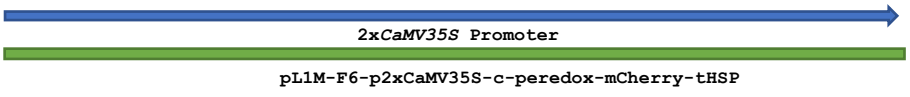


```
2 LS0201                ccactatccttcgcaagacccttcctctatataaggaagttcatttcatttggagaggacacgcaat-ggttgctagcaa
20 LS0201_9_G06         CCACTATCCTTCGCAAGACCCTTCCTCTATATAAGGAAGTTCATTTCATTTGGAGAGGACACGCAAT-GGTTGCTAGCAA
21 LS0201_9_A05         CCACTATCCTTCGCAAGACCCTTCCTCTATATAAGGAAGTTCATTTCATTTGGAGAGGACNCGCAATGGGTTGCTAGCAA
```

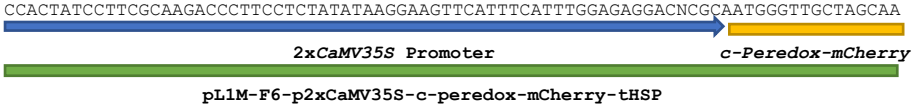


```
2 LS0201                agttcctgaagcagccatttccagactgattacttacctgagaattctggaagagctggaagcccaaggtgtacaccgca
20 LS0201_9_G06         AGTTCCTGAAGCAGCCATTTCCAGACTGATTACTTACCTGNNAATTCTGGAAGAGCTGGAAGCCCAAGGTGTACACCGCA
21 LS0201_9_A05         NGTTCCTGAAGCAGCCATTTCCAGACTGATTACTTACCTGAGAANTCTGGNAAAAANCTGGAANCCCNAAGGNGTACACCG
```

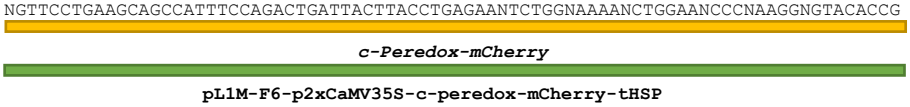


```
2 LS0201                ccgcctccgagcaactgggcgagctggcccaggtcaccgccttccaggttgataaggacctgtcctacttcggctcctac
20 LS0201_9_G06         CCGCCTCCGAGCAACTGGNCGAGCTGGCCCAGGTCACCGCCTTCCAGGTTGANAAGGACCTGTCCTACTTCGGCTCCTAC
22 LS0201_18_G10        NNNNCNNNCNNNCACTGGGCGANCTGG-CCAGGTCACNGCCTTCCAGGTTGATAAGGACCTGTCCTACTTCGGCTCCTAC
```

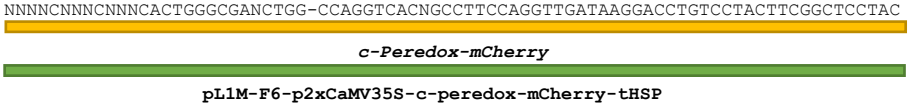


```
2 LS0201                ggcactgacggcgttggctacactgtaccggtcctcaagagagaactgcgccatatcctcggtctgaaccgcaaatgggg
20 LS0201_9_G06         GGCACTGACGGNNTTNGGCTANNNTGTACCGGTCNNNNAAAAAAAANNCTGCCNNANNNNCNNNGGTNNGAACCGCAANTG
22 LS0201_18_G10        GGCACTGACGGCGTTGGCTACACTGTACCGGTCCTNAANNGAGAACTGCGCCATATCCTCGGTCTGAACCGCAAATGGGG
23 LS0201_peredox1_H10  ----------------------------------------------NNNNNNNNNNNNTCNGTCTGACGC---AATGGGG
```

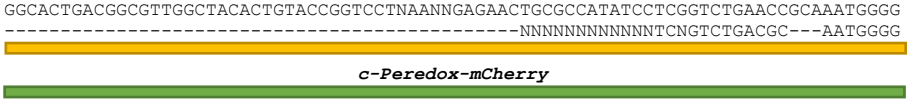


```
2 LS0201                cctgtgcatcgtggggatgggccgcctgggatccgctcttgctgattggcctggttttggcgagagcttcgagctgcgcg
20 LS0201_9_G06         GGGGCCTGNNNNNNCCTGGGGGNATGGGCCCCCNTGGNAATCCNNTTTTNGCTGANTGGNCCTGGTTTTTGGNNAANNNN
22 LS0201_18_G10        CCTGTGCATCGTGGGGATGGGCCGCCTGNNATCNGCTCTTGCTGATTGGCCTGGTTTTGGCGANAGCTTNNANCTGCGCG
23 LS0201_peredox1_H10  CCTGTGCATCGTGGGGATGGGCCGCCTGGGATCCGCTCTTGCTGATTGGCCTGGTTTTGGCGAGAGCTTCGAGCTGCGCG
```

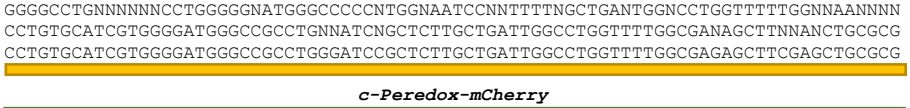


```
2 LS0201                gtttcttcgatgttgacccaggtatggttggtcggccggttcgcggtggtgttatcgaacacgttgatctgctgccccag
22 LS0201_18_G10        GTTTCTTCNATGTTGACCCAGGTATGGTTGGTCGGCCGGTTCGCNGTGGTGTTATCGANNACGTTGATCTGCTGCCCCAG
23 LS0201_peredox1_H10  GTTTCTTCGATGTTGACCCAGGTATGGTTGGTCGGCCGGTTCGCGGTGGTGTTATCGAACACGTTGATCTGCTGCCCCAG
```


```
2 LS0201                cgcgtacctggtcgcatcgaaatcgctctgctgacggttccacgcgaggcagcacagaaggctgccgacctgctggttgc
22 LS0201_18_G10        CGCGTACCTGGTCGCATCGAAATCGCTCTGCTGACGGTTCCACGCGAGGCAGCACAGAAGGCTGCCGACNTGCTGGTTGC
23 LS0201_peredox1_H10  CGCGTACCTGGTCGCATCGAAATCGCTCTGCTGACGGTTCCACGCGAGGCAGCACAGAAGGCTGCCGACCTGCTGGTTGC
```

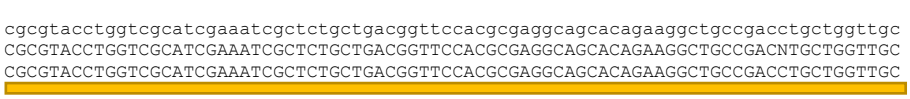


```
2 LS0201                cgctggcatcaagggcatcctgaacttcgctccagttgtactggaggttcccaaggaagtggctgttgagaacgttgaca
22 LS0201_18_G10        CGCTGGCATCAAGGGCATCCTGAACTTCGCTCCAGTTGTACTGGAGGTTCCCAAGGAAGTGGCTGTTGAGAACGTTGACA
23 LS0201_peredox1_H10  CGCTGGCATCAAGGGCATCCTGAACTTCGCTCCAGTTGTACTGGAGGTTCCCAAGGAAGTGGCTGTTGAGAACGTTGACA
```

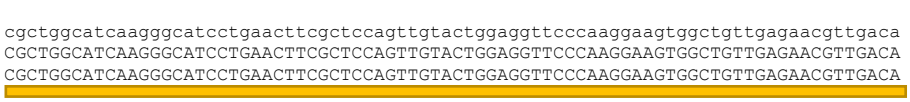

```
2 LS0201                 tcctggccggtctgacgcgtctgagctttgccattctgaaccccacgtggagcgcagcaggtgggcatggtttcactgct
22 LS0201_18_G10         TCCTGGCCGGTCTGACGCGTCTGAACTTTGCCATTCTGAACCCCACGTGGNGCGCANNAAGTGGGCATGNTTTNACTGCT
23 LS0201_peredox1_H10   TCCTGGCCGGTCTGACGCGTCTGAGCTTTGCCATTCTGAACCCCACGTGGAGCGCAGCAGGTGGGCATGGTTTCACTGCT
```

c-Peredox-mCherry

pL1M-F6-p2xCaMV35S-c-peredox-mCherry-tHSP

```
2 LS0201                 cataacgtgtatatcatggctgacaaacagaagaacggtatcaaggccaacttcaagatccgccacaacatcgaagatgg
22 LS0201_18_G10         CATAACGTGNNTNNCATGGCTGACNNNCANAAGAACGGTATCAAGGCCAACTTCAAGATCCGCCACAACATCNAAGATGG
23 LS0201_peredox1_H10   CATAACGTGTATATCATGGCTGACAAACAGAAGAACGGTATCAAGGCCAACTTCAAGATCCGCCACAACATCGAAGATGG
```

c-Peredox-mCherry

pL1M-F6-p2xCaMV35S-c-peredox-mCherry-tHSP

```
2 LS0201                 cggcgttcagctggctgatcactaccagcagaacaccccaatcggcgacggccctgttctgctgcctgacaaccactact
22 LS0201_18_G10         CGNCGTTCAGCTGGCTGATCACTACCAGCANAACACCCCAATCGGCGACGGCCCTGTTCTGCTGCCTGACAACCACTACT
23 LS0201_peredox1_H10   CGGCGTTCAGCTGGCTGATCACTACCAGCAGAACACCCCAATCGGCGACGGCCCTGTTCTGCTGCCTGACAACCACTACT
24 LS0201_peredoxmid2_B06------NNNNNNNNNNTGNNCNCTACCAGCAGACACCCNAATCGGCGACGGCCCTGTTCTGCTGCCTGACAACCACTACT
```

c-Peredox-mCherry

pL1M-F6-p2xCaMV35S-c-peredox-mCherry-tHSP

```
2 LS0201                 taagcatccagtctaaactgtccaaagacccaaacgagaagcgcgaccacatggttctgctggaatttgttaccgccgct
22 LS0201_18_G10         TAAGCATCCAGTCTAAACTGTCCAAAGACCNAAACGAGAAGCGCGACCACATGGTTCTGCTGGAATTTGTTACCGCCGCT
23 LS0201_peredox1_H10   TAAGCATCCAGTCTAAACTGTCCAAAGACCCAAACGAGAAGCGCGACCACATGGTTCTGCTGGAATTTGTTACCGCCGCT
24 LS0201_peredoxmid2_B06TAAGCATCCAGTCTAAACTGTCCAAAGACCCAAACGAGAAGCGCGACCACATGGTTCTGCTGGAATTTGTTACCGCCGCT
```

c-Peredox-mCherry

pL1M-F6-p2xCaMV35S-c-peredox-mCherry-tHSP

```
2 LS0201                 ggcatcacccacggcatggacgaactgtacaagggcggcaccgggggatctatggtttccaaaggcgaggaactgttcac
22 LS0201_18_G10         GGCATCNCCCACGGCATGGACGAACTGTACAAGGGCGGCACCGGGGNGATCTATGGTTTCCAAAGGCGANNAACTGTTCAC
23 LS0201_peredox1_H10   GGCATCACCCACGGCATGGACGAACTGTACAAGGGCGGCACCGGGGGATCTATGGTTTCCAAAGGCGAGGAACTGTTCAC
24 LS0201_peredoxmid2_B06GGCATCACCCACGGCATGGACGAACTGTACAAGGGCGGCACCGGGGGATCTATGGTTTCCAAAGGCGAGGAACTGTTCAC
```

c-Peredox-mCherry

pL1M-F6-p2xCaMV35S-c-peredox-mCherry-tHSP

```
2 LS0201                 tggtgttgttcctatcctggttgaactggacggcgacgttaacggccacaaattcagcgttagcggggaaggcgaaggag
22 LS0201_18_G10         TGGTGTTGTTCCTATCCTGGTTGAACTGGACGGCGACGTTAACGGCCACAAATTCAGCGTTAGCGGGGAAGGCGAAGGAG
23 LS0201_peredox1_H10   TGGTGTTGTTCCTATCCTGGTTGAACTGGACGGCGACGTTAACGGCCACAAATTCAGCGTTAGCGGGGAAGGCGAAGGAG
24 LS0201_peredoxmid2_B06TGGTGTTGTTCCTATCCTGGTTGAACTGGACGGCGACGTTAACGGCCACAAATTCAGCGTTAGCGGGGAAGGCGAAGGAG
```

c-Peredox-mCherry

pL1M-F6-p2xCaMV35S-c-peredox-mCherry-tHSP

```
2 LS0201                 atgctacctacggcaagctgactctgaagttcatctgcaccactggcaagctgcctgttccttggcctaccctggttact
22 LS0201_18_G10         ATGCTACCTACGNCAAGCTGACTCTGAAGTTCATCTGCACCACTGGCAAGCTGCCTGTTCCTTGACCTACCCTGNTNACT
23 LS0201_peredox1_H10   ATGCTACCTACGGCAAGCTGACTCTGAAGTTCATCTGCACCACTGGCAAGCTGCCTGTTCCTTGGCCTACCCTGGTTACT
24 LS0201_peredoxmid2_B06ATGCTACCTACGGCAAGCTGACTCTGAAGTTCATCTGCACCACTGGCAAGCTGCCTGTTCCTTGGCCTACCCTGGTTACT
```

c-Peredox-mCherry

pL1M-F6-p2xCaMV35S-c-peredox-mCherry-tHSP

```
2 LS0201                 accttctcctatggtgttatggttttcgccagatatcctgaccacatgaagcagcacgacttcttcaagagcgccatgcc
22 LS0201_18_G10         ACCTTCTCCTATGGTGTTATGGTTTTCGCCAGATATCCTGANCACATGAATCAGCANGACTTCATCAAGANCGNCATGCC
23 LS0201_peredox1_H10   ACCTTCTCCTATGGTGTTATGGTTTTCGCCAGATATCCTGACCACATGAAGCAGCACGACTTCTTCAAGAGCGCCATGCC
24 LS0201_peredoxmid2_B06ACCTTCTCCTATGGTGTTATGGTTTTCGCCAGATATCCTGACCACATGAAGCAGCACGACTTCTTCAAGAGCGCCATGCC
```

c-Peredox-mCherry

pL1M-F6-p2xCaMV35S-c-peredox-mCherry-tHSP

```
2 LS0201                 tgagggctacgttcaggaacgcaccatctttttcaaggacgacggcaactataagacacgcgctgaggttaagttcgagg
22 LS0201_18_G10         TGAGGNCTACGTTCAGGAACGCACCATCTTTTTCAAGGACGACGGCAACTATAAGACANGCGCTGAGGTTAANTTCGAGG
23 LS0201_peredox1_H10   TGAGGGCTACGTTCAGGAACGCACCATCTTTTTCAAGGACGACGGCAACTATAAGACACGCGCTGAAGTTAAGTTCGAGG
24 LS0201_peredoxmid2_B06TGAGGGCTACGTTCAGGAACGCACCATCTTTTTCAAGGACGACGGCAACTATAAGACACGCGCTGAGGTTAAGTTCGAGG
25 LS0201_peredoxmid3_C06--NNNNNNNNNNNNNNNGACGCACCATCTTTTTC-AGGACGACGGCAACTATAAGACACGCGCTGAGGTTAAGTTCGAGG
```

c-Peredox-mCherry

pL1M-F6-p2xCaMV35S-c-peredox-mCherry-tHSP

```
2 LS0201                gcgacactctggttaaccgcatcgagctgaagggcatcgacttcaaggaggacggcaacatcct-gggccataagcttga
22 LS0201_18_G10        GNNACACTCTGGTTAACNGCATCANNCTNAAGGGCATCGACTTCAANGAAGAACGGCAACATCCTGGNNCCATAANCTTG
23 LS0201_peredox1_H10  GCGACACTCTGGTTAACCGCATCGAGCTGAAGGGCATCGACTTCAAGGAGGACGGCAACATCCTGGGGCCATAAGCTTGA
24 LS0201_peredoxmid2_B06GCGACACTCTGGTTAACCGCATCGAGCTGAAGGGCATCGACTTCAAGGAGGACGGCAACATCCT-GGGCCATAAGCTTGA
25 LS0201_peredoxmid3_C06GCGACACTCTGGTTAACCGCATCGAGCTGAAGGGCATCGACTTCAAGGAGGACGGCAACATCCT-GGGCCATAAGCTTGA
```

c-Peredox-mCherry

pL1M-F6-p2xCaMV35S-c-peredox-mCherry-tHSP

```
2 LS0201                atataacaccaaggtacctgaagcc-gccatcagcc-gcctcatcacttacctccgcatcctgg-aggagctcgaagccc
22 LS0201_18_G10        AATNTAANNCCAAGGTACCTGAANCCNNCNNCANCCGCCTCATNNTTNACCTCCGCATCCTGGAAGAANCTCNAANNCCT
23 LS0201_peredox1_H10  ATATAACACCANGGTACCTGAANCCNGCCATCAGCCNGCCTCATCACTTACCTCCGCATCCTGGAAGGAGCTCGAAGCCC
24 LS0201_peredoxmid2_B06ATATAACACCAAGGTACCTGAAGCC-GCCATCAGCC-GCCTCATCACTTACCTCCGCATCCTGG-AGGAGCTCGAAGCCC
25 LS0201_peredoxmid3_C06ATATAACACCAAGGTACCTGAAGCC-GCCATCAGCC-GCCTCATCACTTACCTCCGCATCCTGG-AGGAGCTCGAAGCCC
```

c-Peredox-mCherry

pL1M-F6-p2xCaMV35S-c-peredox-mCherry-tHSP

```
2 LS0201                aaggcgttcaccgcactgcaagcgagcagctgggcgaactggcacaggttacagcattccaggttgacgaagatctgtcc
22 LS0201_18_G10        AAGGCGTTNNCCGTTTTTNNANGCAANCNNCTTGGNCNAACTNGTNNANG------------------------------
23 LS0201_peredox1_H10  AAGGNCGTTCACCNNNACTGCAAGCCGAACANNTTGGGCNAANTGGNNNNNGGTTACNGCATTNCNGGNTTGACAAAAAN
24 LS0201_peredoxmid2_B06AAGGCGTTCACCGCACTGCAAGCGAGCAGCTGGGCGAACTGGCACAGGTTACAGCATTCCAGGTTGACGAAGATCTGTCC
25 LS0201_peredoxmid3_C06AAGGCGTTCACCGCACTGCAAGCGAGCAGCTGGGCGAACTGGCACAGGTTACAGCATTCCAGGTTGACGAAGATCTGTCC
26 LS0201_pL1R_C06       --------CNNNNTTNNGGNNNTTNNTNNNNNGNNNNCNNNNNNGGNNTTNGNNTNNNNNNNTNCCCNTNCCTTNNNNNN
```

c-Peredox-mCherry

pL1M-F6-p2xCaMV35S-c-peredox-mCherry-tHSP

```
2 LS0201                tatttcggttcctacggcaccgacggtgttggctacacagtccctgtcctgaagcgcgagctgcgccacatcctgggcct
23 LS0201_peredox1_H10  NNNNNCCAATTTCCGGTNCNANNGGCNNCCNACGGGNTTNGGNNANCCNGNCCCNTGNNCNGNAAACNNAANNCNNNCCC
24 LS0201_peredoxmid2_B06TATTTCGGTTCCTACGGCACCGACGGTGTTGGCTACACAGTCCCTGTCCTGAAGCGCGAGCTGCGCCACATCCTGGGCCT
25 LS0201_peredoxmid3_C06TATTTCGGTTCCTACGGCACCGACGGTGTTGGCTACACAGTCCCTGTCCTGAAGCGCGAGCTGCGCCACATCCTGGGCCT
26 LS0201_pL1R_C06       GNNNNNNNNNNGNCCCNNNTTNTTNGGNCCCNNAANNNCCNNAANNNNGGGNNNTTNNGNNNNNNNNTNNCCNNNGGGCC
```

c-Peredox-mCherry

pL1M-F6-p2xCaMV35S-c-peredox-mCherry-tHSP

```
2 LS0201                gaaccgcaagtggggcttatgcatcgttggcatgggccgcctcggtagtgcactggcagactggccgggctttggtgaat
23 LS0201_peredox1_H10  CNATTCCTGGNNCCNGAANCCNNAAATGGNC--------------------------------------------------
24 LS0201_peredoxmid2_B06GAACCGCAAGTGGGGCTTATGCATCGTTGGCATGGGCCGCCTCGGTAGTGCACTGGCAGACTGGCCGGGCTTTGGTGAAT
25 LS0201_peredoxmid3_C06GAACCGCAAGTGGGGCTTATGCATCGTTGGCATGGGCCGCCTCGGTAGTGCACTGGCAGACTGGCCGGGCTTTGGTGAAT
26 LS0201_pL1R_C06       NNCCTNCNGNNANNNNNNNGGCCNNNACTGGCCCNGGGNNTTTGGGGNAANNNNTTTGNAATTNGGGCNGGNTTTTTTGA
```

c-Peredox-mCherry

pL1M-F6-p2xCaMV35S-c-peredox-mCherry-tHSP

```
2 LS0201                ctttcgaactgcgcggcttcttcgacgttgatccaggcatggttgggcgccctgttcgcggtggcgttatcgagcatgtt
24 LS0201_peredoxmid2_B06CTTTCGAACTGCGCGGCTTCTTCGACGTTGATCCAGGCATGGTTGGGCGCCCTGTTCGCGGTGGCGTTATCGAGCATGTT
25 LS0201_peredoxmid3_C06CTTTCGAACTGCGCGGCTTCTTCGACGTTGATCCAGGCATGGTTGGGCGCCCTGTTCGCGGTGGCGTTATCGAGCATGTT
26 LS0201_pL1R_C06       NCNNTGAATNNCAGGNCNNGGNTTGGNNCCCCCNTTTCGNNGGNGGNNTTNNTCGAGCCNTGTTGACCNTCTTGNCCNNA
```

c-Peredox-mCherry

pL1M-F6-p2xCaMV35S-c-peredox-mCherry-tHSP

```
2 LS0201                gacctcctgccacagcgcgtcccgggtcgcatcgagatcgccctgctgaccgttcctcgcgaagctgcacagaaggcagc
24 LS0201_peredoxmid2_B06GACCTCCTGCCACAGCGCGTCCCGGGTCGCATCGAGATCGCCCTGCTGACCGTTCCTCGCGAAGCTGCACAGAAGGCAGC
25 LS0201_peredoxmid3_C06GACCTCCTGCCACAGCGCGTCCCGGGTCGCATCGAGATCGCCCTGCTGACCGTTCCTCGCGAAGCTGCACAGAAGGCAGC
26 LS0201_pL1R_C06       NNGNNGTNCCCNGGTNNCNNNCNNNANNNGNCCTNNTTGANCCGTTCCTTNGGNAAGCTGCNNAGNAAGNNAGCCGGACT
```

c-Peredox-mCherry

pL1M-F6-p2xCaMV35S-c-peredox-mCherry-tHSP

```
2 LS0201                cgacttactagtcgccgctggtatcaagggaattctgaacttcgcccctgttgttctggaggttcct--aaggaagttgc
24 LS0201_peredoxmid2_B06CGACTTACTAGTCGCCGCTGGTATCAAGGGAATTCTGAACTTCGCCCCTGTTGTTCTGGAGGTTCCT--AAGGAAGTTGC
25 LS0201_peredoxmid3_C06CGACTTACTAGTCGCCGCTGGTATCAAGGGAATTCTGAACTTCGCCCCTGTTGTTCTGGAGGTTCCT--AAGGAAGTTGC
26 LS0201_pL1R_C06       TACTTNNTCGNCCNCTGGTATCAANGGGAANNTTTGAANTTCGCCCCCTGTTGTTCTGGAGGTTCCTTAAGGNAAGTTGC
```

c-Peredox-mCherry

pL1M-F6-p2xCaMV35S-c-peredox-mCherry-tHSP

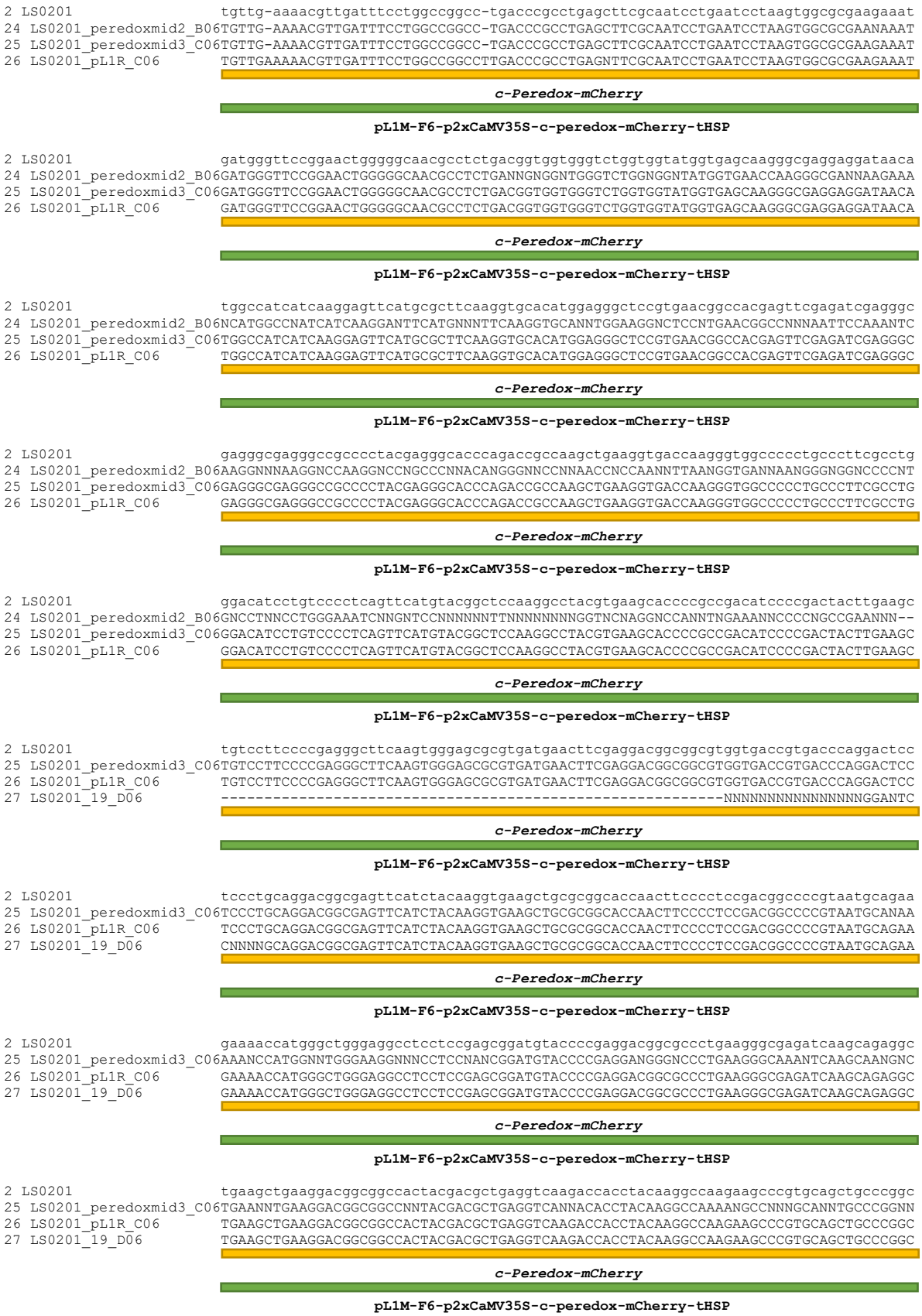
2 LS0201 tgttg-aaaacgttgatttcctggccggcc-tgacccgcctgagcttcgcaatcctgaatcctaagtggcgcgaagaaat
24 LS0201_peredoxmid2_B06 TGTTG-AAAACGTTGATTTCCTGGCCGGCC-TGACCCGCCTGAGCTTCGCAATCCTGAATCCTAAGTGGCGCGAANAAAT
25 LS0201_peredoxmid3_C06 TGTTG-AAAACGTTGATTTCCTGGCCGGCC-TGACCCGCCTGAGCTTCGCAATCCTGAATCCTAAGTGGCGCGAAGAAAT
26 LS0201_pL1R_C06 TGTTGAAAAACGTTGATTTCCTGGCCGGCCTTGACCCGCCTGAGNTTCGCAATCCTGAATCCTAAGTGGCGCGAAGAAAT
c-Peredox-mCherry
pL1M-F6-p2xCaMV35S-c-peredox-mCherry-tHSP
2 LS0201 gatgggttccggaactgggggcaacgcctctgacggtggtgggtctggtggtatggtgagcaagggcgaggaggataaca
24 LS0201_peredoxmid2_B06 GATGGGTTCCGGAACTGGGGGCAACGCCTCTGANNGNGGNTGGGTCTGGNGGNTATGGTGAACCAAGGGCGANNAAGAAA
25 LS0201_peredoxmid3_C06 GATGGGTTCCGGAACTGGGGGCAACGCCTCTGACGGTGGTGGGTCTGGTGGTATGGTGAGCAAGGGCGAGGAGGATAACA
26 LS0201_pL1R_C06 GATGGGTTCCGGAACTGGGGGCAACGCCTCTGACGGTGGTGGGTCTGGTGGTATGGTGAGCAAGGGCGAGGAGGATAACA
c-Peredox-mCherry
pL1M-F6-p2xCaMV35S-c-peredox-mCherry-tHSP
2 LS0201 tggccatcatcaaggagttcatgcgcttcaaggtgcacatggagggctccgtgaacggccacgagttcgagatcgagggc
24 LS0201_peredoxmid2_B06 NCATGGCCNATCATCAAGGANTTCATGNNNTTCAAGGTGCANNTGGAAGGNCTCCNTGAACGGCCNNNAATTCCAAANTC
25 LS0201_peredoxmid3_C06 TGGCCATCATCAAGGAGTTCATGCGCTTCAAGGTGCACATGGAGGGCTCCGTGAACGGCCACGAGTTCGAGATCGAGGGC
26 LS0201_pL1R_C06 TGGCCATCATCAAGGAGTTCATGCGCTTCAAGGTGCACATGGAGGGCTCCGTGAACGGCCACGAGTTCGAGATCGAGGGC
c-Peredox-mCherry
pL1M-F6-p2xCaMV35S-c-peredox-mCherry-tHSP
2 LS0201 gagggcgagggccgcccctacgagggcacccagaccgccaagctgaaggtgaccaagggtggccccctgcccttcgcctg
24 LS0201_peredoxmid2_B06 AAGGNNNAAGGNCCAAGGNCCNGCCCNNACANGGGNNCCNNAACCNCCAANNTTAANGGTGANNAANGGGNGGNCCCCNT
25 LS0201_peredoxmid3_C06 GAGGGCGAGGGCCGCCCCTACGAGGGCACCCAGACCGCCAAGCTGAAGGTGACCAAGGGTGGCCCCCTGCCCTTCGCCTG
26 LS0201_pL1R_C06 GAGGGCGAGGGCCGCCCCTACGAGGGCACCCAGACCGCCAAGCTGAAGGTGACCAAGGGTGGCCCCCTGCCCTTCGCCTG
c-Peredox-mCherry
pL1M-F6-p2xCaMV35S-c-peredox-mCherry-tHSP
2 LS0201 ggacatcctgtcccctcagttcatgtacggctccaaggcctacgtgaagcaccccgccgacatccccgactacttgaagc
24 LS0201_peredoxmid2_B06 GNCCTNNCCTGGGAAATCNNGNTCCNNNNNNTTNNNNNNNNGGTNCNAGGNCCANNTNGAAANNCCCCNGCCGAANNN--
25 LS0201_peredoxmid3_C06 GGACATCCTGTCCCCTCAGTTCATGTACGGCTCCAAGGCCTACGTGAAGCACCCCGCCGACATCCCCGACTACTTGAAGC
26 LS0201_pL1R_C06 GGACATCCTGTCCCCTCAGTTCATGTACGGCTCCAAGGCCTACGTGAAGCACCCCGCCGACATCCCCGACTACTTGAAGC
c-Peredox-mCherry
pL1M-F6-p2xCaMV35S-c-peredox-mCherry-tHSP
2 LS0201 tgtccttccccgagggcttcaagtgggagcgcgtgatgaacttcgaggacggcggcgtggtgaccgtgacccaggactcc
25 LS0201_peredoxmid3_C06 TGTCCTTCCCCGAGGGCTTCAAGTGGGAGCGCGTGATGAACTTCGAGGACGGCGGCGTGGTGACCGTGACCCAGGACTCC
26 LS0201_pL1R_C06 TGTCCTTCCCCGAGGGCTTCAAGTGGGAGCGCGTGATGAACTTCGAGGACGGCGGCGTGGTGACCGTGACCCAGGACTCC
27 LS0201_19_D06 ----------NNNNNNNNNNNNNNNNGGANTC
c-Peredox-mCherry
pL1M-F6-p2xCaMV35S-c-peredox-mCherry-tHSP
2 LS0201 tccctgcaggacggcgagttcatctacaaggtgaagctgcgcggcaccaacttcccctccgacggccccgtaatgcagaa
25 LS0201_peredoxmid3_C06 TCCCTGCAGGACGGCGAGTTCATCTACAAGGTGAAGCTGCGCGGCACCAACTTCCCCTCCGACGGCCCCGTAATGCANAA
26 LS0201_pL1R_C06 TCCCTGCAGGACGGCGAGTTCATCTACAAGGTGAAGCTGCGCGGCACCAACTTCCCCTCCGACGGCCCCGTAATGCAGAA
27 LS0201_19_D06 CNNNNGCAGGACGGCGAGTTCATCTACAAGGTGAAGCTGCGCGGCACCAACTTCCCCTCCGACGGCCCCGTAATGCAGAA
c-Peredox-mCherry
pL1M-F6-p2xCaMV35S-c-peredox-mCherry-tHSP
2 LS0201 gaaaaccatgggctgggaggcctcctccgagcggatgtaccccgaggacggcgccctgaagggcgagatcaagcagaggc
25 LS0201_peredoxmid3_C06 AAANCCATGGNNTGGGAAGGNNNCCTCCNANCGGATGTACCCCGAGGANGGGNCCCTGAAGGGCAAANTCAAGCAANGNC
26 LS0201_pL1R_C06 GAAAACCATGGGCTGGGAGGCCTCCTCCGAGCGGATGTACCCCGAGGACGGCGCCCTGAAGGGCGAGATCAAGCAGAGGC
27 LS0201_19_D06 GAAAACCATGGGCTGGGAGGCCTCCTCCGAGCGGATGTACCCCGAGGACGGCGCCCTGAAGGGCGAGATCAAGCAGAGGC
c-Peredox-mCherry
pL1M-F6-p2xCaMV35S-c-peredox-mCherry-tHSP
2 LS0201 tgaagctgaaggacggcggccactacgacgctgaggtcaagaccacctacaaggccaagaagcccgtgcagctgcccggc
25 LS0201_peredoxmid3_C06 TGAANNTGAAGGACGGCGGCCNNTACGACGCTGAGGTCANNACACCTACAAGGCCAAAANGCCNNNGCANNTGCCCGGNN
26 LS0201_pL1R_C06 TGAAGCTGAAGGACGGCGGCCACTACGACGCTGAGGTCAAGACCACCTACAAGGCCAAGAAGCCCGTGCAGCTGCCCGGC
27 LS0201_19_D06 TGAAGCTGAAGGACGGCGGCCACTACGACGCTGAGGTCAAGACCACCTACAAGGCCAAGAAGCCCGTGCAGCTGCCCGGC
c-Peredox-mCherry
pL1M-F6-p2xCaMV35S-c-peredox-mCherry-tHSP

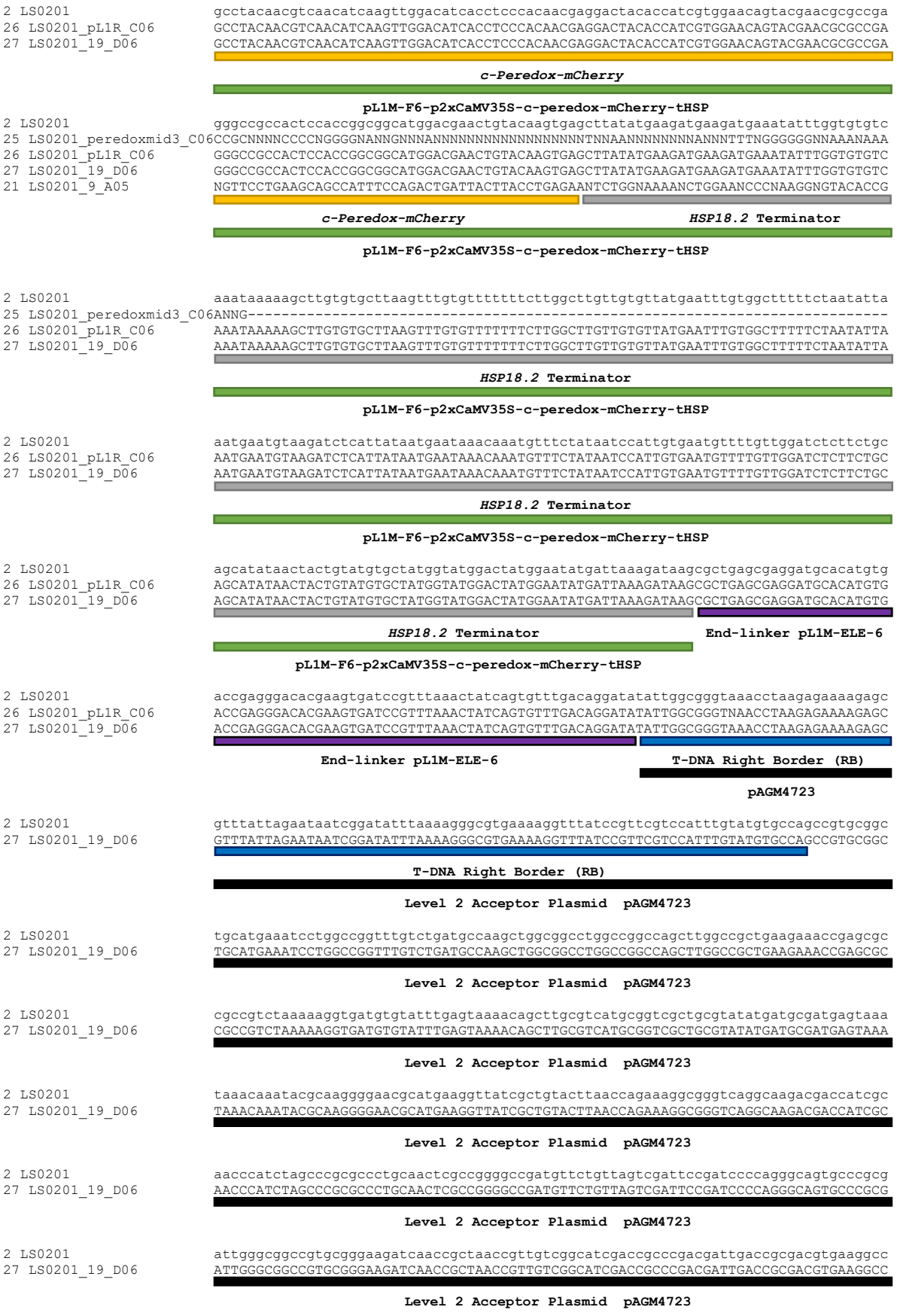
2 LS0201 gcctacaacgtcaacatcaagttggacatcacctcccacaacgaggactacaccatcgtggaacagtacgaacgcgccga
26 LS0201_pL1R_C06 GCCTACAACGTCAACATCAAGTTGGACATCACCTCCCACAACGAGGACTACACCATCGTGGAACAGTACGAACGCGCCGA
27 LS0201_19_D06 GCCTACAACGTCAACATCAAGTTGGACATCACCTCCCACAACGAGGACTACACCATCGTGGAACAGTACGAACGCGCCGA
c-Peredox-mCherry
pL1M-F6-p2xCaMV35S-c-peredox-mCherry-tHSP
2 LS0201 gggccgccactccaccggcggcatggacgaactgtacaagtgagcttatatgaagatgaagatgaaatatttggtgtgtc
25 LS0201_peredoxmid3_C06 CCGCNNNNCCCCNGGGGNANNGNNNANNNNNNNNNNNNNNNNNNTNNAANNNNNNNNANNNTTTNGGGGGGNNAAANAAA
26 LS0201_pL1R_C06 GGGCCGCCACTCCACCGGCGGCATGGACGAACTGTACAAGTGAGCTTATATGAAGATGAAGATGAAATATTTGGTGTGTC
27 LS0201_19_D06 GGGCCGCCACTCCACCGGCGGCATGGACGAACTGTACAAGTGAGCTTATATGAAGATGAAGATGAAATATTTGGTGTGTC
21 LS0201_9_A05 NGTTCCTGAAGCAGCCATTTCCAGACTGATTACTTACCTGAGAANTCTGGNAAAANCTGGAANCCCNAAGGNGTACACCG
c-Peredox-mCherry
HSP18.2 Terminator
pL1M-F6-p2xCaMV35S-c-peredox-mCherry-tHSP
2 LS0201 aaataaaaagcttgtgtgcttaagtttgtgttttttttcttggcttgttgtgttatgaatttgtggctttttctaatatta
25 LS0201_peredoxmid3_C06 ANNG----------
26 LS0201_pL1R_C06 AAATAAAAAGCTTGTGTGCTTAAGTTTGTGTTTTTTTTCTTGGCTTGTTGTGTTATGAATTTGTGGCTTTTTCTAATATTA
27 LS0201_19_D06 AAATAAAAAGCTTGTGTGCTTAAGTTTGTGTTTTTTTTCTTGGCTTGTTGTGTTATGAATTTGTGGCTTTTTCTAATATTA
HSP18.2 Terminator
pL1M-F6-p2xCaMV35S-c-peredox-mCherry-tHSP
2 LS0201 aatgaatgtaagatctcattataatgaataaacaaatgtttctataatccattgtgaatgttttgttggatctcttctgc
26 LS0201_pL1R_C06 AATGAATGTAAGATCTCATTATAATGAATAAACAAATGTTTCTATAATCCATTGTGAATGTTTTGTTGGATCTCTTCTGC
27 LS0201_19_D06 AATGAATGTAAGATCTCATTATAATGAATAAACAAATGTTTCTATAATCCATTGTGAATGTTTTGTTGGATCTCTTCTGC
HSP18.2 Terminator
pL1M-F6-p2xCaMV35S-c-peredox-mCherry-tHSP
2 LS0201 agcatataactactgtatgtgctatggtatggactatggaatatgattaaagataagcgctgagcgaggatgcacatgtg
26 LS0201_pL1R_C06 AGCATATAACTACTGTATGTGCTATGGTATGGACTATGGAATATGATTAAAGATAAGCGCTGAGCGAGGATGCACATGTG
27 LS0201_19_D06 AGCATATAACTACTGTATGTGCTATGGTATGGACTATGGAATATGATTAAAGATAAGCGCTGAGCGAGGATGCACATGTG
HSP18.2 Terminator
End-linker pL1M-ELE-6
pL1M-F6-p2xCaMV35S-c-peredox-mCherry-tHSP
2 LS0201 accgagggacacgaagtgatccgtttaaactatcagtgtttgacaggatatattggcgggtaaacctaagagaaaagagc
26 LS0201_pL1R_C06 ACCGAGGGACACGAAGTGATCCGTTTAAACTATCAGTGTTTGACAGGATATATTGGCGGGTNAACCTAAGAGAAAAGAGC
27 LS0201_19_D06 ACCGAGGGACACGAAGTGATCCGTTTAAACTATCAGTGTTTGACAGGATATATTGGCGGGTAAACCTAAGAGAAAAGAGC
End-linker pL1M-ELE-6
T-DNA Right Border (RB)
pAGM4723
2 LS0201 gtttattagaataatcggatatttaaaagggcgtgaaaaggtttatccgttcgtccatttgtatgtgccagccgtgcggc
27 LS0201_19_D06 GTTTATTAGAATAATCGGATATTTAAAAGGGCGTGAAAAGGTTTATCCGTTCGTCCATTTGTATGTGCCAGCCGTGCGGC
T-DNA Right Border (RB)
Level 2 Acceptor Plasmid pAGM4723
2 LS0201 tgcatgaaatcctggccggtttgtctgatgccaagctggcggcctggccggccagcttggccgctgaagaaaccgagcgc
27 LS0201_19_D06 TGCATGAAATCCTGGCCGGTTTGTCTGATGCCAAGCTGGCGGCCTGGCCGGCCAGCTTGGCCGCTGAAGAAACCGAGCGC
Level 2 Acceptor Plasmid pAGM4723
2 LS0201 cgccgtctaaaaaggtgatgtgtatttgagtaaaacagcttgcgtcatgcggtcgctgcgtatatgatgcgatgagtaaa
27 LS0201_19_D06 CGCCGTCTAAAAAGGTGATGTGTATTTGAGTAAAACAGCTTGCGTCATGCGGTCGCTGCGTATATGATGCGATGAGTAAA
Level 2 Acceptor Plasmid pAGM4723
2 LS0201 taaacaaatacgcaaggggaacgcatgaaggttatcgctgtacttaaccagaaaggcgggtcaggcaagacgaccatcgc
27 LS0201_19_D06 TAAACAAATACGCAAGGGGAACGCATGAAGGTTATCGCTGTACTTAACCAGAAAGGCGGGTCAGGCAAGACGACCATCGC
Level 2 Acceptor Plasmid pAGM4723
2 LS0201 aacccatctagcccgcgccctgcaactcgccggggccgatgttctgttagtcgattccgatccccagggcagtgcccgcg
27 LS0201_19_D06 AACCCATCTAGCCCGCGCCCTGCAACTCGCCGGGGCCGATGTTCTGTTAGTCGATTCCGATCCCCAGGGCAGTGCCCGCG
Level 2 Acceptor Plasmid pAGM4723
2 LS0201 attgggcggccgtgcgggaagatcaaccgctaaccgttgtcggcatcgaccgcccgacgattgaccgcgacgtgaaggcc
27 LS0201_19_D06 ATTGGGCGGCCGTGCGGGAAGATCAACCGCTAACCGTTGTCGGCATCGACCGCCCGACGATTGACCGCGACGTGAAGGCC
Level 2 Acceptor Plasmid pAGM4723

```
2 LS0201                atcggccggcgcgacttcgtagtgatcgacggagcgccccaggcggcggacttggctgtgtccgcgatcaaggcagccga
27 LS0201_19_D06        ATCGGCCGGNGCGACTTCGTAGTGATCGACGGAACGCCCCAGGCGGCGGACTTGGCTGNGTCCGCGATCAAGGCAGCCGA
```

Level 2 Acceptor Plasmid pAGM4723

```
2 LS0201                cttcgtgctgattccggtgcagccaagcccttacgacatatgggccaccgccgacctggtggagctggttaagcagcgca
27 LS0201_19_D06        CTTCGTGCTGATTCCGGNGCAACCAAGCCCTTACGANNTATGGGCCACCNCCAACCTGGNGGAACTGNTTAANCACCGCA
```

Level 2 Acceptor Plasmid pAGM4723

```
2 LS0201                ttgaggtcacggatggaaggctacaagcggcctttgtcgtgtcgcgggcgatcaaaggcacgcgcatcggcggtgaggtt
27 LS0201_19_D06        TTGAGGTCACGGNNGGAAGNNNACAAGCGGCCTTTNNCNNNNCNGGGNNNNTCAAAGGNACCCCNATCCGNCGNNNNGGT
```

Level 2 Acceptor Plasmid pAGM4723

```
2 LS0201                gccgaggcgctggccgggtacgagctgcccattcttgagtcccgtatcacgcagcgcgtgagctacccaggcactgccgc
27 LS0201_19_D06        TGCCAANGGCCNNGGNCCGGGTANANNTNGCCNATTCTTGAATCCNGNNNNNNNANNNNGGTGGACNNNCCAAG------
```

Level 2 Acceptor Plasmid pAGM4723

pLS0207 – c-Peredox-mCherry construct

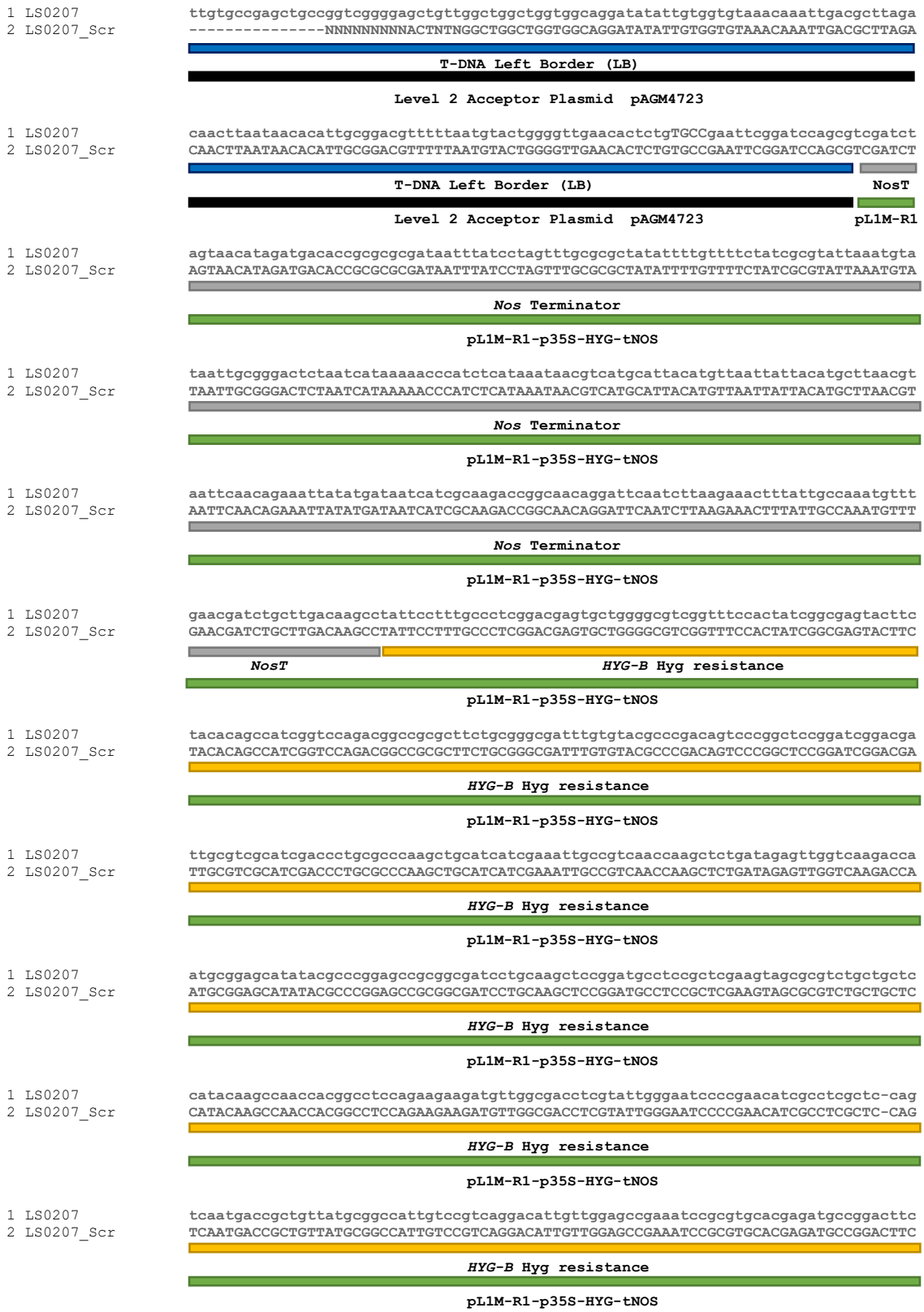

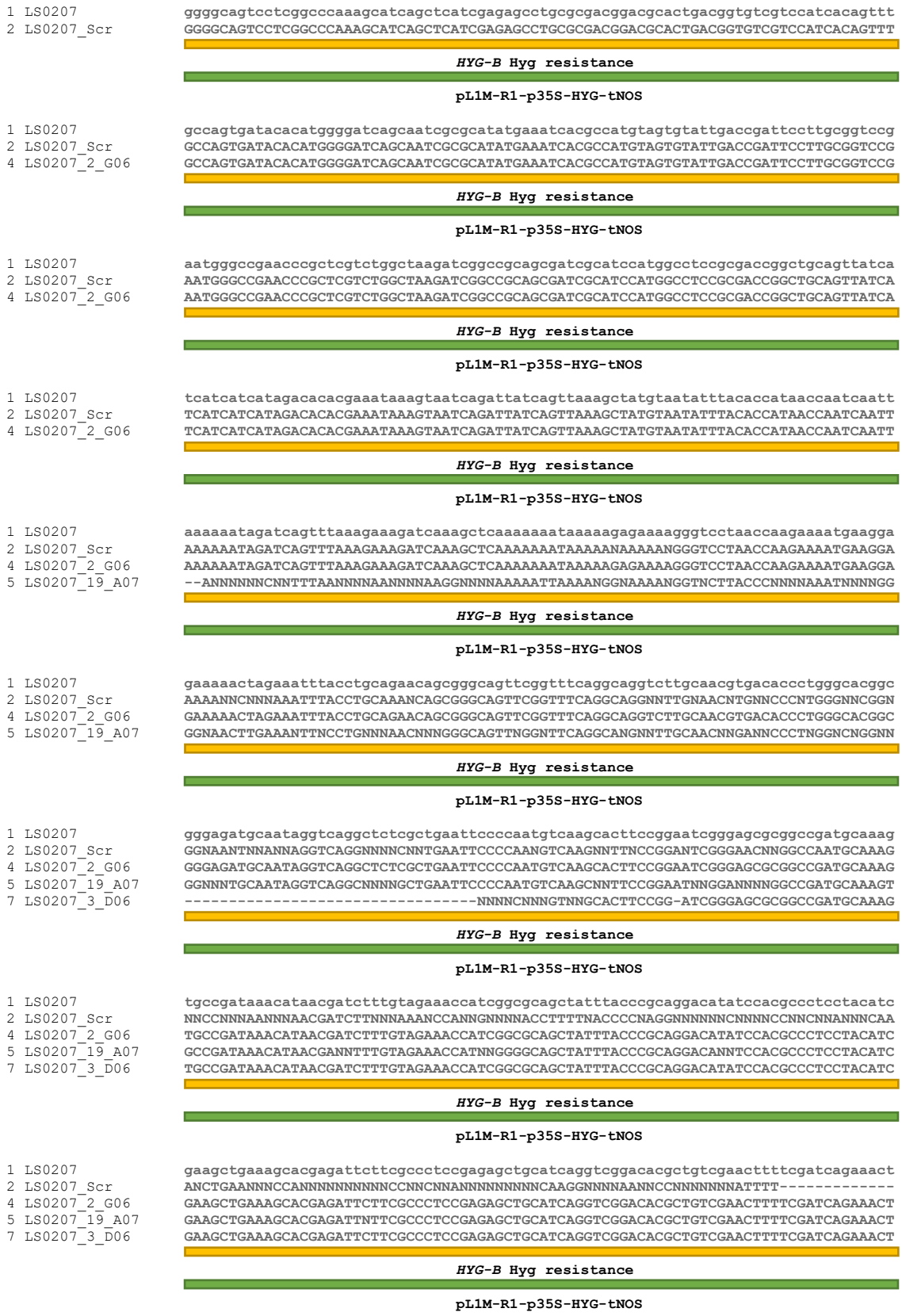
1 LS0207 ggggcagtcctcggcccaaagcatcagctcatcgagagcctgcgcgacggacgcactgacggtgtcgtccatcacagttt
2 LS0207_Scr GGGGCAGTCCTCGGCCCAAAGCATCAGCTCATCGAGAGCCTGCGCGACGGACGCACTGACGGTGTCGTCCATCACAGTTT
HYG-B Hyg resistance
pL1M-R1-p35S-HYG-tNOS
1 LS0207 gccagtgatacacatggggatcagcaatcgcgcatatgaaatcacgccatgtagtgtattgaccgattccttgcggtccg
2 LS0207_Scr GCCAGTGATACACATGGGGATCAGCAATCGCGCATATGAAATCACGCCATGTAGTGTATTGACCGATTCCTTGCGGTCCG
4 LS0207_2_G06 GCCAGTGATACACATGGGGATCAGCAATCGCGCATATGAAATCACGCCATGTAGTGTATTGACCGATTCCTTGCGGTCCG
HYG-B Hyg resistance
pL1M-R1-p35S-HYG-tNOS
1 LS0207 aatgggccgaacccgctcgtctggctaagatcggccgcagcgatcgcatccatggcctccgcgaccggctgcagttatca
2 LS0207_Scr AATGGGCCGAACCCGCTCGTCTGGCTAAGATCGGCCGCAGCGATCGCATCCATGGCCTCCGCGACCGGCTGCAGTTATCA
4 LS0207_2_G06 AATGGGCCGAACCCGCTCGTCTGGCTAAGATCGGCCGCAGCGATCGCATCCATGGCCTCCGCGACCGGCTGCAGTTATCA
HYG-B Hyg resistance
pL1M-R1-p35S-HYG-tNOS
1 LS0207 tcatcatcatagacacacgaaataaagtaatcagattatcagttaaagctatgtaatatttacaccataaccaatcaatt
2 LS0207_Scr TCATCATCATAGACACACGAAATAAAGTAATCAGATTATCAGTTAAAGCTATGTAATATTTACACCATAACCAATCAATT
4 LS0207_2_G06 TCATCATCATAGACACACGAAATAAAGTAATCAGATTATCAGTTAAAGCTATGTAATATTTACACCATAACCAATCAATT
HYG-B Hyg resistance
pL1M-R1-p35S-HYG-tNOS
1 LS0207 aaaaaatagatcagtttaaagaaagatcaaagctcaaaaaaataaaaagagaaaagggtcctaaccaagaaaatgaagga
2 LS0207_Scr AAAAAATAGATCAGTTTAAAGAAAGATCAAAGCTCAAAAAAATAAAAANAAAAANGGGTCCTAACCAAGAAAATGAAGGA
4 LS0207_2_G06 AAAAAATAGATCAGTTTAAAGAAAGATCAAAGCTCAAAAAAATAAAAAGAGAAAAGGGTCCTAACCAAGAAAATGAAGGA
5 LS0207_19_A07 --ANNNNNNCNNTTTAANNNNAANNNNAAGGNNNNAAAAATTAAAANGGNAAAANGGTNCTTACCCNNNNAAATNNNNGG
HYG-B Hyg resistance
pL1M-R1-p35S-HYG-tNOS
1 LS0207 gaaaaactagaaatttacctgcagaacagcgggcagttcggtttcaggcaggtcttgcaacgtgacaccctgggcacggc
2 LS0207_Scr AAAANNCNNNAAATTTACCTGCAAANCAGCGGGCAGTTCGGTTTCAGGCAGGNNTTGNAACNTGNNCCCNTGGGNNCGGN
4 LS0207_2_G06 GAAAAACTAGAAATTTACCTGCAGAACAGCGGGCAGTTCGGTTTCAGGCAGGTCTTGCAACGTGACACCCTGGGCACGGC
5 LS0207_19_A07 GGNAACTTGAAANTTNCCTGNNNAACNNNGGGCAGTTNGGNTTCAGGCANGNNTTGCAACNNGANNCCCTNGGNCNGGNN
HYG-B Hyg resistance
pL1M-R1-p35S-HYG-tNOS
1 LS0207 gggagatgcaataggtcaggctctcgctgaattccccaatgtcaagcacttccggaatcgggagcgcggccgatgcaaag
2 LS0207_Scr GGNAANTNNANNAGGTCAGGNNNNCNNTGAATTCCCCAANGTCAAGNNTTNCCGGANTCGGGAACNNGGCCAATGCAAAG
4 LS0207_2_G06 GGGAGATGCAATAGGTCAGGCTCTCGCTGAATTCCCCAATGTCAAGCACTTCCGGAATCGGGAGCGCGGCCGATGCAAAG
5 LS0207_19_A07 GGNNNTGCAATAGGTCAGGCNNNNGCTGAATTCCCCAATGTCAAGCNNTTCCGGAATNNGGANNNNGGCCGATGCAAAGT
7 LS0207_3_D06 ----------NNNNCNNNGTNNGCACTTCCGG-ATCGGGAGCGCGGCCGATGCAAAG
HYG-B Hyg resistance
pL1M-R1-p35S-HYG-tNOS
1 LS0207 tgccgataaacataacgatctttgtagaaaccatcggcgcagctatttacccgcaggacatatccacgccctcctacatc
2 LS0207_Scr NNCCNNNAANNNAACGATCTTNNNAAANCCANNGNNNNACCTTTTNACCCCNAGGNNNNNNCNNNNCCNNCNNANNNCAA
4 LS0207_2_G06 TGCCGATAAACATAACGATCTTTGTAGAAACCATCGGCGCAGCTATTTACCCGCAGGACATATCCACGCCCTCCTACATC
5 LS0207_19_A07 GCCGATAAACATAACGANNTTTGTAGAAACCATNNGGGGCAGCTATTTACCCGCAGGACANNTCCACGCCCTCCTACATC
7 LS0207_3_D06 TGCCGATAAACATAACGATCTTTGTAGAAACCATCGGCGCAGCTATTTACCCGCAGGACATATCCACGCCCTCCTACATC
HYG-B Hyg resistance
pL1M-R1-p35S-HYG-tNOS
1 LS0207 gaagctgaaagcacgagattcttcgccctccgagagctgcatcaggtcggacacgctgtcgaacttttcgatcagaaact
2 LS0207_Scr ANCTGAANNNCCANNNNNNNNNNCCNNCNNANNNNNNNNNCAAGGNNNNAANNCCNNNNNNNATTTT----------
4 LS0207_2_G06 GAAGCTGAAAGCACGAGATTCTTCGCCCTCCGAGAGCTGCATCAGGTCGGACACGCTGTCGAACTTTTCGATCAGAAACT
5 LS0207_19_A07 GAAGCTGAAAGCACGAGATTNTTCGCCCTCCGAGAGCTGCATCAGGTCGGACACGCTGTCGAACTTTTCGATCAGAAACT
7 LS0207_3_D06 GAAGCTGAAAGCACGAGATTCTTCGCCCTCCGAGAGCTGCATCAGGTCGGACACGCTGTCGAACTTTTCGATCAGAAACT
HYG-B Hyg resistance
pL1M-R1-p35S-HYG-tNOS

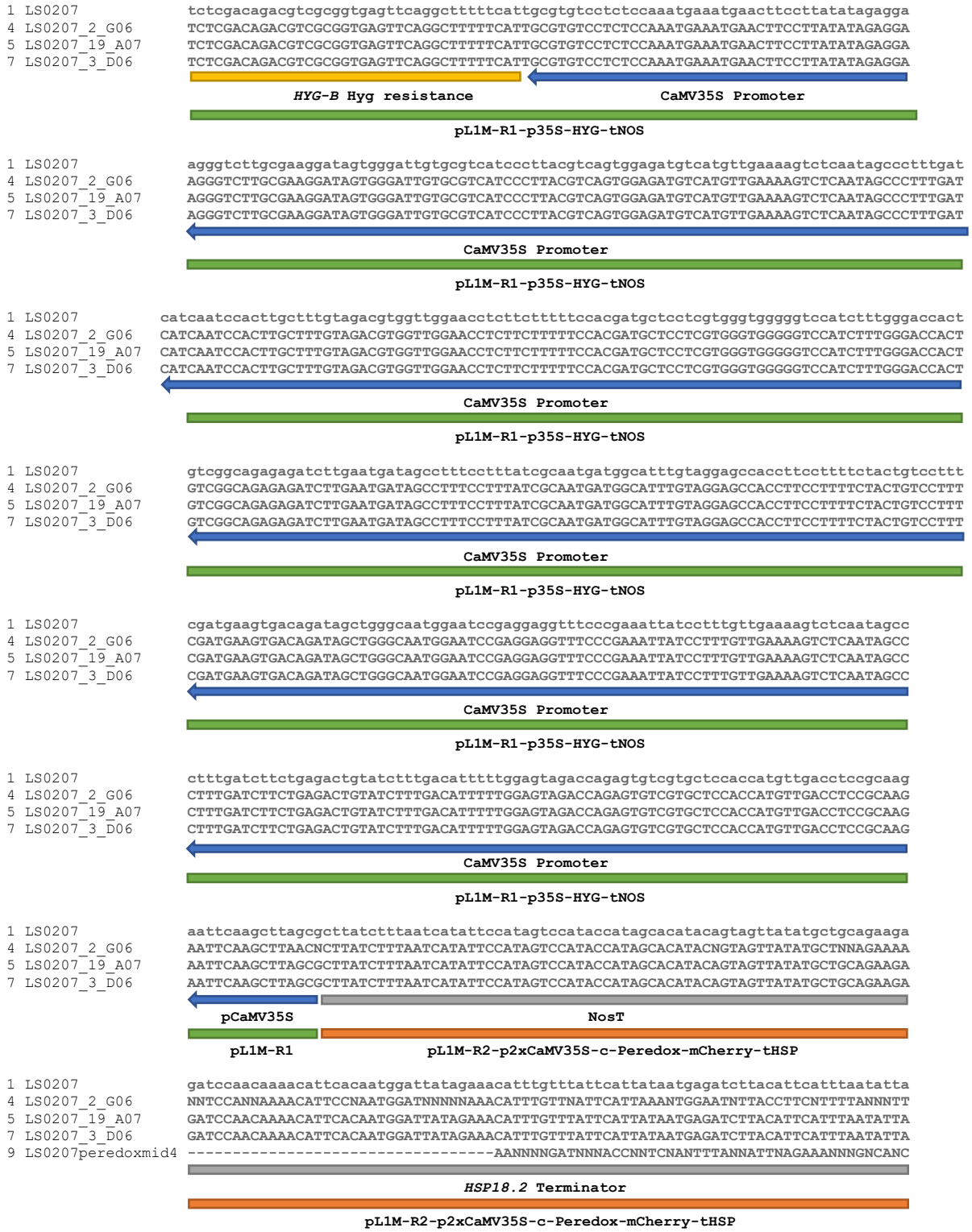
1 LS0207 tctcgacagacgtcgcggtgagttcaggctttttcattgcgtgtcctctccaaatgaaatgaacttccttatatagagga
4 LS0207_2_G06 TCTCGACAGACGTCGCGGTGAGTTCAGGCTTTTTCATTGCGTGTCCTCTCCAAATGAAATGAACTTCCTTATATAGAGGA
5 LS0207_19_A07 TCTCGACAGACGTCGCGGTGAGTTCAGGCTTTTTCATTGCGTGTCCTCTCCAAATGAAATGAACTTCCTTATATAGAGGA
7 LS0207_3_D06 TCTCGACAGACGTCGCGGTGAGTTCAGGCTTTTTCATTGCGTGTCCTCTCCAAATGAAATGAACTTCCTTATATAGAGGA
HYG-B Hyg resistance
CaMV35S Promoter
pL1M-R1-p35S-HYG-tNOS
1 LS0207 agggtcttgcgaaggatagtgggattgtgcgtcatcccttacgtcagtggagatgtcatgttgaaaagtctcaatagccctttgat
4 LS0207_2_G06 AGGGTCTTGCGAAGGATAGTGGGATTGTGCGTCATCCCTTACGTCAGTGGAGATGTCATGTTGAAAAGTCTCAATAGCCCTTTGAT
5 LS0207_19_A07 AGGGTCTTGCGAAGGATAGTGGGATTGTGCGTCATCCCTTACGTCAGTGGAGATGTCATGTTGAAAAGTCTCAATAGCCCTTTGAT
7 LS0207_3_D06 AGGGTCTTGCGAAGGATAGTGGGATTGTGCGTCATCCCTTACGTCAGTGGAGATGTCATGTTGAAAAGTCTCAATAGCCCTTTGAT
CaMV35S Promoter
pL1M-R1-p35S-HYG-tNOS
1 LS0207 catcaatccacttgctttgtagacgtggttggaacctcttctttttccacgatgctcctcgtgggtgggggtccatctttgggaccact
4 LS0207_2_G06 CATCAATCCACTTGCTTTGTAGACGTGGTTGGAACCTCTTCTTTTTCCACGATGCTCCTCGTGGGTGGGGGTCCATCTTTGGGACCACT
5 LS0207_19_A07 CATCAATCCACTTGCTTTGTAGACGTGGTTGGAACCTCTTCTTTTTCCACGATGCTCCTCGTGGGTGGGGGTCCATCTTTGGGACCACT
7 LS0207_3_D06 CATCAATCCACTTGCTTTGTAGACGTGGTTGGAACCTCTTCTTTTTCCACGATGCTCCTCGTGGGTGGGGGTCCATCTTTGGGACCACT
CaMV35S Promoter
pL1M-R1-p35S-HYG-tNOS
1 LS0207 gtcggcagagagatcttgaatgatagcctttccttttatcgcaatgatggcatttgtaggagccaccttccttttctactgtccttt
4 LS0207_2_G06 GTCGGCAGAGAGATCTTGAATGATAGCCTTTCCTTTATCGCAATGATGGCATTTGTAGGAGCCACCTTCCTTTTCTACTGTCCTTT
5 LS0207_19_A07 GTCGGCAGAGAGATCTTGAATGATAGCCTTTCCTTTATCGCAATGATGGCATTTGTAGGAGCCACCTTCCTTTTCTACTGTCCTTT
7 LS0207_3_D06 GTCGGCAGAGAGATCTTGAATGATAGCCTTTCCTTTATCGCAATGATGGCATTTGTAGGAGCCACCTTCCTTTTCTACTGTCCTTT
CaMV35S Promoter
pL1M-R1-p35S-HYG-tNOS
1 LS0207 cgatgaagtgacagatagctgggcaatggaatccgaggaggtttcccgaaattatcctttgttgaaaagtctcaatagcc
4 LS0207_2_G06 CGATGAAGTGACAGATAGCTGGGCAATGGAATCCGAGGAGGTTTCCCGAAATTATCCTTTGTTGAAAAGTCTCAATAGCC
5 LS0207_19_A07 CGATGAAGTGACAGATAGCTGGGCAATGGAATCCGAGGAGGTTTCCCGAAATTATCCTTTGTTGAAAAGTCTCAATAGCC
7 LS0207_3_D06 CGATGAAGTGACAGATAGCTGGGCAATGGAATCCGAGGAGGTTTCCCGAAATTATCCTTTGTTGAAAAGTCTCAATAGCC
CaMV35S Promoter
pL1M-R1-p35S-HYG-tNOS
1 LS0207 ctttgatcttctgagactgtatctttgacatttttggagtagaccagagtgtcgtgctccaccatgttgacctccgcaag
4 LS0207_2_G06 CTTTGATCTTCTGAGACTGTATCTTTGACATTTTTGGAGTAGACCAGAGTGTCGTGCTCCACCATGTTGACCTCCGCAAG
5 LS0207_19_A07 CTTTGATCTTCTGAGACTGTATCTTTGACATTTTTGGAGTAGACCAGAGTGTCGTGCTCCACCATGTTGACCTCCGCAAG
7 LS0207_3_D06 CTTTGATCTTCTGAGACTGTATCTTTGACATTTTTGGAGTAGACCAGAGTGTCGTGCTCCACCATGTTGACCTCCGCAAG
CaMV35S Promoter
pL1M-R1-p35S-HYG-tNOS
1 LS0207 aattcaagcttagcgcttatctttaatcatattccatagtccataccatagcacatacagtagttatatgctgcagaaga
4 LS0207_2_G06 AATTCAAGCTTAACNCTTATCTTTAATCATATTCCATAGTCCATACCATAGCACATACNGTAGTTATATGCTNNAGAAAA
5 LS0207_19_A07 AATTCAAGCTTAGCGCTTATCTTTAATCATATTCCATAGTCCATACCATAGCACATACAGTAGTTATATGCTGCAGAAGA
7 LS0207_3_D06 AATTCAAGCTTAGCGCTTATCTTTAATCATATTCCATAGTCCATACCATAGCACATACAGTAGTTATATGCTGCAGAAGA
pCaMV35S
NosT
pL1M-R1
pL1M-R2-p2xCaMV35S-c-Peredox-mCherry-tHSP
1 LS0207 gatccaacaaaacattcacaatggattatagaaacatttgtttattcattataatgagatcttacattcatttaatatta
4 LS0207_2_G06 NNTCCANNAAAACATTCCNAATGGATNNNNNAAACATTTGTTNATTCATTAAANTGGAATNTTACCTTCNTTTTANNNTT
5 LS0207_19_A07 GATCCAACAAAACATTCACAATGGATTATAGAAACATTTGTTTATTCATTATAATGAGATCTTACATTCATTTAATATTA
7 LS0207_3_D06 GATCCAACAAAACATTCACAATGGATTATAGAAACATTTGTTTATTCATTATAATGAGATCTTACATTCATTTAATATTA
9 LS0207peredoxmid4 ----------AANNNNGATNNNACCNNTCNANTTTANNATTNAGAAANNNGNCANC
HSP18.2 Terminator
pL1M-R2-p2xCaMV35S-c-Peredox-mCherry-tHSP

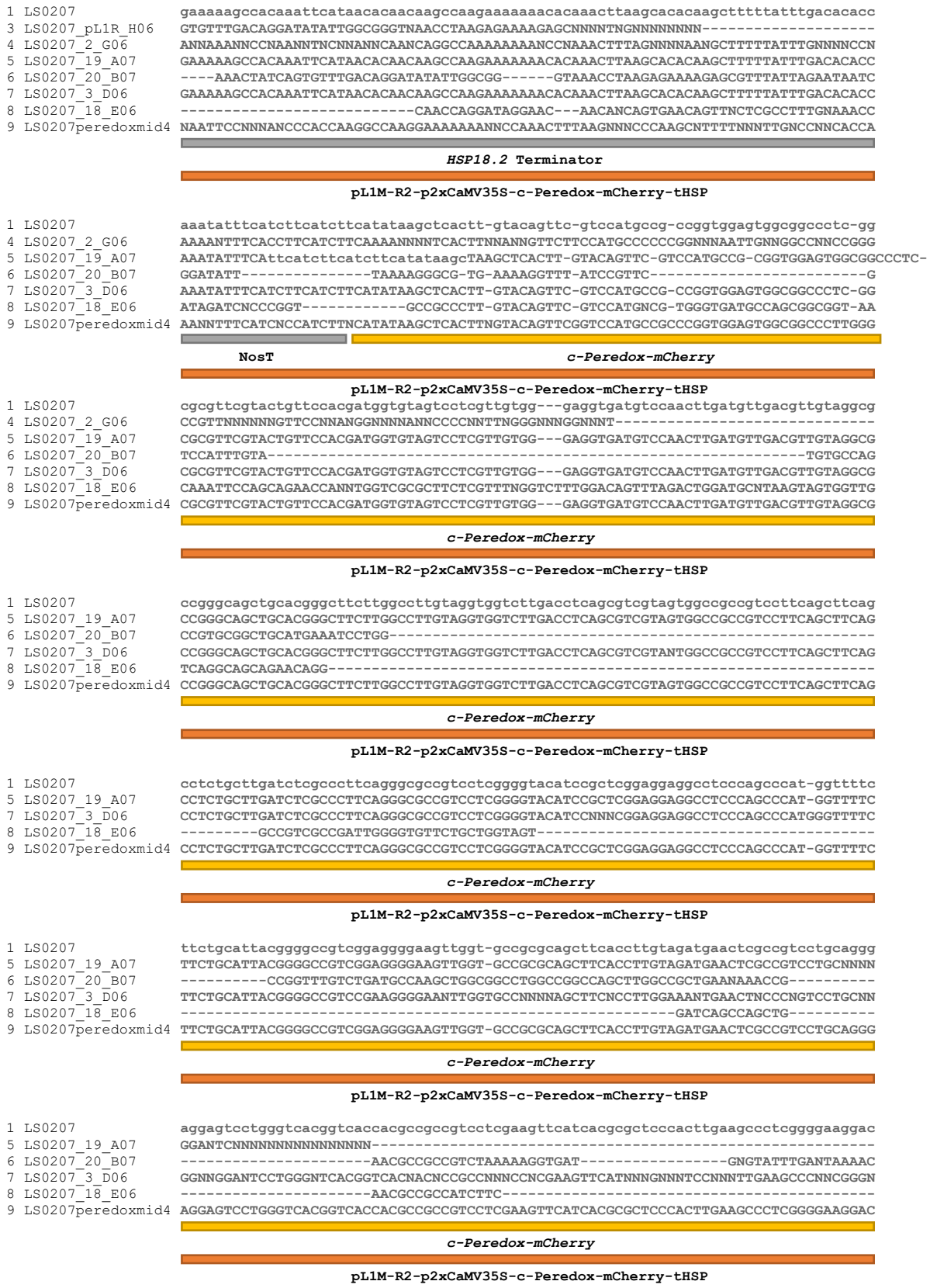
1 LS0207 gaaaaagccacaaattcataacacaacaagccaagaaaaaaacacaaacttaagcacacaagctttttatttgacacacc
3 LS0207_pL1R_H06 GTGTTTGACAGGATATATTGGCGGGTNAACCTAAGAGAAAAGAGCNNNNTNGNNNNNNNN----------
4 LS0207_2_G06 ANNAAANNCCNAANNTNCNNANNCAANCAGGCCAAAAAAAAANCCNAAACTTTAGNNNNAANGCTTTTTATTTGNNNNCCN
5 LS0207_19_A07 GAAAAAGCCACAAATTCATAACACAACAAGCCAAGAAAAAAACACAAACTTAAGCACACAAGCTTTTTATTTGACACACC
6 LS0207_20_B07 ----AAACTATCAGTGTTTGACAGGATATATTGGCGG------GTAAACCTAAGAGAAAAGAGCGTTTATTAGAATAATC
7 LS0207_3_D06 GAAAAAGCCACAAATTCATAACACAACAAGCCAAGAAAAAAACACAAACTTAAGCACACAAGCTTTTTATTTGACACACC
8 LS0207_18_E06 --------------------------CAACCAGGATAGGAAC---AACANCAGTGAACAGTTNCTCGCCTTTGNAAACC
9 LS0207peredoxmid4 NAATTCCNNNANCCCACCAAGGCCAAGGAAAAAAANNCCAAACTTTAAGNNNCCCAAGCNTTTTNNNTTGNCCNNCACCA
HSP18.2 Terminator
pL1M-R2-p2xCaMV35S-c-Peredox-mCherry-tHSP
1 LS0207 aaatatttcatcttcatcttcatataagctcactt-gtacagttc-gtccatgccg-ccggtggagtggcggccctc-gg
4 LS0207_2_G06 AAAANTTTCACCTTCATCTTCAAAANNNNTCACTTNNANNGTTCTTCCATGCCCCCCGGNNNAATTGNNGGCCNNCCGGG
5 LS0207_19_A07 AAATATTTCAttcatcttcatcttcatataagcTAAGCTCACTT-GTACAGTTC-GTCCATGCCG-CGGTGGAGTGGCGGCCCTC-
6 LS0207_20_B07 GGATATT---------------TAAAAGGGCG-TG-AAAAGGTTT-ATCCGTTC-------------------------G
7 LS0207_3_D06 AAATATTTCATCTTCATCTTCATATAAGCTCACTT-GTACAGTTC-GTCCATGCCG-CCGGTGGAGTGGCGGCCCTC-GG
8 LS0207_18_E06 ATAGATCNCCCGGT------------GCCGCCCTT-GTACAGTTC-GTCCATGNCG-TGGGTGATGCCAGCGGCGGT-AA
9 LS0207peredoxmid4 AANNTTTCATCNCCATCTTNCATATAAGCTCACTTNGTACAGTTCGGTCCATGCCGCCCGGTGGAGTGGCGGCCCTTGGG
NosT
c-Peredox-mCherry
pL1M-R2-p2xCaMV35S-c-Peredox-mCherry-tHSP
1 LS0207 cgcgttcgtactgttccacgatggtgtagtcctcgttgtgg---gaggtgatgtccaacttgatgttgacgttgtaggcg
4 LS0207_2_G06 CCGTTNNNNNNGTTCCNNANGGNNNNANNCCCCNNTTNGGGNNNGGNNNT----------
5 LS0207_19_A07 CGCGTTCGTACTGTTCCACGATGGTGTAGTCCTCGTTGTGG---GAGGTGATGTCCAACTTGATGTTGACGTTGTAGGCG
6 LS0207_20_B07 TCCATTTGTA----------TGTGCCAG
7 LS0207_3_D06 CGCGTTCGTACTGTTCCACGATGGTGTAGTCCTCGTTGTGG---GAGGTGATGTCCAACTTGATGTTGACGTTGTAGGCG
8 LS0207_18_E06 CAAATTCCAGCAGAACCANNTGGTCGCGCTTCTCGTTTNGGTCTTTGGACAGTTTAGACTGGATGCNTAAGTAGTGGTTG
9 LS0207peredoxmid4 CGCGTTCGTACTGTTCCACGATGGTGTAGTCCTCGTTGTGG---GAGGTGATGTCCAACTTGATGTTGACGTTGTAGGCG
c-Peredox-mCherry
pL1M-R2-p2xCaMV35S-c-Peredox-mCherry-tHSP
1 LS0207 ccgggcagctgcacgggcttcttggccttgtaggtggtcttgacctcagcgtcgtagtggccgccgtccttcagcttcag
5 LS0207_19_A07 CCGGGCAGCTGCACGGGCTTCTTGGCCTTGTAGGTGGTCTTGACCTCAGCGTCGTAGTGGCCGCCGTCCTTCAGCTTCAG
6 LS0207_20_B07 CCGTGCGGCTGCATGAAATCCTGG----------
7 LS0207_3_D06 CCGGGCAGCTGCACGGGCTTCTTGGCCTTGTAGGTGGTCTTGACCTCAGCGTCGTANTGGCCGCCGTCCTTCAGCTTCAG
8 LS0207_18_E06 TCAGGCAGCAGAACAGG----------
9 LS0207peredoxmid4 CCGGGCAGCTGCACGGGCTTCTTGGCCTTGTAGGTGGTCTTGACCTCAGCGTCGTAGTGGCCGCCGTCCTTCAGCTTCAG
c-Peredox-mCherry
pL1M-R2-p2xCaMV35S-c-Peredox-mCherry-tHSP
1 LS0207 cctctgcttgatctcgcccttcagggcgccgtcctcggggtacatccgctcggaggaggcctcccagcccat-ggttttc
5 LS0207_19_A07 CCTCTGCTTGATCTCGCCCTTCAGGGCGCCGTCCTCGGGGTACATCCGCTCGGAGGAGGCCTCCCAGCCCAT-GGTTTTC
7 LS0207_3_D06 CCTCTGCTTGATCTCGCCCTTCAGGGCGCCGTCCTCGGGGTACATCCNNNCGGAGGAGGCCTCCCAGCCCATGGGTTTTC
8 LS0207_18_E06 ---------GCCGTCGCCGATTGGGGTGTTCTGCTGGTAGT----------
9 LS0207peredoxmid4 CCTCTGCTTGATCTCGCCCTTCAGGGCGCCGTCCTCGGGGTACATCCGCTCGGAGGAGGCCTCCCAGCCCAT-GGTTTTC
c-Peredox-mCherry
pL1M-R2-p2xCaMV35S-c-Peredox-mCherry-tHSP
1 LS0207 ttctgcattacggggccgtcggaggggaagttggt-gccgcgcagcttcaccttgtagatgaactcgccgtcctgcaggg
5 LS0207_19_A07 TTCTGCATTACGGGGCCGTCGGAGGGGAAGTTGGT-GCCGCGCAGCTTCACCTTGTAGATGAACTCGCCGTCCTGCNNNN
6 LS0207_20_B07 ----------CCGGTTTGTCTGATGCCAAGCTGGCGGCCTGGCCGGCCAGCTTGGCCGCTGAANAAACCG----------
7 LS0207_3_D06 TTCTGCATTACGGGGCCGTCCGAAGGGGAANTTGGTGCCNNNNAGCTTCNCCTTGGAAANTGAACTNCCCNGTCCTGCNN
8 LS0207_18_E06 ----------GATCAGCCAGCTG----------
9 LS0207peredoxmid4 TTCTGCATTACGGGGCCGTCGGAGGGGAAGTTGGT-GCCGCGCAGCTTCACCTTGTAGATGAACTCGCCGTCCTGCAGGG
c-Peredox-mCherry
pL1M-R2-p2xCaMV35S-c-Peredox-mCherry-tHSP
1 LS0207 aggagtcctgggtcacggtcaccacgccgccgtcctcgaagttcatcacgcgctcccacttgaagccctcggggaaggac
5 LS0207_19_A07 GGANTCNNNNNNNNNNNNNNNN----------
6 LS0207_20_B07 ----------AACGCCGCCGTCTAAAAAGGTGAT----------GNGTATTTGANTAAAAC
7 LS0207_3_D06 GGNNGGANTCCTGGGNTCACGGTCACNACNCCGCCNNNCCNCGAAGTTCATNNNGNNNTCCNNNTTGAAGCCCNNCGGGN
8 LS0207_18_E06 ----------AACGCCGCCATCTTC----------
9 LS0207peredoxmid4 AGGAGTCCTGGGTCACGGTCACCACGCCGCCGTCCTCGAAGTTCATCACGCGCTCCCACTTGAAGCCCTCGGGGAAGGAC
c-Peredox-mCherry
pL1M-R2-p2xCaMV35S-c-Peredox-mCherry-tHSP


1 LS0207 agcttcaagtagtcggggatgtcggcggggtgcttcacgtaggccttggagccgtacatgaactgaggggacaggatgtc
6 LS0207_20_B07 AGCT----------TGCGTCATGCGGTCCNTGCGNANNTGATGCGATGAGTAAATAANCCAATN
8 LS0207_18_E06 ----------GATGTTGTGGCGGATCTTGAAGTTGGCCTTGATACCGT----------
9 LS0207peredoxmid4 AGCTTCAAGTAGTCGGGGATGTCGGCGGGGTGCTTCACGTAGGCCTTGGAGCCGTACATGAACTGAGGGGACAGGATGTC
10 LS0207peredoxmid3 ----------GNNNNNNTNNNNNNAGACTTNNNNNNNNGTTCANGNNNNNNNGNNACTNNATNNN
11 LS0207peredoxmid2 ----------GG
c-Peredox-mCherry
pL1M-R2-p2xCaMV35S-c-Peredox-mCherry-tHSP
1 LS0207 ccaggcgaagggcaggggggccaccccttggtcaccttcagcttggcggtctgggtgcccctcgtaggggcggcccctcgccct
6 LS0207_20_B07 CCCNAGGGGNAACGCATGAAGGTTATCNNTGTACTTAACCANAAAGGCGGGTCAGGCAANNNAACATNNNAACCCATCTA
8 LS0207_18_E06 ----------TCTTCTGTTTGTCAGCC----------
9 LS0207peredoxmid4 CCAGGCGAAGGGCAGGGGGCCACCCTTGGTCACCTTCAGCTTGGCGGTCTGGGTGCCCTCGTAGGGGCGGCCCTCGCCCT
10 LS0207peredoxmid3 NNAGANNAANNNCANNGGNNNATCCTTNNTCANNNTCAGNNNGGCNNTTAGGATGCCNTNGTANNGNNGGCCTTTGCCCT
11 LS0207peredoxmid2 GGNCCCCCNTTNNNNCCCTTTAANTTNGGGGGTTTNGGGGNCCCNNNNNANGGGGGGNCCNTTGNCCTTTGNCCNTTGAN
c-Peredox-mCherry
pL1M-R2-p2xCaMV35S-c-Peredox-mCherry-tHSP
1 LS0207 cgccctcgatctcgaactcgtggccgttcacggagccctccatgtgcaccttgaagcgcatgaactccttgatgatggcc
6 LS0207_20_B07 GCCCNNNCCCTGCAANNCCCNGGGGCCAANNTTNNGTTNTTCNNTTCCANTCCCNAGGGCAATGCCCCNANTTGGGCNNC
8 LS0207_18_E06 ----------ATGNNANAC
9 LS0207peredoxmid4 CGCCCTCGATCTCGAACTCGTGGCCGTTCACGGAGCCCTCCATGTGCACCTTGAAGCGCATGAACTCCTTGATGATGGCC
10 LS0207peredoxmid3 CGCCCTCGATCTCGAACTCGTGGCCGTTCACGGAGCCCTCCATGTGCACCTTGAAGCGCATGAACTCCTTGATGATGGNC
11 LS0207peredoxmid2 TTTGNAANTTNGGGCCGNTTNNNGGNNNCCTNCCANNNNNNCCTTGAANGGNCNNGAANNCCTTGAANNNGGCCNANGNT
9 LS0207peredoxmid4 CGCGTTCGTACTGTTCCACGATGGTGTAGTCCTCGTTGTGG---GAGGTGATGTCCAACTTGATGTTGACGTTGTAGGCG
c-Peredox-mCherry
pL1M-R2-p2xCaMV35S-c-Peredox-mCherry-tHSP
1 LS0207 atgttatcctcctcgccctgctcaccataccaccagacccaccaccgtcagaggcgttgccccagttccggaacccat
6 LS0207_20_B07 CNNCNGGNAANNNNNCNNNTAACCGTTNNCNGGNNCNNNCCNCCNAAAANTTGACCNNNNNNANNGGCCNNCGCCNGGNN
8 LS0207_18_E06 ACGTTAT----------GAGCAGTNAAACCATGCCCAC----------
9 LS0207peredoxmid4 ATGTTATCCTCCTCGCCCTTGCTCACCATACCACCAGACCCACCACCGTCAGAGGCGTTGCCCCCAGTTCCGGAACCCAT
10 LS0207peredoxmid3 ATGTTATCCTCCTCGCCCTTGCTCACCATACCACCAGACCCACCACCGTCAGAGGCGTTGCCCCCAGTTCCGGAACCCAT
11 LS0207peredoxmid2 NTNNNNNNTTGCCCNTTNNTNNCCNNNANNNCCNNANNCCCNNNCCGNTCNNNNGNGTTGNCCCCAGTTCCGGAACCNNN
c-Peredox-mCherry
pL1M-R2-p2xCaMV35S-c-Peredox-mCherry-tHSP
1 LS0207 catttcttcgcgccacttaggattcaggattgcgaagctcaggcgggtcaggcc-ggccaggaaatcaacgttttcaaca
6 LS0207_20_B07 NNNNTNNNNAAGGTTNNNGG----------
8 LS0207_18_E06 --TTNCTGCGCTCCACGTGGGGTTCAGAATGGCAAAGCTCAGACGCGTCAGACC-GGCCAGGATGTCAACGTTCTCAACA
9 LS0207peredoxmid4 CATTTCTTCGCGCCACTTAGGATTCAGGATTGCGAAGCTCAGGCGGGTCAGGCC-GGCCAGGAAATCAACGTTTTCAACA
10 LS0207peredoxmid3 CATTTCTTCGCGCCACTTAGGATTCAGGATTGCGAAGCTCAGGCGGGTCAGGCC-GGCCAGGAAATCAACGTTTTCAACA
11 LS0207peredoxmid2 CATTTTTTNNNNCCNNTTAGGATTCAGGATTNNGAAGTTCAGGCGGGTCAGGCCNGGCCAGGAAATCAACGTTTTCAACA
c-Peredox-mCherry
pL1M-R2-p2xCaMV35S-c-Peredox-mCherry-tHSP
1 LS0207 gcaacttccttaggaacctccagaacaacaggggcgaagttcagaattcccttgataccagcggcgactagtaagtcggc
8 LS0207_18_E06 GCCACTTCCTTGGGAACCTCCAGTACAACTGGAGCGAAGTTCAGG----------
9 LS0207peredoxmid4 GCAACTTCCTTAGGAACCTCCAGAACAACAGGGGCGAAGTTCAGAATTCCCTTGATACCAGCGGCGACTAGTAAGTCGGC
10 LS0207peredoxmid3 GCAACTTCCTTAGGAACCTCCAGAACAACAGGGGCGAAGTTCAGAATTCCCTTGATACCAGCGGCGACTAGTAAGTCGGC
11 LS0207peredoxmid2 GCAACTTCCTTAGGAACCTCCAGAACAACAGGGGNGAAGTTCAGAATTCCCTTGATACCAGCNGGGACTAGTAAGTCGGC
c-Peredox-mCherry
pL1M-R2-p2xCaMV35S-c-Peredox-mCherry-tHSP
1 LS0207 tgccttctgtgcagcttcgcgaggaacggtcagcagggcgatctcgatgcgacccgggacgcgctgtggcaggaggtcaa
9 LS0207peredoxmid4 TGCCTTCTGTGCAGCTTCGCGAGGAACGGTCAGCAGGGCGATCTCGATGCGACCCGGGACGCGCTGNGGCAGGAGGTCAA
10 LS0207peredoxmid3 TGCCTTCTGTGCAGCTTCGCGAGGAACGGTCAGCAGGGCGATCTCGATGCGACCCGGGACGCGCTGTGGCAGGAGGTCAA
11 LS0207peredoxmid2 TGCCNTTTNTGCAGCTTCGCGAGGAACGGTCAGCAGGGCGATCTCGATGCGACCCGGGACGCGCTGTGGCAGGAGGTCAA
c-Peredox-mCherry
pL1M-R2-p2xCaMV35S-c-Peredox-mCherry-tHSP
1 LS0207 catgctcgataacgccaccgcgaacagggcgcccaaccatgcctggatcaacgtcgaagaagccgcgcagttcgaaagat
9 LS0207peredoxmid4 CATGCTCGATAACGCCACCGCGAACNNNNNCCCANNANGNNNNNNNNNNNNNNNNNNN----------
10 LS0207peredoxmid3 CATGCTCGATAACGCCACCGCGAACAGGGCGCCCAACCATGCCTGGATCAACGTCGAAGAAGCCGCGCAGTTCGAAAGAT
11 LS0207peredoxmid2 CATGCTCGATAACGCCACCGCGAACAGGGCGCCCAACCATGCCTGGATCAACGTCGAAGAAGCCGCGCAGTTCGAAAGAT
c-Peredox-mCherry
pL1M-R2-p2xCaMV35S-c-Peredox-mCherry-tHSP

```
 1 LS0207             tcaccaaagcccggccagtctgccagtgcactaccgaggcggcccatgccaacgatgcataagccccacttgcggttcag
10 LS0207peredoxmid3 TCACCAAAGCCCGGCCAGTCTGCCAGTGCACTACCGAGGCGGCCCATGCCAACGATGCATAAGCCCCACTTGCGGTTCAG
11 LS0207peredoxmid2 TCACCAAAGCCCGGCCAGTCTGCCAGTGCACTACCGAGGCGGCCCATGCCAACGATGCATAAGCCCCACTTGCGGTTCAG
```

c-Peredox-mCherry

pL1M-R2-p2xCaMV35S-c-Peredox-mCherry-tHSP

```
 1 LS0207             gcccaggatgtggcgcagctcgcgcttcaggacagggactgtgtagccaacaccgtcggtgccgtaggaaccgaaatagg
10 LS0207peredoxmid3 GCCCAGGATGTGGCGCAGCTCGCGCTTCAGGACAGGGACTGTGTAGCCAACACCGTCGGTGCCGTAGGAACCGAAATAGG
11 LS0207peredoxmid2 GCCCAGGATGTGGCGCAGCTCGCGCTTCAGGACAGGGACTGTGTAGCCAACACCGTCGGTGCCGTAGGAACCGAAATAGG
```

c-Peredox-mCherry

pL1M-R2-p2xCaMV35S-c-Peredox-mCherry-tHSP

```
 1 LS0207             acagatcttcgtcaacctggaatgctgtaacctgtgccagttcgcccagctgctcgcttgcagtgcggtgaacgccttgg
10 LS0207peredoxmid3 ACAGATCTTCGTCAACCTGGAATGCTGTAACCTGTGCCAGTTCGCCCAGCTGCTCGCTTGCAGTGCGGTGAACGCCTTGG
11 LS0207peredoxmid2 ACAGATCTTCGTCAACCTGGAATGCTGTAACCTGTGCCAGTTCGCCCAGCTGCTCGCTTGCAGTGCGGTGAACGCCTTGG
```

c-Peredox-mCherry

pL1M-R2-p2xCaMV35S-c-Peredox-mCherry-tHSP

```
 1 LS0207             gcttcgagctcctccaggatgcggaggtaagtgatgaggcggctgatggcggcttcaggtaccttggtgttatattcaag
10 LS0207peredoxmid3 GCTTCGAGCTCCTCCAGGATGCGGAGGTAAGTGATGAGGCGGCTGATGGCGGCTTCAGGTACCTTGGTGTTATATTCAAG
11 LS0207peredoxmid2 GCTTCGAGCTCCTCCAGGATGCGGAGGTAAGTGATGAGGCGGCTGATGGCGGCTTCAGGTACCTTGGTGTTATATTCAAG
```

c-Peredox-mCherry

pL1M-R2-p2xCaMV35S-c-Peredox-mCherry-tHSP

```
 1 LS0207             cttatggcccaggatgttgccgtcctccttgaagtcgatgcccttcagctcgatgcggttaaccagagtgtcgccctcga
10 LS0207peredoxmid3 CTTATGGCCCAGGATGTTGCCGTCCTCCTTGAAGTCGATGCCCTTCAGCTCGATGCGGTTAACCAGAGTGTCGCCCTCGA
11 LS0207peredoxmid2 CTTATGGCCCAGGATGTTGCCGTCCTCCTTGAAGTCGATGCCCTTCAGCTCGATGCGGTTAACCAGAGTGTCGCCCTCGA
```

c-Peredox-mCherry

pL1M-R2-p2xCaMV35S-c-Peredox-mCherry-tHSP

```
 1 LS0207             acttaacctcagcgcgtgtcttatagttgccgtcgtccttgaaaaagatggtgcgttcctgaacgtagccctcaggcatg
10 LS0207peredoxmid3 ACTTAACCTCAGCGCGTGTCTTATAGTTGCCGTCGTCC-TGAAAAAGATGGTGCGTCNNNNNNNNNNNNNN---------
11 LS0207peredoxmid2 ACTTAACCTCAGCGCGTGTCTTATAGTTGCCGTCGTCCTTGAAAAAGATGGTGCGTTCCTGAACGTAGCCCTCAGGCATG
```

c-Peredox-mCherry

pL1M-R2-p2xCaMV35S-c-Peredox-mCherry-tHSP

```
 1 LS0207             gcgctcttgaagaagtcgtgctgcttcatgtggtcaggatatctggcgaaaaccataacaccataggagaaggtagtaac
11 LS0207peredoxmid2 GCGCTCTTGAAGAAGTCGTGCTGCTTCATGTGGTCAGGATATCTGGCGAAAACCATAACACCATAGGAGAAGGTAGTAAC
```

c-Peredox-mCherry

pL1M-R2-p2xCaMV35S-c-Peredox-mCherry-tHSP

```
 1 LS0207             cagggtaggccaaggaacaggcagcttgccagtggtgcagatgaacttcagagtcagcttgccgtaggtagcatctcctt
11 LS0207peredoxmid2 CAGGGTAGGCCAAGGAACAGGCAGCTTGCCAGTGGTGCAGATGAACTTCAGAGTCAGCTTGCCGTAGGTAGCATCTCCTT
```

c-Peredox-mCherry

pL1M-R2-p2xCaMV35S-c-Peredox-mCherry-tHSP

```
 1 LS0207             cgccttccccgctaacgctgaatttgtggccgttaacgtcgccgtccagttcaaccaggataggaacaacaccagtgaac
 9 LS0207peredoxmid4 CGCGTTCGTACTGTTCCACGATGGTGTAGTCCTCGTTGTGG---GAGGTGATGTCCAACTTGATGTTGACGTTGTAGGCG
```

c-Peredox-mCherry

pL1M-R2-p2xCaMV35S-c-Peredox-mCherry-tHSP

```
 1 LS0207             agttcctcgcctttggaaaccatagatcccccggtgccgcccttgtacagttcgtccatgccgtgggtgatgccagcggc
11 LS0207peredoxmid2 AGTTCCTCGCCTTTGGAAACCATAGATCCCCCGGTGCCGCCCTTGTACAGTTCGTCCATGCCGTGGGTGATGCCAGCGGC
```

c-Peredox-mCherry

pL1M-R2-p2xCaMV35S-c-Peredox-mCherry-tHSP

```
 1 LS0207             ggtaacaaattccagcagaaccatgtggtcgcgcttctcgtttgggtctttggacagtttagactggatgcttaagtagt
11 LS0207peredoxmid2 GGTAACAAATTCCAGCAGAACCATGTGGTCGCGCTTCTCGTTTGGGTCTTTGGACAGTTTAGACTGGATGCTTAAGTAGT
```

c-Peredox-mCherry

pL1M-R2-p2xCaMV35S-c-Peredox-mCherry-tHSP

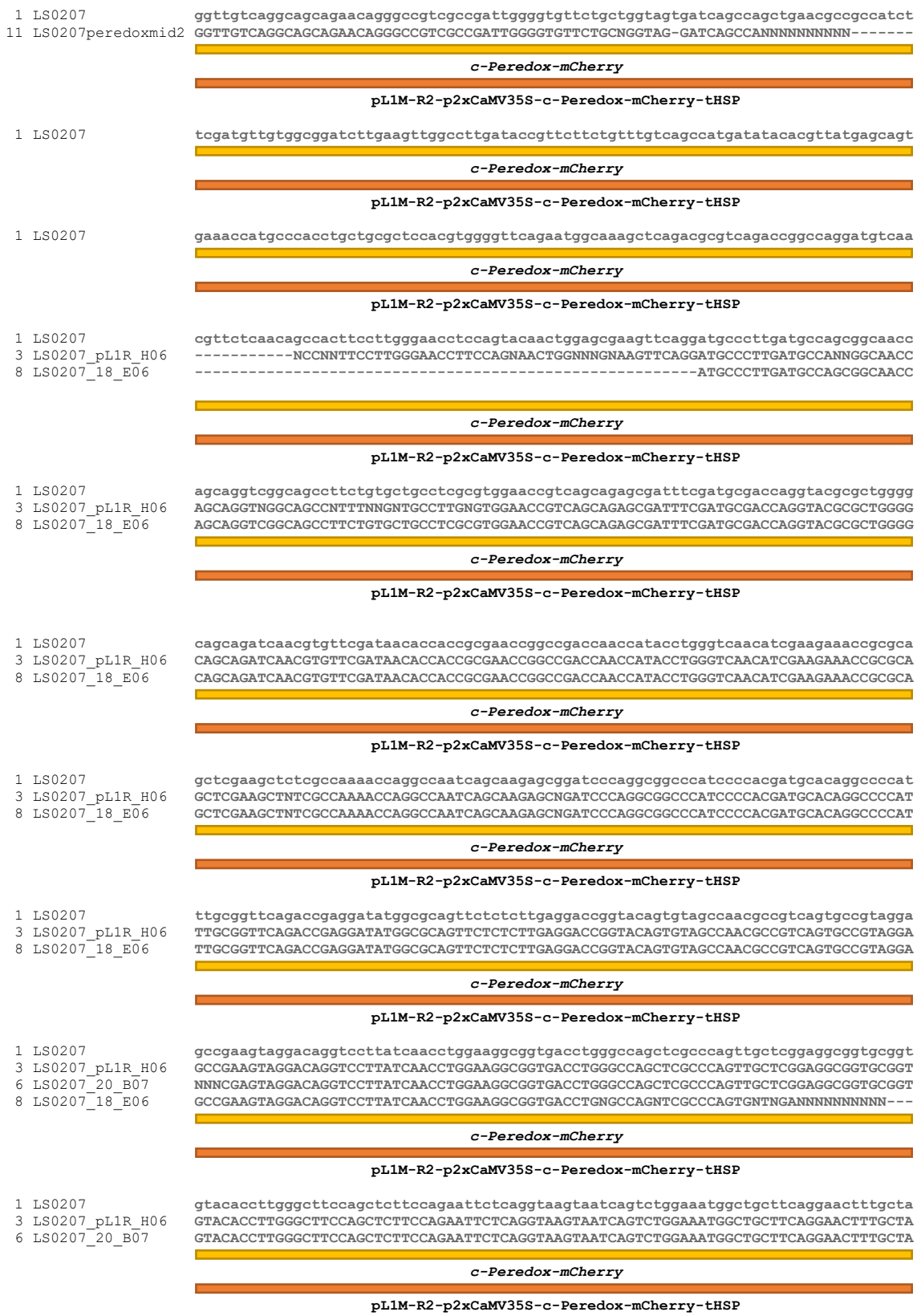
1 LS0207 ggttgtcaggcagcagaacagggccgtcgccgattggggtgttctgctggtagtgatcagccagctgaacgccgccatct
11 LS0207peredoxmid2 GGTTGTCAGGCAGCAGAACAGGGCCGTCGCCGATTGGGGTGTTCTGCNGGTAG-GATCAGCCANNNNNNNNNN-------
c-Peredox-mCherry
pL1M-R2-p2xCaMV35S-c-Peredox-mCherry-tHSP
1 LS0207 tcgatgttgtggcggatcttgaagttggccttgataccgttcttctgtttgtcagccatgatatacacgttatgagcagt
c-Peredox-mCherry
pL1M-R2-p2xCaMV35S-c-Peredox-mCherry-tHSP
1 LS0207 gaaaccatgcccacctgctgcgctccacgtggggttcagaatggcaaagctcagacgcgtcagaccggccaggatgtcaa
c-Peredox-mCherry
pL1M-R2-p2xCaMV35S-c-Peredox-mCherry-tHSP
1 LS0207 cgttctcaacagccacttccttgggaacctccagtacaactggagcgaagttcaggatgcccttgatgccagcggcaacc
3 LS0207_pL1R_H06 ----------NCCNNTTCCTTGGGAACCTTCCAGNAACTGGNNNGNAAGTTCAGGATGCCCTTGATGCCANNGGCAACC
8 LS0207_18_E06 ----------ATGCCCTTGATGCCAGCGGCAACC
c-Peredox-mCherry
pL1M-R2-p2xCaMV35S-c-Peredox-mCherry-tHSP
1 LS0207 agcaggtcggcagccttctgtgctgcctcgcgtggaaccgtcagcagagcgatttcgatgcgaccaggtacgcgctgggg
3 LS0207_pL1R_H06 AGCAGGTNGGCAGCCNTTTNNGNTGCCTTGNGTGGAACCGTCAGCAGAGCGATTTCGATGCGACCAGGTACGCGCTGGGG
8 LS0207_18_E06 AGCAGGTCGGCAGCCTTCTGTGCTGCCTCGCGTGGAACCGTCAGCAGAGCGATTTCGATGCGACCAGGTACGCGCTGGGG
c-Peredox-mCherry
pL1M-R2-p2xCaMV35S-c-Peredox-mCherry-tHSP
1 LS0207 cagcagatcaacgtgttcgataacaccaccgcgaaccggccgaccaaccatacctgggtcaacatcgaagaaaccgcgca
3 LS0207_pL1R_H06 CAGCAGATCAACGTGTTCGATAACACCACCGCGAACCGGCCGACCAACCATACCTGGGTCAACATCGAAGAAACCGCGCA
8 LS0207_18_E06 CAGCAGATCAACGTGTTCGATAACACCACCGCGAACCGGCCGACCAACCATACCTGGGTCAACATCGAAGAAACCGCGCA
c-Peredox-mCherry
pL1M-R2-p2xCaMV35S-c-Peredox-mCherry-tHSP
1 LS0207 gctcgaagctctcgccaaaaccaggccaatcagcaagagcggatcccaggcggcccatccccacgatgcacaggccccat
3 LS0207_pL1R_H06 GCTCGAAGCTNTCGCCAAAACCAGGCCAATCAGCAAGAGCNGATCCCAGGCGGCCCATCCCCACGATGCACAGGCCCCAT
8 LS0207_18_E06 GCTCGAAGCTNTCGCCAAAACCAGGCCAATCAGCAAGAGCNGATCCCAGGCGGCCCATCCCCACGATGCACAGGCCCCAT
c-Peredox-mCherry
pL1M-R2-p2xCaMV35S-c-Peredox-mCherry-tHSP
1 LS0207 ttgcggttcagaccgaggatatggcgcagttctctcttgaggaccggtacagtgtagccaacgccgtcagtgccgtagga
3 LS0207_pL1R_H06 TTGCGGTTCAGACCGAGGATATGGCGCAGTTCTCTCTTGAGGACCGGTACAGTGTAGCCAACGCCGTCAGTGCCGTAGGA
8 LS0207_18_E06 TTGCGGTTCAGACCGAGGATATGGCGCAGTTCTCTCTTGAGGACCGGTACAGTGTAGCCAACGCCGTCAGTGCCGTAGGA
c-Peredox-mCherry
pL1M-R2-p2xCaMV35S-c-Peredox-mCherry-tHSP
1 LS0207 gccgaagtaggacaggtccttatcaacctggaaggcggtgacctgggccagctcgcccagttgctcggaggcggtgcggt
3 LS0207_pL1R_H06 GCCGAAGTAGGACAGGTCCTTATCAACCTGGAAGGCGGTGACCTGGGCCAGCTCGCCCAGTTGCTCGGAGGCGGTGCGGT
6 LS0207_20_B07 NNNCGAGTAGGACAGGTCCTTATCAACCTGGAAGGCGGTGACCTGGGCCAGCTCGCCCAGTTGCTCGGAGGCGGTGCGGT
8 LS0207_18_E06 GCCGAAGTAGGACAGGTCCTTATCAACCTGGAAGGCGGTGACCTGNGCCAGNTCGCCCAGTGNTNGANNNNNNNNNN---
c-Peredox-mCherry
pL1M-R2-p2xCaMV35S-c-Peredox-mCherry-tHSP
1 LS0207 gtacaccttgggcttccagctcttccagaattctcaggtaagtaatcagtctggaaatggctgcttcaggaactttgcta
3 LS0207_pL1R_H06 GTACACCTTGGGCTTCCAGCTCTTCCAGAATTCTCAGGTAAGTAATCAGTCTGGAAATGGCTGCTTCAGGAACTTTGCTA
6 LS0207_20_B07 GTACACCTTGGGCTTCCAGCTCTTCCAGAATTCTCAGGTAAGTAATCAGTCTGGAAATGGCTGCTTCAGGAACTTTGCTA
c-Peredox-mCherry
pL1M-R2-p2xCaMV35S-c-Peredox-mCherry-tHSP

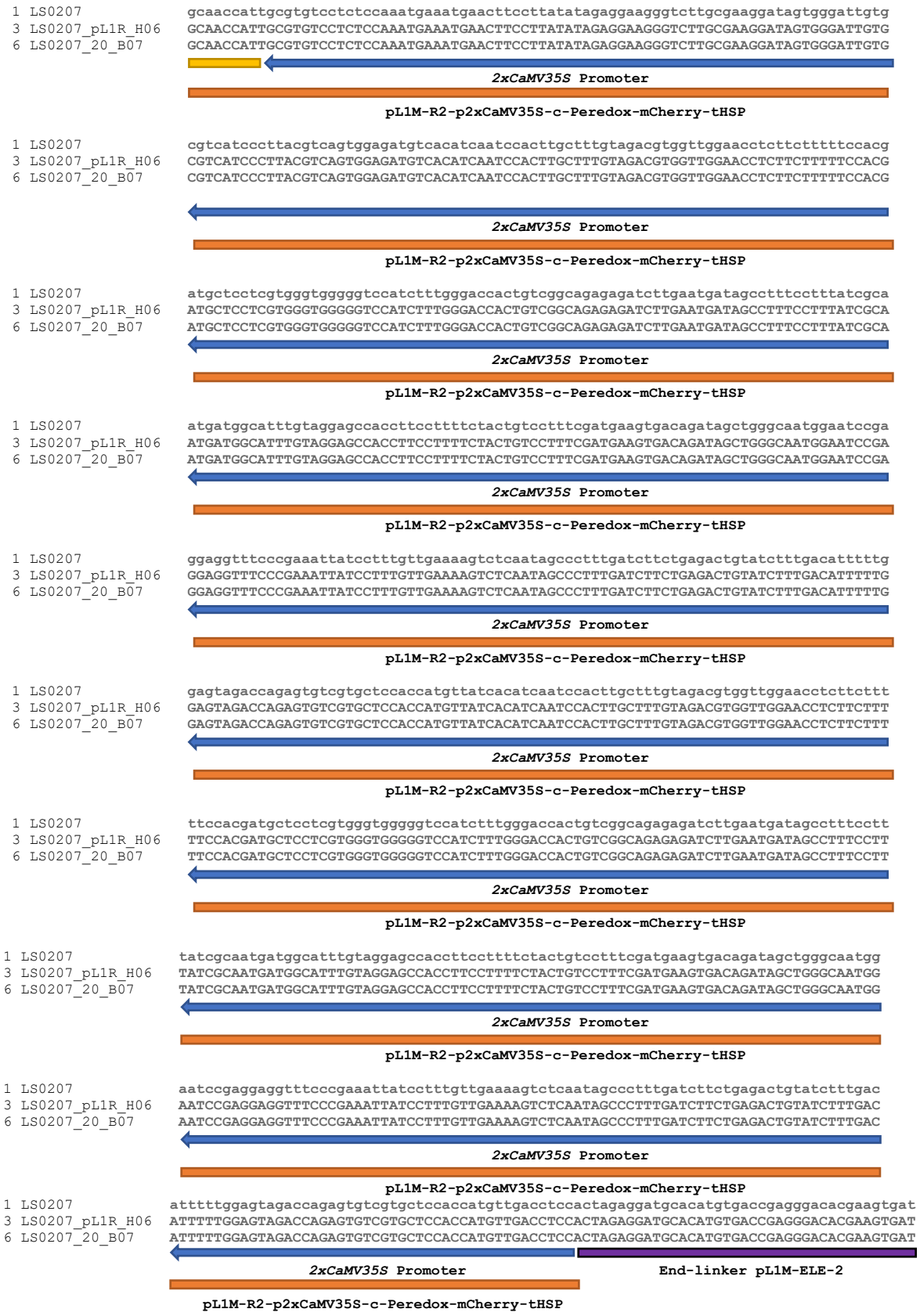
1 LS0207 gcaaccattgcgtgtcctctccaaatgaaatgaacttccttatatagaggaagggtcttgcgaaggatagtgggattgtg
3 LS0207_pL1R_H06 GCAACCATTGCGTGTCCTCTCCAAATGAAATGAACTTCCTTATATAGAGGAAGGGTCTTGCGAAGGATAGTGGGATTGTG
6 LS0207_20_B07 GCAACCATTGCGTGTCCTCTCCAAATGAAATGAACTTCCTTATATAGAGGAAGGGTCTTGCGAAGGATAGTGGGATTGTG
2xCaMV35S Promoter
pL1M-R2-p2xCaMV35S-c-Peredox-mCherry-tHSP
1 LS0207 cgtcatcccttacgtcagtggagatgtcacatcaatccacttgctttgtagacgtggttggaacctcttctttttccacg
3 LS0207_pL1R_H06 CGTCATCCCTTACGTCAGTGGAGATGTCACATCAATCCACTTGCTTTGTAGACGTGGTTGGAACCTCTTCTTTTTCCACG
6 LS0207_20_B07 CGTCATCCCTTACGTCAGTGGAGATGTCACATCAATCCACTTGCTTTGTAGACGTGGTTGGAACCTCTTCTTTTTCCACG
2xCaMV35S Promoter
pL1M-R2-p2xCaMV35S-c-Peredox-mCherry-tHSP
1 LS0207 atgctcctcgtgggtgggggtccatctttgggaccactgtcggcagagagatcttgaatgatagcctttccttttatcgca
3 LS0207_pL1R_H06 ATGCTCCTCGTGGGTGGGGGTCCATCTTTGGGACCACTGTCGGCAGAGAGATCTTGAATGATAGCCTTTCCTTTATCGCA
6 LS0207_20_B07 ATGCTCCTCGTGGGTGGGGGTCCATCTTTGGGACCACTGTCGGCAGAGAGATCTTGAATGATAGCCTTTCCTTTATCGCA
2xCaMV35S Promoter
pL1M-R2-p2xCaMV35S-c-Peredox-mCherry-tHSP
1 LS0207 atgatggcatttgtaggagccaccttccttttctactgtcctttcgatgaagtgacagatagctgggcaatggaatccga
3 LS0207_pL1R_H06 ATGATGGCATTTGTAGGAGCCACCTTCCTTTTCTACTGTCCTTTCGATGAAGTGACAGATAGCTGGGCAATGGAATCCGA
6 LS0207_20_B07 ATGATGGCATTTGTAGGAGCCACCTTCCTTTTCTACTGTCCTTTCGATGAAGTGACAGATAGCTGGGCAATGGAATCCGA
2xCaMV35S Promoter
pL1M-R2-p2xCaMV35S-c-Peredox-mCherry-tHSP
1 LS0207 ggaggtttcccgaaattatcctttgttgaaaagtctcaatagccctttgatcttctgagactgtatctttgacatttttg
3 LS0207_pL1R_H06 GGAGGTTTCCCGAAATTATCCTTTGTTGAAAAGTCTCAATAGCCCTTTGATCTTCTGAGACTGTATCTTTGACATTTTTG
6 LS0207_20_B07 GGAGGTTTCCCGAAATTATCCTTTGTTGAAAAGTCTCAATAGCCCTTTGATCTTCTGAGACTGTATCTTTGACATTTTTG
2xCaMV35S Promoter
pL1M-R2-p2xCaMV35S-c-Peredox-mCherry-tHSP
1 LS0207 gagtagaccagagtgtcgtgctccaccatgttatcacatcaatccacttgctttgtagacgtggttggaacctcttcttt
3 LS0207_pL1R_H06 GAGTAGACCAGAGTGTCGTGCTCCACCATGTTATCACATCAATCCACTTGCTTTGTAGACGTGGTTGGAACCTCTTCTTT
6 LS0207_20_B07 GAGTAGACCAGAGTGTCGTGCTCCACCATGTTATCACATCAATCCACTTGCTTTGTAGACGTGGTTGGAACCTCTTCTTT
2xCaMV35S Promoter
pL1M-R2-p2xCaMV35S-c-Peredox-mCherry-tHSP
1 LS0207 ttccacgatgctcctcgtgggtgggggtccatctttgggaccactgtcggcagagagatcttgaatgatagcctttcctt
3 LS0207_pL1R_H06 TTCCACGATGCTCCTCGTGGGTGGGGGTCCATCTTTGGGACCACTGTCGGCAGAGAGATCTTGAATGATAGCCTTTCCTT
6 LS0207_20_B07 TTCCACGATGCTCCTCGTGGGTGGGGGTCCATCTTTGGGACCACTGTCGGCAGAGAGATCTTGAATGATAGCCTTTCCTT
2xCaMV35S Promoter
pL1M-R2-p2xCaMV35S-c-Peredox-mCherry-tHSP
1 LS0207 tatcgcaatgatggcatttgtaggagccaccttccttttctactgtcctttcgatgaagtgacagatagctgggcaatgg
3 LS0207_pL1R_H06 TATCGCAATGATGGCATTTGTAGGAGCCACCTTCCTTTTCTACTGTCCTTTCGATGAAGTGACAGATAGCTGGGCAATGG
6 LS0207_20_B07 TATCGCAATGATGGCATTTGTAGGAGCCACCTTCCTTTTCTACTGTCCTTTCGATGAAGTGACAGATAGCTGGGCAATGG
2xCaMV35S Promoter
pL1M-R2-p2xCaMV35S-c-Peredox-mCherry-tHSP
1 LS0207 aatccgaggaggtttcccgaaattatcctttgttgaaaagtctcaatagcccttgatcttctgagactgtatctttgac
3 LS0207_pL1R_H06 AATCCGAGGAGGTTTCCCGAAATTATCCTTTGTTGAAAAGTCTCAATAGCCCTTTGATCTTCTGAGACTGTATCTTTGAC
6 LS0207_20_B07 AATCCGAGGAGGTTTCCCGAAATTATCCTTTGTTGAAAAGTCTCAATAGCCCTTTGATCTTCTGAGACTGTATCTTTGAC
2xCaMV35S Promoter
pL1M-R2-p2xCaMV35S-c-Peredox-mCherry-tHSP
1 LS0207 atttttggagtagaccagagtgtcgtgctccaccatgttgacctccactagaggatgcacatgtgaccgagggacacgaagtgat
3 LS0207_pL1R_H06 ATTTTTGGAGTAGACCAGAGTGTCGTGCTCCACCATGTTGACCTCCACTAGAGGATGCACATGTGACCGAGGGACACGAAGTGAT
6 LS0207_20_B07 ATTTTTGGAGTAGACCAGAGTGTCGTGCTCCACCATGTTGACCTCCACTAGAGGATGCACATGTGACCGAGGGACACGAAGTGAT
2xCaMV35S Promoter
End-linker pL1M-ELE-2
pL1M-R2-p2xCaMV35S-c-Peredox-mCherry-tHSP

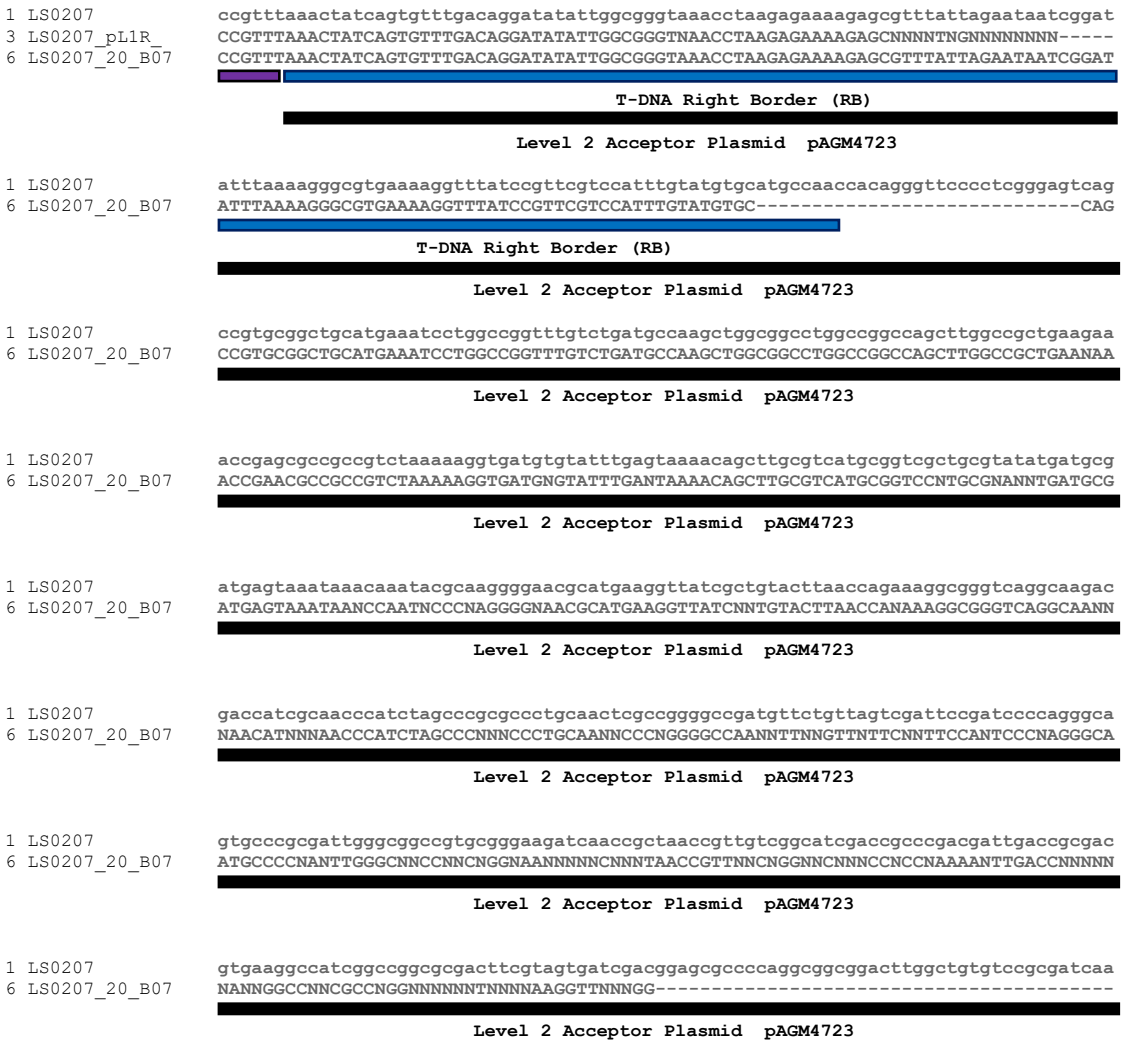
1 LS0207 ccgtttaaactatcagtgtttgacaggatatattggcgggtaaacctaagagaaaagagcgtttattagaataatcggat
3 LS0207_pL1R_ CCGTTTAAACTATCAGTGTTTGACAGGATATATTGGCGGGTNAACCTAAGAGAAAAGAGCNNNNTNGNNNNNNNN-----
6 LS0207_20_B07 CCGTTTAAACTATCAGTGTTTGACAGGATATATTGGCGGGTAAACCTAAGAGAAAAGAGCGTTTATTAGAATAATCGGAT
T-DNA Right Border (RB)
Level 2 Acceptor Plasmid pAGM4723
1 LS0207 atttaaaagggcgtgaaaaggtttatccgttcgtccatttgtatgtgcatgccaaccacagggttcccctcgggagtcag
6 LS0207_20_B07 ATTTAAAAGGGCGTGAAAAGGTTTATCCGTTCGTCCATTTGTATGTGC----------CAG
T-DNA Right Border (RB)
Level 2 Acceptor Plasmid pAGM4723
1 LS0207 ccgtgcggctgcatgaaatcctggccggtttgtctgatgccaagctggcggcctggccggccagcttggccgctgaagaa
6 LS0207_20_B07 CCGTGCGGCTGCATGAAATCCTGGCCGGTTTGTCTGATGCCAAGCTGGCGGCCTGGCCGGCCAGCTTGGCCGCTGAANAA
Level 2 Acceptor Plasmid pAGM4723
1 LS0207 accgagcgccgccgtctaaaaaggtgatgtgtatttgagtaaaacagcttgcgtcatgcggtcgctgcgtatatgatgcg
6 LS0207_20_B07 ACCGAACGCCGCCGTCTAAAAAGGTGATGNGTATTTGANTAAAACAGCTTGCGTCATGCGGTCCNTGCGNANNTGATGCG
Level 2 Acceptor Plasmid pAGM4723
1 LS0207 atgagtaaataaacaaatacgcaaggggaacgcatgaaggttatcgctgtacttaaccagaaaggcgggtcaggcaagac
6 LS0207_20_B07 ATGAGTAAATAANCCAATNCCCNAGGGGNAACGCATGAAGGTTATCNNTGTACTTAACCANAAAGGCGGGTCAGGCAANN
Level 2 Acceptor Plasmid pAGM4723
1 LS0207 gaccatcgcaacccatctagcccgcgccctgcaactcgccggggccgatgttctgttagtcgattccgatccccagggca
6 LS0207_20_B07 NAACATNNNAACCCATCTAGCCCNNNCCCTGCAANNCCCNGGGGCCAANNTTNNGTTNTTCNNTTCCANTCCCNAGGGCA
Level 2 Acceptor Plasmid pAGM4723
1 LS0207 gtgcccgcgattgggcggccgtgcgggaagatcaaccgctaaccgttgtcggcatcgaccgcccgacgattgaccgcgac
6 LS0207_20_B07 ATGCCCCNANTTGGGCNNCCNNCNGGNAANNNNNCNNNTAACCGTTNNCNGGNNCNNNCCNCCNAAAANTTGACCNNNNN
Level 2 Acceptor Plasmid pAGM4723
1 LS0207 gtgaaggccatcggccggcgcgacttcgtagtgatcgacggagcgccccaggcggcggacttggctgtgtccgcgatcaa
6 LS0207_20_B07 NANNGGCCNNCGCCNGGNNNNNNTNNNNAAGGTTNNNGG----------
Level 2 Acceptor Plasmid pAGM4723

References

1. Tilman, D., Balzer, C., Hill, J. & Befort, B. L. Global food demand and the sustainable intensification of agriculture. *Proceedings of the National Academy of Sciences of the United States of America* **108,** 20260–20264 (2011).
2. Hunter, M. C., Smith, R. G., Schipanski, M. E., Atwood, L. W. & Mortensen, D. A. Agriculture in 2050: Recalibrating targets for sustainable intensification. *BioScience* **67,** 386–391 (2017).
3. Wu, A., Hammer, G. L., Doherty, A., von Caemmerer, S. & Farquhar, G. D. Quantifying impacts of enhancing photosynthesis on crop yield. *Nature Plants* **5,** 380–388 (2019).
4. Long, S. P., Zhu, X.-G., Naidu, S. L. & Ort, D. R. Can improvement in photosynthesis increase crop yields? *Plant, Cell & Environment* **29,** 315–330 (2006).
5. Reynolds, M. *et al.* Raising yield potential in wheat. *Journal of Experimental Botany* **60,** 1899–1918 (2009).
6. Nowicka, B. Target genes for plant productivity improvement. *Journal of Biotechnology* **298,** 21–34 (2019).
7. Bailey-Serres, J., Parker, J. E., Ainsworth, E. A., Oldroyd, G. E. & Schroeder, J. I. Genetic strategies for improving crop yields. *Nature* **575,** 109–118 (2019).
8. Von Caemmerer, S. & Evans, J. R. Enhancing C_3 photosynthesis. *Plant Physiology* **154,** 589–592 (2010).
9. Raines, C. A. Increasing photosynthetic carbon assimilation in C_3 plants to improve crop yield: Current and future strategies. *Plant Physiology* **155,** 36–42 (2011).
10. Ainsworth, E. A., Yendrek, C. R., Skoneczka, J. A. & Long, S. P. Accelerating yield potential in soybean: Potential targets for biotechnological improvement. *Plant, Cell & Environment* **35,** 38–52 (2012).
11. Yamori, W. Improving photosynthesis to increase food and fuel production by biotechnological strategies in crops. *Journal of Plant Biochemistry & Physiology* **1,** 113–115 (2013).
12. Singh, J. *et al.* Enhancing C_3 photosynthesis: An outlook on feasible interventions for crop improvement. *Plant Biotechnology Journal* **12,** 1217–1230 (2014).

13. Furbank, R. T., Quick, W. P. & Sirault, X. R. R. Improving photosynthesis and yield potential in cereal crops by targeted genetic manipulation: Prospects, progress and challenges. *Field Crops Research* **182,** 19–29 (2015).

14. Long, S. P., Marshall-Colon, A. & Zhu, X. G. Meeting the global food demand of the future by engineering crop photosynthesis and yield potential. *Cell* **161,** 56–66 (2015).

15. Ort, D. R. *et al.* Redesigning photosynthesis to sustainably meet global food and bioenergy demand. *Proceedings of the National Academy of Sciences of the United States of America* **112,** 8529–8536 (2015).

16. Orr, D. J. *et al.* Engineering photosynthesis: progress and perspectives. *F1000 Research* **6,** 1891–1902 (2017).

17. South, P. F., Cavanagh, A. P., Lopez-Calcagno, P. E., Raines, C. A. & Ort, D. R. Optimizing photorespiration for improved crop productivity. *Journal of Integrative Plant Biology* **60,** 1217–1230 (2018).

18. Éva, C., Oszvald, M. & Tamás, L. Current and possible approaches for improving photosynthetic efficiency. *Plant Science* **280,** 433–440 (2019).

19. Simkin, A. J., López-Calcagno, P. E. & Raines, C. A. Feeding the world: improving photosynthetic efficiency for sustainable crop production. *Journal of Experimental Botany* **70,** 1119–1140 (2019).

20. Weber, A. P. & Bar-Even, A. Improving the efficiency of photosynthetic carbon reactions. *Plant Physiology* **179,** 803–812 (2019).

21. Zhu, X.-G., Long, S. P. & Ort, D. R. Improving photosynthetic efficiency for greater yield. *Annual Review of Plant Biology* **61,** 235–261 (2010).

22. Simkin, A. J., McAusland, L., Lawson, T. & Raines, C. A. Overexpression of the RieskeFeS protein increases electron transport rates and biomass yield. *Plant Physiology* **175,** 134–145 (2017).

23. López-Calcagno, P. E. *et al.* Stimulating photosynthetic processes increases productivity and water-use efficiency in the field. *Nature Plants* **6,** 1054–1063 (2020).

24. South, P. F., Cavanagh, A. P., Liu, H. W. & Ort, D. R. Synthetic glycolate metabolism pathways stimulate crop growth and productivity in the field. *Science* **363,** eaat9077 (2019).

25. Shen, B. R. *et al.* Engineering a new chloroplastic photorespiratory bypass to increase photosynthetic efficiency and productivity in rice. *Molecular Plant* **12,** 199–214 (2019).

26. Food and Agriculture Organisation. *Declaration of the World Summit on Food Security* tech. rep. (2009).

27. United Nations. *Transforming Our World: The 2030 Agenda for Sustainable Development* tech. rep. (General Assembly, 2015).

28. United Nations. *World population prospects: Key findings & advice tables* tech. rep. (Department of Economic and Social Affairs, Population Division, 2019).

29. Alexandratos, N. & Bruinsma, J. *World agriculture towards 2030/2050* tech. rep. 12–03 (Food and Agriculture Organisation, 2012).

30. Tilman, D. & Clark, M. Food, agriculture & the environment: Can we feed the world & save the earth? *Daedalus* **144,** 8–23 (2015).

31. Organisation for Economic Co-Operation and Development (OECD). *Crop Production - definition.* 2020.

32. Ray, D. K., Mueller, N. D., West, P. C. & Foley, J. A. Yield trends are insufficient to double global crop production by 2050. *PLoS ONE* **8,** e66428 (2013).

33. Food & Organisation, A. *FAOSTAT: Statistical database.* 2020.

34. Tilman, D., Cassman, K. G., Matson, P. A., Naylor, R. & Polasky, S. Agricultural sustainability and intensive production practices. *Nature* **418,** 671–677 (2002).

35. Godfray, H. C. J. *et al.* Food security: The challenge of feeding 9 billion people. *Science* **327,** 812–818 (2010).

36. Evans, L. T. & Fisher, R. A. Yield potential: Its definition, measurement, and significance. *Crop Science* **39,** 1544–1551 (1999).

37. Monteith, J. L. Climate and the efficiency of crop production in Britain. *Philosophical Transactions of the Royal Society B: Biological Sciences* **281,** 277–294 (1977).

38. Evenson, R. E. & Gollin, D. Assessing the impact of the Green Revolution, 1960 to 2000. *Science* **300,** 758–762 (2003).

39. Rossi, M., Bermudez, L. & Carrari, F. Crop yield: Challenges from a metabolic perspective. *Current Opinion in Plant Biology* **25,** 79–89 (2015).

40. Slattery, R. A. & Ort, D. R. Photosynthetic energy conversion efficiency: Setting a baseline for gauging future improvements in important food and biofuel crops. *Plant Physiology* **168,** 383–392 (2015).

41. Long, S. P. & Zhu, X. G. Photosynthesis: The final frontier. *CSA News* **59,** 12–13 (2014).

42. Sinclair, T. R., Purcell, L. C. & Sneller, C. H. Crop transformation and the challenge to increase yield potential. *Trends in Plant Science* **9,** 70–75 (2004).

43. Kirschbaum, M. U. F. Does enhanced photosynthesis enhance growth? Lessons learned from CO_2 enrichment studies. *Plant Physiology* **155,** 117–124 (2011).

44. Sinclair, T. R., Rufty, T. W. & Lewis, R. S. Increasing photosynthesis: Unlikely solution for world food problem. *Trends in Plant Science* **24,** 1032–1039 (2019).

45. Walker, B. J., Busch, F. A., Driever, S. M., Kromdijk, J. & Lawson, T. in *Methods in Molecular Biology* (ed Covshoff, S.) 3–24 (Humana Press Inc., 2018).

46. Farquhar, G. D., von Caemmerer, S. & Berry, J. A. A biochemical model of photosynthetic CO_2 assimilation in leaves of C_3 species. *Planta* **149,** 78–90 (1980).

47. Murchie, E. & Lawson, T. Chlorophyll fluorescence analysis: a guide to good practice and understanding some new applications. *Journal of Experimental Botany* **64,** 3983–3998 (2013).

48. Maxwell, K. & Johnson, G. N. Chlorophyll fluorescence — a practical guide. *Journal of Experimental Botany* **51,** 659–668 (2000).

49. Chang, H., Huang, H. E., Cheng, C. F., Ho, M. H. & Ger, M. J. Constitutive expression of a plant ferredoxin-like protein (pflp) enhances capacity of photosynthetic carbon assimilation in rice (*Oryza sativa*). *Transgenic Research* **26,** 279–289 (2017).

50. Hill, J. F. in *Photosynthesis: Plastid Biology, Energy Conversion and Carbon Assimilation, Advances in Photosynthesis and Respiration* (eds Eaton-Rye, J. J., Tripathy, B. & Sharkey, T.) 771–800 (Springer, 2012).

51. Stirbet, A., Lazár, D., Guo, Y. & Govindjee. Photosynthesis: Basics, history and modelling. **126,** 511–537 (2020).

52. Benson, A. A. *et al.* The path of carbon in photosynthesis. V. Paper chromatography and radioautography of the products. *Journal of the American Chemical Society* **72,** 1710–1718 (1950).

53. Yamori, W. *et al.* The roles of ATP synthase and the cytochrome b6/f complexes in limiting chloroplast electron transport and determining photosynthetic capacity. *Plant Physiology* **155,** 956–962 (2011).

54. Lin, M. T., Occhialini, A., Andralojc, P. J., Parry, M. A. J. & Hanson, M. R. A faster Rubisco with potential to increase photosynthesis in crops. *Nature* **513,** 547–550 (2014).

55. Salesse-Smith, C. E. *et al.* Overexpression of Rubisco subunits with RAF1 increases Rubisco content in maize. *Nature Plants* **4,** 802–810 (2018).

56. Parry, M. A. *et al.* Rubisco activity and regulation as targets for crop improvement. *Journal of Experimental Botany* **64,** 717–730 (2013).

57. Lefebvre, S., Lawson, T., Zakhleniuk, O. V., Lloyd, J. C. & Raines, C. A. Increased sedoheptulose-1,7-bisphosphatase activity in transgenic tobacco plants stimulates photosynthesis and growth from an early stage in development. *Plant Physiology* **138,** 451–460 (2005).

58. Rosenthal, D. M. *et al.* Over-expressing the C_3 photosynthesis cycle enzyme Sedoheptulose-1-7 Bisphosphatase improves photosynthetic carbon gain and yield under fully open air CO_2 fumigation (FACE). *BMC Plant Biology* **11,** 123–135 (2011).

59. Simkin, A. J. *et al.* Simultaneous stimulation of the SBPase, FBP aldolase and the photorespiratory GDC-H protein increases CO_2 assimilation, vegetative biomass and seed yield in Arabidopsis. *Plant Biotechnology Journal* **15,** 805–816 (2016).

60. Price, G. D., Badger, M. R. & von Caemmerer, S. The prospect of using cyanobacterial bicarbonate transporters to improve leaf photosynthesis in C_3 crop plants. *Plant Physiology* **155,** 20–6 (2011).

61. Price, G. D. *et al.* The cyanobacterial CCM as a source of genes for improving photosynthetic CO_2 fixation in crop species. *Journal of Experimental Botany* **64,** 753–768 (2013).

62. McGrath, J. M. & Long, S. P. Can the cyanobacterial carbon-concentrating mechanism increase photosynthesis in crop species? A theoretical analysis. *Plant Physiology* **164,** 2247–2261 (2014).

63. Hay, W. T. *et al.* Enhancing soybean photosynthetic CO_2 assimilation using a cyanobacterial membrane protein, ictB. *Plant Physiology* **212,** 58–68 (2017).

64. Rae, B. D. *et al.* Progress and challenges of engineering a biophysical carbon dioxide-concentrating mechanism into higher plants. *Journal of Experimental Botany* **68,** 3717–3737 (2017).

65. Atkinson, N., Mao, Y., Chan, K. X. & McCormick, A. J. Condensation of Rubisco into a proto-pyrenoid in higher plant chloroplasts. *Nature Communications* **11,** 6303 (2020).

66. Kromdijk, J. *et al.* Improving photosynthesis and crop productivity by accelerating recovery from photoprotection. *Science* **354,** 857–861 (2016).

67. Kebeish, R. *et al.* Chloroplastic photorespiratory bypass increases photosynthesis and biomass production in *Arabidopsis thaliana*. *Nature Biotechnology* **25,** 593–599 (2007).

68. Carvalho, J. F. *et al.* An engineered pathway for glyoxylate metabolism in tobacco plants aimed to avoid the release of ammonia in photorespiration. *BMC Biotechnology* **11,** 111–128 (2011).

69. Maier, A. *et al.* Transgenic introduction of a glycolate oxidative cycle into *A. thaliana* chloroplasts leads to growth improvement. *Frontiers in Plant Science* **3,** 1–12 (2012).

70. Dalal, J. *et al.* A photorespiratory bypass increases plant growth and seed yield in biofuel crop *Camelina sativa*. *Biotechnology for Biofuels* **8,** 175–197 (2015).

71. López-Calcagno, P. E. *et al.* Overexpressing the H-protein of the glycine cleavage system increases biomass yield in glasshouse and field-grown transgenic tobacco plants. *Plant Biotechnology Journal* **17,** 141–151 (2019).

72. Ainsworth, E. A. & Bush, D. R. Carbohydrate export from the leaf: A highly regulated process and target to enhance photosynthesis and productivity. *Plant Physiology* **155,** 64–69 (2011).

73. Langdale, J. A. C_4 Cycles: Past, present, and future research on C_4 photosynthesis. *Plant Cell* **23,** 3879–3892 (2011).

74. Wang, P. *et al.* Re-creation of a key step in the evolutionary switch from C_3 to C_4 leaf anatomy. *Current Biology* **27,** 3278–3287 (2017).

75. Allen, J. F., de Paula, W. B., Puthiyaveetil, S. & Nield, J. A structural phylogenetic map for chloroplast photosynthesis. *Trends in Plant Science* **16,** 645–655 (2011).

76. Chida, H. *et al.* Expression of the algal cytochrome c_6 gene in Arabidopsis enhances photosynthesis and growth. *Plant and Cell Physiology* **48,** 948–957 (2007).

77. Kerfeld, C. A. & Krogmann, D. W. Photosynthetic cytochromes *c* in cyanobacteria, algae, and plants. *Annual Review of Plant Physiology and Plant Molecular Biology* **49,** 397–425 (1998).

78. Yadav, S. K., Khatri, K., Rathore, M. S. & Jha, B. Introgression of *UfCyt* c_6, a thylakoid lumen protein from a green seaweed *Ulva fasciata* Delile enhanced photosynthesis and growth in tobacco. *Molecular Biology Reports* **45,** 1745–1758 (2018).

79. Kirchhoff, H., Horstmann, S. & Weis, E. Control of the photosynthetic electron transport by PQ diffusion microdomains in thylakoids of higher plants. *Biochimica et Biophysica Acta - Bioenergetics* **1459,** 148–168 (2000).

80. Price, G. D. *et al.* Photosynthesis is strongly reduced by antisense suppression of chloroplastic cytochrome bf complex in transgenic tobacco. *Australian Journal of Plant Physiology* **25,** 445–452 (1998).

81. Ruuska, S. A., Andrews, T. J., Badger, M. R., Price, G. D. & Von Caemmerer, S. The role of chloroplast electron transport and metabolites in modulating Rubisco activity in tobacco. Insights from transgenic plants with reduced amounts of cytochrome *b/f* complex or glyceraldehyde 3-phosphate dehydrogenase. *Plant Physiology* **122,** 491–504 (2000).

82. Yamori, W. *et al.* Enhanced leaf photosynthesis as a target to increase grain yield: Insights from transgenic rice lines with variable Rieske FeS protein content in the cytochrome b_6/f complex. *Plant, Cell & Environment* **39,** 80–87 (2016).

83. Raines, C. A. The Calvin cycle revisited. *Photosynthesis Research* **75,** 1–10 (2003).

84. Tang, K. *et al.* Transgenic rice plants expressing the ferredoxin-like protein (AP1) from sweet pepper show enhanced resistance to *Xanthomonas oryzae* pv. *oryzae*. *Plant Science* **160,** 1035–1042 (2001).

85. Namukwaya, B. *et al.* Transgenic banana expressing *Pflp* gene confers enhanced resistance to Xanthomonas wilt disease. *Transgenic Research* **21,** 855–865 (2012).

86. Ger, M. J., Louh, G. Y., Lin, Y. H., Feng, T. Y. & Huang, H. E. Ectopically expressed sweet pepper ferredoxin PFLP enhances disease resistance to *Pectobacterium carotovorum* subsp. *carotovorum* affected by harpin and protease-mediated hypersensitive response in Arabidopsis. *Molecular Plant Pathology* **15,** 892–906 (2014).

87. Stitt, M., Sulpice, R. & Keurentjes, J. Metabolic networks: How to identify key components in the regulation of metabolism and growth. *Plant Physiology* **152,** 428–444 (2010).

88. Forrester, M. L., Krotkov, G. & Nelson, C. D. Effect of oxygen on photosynthesis, photorespiration and respiration in detached leaves. I. Soybean. *Plant Physiology* **41,** 422–427 (1966).

89. Ogren, W. L. & Bowes, G. Ribulose diphosphate carboxylase regulates soybean photorespiration. *Nature New Biology* **230,** 159–160 (1971).

90. Evans J.R. & Seemann J.R. The allocation of protein nitrogen in the photosynthetic apparatus: costs, consquences, and control. *Plant Biology* **8,** 183–205 (1989).

91. Raven, J. A. Rubisco: Still the most abundant protein of Earth? *New Phytologist* **198,** 1–3 (2013).

92. Carmo-Silva, E., Scales, J. C., Madgwick, P. J. & Parry, M. A. Optimizing Rubisco and its regulation for greater resource use efficiency. *Plant, Cell & Environment* **38,** 1817–1832 (2015).

93. Parry, M. A., Madgwick, P. J., Carvalho, J. F. & Andralojc, P. J. Prospects for increasing photosynthesis by overcoming the limitations of Rubisco. *Journal of Agricultural Science* **145,** 31–43 (2007).

94. Stitt, M. & Schulze, D. Does Rubisco control the rate of photosynthesis and plant growth? An exercise in molecular ecophysiology. *Plant, Cell & Environment* **17,** 465–487 (1994).

95. Zhu, X. G., De Sturler, E. & Long, S. P. Optimizing the distribution of resources between enzymes of carbon metabolism can dramatically increase photosynthetic rate: A numerical simulation using an evolutionary algorithm. *Plant Physiology* **145,** 513–526 (2007).

96. Yoon, D.-K. *et al.* Transgenic rice overproducing Rubisco exhibits increased yields with improved nitrogen-use efficiency in an experimental paddy field. *Nature Food* **1,** 134–139 (2020).

97. Miyagawa, Y., Tamoi, M. & Shigeoka, S. Overexpression of a cyanobacterial fructose-1,6-/sedoheptulose-1,7-bisphosphatase in tobacco enhances photosynthesis and growth. *Nature Biotechnology* **19,** 965–969 (2001).

98. Uematsu, K., Suzuki, N., Iwamae, T., Inui, M. & Yukawa, H. Increased fructose 1,6-bisphosphate aldolase in plastids enhances growth and photosynthesis of tobacco plants. *Journal of Experimental Botany* **63,** 3001–3009 (2012).

99. Driever, S. M. *et al.* Increased SBPase activity improves photosynthesis and grain yield in wheat grown in greenhouse conditions. *Philosophical Transactions of the Royal Society B: Biological Sciences* **372,** 20160384 (2017).

100. Simkin, A. J., McAusland, L., Headland, L. R., Lawson, T. & Raines, C. A. Multigene manipulation of photosynthetic carbon assimilation increases CO_2 fixation and biomass yield in tobacco. *Journal of Experimental Botany* **66,** 4075–4090 (2015).

101. Lieman-Hurwitz, J., Rachmilevitch, S., Mittler, R., Marcus, Y. & Kaplan, A. Enhanced photosynthesis and growth of transgenic plants that express *ictB*, a gene involved in HCO_3^- accumulation in cyanobacteria. *Plant Biotechnology Journal* **1,** 43–50 (2003).

102. Gong, H. Y. *et al.* Transgenic rice expressing *Ictb* and *FBP/Sbpase* derived from cyanobacteria exhibits enhanced photosynthesis and mesophyll conductance to CO_2. *PLoS ONE* **10,** e0140928 (2015).

103. Bonfil, D. J. *et al.* A putative HCO_3^- transporter in the cyanobacterium *Synechococcus* sp. strain PCC 7942. *FEBS letters* **430,** 236–240 (1998).

104. Xu, H. *et al.* Inducible antisense suppression of glycolate oxidase reveals its strong regulation over photosynthesis in rice. *Journal of Experimental Botany* **60,** 1799–1809 (2009).

105. Khozaei, M. *et al.* Overexpression of plastid transketolase in tobacco results in a thiamine auxotrophic phenotype. *Plant Cell* **27,** 432–447 (2015).

106. Peterhansel, C. *et al.* Photorespiration. *The Arabidopsis Book* **8,** e0130 (2010).

107. Fernie, A. R. *et al.* Perspectives on plant photorespiratory metabolism. *Plant Biology* **15,** 748–753 (2013).

108. Busch, F. A. Photorespiration in the context of Rubisco biochemistry, CO_2 diffusion and metabolism. *The Plant Journal* **101,** 919–939 (2020).

109. Timm, S. & Bauwe, H. The variety of photorespiratory phenotypes - employing the current status for future research directions on photorespiration. *Plant Biology* **15,** 737–747 (2013).

110. Walker, B. J., VanLoocke, A., Bernacchi, C. J. & Ort, D. R. The costs of photorespiration to food production now and in the future. *Annual Review of Plant Biology* **67,** 107–129 (2016).

111. Betti, M. *et al.* Manipulating photorespiration to increase plant productivity: Recent advances and perspectives for crop improvement. *Journal of Experimental Botany* **67,** 2977–2988 (2016).

112. Timm, S. *et al.* Glycine decarboxylase controls photosynthesis and plant growth. *FEBS Letters* **586,** 3692–3697 (2012).

113. Timm, S. *et al.* Mitochondrial dihydrolipoyl dehydrogenase activity shapes photosynthesis and photorespiration of *Arabidopsis thaliana*. *Plant Cell* **27,** 1968–84 (2015).

114. Häusler, R. E. *et al.* Control of carbon partitioning and photosynthesis by the triose phosphate/phosphate translocator in transgenic tobacco plants (*Nicotiana tabacum* L.). I. Comparative physiological analysis of tobacco plants with antisense repression and overexpression of the triose phosphate/phosphate translocator. *Planta* **210,** 371–382 (2000).

115. Stitt, M., Lunn, J. & Usadel, B. Arabidopsis and primary photosynthetic metabolism — more than the icing on the cake. *The Plant Journal* **61,** 1067–1091 (2010).

116. Cho, M. H., Jang, A., Bhoo, S. H., Jeon, J. S. & Hahn, T. R. Manipulation of triose phosphate/phosphate translocator and cytosolic fructose-1,6-bisphosphatase, the key components in photosynthetic sucrose synthesis, enhances the source capacity of transgenic *Arabidopsis* plants. *Photosynthesis Research* **111,** 261–268 (2012).

117. Schlosser, A. J., Martin, J. M., Beecher, B. S. & Giroux, M. J. Enhanced rice growth is conferred by increased leaf ADP-glucose pyrophosphorylase activity. *Journal of Plant Physiology and Pathology* **2,** 1–10 (2014).

118. Jonik, C., Sonnewald, U., Hajirezaei, M. R., Flügge, U. I. & Ludewig, F. Simultaneous boosting of source and sink capacities doubles tuber starch yield of potato plants. *Plant Biotechnology Journal* **10,** 1088–1098 (2012).

119. Chen, L. Q. *et al.* Sucrose efflux mediated by SWEET proteins as a key step for phloem transport. *Science* **335,** 207–211 (2012).

120. Sauer, N. & Stolz, J. SUC1 and SUC2: two sucrose transporters from *Arabidopsis thaliana*; expression and characterization in baker's yeast and identification of the histidine-tagged protein. *The Plant Journal* **6,** 67–77 (1994).

121. Gottwald, J. R., Krysan, P. J., Young, J. C., Evert, R. F. & Sussman, M. R. Genetic evidence for the *in planta* role of phloem-specific plasma membrane sucrose transporters. *Proceedings of the National Academy of Sciences of the United States of America* **97,** 13979–13984 (2000).

122. Srivastava, A. C., Ganesan, S., Ismail, I. O. & Ayre, B. G. Functional characterization of the Arabidopsis AtSUC2 sucrose/H^+ symporter by tissue-specific complementation reveals an essential role in phloem loading but not in long-distance transport. *Plant Physiology* **148,** 200–211 (2008).

123. Dasgupta, K. *et al.* Expression of sucrose transporter cDNAs specifically in companion cells enhances phloem loading and long-distance transport of sucrose but leads to an inhibition of growth and the perception of a phosphate limitation. *Plant Physiology* **165,** 715–731 (2014).

124. Trethewey, R. N. Metabolite profiling as an aid to metabolic engineering in plants. *Current Opinion in Plant Biology* **7,** 196–201 (2004).

125. Sweetlove, L. J., Nielsen, J. & Fernie, A. R. Engineering central metabolism — a grand challenge for plant biologists. *The Plant Journal* **90,** 749–763 (2017).

126. Kacser, H. & Burns, J. A. The control of flux. *Biochemical Society Transactions* **23,** 341–366 (1973).

127. Fell, D. A. Metabolic control analysis: A survey of its theoretical and experimental development. *Biochemical Journal* **286,** 313–330 (1992).

128. Fell, D. A. & Thomas, S. Physiological control of metabolic flux: the requirement for multisite modulation. *Biochemical Journal* **311,** 35–39 (1995).

129. Morandini, P. Control limits for accumulation of plant metabolites: Brute force is no substitute for understanding. *Plant Biotechnology Journal* **11,** 253–267 (2013).

130. Farré, G. *et al.* Engineering complex metabolic pathways in plants. *Annual Review of Plant Biology* **65,** 187–223 (2014).

131. Baghalian, K., Hajirezaei, M. & Schreiber, F. Plant metabolic modeling: Achieving new insight into metabolism and metabolic engineering. *Plant Cell* **26,** 3847–3866 (2014).

132. Small, J. R. & Kacser, H. Responses of metabolic systems to large changes in enzyme activities and effectors: 1. The linear treatment of unbranched chains. *European Journal of Biochemistry* **213,** 613–624 (1993).

133. Evans, J. R. Improving photosynthesis. *Plant Physiology* **162,** 1780–1793 (2013).

134. Shehryar, K. *et al.* Transgene stacking as effective tool for enhanced disease resistance in plants. *Molecular Biotechnology* **62,** 1–7 (2020).

135. Samis, K., Bowley, S. & McKersie, B. Pyramiding Mn-superoxide dismutase transgenes to improve persistence and biomass production in alfalfa. *Journal of Experimental Botany* **53,** 1343–1350 (2002).

136. International Service for the Acquisition of Agri-biotech Applications. *Global Status of Commercialized Biotech/GM Crops: 2018 - ISAAA Brief 54-2018* tech. rep. (2020).

137. Bock, R. Strategies for metabolic pathway engineering with multiple transgenes. *Plant Molecular Biology* **83,** 21–31 (2013).

138. Halpin, C., Barakate, A., Askari, B. M., Abbott, J. C. & Ryan, M. D. Enabling technologies for manipulating multiple genes on complex pathways. *Plant Molecular Biology* **47,** 295–310 (2001).

139. Naqvi, S. *et al.* When more is better: multigene engineering in plants. *Trends in Plant Science* **15,** 48–56 (2010).

140. Dafny-Yelin, M. & Tzfira, T. Delivery of multiple transgenes to plant cells. *Plant Physiology* **145,** 1118–1128 (2007).

141. Engler, C., Kandzia, R. & Marillonnet, S. A one pot, one step, precision cloning method with high throughput capability. *PLoS ONE* **3,** e3647 (2008).

142. Weber, E., Engler, C., Gruetzner, R., Werner, S. & Marillonnet, S. A modular cloning system for standardized assembly of multigene constructs. *PLoS ONE* **6,** e16765 (2011).

143. Engler, C. & Marillonnet, S. Combinatorial DNA assembly using Golden Gate cloning. *Methods in Molecular Biology* **1073,** 141–156 (2013).

144. Engler, C. *et al.* A Golden Gate modular cloning toolbox for plants. *ACS Synthetic Biology* **3,** 839–843 (2014).

145. Hadi, M. Z., McMullen, M. D. & Finer, J. J. Transformation of 12 different plasmids into soybean via particle bombardment. *Plant Cell Reports* **15,** 500–505 (1996).

146. Chen, L. *et al.* Expression and inheritance of multiple transgenes in rice plants. *Nature Biotechnology* **16,** 1060–1064 (1998).

147. Naqvi, S. *et al.* Transgenic multivitamin corn through biofortification of endosperm with three vitamins representing three distinct metabolic pathways. *Proceedings of the National Academy of Sciences of the United States of America* **106,** 7762–7767 (2009).

148. Fuentes, P. *et al.* A new synthetic biology approach allows transfer of an entire metabolic pathway from a medicinal plant to a biomass crop. *eLife* **5,** e13664 (2016).

149. Christou, P., Murphy, J. E. & Swain, W. F. Stable transformation of soybean by electroporation and root formation from transformed callus. *Proceedings of the National Academy of Sciences* **84,** 3962–3966 (1987).

150. Christou, P., Swain, W. F., Yang, N. S. & McCabe, D. E. Inheritance and expression of foreign genes in transgenic soybean plants. *Proceedings of the National Academy of Sciences* **86,** 7500–7504 (1989).

151. Christou, P., Ford, T. L. & Kofron, M. Production of transgenic rice (*Oryza sativa* L.) plants from agronomically important indica and japonica varieties via electric discharge particle acceleration of exogenous DNA into immature zygotic embryos. *Nature Biotechnology* **9,** 957–962 (1991).

152. Christou, P. & Swain, W. F. Cotransformation frequencies of foreign genes in soybean cell cultures. *Theoretical and Applied Genetics* **79,** 337–341 (1990).

153. Li, L., Qu, R., de Kochko, A., Fauquet, C. & Beachy, R. N. An improved rice transformation system using the biolistic method. *Plant Cell Reports* **12,** 250–255 (1993).

154. Qu, R. *et al.* Analysis of a large number of independent transgenic rice plants produced by the biolistic method. *In Vitro Cellular and Developmental Biology - Plant* **32,** 233–240 (1996).

155. Kohli, A., Leech, M., Vain, P., Laurie, D. A. & Christou, P. Transgene organization in rice engineered through direct DNA transfer supports a two-phase integration mechanism mediated by the establishment of integration hot spots. *Proceedings of the National Academy of Sciences of the United States of America* **95,** 7203–7208 (1998).

156. Gelvin, S. B. Multigene plant transformation: More is better! *Nature Biotechnology* **16,** 1009–1010 (1998).

157. Baxter, I. We aren't good at picking candidate genes, and it's slowing us down. *Current Opinion in Plant Biology* **54,** 57–60 (2020).

158. Li, L. *et al.* Combinatorial modification of multiple lignin traits in trees through multigene cotransformation. *Proceedings of the National Academy of Sciences of the United States of America* **100,** 4939–4944 (2003).

159. Vallarino, J. G. *et al.* Multi-gene metabolic engineering of tomato plants results in increased fruit yield up to 23%. *Scientific Reports* **10,** 17219 (2020).

160. Zhu, C. *et al.* Combinatorial genetic transformation generates a library of metabolic phenotypes for the carotenoid pathway in maize. *Proceedings of the National Academy of Sciences of the United States of America* **105,** 18232–18237 (2008).

161. Sonnewald, U. & Fernie, A. R. Next-generation strategies for understanding and influencing source–sink relations in crop plants. *Current Opinion in Plant Biology* **43,** 63–70 (2018).

162. Clark, T. J., Guo, L., Morgan, J. & Schwender, J. Modeling plant metabolism: From network reconstruction to mechanistic models. *Annual Review of Plant Biology* **71,** 303–326 (2020).

163. Farquhar, G. D., Von Caemmerer, S. & Berry, J. A. Models of photosynthesis. *Plant Physiology* **125,** 42–45 (2001).

164. Pettersson, G. & Ryde-Pettersson, U. A mathematical model of the Calvin photosynthesis cycle. *European Journal of Biochemistry* **175,** 661–672 (1988).

165. Woodrow, I. E. Control of the rate of photosynthetic carbon dioxide fixation. *Biochimica et Biophysica Acta - Bioenergetics* **851,** 181–192 (1986).

166. Sage, R. F. A model describing the regulation of ribulose-1,5-bisphosphate carboxylase, electron transport, and triose phosphate use in response to light intensity and CO_2 in C_3 plants. *Plant Physiology* **94,** 1728–1734 (1990).

167. Poolman, M. G., Fell, D. A. & Thomas, S. Modelling photosynthesis and its control. *Journal of Experimental Botany* **51,** 319–328 (2000).

168. Zhu, X. G., Wang, Y., Ort, D. R. & Long, S. P. e-photosynthesis: A comprehensive dynamic mechanistic model of C_3 photosynthesis: From light capture to sucrose synthesis. *Plant, Cell & Environment* **36,** 1711–1727 (2013).

169. Niklas, J., Schneider, K. & Heinzle, E. Metabolic flux analysis in eukaryotes. *Current Opinion in Biotechnology* **21,** 63–69 (2010).

170. Kruger, N. J. & Ratcliffe, R. G. Fluxes through plant metabolic networks: Measurements, predictions, insights and challenges. *Biochemical Journal* **465,** 27–38 (2015).

171. Sweetlove, L. J. & George Ratcliffe, R. Flux-balance modeling of plant metabolism. *Frontiers in Plant Science* **2,** 38 (2011).

172. Stalidzans, E., Seiman, A., Peebo, K., Komasilovs, V. & Pentjuss, A. Model-based metabolism design: Constraints for kinetic and stoichiometric models. **46,** 261–267 (2018).

173. Cheung, C. Y. M. *Genome scale metabolic models of plant tissues.* PhD thesis (University of Oxford, 2013), 15–16.

174. Poolman, M. G., Miguet, L., Sweetlove, L. J. & Fell, D. A. A genome-scale metabolic model of Arabidopsis and some of its properties. *Plant Physiology* **151,** 1570–1581 (2009).

175. Dal'Molin, C. G. O., Quek, L. E., Palfreyman, R. W., Brumbley, S. M. & Nielsen, L. K. AraGEM, a genome-scale reconstruction of the primary metabolic network in Arabidopsis. *Plant Physiology* **152,** 579–589 (2010).

176. Mintz-Oron, S. *et al.* Reconstruction of Arabidopsis metabolic network models accounting for subcellular compartmentalization and tissue-specificity. *Proceedings of the National Academy of Sciences of the United States of America* **109,** 339–344 (2012).

177. Saha, R., Suthers, P. F. & Maranas, C. D. *Zea mays* iRS1563: A comprehensive genome-scale metabolic reconstruction of maize metabolism. *PLoS ONE* **6,** e21784 (2011).

178. Grafahrend-Belau, E. *et al.* Multiscale metabolic modeling: dynamic flux balance analysis on a whole-plant scale. *Plant Physiology* **163,** 637–647 (2013).

179. Cheung, C. Y. M., Poolman, M. G., Fell, D. A., Ratcliffe, R. G. & Sweetlove, L. J. A diel flux balance model captures interactions between light and dark metabolism during day-night cycles in C_3 and crassulacean acid metabolism leaves. *Plant Physiology* **165,** 917–929 (2014).

180. Cheung, C. M., Ratcliffe, R. G. & Sweetlove, L. J. A method of accounting for enzyme costs in flux balance analysis reveals alternative pathways and metabolite stores in an illuminated Arabidopsis leaf. *Plant Physiology* **169,** 1671–1682 (2015).

181. Shameer, S., Baghalian, K., Cheung, C. Y. M., Ratcliffe, R. G. & Sweetlove, L. J. Computational analysis of the productivity potential of CAM. *Nature Plants* **4,** 165–171 (2018).

182. Shameer, S., Ratcliffe, R. G. & Sweetlove, L. J. Leaf energy balance requires mitochondrial respiration and export of chloroplast NADPH in the light. *Plant Physiology* **180,** 1947–1961 (2019).

183. Kromer, S. Respiration during photosynthesis. *Annual Review of Plant Physiology and Plant Molecular Biology* **46,** 45–70 (1995).

184. Hoefnagel, M. H., Atkin, O. K. & Wiskich, J. T. Interdependence between chloroplasts and mitochondria in the light and the dark. *Biochimica et Biophysica Acta - Bioenergetics* **1366,** 235–255 (1998).

185. Selinski, J. & Scheibe, R. Malate valves: old shuttles with new perspectives. *Plant Biology* **21,** 21–30 (2019).

186. Bauwe, H., Hagemann, M. & Fernie, A. R. Photorespiration: players, partners and origin. *Trends in Plant Science* **15,** 330–336 (2010).

187. Lindén, P., Keech, O., Stenlund, H., Gardeström, P. & Moritz, T. Reduced mitochondrial malate dehydrogenase activity has a strong effect on photorespiratory metabolism as revealed by ^{13}C labelling. *Journal of Experimental Botany* **67,** 3123–3135 (2016).

188. Kinoshita, H. *et al.* The chloroplastic 2-oxoglutarate/malate transporter has dual function as the malate valve and in carbon/nitrogen metabolism. *The Plant Journal* **65,** 15–26 (2011).

189. Noguchi, K. & Yoshida, K. Interaction between photosynthesis and respiration in illuminated leaves. *Mitochondrion* **8,** 87–99 (2008).

190. Taniguchi, M. *et al.* Identifying and characterizing plastidic 2-oxoglutarate/malate and dicarboxylate transporters in *Arabidopsis thaliana*. *Plant and Cell Physiology* **43,** 706–717 (2002).

191. Kramer, D. M. & Evans, J. R. The importance of energy balance in improving photosynthetic productivity. *Plant Physiology* **155,** 70–78 (2011).

192. Bailleul, B. *et al.* Energetic coupling between plastids and mitochondria drives CO_2 assimilation in diatoms. *Nature* **524,** 366–369 (2015).

193. Sambrook, J., Fritsch, E. F. & Maniatis, T. *Molecular Cloning: A Laboratory Manual, Second Edition* (1989).

194. Hanahan, D. Studies on transformation of *Escherichia coli* with plasmids. *Journal of Molecular Biology* **166,** 557–580 (1983).

195. Green, M. R. & Sambrook, J. The Hanahan method for preparation and transformation of competent *Escherichia coli*: High-efficiency transformation. *Cold Spring Harbor Protocols* **2018,** 183–190 (2018).

196. Weigel, D. & Glazebrook, J. Transformation of *Agrobacterium* using the freeze-thaw method. *Cold Spring Harbor Protocols* **2006,** pdb.prot4666 (2006).

197. NCBI Resource Coordinators. Database Resources of the National Center for Biotechnology Information. *Nucleic Acids Research* **45,** D12–D17 (2017).

198. Hung, Y. P., Albeck, J. G., Tantama, M. & Yellen, G. Imaging cytosolic NADH-NAD^+ redox state with a genetically encoded fluorescent biosensor. *Cell Metabolism* **14,** 545–554 (2011).

199. Berardini, T. Z. *et al.* The Arabidopsis information resource: Making and mining the "gold standard" annotated reference plant genome. *Genesis* **53,** 474–485 (2015).

200. Sierro, N. *et al.* The tobacco genome sequence and its comparison with those of tomato and potato. *Nature Communications* **5,** 3833 (2014).

201. Fernandez-Pozo, N. *et al.* The Sol Genomics Network (SGN)-from genotype to phenotype to breeding. *Nucleic Acids Research* **43,** D1036–D1041 (2015).

202. Karimi, M., Inzé, D. & Depicker, A. GATEWAY™ vectors for *Agrobacterium*-mediated plant transformation. *Trends in Plant Science* **7,** 193–195 (2002).

203. Doyle, J. & Doyle, J. DNA isolation from small amount of plant tissue. *Phytochemical Bulletin* **19,** 11–15 (1991).

204. Schmidt, G. W. & Delaney, S. K. Stable internal reference genes for normalization of real-time RT-PCR in tobacco (*Nicotiana tabacum*) during development and abiotic stress. *Molecular Genetics and Genomics* **283,** 233–241 (2010).

205. Pfaffl, M. W. A new mathematical model for relative quantification in real-time RT-PCR. *Nucleic Acids Research* **29,** 2003–2007 (2001).

206. Sievers, F. *et al.* Fast, scalable generation of high-quality protein multiple sequence alignments using Clustal Omega. *Molecular Systems Biology* **7,** 539–539 (2014).

207. Katoh, K. & Standley, D. M. MAFFT multiple sequence alignment software version 7: Improvements in performance and usability. *Molecular Biology and Evolution* **30,** 772–780 (2013).

208. Brown, N. P., Leroy, C. & Sander, C. MView: A web-compatible database search or multiple alignment viewer. *Bioinformatics* **14,** 380–381 (1998).

209. Elghabi, Z., Ruf, S. & Bock, R. Biolistic co-transformation of the nuclear and plastid genomes. *The Plant Journal* **67,** 941–948 (2011).

210. Clough, S. J. & Bent, A. F. Floral dip: A simplified method for *Agrobacterium*-mediated transformation of *Arabidopsis thaliana*. *The Plant Journal* **16,** 735–743 (1998).

211. Horsch, R. B. *et al.* Inheritance of functional genes in plants. *Science* **223,** 496–498 (1984).

212. Kuhlgert, S. *et al.* MultispeQ Beta: A tool for large-scale plant phenotyping connected to the open photosynQ network. *Royal Society Open Science* **3,** 160592 (2016).

213. Stirbet, A. & Govindjee. On the relation between the Kautsky effect (chlorophyll *a* fluorescence induction) and Photosystem II: Basics and applications of the OJIP fluorescence transient. *Journal of Photochemistry and Photobiology B: Biology* **104,** 236–257 (2011).

214. Strasser, R. J., Srivastava, A. & Tsimilli-Michael, M. in *Probing Photosynthesis: Mechanism, Regulation and Adaptation* (eds Yunus, M., Pathre, U. & Mohanty, P.) 445–483 (Taylor & Francis, 2000).

215. Porra, R. J., Thompson, W. A. & Kriedemann, P. E. Determination of accurate extinction coefficients and simultaneous equations for assaying chlorophylls *a* and *b* extracted with four different solvents: verification of the concentration of chlorophyll standards by atomic absorption spectroscopy. *Biochimica et Biophysica Acta - Bioenergetics* **975,** 384–394 (1989).

216. Palikaras, K. & Tavernarakis, N. Measuring oxygen consumption rate in *Caenorhabditis elegans*. *Bio Protocol* **6,** e2049 (2016).

217. O'Leary, B. M. *et al.* Variation in leaf respiration rates at night correlates with carbohydrate and amino acid supply. *Plant Physiology* **174,** 2261–2273 (2017).

218. Sew, Y. S., Harvey Millar, A. & Stroeher, E. in *Plant Mitochondria: Methods and Protocols* 187–196 (Springer, 2015).

219. Sew, Y. S. *et al.* Multiplex micro-respiratory measurements of Arabidopsis tissues. *New Phytologist* **200,** 922–932 (2013).

220. Wagner, S. *et al.* Multiparametric real-time sensing of cytosolic physiology links hypoxia responses to mitochondrial electron transport. *New Phytologist* **224,** 1668–1684 (2019).

221. Steinbeck, J. *et al.* In vivo NADH/NAD^+ biosensing reveals the dynamics of cytosolic redox metabolism in plants. *Plant Cell* **32,** 3324–3345 (2020).

222. Osorio, S., Do, T. & Fernie, A. R. Profiling primary metabolites of tomato fruit with gas chromatography/mass spectrometry. *Methods in Molecular Biology* **860,** 101–109.

223. Luedemann, A., Strassburg, K., Erban, A. & Kopka, J. TagFinder for the quantitative analysis of gas chromatography-mass spectrometry (GC-MS)-based metabolite profiling experiments. *Bioinformatics* **24,** 732–737 (2008).

224. Kopka, J. *et al.* GMD@CSB.DB: the Golm Metabolome Database. *Bioinformatics* **21,** 1635–1638 (2005).

225. R Core Team. *R: A Language and Environment for Statistical Computing* R Foundation for Statistical Computing (Vienna, Austria, 2017).

226. RStudio Team. *RStudio: Integrated Development Environment for R.* RStudio, PBC. (Boston, MA, 2020).

227. Horsch, R. B. *et al.* A simple and general method for transferring genes into plants. *Science* **227,** 1229–1230 (1985).

228. Yang, S.-M. *et al.* in *Photosynthesis. Energy from the Sun* (eds Allen, J., Gantt, E., Golbeck, J. & Osmond, B.) 1243–1246 (Springer, 2008).

229. Sonnewald, U. Expression of *E. coli* inorganic pyrophosphatase in transgenic plants alters photoassimilate partitioning. *The Plant Journal* **2,** 571–581 (1992).

230. Fladung, M., Ballvora, A. & Schmülling, T. Constitutive or light-regulated expression of the *rolC* gene in transgenic potato plants has different effects on yield attributes and tuber carbohydrate composition. *Plant Molecular Biology* **23,** 749–757 (1993).

231. Lloyd, J. C., Raines, C. A., John, U. P. & Dyer, T. A. The chloroplast FBPase gene of wheat: structure and expression of the promoter in photosynthetic and meristematic cells of transgenic tobacco plants. *Molecular and General Genetics* **225,** 209–216 (1991).

232. Matsuda, Y. *et al.* The Commelina yellow mottle virus promoter drives companion-cell-specific gene expression in multiple organs of transgenic tobacco. *Protoplasma* **220,** 51–58 (2002).

233. Medberry, S. L., Lockhart, B. E. & Olszewski, N. E. The Commelina yellow mottle virus promoter is a strong promoter in vascular and reproductive tissues. *Plant Cell* **4,** 185–192 (1992).

234. Huang, W., Zhang, S. B. & Hu, H. Sun leaves up-regulate the photorespiratory pathway to maintain a high rate of CO_2 assimilation in tobacco. *Frontiers in Plant Science* **5,** 688 (2014).

235. Baroli, I., Price, G. D., Badger, M. R. & Von Caemmerer, S. The contribution of photosynthesis to the red light response of stomatal conductance. *Plant Physiology* **146,** 737–747 (2008).

236. Srinivasan, V., Kumar, P. & Long, S. P. Decreasing, not increasing, leaf area will raise crop yields under global atmospheric change. *Global Change Biology* **23,** 1626–1635 (2017).

237. Yui, R., Iketani, S., Mikami, T. & Kubo, T. Antisense inhibition of mitochondrial pyruvate dehydrogenase E1α subunit in anther tapetum causes male sterility. *The Plant Journal* **34,** 57–66 (2003).

238. Agrawal, P. K., Kohli, A., Twyman, R. M. & Christou, P. Transformation of plants with multiple cassettes generates simple transgene integration patterns and high expression levels. *Molecular Breeding* **16,** 247–260 (2005).

239. Maqbool, S. B. & Christou, P. Multiple traits of agronomic importance in transgenic indica rice plants: Analysis of transgene integration patterns, expression levels and stability. *Molecular Breeding* **5,** 471–480 (1999).

240. Poorter, H., Bühler, J., Van Dusschoten, D., Climent, J. & Postma, J. A. Pot size matters: A meta-analysis of the effects of rooting volume on plant growth. *Functional Plant Biology* **39,** 839–850 (2012).

241. Poorter, H. *et al.* Pampered inside, pestered outside? Differences and similarities between plants growing in controlled conditions and in the field. *New Phytologist* **212,** 838–855 (2016).

242. White, A. C., Rogers, A., Rees, M. & Osborne, C. P. How can we make plants grow faster? A source-sink perspective on growth rate. *Journal of Experimental Botany* **67,** 31–45 (2016).

243. Tang, Y.-j. & Liesche, J. The molecular mechanism of shade avoidance in crops – How data from Arabidopsis can help to identify targets for increasing yield and biomass production. **16,** 1244–1255 (2017).

244. Zhu, X. G., Long, S. P. & Ort, D. R. What is the maximum efficiency with which photosynthesis can convert solar energy into biomass? *Current Opinion in Biotechnology* **19,** 153–159 (2008).

245. Kohli, A. *et al.* The quest to understand the basis and mechanisms that control expression of introduced transgenes in crop plants. *Plant Signaling & Behavior* **1,** 185–195 (2006).

246. Altpeter, F. *et al.* Particle bombardment and the genetic enhancement of crops: Myths and realities. *Molecular Breeding* **15,** 305–327 (2005).

247. Datta, K. *et al.* Bioengineered 'golden' indica rice cultivars with β-carotene metabolism in the endosperm with hygromycin and mannose selection systems. *Plant Biotechnology Journal* **1,** 81–90 (2003).

248. Kohli, A. *et al.* Transgene integration, organization and interaction in plants. *Plant Molecular Biology* **52,** 247–258. arXiv: `0005074v1 [astro-ph]` (2003).

249. Mehlo, L. *et al.* Structural analysis of transgene rearrangements and effects on expression in transgenic maize plants generated by particle bombardment. *Maydica* **45,** 277–287 (2000).

250. Kohli, A., Gahakwa, D., Vain, P., Laurie, D. A. & Christou, P. Transgene expression in rice engineered through particle bombardment: molecular factors controlling stable expression and transgene silencing. **208,** 88–97 (1999).

251. Kalaji, H. M. *et al.* Frequently asked questions about chlorophyll fluorescence, the sequel. *Photosynthesis Research* **132,** 13–66 (2017).

252. Peterhansel, C., Blume, C. & Offermann, S. Photorespiratory bypasses: how can they work? *Journal of Experimental Botany* **64,** 709–715 (2013).

253. Yin, Z., Plader, W. & Malepszy, S. Transgene inheritance in plants. *Journal of Applied Genetics* **45,** 127–144 (2004).

254. Sulpice, R. *et al.* Starch as a major integrator in the regulation of plant growth. *Proceedings of the National Academy of Sciences of the United States of America* **106,** 10348–10353 (2009).

255. Niittylä, T. *et al.* A previously unknown maltose transporter essential for starch degradation in leaves. *Science* **303,** 87–89 (2004).

256. Yu, T.-S. *et al.* The Arabidopsis sex1 mutant is defective in the R1 protein, a general regulator of starch degradation in plants, and not in the chloroplast hexose transporter. *The Plant Cell* **13,** 1907–1918 (2001).

257. Adams, W. W., Muller, O., Cohu, C. M. & Demmig-Adams, B. May photoinhibition be a consequence, rather than a cause, of limited plant productivity? *Photosynthesis Research* **117,** 31–44 (2013).

258. Paul, M. J. & Foyer, C. H. Sink regulation of photosynthesis. *Journal of Experimental Botany* **52,** 1383–1400 (2001).

259. Adams, W. W., Muller, O., Cohu, C. M. & Demmig-Adams, B. in *Non-Photochemical Quenching and Energy Dissipation in Plants, Algae and Cyanobacteria* (eds B., D.-A., G., G., W., A. I. & Govindjee) 503–529 (2014).

260. Nunes-Nesi, A., Fernie, A. R. & Stitt, M. Metabolic and signaling aspects underpinning the regulation of plant carbon nitrogen interactions. *Molecular Plant* **3,** 973–996 (2010).

261. Osmond, C. & Grace, S. Perspectives on photoinhibition and photorespiration in the field: quintessential inefficiencies of the light and dark reactions of photosynthesis? *Journal of Experimental Botany* **46,** 1351–1362 (1995).

262. Głowacka, K. *et al.* An evaluation of new and established methods to determine T-DNA copy number and homozygosity in transgenic plants. *Plant Cell & Environment* **39,** 908–917 (2016).

263. Ermakova, M., Lopez-Calcagno, P. E., Raines, C. A., Furbank, R. T. & von Caemmerer, S. Overexpression of the Rieske FeS protein of the cytochrome b6f complex increases C_4 photosynthesis in *Setaria viridis*. *Communications Biology* **2,** 314–326 (2019).

264. Dai, S. *et al.* Comparative analysis of transgenic rice plants obtained by *Agrobacterium*-mediated transformation and particle bombardment. *Molecular Breeding* **7,** 25–33 (2001).

265. Fernie, A. R. *et al.* Synchronization of developmental, molecular and metabolic aspects of source–sink interactions. *Nature Plants* **6,** 55–66 (2020).

266. Körner, C. Paradigm shift in plant growth control. *Current Opinion in Plant Biology* **25,** 107–114 (2015).

267. Ruiz-Vera, U. M., De Souza, A. P., Long, S. P. & Ort, D. R. The role of sink strength and nitrogen availability in the down-regulation of photosynthetic capacity in field-grown *Nicotiana tabacum* L. at elevated CO_2 concentration. *Frontiers in Plant Science* **8,** 998 (2017).

268. Tomaz, T. *et al.* Mitochondrial malate dehydrogenase lowers leaf respiration and alters photorespiration and plant growth in Arabidopsis. *Plant Physiology* **154,** 1143–1157 (2010).

269. Nunes-Nesi, A. *et al.* Enhanced photosynthetic performance and growth as a consequence of decreasing mitochondrial malate dehydrogenase activity in transgenic tomato plants. *Plant Physiology* **137,** 611–22 (2005).

270. Nunes-Nesi, A., Sulpice, R., Gibon, Y. & Fernie, A. R. The enigmatic contribution of mitochondrial function in photosynthesis. *Journal of Experimental Botany* **59,** 1675–1684 (2008).

271. Zhao, Y. *et al.* Malate transported from chloroplast to mitochondrion triggers production of ROS and PCD in *Arabidopsis thaliana*. *Cell Research* **28,** 448–461 (2018).

272. Fujimoto, M. *et al.* Arabidopsis dynamin-related proteins DRP3A and DRP3B are functionally redundant in mitochondrial fission, but have distinct roles in peroxisomal fission. *The Plant Journal* **58,** 388–400 (2009).

273. Zhang, X. C. & Hu, J. P. Two small protein families, DYNAMIN-RELATED PROTEIN3 and FISSION1, are required for peroxisome fission in Arabidopsis. *The Plant Journal* **57,** 146–159 (2009).

274. Zhang, X. C. & Hu, J. P. FISSION1A and FISSION1B proteins mediate the fission of peroxisomes and mitochondria in Arabidopsis. *Molecular Plant* **1,** 1036–1047 (2008).

275. Arimura, S. *et al.* Arabidopsis ELONGATED MITOCHONDRIA1 is required for localization of DYNAMIN-RELATED PROTEIN3A to mitochondrial fission sites. *Plant Cell* **20,** 1555–1566 (2008).

276. Aung, K. & Hu, J. Differential roles of Arabidopsis dynamin-related proteins DRP3A, DRP3B, and DRP5B in organelle division. *Journal of Integrative Plant Biology* **54,** 921–931 (2012).

277. Elgass, K., Pakay, J., Ryan, M. T. & Palmer, C. S. Recent advances into the understanding of mitochondrial fission. *Biochimica et Biophysica Acta - Molecular Cell Research* **1833,** 150–161 (2013).

278. Lingard, M. J. *et al.* Arabidopsis PEROXIN11c-e, FISSION1b, and DYNAMIN-RELATED PROTEIN3A cooperate in cell cycle-associated replication of peroxisomes. *Plant Cell* **20,** 1567–1585 (2008).

279. Scheibe, R. Malate valves to balance cellular energy supply. *Physiologia Plantarum* **120,** 21–26 (2004).

280. Taniguchi, M. & Miyake, H. Redox-shuttling between chloroplast and cytosol: Integration of intra-chloroplast and extra-chloroplast metabolism. *Current Opinion in Plant Biology* **15,** 252–260 (2012).

281. Rius, S. P., Casati, P., Iglesias, A. A. & Gomez-Casati, D. F. Characterization of an *Arabidopsis thaliana* mutant lacking a cytosolic non-phosphorylating glyceraldehyde-3-phosphate dehydrogenase. *Plant Molecular Biology* **61,** 945–957 (2006).

282. Hajirezaei, M. R. *et al.* The influence of cytosolic phosphorylating glyceraldehyde 3-phosphate dehydrogenase (GAPC) on potato tuber metabolism. *Journal of Experimental Botany* **57,** 2363–2377 (2006).

283. Muñoz-Bertomeu, J. *et al.* Plastidial glyceraldehyde-3-phosphate dehydrogenase deficiency leads to altered root development and affects the sugar and amino acid balance in Arabidopsis. *Plant Physiology* **151,** 541–558 (2009).

284. Guo, L. *et al.* Cytosolic glyceraldehyde-3-phosphate dehydrogenases interact with phospholipase D to transduce hydrogen peroxide signals in the Arabidopsis response to stress. *Plant Cell* **24,** 2200–2212 (2012).

285. Rius, S. P., Casati, P., Iglesias, A. A. & Gomez-Casati, D. F. Characterization of Arabidopsis lines deficient in GAPC-1, a cytosolic NAD-dependent glyceraldehyde-3-phosphate dehydrogenase. *Plant Physiology* **148,** 1655–1667 (2008).

286. Gardeström, P. & Igamberdiev, A. U. The origin of cytosolic ATP in photosynthetic cells. *Physiologia Plantarum* **157,** 367–379 (2016).

287. Zhu, X. G., De Sturler, E. & Long, S. P. Optimizing the distribution of resources between enzymes of carbon metabolism can dramatically increase photosynthetic rate: A numerical simulation using an evolutionary algorithm. *Plant Physiology* **145,** 513–526 (2007).

288. Elsässer, M. *et al.* Photosynthetic activity triggers pH and NAD redox signatures across different plant cell compartments. *bioRxiv,* 2020.10.31.363051 (2020).

289. Feitosa-Araujo, E. *et al.* Changes in intracellular NAD status affect stomatal development in an abscisic acid-dependent manner. *The Plant Journal* **104,** 1149–1168 (2020).

290. Knupp, J., Arvan, P. & Chang, A. Increased mitochondrial respiration promotes survival from endoplasmic reticulum stress. *Cell Death and Differentiation* **26,** 487–501 (2019).

291. Lee, C. P., Eubel, H., O'Toole, N. & Millar, A. H. Heterogeneity of the mitochondrial proteome for photosynthetic and non-photosynthetic Arabidopsis metabolism. *Molecular and Cellular Proteomics* **7,** 1297–1316 (2008).

292. Millar, A. H., Sweetlove, L. J., Giege, P. & Leaver, C. J. Analysis of the Arabidopsis mitochondrial proteome. *Plant Physiology* **127,** 1711–1727 (2001).

293. Collier, R. *et al.* Accurate measurement of transgene copy number in crop plants using droplet digital PCR. *The Plant Journal* **90,** 1014–1025 (2017).

294. Passricha, N., Saifi, S., Khatodia, S. & Tuteja, N. Assessing zygosity in progeny of transgenic plants: current methods and perspectives. *Journal of Biological Methods* **3,** 46 (2016).

295. Lu, M.-Z., Snyder, R., Grant, J. & Tegeder, M. Manipulation of sucrose phloem and embryo loading affects pea leaf metabolism, carbon and nitrogen partitioning to sinks as well as seed storage pools. *The Plant Journal* **101,** 217–236 (2020).

296. Paul, M. J., Watson, A. & Griffiths, C. A. Linking fundamental science to crop improvement through understanding source and sink traits and their integration for yield enhancement. *Journal of Experimental Botany* **71,** 2270–2280 (2020).

297. Furbank, R. T., Sharwood, R., Estavillo, G. M., Silva-Perez, V. & Condon, A. G. Photons to food: genetic improvement of cereal crop photosynthesis. *Journal of Experimental Botany* **71,** 2226–2238 (2020).

298. Kacser, H. & Acerenza, L. A universal method for achieving increases in metabolite production. *European Journal of Biochemistry* **216,** 361–367 (1993).

299. Pego, J. V., Kortstee, A. J., Huijser, C. & Smeekens, S. C. Photosynthesis, sugars and the regulation of gene expression. *Journal of Experimental Botany* **51,** 407–416 (2000).

300. Krapp, A., Hofmann, B., Schäfer, C. & Stitt, M. Regulation of the expression of rbcS and other photosynthetic genes by carbohydrates: A mechanism for the 'sink regulation' of photosynthesis? *Plant Journal* **3,** 817–828 (1993).

301. Tao, R. *et al.* Genetically encoded fluorescent sensors reveal dynamic regulation of NADPH metabolism. *Nature Methods* **14,** 720–728 (2017).

302. De Col, V. *et al.* ATP sensing in living plant cells reveals tissue gradients and stress dynamics of energy physiology. *eLife* **6,** e26770 (2017).

303. Flexas, J. Genetic improvement of leaf photosynthesis and intrinsic water use efficiency in C_3 plants: Why so much little success? *Plant Science* **251,** 155–161 (2016).

304. Dey, N., Sarkar, S., Acharya, S. & Maiti, I. B. Synthetic promoters *in planta*. *Planta* **242,** 1077–1094 (2015).

305. De Lange, O., Klavins, E. & Nemhauser, J. Synthetic genetic circuits in crop plants. *Current Opinion in Biotechnology* **49,** 16–22 (2018).

306. Cai, Y.-M. *et al.* Rational design of minimal synthetic promoters for plants. *Nucleic Acids Research* **48,** 11845–11856 (2020).

307. Moradpour, M., Nor, S. & Abdulah, A. CRISPR/dCas9 platforms in plants: strategies and applications beyond genome editing. *Plant Biotechnology Journal* **18,** 32–44.

308. Maher, M. F. *et al.* Plant gene editing through de novo induction of meristems. *Nature Biotechnology* **38,** 84–89 (2020).

309. He, Y., Zhang, T., Sun, H., Zhan, H. & Zhao, Y. A reporter for noninvasively monitoring gene expression and plant transformation. *Horticulture Research* **7,** 152 (2020).

310. Lu, Y. *et al.* Horizontal transfer of a synthetic metabolic pathway between plant species. *Current Biology* **27,** 3034–3041 (2017).

311. Zhang, Y. *et al.* A highly efficient *Agrobacterium*-mediated method for transient gene expression and functional studies in multiple plant species. *Plant Communications* **1,** 100028 (2020).